Design und Synthese neuer Azoimidazol-Liganden für die Licht-Induzierte Spinschaltung von Nickel(II)-Porphyrinen

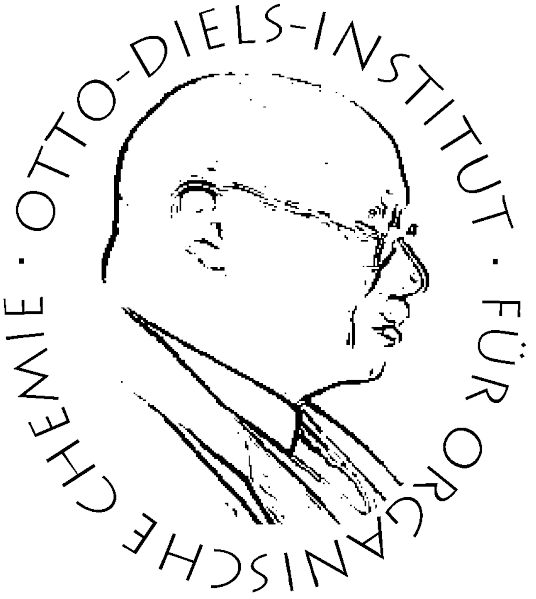

DISSERTATION

zur Erlangung des Doktorgrades
der Mathematisch-Naturwissenschaftlichen-Fakultät
der Christian-Albrechts-Universität
zu Kiel

vorgelegt von

Gernot Heitmann

Otto Diels-Institut für Organische Chemie
Kiel 2016

Referent: Prof. Dr. Rainer Herges
Koreferent: Prof. Dr. Felix Tuczek

Tag der mündlichen Prüfung: 16.12.2016
Zum Druck genehmigt: 16.12.2016

gez. Prof. Dr. Natascha Oppelt, Dekanin

Die vorliegende Arbeit wurde unter Anleitung von
Prof. Dr. Rainer Herges
am Otto-Diels-Institut für Organische Chemie
der Christian-Albrechts-Universität
sowie im Rahmen des Sonderforschungsbereichs 677
``Funktion durch Schalten´´
im Zeitraum von April 2012 bis November 2016 angefertigt.

Hiermit erkläre ich, Gernot Heitmann, dass ich die vorliegende Dissertation selbstständig und nur mit den angegebenen Hilfsmitteln angefertigt habe. Diese Doktorarbeit ist nach Inhalt und Form, abgesehen von der Beratung durch meinen Betreuer Herrn Prof. Dr. Rainer Herges, durch mich eigenständig nach den Regeln guter wissenschaftlicher Praxis der Deutschen Forschungsgemeinschaft verfasst worden. Sie wurde weder in Auszügen noch vollständig einer anderen Stelle im Rahmen eines Prüfungsverfahrens vorgelegt. Es handelt sich um meinen ersten Promotionsversuch.

Kiel, 08.11.2016

Gernot Heitmann

Kurzdarstellung

Magnetische Bistabilität in Einzelmolekülen ist für eine Vielzahl von Anwendung interessant, beispielsweise für die Realisierung eines schaltbaren Kontrastmittels für die Magnetresonanztomographie (MRT). Das *Light-Driven Coordination-Induced Spin State Switch* (LD-CISSS) Konzept ist der erfolgreichste Ansatz für die reversible Spinschaltung bei Raumtemperatur in homogener Lösung. Es beruht auf der Änderung der Koordinationszahl (*KZ*) eines Metallions durch die lichtgetriebene Assoziation bzw. Dissoziation von photochromen Liganden. In einer quadratisch-planaren Koordinationsumgebung (*KZ* 4) ist Ni(II) stets diamagnetisch ($S = 0$), während quadratisch-pyramidale oder oktaedrische Ni(II)-Komplexe (*KZ* 5, bzw. 6) einen paramagnetischen High-Spin-Zustand ($S = 1$) einnehmen. In dieser Arbeit wurden photoschaltbare Liganden auf Basis von *N*-Methylimidazol eingesetzt, um den Spinzustand von Ni(II)porphyrinen zu kontrollieren. Die verwendeten Phenylazoimidazole zeigen eine lichtinduzierbare *cis*/*trans*-Isomerisierung und wurden so konzipiert, dass nur eines der Photoisomere in der Lage ist, an das quadratisch-planare Ni(II)porphyrin zu koordinieren.
Eine quantenchemisch gestütze Designoptimierung führte zur Synthese eines äußerst effizienten, photodissoziierbaren Liganden. In seiner *trans*-Konfiguration koordiniert dieser sehr stark an das Ni(II)porphyrin, während sein *cis*-Isomer durch sterisch anspruchsvolle Substituenten effektiv an der Assoziation gehindert wird. Der Anteil der paramagnetischen Ni(II)-Spezies konnte mit diesem Liganden lichtinduziert zwischen 19 % und 89 % über mehrere Zyklen vollständig reversibel geschaltet werden. Die Schalteffizienz (SE) von 70 % ist für den intermolekularen LD-CISSS mit einem photodissoziierbaren Liganden bislang Rekord.
Durch die kovalente Anbindung der Phenylazoimidazol-Einheit an das Porphyrin konnte des Weiteren eine intramolekulare Spinschaltung realisiert werden. Um die Voraussetzungen für eine optimale Koordination des Liganden zu eruieren, wurden drei verschiedene Zielstrukturen mit variierender Verknüpfungseinheit designt und anschließend synthetisiert. Das Derivat, für das theoretisch die beste Performance vorhergesagt wurde, zeigte auch im Experiment die höchste Schalteffizienz (55 %). Die Verfolgung der Spinschaltung mittels MRT sowie erfolgreiche Schaltversuche in Gegenwart von Wasser beweisen, dass die vorgestellten molekularen Spinschalter für die Entwicklung eines photoschaltbaren MRT-Kontrastmittels ein sehr vielversprechender Ansatz sind.
In einem weiteren Projekt wurde eine effiziente Synthesestrategie für die kovalente Anbindung des schaltbaren Liganden an das Ni(II)porphyrin entwickelt. Durch die Verwendung eines sehr gut zugänglichen Precursor-Porphyrins gelang es, molekulare Spinschalter nach dem Baukastenprinzip zu synthetisieren und zu derivatisieren. Die Zielverbindungen konnten im Vergleich zu vorher angewandten Synthesestrategien zeitsparend und in deutlich höheren Ausbeuten erhalten werden. Für die weitere Entwicklung hinsichtlich medizinischer oder technischer Anwendungen ist diese neue modulare Synthesestrategie von hoher Bedeutung.

Abstract

Magnetic bistability in single molecules is of great interest for a number of different applications, e.g. for switchable contrast agents for magnetic resonance imaging (MRI). The *Light-Driven Coordination-Induced Spin State Switch* (LD-CISSS) concept is the most successful approach for reversible spin switching at room temperature in homogeneous solution. The LD-CISSS is based on a change of the coordination number (*CN*) in a transition metal complex by light-driven association or dissocation of photochromic ligands. Ni(II) in a square-planar coordination environment (*CN* 4) is always diamagnetic ($S = 0$) whereas a square-pyramidal or octahedral coordination sphere (*CN* 5 or 6) gives rise to a paramagnetic high spin state ($S = 1$). Within this thesis, photoswitchable ligands based on *N*-methylimidazole were used to control the spin state of Ni(II)porpyhrins. The applied phenylazoimidazoles exhibit photoinduced *cis*/*trans* isomerization and were designed for permitting only one of the photoisomers to coordinate to the Ni(II) center.

Quantum chemical design led to the synthesis of a very efficient photodissociable ligand. Its *trans* isomer coordinates extraordinary strongly to the Ni(II)porphyrin whereas the *cis* isomer is hindered efficiently from binding by sterically demanding substituents. Upon light-induced isomerization of this ligand in the presence of a Ni(II)porpyhrin, the percentage of paramagnetic Ni(II) species was switched reversibly from 19 % to 89 % over several cycles without a sign of fatigue. With a switching efficiency (SE) of 70 % it is by far the most efficient photodissociable ligand for the intermolecular LD-CISSS to date.

Furthermore, an intramolecular LD-CISSS was attained by covalently attaching the phenylazoimidazole unit to the porphyrin. To elucidate the prerequisites for optimal coordination of the ligand, three different target structures with varying tether units between porphyrin and azoimidazole were quantum chemically designed and subsequently synthesized. The theoretically most promising derivative also performed best in actual switching experiments (SE = 55 %). Visualization of the spin transition event by MRI, as well as sucessful switching experiments in the presence of water clearly proved that the reported molecular spin switches are a very promising approach for the development of a photoswitchable MRI contrast agent.

Another project of this thesis was devoted to the establishment of an efficient synthetic strategy for the tethering of the switching unit to the Ni(II)porphyrin. The development of an easily accessible precursor porphyrin as building block allowed for the synthesis and derivatization of molecular spin switches in a modular way. Compared to previously applied synthetic strategies, the respective target molecules were obtained more expeditiously and in significantly higher yields. The novel, modular synthetic approach is of utmost importance for further steps towards medicinal or technical applications.

Danksagung

Zunächst möchte ich meinem Doktorvater Prof. Dr. Rainer Herges für die Bereitstellung des außerordentlich interessanten Themas und seinem steten Interesse an meiner Forschungsarbeit danken. Ohne den Freiraum, den er mir für die Verfolgung eigener Ansätze gelassen hat und seinen hilfreichen Anregungen und Ideen zur richtigen Zeit wäre diese Arbeit sicherlich nicht so erfolgreich verlaufen. Auch für die Möglichkeit, eine Vielzahl an hochklassigen internationalen Konferenzen besuchen zu können, bin ich ihm sehr dankbar.
Allen aktuellen und ehemaligen Mitarbeitern des Arbeitskreis Herges danke ich für die lockere und entspannte Arbeitsatmosphäre und die große Hilfsbereitschaft. Die Kaffeepausen und diverse Feierabend- oder Freizeitaktivitäten werde ich sehr vermissen. Auch den Mitgliedern der weiteren Arbeitskreise des Otto Diels-Instituts und des Sonderforschungsbereichs 677 sei für die gute Zusammenarbeit gedankt.
Prof. Dr. Frank Sönnichsen und den Mitarbeitern der spektroskopischen Abteilung des Otto Diels-Instituts gebührt mein Dank für die Aufnahme zahlloser Spektren und das offene Ohr bei kniffligen spektroskopischen Fragen. Dr. Claus Gernert und Prof. Dr. Jürgen Grotemeyer danke ich für das Anfertigen hochaufgelöster Massespektren. Vanessa Kahl und den anderen nicht-wissenschaftlichen Mitarbeitern des Instituts danke ich für die organisatorische Hilfe und die großzügige Bereitstellung von Verbrauchsmaterialien.
Meinen Bachelor Studenten und F3 Praktikanten Andrei Kindjajev, Florian Borchert, Jannis Ludwig, Roland Löw und Fabian Kruse danke ich für ihr Interesse und die fruchtbare Mitarbeit an meiner Forschung. . . teilweise.
Dr. Torsten Winkler, Dr. Marcel Dommaschk, Dr. Christian Schütt, Dr. Jens Gröbner und Anne Heitmann sei für das Lektorat und den damit verbundenen Feinschliff dieser Arbeit gedankt.
Die Jahre in Kiel wären ohne Freunde wie Christian, Marcel, Melanie, Kim, Carolin, Joanna oder Michael mit Sicherheit deutlich weniger spaßig und ereignisreich verlaufen. Ihnen und den vielen anderen Menschen, die ich während des Studiums und der Promotion kennenlernen durfte, danke ich für die tolle Zeit. Die Squash- und Fußballspiele, die Donnerstagstreffen und Semesteressen, zahlreiche Pub-Abende oder auch einfach nur schöne Gespräche bei einer Tasse Kaffee haben mich so manchen Frust über fehlgeschlagene Synthesen vergessen lassen. Auch „meinen Hamburgern“ möchte ich für ihre jahrelange Freundschaft und ihr Verständnis danken, wenn ich in den letzten Jahren mal nicht so viel Zeit für sie hatte.
Ein besonderer Dank gebührt meinen Eltern und meinen Geschwistern, sowie den Familien Müller, Gottschald und Krenz für die tolle Unterstützung in jeglicher Form.
Ganz besonders danke ich meiner Anne, die in den letzten Jahren immer mein größter Rückhalt war und der ich so viel verdanke. Ich bin unsagbar glücklich, dich gefunden zu haben und freue mich auf das, was vor uns liegt.

Inhaltsverzeichnis

1 Einleitung

Im Zuge der Miniaturisierung der technischen Welt gewinnt auch das Schalten magnetischer Eigenschaften auf molekularer Ebene immer weiter an Bedeutung. Materialien und Einzelmoleküle, die bezüglich ihres magnetischen Zustands responsiv auf äußere Parameter reagieren oder durch Stimuli gezielt beeinflusst werden können, werden zukünftig in vielen Bereichen Anwendung finden.[1,2] Der seit mehr als 80 Jahren bekannte Spin Crossover (SCO) bildet die Grundlage für molekulare Bistabilität in Festkörpern und Polymeren. Solche Systeme sind unter Anderem für neuartige elektronische Speichermedien und Displays,[3–5] Sensoren[6] oder für Spintronics[7] interessant. Auch das Schalten magnetischer Zustände in Lösung oder auf Oberflächen ist von großer Bedeutung und gleichzeitig mit besonderen Herausforderungen verbunden. Da kooperative Effekte in diesen Fällen keine Rolle spielen, müssen neue Konzepte zur Realisierung der magnetischen Bistabilität in isolierten Einzelmolekülen entwickelt und erforscht werden. Anwendungsmöglichkeiten für solche Systeme reichen von der Beeinflussung magnetischer Levitation,[8] Entwicklung schaltbarer Spinlabel für die Aufklärung von Proteinstrukturen mittels PRE (*Paramagnetic Relaxation Enhancement*)[9] bis hin zur Realisierung von responsiven bzw. schaltbaren Kontrastmitteln für die Magnetresonanztomographie (MRT).[10,11]

1.1 Magnetresonanztomographie

Die Magnetresonanztomographie (MRT) ist neben der Computertomographie (CT) das wichtigste bildgebende Verfahren in der modernen medizinischen Diagnostik. Im Gegensatz zu Projektionsverfahren wie der herkömmlichen Röntgentechnik oder der Ultraschallbildgebung liefern beide Verfahren überlagerungsfreie Schnittbilder, die sogenannten Tomogramme, welche im Anschluss mittels Computertechniken zu einer dreidimensionalen Abbildung des Körperinneren zusammengesetzt werden können. Die Magnetresonanztomographie kommt anders als die CT ohne ionisierende Röntgenstrahlung aus. Die verwendeten Frequenzen im Radiowellenbereich sind nach heutigem Wissensstand unbedenklich. Des Weiteren bietet sie den besten Weichteilkontrast aller derzeit verfügbaren Bildgebungsmethoden, weshalb sie sich hervorragend für die Diagnostik von Tumoren und Entzündungsherden eignet. Die MRT basiert auf den physikalischen Grundlagen der Kernspinresonanz und ist eng mit der NMR-Spektroskopie verwandt.[12] Der wesentliche Unterschied zur NMR-Spektroskopie besteht in der Ortskodierung, also der räumlichen Zuordnung des MR-Signals, welche in der MRT mithilfe von Magnetfeldgradienten

erreicht wird. Die wesentlichen Grundlagen, die den Einsatz der Magnetresonanz als Routineverfahren in der medizinischen Bildgebung ermöglichten, wurden von LAUTERBUR[13] und MANSFIELD[14,15] entwickelt. Ihre Leistungen wurden 2003 mit dem Nobelpreis für Physiologie oder Medizin ausgezeichnet.[16]

In der MRT werden anhand der Relaxationszeiten von Kernspins Gewebearten und Körperstrukturen unterschieden.[17] Aufgrund seines ubiquitären Vorkommens in biologischen Systemen (v.a. Wasser, aber auch Biomoleküle) und seiner günstigen Eigenschaften für die Magnetresonanz wird in der Regel der ^{1}H-Kern gemessen. Die Relaxationszeit des ^{1}H-Kerns ist von vielen Umgebungsfaktoren abhängig,[18] unter anderem von der Viskosität und von der strukturellen Ordnung des Mediums, in dem sich die zu messenden Kernspins befinden. So besitzt beispielsweise Tumorgewebe aufgrund der unkontrollierten Teilung der betroffenen Zellen eine geringe strukturelle Ordnung, was im Vergleich zum gesunden Gewebe zu einer starken Verkürzung der Relaxationszeiten von Wasserprotonen führt.[19] In MRT-Aufnahmen zeichnet sich das Tumorgewebe als heller Bereich ab, da kurze Relaxationszeiten per Konvention zu einer Kontrastaufhellung führen.

Kernspin-Relaxationszeiten werden des Weiteren stark durch paramagnetische Substanzen beschleunigt.[20,21] Dies ist auf das lokale magnetische Störfeld zurückzuführen, welches paramagnetische Verbindungen aufgrund ihres eigenen magnetischen Moments erzeugen. Die Verwendung von paramagnetischen Substanzen als MRT-Kontrastmittel für die Steigerung des Informationsgehalts einer MRT-Aufnahme ist inzwischen gängige Praxis.[22] Bis heute wurden

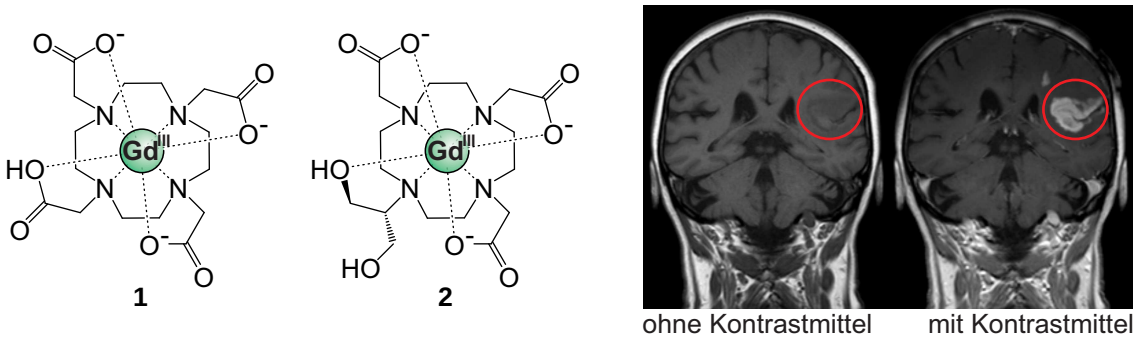

Abb. 1.1: Links: Die gängigen, klinisch zugelassenen Gd(III) Kontrastmittel Gadotersäure (**1**) und Gadobutrol (**2**). Rechts: T1-gewichtete MRT-Aufnahme des Kopfes nach einem ischämischen Hirninfarkt mit und ohne Kontrastmittel.[23] Das Eindringen des Kontrastmittels in das Hirngewebe ist auf eine Störung der Blut-Hirn-Schranke zurückzuführen.

in medizinischen Untersuchungen bereits über 200 Millionen Dosen Kontrastmittel verabreicht. Die Effektivität, mit der ein Kontrastmittel Kernspin-Relaxationszeiten beschleunigt, wird durch dessen Relaxivität quantifiziert.[24] Die meisten klinisch relevanten MRT-Kontrastmittel enthalten Gd(III) als paramagnetisches Zentrum.[25] Gd(III) besitzt mit einem Gesamtspin von $S = 7/2$ ein sehr großes magnetisches Moment, sodass hohe Relaxivitäten erreicht werden. Aufgrund der hohen Toxizität wird Gd(III) in Form von sehr stabilen Komplexverbindungen als Kontrastmittel

verabreicht. Die Freisetzung von ungebundenem Gd(III) wird im Körper durch multidentat koordinierende Chelatliganden verhindert (siehe Abb. 1.1).[26,27] Gadotersäure (**1**) mit dem extrem stark komplexierenden Chelat-Liganden 1,4,7,10-Tetraazacyclododecan-1,4,7,10-tetraessigsäure (DOTA) stellt die Basis für die meisten klinischen Gd(III)-Kontrastmittel dar. Das ähnlich stabile Derivat Gadobutrol (**2**) weist verbesserte physikochemische Eigenschaften auf und kann konzentrierter verabreicht werden. Beide Kontrastmittel sind hoch polar und besitzen ein relativ großes Molekulargewicht, sodass sie bei einem gesunden Menschen die Blut-Hirn-Schranke nicht passieren können. Tritt nach Applikation einer dieser Verbindungen eine Kontrastverstärkung im Gehirn auf, kann demnach mit großer Sicherheit auf eine krankheitsbedingte Ursache geschlossen werden (siehe Abb. 1.1).

1.2 Intelligente MRT-Kontrastmittel

Herkömmliche Kontrastmittel sind permanent aktiv und können lediglich statische anatomische Details hervorheben. Neuere Entwicklungen beschäftigen sich mit der Entwicklung sogenannter intelligenter Kontrastmittel, die responsiv auf metabolische Aktivität oder einen physiologischen Parameter mit einer Änderung ihrer Relaxivität reagieren.[28–30] Bereits adressierte Parameter sind beispielsweise der pH-Wert,[31–36] die Temperatur,[37,38] die Aktivität bestimmter Enzyme[39–46] oder die Konzentration von Thiolen,[47] Kohlenhydraten[48,49] und Ionen.[50–56]
Die Relaxivität eines Kontrastmittels kann auf verschiedenen Wegen beeinflusst werden.[11,57,58] Die zwei interessantesten Mechanismen sind in Abb. 1.2 schematisch dargestellt. Im ersten Fall erfolgt die Änderung der Relaxivität durch eine Beeinflussung der Wechselwirkung zwischen Kernspin und Kontrastmittel. Durch eine vollständige Absättigung der Koordinationssphäre wird ein direkter Kontakt zwischen Wassermolekülen und Metallion verhindert. Der adressierte Stimulus öffnet die Koordinationssphäre partiell, sodass das Wasser Zugang zum paramagnetischen Zentrum erhält und folglich die sogenannte *inner sphere* Relaxation aktiviert wird. Diese stellt in der Regel den effektivsten Relaxationsprozess dar. Allerdings gibt es mit der *second sphere* sowie der *outer sphere* Relaxation weitere Mechanismen, über die das Kontrastmittel wirksam ist. Gd(III)-Komplexe sind demzufolge bezüglich ihrer Relaxivität beeinflussbar, ein vollständiges Abschalten des Kontrastmittels ist jedoch nicht möglich.
Die zweite Strategie beruht auf einer Änderung des magnetischen Moments des paramagnetischen Zentrums mittels eines Spinübergangs. Bestimmte Metallionen können sowohl in einem sogenannten Low-Spin (LS) als auch in einem High-Spin (HS) Zustand vorliegen, wobei die LS-Spezies einen geringeren Gesamtspin und somit auch ein kleineres magnetisches Moment aufweist. Der LS-Zustand stellt somit den inaktiven Zustand des Kontrastmittels mit der geringeren Relaxivität dar. Ein bereits heute eingesetztes responsives Kontrastmittel, welches diesem Prinzip folgt, ist natürlichen Ursprungs. Das sauerstofftransportierende Protein Hämoglobin enthält als prosthetische Gruppe das Fe(II)-Porphyrin-Derivat Häm *b*, dessen Spinzustand sich

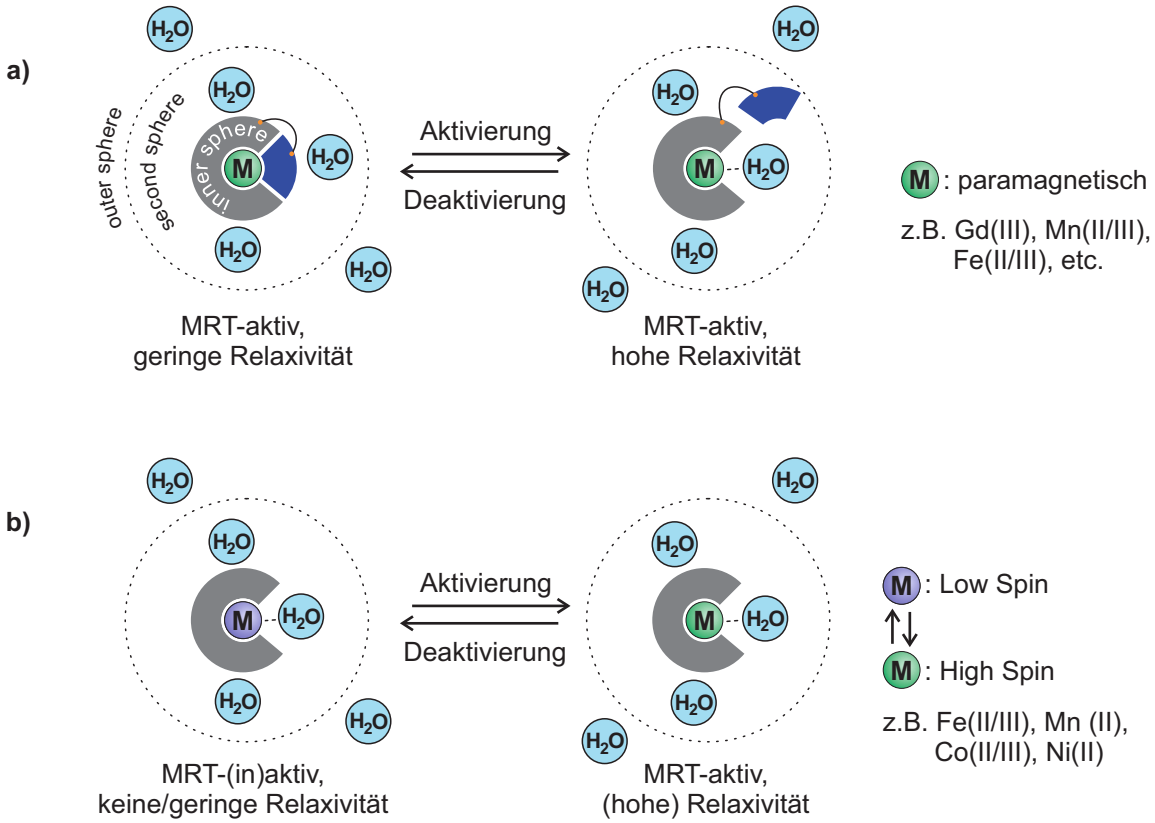

Abb. 1.2: Gezeigt sind zwei Mechanismen, mittels derer die Relaxivität von MRT-Kontrastmitteln beeinflusst werden. a) Die Relaxivität des Kontrastmittels ist von der Art der Wechselwirkung zwischen paramagnetischem Zentrum und Kernspin abhängig. Im vollständig abgesättigten Komplex ist die sogenannte *inner sphere* Relaxation verhindert und folglich das Kontrastmittel weniger aktiv. b) Ein Übergang des Metallions zwischen einer High-Spin und einer Low-Spin Form ändert das magnetische Moment des Komplexes und folglich seine Relaxivität.

bei der Aufnahme bzw. Abgabe von Sauerstoff ändert. Folglich sind die Relaxationszeiten von im Blut vorhandenen Kernspins vom Oxygenierungsgrad des Hämoglobins abhängig.[59] In der funktionellen MRT (fMRT) dient dieser sogenannte BOLD (*blood oxygenation level dependent*) Kontrast der Identifizierung von neuronal aktiven Hirnarealen mit einem erhöhten Sauerstoffverbrauch.[60–63]

Neben der Responsivität auf einen physiologischen Parameter ist auch das gezielte Ein- und Ausschalten eines Kontrastmittels durch einen externen Stimulus höchst interessant, insbesondere in der interventionellen Radiologie.[64] Die Kontrolle von katheterbasierten, minimalinvasiven Eingriffen zur Behandlung von Gefäßverengungen oder Aneurysmen erfolgt heutzutage größtenteils mittels Röntgen-Angiographie. Die Belastung mit ionisierender Strahlung ist bei solchen Untersuchungen immens, sodass die Verwendung von MRT-Techniken ein großes Verbesserungspotential birgt. Als Stimulus für die Schaltung eines solchen Kontrastmittels bietet sich in erster Linie Licht an. Licht gewährleistet eine exzellente zeitliche und räumliche Auflösung, kann bezüglich Wellenlänge und Intensität sehr gut auf die Anforderungen des zu schaltenden Systems eingestellt

werden, hinterlässt keine unerwünschten Nebenprodukte oder chemische Rückstände und ist nicht-invasiv einsetzbar.[65] Die Verwendung von Licht zur Kontrolle bestimmter Funktionen in biologischen Systemen und *in vivo* ist des Weiteren bereits gut etabliert.[66–70] Photoresponsive MRT-Kontrastmittel wurden schon beschrieben, jedoch beruhen diese auf der Beeinflussung der *inner sphere* Relaxation von Gd(III) Komplexen.[71,72] Folglich weisen diese Verbindungen keine vollständig MRT-inaktive Form auf. Diese sehr erstrebenswerte Eigenschaft lässt sich durch Metallkomplexe realisieren, die sich zwischen einer diamagnetischen (Gesamtspin $S = 0$) und einer paramagnetischen ($S > 0$) Spezies schalten lässt.

1.3 Spin Crossover

Übergangsmetallionen mit einer $3d^2$-$3d^8$ Elektronenkonfiguration können in Abhängigkeit der Stärke und der Geometrie ihres Ligandenfeldes verschiedene elektronische Zustände einnehmen. Unter bestimmten Voraussetzungen sind diese durch einen physikalischen oder chemischen Stimulus ineinander überführbar. Der bekannteste Mechanismus für einen solchen Spinübergang ist der sogenannte Spin Crossover, welcher in einigen oktaedrischen Metallkomplexen (Elektronenkonfiguration $3d^4$-$3d^7$) auftritt (siehe Abb. 1.3).

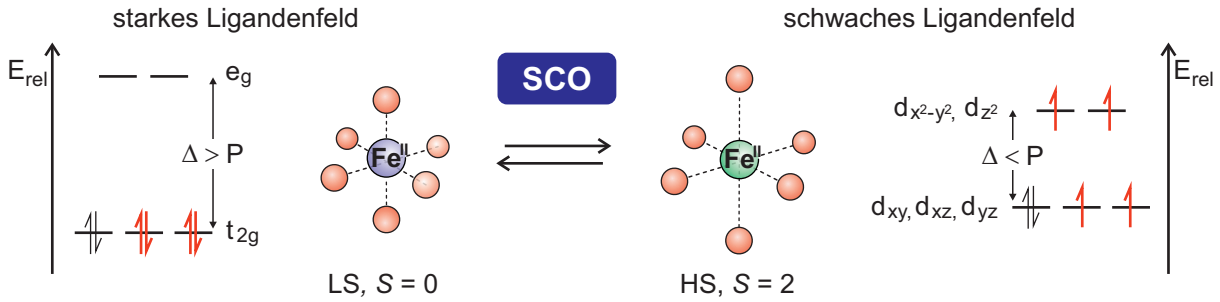

Abb. 1.3: Schematische Darstellung des Spin Crossovers in oktaedrischen Fe(II)-Komplexen. Ein starkes Ligandenfeld führt zu einer großen Ligandenfeldaufspaltung (Δ) und zur bevorzugten Doppelbesetzung der energetisch günstigen t_{2g}-Orbitale. Im schwachen Ligandenfeld ist Δ kleiner als die Spinpaarungsenergie (P), sodass es zur Besetzung der energetisch ungünstigen e_g-Orbitale kommt. Wenn Δ und P vergleichbar groß sind, kann ein thermischer Spinübergang induziert werden.

Im oktaedrischen Ligandenfeld kommt es gemäß der Ligandenfeldtheorie zur energetischen Aufspaltung der d-Orbitale des Metallions in die t_{2g}-Orbitale (d_{xy}, d_{xz}, d_{yz}) und die e_g-Orbitale (d_{z^2}, $d_{x^2-y^2}$). Die Energiedifferenz zwischen t_{2g}- und e_g-Orbitalen wird als Ligandenfeldaufspaltung (Δ) bezeichnet. In einem starken Ligandenfeld ist Δ größer als die Spinpaarungsenergie (P). Folglich werden entgegen der 2. Hund'schen Regel[73] zunächst die t_{2g}-Orbitale doppelt besetzt, sodass sich ein Low-Spin (LS) Zustand ergibt. Ist hingegen P größer als Δ, erfolgt zunächst die Einfachbesetzung aller d-Orbitale und erst im Anschluss gegebenenfalls die Doppelbesetzung. Der Komplex befindet sich im High-Spin (HS) Zustand. Ist die Differenz von Δ und P in

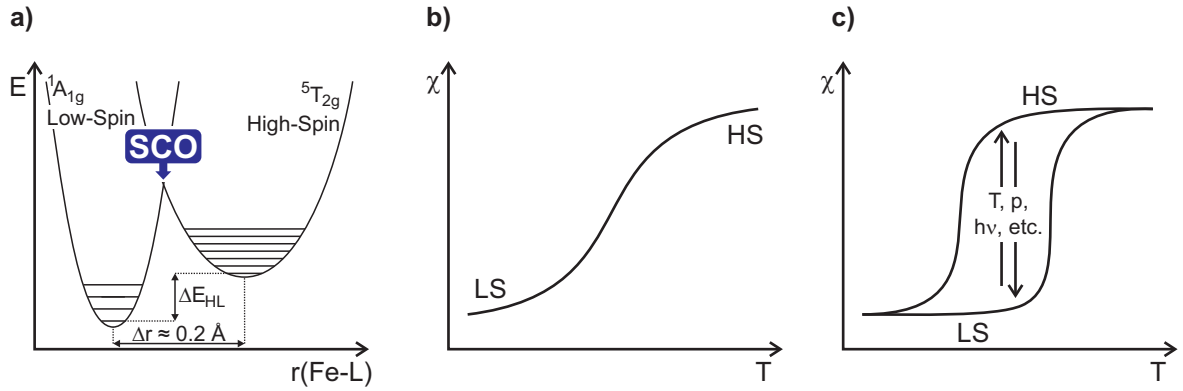

Abb. 1.4: Spin Crossover in Fe(II)-Komplexen. a) Der LS-Zustand ($^1A_{1g}$) ist enthalpisch begünstigt und somit bei tiefen Temperaturen stabil. Der HS-Zustand ($^5T_{2g}$) besitzt eine höhere Schwingungszustandsdichte und ist folglich entropisch bevorzugt. b) Wird ein SCO-Komplex einem Temperaturgradienten ausgesetzt, kommt es gemäß der Boltzmann-Verteilung zu einem graduellen, thermischen SCO vom LS- in den HS-Zustand. c) Im Festkörper stabilisieren kooperative Effekte des Kristallgitters beide Spinzustände, sodass es zur Hysterese kommt. Innerhalb der Hystereseschleife kann der Spinübergang durch verschiedene externe Stimuli induziert werden.

der Größenordnung der thermischen Energie (k_BT), kann es zu einem Spinübergang zwischen LS- und HS-Zustand kommen, welcher als Spin Crossover (SCO) bezeichnet wird. Der SCO ist erstmals 1931 durch CAMBI *et al.* für einen Fe(III)-Komplex beschrieben worden.[74,75] Seitdem ist eine große Zahl an Originalarbeiten und Reviewartikeln über SCO-Systeme erschienen.[1,76–88] Die meisten SCO-Komplexe sind für Fe(II) bekannt.[89–92] Der LS-Zustand ($^1A_{1g}$) von Fe(II) besitzt eine geringere Nullpunktsenergie als der HS-Zustand ($^5T_{2g}$) und ist folglich enthalpisch bevorzugt. Mit steigender Temperatur werden höher liegende Schwingungszustände zugänglich und die Bindungen zwischen Zentralion und Liganden (r(Fe-L)) werden länger (siehe Abb. 1.4a). Dies begünstigt den entropisch bevorzugten HS-Zustand. Die Folge der sich einstellenden Boltzmann-Verteilung ist ein gradueller Spinübergang vom LS- zum HS-Zustand (siehe Abb. 1.4b). Kooperative Effekte im Festkörper oder in Polymerverbindungen können beide Spinzustände über einen relativ weiten Temperaturbereich stabilisieren, wodurch es zu zwei Effekten kommt. Der Spinübergang findet zum einen sprunghaft innerhalb eines kleinen Temperaturintervalls statt und unterliegt zum anderen einer Hysterese (siehe Abb. 1.4c).[91] Dies lässt sich mit den starken strukturellen Anpassungen aufgrund der sich ändernden Metall-Ligand-Bindungen erklären, die der Festkörper während des Spinübergangs vollziehen muss. Innerhalb der Hystereseschleife, welche zum Teil mehr als 100 K umfasst[93,94] und den für die meisten Anwendungen interessanten Bereich um Raumtemperatur abdecken kann,[3,81,84] weisen SCO-Festkörper magnetische Bistabilität auf. Der Spinübergang kann unter Anderem durch Änderungen der Temperatur, des Drucks oder durch die Bestrahlung mit Licht induziert werden.[95–99] Die erwünschte Eigenschaft eines diamagnetischen (MRT-inaktiven) LS-Zustands des zu entwickelnden photoresponsiven Kontrastmittels schränkt die Auswahl an geeigneten

Metallionen stark ein. Das vergleichsweise große magnetische Moment des paramagnetischen HS-Zustands ($S = 2$) prädestiniert insbesondere Fe(II). Auch Co(III) und Ni(II) weisen einen diamagnetischen LS-Zustand auf. Für alle drei Metallionen wurden bereits Strategien bezüglich einer lichtinduzierten Spinschaltung entwickelt.

1.4 Lichtinduzierte Spinschaltung

Die Spinschaltung von oktaedrischen Fe(II)-Komplexen durch elektronische Anregung des Metallzentrums mittels Licht wird durch den seit 1984 bekannten LIESST (*Light-Induced Excited Spin State Trapping*) Effekt beschrieben (siehe Abb. 1.5, links).[80,100] Bei Temperaturen unterhalb der Spinübergangstemperatur liegt Fe(II) erwartungsgemäß im LS-Zustand vor. Durch Bestrahlung mit grünem Licht erfolgt unter Berücksichtigung des Franck-Condon-Prinzips ein elektronischer Übergang in einen angeregten LS-Zustand ($^1T_2$). Über zwei Intersystem-Crossing-Prozesse relaxiert der angeregte Komplex in den bei tiefen Temperaturen metastabilen HS-Zustand und kann mittels der üblichen spektroskopischen Methoden charakterisiert werden. Durch Bestrahlung mit rotem Licht kann der Komplex zurück in den LS-Grundzustand überführt werden. Dieser Effekt ist als reverse-LIESST bekannt.[101] Die Spinschaltung von Fe(II) mittels LIESST ist effizient und reversibel, jedoch ist sie auf Festkörperverbindungen bzw. sehr niedrige Temperaturen beschränkt. Die Energiebarriere zwischen den elektronischen Zuständen des Metallions ist sehr klein, sodass es ohne die stabilisierenden kooperativen Effekte des Festkörpers bei höheren Temperaturen immer zu einem graduellen SCO kommt. In Lösung liegen die Metallkomplexe isoliert und somit frei von jeglichen kooperativen Effekten vor. Hier lässt sich der HS Zustand nur für eine extrem geringe Zeitspanne anreichern und das auch nur bei sehr geringen Temperaturen.[102]

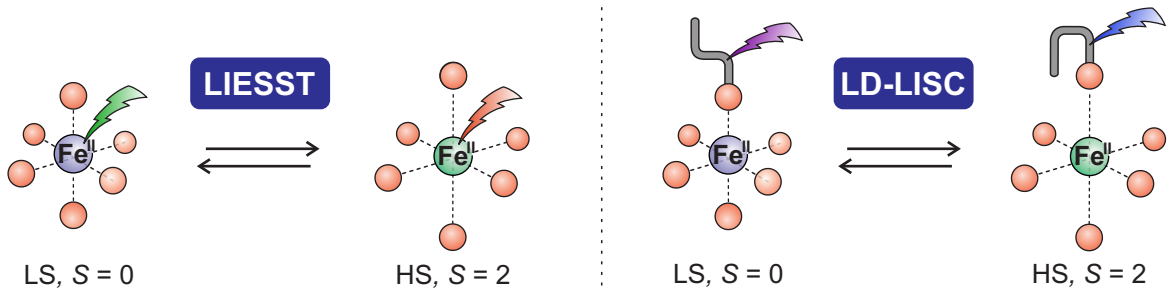

Abb. 1.5: Lichtinduzierte Spinschaltung in oktaedrischen Fe(II)-Komplexen. Beim sogenannten LIESST (*Light-Induced Excited Spin State Trapping*, links) erfolgt die Spinschaltung durch eine elektronische Anregung des Metallzentrums. Der LD-LISC (*Ligand-Driven Light-Induced Spin Change*, rechts) beruht auf einer Änderung der Ligandenfeldstärke durch photochrome Liganden, deren Photoisomere unterschiedliche Donorstärken aufweisen.

Der LD-LISC (*Ligand-Driven Light-Induced Spin Change*) Effekt beruht ebenfalls auf dem SCO Phänomen.[83,103,104] Statt mittels einer direkten elektronischen Anregung des Metallzentrums erfolgt der Spinübergang durch eine photoinduzierte Änderung der Ligandenfeldstärke (siehe Abb. 1.5, rechts). Hiefür werden photochrome Liganden verwendet, deren Photoisomere unterschiedliche Koordinationsstärken aufweisen und somit zu einer Verschiebung der Spinübergangstemperatur des Metallions führen. Im Temperaturbereich zwischen diesen Spinübergängen ist mittels Photoisomerisierung des Liganden eine lichtgetriebene Spinschaltung möglich. Durch Variation der photochromen Liganden gelang die Spinschaltung von Fe(II) bei Raumtemperatur[105,106] und in Lösung.[107] Die mittels LD-LISC erreichbaren Schalteffizienzen sind allerdings meist gering. Des Weiteren sind die Komplexe in der Regel nur unter inerten Bedingungen verwendbar und weisen eine unzureichende Photostabilität auf. Weder LIESST noch LD-LISC stellen für die Entwicklung eines photoschaltbaren MRT-Kontrastmittels geeignete Ansätze dar. Eine effiziente und ermüdungsfreie Spinschaltung bei Raumtemperatur und in Lösung ist nicht gegeben. Für die lichtinduzierte *in vivo* Spinschaltung von Fe(II) stehen somit nach heutigem Stand keine geeigneten Konzepte zur Verfügung.

Die lichtinduzierte Spinschaltung von Cobalt kann mittels einer sogenannten Valenztautomerie (VT) erreicht werden.[108,109] Hierbei kommt es zu einer intramolekularen Elektronenübertragung zwischen dem Metallzentrum und einem redox-aktiven Liganden.[110] Am häufigsten werden Catecholat/Semichinon-Liganden für die VT von Cobalt verwendet. Die diamagnetische LS-Spezies ($S = 0$) ist ein Co(III)catecholat-Komplex, welcher im Gleichgewicht mit einer paramagnetischen Co(II)semichinon-Form steht. Das Gleichgewicht zwischen beiden Spezies kann durch Temperaturveränderung oder Bestrahlung mit Licht verschoben und folglich ein Spinübergang induziert werden.[111–113] Durch den Einsatz von photoschaltbaren Co-Liganden kann das VT-Gleichgewicht im Bereich der Raumtemperatur beeinflusst werden. Dieser Effekt wurde als *Light-Driven Ligand-Induced Valence Tautomerism* (LD-LIVT) bezeichnet (siehe Abb. 1.6).[114,115] Allerdings ist auch die Spinschaltung mittels LD-LIVT lediglich unter inerten Bedingungen durchführbar und zeigt bisher keine zufriedenstellende Schalteffizienz.

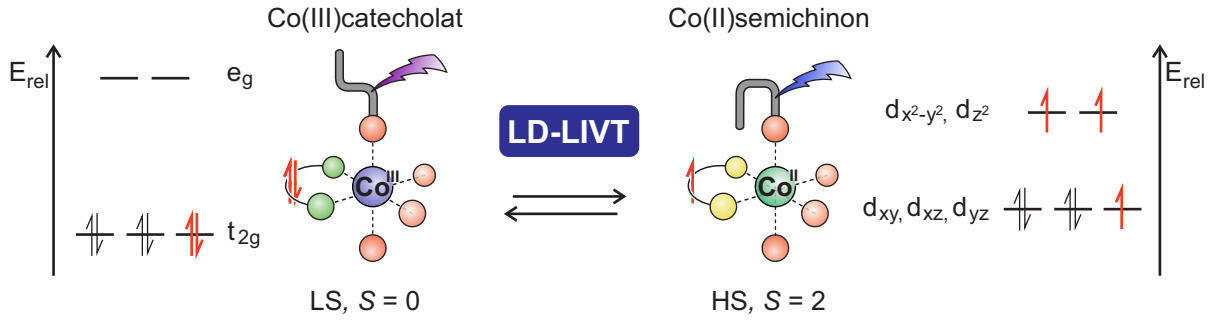

Abb. 1.6: Der LD-LIVT (*Light-Driven Ligand-Induced Valence Tautomerism*) Effekt beruht auf der Beeinflussung des valenztautomeren Gleichgewichts in einem Co(II/III)semichinon/catecholat Komplex mittels photoresponsiver Co-Liganden.

Für die Spinschaltung von Ni(II) wurde ein Konzept verfolgt, das auf der lichtgetriebenen Assoziation bzw. Dissoziation von Liganden beruht. Dieser Spinübergang ist unter der Abkürzung LD-CISSS (*Light-Driven Coordination-Induced Spin State Switch*) bekannt.[116,117] Anders als der vom SCO abgeleitete LD-LISC basiert der LD-CISSS nicht auf einer Änderung der Ligandenfeldstärke, sondern auf einer Änderung der Ligandenfeldgeometrie. Dies stellt einen wesentlich stärkeren Eingriff in die energetische Aufspaltung der d-Orbitale des Metallions dar, sodass der LD-CISSS deutlich weniger anfällig für Schwankungen von Umgebungsparametern wie der Temperatur oder des Drucks ist. Ni(II) ist chemisch äußerst robust, kann in beiden Spinzuständen gut mittels NMR-Spektroskopie charakterisiert werden und ist quantenchemisch (Dichtefunktionaltheorie) vergleichsweise einfach beschreibbar. Die erforderlichen Komplexgeometrien sind bereits gut etabliert (siehe Kap. 1.5.1). Nachteilig ist lediglich das im Vergleich zu Fe(II) kleine magnetische Moment des HS-Zustands ($S = 1$) und die daraus folgende geringere Relaxivität des MRT-aktiven Zustands.

1.5 Spinschaltung von Nickel(II)

In einem quadratisch-planaren Ligandenfeld ist Ni(II) stets diamagnetisch ($S = 0$), während eine quadratisch-pyramidale oder oktaedrische Koordinationssphäre zu einem paramagnetischen Spinzustand ($S = 1$) führt. Die entsprechenden Orbitalschemata sind in Abb 1.7 gezeigt. Im quadratisch-planaren Ni(II)-Komplex sind die vier Liganden direkt auf das $d_{x^2-y^2}$ Orbital

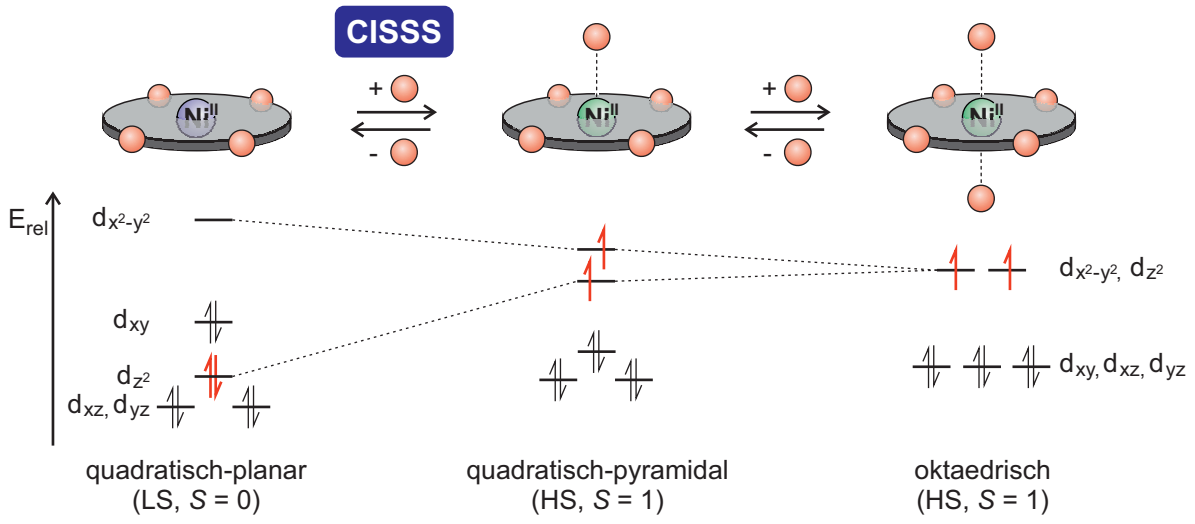

Abb. 1.7: Coordination-Induced Spin State Switching in Ni(II)-Komplexen. Ein quadratisch-planares Ligandenfeld führt zu einem diamagnetischen LS-Zustand ($S = 0$). Die Addition eines axialen Liganden ergibt eine quadratisch-pyramidale Koordinationssphäre und aufgrund der drastischen Änderung der Orbitalaufspaltung einen paramagnetischen HS-Zustand ($S = 1$). Durch die Addition eines weiteren axialen Liganden wird die bekannte Orbitalaufspaltung der oktaedrischen Koordinationssphäre erhalten, in der Ni(II) ebenfalls im HS-Zustand vorliegt.

ausgerichtet, welches deshalb energetisch sehr ungünstig ist und unbesetzt bleibt. Die acht d-Elektronen verteilen sich auf die übrigen vier d-Orbitale, wobei jene mit z-Charakter (d_{z^2}, d_{xz}, d_{yz}) energetisch bevorzugt sind. Bei der Addition eines axialen Liganden ändert sich die energetische Aufspaltung der d-Orbitale drastisch. Das d_{z^2}-Orbital wird durch den zusätzlichen Liganden relativ zu den übrigen Orbitalen so stark angehoben, dass die energetische Aufspaltung zwischen d_{z^2} und $d_{x^2-y^2}$ geringer wird als die Spinpaarungsenergie. Folglich kommt es zur Einfachbesetzung beider Orbitale und zum sogenannten *Coordination-Induced Spin State Switch* (CISSS).[118–121] Ein weiterer axialer Ligand führt zur bekannten Ligandenfeldaufspaltung im Oktaeder, in der Ni(II) ebenfalls im HS-Zustand vorliegt.
Die Koordinationsstärke von Liganden wird durch deren Assoziationskonstanten (K) quantifiziert. Die Assoziationskonstante der ersten axialen Koordination (Ausbildung des quadratisch-pyramidalen Komplexes) wird als K_{1S}, die der zweiten Koordination (Ausbildung des oktaedrischen Komplexes) als K_2 bezeichnet. Der Index S der ersten Assoziationskonstante (K_{1S}) kennzeichnet den dabei stattfindenden Spinübergang. In Ni(II)-Komplexen sind die Assoziationskonstanten K_{1S} und K_2 eines Liganden in der Regel nicht identisch (siehe Kap. 1.5.1). Bei der Verwendung schwacher Donorliganden ist der quadratisch-pyramidale Komplex energetisch ungünstig und die erste Koordination wird durch einen weiteren axialen Liganden unter Ausbildung des oktaedrischen Komplexes stabilisiert ($K_{1S}<K_2$). Bei starken Donorliganden ist die Elektronendichte am Ni(II) nach der Koordination des ersten Liganden hingegen bereits so hoch, dass eine weitere Koordination energetisch weniger bevorzugt ist ($K_{1S}>K_2$).

1.5.1 Coordination-Induced Spin State Switch von Ni(II)porphyrinen

Der CISSS mit Ni(II) erfordert als strukturelle Basis eine stabile, quadratisch-planare Koordinationsumgebung, welche zudem ausreichend Raum für die zusätzliche Koordination axialer Liganden gewährleistet. Die Porphyrin- und porphyrinverwandten Makrozyklen stellen hinsichtlich des angestrebten CISSS die interessantesten Liganden dar.[118–120,122–130] Tetraarylporphyrine mit aromatischen Substituenten in den *meso*-Positionen des Porphyrins sind synthetisch mittels einer säurekatalysierten Kondensation von Pyrrol und Benzaldehyd-Derivaten gut zugänglich. Die elektronischen Eigenschaften des Porphyrins und damit die Affinität für die Koordination axialer Liganden kann über die *meso*-Substituenten sehr genau eingestellt werden. Elektronenziehende *meso*-Substituenten führen zu einer Elektronenarmut des Ni(II) und begünstigen die axiale Koordination von Donorliganden.[122,123,131] Das elektronenarme *meso*-Tetrakis(pentafluorphenyl)nickel(II)porphyrin ($NiTPPF_{20}$, **3**) hat sich als quadratisch-planar koordinierender Ni(II)-Plattform für den CISSS bewährt (siehe Abb. 1.8).[118,131]
Funktionalisierungen an den *meso*-Substituenten oder den β-Positionen des Porphyrins ermöglichen eine zusätzliche Anpassung der molekularen Eigenschaften. Es wurden bereits mehrere

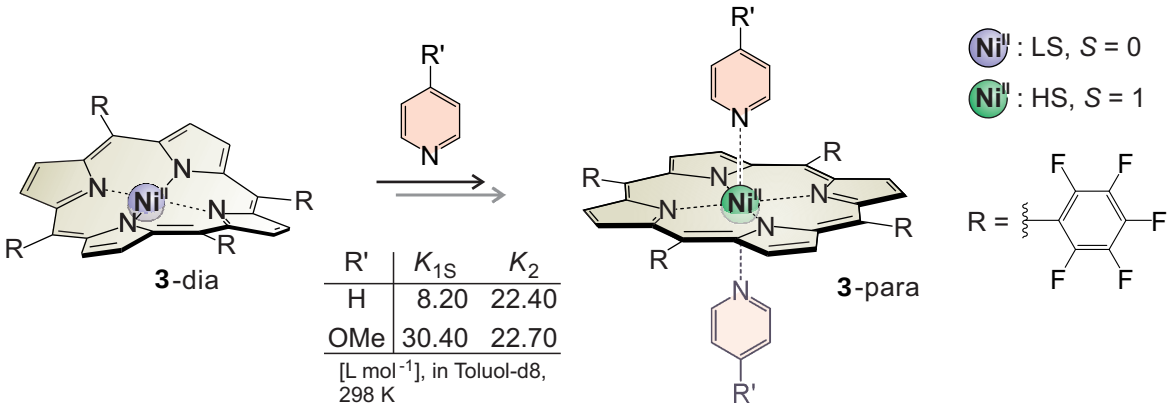

Abb. 1.8: Coordination-Induced Spin State Switching von *meso*-Tetrakis-(pentafluorphenyl)nickel(II)porphyrin ($NiTPPF_{20}$, **3**) mit Pyridinliganden. Die Assoziationskonstanten (K_{1S}, K_2) von Pyridin und damit die bevorzugte Geometrie des paramagnetischen Komplexes (quadratisch-pyramidal oder oktaedrisch) können durch *para*-Substitution beeinflusst werden.

von **3** abgeleitete Ni(II)-Komplexe realisiert, welche wichtige Zwischenschritte für die Entwicklung von Spinschaltern für zukünftige medizinische Anwendungen darstellen (siehe Abb. 1.8). So konnten durch 1,3-dipolare Cycloadditionsreaktionen an einer oder zwei Doppelbindungen des Porphyrinsystems die entsprechenden Chlorin- bzw. Isobakteriochlorin-Derivate **4** und **5** erhalten werden, welche im Vergleich zum Porphyrin-Stammsystem stark bathochrom verschobene UV/Vis-Absorptionsbanden aufweisen und insbesondere für zukünftige *in vivo* Belichtungsexperimente interessant sind.[120] In CISSS-Experimenten zeigten diese Systeme zudem eine deutlich höhere Affinität für die Koordination axialer Liganden. Mit dem dendronisierten $NiTPPF_{16}$-Derivat **6** konnte des Weiteren ein CISSS in Wasser realisiert werden. Die Einführung der Glycerin-Dendrimere mittels nukleophiler Aromatensubstitution an den *meso*-Pentafluorphenylsubstituenten von **3** führt zur erwünschten Wasserlöslichkeit des Porphyrins. Außerdem wird durch die leicht erhöhte Elektronendichte am Ni(II) die Koordination von Wasser ans Ni(II) und damit eine unerwünschte Spinschaltung durch das Lösungsmittel verhindert.[119] Als Liganden für den CISSS mit Ni(II)porphyrinen haben sich Stickstoffbasen bewährt.[118–120] Pyridin ist ein relativ schwacher Ligand, allerdings kann seine Donorstärke durch elektronenschiebende Substituenten in *para*-Position zum koordinierenden Stickstoff verbessert werden.[118] Die aliphatische Base Piperidin ist ein extrem starker Ligand und wurde für den CISSS in Wasser verwendet.[119] Für die Entwicklung von lichtresponsiven CISSS-Systemen sind aufgrund ihrer rigideren Struktur dennoch die Pyridin-Liganden vorzuziehen.

1.5.2 Lichtgetriebener CISSS mit Photodissoziierbaren Liganden

Für einen mit Licht steuerbaren CISSS (*engl. Light-Driven* CISSS, LD-CISSS) wurden im Arbeitskreis HERGES die als axiale Liganden verwendeten Pyridine mit einer photoschaltbaren Azoeinheit versehen. Azopyridine können eine *cis*- sowie eine *trans*-Konfiguration einnehmen.

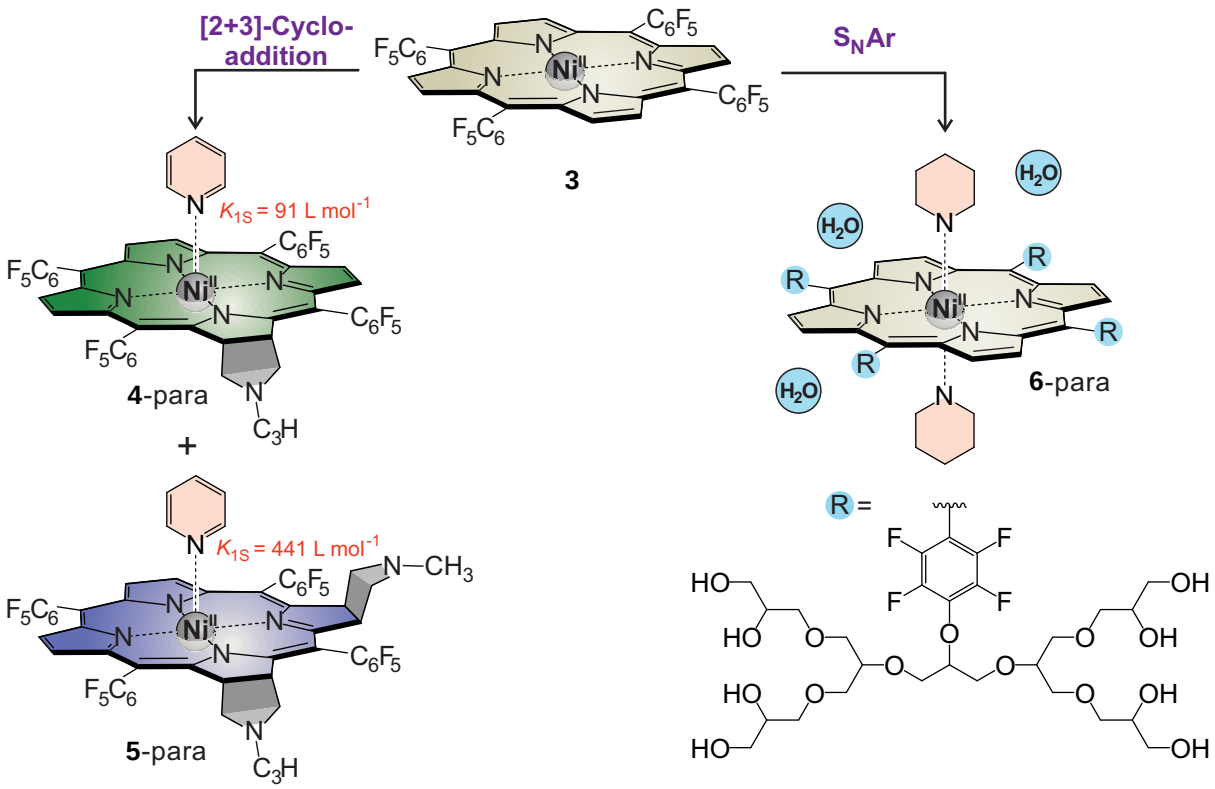

Abb. 1.9: Derivate von $NiTPPF_{20}$ **3** als wichtige Zwischenschritte für die angestrebte *in vivo* Anwendung. Die durch Cycloadditionen an **3** erhaltenen Chlorin- bzw. Isobakteriochlorin-Derivate **4** und **5** weisen im Vergleich zum Porphyrin **3** stark bathochrom verschobene Absorptionsbanden auf, was durch die Färbung ihrer Lösungen gut zu beobachten ist (**4**: grün, **5**: blau). Des weiteren zeigen **4** und **5** in CISSS-Experimenten mit Pyridin eine wesentlich höhere Affinität für die axiale Koordination. Ein CISSS in Wasser konnte mit dem dendronisierten $NiTPPF_{20}$-Derivat **6** realisiert werden. Die Einführung der solvatisierenden Glycerin-Dendrimere gelang mittels nukleophiler Aromatensubstitution an den Pentafluorphenylgruppen von **3**.

Die entsprechenden Isomere lassen sich photochemisch durch die Bestrahlung mit UV-Licht (ca. 365 nm, *trans*→*cis*) beziehungsweise blauem Licht (ca. 440 nm, *cis*→*trans*) ineinander überführen. Bei der *cis*/*trans*-Isomerisierung von Azopyridinen kommt es zu einer großen strukturellen Änderung des Moleküls, die sich sehr gut für die Realisierung eines bindenden und eines nicht-bindenden Schaltzustands nutzen lässt. Das *trans*-Isomer weist eine planare Struktur auf, während die *cis*-Konfiguration bevorzugt in einer verdrillten Konformation vorliegt, in der die aromatischen Systeme parallel zueinander orientiert sind. Der Abstand zwischen den *para*-Kohlenstoffatomen verändert sich dabei von 9 Å (*trans*) auf 6 Å (*cis*).[132–134]

THIES *et al.* verwendeten für den LD-CISSS an $NiTPPF_{20}$ (**3**) photodissoziierbare Liganden (PDLs) auf Basis von Azobipyridinen und Phenylazopyridinen (siehe Abb. 1.10).[116,135] Das Vorgehen für das Design eines effizienten PDLs ist für beide Ligandenklassen in den entscheidenden Punkten identisch. Die regiospezifische Anknüpfung der Azoeinheit in *meta*-Position zum koordinierenden Stickstoffatom gewährleistet, dass der Ligand im *trans*-Isomer ungehindert

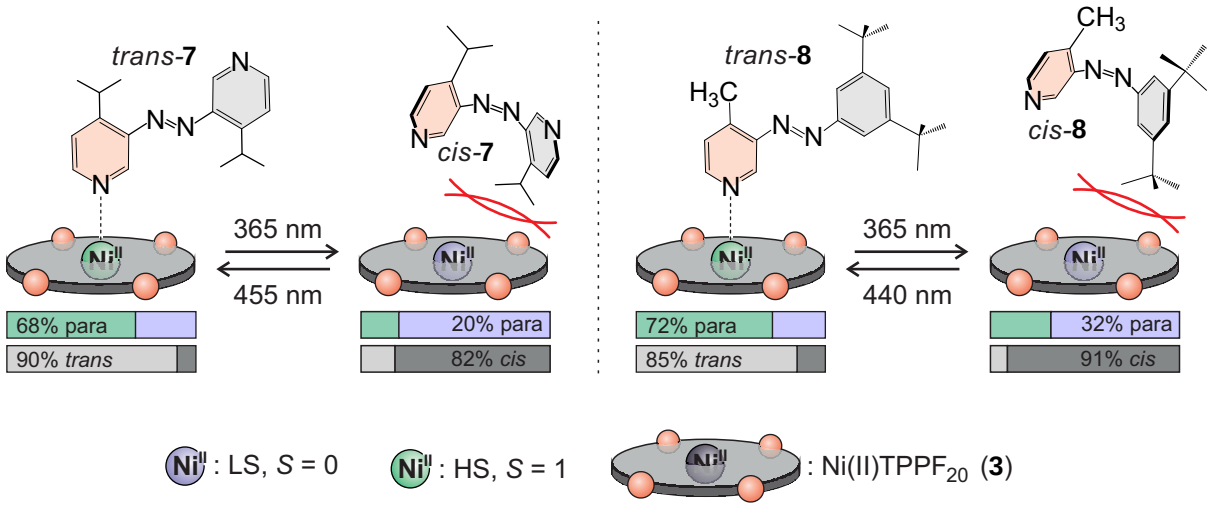

Abb. 1.10: Effizienter intermolekularer LD-CISSS mit pyridinbasierten PDLs **7** und **8**. Die Azoeinheit in *meta*-Position und die Alkylsubstituenten bedingen die effektive Dissoziation des *cis*-Isomers. Eine Koordination des *trans*-Isomers ist hingegen weiterhin möglich.

koordinieren kann, während es im Falle des *cis*-Isomers zu sterischen Wechselwirkungen mit dem Porphyrin kommt. Um diese Repulsion zu verstärken, tragen die PDLs weitere sterisch anspruchsvolle Substituenten.

Das *meta*-Azo-(4,4'-di-isopropyl)bipyridin (**7**) ist als PDL für $NiTPPF_{20}$ (**3**) bereits sehr effizient.[116] Der Anteil an paramagnetischer Ni(II)-Spezies konnte lichtinduziert mit **7** in Toluol zwischen 68 % (Belichtung mit 455 nm, 90 % *trans*-Isomer) und 20 % (Belichtung mit 365 nm, 82 % *cis*-Isomer) geschaltet werden, was einer Schalteffizienz von 48 % entspricht. Da das Azobipyridin-System zwei koordinative Pyridin-Einheiten enthält, bildet es allerdings als *trans*-Isomer paramagnetische Koordinationpolymere und -oligomere mit **3** aus, welche aus konzentrierten Lösungen leicht ausfallen. Diesbezüglich stellen die Phenylazopyridine mit nur noch einer koordinierenden Einheit eine Weiterentwicklung dar.[135] Das 3-(3',5'-di-*tert*-butylphenylazo)-4-methylpyridin (**8**) ist der effizienteste PDL auf Basis eines Phenylazopyridins. Die Koordination von *trans*-**8** wird durch die sterisch anspruchsvollen Substituenten nicht negativ beeinflusst, die von *cis*-**8** hingegen gut unterbunden. Die Verwendung von **8** als PDL für $NiTPPF_{20}$ (**3**) erlaubte die Schaltung des Anteils an paramagnetischen Ni(II)-Spezies zwischen 72 % (Belichtung mit 440 nm, 85 % *trans*-Isomer) und 32 % (Belichtung mit 365 nm, 91 % *cis*-Isomer), sodass eine Schalteffizienz von 40 % erreicht wurde.

Der LD-CISSS von $NiTPPF_{20}$ (**3**) mit photodissoziierbaren Liganden ist sehr effizient und über eine große Zahl von Schaltzyklen vollständig reversibel. Eine hohe Schalteffizienz mit diesen Systemen wird jedoch nur dann erreicht, wenn der Ligand im hohen Überschuss und in einer Gesamtkonzentration nahe der optimalen Ligandenkonzentration (L_{opt}, siehe Kap. 3) vorliegt. Der supramolekulare Ansatz mit PDLs ist folglich für eine medizinische Anwendung als photoresponsives MRT-Kontrastmittel nicht geeignet. Die starke Abhängigkeit der Spinschaltung von der Ligandenkonzentration würde die Verabreichung sehr großer Mengen freier Azover-

bindung erfordern, was aus toxikologischen Gesichtspunkten äußerst bedenklich wäre.[136,137] Zudem ist eine exakte Einstellung der optimalen Ligandenkonzentration im biologischen System vermutlich nahezu unmöglich. Die Anwendung eines LD-CISSS-Systems als photoschaltbares MRT-Kontrastmittel erfordert zwingend die Unabhängigkeit der Spinschaltung von der Ligandenkonzentration, was nur mit einem intramolekularen Mechanismus realisiert werden kann.

1.5.3 Das *Recordplayer*-Konzept

Das erste System, welches zu einem intramolekularen LD-CISSS befähigt ist, konnte 2011 durch VENKATARAMANI *et al.* mittels einer kovalenten Anbindung des Azopyridin-Liganden an das Porphyrin-Gerüst realisiert werden.[117] Die photoinduzierte *trans*→*cis* Isomerisierung der Azopyridin-Einheit mit grünem Licht (495 – 530 nm) senkt den Liganden auf das Ni(II)-Ion und führt somit zu einer Bewegung, die an das Aufsetzen eines Plattenspieler-Tonarms auf eine Schallplatte erinnert. Aus diesem Grund wurde die Bezeichnung als *Recordplayer* für diese Verbindungklasse gewählt. Bestrahlung mit blauem Licht (420 – 435 nm) kehrt diesen Prozess um und überführt das Azopyridin in den nicht-koordinierenden *trans*-Zustand (siehe Abb. 1.11).

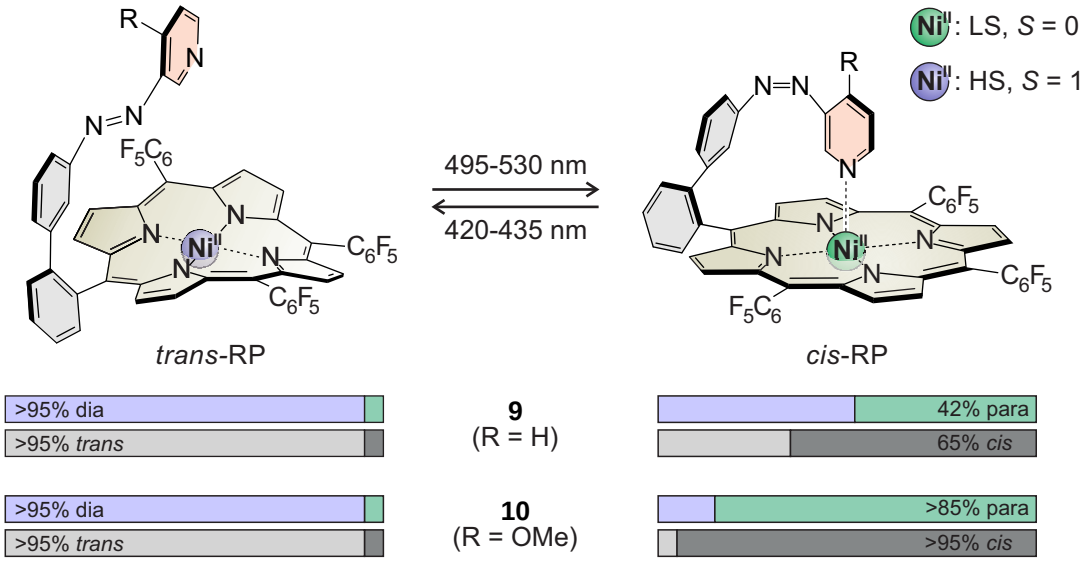

Abb. 1.11: Intramolekularer LD-CISSS mit *Recordplayer*-Molekülen **9** und **10** in Aceton. Eine intramolekulare Koordination des Pyridins ist ausschließlich im *cis*-Isomer möglich. Die Anreicherung des *cis*-Isomers gelingt photoinduziert mit grünem Licht (495-530 nm), während das *trans*-Isomer nahezu quantitativ durch Bestrahlung mit blauem Licht (420-435 nm) erhalten wird. Der methoxysubstituierte Pyridin-*Recordplayer* **10** weist gegenüber dem Stammsystem **9** deutlich verbesserte Schalteigenschaften auf und ist der bislang effektivste Spinschalter in homogener Lösung bei Raumtemperatur.

Die Schalteffizienz des Pyridin-*Recordplayer*s **9** ist analog zu den intermolekularen LD-CISSS-Systemen von der Effektivität der Photoisomerisierung sowie von den Assoziationskonstanten des lichtresponsiven Liganden abhängig. Der Anteil an paramagnetischer Ni(II)-Spezies konnte

mit **9** zwischen <5 % (Belichtung mit 430 nm, <5 % *cis*) und 42 % (Belichtung mit 530 nm, 65 *cis*) geschaltet werden. DOMMASCHK *et al.* konnten im Folgenden die erreichte Schalteffizienz von >37 % deutlich verbessern.[138,139] Die elektronischen Eigenschaften des Porphyrins und des photoschaltbaren Liganden haben einen großen Einfluss auf die Koordination des Pyridins und somit auf die Schalteffizienz. Elektronenziehende *meso*-Substituenten am Porphyrin verstärken die Assoziation des Pyridins und sorgen für eine effizientere SpinSchaltung.[139,140] Eine weitere Möglichkeit zur Verbesserung der Schalteffizienz von *Recordplayer*-Molekülen besteht in der Erhöhung der Donorstärke des Pyridins durch eine Substitution mit elektronenschiebenden Gruppen in *para*-Position zum koordinierenden Pyridin-Stickstoff. Entsprechende *Recordplayer*-Derivate weisen eine verbesserte *trans*→*cis* Photoisomerisierung sowie deutlich höhere Anteile der koordinierten und somit paramagnetischen *cis*-Spezies auf.[138] Der zurzeit effektivste Spinschalter auf Basis eines LD-CISSS-Systems ist der Methoxypyridin-*Recordplayer* **10** (siehe Abb. 1.11). Neben der hohen magnetischen Schalteffizienz von über 80 % zeichnet er sich durch eine extrem hohe Photostabilität und eine sehr lange thermische Halbwertszeit des metastabilen *cis*-Isomers aus.

2 Aufgabenstellung

Diese Arbeit ist dem Design sowie der Synthese und Charakterisierung neuer photoresponsiver Liganden für den *Light-Driven Coordination-Induced Spin State Switch* (LD-CISSS) von Ni(II) gewidmet. Um den LD-CISSS weiterzuentwickeln und zu verbessern, sollen die bislang verwendeten Azopyridine durch geeignete Azoimidazole ersetzt werden.

Das LD-CISSS-Konzept und insbesondere der *Recordplayer*-Ansatz ist für die Entwicklung eines mit Licht schaltbaren MRT-Kontrastmittels sehr vielversprechend. Eine Anwendung unter physiologischen Bedingungen setzt allerdings voraus, dass diese Spinschalter auch in Gegenwart von Wasser hoch effizient sind. Dies können die bisher bekannten Systeme nicht gewährleisten. Wasser kann im Gegensatz zu organischen Lösungsmitteln die Assoziationsfähigkeit des schaltbaren Donorliganden durch die Ausbildung von Wasserstoffbrücken oder sogar durch Protonierung drastisch herabsetzen. *N*-Methylimidazol ist mit seiner vergleichsweise moderaten Basizität und seinen hervorragenden Eigenschaften als Donorligand für Ni(II)porphyrine für weitere Optimierungsschritte auf dem Weg zu effizienten wasserlöslichen LD-CISSS Systemen sehr gut geeignet.[141]

Das bereits bekannte 5-Phenylazo-1-methylimidazol (**11**) ist als Grundgerüst für die Entwicklung von LD-CISSS Liganden prädestiniert.[142,143] Die 1,5-Substitution am Imidazolring gewährleistet, dass dessen Koordination ans Ni(II)porphyrin weder durch die Azogruppe noch durch den Alkylrest sterisch behindert wird, während die Methylgruppe die bei unsubstituierten Phenylazoimidazolen auftretende, schnelle thermische *cis*→*trans*-Isomerisierung über einen tautomeren Mechanismus verhindert.[144] Der Fokus dieser Arbeit liegt auf der Modifizierung des Stammsystems **11** mit dem Ziel, hocheffiziente photodissoziierbare Liganden (PDLs) und *Recordplayer*-Moleküle für den LD-CISSS von Ni(II) zu erhalten (siehe Abb. 2.1).

Der intermolekulare LD-CISSS mit PDLs erfordert eine zielgerichtete Substitution von **11**, sodass eines seiner Photoisomere möglichst effektiv an der Koordination ans Ni(II)porphyrin gehindert wird. Vorherige Arbeiten haben gezeigt, dass sich das optimale Substitutionsmuster eines PDLs mittels quantenchemischer Rechnungen sehr gut theoretisch ermitteln lässt.[116,135] Die so gefundenen und synthetisierten Kandidaten sollen hinsichtlich ihrer Eigenschaften als PDL für den LD-CISSS an dem gut etablierten Ni(II)porphyrin $NiTPPF_{20}$ (**3**) untersucht werden.

Der *Recordplayer*-Ansatz erfordert für eine optimale intramolekulare Spinschaltung in erster Linie ein äußerst akkurates Design des bindenden Schaltzustands.[140] Es ist zu erwarten, dass eine einfache Adaption der Pyridin-*Recordplayer*-Struktur nicht ausreicht, um einen effizienten

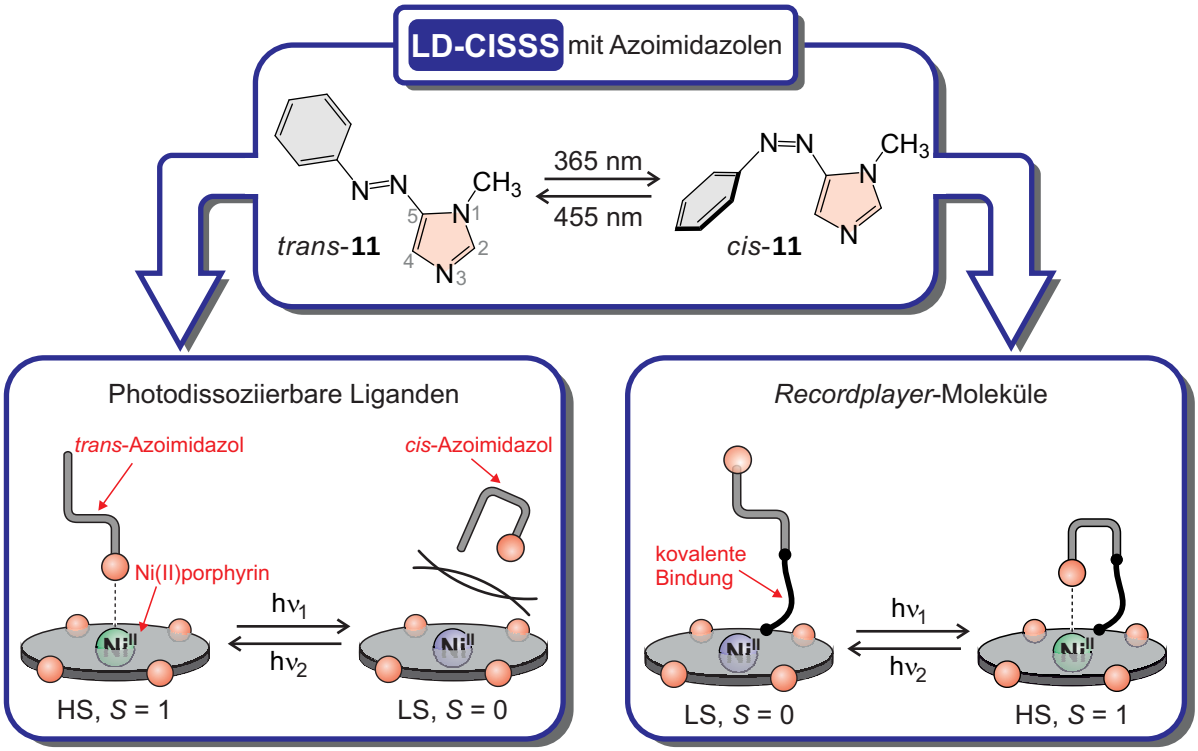

Abb. 2.1: Das bereits bekannte 5-Phenylazo-1-methylimidazol (**11**) stellt das Stammsystem einer neuen Klasse photoresponsiver Donorliganden für Metallionen dar. Ziel dieser Arbeit ist die Implementierung von **11** in das LD-CISSS (*Light-Driven Coordination-Induced Spin State Switch*) Konzept. Es sollen sowohl photodissoziierbare Liganden (PDLs) als auch *Recordplayer*-Moleküle entwickelt, synthetisiert und hinsichtlich ihrer Eignung als Spinschalter untersucht werden.

Schalter zu erhalten. Mit Hilfe von quantenmechanische Rechnungen sollen neue molekulare Designs für *Recordplayer* entwickelt werden, die die veränderten geometrischen Gegebenheiten durch die Verwendung des Imidazol-Liganden berücksichtigen. Die Synthese und Charakterisierung der so erhaltenen *Recordplayer*-Strukturen sind zentrale Aspekte dieser Arbeit.

Bezüglich der angestrebten Anwendung als MRT-Kontrastmittel ist des Weiteren die ökonomische Herstellung von *Recordplayer*-Molekülen von großer Wichtigkeit. Die bislang angewandten Syntheseprotokolle für *Recordplayer*-Moleküle sind sehr zeit-, kosten- und materialintensiv. Um *Recordplayer*-Moleküle zukünftig effizient und mit deutlich reduziertem Aufwand herstellen und derivatisieren zu können, wird die Entwicklung einer modularen Synthesestrategie verfolgt. Dem Baukastenprinzip folgend soll ein geeignetes Vorläufer-Porphyrin identifiziert und hergestellt werden, welches erst im letzten Syntheseschritt mit der gewünschten Schalteinheit versehen wird.

3 Intermolekularer LD-CISSS mit Azoimidazolen

Das Prinzip der photodissoziierbaren Liganden (PDLs) beschreibt die lichtinduzierte Änderung einer bestimmten physikalischen oder chemischen Eigenschaft als Folge der Assoziation bzw. Dissoziation eines Rezeptors und eines photochromen Liganden. Ein perfektes System würde das vollständige Schalten zwischen Assoziation und Dissoziation von Ligand und Rezeptor erlauben. Die Schalteffizienz (SE), also die Differenz des adressierten Parameters zwischen beiden Schaltzuständen, betrüge in diesem Fall 100 %. Dies ist in der Realität im Allgemeinen nicht erreichbar. Die SE wird durch eine unvollständige Assoziation des bindenden Photoisomers, eine geringe Assoziationsfähigkeit des nicht-bindenden Isomers, sowie eine unvollständige Photoisomerisierung des Liganden herabgesetzt.
Die Effizienz eines PDL-Systems wird im Wesentlichen durch zwei Parameter charakterisiert, der maximal erreichbaren Schalteffizienz SE_{max} und der dazugehörigen optimalen Konzentration des Liganden $[L]_{opt}$. Diese werden, sofern ein großer Überschuss des Liganden vorliegt, sehr gut durch die Gleichungen 3.1 und 3.2 beschrieben.[135]

$$SE_{max} = 100 \cdot \frac{1 - \sqrt{K_b/K_a}}{1 + \sqrt{K_b/K_a}} \tag{3.1}$$

$$[L]_{opt} = \frac{1}{\sqrt{K_a \cdot K_b}} \tag{3.2}$$

Hierbei bezeichnet K_a die Assoziationskonstante des bindenden Photoisomers und K_b die Assoziationskonstante des nicht-bindenden Zustands.
Überraschenderweise sind beide Parameter in dieser Näherung ausschließlich von den Assoziationskonstanten des PDLs abhängig, während die Konzentration des Rezeptors keine Rolle spielt. Aus Gleichung 3.1 folgt, dass eine hohe SE_{max} erhalten wird, wenn die Differenz der Assoziationskonstanten möglichst groß ist. Bei dem Design eines effektiven PDLs wird in erster Linie die Optimierung des nicht-bindenden Schaltzustands angestrebt (Verkleinerung von K_b). Dies wird beispielsweise durch geeignete Substitution mit sterisch anspruchsvollen Gruppen erreicht, welche seine Assoziation verhindern und die Assoziation des bindenden Isomers unbeeinflusst lassen. Eine möglichst hohe Assoziationskonstante K_a für den bindenden Schaltzustand ist jedoch trotzdem erstrebenswert, da $[L]_{opt}$ umso geringer ausfällt, je größer das Produkt der

Assoziationskonstanten ist (siehe Gleichung 3.2). Eine niedrige $[L]_{opt}$ ist aus ökonomischen Gründen sinnvoll, da geringere Substanzmengen des Liganden benötigt werden. Außerdem werden Probleme vermieden, die sich aus einer unzureichenden Löslichkeit des Liganden sowie aus langen Belichtungszeiten für das Erreichen des gewünschten photostationären Gleichgewichts des Liganden ergeben. Letztendlich spielt auch die Photoisomerisierung des PDLs eine wichtige Rolle für seine Effektivität. Selbst wenn beide Schaltzustände perfekt designt sind, stellt der Ligand dennoch einen ineffizienten PDL dar, sofern sich die Isomere des Liganden photochemisch nicht anreichern lassen. Aus diesem Grund müssen auch die prozentualen Anteile beider Isomere in den jeweiligen photostationären Gleichgewichten berücksichtigt werden. Insbesondere die effektive Anreicherung des nicht-bindenden Zustands ist hierbei von Bedeutung.
Das Konzept der photodissoziierbaren Liganden ist für eine ganze Reihe von Anwendungen interessant, bei der die Wechselwirkung eines Liganden mit seinem Rezeptor zu einer Zustandsänderung des Systems führt.[69,145–149] Besonders interessante Einsatzgebiete für das PDL-Konzept stellen die Photopharmakologie, in der die lichtinduzierte Aktivierung bzw. Deaktivierung von medizinischen Wirkstoffen verfolgt wird,[150–158] sowie die durch den LD-CISSS Effekt beschriebene Schaltung des Spinzustands eines Übergangsmetallions in homogener Lösung dar.[116,135]
Die von THIES verwendeten pyridinbasierten PDLs für den LD-CISSS an $NiTPPF_{20}$ (**3**) zeichnen sich in erster Linie durch die fast vollständige Verhinderung der Assoziation des *cis*-Isomers aus, wohingegen sowohl die Assoziation des *trans*-Isomers als auch die Photoisomerisierung zum *cis*-Isomer nicht zufriedenstellend sind. Beide Nachteile werden optimal durch das bereits bekannte Stammsystem **11** der 5-Phenylazo-1-methylimidazole adressiert, welches die sehr guten Donoreigenschaften des *N*-Methylimidazols mit einer nahezu quantitativen photochemischen Anreicherung des *cis*-Isomers kombiniert.[142] Die Ergebnisse früherer Arbeiten zeigen zudem, dass sich **11** durch gezielte Derivatisierung sehr gut für die Anwendung als PDL anpassen lässt.[143]

3.1 Design and Synthesis of Photodissociable Ligands Based on Azoimidazoles for Light-Driven Coordination-Induced Spin State Switching in Homogeneous Solution

Christian Schütt, Gernot Heitmann, Thore Wendler, Bahne Krahwinkel und Rainer Herges

J. Org. Chem. **2016**, *81*, 1206-1215.
http://dx.doi.org/10.1021/acs.joc.5b02817

Zusammenfassung

Das Stammsystem **11** der 5-Phenylazo-1-methylimidazole wurde hinsichtlich der Anwendung als photodissoziierbarer Ligand (PDL) optimiert. Mittels umfangreicher quantenchemischer Rechnungen wurde das für die Dissoziation des *cis*-Isomers benötigte Substitutionsmuster am Imidazol- und am Phenylring ermittelt. Hierzu wurden die Komplexbildungsenergien des jeweils günstigsten *trans*- und *cis*-Konformers eines substituierten Azoimidazols mit $NiTPPF_{20}$ (**3**) berechnet und deren Differenz durch Variation der Substituenten maximiert. Der aus der computergestützen Design-Studie erhaltene vielversprechendste Kanditat ist 5-(3',5'-Di-*tert*-butyl-4'-methoxyphenylazo)-1-methylimidazol (**12**). Die Methylgruppe am Imidazol verhindert die Bildung einer bindenden *cis*-Konformation, während die *tert*-Butylsubstituenten am Phenylring für die sterische Abstoßung zwischen *cis*-Isomer des Liganden und Porphyrin sorgen. Die Methoxygruppe am Phenylring wurde eingeführt, da sich in Vorversuchen zeigte, dass diese die Photoisomerisierung zum bindenden *trans*-Isomer verbessert. Azoimidazol **12** wurde synthetisiert und hinsichtlich seiner Effektivität als PDL an $NiTPPF_{20}$ (**3**) untersucht (siehe Abb. 3.1). Die

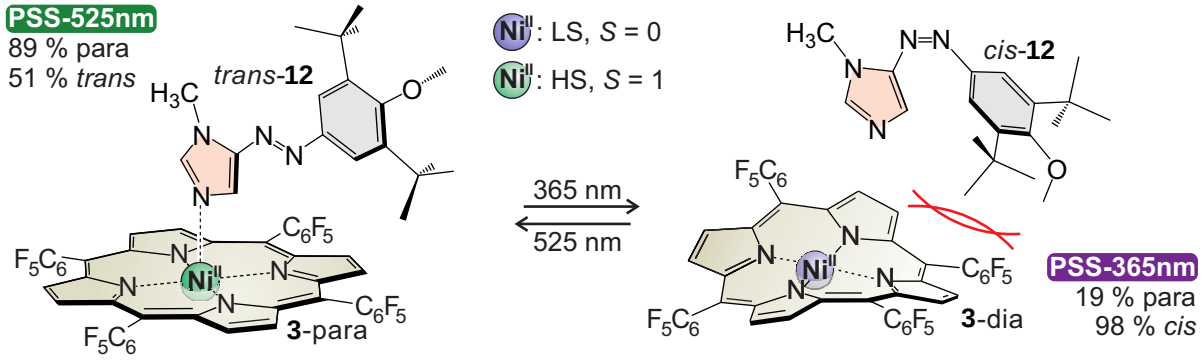

Abb. 3.1: 5-(3',5'-Di-*tert*-butyl-4'-methoxyphenylazo)-1-methylimidazol (**12**) ist der bisher effektivste PDL für den intermolekularen LD-CISSS von $NiTPPF_{20}$ (**3**).

Anreicherung des nicht-bindenden *cis*-Isomers ist mit UV-Licht (365 nm) äußerst effektiv (98 % *cis*). Somit erfüllt **12** eine der Grundvoraussetzungen eines effizienten PDLs. Die Assoziationskonstanten von **12** wurden anhand von ^{1}H-NMR-Titrationsreihen mithilfe nichtlinearer Regression ermittelt. Das bindende *trans*-Isomer zeichnet sich durch eine im Vergleich zu Pyridin-Liganden stark verbesserte Koordination aus ($K_{1S} = 60.0\,\mathrm{L\,mol^{-1}}$). Die Assoziation des *cis*-Isomers wird durch die eingeführten Substituenten sehr gut unterbunden ($K_{1S} = 1.37\,\mathrm{L\,mol^{-1}}$). Aus der Temperaturabhängigkeit der Assoziationskonstanten wurden außerdem die thermodynamischen Parameter ΔH und ΔS der Koordination bestimmt. Die theoretisch vorhergesagten Energiedifferenzen konnten im Experiment bestätigt werden. Der Anteil an paramagnetischer Ni(II)-Spezies konnte in ^{1}H-NMR-Experimenten reversibel über mehrere Zyklen zwischen 19 % und 89 % geschaltet werden. Die Schalteffizienz von 70 % ist eine Verbesserung um mehr als 20 % im Vergleich zum bisher besten System **7** auf Basis der Azopyridine. Gleichzeitig konnte aufgrund der deutlich größeren Assoziationskonstante des bindenden *trans*-Isomers die optimale Ligandenkonzentration von 92 mM (**7**) auf 65 mM (**12**) gesenkt werden. Somit stellt **12** den bisher effektivsten PDL für den intermolekularen LD-CISSS dar.

JOC The Journal of Organic Chemistry

Article

pubs.acs.org/joc

Design and Synthesis of Photodissociable Ligands Based on Azoimidazoles for Light-Driven Coordination-Induced Spin State Switching in Homogeneous Solution

Christian Schütt, Gernot Heitmann, Thore Wendler, Bahne Krahwinkel, and Rainer Herges*

Otto Diels-Institute for Organic Chemistry, University of Kiel, Otto-Hahn-Platz 4, Kiel D-24119, Germany

Supporting Information

ABSTRACT: Light-switchable azoimidazoles were rationally designed and synthesized, and their performance was investigated as photodissociable ligands (PDL) and for spin state switching of Ni porphyrins. The rationally designed ligands exhibit a high photochemical conversion rate (*trans* → *cis* > 98%) and no measurable fatigue over a large number of switching cycles at room temperature under air. As compared to the known phenylazopyridines, the phenylazoimidazoles exhibit a much stronger affinity as axial ligands to Ni porphyrin in the binding *trans* configuration and a low affinity in their *cis* form. This affinity switching was used to control the coordination number of Ni^{2+}. Concomitant with the change in coordination number is the change of the spin state from triplet (high spin) to singlet state (low spin). We report on phenylazoimidazole-based PDLs that switch the paramagnetic ratio of the investigated nickel species by up to 70%. Consequently, azoimidazoles exhibit considerably higher switching efficiencies than previously described pyridine-based PDLs.

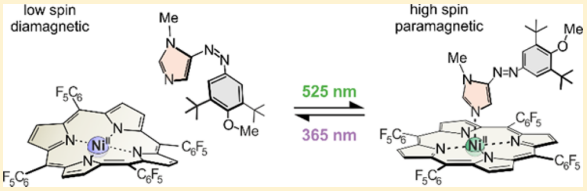

INTRODUCTION

Switchable ligands for photocontrolled binding are of general interest in a large number of fields. Practical applications range from the reversible switching of the activity of drugs, inhibitors, ion channels, and chemical optogenetics.[1−3] Particularly important as well is the light control of optical, electric, and magnetic properties of materials (such as the orientation of the magnetization or the magnetic susceptibility). Magnetic bistability at room temperature is a typical materials property. Cooperative effects between a large number of spin centers in the solid state stabilize the magnetic states and lead to hysteresis.[4] Notably, spin crossover and the light-induced excited spin state trapping (LIESST) phenomenon have been used to switch the spin state in crystals of transition metal complexes.[5] Until recently, however, there was little work on spin switching in the solution phase[6,7] or on single molecules at surfaces,[8,9] even though this would open a number of interesting applications, such as data storage or their use as switchable contrast agents in MRI. For achieving bistability in isolated molecules, the solid state cooperative effects have to be replaced by molecule inherent mechanisms. We have recently demonstrated that the spin state of isolated molecules can be switched between low spin (diamagnetic) and high spin (paramagnetic) using light.[10−13] Our approach is based on the fact that a number of transition metal ions (e.g., Fe^{2+}, Fe^{3+}, Co^{2+}, Ni^{2+}) change the spin state upon changing their coordination number. We chose Ni^{2+} because it is stable in its oxidation state and the spin state change is reliable and predictable. Square planar (4-coordinate) Ni^{2+} is low spin (S = 0), and square pyramidal (5-coordinate) or square bipyramidal (6-coordinate) Ni^{2+} are high spin (S = 1).[14−19] Coordination change, and thus spin change, is achieved by adding and removing axial ligands from a square planar Ni porphyrin (Figure 1).[20]

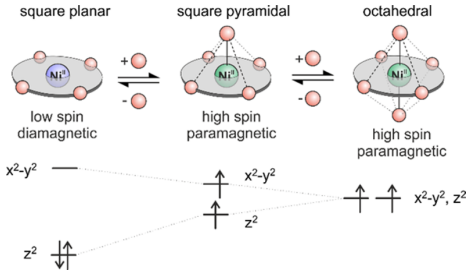

Figure 1. Coordination-induced spin state switch (CISSS) in Ni(II) complexes.

Light-induced axial ligand association and dissociation is operated either by tethering the switchable ligands to the square planar Ni porphyrin (record player design)[11,13,21] or by properly designed photodissociable ligands (PDLs).[10,12] Both designs have pros and cons. "Record player" complexes that move the coordinating nitrogen up and down like a tone arm the needle exhibit a large switching efficiency; however, at large concentrations, they undergo intermolecular coordination. PDLs, if properly designed, are sterically hindered in one of the two photoisomers, which prevents inter- as well as intramolecular coordination. Moreover, new types of PDLs

Received: December 11, 2015
Published: January 13, 2016

DOI: 10.1021/acs.joc.5b02817
J. Org. Chem. 2016, 81, 1206−1215

might also find applications as switchable drugs, inhibitors, or other biochemical probes. The most frequently used PDLs are probably azopyridines.[22−25] They combine the photochromism of azobenzene and the coordination properties of pyridine in one small molecule and are easy to synthesize. Other heterocyclic azo compounds are scarce.[26] Azo heterocycles with a higher basicity, nucleophilicity, and coordination power than azopyridines would be particularly valuable for the switching of functions, such as spin state switching, or the control of binding properties, e.g., in active sites of enzymes. We chose imidazole as the heterocycle, replacing one phenyl group in azobenzene. The binding constant of *N*-methylimidiazole to Ni porphyrins is more than an order of magnitude higher compared to pyridine and three times the value of 4-methoxypyridine.[27] There are three regioisomers of phenyl azoimidazoles (azo group in 2, 4, and 5 position if tautomerism is prevented by substitution at N-1). However, imidazoles that bear substituents adjacent to the coordinating nitrogen (in 2- and 4-position) do not coordinate to metal porphyrins for steric reasons (Figure 2).[28,29] Only 5-phenylazoimidazoles are potential candidates for coordination switching (see also coordination of histidine to iron in hemoglobin as an example in nature).

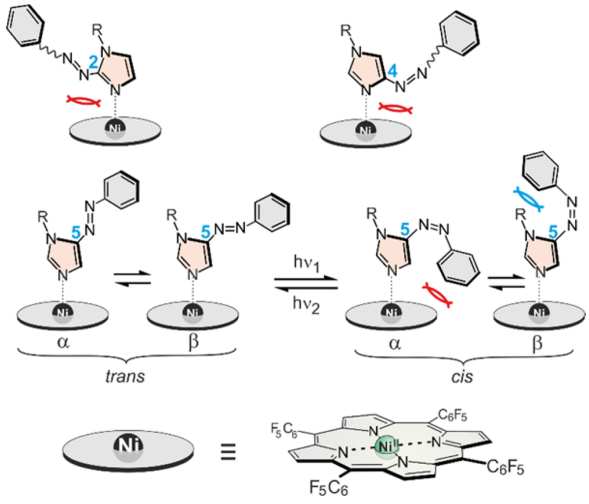

Figure 2. Schematic representation of the steric implications upon coordination of different phenylazoimidazoles to metal porphyrins. Imidazoles with substituents next to the coordinating nitrogen (2- and 4-phenylazoimidazole) do not bind to the metal for steric reasons (red arcs). Only 5-phenylazoimidazole provides a basis for the development of PDLs. The *trans* and the *cis* isomers each can adopt two conformations (α and β). Both *trans* conformations are binding. One of the *cis* conformations (α) exhibits sterical problems upon coordination (red arcs); however, the β conformation does not. The *cis*-β conformer would still bind, and photoisomerization of the ligand would not lead to photodissociation. However, formation of the *cis*-β conformation could be hampered by steric interaction of the substituent R at N-1 and the phenyl ring (blue arcs).

We recently published a convenient synthesis for the hitherto unknown 5-phenylazoimidazoles using a novel type of azocoupling of lithiated imidazole with benzene diazonium salts.[30] We now report on the rational design of substituted 5-phenylazoimidazoles, which are structurally optimized with respect to their switching efficiency (SE). The switching efficiency is defined as the difference of a target parameter in the two switching states. In a two-component system (metal complex/photodissociable ligand or receptor/photoswitchable inhibitor), it seems obvious that the maximum switching efficiency (SE_{max}) depends on the concentration of both components. Surprisingly, this is not the case. There is an optimal ligand concentration ($[L]_{opt}$) that leads to the maximum switching efficiency (SE_{max}) independent of the metal complex (receptor) concentration.[12] The maximum switching efficiency and the optimal ligand concentration are system parameters. The most important conclusion that we draw from this finding is that it is more important to optimize the conversion to the non-binding isomer and to reduce its coordination by steric hindrance than optimizing the binding state.

RESULTS AND DISCUSSION

Steric Design at the Imidazole. The starting point of our design was the introduction of bulky substituents in such a way that the binding of the *cis* isomer would be impaired while leaving the coordination of the *trans* form unaffected. To achieve this goal, one has to consider that both isomers have two conformations. To prevent the *cis* isomer from binding, both conformations (*cis*-α and *cis*-β, Figure 2) have to be included in the design process. In contrast to the *cis*-α conformer, the coordination of the *cis*-β conformer to the porphyrin is not sterically hindered because the phenyl group points away from the porphyrin (Figure 2, right). Thus, it is obvious that steric constraints have to be introduced at the N-1 position (Figure 2, right, blue arcs) to disfavor the formation of the *cis*-β conformation. For predicting which substituent would be needed to sufficiently disfavor the *cis*-β conformer, quantum chemical calculations were performed using the program TURBOMOLE[31] 6.3 at the PBE/SVP level of DFT. The relative energies show that in the parent system (R^1 = H, **1**) both conformations *cis*-α and *cis*-β are almost equal in energy (Figure 3). Upon introducing a methyl group (R^1 = Me, **2**) in the 1-position of the imidazole, the formation of the *cis*-β conformer is already disfavored by more than 5 kcal mol^{-1}.

Further increasing the steric repulsion between the 1-position and the phenyl ring leads to a larger energy difference of the two

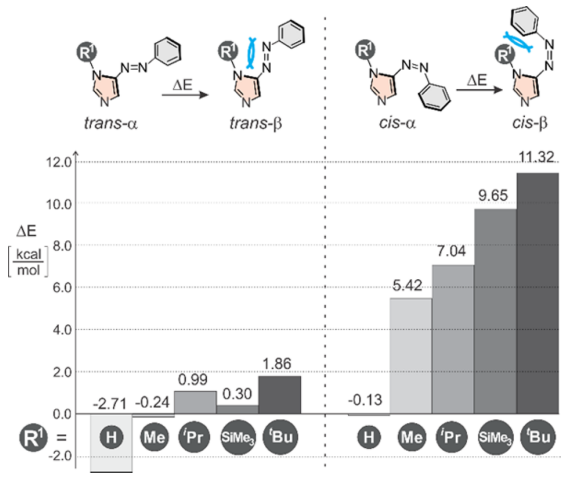

Figure 3. Bar diagram of the energy difference ($E_\beta - E_\alpha$) of the α and β conformation of several N-1-substituted azoimidazoles at the PBE/SVP level of theory. Energies are given in kcal mol^{-1}. Intramolecular steric repulsion is indicated by blue arcs.

DOI: 10.1021/acs.joc.5b02817
J. Org. Chem. 2016, 81, 1206−1215

The Journal of Organic Chemistry Article

cis conformers. The introduction of an isopropyl group in the 1-position (**3**, ΔE = 7.04 kcal mol^{-1}) disfavors the formation of the *cis*-β conformer roughly by an additional 1.5 kcal mol^{-1}, whereas substitution with a trimethylsilyl- (**4**, ΔE = 9.65 kcal mol^{-1}) or *tert*-butyl-group (**5**, ΔE = 11.32 kcal mol^{-1}) leads to a significantly larger energy difference compared to phenyl-azoimidazole **2** (see Figure 3). As a result, the non-binding *cis*-α conformer should be the predominant species in solution in all cases except R = H. To gain information on how substitution (R^1) at N-1 would affect the coordination of the *trans* and the *cis* ligands to Ni porphyrins, and more specifically, if disfavoring the binding *cis*-β conformation would be sufficient to obtain an efficient photodissociable ligand, we calculated the binding energy of the four species (*trans*-α, *trans*-β, *cis*-α, and *cis*-β) of azoimidazoles **1**−**5** to the Ni porphyrin $NiTPPF_{20}$ at the B3LYP/def2TZVP//PBE/SVP level of density functional theory. This level has proven to yield reliable results for the formation of complexes of 1-methylimidazole (see Supporting Information) with $NiTPPF_{20}$ (Table 1). Because the α and β conformations are

Table 1. Calculated Complex Formation Energies (ΔE_f, kcal mol^{-1}) of 1−5 (see Figure 4) with $NiTPPF_{20}$ at the B3LYP/def2TZVP//PBE/SVP Level of Theory

	R^1	*trans*-α	*trans*-β	*cis*-α	*cis*-β	$\Delta\Delta E_{f,calc}$ [a]
1	H	−4.35	−7.70	−5.18	−6.67	1.03
2	Me	−7.70	−8.08	−5.20	−0.65	2.88
3	^{i}Pr	−8.54	−7.07	−6.66	−0.79	1.88
4	$SiMe_3$	−7.42	−6.79	−6.86	3.63	0.57
5	^{t}Bu	−8.24	−4.26	−6.44	3.44	1.80

[a]Energy difference of ΔE_f of the strongest binding *trans* and *cis* conformer.

in fast equilibrium, the complex formation energies listed in Table 1 are relative to the most stable conformation. The calculated binding energies in Table 1 and Figure 4 clearly predict that the parent system (R = H) would bind strongly in all configurations and conformations, and therefore, it would be a very inefficient photodissociable ligand. Introduction of a methyl group at N-1, as expected, prevents the formation of the complex of the *cis*-β species with $NiTPPF_{20}$ almost completely (ΔE_f = −0.65 kcal mol^{-1}). For the larger substituents $SiMe_3$ and ^{t}Bu, complex formation of the *cis*-β species is predicted to be endothermic (3.63 and 3.44 kcal mol^{-1}).

Even though introduction of substituents such as Me, ^{i}Pr, $SiMe_3$, and ^{t}Bu at the imidazole nitrogen efficiently prevent the formation of the complexes with the β-*cis* ligand, the α-*cis* ligands still bind with $\Delta E_f < -5$ kcal mol^{-1}. Obviously, steric interaction of the phenyl group with the porphyrin (red arcs in Figure 4) is not sufficient to disfavor complex formation. Therefore, the steric hindrance of the phenyl group has to be increased by substitution of the phenyl ring with bulky substituents.

Photophysical Design of the Ligand. The photophysical properties of the parent azoimidazole switch, 1-methyl-5-phenylazoimidazole (**2**), have been recently investigated.[30] The light-induced conversion (365 nm) of the more stable *trans* to *cis* state is extremely efficient (>99%), and the thermal back reaction is very slow ($t_{1/2}$ = 22 days at 25 °C). Unfortunately, the light-induced isomerization of the *cis* isomer back to the *trans* form with visible light (455 nm) is incomplete (40%) because there is a considerable overlap of the π−π^* and n−π^* bands in the *cis* configuration. To improve the photochemical back reaction, we synthesized several derivatives of 1-methyl-5-phenyl azoimidazole (**2a**−**c**, Figure 5). Electron-donating and -withdrawing groups were introduced at the phenyl group. Substitution with

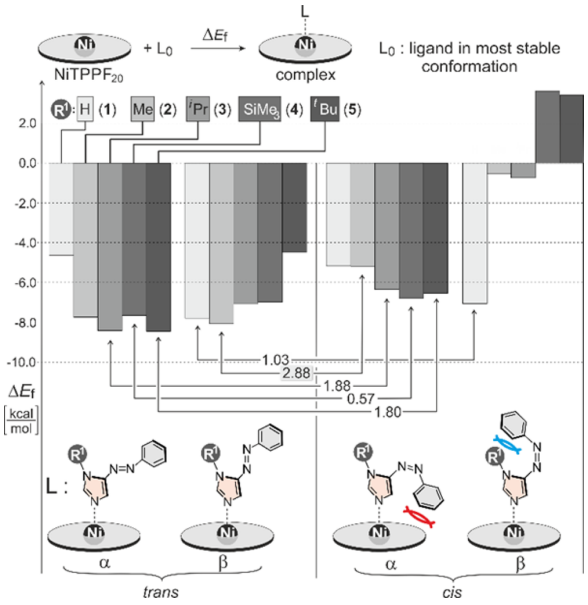

Figure 4. Calculated (B3LYP/def2TZVP//PBE/SVP) complex formation energies (ΔE_f in kcal mol^{-1}) of phenylazoimidazole derivatives (**1**−**5**) with $NiTPPF_{20}$. The definition of the complexation energy (ΔE_f) is given on top. Intermolecular and intramolecular steric hindrance is indicated with red and blue arcs. The energy differences between the strongest binding *trans* and *cis* conformations of each ligand are indicated by arrows. The *N*-methyl-substituted ligand (**2**) exhibits the largest change in binding energy ($\Delta\Delta E_f$ = 2.88 kcal mol^{-1}) upon *trans*-*cis* isomerization.

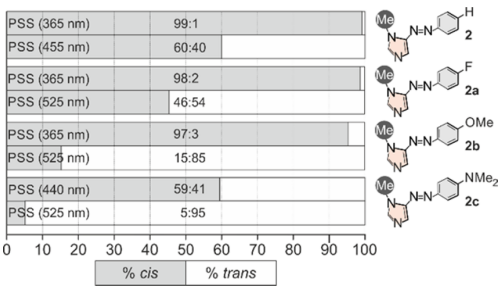

Figure 5. Photostationary states of 4′-substituted 1-methyl-5-phenyl-azoimidazoles determined by UV spectroscopy. Irradiation times: 20 min.

fluorine in the *para* position (**2a**) improves the photostationary state (PSS) at 525 nm from 40 to 54% *trans*, whereas the *trans* to *cis* isomerization (PSS 365 nm) is almost unchanged. The introduction of electron-donating groups in the *para* position further improves the *cis* to *trans* conversion (PSS 525 nm) with increasing donor strength from 85% (OMe, **2b**) to 95% (NMe_2, **2c**). However, although the *trans* to *cis* conversion is almost unchanged for **2b** (97%), the photo-induced switching to the *cis* isomer in **2c** decreases to 59% (Figure 5). TD-DFT calculations (see Supporting Information) provide a rational understanding of the experimental results. They predict the largest separation of the π−π^* and n−π^* bands for **2b**.

DOI: 10.1021/acs.joc.5b02817
J. Org. Chem. 2016, 81, 1206−1215

The Journal of Organic Chemistry Article

The results of the experimental and theoretical investigations lead to the conclusion that a methoxy group in the *para* position of the phenyl ring is the most effective substituent to improve the switching efficiency of 5-phenyl-azoimidazoles. Therefore, **2b** is a promising starting point for the further design of PDLs.

Steric Design at the Phenyl Group. As stated before, the PDL design has to include both conformations (α and β) of the *cis* isomer. For preventing the *cis* isomer from binding, the formation of the β conformation was suppressed by introduction of a methyl group at the imidazole ring (Figure 3). However, as predicted by theoretical calculations, steric hindrance in the α conformation obviously is not sufficient to prevent the parent system **2** from binding (Table 1, Figure 4). Therefore, we have to increase the steric demand of the phenyl group by the introduction of bulky substituents (Figure 6).

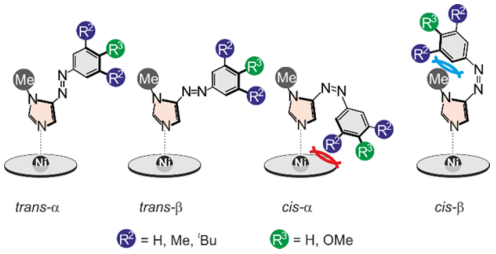

Figure 6. Binding modes of *trans*- and *cis*-1-methylphenylazoimidazole derivatives. Intermolecular steric hindrance of the *cis* isomer with $NiTPPF_{20}$ is indicated with red curved lines. Intramolecular hindrance is indicated by blue arcs.

We calculated the complex formation energies of the photophysically optimized methoxy derivative **2b** and the sterically more demanding systems **2d** and **2e** with $NiTPPF_{20}$ at the B3LYP/def2TZVP//PBE/SVP level of theory to quantify the effect of the steric bulk (Figure 7 and Table 2).

The calculations predict that two *t*-butyl groups in the *meta* position are most effective in preventing the α conformation from binding to the Ni porphyrin. Methyl substituents in the *meta* position or the methoxy group in the *para* position are considerably less effective.

Thus, **2e** is the most promising candidate for an effective PDL. The methoxy group in the *para* position improves the photophysical properties; the methyl group at the imidazole ring suppresses the formation of the β conformation, and the two *t*-butyl substituents prevent the α conformation from binding.

Synthesis and Properties of the Improved PDL. Azoimidazole **2e** was synthesized analogously to a previously published strategy.[30] The key step is the directed lithiation of a doubly protected imidazole and the reaction with a phenyldiazonium salt (prepared as tetrafluoroborate in five steps out of 3,5-di-*tert*-butyl-4-hydroxybenzoic acid; overall yield of 31%), forming the azo compound by a polar C−N bond formation (Scheme 1). Both protecting groups at the imidazole are then removed. A trityl (Tr) group is regioselectively introduced at the sterically less hindered nitrogen. Subsequent methylation of the second nitrogen leads to the imidazolium ion, which easily cleaves the Tr group leading to the desired 1,5 substitution pattern at the imidazole ring. The overall yield over nine steps (starting from sulfamoyl imidazole) is 37%. The preparation is quite convenient because only two intermediate compounds have to be isolated in the three pot reaction.

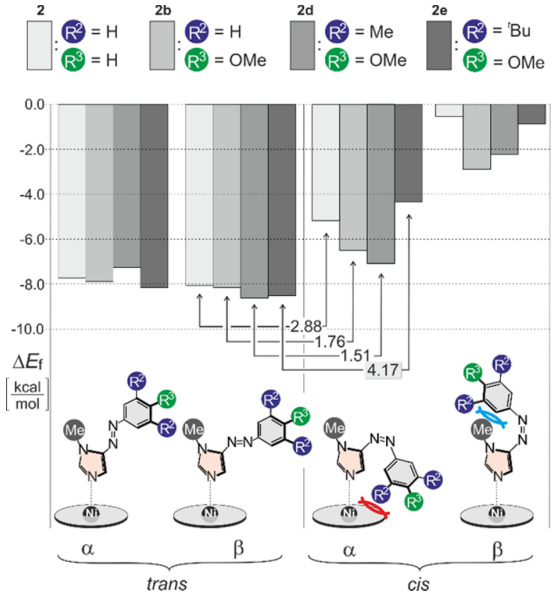

Figure 7. Calculated (B3LYP/def2TZVP//PBE/SVP) complex formation energies. The energy difference between the *trans*-β conformer and strongest binding *cis* configuration of the considered ligands are indicated by arrows. Ligand **2e** exhibits the largest change in binding energy ($\Delta\Delta E_f$ = 4.17 kcal mol^{-1}) upon *trans*-*cis* isomerization. Energies are given in kcal mol^{-1}. Intermolecular and intramolecular steric repulsion is indicated with red and blue arcs.

Table 2. Calculated Complex Formation Energies (ΔE_f, kcal mol^{-1}) of 2, 2b, 2d, and 2e (see Figure 7) with $NiTPPF_{20}$ (B3LYP/def2TZVP//PBE/SVP)

	trans-α	*trans*-β	*cis*-α	*cis*-β	$\Delta\Delta E_{f,calc}$ [a]
2	−7.70	−8.08	−5.20	−0.65	2.88
2b	−7.86	−8.16	−6.40	−2.98	1.76
2d	−7.15	−8.45	−6.94	−2.07	1.51
2e	−8.20	−8.43	−4.26	−0.79	4.17

[a]Energy difference of ΔE_f of the strongest binding *trans* and *cis* conformer.

We determined the association constants (K) and enthalpies of complex formation (ΔH) of the *cis* and *trans* isomer of **2e** with $NiTPPF_{20}$ using a previously developed NMR titration method (for details, see the Supporting Information).[10] For comparison with the theoretically predicted energies of complex formation and to quantify the improvement of the switching efficiency by our molecular design, we also included the parent system **2** and **2b** in our experimental studies. Table 3 summarizes the experimental values for K_{1S} and ΔH_{1S} (formation of the 1:1 complex) for **2**, **2b**, and **2c** in *cis* and *trans* configurations. Our molecular design strategy aims at increasing the difference in binding energy of the *cis* and *trans* isomer ($\Delta\Delta H_{1S}$). Introduction of the two *tert*-butyl substituents in **2e** indeed decreases the binding energy of the *cis* isomer substantially while having little effect on the association of the *trans* form. The ratio between the *trans* and *cis* association constants ($K_{1S,trans}/K_{1S,cis}$) in the parent system (**2**) is 3.60 and increases to 43.8 in the sterically hindered system **2e** (Table 3). It is noteworthy that the experimentally derived binding enthalpy differences are in good agreement with the calculated values (Table 3).

DOI: 10.1021/acs.joc.5b02817
J. Org. Chem. 2016, 81, 1206−1215

The Journal of Organic Chemistry Article

Scheme 1. Synthesis of Azoimidazole 2e[a]

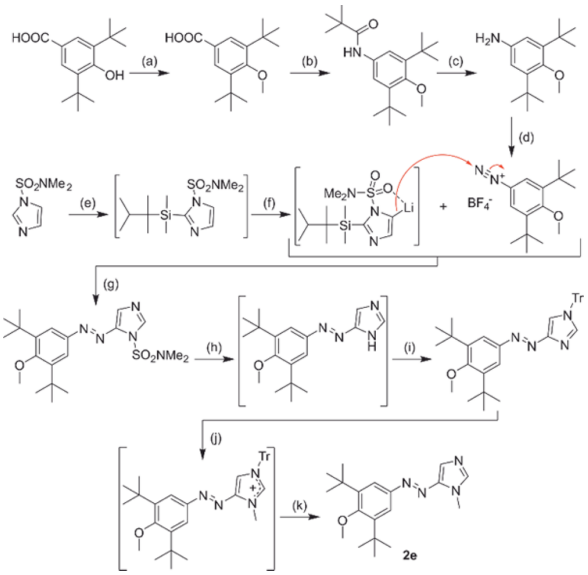

[a]Reagents and conditions. (a) 1. MeI, KOH, acetone, 60 °C, 18 h; 2. LiOH, THF, H_2O, 60 °C, 18 h, 71%; (b) DPPA, Et_3N, ^tBuOH, 85 °C, 18 h, 72%; (c) TFA, CH_2Cl_2, rt, overnight, 92%; (d) isopentyl nitrite, HBF_4 (aq), EtOH, rt, 15 min, 65%; (e) 1. *n*-BuLi, THF, −78 °C, 30 min; 2. dimethylthexylchlorosilane, THF, −78 °C to rt, overnight; (f) *n*-BuLi, THF, −78 °C, 30 min; (g) 1. THF, −78 °C to rt, overnight; 2. TBAF trihydrate, CsF, THF, rt, overnight, 58% (5 steps, 1 pot); (h) HCl, EtOH, 50 °C, 3 h; (i) trityl chloride, Et_3N, CH_2Cl_2, rt, overnight, 77% (2 steps, 1 pot); (j) 1. methyl triflate, CH_2Cl_2, rt, overnight; (k) H_2O, acetone, CH_2Cl_2, rt, 3 h, 82%.

Table 3. Experimentally Determined Association Constants (K_{1S}) and Binding Enthalpies (ΔH_{1S}) for Coordination of the *trans* and *cis* Isomers of 2, 2b, and 2e to NiTPPF$_{20}$

	2	2b	2e
$K_{1S,trans}$ [a]	38.31	59.14	60.03
$\Delta H_{1S,trans}$ [b]	−6.84	−6.63	−7.10
$K_{1S,cis}$ [a]	10.76	15.83	1.37
$\Delta H_{1S,cis}$ [b]	−4.69	−4.97	−3.01
$\Delta\Delta H_{1S}$ [c]	2.15	1.66	4.09
$\Delta\Delta E_{1S}$ [d]	2.88	1.75	4.18

[a]At 298 K for **2** and **2b**, 300 K for **2e**, toluene-d_8, [L mol^{-1}]. [b]In [kcal mol^{-1}]. [c]Experimental binding enthalpy differences to NiTPPF$_{20}$ ($\Delta\Delta H_{1S} = \Delta H_{1S,cis} - \Delta H_{1S,trans}$) [kcal mol^{-1}]. [d]Calculated binding energy differences (B3LYP/def2TZVP//PBE/SVP) to NiTPPF$_{20}$ ($\Delta\Delta E_{1S} = \Delta E_{1S,cis} - \Delta E_{1S,trans}$) [kcal mol^{-1}].

Switching Experiments. On the basis of the experimentally determined association constants (K_{1s}, K_2, for data, see the Supporting Information) of the *trans* and *cis* configurations of **2**, **2b**, and **2e**, the conditions for achieving the maximum switching efficiency SE$_{max}$ can be theoretically calculated. The switching efficiency is defined as the difference of the properties of a system in the two switching states. The properties of interest are the amount of *cis* isomer, or in our case, even more interesting is the amount of paramagnetic species in solution in both photostationary states. A perfect system would exhibit 0% paramagnetic species in one switching state and 100% in the other state. SE$_{max}$, thus, would be 100%. Parameters that lower SE$_{max}$ are incomplete photochemical conversions between *cis* and *trans*, incomplete binding of the *trans*, and residual binding of the *cis* isomer. Using a mathematical analysis, we have previously shown that there is an optimum ligand (PDL) concentration $[L]_{opt}$ that leads to a maximum switching efficiency (SE$_{max}$).[10] A plot of the switching efficiency as a function of the ligand (PDL) concentration of **2e** is given in Figure 8.

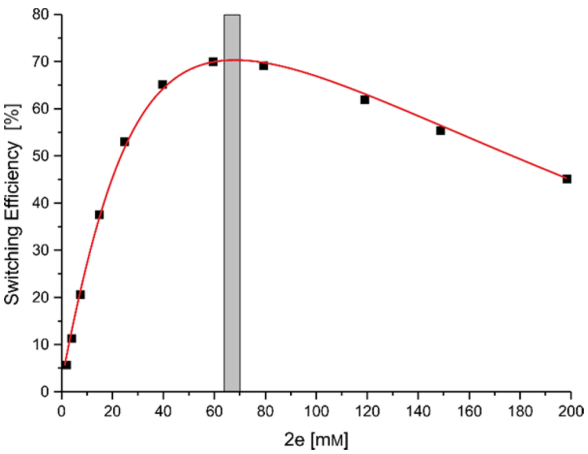

Figure 8. Switching efficiency (SE) (black squares) as a function of the ligand concentration of **2e** calculated from the experimentally determined association constants.[10] The maximum switching efficiency (SE$_{max}$ = 70%) is predicted at a ligand concentration ($[L]_{opt}$) of 64.3 mM. The gray bar indicates the concentration used in our experiments (67.9 mM), which is close to the optimum ligand concentration.

The maximum switching efficiency SE$_{max}$ for the system NiTPPF$_{20}$/**2e** is obtained at the optimum ligand concentration of **2e** ($[L]_{opt}$ = 64.3 mM). The optimum ligand concentrations for **2** and **2b** are 35.1 and 21.9 mM. Surprisingly, a rigorous mathematical treatment proves that $[L]_{opt}$ is independent of the receptor (NiTPPF$_{20}$) concentration over a concentration range from 0 to 4 mM. (Figure 9).

The switching experiments including **2**, **2b**, and **2e** were performed with concentrations close to the optimum ligand

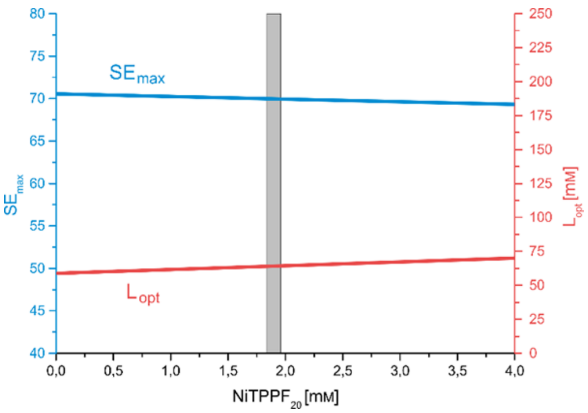

Figure 9. Maximum switching efficiency (SE$_{max}$) and optimal ligand concentration ($[L]_{opt}$) of **2e** as a function of the concentration of NiTPPF$_{20}$ (concentration range: 0−4 mM). In this region, SE$_{max}$ and L_{opt} are independent from the concentration of NiTPPF$_{20}$. The gray bar indicates the concentration of **2e** used in our experiments (67.9 mM).

DOI: 10.1021/acs.joc.5b02817
J. Org. Chem. 2016, 81, 1206−1215

Table 4. Important Photochemical and Magnetic Switching Properties of Three Azoimidazoles (2, 2b, and 2e) and the to Date Most Efficient Azopyridine PDL 6[10] at Photostationary States PSS-365 and PSS-vis

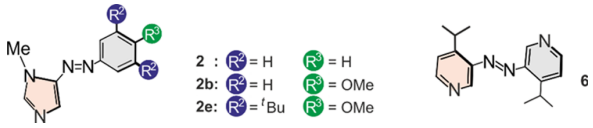

	% *cis* isomer[a]								% para. Ni^{2+}[f]		
	PSS-365	PSS-vis	$t_{1/2}$[b] [h]	$K_{1S\text{-}trans}$[c] [L mol^{-1}]	$K_{1S\text{-}cis}$[c] [L mol^{-1}]	$[L]_{opt}$[d] [mM]	SE_{max}[d] [%]	$[L]_{exptl}$[e] [mM]	$PSS_{365\ nm}$	PSS_{vis}	SE_{exptl}[f] [%]
2	98	67[g]	528	38.3	10.8	35.1	16	34.9	43	64	21
2b	95	22[h]	37.5	59.1	15.8	21.9	26	19.4	36	66	30
2e	98	49[h]	158	60.0	1.37	64.9	70	67.9	19	89	70
6	82	10[g]	262	9.99	0.30	91.9	50	69.2	21	68	48

[a]Amount of *cis* isomer in both photostationary states (PSS-365 and PSS-vis), 298 K, toluene-d_8, in the presence of $NiTPPF_{20}$ (1.94 mM for **2**, **2b**, and **2e**, 0.106 mM for **6**). [b]Thermal half-life of *cis* isomer, 298 K, toluene-d_8. [c]Association constants (K_{1S}) for *cis* and *trans* isomers determined from ^{1}H NMR titration experiments (for a full list of association constants, see the Supporting Information), 298 K for **2**, **2b**, and **6**, 300 K for **2e**, toluene-d_8, $NiTPPF_{20}$ (1.94 mM for **2**, **2b**, and **2e**, 0.106 mM for **6**). [d]Theoretically calculated optimal ligand concentrations ($[L]_{opt}$) and maximum switching efficiencies (SE_{max}) on the basis of experimentally determined association constants. [e]Ligand concentration used in the switching experiment. [f]Ratios of paramagnetic Ni^{2+} (% para. Ni^{2+}) in both photostationary states; the experimental switching efficiencies (SE_{exptl}) are determined on the basis of the porphyrin pyrrole shifts. [g]Irradiation with 455 nm. [h]Irradiation with 525 nm. Irradiation times were 20 min.

concentrations ($[L]_{opt}$). The experimental maximum switching efficiencies (SE_{exptl}) under these conditions are in good agreement with the theoretically predicted values (SE_{max}), supporting our mathematical model. Table 4 summarizes important properties of **2**, **2b**, and **2e**, including the parameters of azopyridine **6**, which has been the most efficient system so far.[10] Figure 10 shows a comparison of **6** with compound **2e**. The light-induced switching process is fully reversible without any sign of fatigue for both ligands over a large number of cycles.

To gain further insight into the compositions and concentrations of the complexes that are actually present in the solutions, we calculated the concentrations of the five possible complex species as a function of the ligand concentration (speciation plots, Figure 11). At the experimentally used ligand concentration ([**2e**] = $[L]_{exptl} \cong [L]_{opt}$), the prevalent complex at PSS-365 is the bare $NiTPPF_{20}$ (81%, Figure 11a), and at PSS-525, the predominant species is the six-coordinate complex of $NiTPPF_{20}$ with two axial *trans*-**2e** ligands (55%, Figure 11b).

■ CONCLUSIONS

We present the most efficient photodissociable ligand (PDL) to date for light-driven, coordination-induced spin state switching (LD-CISSS). The coordination properties of imidazole were combined with the photochromic properties of azo compounds in a 5-phenylazoimidazole. The starting point of our design was the already published parent system,[30] which however exhibits an unsatisfying switching efficiency. We extensively used quantum chemical calculations to improve the properties by suitable substitution. The most promising candidates were synthesized and investigated. Azoimidazole **2e** turned out to be superior to previously used azopyridines (e.g., **6**)[10,12] in most aspects. The coordination power of the binding isomer is substantially higher, and smaller concentrations of the ligand are necessary for optimal switching. The photochemical conversion to the non-binding *cis* form is almost quantitative (98% as compared to 82% in azopyridine). Consequently, the switching efficiency was improved to 70% (as compared to 48% in azopyridine). Azoimidazoles are promising candidates to expand the coordination-induced spin state switching concept to other transition metal ions, such as Fe(II), Fe(III), and Mn(III). They are also suitable to be covalently tethered to the porphyrin core, a

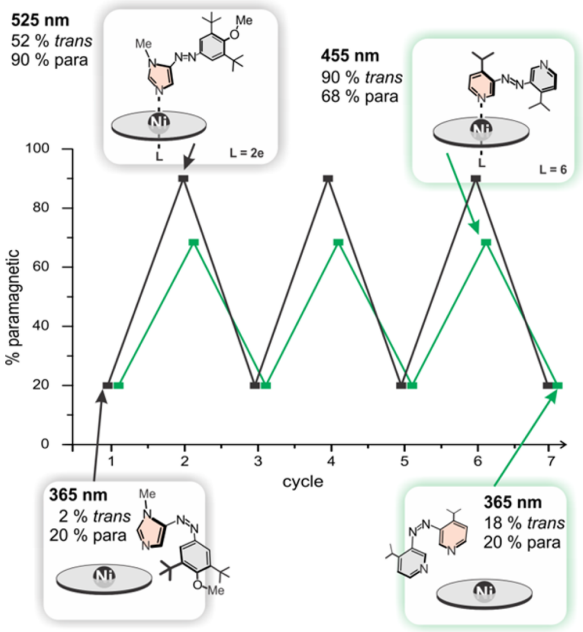

Figure 10. Reversible spin state switching of $NiTPPF_{20}$ with the PDL **2e** (azoimidazole, black curve) and **6**[10] (azopyridine, green curve). The proportion of paramagnetic nickel species is plotted as a function of the switching cycles. Switching was performed by irradiation with 365 nm (*trans* → *cis*) and 525 nm (**2e**) or 455 nm (**6**) (*cis* → *trans*). The azoimidazole ([**2e**] = 67.9 mM, $[NiTPPF_{20}]$ = 1.94 mM, toluene-d_8) exhibits a switching efficiency (SE) of 70%, whereas the azopyridine ([**6**] = 69.2 mM, $[NiTPPF_{20}]$ = 0.106 mM, toluene-d_8) is less efficient with SE = 48%. The predominant species at both PSSs are shown as simplified structures.

strategy that has been successfully used with azopyridines.[11,13] This so-called "record player" design has already been used to switch MRI contrasts.[21] Contrast agents based on the CISSS concept have a high potential for functional imaging in MRI and interventional radiology (minimal invasive, catheter-based

DOI: 10.1021/acs.joc.5b02817
J. Org. Chem. 2016, 81, 1206−1215

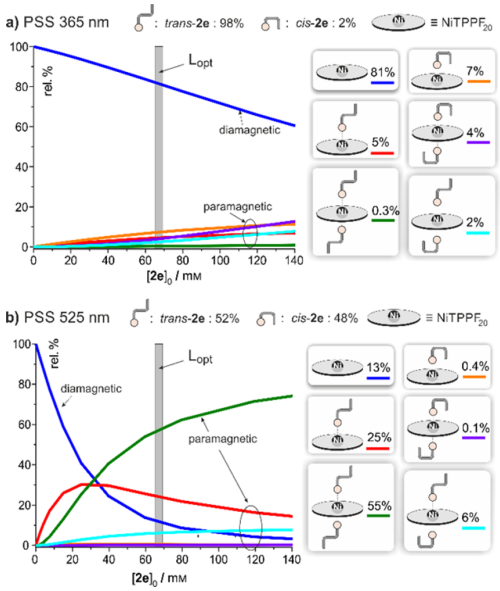

Figure 11. (a) Speciation plot of the six species in a solution of $NiTPPF_{20}$ (1.94 mM) in the presence of the *cis*/*trans* mixture of the ligand **2e** at PSS-365 (98% *cis*, 2% *trans*) and (b) speciation plot of the same solution at PSS-525 (48% *cis*, 52% *trans*). Both are given as a function of the total concentration of **2e** ($[\mathbf{2e}]_0 = [trans\text{-}\mathbf{2e}] + [cis\text{-}\mathbf{2e}]$). The proportion of the five complexes and free porphyrin at the ligand concentration used in the experiment $[\mathbf{2e}]_0 = [L]_{exptl} = 67.9$ mM, are given on the right. Note that only the free porphyrin is diamagnetic. All other complexes are paramagnetic.

surgery).[32−34] Azoimidazoles could improve and expand applications toward this end.

EXPERIMENTAL SECTION

General Experimental Methods. THF was dried and distilled from sodium/benzophenone. Dichloromethane was dried and distilled from CaH_2. *N,N*-Dimethylsulfamoylimidazole was synthesized analogously to the procedure of Chadwick et al.[35]

General Synthetic Procedure A. Synthesis of benzenediazonium tetrafluoroborates. If not stated otherwise, diazonium salts were prepared analogously to the procedure of Dunker et al.[36] Aniline (10.0 mmol) was suspended in tetrafluoroboric acid (20.0 mL, 50 wt % in water), and water was added until a clear solution was obtained. It was cooled to 0 °C, and sodium nitrite (10.0 mmol in 1.50 mL of water) was added dropwise. The precipitate was filtered off and washed subsequently with water, ethanol, and diethyl ether before being dried in vacuo. Because of the low thermal stability, we solely performed ^{1}H NMR spectroscopy on the diazonium salts and used them in the following step immediately after preparation.

General Synthetic Procedure B. Synthesis of 1-*N,N*-dimethylsulfamoyl-5-phenylazoimidazoles.[30] 1-*N,N*-Dimethylsulfamoylimidazole was dissolved under a nitrogen atmosphere in dry THF (6 mL per mmol) and cooled to −78 °C. Then, *n*-BuLi (2.5 M in hexane, 1.0 equiv) was added slowly over 15 min, and the solution was stirred at −78 °C for 30 min. Dimethylthexylchlorosilane (1.0 equiv) was added; the cooling bath was removed, and stirring was continued at room temperature overnight. The solution was again cooled to −78 °C; *n*-BuLi (2.5 M in hexane, 1.1 equiv) was added slowly over 10 min, and the mixture was stirred at −78 °C for 30 min. Then, diazonium tetrafluoroborate (1.0 equiv) was added, and the reaction mixture immediately turned from light yellow to deep red. The cooling bath was removed, and the mixture was stirred at room temperature overnight. The reaction mixture was quenched with diluted aq $NaHCO_3$, layers were separated, and the aqueous layer was extracted once with THF. The combined organic layers were treated with TBAF trihydrate (1.5 equiv) and a spatula tip of cesium fluoride and were stirred at room temperature overnight. Diluted aq NaHCO3 was added; layers were separated, and the aqueous layer was extracted with DCM (3×). The combined organic layers were dried over $MgSO_4$ and evaporated. Purification was achieved via column chromatography on silica gel.

General Synthetic Procedure C. Synthesis of 1-trityl-4-phenylazoimidazoles.[30] The sulfamoyl-protected azo-imidazole was dissolved in EtOH/HCl (4:1) (25 mL/mmol), and the mixture was stirred at 50 °C for 3 h. After cooling to 0 °C (ice bath), the mixture was basified with 40% KOH (aq) (pH ∼10). The solution was extracted with $CHCl_3$ (3 × 25 mL); the combined organic layers were dried over $MgSO_4$ and evaporated to dryness. The residue was taken up in DCM (15 mL/mmol), treated with trityl chloride (1.1 equiv) and triethylamine (1.3 equiv), and stirred at room temperature overnight. The organic layer was washed with aq $NaHCO_3$ (2×), and the combined aq layers were extracted with DCM (2×). The combined organic layers were dried over $MgSO_4$, and the solvent was removed. Purification was achieved via column chromatography on silica gel.

General Synthetic Procedure D. Synthesis of 1-methyl-5-phenylazoimidazoles.[30] 1-Trityl-5-phenyl-azoimidazole was dissolved under nitrogen atmosphere in dry DCM (7.5 mL/mmol), and methyl triflate (1.2 equiv) was added via a syringe at room temperature. The reaction mixture was stirred at room temperature overnight; acetone/water (1:1, 15 mL/mmol) was added, and stirring was continued for an additional 4 h. Then, saturated $NaHCO_3$ was added, and the layers were separated. The aq layer was extracted with DCM (3×); the combined organic layers were dried over $MgSO_4$, and the solvent was removed. Purification was achieved via column chromatography on silica gel.

Synthesis of 1-Methyl-5-(phenylazo)imidazole (2). 1-Methyl-5-(phenylazo)imidazole (**2**) was synthesized and characterized as previously reported.[30]

*Synthesis of 1-Methyl-5-(4′-fluorophenylazo)imidazole (**2a**).* Step 1: 4-Fluorodiazoniumbenzene tetrafluoroborate. 4-Fluoroaniline (4.30 g, 45.0 mmol) was converted to the desired diazonium compound following general procedure A. The product was obtained as a white solid (7.31, 34.8 mmol, 77%). ^{1}H NMR (200 MHz, 300 K, CD_3CN): δ 8.72−8.50 (m, 2 H, 2,6-H), 7.78−7.55 (m, 2 H, 3,5-H) ppm. Step 2: 1-Dimethylsulfamoyl-5-(4′-fluorophenylazo)imidazole. Starting from 1-*N,N*-dimethyl-sulfamoylimidazole (2.00 g, 11.4 mmol), general procedure B was applied. Purification via column chromatography on silica gel (CH_2Cl_2/EtOAc (9:1), R_f = 0.51) gave the desired product as an orange-yellow solid (2.01 g, 6.75 mmol, 59%). Mp: 98 °C. FT-IR (layer) ν: 3142 (w), 2931 (w), 1592 (m), 1518 (w), 1501 (m), 1457 (m), 1388 (m), 1336 (m), 1226 (m), 1168 (s), 1143 (m), 1115 (m), 1091 (s), 1055 (m), 969 (s), 850 (s), 820 (s), 748 (m), 723 (s), 649 (m), 629 (m), 584 (s), 518 (s) cm^{-1}. ^{1}H NMR (500 MHz, 300 K, $CDCl_3$, TMS): δ 8.13 (s, 1 H, 2-H), 7.88−7.83 (m, 2 H, 2′,6′-H), 7.50 (s, 1 H, 4-H), 7.22−7.17 (m, 2 H, 3′,5′-H), 2.97 (s, 6 H, -N(CH_3)$_2$) ppm. ^{13}C NMR (125 MHz, 300 K, $CDCl_3$, TMS): δ 164.8 (C-4′), 149.6 (C-1′), 145.1 (C-5), 141.1 (C-2), 125.2 (C-2′,6′), 119.0 (C-4), 116.6 (C-3′,5′), 38.5 (-N(CH_3)$_2$) ppm. ^{19}F-NMR (470 MHz, 300 K, $CDCl_3$): δ −107.52 (s, 4′-F) ppm. MS (EI, 70 eV) *m*/*z* (%): 297 (42) $[M]^+$, 190 (44) $[M - DMS]^+$, 134 (100), 108 (40) $[SO_2NMe_2]^+$. MS (CI, isobutane) *m*/*z* (%): 298 (100) $[M + H]^+$, 123 (11). UV−vis (toluene) λ_{max} (lg ε): 357 nm (4.214). Anal. Calcd for $C_{11}H_{12}N_5O_2FS$: C, 44.44; H, 4.07; N, 23.56; S, 10.79. Found: C, 44.79; H, 4.04; N, 23.42; S, 10.71. Step 3: 1-Trityl-4-(4′-fluorophenylazo)imidazole. Starting from 1-dimethylsulfamoyl-5-(4′-fluoro-phenylazo)imidazole (1.00 g, 3.36 mmol), general procedure C was applied. Purification via column chromatography on silica gel (CH_2Cl_2/EtOAc (1:1), R_f = 0.80) gave the desired product as a yellow solid (884 mg, 2.04 mmol, 61%). Mp: 234 °C. FT-IR (layer) ν: 3059 (w), 1593 (m), 1492 (m), 1444 (m), 1322 (w), 1299 (m), 1222 (m), 1124 (m), 1090 (w), 1038 (w), 1001 (w), 846 (m), 749 (s), 702 (s), 658 (s), 639 (m), 528 (s) cm^{-1}. ^{1}H NMR (500 MHz, 300 K, $CDCl_3$, TMS): δ 7.92−7.88 (m, 2 H, 2′,6′-H), 7.54 (s, 1 H, 5-H), 7.52 (s, 1 H, 2-H), 7.39−7.36 (m, 9 H, *m*-Tr-H, *p*-Tr-H), 7.22−7.18 (m, 6 H, *o*-Tr-H), 7.16−7.10 (m, 2 H, 3′,5′-H) ppm. ^{13}C NMR (125 MHz, 300 K, $CDCl_3$, TMS): δ 164.1 (C-4′), 153.2 (C-4), 149.7 (C-1′), 141.9 (-CPh_3), 139.5 (C-2), 129.9 (C-*o*-Tr), 128.6 (C-*m*-Tr), 128.5 (C-*p*-Tr), 124.7 (C-

DOI: 10.1021/acs.joc.5b02817
J. Org. Chem. 2016, 81, 1206−1215

2′,6′), 122.5 (C-5), 116.0 (C-3′,5′) 76.4 (C-*i*-Tr) ppm. ^{19}F-NMR (470 MHz, 300 K, $CDCl_3$): δ −110.40 (s, 4′-F) ppm. MS (EI, 70 eV) *m*/*z* (%): 432 (1) $[M]^+$, 243 (100) $[Tr]^+$, 165 (42) $[Tr\text{-}Ph]^+$. MS (CI, isobutane) *m*/*z* (%): 433 (1) $[M + H]^+$, 243 (100) $[Tr]^+$, 191 (20) $[M - Tr + H]^+$, 167 (31) $[Tr - Ph + 2H]^+$. UV−vis (toluene) λ_{max} (lg ε): 336 nm (4.246). Anal. Calcd for $C_{28}H_{21}N_4F$: C, 77.76; H, 4.89; N, 12.95. Found: C, 77.80; H, 5.21; N, 12.96. Step 4: 1-Methyl-5-(4′-fluorophenylazo)imidazole (**2a**). Starting from 1-trityl-4-(4′-fluorophenylazo)-imidazole (400 mg, 925 μmol), general procedure D was applied. Purification via column chromatography on silica gel (EtOAc, R_f = 0.30) gave the desired product **2a** as a yellow solid (150 mg, 735 μmol, 79%). Mp: 113 °C. FT-IR (layer) ν: 3089 (w), 1588 (m), 1496 (m), 1429 (m), 1402 (w), 1345 (m), 1284 (m), 1232 (s), 1207 (s), 1170 (m), 1119 (s), 1096 (m), 1034 (m), 894 (w), 842 (s), 750 (m), 717 (m), 682 (m), 663 (s), 646 (s), 552 (m), 514 (s) cm^{-1}. ^{1}H NMR (500 MHz, 300 K, $CDCl_3$, TMS): δ 7.87−7.80 (m, 2 H, 2′,6′-H), 7.69 (s, 1 H, 2-H), 7.57 (s, 1 H, 4-H), 7.20−7.12 (m, 2 H, 3′,5′-H), 3.96 (s, 3 H, N-CH_3) ppm. ^{13}C NMR (125 MHz, 300 K, $CDCl_3$, TMS): δ 164.3 (C-4′), 149.7 (C-1′), 145.2 (C-5), 140.4 (C-2), 124.4 (C-2′,6′), 122.8 (C-4), 116.2 (C-3′,5′), 32.7 (N-CH_3) ppm. ^{19}F-NMR (470 MHz, 300 K, $CDCl_3$): δ −109.48 (s, br, 4′-F) ppm. MS (EI, 70 eV) *m*/*z* (%): 204 (100) $[M]^+$, 124 (15), 109 (39). MS (CI, isobutane) *m*/*z* (%): 205 (100) $[M + H]^+$. HR-MS (EI, 70 eV): *m*/*z* $[M]^+$ calcd for $C_{10}H_9N_4F$, 204.0811; found 204.0811. UV−vis (toluene) λ_{max} (lg ε): 362 nm (4.230).

*Synthesis of 1-Methyl-5-(4′-methoxyphenylazo)imidazole (**2b**).* Step 1: 4-Methoxydiazoniumbenzene tetrafluoroborate. 4-Anisidine (5.00 g, 40.6 mmol) was converted to the desired diazonium compound following general procedure A. The product was obtained as light purple solid (6.70, 30.2 mmol, 74%). ^{1}H NMR (200 MHz, 300 K, CD_3CN): δ 8.43 (s, 2 H, 2,6-H), 7.36 (s, 2 H, 3,5-H), 4.06 (s, 3 H, -OCH_3) ppm. Step 2: 1-Dimethylsulfamoyl-5-(4′-methoxyphenylazo)imidazole. Starting from 1-*N*,*N*-dimethyl-sulfamoylimidazole (2.00 g, 11.4 mmol), general procedure B was applied. Purification via column chromatography on silica gel (CH_2Cl_2/EtOAc (9:1), R_f = 0.49) gave the desired product as an orange-red solid (2.35 g, 7.60 mmol, 67%). Mp: 125 °C. FT-IR (layer) ν: 3134 (w), 2943 (w), 2838 (w), 1602 (m), 1582 (m), 1419 (m), 1454 (m), 1385 (s), 1251 (s), 1166 (s), 1138 (s), 1090 (s), 1023 (s), 972 (s), 890 (m), 841 (m), 808 (m), 723 (s), 651 (m), 634 (m), 584 (s), 551 (s), 529 (s) cm^{-1}. ^{1}H NMR (500 MHz, 300 K, $CDCl_3$, TMS): δ 8.09 (d, ^4J = 0.8 Hz, 1 H, 2-H), 7.85−7.82 (m, 2 H, 2′,6′-H), 7.45 (d, ^4J = 0.8 Hz, 1 H, 4-H), 7.02−6.98 (m, 2 H, 3′,5′-H), 3.90 (s, 3 H, -OCH_3), 2.97 (s, 6 H, -N(CH_3)$_2$) ppm. ^{13}C NMR (125 MHz, 300 K, $CDCl_3$, TMS): δ 162.7 (C-4′), 147.3 (C-1′), 145.1 (C-5), 140.3 (C-2), 125.0 (C-2′,6′), 118.1 (C-4), 114.5 (C-3′,5′), 55.7 (-OCH_3), 38.4 (-N(CH_3)$_2$) ppm. MS (EI, 70 eV) *m*/*z* (%): 309 (72) $[M]^+$, 202 (27) $[M - DMS + H]^+$. MS (CI, isobutane) *m*/*z* (%): 310 (100) $[M + H]^+$. UV−vis (toluene) λ_{max} (lg ε): 371 nm (4.314). Step 3: 1-Trityl-4-(4′-methoxyphenylazo)imidazole. Starting from 1-dimethylsulfamoyl-5-(4′-meth-oxyphenylazo)imidazole (1.00 g, 3.23 mmol), general procedure C was applied. Purification via column chromatography on silica gel (EtOAc, R_f = 0.74) gave the desired product as a yellow solid (1.30 g, 2.92 mmol, 90%). Mp: 190 °C. FT-IR (layer) ν: 3057 (w), 2838 (w), 1597 (m), 1578 (m), 1491 (m), 1442 (m), 1298 (w), 1244 (s), 1184 (m), 1143 (m), 1119 (m), 1029 (m), 991 (m), 839 (s), 808 (m), 747 (s), 700 (s), 655 (s), 536 (m) cm^{-1}. ^{1}H NMR (500 MHz, 300 K, $CDCl_3$, TMS): δ 7.91−7.86 (m, 2 H, 2′,6′-H), 7.50 (d, ^4J = 1.4 Hz, 1 H, 5-H), 7.49 (d, ^4J = 1.3 Hz, 1 H, 2-H), 7.39−7.36 (m, 9 H, *m*-Tr-H, *p*-Tr-H), 7.22−7.18 (m, 6 H, *o*-Tr-H), 6.98−6.94 (m, 2 H, 3′,5′-H), 3.86 (s, 3 H, -OCH_3) ppm. ^{13}C NMR (125 MHz, 300 K, $CDCl_3$, TMS): δ 161.5 (C-1′), 153.4 (C-4), 147.4 (C-3′,5′), 141.9 (C-*i*-Tr), 139.1 (C-2), 129.8 (C-*o*-Tr), 128.3 (C- *p*-Tr), 128.3 (C-*m*-Tr), 124.4 (C-2′,6′), 121.0 (C-5), 114.1 (C-3′,5′), 76.1 (-CPh_3), 55.5 (-OCH_3) ppm. MS (EI, 70 eV) *m*/*z* (%): 444 (1) $[M]^+$, 243 (100) $[Tr]^+$, 202 (15) $[M - Tr + H]^+$, 165 (42) $[Tr - Ph]^+$. MS (CI, isobutane) *m*/*z* (%): 445 (1) $[M + H]^+$, 243 (100) $[Tr]^+$, 203 (20) $[M - Tr + 2H]^+$. UV−vis (toluene) λ_{max} (lg ε): 360 nm (4.349). Anal. Calcd for $C_{29}H_{24}N_4O$: C, 78.36; H, 5.44; N, 12.60. Found: C, 78.15; H, 5.77; N, 12.36. Step 4: 1-Methyl-5-(4′-methoxyphenylazo)imidazole (**2b**). Starting from 1-trityl-4-(4′-methoxyphenyl-azo)imidazole (400 mg, 900 μmol), general procedure D was applied. Purification via column chromatography on silica gel (EtOAc, R_f = 0.32) gave desired product **2b** as an orange-yellow solid (179 mg, 828 μmol, 92%). Mp: 103 °C. FT-IR (layer) ν: 2916 (w), 1599 (m), 1581 (m), 1525 (w), 1495 (m), 1444 (m), 1343 (m), 1240 (s), 1143 (s), 1107 (m), 909 (m), 844 (s), 812 (s), 758 (m), 699 (m), 640 (s), 559 (s), 524 (s) cm^{-1}. ^{1}H NMR (500 MHz, 300 K, $CDCl_3$, TMS): δ 7.85−7.80 (m, 2 H, 2′,6′-H), 7.77 (s, 1 H, 2-H), 7.52 (s, 1 H, 4-H), 7.01−6.97 (m, 2 H, 3′,5′-H), 3.98 (s, 3 H, N-C H_3), 3.89 (s, 3 H, -OCH_3) ppm. ^{13}C NMR (125 MHz, 300 K, $CDCl_3$, TMS): δ 162.2 (C-1′), 147.5 (C-4′), 145.4 (C-5), 139.5 (C-2), 124.5 (C-2′,6′), 120.5 (C-4), 114.5 (C-3′,5′), 55.8 (-OCH_3), 32.6 (N-CH_3) ppm. MS (EI, 70 eV) *m*/*z* (%): 216 (100) $[M]^+$, 122 (15), 109 (16), 107 (60) $[C_7H_7O]^+$. MS (CI, isobutane) *m*/*z* (%): 217 (100) $[M + H]^+$. HR-MS (EI, 70 eV): *m*/*z* $[M]^+$ calcd for $C_{11}H_{12}N_4O$, 216.1011; found, 216.1020. UV−vis (toluene) λ_{max} (lg ε): 372 nm (4.284).

*Synthesis of 1-Methyl-5-(4′-N,N-dimethylaminophenylazo)-imidazole (**2c**).* Step 1: 4-*N*,*N*-Dimethylaminodiazoniumbenzene tetrafluoroborate. 4-*N*,*N*-Dimethylaminoaniline (3.70 g, 27.2 mmol) was converted into the desired diazonium compound following general procedure A. The product was obtained as a white solid (3.26 g, 13.9 mmol, 51%). ^{1}H NMR (200 MHz, 300 K, CD_3CN): δ 8.08−7.94 (m, 2 H, 2,6-H), 7.00−6.89 (m, 2 H, 3,5-H), 3.27 (s, 6 H, -N(CH_3)$_2$) ppm. Step 2: 1-Dimethylsulfamoyl-5-(4′-*N*,*N*-dimethylaminophenylazo)-imidazole. Starting from 1-*N*,*N*-dimethylsulfamoylimidazole (1.50 g, 8.57 mmol), general procedure B was applied. Purification via column chromatography on silica gel (CH_2Cl_2/EtOAc (9:1), R_f = 0.34) gave the desired product as a red solid (1.30 g, 4.03 mmol, 47%). Mp: 157 °C. FT-IR (layer) ν: 3116 (w), 2901 (w), 1598 (m), 1514 (m), 1460 (w), 1432 (m), 1417 (m), 1388 (m), 1353 (m), 1272 (m), 1231 (m), 1170 (m), 1087 (s), 959 (s), 886 (m), 844 (m), 823 (s), 725 (s), 702 (m), 631 (m), 594 (s), 524 (s) cm^{-1}. ^{1}H NMR (600 MHz, 300 K, $CDCl_3$, TMS): δ 8.04 (d, ^4J = 0.7 Hz, 1 H, 2-H), 7.80−7.77 (m, 2 H, 2′,6′-H), 7.36 (d, ^4J = 0.7 Hz, 1 H, 4-H), 6.75−6.71 (m, 2 H, 3′,5′-H), 3.11 (s, 6 H, C$^{4'}$-N(CH_3)$_2$), 2.96 (s, 6 H, -SO_2N(CH_3)$_2$) ppm. ^{13}C NMR (125 MHz, 300 K, $CDCl_3$, TMS): δ 152.8 (C-1′), 145.6 (C-5), 144.0 (C-4′), 139.2 (C-2), 125.4 (C-2′,6′), 116.9 (C-4), 111.6 (C-3′,5′), 40.3 (C$^{4'}$-N(CH_3)$_2$), 38.4 (-SO_2N(CH_3)$_2$) ppm. MS (EI, 70 eV) *m*/*z* (%): 322 (100) $[M]^+$, 214 (20) $[M\text{-}SO_2NMe_2]^+$. MS (CI, isobutane) *m*/*z* (%): 323 (100) $[M + H]^+$, 216 (13) $[M - SO_2NMe_2 + H]^+$. UV−vis (toluene) λ_{max} (lg ε): 455 nm (4.395). Anal. Calcd for $C_{13}H_{18}N_6O_2S$: C, 48.43; H, 5.63; N, 26.07; S, 9.95. Found: C, 48.85; H, 5.46; N, 25.79; S, 10.22. Step 3: 4(5)-(4′-*N*,*N*-Dimethylaminophenylazo)imidazole. 1-Dimethylsulfamoyl-5-(4′-*N*,*N*-dimethylaminophenylazo)imidazole (100 mg, 310 μmol) was dissolved in THF/HCl (4:1) (16 mL), and the mixture was heated to reflux for 1 h. The mixture was basified with 40% KOH (aq) (pH ∼10) and extracted with CH_2Cl_2 (3 × 50 mL). The combined organic layers were dried over $MgSO_4$ and evaporated to dryness. Purification via column chromatography on silica gel (EtOAc/acetone, 1:1) gave a red solid (33.0 mg, 153 μmol, 49%). ^{1}H NMR (500 MHz, 300 K, $CDCl_3$): δ 7.81−7.77 (m, 2 H, 2′,6′-H), 7.67 (d, ^4J = 0.8 Hz, 1 H, 5(4)-H), 7.64 (d, ^4J = 0.8 Hz, 1 H, 2-H), 6.75−6.71 (m, 2 H, 3′,5′-H), 3.06 (s, 6 H, -N(CH_3)$_2$) ppm. MS (EI, 70 eV) *m*/*z* (%): 215 (100) $[M]^+$, 149 (18) $[M - Im + H]^+$, 120 (19) $[C_8H_{10}N]^+$. MS (CI, isobutane) *m*/*z* (%): 216 (10) $[M + H]^+$. Step 4: 1-Trityl-4-(4′-*N*,*N*-dimethylaminophenylazo)-imidazole. 4(5)-(4′-*N*,*N*-Dimethylaminophenylazo)imidazole (186 mg, 767 μmol) was dissolved in CH_2Cl_2 (10 mL). The solution was treated with trityl chloride (235 mg, 844 μmol) and triethylamine (140 μL, 997 μmol) and stirred at room temperature overnight. The organic layer was washed twice with water, and the combined aq layers were extracted with DCM (2 × 20 mL). The combined organic layers were dried over $MgSO_4$, and the solvent was removed. Purification via column chromatography on silica gel (CH_2Cl_2/EtOAc (1:1), R_f = 0.67) gave the desired product as a yellow solid (230 mg, 503 μmol, 66%). Mp: 263 °C. FT-IR (layer) ν: 2906 (w), 1595 (s), 1511 (m), 1488 (m), 1442 (m), 1406 (w), 1361 (s), 1224 (m), 1147 (s), 1113 (m), 1035 (w), 986 (m), 942 (m), 865 (w), 823 (s), 751 (s), 704 (s), 655 (s), 526 (s) cm^{-1}. ^{1}H NMR (600 MHz, 300 K, $CDCl_3$, TMS): δ 7.86−7.84 (m, 2 H, 2′,6′-H), 7.46 (d, ^4J = 1.4 Hz, 1 H, 2-H), 7.41 (d, ^4J = 1.5 Hz, 1 H, 5-H), 7.37−7.34 (m, 9 H, *m*-Tr-H, *p*-Tr-H), 7.22−7.19 (m, 6 H, *o*-Tr-H), 6.73−6.70 (m, 2 H, 3′,5′-H), 3.03 (s, 6 H, -N(CH_3)$_2$) ppm. ^{13}C NMR (150 MHz, 300 K, $CDCl_3$, TMS): δ 153.6 (C-4), 152.0 (C-4′), 143.9 (C-1′), 142.0 (C-*i*-

DOI: 10.1021/acs.joc.5b02817
J. Org. Chem. 2016, 81, 1206−1215

Tr), 138.8 (C-2), 129.8 (C-*o*-Tr), 128.2 (C-*m*-Tr), 127.9 (C-*p*-Tr), 124.6 (C-2′,6′), 119.2 (C-5), 111.5 (C-3′,5′), 76.0 (-CPh_3), 40.3 (-$N(CH_3)_2$) ppm. MS (EI, 70 eV) *m*/*z* (%): 457 (5) $[M]^+$, 243 (100) $[Tr]^+$, 215 (10) $[M\text{-}Tr]^+$, 165 (41) $[Tr\text{-}Ph]^+$. MS (CI, isobutane) *m*/*z* (%): 458 (1) $[M + H]^+$, 243 (100) $[Tr]^+$, 216 (10) $[M - Tr + 2H]^+$, 167 (18) $[Tr - Ph + 2H]^+$. UV−vis (toluene) λ_{max} (lg ε): 402 nm (4.146). Step 5: 1-Methyl-5-(4′-*N*,*N*-dimethylaminophenylazo)imidazole (**2c**). Starting from 1-trityl-4-(4′-*N*,*N*-dimethylaminophenylazo)-imidazole (220 mg, 481 μmol), general procedure D was applied. Purification via column chromatography on silica gel (acetone, R_f = 0.52) gave desired product **2c** as a red solid (60.0 mg, 262 μmol, 54%). Mp: 126 °C. FT-IR (layer) ν: 3120 (w), 2917 (m), 2820 (w), 2652 (w), 1600 (s), 1557 (m), 1506 (m), 1445 (m), 1367 (s), 1311 (m), 1278 (m), 1231 (m), 1144 (s), 1108 (s), 1069 (s), 942 (m), 892 (m), 821 (s), 796 (s), 711 (m), 669 (s), 642 (s), 529 (s) cm^{-1}. ^1H NMR (500 MHz, 300 K, $CDCl_3$, TMS): δ 7.80−7.76 (m, 2 H, 2′,6′-H), 7.54 (s, 1 H, 2-H), 7.42 (d, ^4J = 0.9 Hz, 1 H, 4-H), 6.76−6.72 (m, 2 H, 3′,5′-H), 3.92 (s, 3 H, -CH_3), 3.08 (s, 6 H, $C^{4\prime}$-$N(CH_3)_2$) ppm. ^{13}C NMR (125 MHz, 300 K, $CDCl_3$, TMS): δ 152.3 (C-1′), 145.8 (C-5), 144.2 (C-4′), 139.0 (C-2), 124.5 (C-2′,6′), 120.1 (C-4), 111.7 (C-3′,5′), 40.5 ($C^{4\prime}$-$N(CH_3)_2$), 32.2 (−CH_3) ppm. MS (EI, 70 eV) *m*/*z* (%): 229 (100) $[M]^+$, 105 (10) $[C_6H_5N_2]^+$. MS (CI, isobutane) *m*/*z* (%): 230 (100) $[M + H]^+$. HR-MS (EI, 70 eV): *m*/*z* $[M]^+$ calcd for $C_{12}H_{15}N_5$, 229.1328; found, 229.1323. UV−vis (toluene) λ_{max} (lg ε): 440 nm (4.339).

*Synthesis of 1-Methyl-5-(3′,5′-di-tert-butyl-4′-methoxyphenylazo)imidazole (**2e**).* Step 1: 3,5-Di-*tert*-butyl-4-methoxybenzoic acid. 3,5-Di-*tert*-butyl-4-hydroxybenzoic acid (10.0 g, 39.9 mmol) was dissolved in acetone (200 mL) and treated with potassium hydroxide (5.60 g, 100 mmol) and iodomethane (7.40 mL, 120 mmol). The reaction mixture was heated to 60° and stirred under reflux for 18 h. The mixture was partially evaporated and treated with ethyl acetate and water. Layers were separated, and the aqueous layer was extracted three times with ethyl acetate. The combined organic layers were dried over magnesium sulfate and evaporated to dryness. The residue was dissolved in THF/water (1:1, 100 mL) and treated with lithium hydroxide monohydrate (5.00 g, 119 mmol). The reaction mixture was stirred at 60 °C for 18 h. The solution was partially evaporated and acidified with concd HCl. The precipitate was filtered off and recrystallized from CH_2Cl_2/*n*-hexane (1:1). The desired product was obtained as a colorless solid (7.49 g, 26.7 mmol, 71%). ^1H NMR (200 MHz, 300 K, $CDCl_3$, TMS): δ 8.04 (d, ^4J = 0.4 Hz, 2 H, 2-H), 3.74 (s, 3 H, -OCH_3), 1.47 (s, 18 H, 2x -$C(CH_3)_3$) ppm. Step 2: 3,5-Di-*tert*-butyl-4-methoxyphenylcarbamic *tert*-butylester. 3,5-Di-*tert*-butyl-4-methoxybenzoic acid (3.00 g, 11.4 mmol) was treated with triethylamine (1.66 mL, 11.4 mmol) and DPPA (2.60 mL, 11.4 mmol) in *tert*-butanol (50.0 mL). The mixture was stirred at 85 °C overnight, and after cooling, the precipitate was filtered off multiple times and washed with little EtOH to yield 3,5-di-*tert*-butyl-4-methoxyphenylcarbamic *tert*-butylester as a white solid (2.75 g, 8.2 mmol, 72%). ^1H NMR (500 MHz, 300 K, $CDCl_3$, TMS): δ 7.21 (s, 2 H, 2,6-H), 6.32 (br s, 1 H, NH), 3.66 (s, 3 H, -OCH_3), 1.51 (s, 9 H, -$OC(CH_3)_3$), 1.42 (s, 18 H, 2x Ar-$C(CH_3)_3$) ppm. ^{13}C NMR (125 MHz, 300 K, $CDCl_3$, TMS): δ 223.7 (-N-CO-O-), 155.3 (C-4), 144.1 (C-3,5), 123.9 (C-1), 117.5 (C-2,6), 80.0 (O-$C(CH_3)_3$), 64.2 (-OCH_3), 35.9 (2x Ar-$C(CH_3)_3$), 32.0 (2x Ar-$C(CH_3)_3$), 28.4 (O-$C(CH_3)_3$) ppm. MS (EI, 70 eV) *m*/*z* (%): 335 (17) $[M]^+$, 279 (100) $[M - {}^tBu + H]^+$, 220 (21) $[C_{15}H_{24}O]^+$. MS (CI, isobutane) *m*/*z* (%): 336 (18) $[M + H]^+$, 280 (100) $[M - {}^tBu + 2H]^+$. Step 3:3,5-Di-*tert*-butyl-4-methoxyaniline. 3,5-Di-*tert*-butyl-4-methoxyphenylcarbamic *tert*-butylester (335 mg, 10.0 mmol) was dissolved in DCM (6.0 mL) and treated with trifluoracetic acid (1.0 mL). After stirring overnight at room temperature, the mixture was treated with sodium hydroxide (1.00 g) in water (6.0 mL) and extracted with DCM (3 × 30 mL). The organic layer was separated and dried over magnesium sulfate, and the solvent was evaporated in vacuo to give 3,5-di-*tert*-butyl-4-methoxy-aniline as a white solid (217 mg, 923 μmol, 92%). ^1H NMR (200 MHz, 300 K, $CDCl_3$, TMS): δ 6.55 (s, 2 H, 2,6-H), 3.57 (s, 3 H, -OCH_3), 3.41 (s, br, 2 H, NH_2), 1.33 (s, 18 H, 2x -$C(CH_3)_3$) ppm. Step 4: 3,5-Di-*tert*-butyl-4-methoxydiazoniumbenzene tetrafluoroborate. 3,5-Di-*tert*-butyl-4-methoxyaniline (2.25 g, 9.57 mmol) was dissolved in EtOH (22.5 mL) and 50% HBF_4 (2.00 mL). Isopentyl nitrite (1.35 mL, 10.1 mmol) was added dropwise and stirred for 15 min at room temperature. Then, 50% HBF_4 (5.0 mL) and water (30.0 mL) were added. The precipitate was filtered off and washed with little EtOH. The desired product was obtained as a light purple solid (2.07 g, 9.57 mmol, 65%), which was rather unstable and therefore was immediately used after preparation. ^1H NMR (200 MHz, 300 K, CD_3CN): δ 8.48 (s, 2 H, 2,6-H), 3.47 (s, 3 H, -OCH_3), 1.53 (s, 18 H, 2x -$C(CH_3)_3$) ppm. Step 5: 1-Dimethylsulfamoyl-5-(3′,5′-di-*tert*-butyl-4′-methoxyphenylazo)-imidazole. Starting from 1-*N*,*N*-dimethylsulfamoylimidazole (1.00 g, 5.71 mmol), general procedure B was applied. Purification via column chromatography on silica gel (CH_2Cl_2/EtOAc (19:1), R_f = 0.43) gave the desired product as an orange-red solid (1.40 g, 3.32 mmol, 58%). Mp: 114 °C. FT-IR (layer) ν: 3142 (w), 2956 (m), 1455 (m), 1387 (s), 1223 (m), 1162 (s), 1093 (s), 1003 (m), 972 (m), 889 (w), 834 (w), 750 (w), 726 (s), 638 (m), 591 (s), 537 (m), 513 (s) cm^{-1}. ^1H NMR (500 MHz, 300 K, $CDCl_3$, TMS): δ 8.12 (s, 1 H, 2-H), 7.81 (s, 2 H, 2′,6′-H), 7.46 (s, 1 H, 4-H), 3.75 (s, 3 H, -OCH_3), 3.01 (s, 6 H, -$SO_2N(CH_3)_2$), 1.47 (s, 18 H, 2x -$C(CH_3)_3$) ppm. ^{13}C NMR (125 MHz, 300 K, $CDCl_3$, TMS): δ 163.3 (C-4′), 148.2 (C-1′), 145.2 (C-3′,5′), 145.1 (C-5), 140.3 (C-2), 121.9 (C-2′,6′), 117.8 (C-4), 64.5 (-OCH_3), 38.4 (-$SO_2N(CH_3)_2$), 36.0 (2x -$C(CH_3)_3$), 31.9 (2x -$C(CH_3)_3$) ppm. MS (EI, 70 eV) *m*/*z* (%): 421 (100) $[M]^+$, 314 (30) $[M - SO_2NMe_2 + H]^+$, 257 (35) $[M - SO_2NMe_2 - {}^tBu + H]^+$, 234 (10). MS (CI, isobutane) *m*/*z* (%): 422 (100) $[M + H]^+$. UV−vis (toluene) λ_{max} (lg ε): 368 nm (4.204). Step 6: 1-Trityl-4-(3′,5′-di-*tert*-butyl-4′-methoxyphenylazo)imidazole. Starting from 1-dimethyl-sulfamoyl-5-(3′,5′-di-*tert*-butyl-4′-methoxyphenylazo)imidazole (1.10 g, 2.61 mmol), general procedure C was applied. Purification via column chromatography on silica gel ($CHCl_3$, R_f = 0.75) gave the desired product as an orange-yellow solid (1.12 g, 2.01 mmol, 77%). Mp: 208 °C. FT-IR (layer) ν: 2956 (w), 1491 (w), 1444 (m), 1407 (w), 1282 (w), 1218 (m), 1157 (w), 1119 (m), 1009 (m), 893 (w), 859 (w), 754 (s), 700 (s), 660 (m), 639 (m), 504 (m) cm^{-1}. ^1H NMR (500 MHz, 300 K, $CDCl_3$, TMS): δ 7.85 (s, 2 H, 2′,6′-H), 7.80 (d, ^4J = 1.6 Hz, 1 H, 5-H), 7.52 (d, ^4J = 1.4 Hz, 1 H, 2-H), 7.42−7.38 (m, 9 H, *m*-Tr-H, *p*-Tr-H), 7.21−7.17 (m, 6 H, *o*-Tr-H), 3.72 (s, 3 H, -OCH_3), 1.44 (s, 18 H, 2x -$C(CH_3)_3$) ppm. ^{13}C NMR (125 MHz, 300 K, $CDCl_3$, TMS): δ 162.1 (C-4′), 153.3 (C-4), 148.4 (C-1′), 144.5 (C-3′,5′), 142.0 (C-*i*-Tr), 139.0 (C-2), 129.9 (C-*o*-Tr), 128.4 (C-*m*-Tr), 128.0 (C-*p*-Tr), 121.6 (C-2′,6′), 121.3 (C-5), 76.3 (-CPh_3), 64.5 (-OCH_3), 36.2 (2x -$C(CH_3)_3$), 32.1 (2x -$C(CH_3)_3$) ppm. MS (EI, 70 eV) *m*/*z* (%): 260 (34), 243 (100) $[Tr]^+$, 183 (100), 165 (31) $[Tr\text{-}Ph]^+$, 105 (92). MS (CI, isobutane) *m*/*z* (%): 557 (4) $[M + H]^+$, 315 (14) $[M - Tr + H]^+$, 243 (100) $[Tr]^+$, 236 (17). UV−vis (toluene) λ_{max} (lg ε): 344 nm (4.152). Step 7: 1-Methyl-5-(3′,5′-di-*tert*-butyl-4′-methoxyphenylazo)imidazole (**2e**). Starting from 1-trityl-4-(3′,5′-di-*tert*-butyl-4′-methoxyphenylazo)imidazole (800 mg, 1.44 mmol), general procedure D was applied. Purification via column chromatography on silica gel (EtOAc, R_f = 0.55) gave desired product **2e** as an orange-yellow solid (388 mg, 1.18 mmol, 82%). Mp: 107 °C. FT-IR (layer) ν: 3102 (w), 2956 (m), 1503 (m), 1405 (m), 1340 (m), 1246 (w), 1219 (s), 1169 (m), 1114 (s), 996 (m), 893 (m), 809 (m), 643 (m), 597 (m), 535 (m) cm^{-1}. ^1H NMR (500 MHz, 300 K, toluene-d_8, toluene-d_8): δ 7.98 (s, 2 H, 2′,6′-H), 7.84 (s, br, 1 H, 4-H), 6.94 (s, br, 1 H, 2-H), 3.40 (s, 3 H, -OCH_3), 3.09 (s, 3 H, N-CH_3), 1.44 (s, 18 H, 2x -$C(CH_3)_3$) ppm. ^{13}C NMR (125 MHz, 300 K, toluene-d_8, toluene-d_8): δ 162.3 (C-4′), 149.3 (C-1′), 145.8 (C-5), 144.8 (C-3′,5′), 140.5 (C-2), 124.0 (C-4), 121.5 (C-2′,6′), 64.3 (-OCH_3), 36.2 (2x -$C(CH_3)_3$), 32.1 (2x -$C(CH_3)_3$), 31.4 (N-CH_3) ppm. MS (EI, 70 eV) *m*/*z* (%): 328 (74) $[M]^+$. MS (CI, isobutane) *m*/*z* (%): 329 (33) $[M + H]^+$. HR-MS (EI, 70 eV): *m*/*z* $[M]^+$ calcd for $C_{19}H_{28}N_4O$, 328.2263; found, 328.2261. UV−vis (toluene) λ_{max} (lg ε): 369 nm (4.156). Anal. Calcd for $C_{19}H_{28}N_4O$: C, 69.48; H, 8.59; N, 17.06. Found: C, 69.38; H, 8.61; N, 16.88.

■ ASSOCIATED CONTENT

Supporting Information

The Supporting Information is available free of charge on the ACS Publications website at DOI: 10.1021/acs.joc.5b02817.

Details of computational studies, ^1H NMR, ^{13}C NMR, and UV−vis spectra for compounds **2a**−**c** and **2e**, details of ^1H

DOI: 10.1021/acs.joc.5b02817
J. Org. Chem. 2016, 81, 1206−1215

NMR titration experiments, and details of ^{1}H NMR LD-CISSS experiments (PDF)

AUTHOR INFORMATION

Corresponding Author

*E-mail: rherges@oc.uni-kiel.de.

Notes

The authors declare no competing financial interest.

ACKNOWLEDGMENTS

We gratefully acknowledge financial support by the Deutsche Forschungsgemeinschaft via the collaborative research center SFB 677 "Function by Switching".

REFERENCES

(1) Szymanski, W.; Beierle, J. M.; Kistemaker, H. A. V.; Velema, W. A.; Feringa, B. L. *Chem. Rev.* **2013**, *113*, 6114−6178.
(2) Hilf, R. J. C.; Bertozzi, C.; Zimmermann, I.; Reiter, A.; Trauner, D.; Dutzler, R. *Nat. Struct. Mol. Biol.* **2010**, *17*, 1330−1336.
(3) Polosukhina, A.; Litt, J.; Tochitsky, I.; Nemargut, J.; Sychev, Y.; De Kouchkovsky, I.; Huang, T.; Borges, K.; Trauner, D.; Van Gelder, R.; Kramer, R. *Neuron* **2012**, *75*, 271−282.
(4) Kahn, O. *Molecular Magnetism*; VCH, 1993; p 380.
(5) Decurtins, S.; Gütlich, P.; Köhler, C. P.; Spiering, H.; Hauser, A. *Chem. Phys. Lett.* **1984**, *105*, 1−4.
(6) Gütlich, P.; Garcia, Y.; Goodwin, H. A. *Chem. Soc. Rev.* **2000**, *29*, 419−427.
(7) Gütlich, P.; Goodwin, H. A. *Spin Crossover in Transition Metal Compounds I*; Springer, 2004.
(8) Gopakumar, T. G.; Matino, F.; Naggert, H.; Bannwarth, A.; Tuczek, F.; Berndt, R. *Angew. Chem.* **2012**, *124*, 6367−6371.
(9) Gopakumar, T. G.; Matino, F.; Naggert, H.; Bannwarth, A.; Tuczek, F.; Berndt, R. *Angew. Chem., Int. Ed.* **2012**, *51*, 6262−6266.
(10) Thies, S.; Sell, H.; Schütt, C.; Bornholdt, C.; Näther, C.; Tuczek, F.; Herges, R. *J. Am. Chem. Soc.* **2011**, *133*, 16243−16250.
(11) Venkataramani, S.; Jana, U.; Dommaschk, M.; Sönnichsen, F. D.; Tuczek, F.; Herges, R. *Science* **2011**, *331*, 445−448.
(12) Thies, S.; Sell, H.; Bornholdt, C.; Schütt, C.; Köhler, F.; Tuczek, F.; Herges, R. *Chem. - Eur. J.* **2012**, *18*, 16358−16368.
(13) Dommaschk, M.; Schütt, C.; Venkataramani, S.; Jana, U.; Näther, C.; Sönnichsen, F. D.; Herges, R. *Dalton Trans.* **2014**, *43*, 17395−17405.
(14) Caughey, W. S.; Deal, R. M.; McLees, B. D.; Alben, J. O. *J. Am. Chem. Soc.* **1962**, *84*, 1735−1736.
(15) Caughey, W. S.; Fujimoto, W. Y.; Johnson, B. P. *Biochemistry* **1966**, *5*, 3830−3843.
(16) McLees, B. D.; Caughey, W. S. *Biochemistry* **1968**, *7*, 642−652.
(17) Cole, S. J.; Curthoys, G. C.; Magnusson, E. A.; Phillips, J. N. *Inorg. Chem.* **1972**, *11*, 1024−1028.
(18) Kim, D.; Su, Y. O.; Spiro, T. G. *Inorg. Chem.* **1986**, *25*, 3988−3993.
(19) Song, Y.; Haddad, R. E.; Jia, S.-L.; Hok, S.; Olmstead, M. M.; Nurco, D. J.; Schore, N. E.; Zhang, J.; Ma, J.-G.; Smith, K. M.; Gazeau, S.; Pécaut, J.; Marchon, J.-C.; Medforth, C. J.; Shelnutt, J. A. *J. Am. Chem. Soc.* **2005**, *127*, 1179−1192.
(20) Thies, S.; Bornholdt, C.; Köhler, F.; Sönnichsen, F. D.; Näther, C.; Tuczek, F.; Herges, R. *Chem. - Eur. J.* **2010**, *16*, 10074−10083.
(21) Dommaschk, M.; Peters, M.; Gutzeit, F.; Schütt, C.; Näther, C.; Sönnichsen, F. D.; Tiwari, S.; Riedel, C.; Boretius, S.; Herges, R. *J. Am. Chem. Soc.* **2015**, *137*, 7552−7555.
(22) Otsuki, J.; Narutaki, K. *Bull. Chem. Soc. Jpn.* **2004**, *77*, 1537−1544.
(23) Otsuki, J.; Narutaki, K.; Bakke, J. M. *Chem. Lett.* **2004**, *33*, 356−357.
(24) Suwa, K.; Otsuki, J.; Goto, K. *Tetrahedron Lett.* **2009**, *50*, 2106−2108.
(25) Suwa, K.; Otsuki, J.; Goto, K. *J. Phys. Chem. A* **2010**, *114*, 884−890.
(26) Weston, C. E.; Richardson, R. D.; Haycock, P. R.; White, A. J. P.; Fuchter, M. J. *J. Am. Chem. Soc.* **2014**, *136*, 11878−11881.
(27) Tabata, M.; Nishimoto, J. Equilibrium data of porphyrins and metalloporphyrins. *Porphyrin Handb.* **2000**, 221−419.
(28) Walker, F. A.; Lo, M.-W.; Ree, M. T. *J. Am. Chem. Soc.* **1976**, *98*, 5552−5560.
(29) Portela, C. F.; Magde, D.; Traylor, T. G. *Inorg. Chem.* **1993**, *32*, 1313−1320.
(30) Wendler, T.; Schütt, C.; Näther, C.; Herges, R. *J. Org. Chem.* **2012**, *77*, 3284−3287.
(31) *TURBOMOLE*, V6.3, 2011; a development of University of Karlsruhe and Forschungszentrum Karlsruhe GmbH, 1989−2007, TURBOMOLE GmbH, since 2007; available from http://www.turbomole.com.
(32) Herges, R.; Jansen, O.; Tuczek, F.; Venkatamarani, S. Photosensitive metal porphyrin complexes with pendant photoisomerizable chelate arm as photochromic molecular switches undergoing photo-induced spin transition. Patent DE 102010034496 A1, Feb 16, 2012.
(33) Herges, R.; Jansen, O.; Tuczek, F.; Venkatamarani, S. Transition metal complexes with photosensitive tethered ligands as visible light-induced spin-crossover magnetic molecular switches. Patent WO 2012022299 A1, Feb 23, 2012.
(34) Dommaschk, M.; Gutzeit, F.; Boretius, S.; Haag, R.; Herges, R. *Chem. Commun.* **2014**, *50*, 12476−12478.
(35) Chadwick, D. J.; Ngochindo, R. I. *J. Chem. Soc., Perkin Trans. 1* **1984**, 481−486.
(36) Dunker, M. F. W.; Starkey, E. B.; Jenkins, G. L. *J. Am. Chem. Soc.* **1936**, *58*, 2308−2309.

DOI: 10.1021/acs.joc.5b02817
J. Org. Chem. 2016, 81, 1206−1215

4 Intramolekularer LD-CISSS mit Azoimidazolen

Der LD-CISSS mit *Recordplayer*-Molekülen erfordert ein äußerst akkurates Design des bindenden Schaltzustands. Bereits kleine strukturelle Veränderungen können die Geometrie der intramolekular koordinierten Spezies so stark beeinflussen, dass eine spannungsfreie Assoziation des Liganden nicht mehr möglich ist und folglich dessen Bindungsstärke deutlich abgeschwächt wird. Die molekulare *Recordplayer*-Struktur wurde mittels quantenchemischer Rechnungen so konzipiert, dass die Koordination der Pyridineinheit an das zentrale Ni(II)-Ion ausschließlich im *cis*-Isomer möglich ist.[117,140] Im thermodynamisch bevorzugten *trans*-Isomer ist der Nickel-Stickstoff-Abstand in jeder denkbaren stabilen Konformation größer als 6 Å, sodass eine intramolekulare Koordination ausgeschlossen werden kann. Im *cis*-Isomer sinkt dieser minimale Abstand auf unter 2.2 Å, was für die Ausbildung einer koordinativen Bindung ein sehr guter Wert ist. Bei der Koordination an das Ni(II)-Ion steht der Pyridinligand zudem fast orthogonal zur Porphyrinebene, sodass die geometrischen Voraussetzung für die intramolekulare Koordination nahezu optimal sind. Vom *para*-Methylpyridin-Derivat **13** konnte eine Einkristallstruktur des koordinierten *cis*-Isomers erhalten werden, anhand derer die sehr gute Vorhersage des theoretischen Modells bewiesen werden konnte (siehe Abb. 4.1).[138]

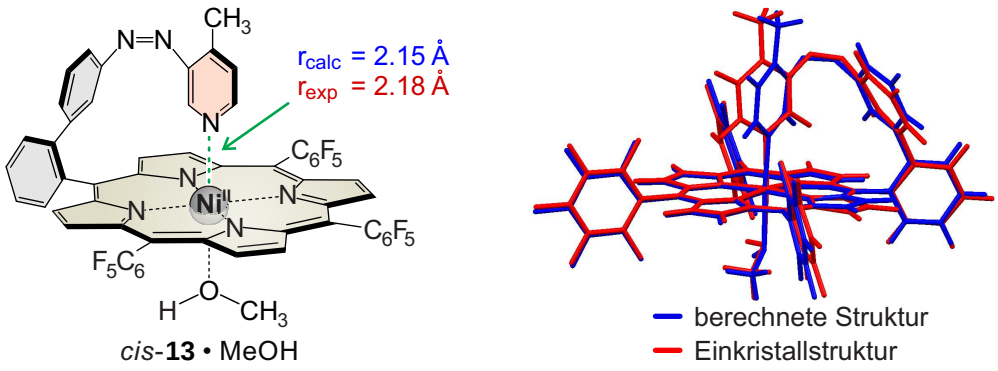

Abb. 4.1: Die molekulare Struktur für Pyridin-*Recordplayer* wurde mithilfe quantenchemischer Rechnungen für die optimale Koordination des *cis*-Isomers konzipiert. Eine Einkristallstruktur, die vom *cis*-Isomer des *para*-Methylpyridin-Derivats **13** erhalten wurde, konnte die sehr gute Vorhersage der theoretisch ermittelten Struktur (Dichtefunktionaltheorie, Theorielevel: PBE/SVP) bestätigen.[138]

Die Versuche zum intermolekularen LD-CISSS haben gezeigt, dass sich die Effizienz der Spinschaltung durch die Verwendung von photoresponsiven Liganden auf Basis von Azoimidazolen stark verbessern lässt.[159] Sowohl die Donorstärke des Liganden als auch die Photoisomerisierung ins *cis*-Isomer sind im Vergleich zu den Pyridin-Systemen klar verbessert. Ein einfacher Austausch von Pyridin durch *N*-Methylimidazol im bestehenden molekularen *Recordplayer*-Design führt allerdings nicht zwangsläufig zu einem effizienten Spinschalter. Die kleinere Ringgröße des Imidazols bewirkt, dass sich sowohl der Abstand als auch der Winkel zwischen den möglichen Anknüpfungspunkten des koordinierten Liganden und des Porphyrins ändern. Des Weiteren bevorzugen *cis*-Phenylazoimidazole eine Konformation, bei der die aromatischen Systeme vom Phenyl- und vom Imidazolring orthogonal zueinander orientiert sind.[142] Diese strukturellen Grundvoraussetzungen des Phenylazoimidazols müssen bei der kovalenten Anbindung der neuen Schalteinheit an das Nickel(II)porphyrin berücksichtigt werden.

4.1 Azoimidazole functionalized Ni-porphyrins for molecular spin switching and light responsive MRI contrast agents.

Gernot Heitmann, Christian Schütt, Jens Gröbner, Lukas Huber und Rainer Herges

Dalton Trans. **2016**, *45*, 11407-11412.
http://dx.doi.org/10.1039/c6dt01727d

Zusammenfassung

Die molekularen Designs, die Synthesen sowie die Schalteigenschaften der Imidazol-*Recordplayer*-Moleküle **14** und **15** werden vorgestellt. Das Derivat **14**, in dem Porphyrin und schaltbarer Ligand über eine Biphenyleinheit verbunden sind, weist in den quantenchemischen Rechnungen eine eher gespannte Geometrie für das koordinierende *cis*-Konformer auf. Eine einatomige Verlängerung der Verbindungseinheit ergab das Thioether-Derivat **15**, für das rechnerisch eine nahezu optimale intramolekulare Koordination vorhergesagt wird. Nachteilig bei diesem Design ist die höhere Flexibilität der Verbindungseinheit. Die Synthese beider *Recordplayer*-Derivate **14** und **15** gelang mittels des gut etablierten Schaltarm-Ansatzes. Das koordinierende *cis*-Isomer beider Imidazol-*Recordplayer* lässt sich am effektivsten durch Belichtung mit UV-Licht ($\lambda_a = 365\,\text{nm}$) anreichern (85 % *cis*). Die Rückschaltung mit blauem Licht ($\lambda_b = 435\,\text{nm}$) ergibt große Überschüsse der diamagnetischen Spezies (86-87 % *trans*). Die intramolekulare Koordination des *cis*-Isomers ist im Falle von **15** stärker (77 % koordiniertes *cis*-**15**, 72 % koordiniertes *cis*-**14**), allerdings ist die Verbesserung weniger stark als durch die theoretische Vorhersage erwartet. Temperaturabhängige ^{1}H-NMR-Messungen bestätigten die Ergebnisse der quantenchemischen Rechnungen und ergaben, dass die Koordination von *cis*-**15** im Vergleich zu *cis*-**14** mit einem höheren Energiegewinn (ΔH) verbunden ist. Dies wird jedoch durch eine entropische Benachteiligung (ΔS) aufgrund der höheren Flexibilität der Thioethereinheit, welche anhand der experimentellen Daten festgestellt werden konnte, teilweise wieder ausgelöscht. Nichtsdestotrotz konnte die Schalteffizienz des paramagnetischen Anteils in Acetonitril mithilfe des Thioether-Derivats **15** im Vergleich zum bereits bekannten Pyridin-System von 52 % auf 55 % erhöht werden. Durch erfolgreiche Spinschaltungsversuche in Gegenwart von Wasser und die Visualisierung des Spinwechsels in MRT-Aufnahmen konnte das Potential der Imidazol-*Recordplayer* für zukünftige medizinische Anwendungen als MRT-Kontrastmittel eindrucksvoll aufgezeigt werden (siehe Abb. 4.2).

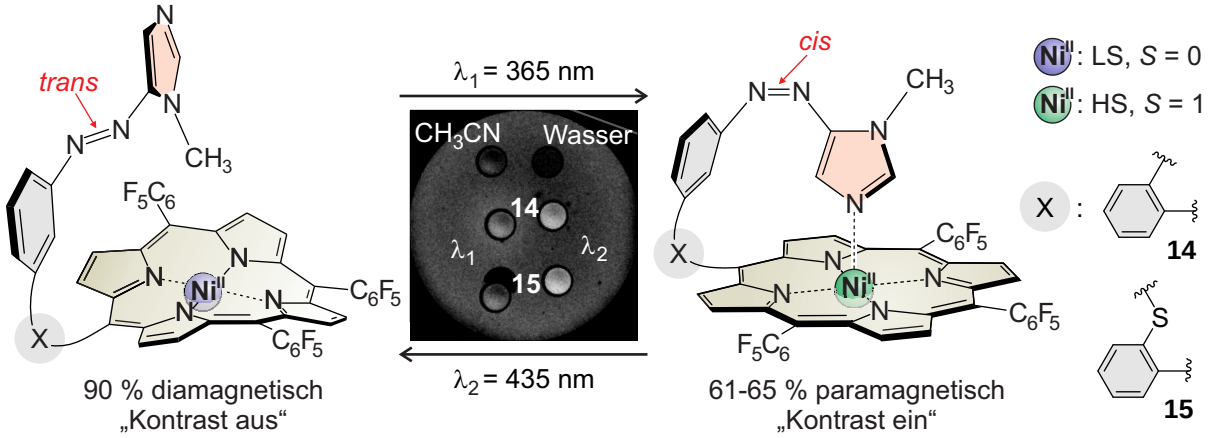

Abb. 4.2: Die Imidazol-*Recordplayer* **14** und **15** zeigen bei Belichtung mit ultraviolettem (365 nm) und blauem (435 nm) Licht den gewünschten intramolekularen LD-CISSS, was unter Anderem mittels MRT visualisiert werden konnte.

Dalton Transactions

PAPER

Cite this: *Dalton Trans.*, 2016, **45**, 11407

Azoimidazole functionalized Ni-porphyrins for molecular spin switching and light responsive MRI contrast agents†

Gernot Heitmann,[a] Christian Schütt,[a] Jens Gröbner,[a] Lukas Huber[b] and Rainer Herges*[a]

Received 2nd May 2016,
Accepted 14th June 2016

DOI: 10.1039/c6dt01727d

www.rsc.org/dalton

Azo-*N*-methylimidazole functionalized Ni(II)porphyrins were rationally designed and synthesized and their performance as molecular spin switches was investigated. They perform intramolecular light-driven coordination-induced spin state switching (LD-CISSS) in the presence of water and therefore are an important step towards spin switches for medicinal applications, particularly functional MRI contrast agents.

Introduction

The manipulation of magnetic properties in bulk materials as well as in molecular systems has gained increasing attention due to numerous promising applications,[1,2] *e.g.* spintronics, data storage,[3,4] switchable diamagnetic levitation[5] or responsive ("smart") contrast agents for magnetic resonance imaging (MRI).[6–10] However, spin switching of single molecules in solution or on surfaces at ambient temperatures is still challenging and only a few examples are known in the literature.[11–14] Ni^{2+} complexes change their spin state from diamagnetic ($S = 0$) to paramagnetic ($S = 1$) when the coordination sphere is changed from square planar (CN = 4) to square pyramidal (CN = 5) or square bipyramidal (CN = 6).[15–21] We have demonstrated highly efficient and fatigue resistant light-driven coordination-induced spin state switching (LD-CISSS) by adding photodissociable ligands[22–24] to a solution of a Ni^{2+}-porphyrin (PDL approach) as well as by tethering azopyridines directly to the porphyrin ("record player" approach).[10,25–27] In both concepts the photoresponsive axial ligands are designed in such a way that only one photo isomer is capable of coordinating to the Ni^{2+}. Recently, we were able to show the photo switching of MRI contrasts with record player molecules.[10] Thus, the "record player" concept is a promising approach for the development of "smart" MRI contrast agents that can be switched on and off with light for interventional radiology. A number of diseases such as stroke and heart attack are increasingly treated with minimal invasive, catheter-based interventions under X-ray imaging control (*e.g.* placing stents). Replacing X-ray imaging by MRI would have several advantages: avoidance of ionizing radiation, better soft tissue contrast, and 3D control.[28] However, for MRI guided interventions switchable contrast agents are needed to continuously check the dynamic blood flow. Light is the ideal stimulus for switching because it can be applied with temporal and spatial control, it is traceless and, regarding practical applications, even a micro-catheter can easily accommodate optical fibers that carry sufficient light energy to the site of intervention.[29] Our "record player" molecules are the most promising candidates for light-controlled contrast switching, however, their function is restricted to organic solvents, thus precluding medical applications. Aiming at the extension of the "record player" concept towards operation in aqueous solution one has to consider that water severely reduces the ligand's donor strength by hydrogen bonding or, in the worst case, by protonation. An appropriate ligand for coordination-induced spin state switching (CISSS) in water[30] therefore has to provide a high binding affinity (K_L) to the metal centre while exhibiting a rather low basicity (corresponding to a low pK_a). In toluene, the coordination strength K_L of pyridine based ligands to the highly electron deficient Ni^{2+}-porphyrin $NiTPPF_{20}$ can be increased effectively by introducing electron releasing groups in *para* position to the coordinating nitrogen.[21] However, electron releasing substituents also increase the basicity of the pyridine. The pK_a and K_L follow a linear free energy relationship (see Fig. 1). To avoid protonation (*e.g.* in blood), the pK_a of the ligand should be <7. Methoxypyridine (**1**) (pK_a 6.55) is just within this range, however, dimethylamino pyridine (**2**) which is an extremely strong ligand in toluene[31] would be completely

[a]*Otto Diels-Institut für Organische Chemie, Christian-Albrechts-Universität zu Kiel, Otto-Hahn-Platz 4, D-24098 Kiel, Germany. E-mail: rherges@oc.uni-kiel.de*
[b]*Molecular Imaging North Competence Center, Christian-Albrechts-Universität zu Kiel, Am Botanischen Garten 14, 24118 Kiel, Germany*

†Electronic supplementary information (ESI) available: Details of computational studies, experimental procedures, analytical data. See DOI: 10.1039/c6dt01727d

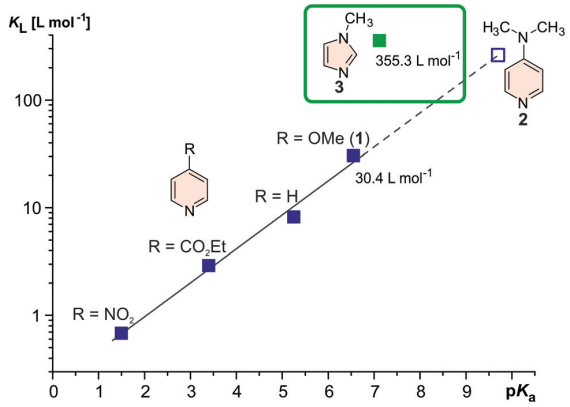

Fig. 1 Association constants of pyridine derivatives[21] and 1-methylimidazole (**3**)[22] with Ni(II)TPPF$_{20}$ (in toluene) as a function of their pK_a value. Electron releasing *para* substituents at the pyridine ring improve the association to the nickel but also give rise to substantially higher basicity. DMAP[31] strongly coordinates to Ni^{2+} in organic solvents, however, in water at pH 7 it would be almost completely protonated and not bind at all. 1-Methylimidazole (**3**) on the other hand exhibits an extremely high association constant and nevertheless a low basicity (pK_a 7.12). Considering the fact that the imidazole ring would bear an additional electron withdrawing azo group, the record player molecule would not be protonated at pH 7.

protonated in water (pK_a 9.7), and not bind at all. We therefore decided to replace pyridine by 1-methylimidazole (**3**) in our record player design. While having a similar basicity as methoxy pyridine (**1**) (pK_a 6.55), 1-methylimidazole (**3**) (pK_a 7.12) has an almost 12-fold higher binding affinity to NiTPPF$_{20}$.[22] We attribute this fact to a reduced steric hindrance of the hydrogen atoms in *ortho* position with respect to the coordinating nitrogen in the 5-membered ring. The same trends were also observed with the photoswitchable 3-phenylazo-substituted pyridines[24] and 5-phenylazo-substituted imidazoles[22] (PDLs, see the ESI†). The (electron withdrawing) azo group in 5-position of the 1-methylimidazol (**3**) should further reduce the pK_a to <6, and protonation under physiological conditions should not occur. This provides further arguments to replace the phenylazopyridine by a phenylazoimidazole unit in our "record player" approach. Consequently, we set out to design new "record player" structures that allow optimal intramolecular coordination of the imidazole of the *cis* isomer, and a weak or no coordination in the *trans* form.

Results and discussion

Previous ligand design studies have shown that even small changes in geometry (bond lengths ~0.01 Å, bond angles ~5°) can have a large effect on functionality and switching efficiency. So, it was to be expected that a simple replacement of the pyridine ring by an imidazole ring would not necessarily lead to a successful spin switch, because the change in ring size would change the length and the angle of the coordinative bond to the Ni^{2+}. Moreover, *cis*-azopyridines prefer a conformation with the phenyl and pyridine ring only slightly twisted with respect to each other, whereas in the *cis*-azoimidazoles the phenyl and the heterocyclic ring are exactly orthogonal.[32] Our record player design is based on three structural elements (Fig. 2): the porphyrin platform (beige), the switchable ligand (red) and the tether (cyan), connecting the former two units.[26] Porphyrin (Ni-tris(pentafluorophenyl)porphyrin) and the photoswitchable ligand (phenylazoimidazole) are already set. So, the tether remains to be optimized. Quantum chemical calculations were performed using the program TURBOMOLE 6.6[33] at the TPSSh/def2TZVP//TPSSh/SVP level of density functional theory (DFT). This level of theory was chosen because, according to an empirical study, it performed best in predicting the coordination energy of axial ligands to nickel porphyrins.[34] Among a number of promising candidates that were initially considered, two structures were selected (Fig. 2, middle and right). A reference structure was calculated as well (Fig. 2, left). In the reference structure ligand and porphyrin are not covalently connected. The reference structure, therefore, exhibits an unstrained geometry with the maximum binding energy. The tether was designed in such a way that this optimum geometry for binding is retained. Structure **4** (Fig. 2, middle) corresponds to the original design.[25,26] The pyridine ring is just replaced by an imidazole ring. The geometry exhibits a strong deviation from ideal binding (*cf.* reference compound) which also leads to a weaker coordination (ΔH_{calc} = −2.15 kcal mol^{-1}) as compared to the reference compound (−6.28 kcal mol^{-1}). Inspection of structure **4** reveals

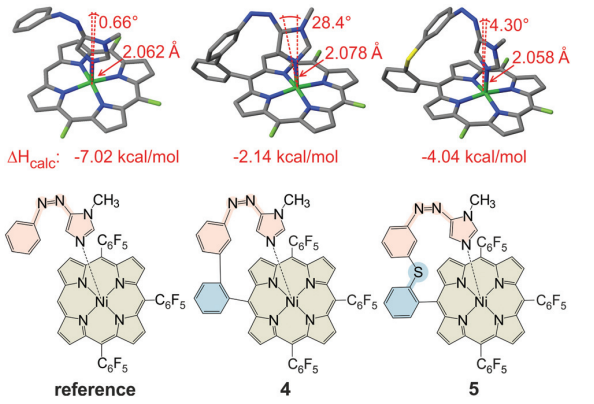

Fig. 2 Calculated (TPSSh/SVP) geometries, ligand binding energies (ΔH_{calc}, TPSSh/def2TZVP//TPSSh/SVP) and schematic 2D structures for the reference structure (left, without a tether) imidazole record player structure **4** (middle, phenyl tether) and **5** (left, thiophenol tether). The reference structure with no constraints represents the ideal binding situation, and therefore exhibits the highest binding energy (ΔH_{calc}). The phenyl tether in **4** imposes a large deviation from the ideal binding geometry and therefore has the lowest binding energy. Obviously the tether is too short. Insertion of a sulphur atom into the tether almost restores the ideal binding geometry. Consequently, the binding energy increases substantially. For the sake of clarity, the pentafluorophenyl substituents are depicted as fluorine substituents in the geometry plots.

that the tether is obviously too short. Therefore we inserted several different atoms and groups into the tether of which sulphur between the two phenyl rings proved to be optimal (Fig. 2, structure **5**). This structure matches the ideal binding conformation almost perfectly and the phenylazoimidazole moiety can obtain a relaxed binding conformation, giving rise to a considerably higher binding energy (−4.04 kcal mol^{-1}). However, an additional rotational degree of freedom is introduced which might disfavour the coordinating *cis* species entropically. Since both structures have pros and cons we were not able to decide at this point which design would be more advantageous. Therefore, we decided to synthesize both "record players" **4** and **5** following the synthetic protocols for the pyridine "record player"[10,25] and for the imidazole based PDLs.[22,32]

The porphyrins were prepared *via* mixed aldehyde syntheses ("tone arm" approach; see Scheme 1; for experimental details see the ESI†). Intermediate for both asymmetric aldehydes ("record player tone arms") **13** and **16** is the tritylated azoimidazole **11** which is prepared from 3-bromoaniline (**6**) and *N*,*N*-dimethylsulfamoylimidazole (**7**) in 8 steps (4 pots) according to a general procedure that we published recently.[22,32] The azo moiety is then connected to the respective benzaldehyde, either by Suzuki cross coupling with 2-formylphenylboronic acid (for biphenyl tone arm **13**), or by Pd-catalyzed thiol functionalization followed by nucleophilic aromatic substitution with 2-fluorobenzaldehyde (for thioether tone arm **16**). Afterwards, the tritylated "tone arms" **12** and **15** are methylated and trityl-deprotected in a one-pot procedure to obtain **13** and **16**. Mixed aldehyde porphyrin syntheses under Lindsey conditions with **13** or **16**, respectively, pentafluoro-benzaldehyde and pentafluorophenyl dipyrromethane gave the porphyrins as free bases which were then treated with nickel(II) acetylacetonate to obtain *N*-methylimidazole "record players" **4** and **5**.

Imidazole "record players" **4** and **5** exhibit considerable differences regarding the photochromism compared to the already known pyridine derivatives (for UV-vis spectra see the ESI†). Pyridine "record players" are switching to the coordinating *cis* isomer upon irradiation into the porphyrin Q bands (~500 nm).[10,25–27] At 365 nm no *trans* → *cis* switching is observed which is peculiar because 365 nm is the usual wavelength for *trans* → *cis* isomerization of azobenzenes and azopyridines. Imidazole "record players" **4** and **5**, however, switch both at 505 nm and 365 nm. Direct excitation of the azo unit with 365 nm or 385 nm is much more efficient (up to 85% *cis*). We assign this improved *trans* → *cis* photoisomerization of **4** and **5** to the bathochromic shift of the azoimidazole π–π* bands in comparison with azopyridines. Unfortunately, this shift also gives rise to a somewhat impaired back-switching to the *trans*-species by irradiation into the *cis* Soret band with 435 nm (14% residual *cis* for **4**; 13% residual *cis* for **5**) which surprisingly is even more pronounced at higher concentrations (for details see the ESI†). The thermal half-life times of *cis*-**4** ($t_{1/2}$ = 69 d) and *cis*-**5** ($t_{1/2}$ = 23 d) exceed those of the free ligands **13** and **16** (18.9 and 19.4 d, measured with ^{1}H NMR, for details see the ESI†). Obviously, coordination increases the stability of the *cis* isomer.

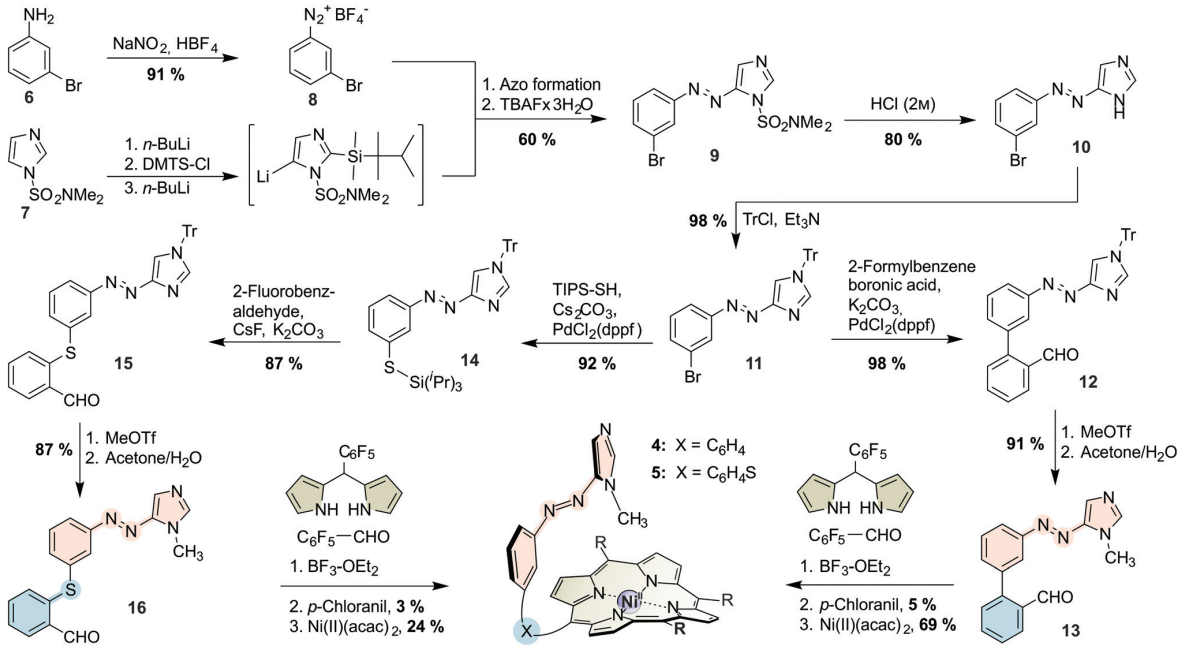

Scheme 1 Synthesis of 1-methylimidazole "record player" molecules **4** and **5**.

The switching performance of our spin switches does not only depend on the conversion rate of *trans* to *cis* and back to the *trans* isomer (complete conversion in an ideal system) but also to what extend the *cis* isomer would be paramagnetic (100% in an ideal system with a strongly coordinating ligand). As we described earlier, the ratio of paramagnetic to diamagnetic *cis*-species can be easily derived from the NMR shift (δ) of the pyrrole protons of the porphyrin system.[23] As expected for the strongly coordinating imidazole ligand, we determined a high amount of paramagnetic *cis* species for **5** (*cis*-$\mathbf{5}_{para}$: 77%) whereas the *cis* isomer of **4** with its more strained binding geometry (Fig. 2 middle) exhibits a lower percentage of paramagnetic species (*cis*-$\mathbf{4}_{para}$: 72%; for details see the ESI†). The measured ratios of paramagnetic *cis* species are in good agreement to the results of our computational studies; however, the performance of thioether "record player" **5** fell somewhat short of our expectations. Temperature dependent NMR experiments provided the thermodynamic parameters ΔH and ΔS of the coordination event, and revealed the reason for this less than optimum performance of **5** (see Table 1, for details see the ESI†). The binding enthalpy ΔH_{exp} for *cis*-**5**, indeed, is much higher than for *cis*-**4**. However, part of the enthalpy gain is cancelled by a more negative coordination entropy ΔS. Insertion of the sulphur atom into the tether introduces an additional degree of conformational freedom in the unbound state (rotation around the C–S bond) which is frozen upon coordination. At 300 K, the free Gibbs enthalpy of coordination (ΔG_{300}) of **5** is only 0.21 kcal mol^{-1} more negative than in **4**. Note that the experimentally determined binding enthalpies of **4** and **5** are in good agreement with the theoretically obtained values (ΔH_{calc}, for details see the ESI†).

The overall performance of a molecular switch is defined as switching efficiency (SE), which in the case of "record player" molecules is the difference of the percentage of the paramagnetic nickel ions in both switching states. The percentage of paramagnetic Ni^{2+} in **4** can be switched between 10% and 61% (SE = 51%) whereas the sulphur derivative is superior with a SE of 55% (10% to 65% paramagnetic Ni^{2+}) (see Fig. 3). Thus, the SE of the imidazole record player **5** in acetonitrile is higher than the SE of the parent pyridine record player in the same solvent (52%).[26]

Encouraged by these results and in view of the development of water soluble spin switches and particularly of functional MRI contrast agents, we performed UV-vis switching experiments with **4** and **5** in a 1 : 1 mixture of phosphate-buffered saline (PBS, pH 7.4) and acetonitrile. The UV-vis spectra of thioether "record player" **5** are depicted in Fig. 4 (for spectra of **4**, see the ESI†). With respect to measurements in pure acetonitrile the MRI "off-state" (PSS-435) is nearly unchanged (~10% *para*) whereas the amount of paramagnetic species in the MRI "on-state" (PSS-365) is somewhat reduced. However, since the paramagnetic species still is formed to 47–48% in **5** (estimated from UV-vis extinction, see the ESI†) we are confident that switching under physiological conditions will be feasible if the solubility in water would be improved.

To take a further step towards application as photoswitchable MRI contrast agents we performed magnetic resonance measurements with **4** and **5** in acetonitrile (~2 mM solutions) in a "small animal" 7T MRI system. The contrast enhancement (corresponding to an accelerated relaxation time of the solvent protons) in the "on-state" (PSS at 365 nm) is clearly visible, proving the applicability of our concept for functional MRI (see Fig. 5, for details see the ESI†). It is noteworthy that acetonitrile is in fact a rather adverse solvent for MRI because of its low proton density, its low coordination affinity to the paramagnetic Ni^{2+}, and the large distance of the methyl protons from the paramagnetic metal ion during coordination. Nevertheless, the MRI contrast of a 2 mM solution of **5** can be switched with UV and visible light by 24%. Previously reported light-responsive MRI contrast agents exhibit switching efficiencies of ~20% in water.[35,36] Corresponding water soluble record

Table 1 Thermodynamic parameters (ΔG at 300 K, ΔH and ΔS) of the coordination event and calculated (TPSSh/def2TZVP//TPSSh/SVP) energy differences (ΔH_{calc}) of the uncoordinated *cis* (singlet) and coordinated *cis* (triplet) species for **4** and **5**

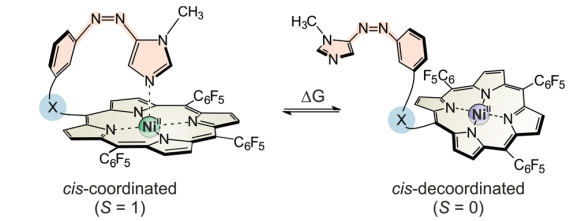

	4 (X = C_6H_4)	**5** (X = C_6H_4S)
ΔH_{exp}/kcal mol^{-1}	−1.96	−2.76
ΔS/cal mol^{-1}	−4.64	−6.84
ΔG_{300}/kcal mol^{-1}	−0.57	−0.71
ΔH_{calc}/kcal mol^{-1}	−2.14	−4.04

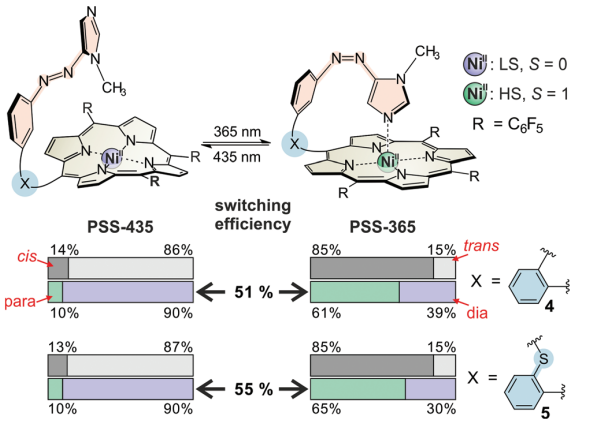

Fig. 3 Switching parameters and switching efficiencies for imidazole record players **4** and **5** in acetonitrile. For the sake of simplicity only the predominant species of each PSS is shown as molecular structure.

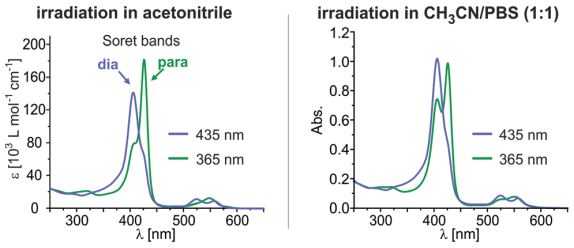

Fig. 4 UV-vis switching experiments of **5** in acetonitrile (left) and in acetonitrile/PBS (1 : 1) (right). Intramolecular coordination of the *cis* species is largely maintained in the presence of water (pH 7.4).

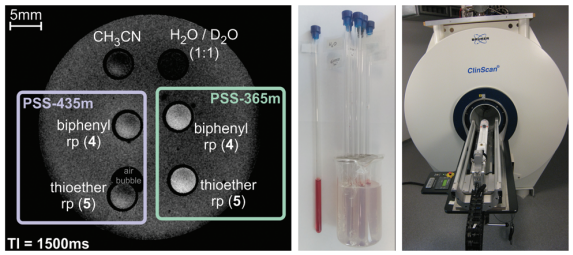

Fig. 5 Left: 7T magnetic resonance image (gradient echo sequence, for details see the ESI†) of record players **4** and **5** in both switching states. The contrast enhancement (corresponding to an accelerated relaxation time of the solvent protons) in the "on-state" (PSS-365 nm) of **4** and **5** is clearly visible. Right: Experimental setup for the MRI measurements. NMR tubes were used as sample carriers and immobilized in an agarose phantom. MRI measurements were carried out on a 7T MRI system (ClinScan by co. Bruker) for "small animals" with a mouse body coil.

player molecules can be expected to be considerably more effective.

Conclusions

In summary, we present two new and very efficient molecular spin switches (**4** and **5**) based on the light-driven coordination-induced spin state switching (LD-CISSS) principle. The molecules are constructed from three building blocks: (a) Ni-porphyrin (disk), (b) azoimidazole (tone arm), (c) tether that connects both units. Upon irradiation with 365 nm the azoimidazole undergoes *trans–cis* isomerization. The associated geometry movement puts the imidazole nitrogen on top of the Ni ion ("record player" design) which changes its coordination number (from 4 to 5), and in turn changes the spin state from diamagnetic to paramagnetic. Irradiation with 435 nm reverses the process. The light-driven spin state switching is completely reversible at room temperature, in solution, and under air. Azo-methylimidazole is a hitherto scarcely used photochromic compound but it combines two properties that are important for the design of spin switches: it's a very efficient photoswitch and the imidazole unit is a very strong ligand that binds to Ni^{2+} even in water. Equally important for the construction of efficient molecular spin switches is a careful design of the tether connecting the azoimidazole with the porphyrin. Quantum chemical calculations and experimental properties of **4** and **5** prove that even very small changes in geometry have a large impact on the switching efficiency. Particularly, the carefully designed "record player" molecule **5** exhibits most prerequisites that are necessary to perform spin switching in water. The spin switching efficiency in a 1 : 1 mixture of water/acetonitrile was determined as 40%. There are a number of potential applications for spin switching in solution. Most obvious is the control of relaxation times of protons. In NMR this could be used to reduce acquisition times, particularly in 2D experiments, whereas in magnetic resonance imaging (MRI) our compounds could be applied as switchable contrast agents in catheter based interventions.[37,38] To demonstrate the efficiency of our "record player" molecules as light controlled contrast agents we performed MRI experiments. Upon irradiation of a 2 mM solution of **5** in acetonitrile the proton relaxation time of the bulk solvent could be reversibly changed, giving rise to a contrast change of 24%.

Acknowledgements

The authors thank Claus Gernert and Jürgen Grotemeyer (Institute for Physical Chemistry, Christian-Albrechts-Universität zu Kiel) for the measurement of high-resolution mass spectra of the compounds **4** and **5**.

This work was funded by the "Deutsche Forschungsgemeinschaft" (DFG) *via* the collaborative research center 677 (SFB 677) "Function by Switching".

Notes and references

1 S. Hayami, S. M. Holmes and M. A. Halcrow, *J. Mater. Chem. C*, 2015, **3**, 7775–7778.
2 M. A. Halcrow, *Spin-Crossover Materials: Properties and Applications*, John Wiley & Sons Ltd, 2013.
3 L. Bogani and W. Wernsdorfer, *Nat. Mater.*, 2008, **7**, 179–186.
4 *J. Mater. Chem.*, 2009, **19**, 1670–1695, themed issue on "Molecular Spintronics and Quantum Computing".
5 K. A. Mirica, S. S. Shevkoplyas, S. T. Phillips, M. Gupta and G. M. Whitesides, *J. Am. Chem. Soc.*, 2009, **131**, 10049–10058.
6 J. Hasserodt, *New J. Chem.*, 2012, **36**, 1707–1712.
7 R. Herges, *Nachr. Chem.*, 2011, **59**, 817–821.
8 I.-R. Jeon, J. G. Park, C. R. Haney and T. D. Harris, *Chem. Sci.*, 2014, **5**, 2461–2465.
9 R. N. Muller, L. Vander Elst and S. Laurent, *J. Am. Chem. Soc.*, 2003, **125**, 8405–8407.
10 M. Dommaschk, M. Peters, F. Gutzeit, C. Schütt, C. Näther, F. D. Sönnichsen, S. Tiwari, C. Riedel, S. Boretius and R. Herges, *J. Am. Chem. Soc.*, 2015, **137**, 7552–7555.

11 A. Witt, F. W. Heinemann and M. M. Khusniyarov, *Chem. Sci.*, 2015, **6**, 4599–4609.
12 M.-L. Boillot, S. Chantraine, J. Zarembowitch, J.-Y. Lallemand and J. Prunet, *New J. Chem.*, 1999, **23**, 179–184.
13 A. Sour, M.-L. Boillot, E. Rivière and P. Lesot, *Eur. J. Inorg. Chem.*, 1999, **1999**, 2117–2119.
14 Y. Hasegawa, S. Kume and H. Nishihara, *Dalton Trans.*, 2009, 280–284.
15 W. S. Caughey, R. M. Deal, B. D. McLees and J. O. Alben, *J. Am. Chem. Soc.*, 1962, **84**, 1735–1736.
16 W. S. Caughey, W. Y. Fujimoto and B. P. Johnson, *Biochemistry*, 1966, **5**, 3830–3843.
17 S. J. Cole, G. C. Curthoys, E. A. Magnusson and J. N. Phillips, *Inorg. Chem.*, 1972, **11**, 1024–1028.
18 D. Kim, Y. O. Su and T. G. Spiro, *Inorg. Chem.*, 1986, **25**, 3988–3993.
19 B. D. McLees and W. S. Caughey, *Biochemistry*, 1968, **7**, 642–652.
20 Y. Song, R. E. Haddad, S.-L. Jia, S. Hok, M. M. Olmstead, D. J. Nurco, N. E. Schore, J. Zhang, J.-G. Ma, K. M. Smith, S. Gazeau, J. Pécaut, J.-C. Marchon, C. J. Medforth and J. A. Shelnutt, *J. Am. Chem. Soc.*, 2005, **127**, 1179–1192.
21 S. Thies, C. Bornholdt, F. Köhler, F. D. Sönnichsen, C. Näther, F. Tuczek and R. Herges, *Chem. – Eur. J.*, 2010, **16**, 10074–10083.
22 C. Schütt, G. Heitmann, T. Wendler, B. Krahwinkel and R. Herges, *J. Org. Chem.*, 2016, **81**, 1206–1215.
23 S. Thies, H. Sell, C. Schütt, C. Bornholdt, C. Näther, F. Tuczek and R. Herges, *J. Am. Chem. Soc.*, 2011, **133**, 16243–16250.
24 S. Thies, H. Sell, C. Bornholdt, C. Schütt, F. Köhler, F. Tuczek and R. Herges, *Chem. – Eur. J.*, 2012, **18**, 16358–16368.
25 S. Venkataramani, U. Jana, M. Dommaschk, F. D. Sönnichsen, F. Tuczek and R. Herges, *Science*, 2011, **331**, 445–448.
26 M. Dommaschk, C. Schütt, S. Venkataramani, U. Jana, C. Näther, F. D. Sönnichsen and R. Herges, *Dalton Trans.*, 2014, **43**, 17395–17405.
27 M. Dommaschk, C. Näther and R. Herges, *J. Org. Chem.*, 2015, **80**, 8496–8500.
28 J.-M. Serfaty, X. Yang, P. Aksit, H. H. Quick, M. Solaiyappan and E. Atalar, *J. Magn. Reson. Imaging*, 2000, **12**, 590–594.
29 K. D. Taylor and C. Reiser, in *Lasers in Cardiovascular Interventions*, ed. O. Topaz, Springer-Verlag, London, 2015, ch. 1, pp. 1–14.
30 M. Dommaschk, F. Gutzeit, S. Boretius, R. Haag and R. Herges, *Chem. Commun.*, 2014, **50**, 12476–12478.
31 The association constant (K_L) of DMAP (**2**) to $NiTPPF_{20}$ in toluene could not be measured due to solubility problems and was extrapolated from the values of the other pyridine derivatives.
32 T. Wendler, C. Schütt, C. Näther and R. Herges, *J. Org. Chem.*, 2012, **77**, 3284–3287.
33 TURBOMOLE V6.6 2014, a development of University of Karlsruhe and Forschungszentrum Karlsruhe GmbH, 1989–2007, TURBOMOLE GmbH, since 2007; available from http://www.turbomole.com.
34 Unpublished results.
35 C. Tu and A. Y. Louie, *Chem. Commun.*, 2007, 1331–1333.
36 C. Tu, E. A. Osborne and A. Y. Louie, *Tetrahedron*, 2009, **65**, 1241–1246.
37 R. Herges, O. Jansen, F. Tuczek and S. Venkatamarani, Molecular Switch., *WO Pat.*, 2012022299 A1, 2012.
38 R. Herges, O. Jansen, F. Tuczek and S. Venkatamarani, Photosensitive metal porphyrin complexes with pendant photoisomerizable chelate arm as photochromic molecular switches undergoing photoinduced spin transition, *DE Pat.*, 102010034 A1, 2012.

4.2 Spin State Switching in Solution with an Azoimidazole-Functionalized Nickel(II)-Porphyrin

Gernot Heitmann, Christian Schütt und Rainer Herges

Eur. J. Org. Chem **2016**, *22*, 3817-3823.
http://dx.doi.org/10.1002/ejoc.201600548

Zusammenfassung

Die theoretische Designstudie aus der in 4.1 vorgestellten Arbeit lieferte einen weiteren Imidazol-*Recordplayer*, dessen Synthese und Schalteigenschaften in dieser Veröffentlichung präsentiert wurden. Die quantenchemischen Rechnungen ergaben, dass eine einatomige Verlängerung der ursprünglich verwendeten Biphenyl-Verknüpfungseinheit notwendig ist, um für *N*-Methylimidazol eine optimale Geometrie für die Koordination des *cis*-Isomers zu erhalten. Im bereits behandelten Thioether-Derivat **15** wird dies durch eine Schwefelbrücke zwischen den Phenylringen des Schaltarms realisiert, jedoch bietet sich auch ein Sauerstoffatom an gleicher Position an. Das entsprechende Diphenylether-Derivat **16** weist in den quantenchemischen Rechnungen eine ähnlich gute Geometrie und dementsprechend eine ebenfalls hohe energetische Bevorzugung der koordinierenden *cis*-Spezies auf. Die Synthese von Diphenylether-*Recordplayer* **16** gelang mittels des Schaltarm-Ansatzes. Der Aufbau der Diphenylether-Einheit mittels nukleophiler Aromatensubstitution erforderte aufgrund unzureichender Reaktivität die Einführung einer Nitrogruppe, welche im ursprünglichen Design nicht vorgesehen war. Eine negative Beeinflussung des angestrebten LD-CISSS wurde jedoch erwartungsgemäß nicht beobachtet. In Schaltexperimenten zeigte *Recordplayer* **16** bei Bestrahlung mit UV Licht (365 nm) eine außergewöhnlich effektive *trans*→*cis* Photoisomerisierung, die in allen untersuchten Lösungsmitteln etwa 90 % des *cis*-Isomers ergab. Die Rückschaltung zum diamagnetische *trans*-Isomer mit blauem Licht (430 nm) verläuft unvollständig und ist lösungsmittelabhängig. Das beste Resultat wurde in Toluol und Methanol (73 % *trans*) beobachtet. Der Anteil des koordinierten, paramagnetischen *cis*-Konformers wird ebenfalls stark vom verwendeten Lösungsmittel bestimmt. Toluol, welches sich bereits bezüglich der *cis*/*trans*-Photoisomerisierung als besonders geeignet erwies, stabilisiert auch die intramolekulare Koordination des *N*-Methylimidazols sehr effektiv (86 % paramagnetische *cis*-Spezies). Folglich lässt sich der Anteil der paramagnetischen Ni(II)-Spezies von **16** in Toluol zwischen 23 % und 81 % schalten (siehe Abb. 4.3).

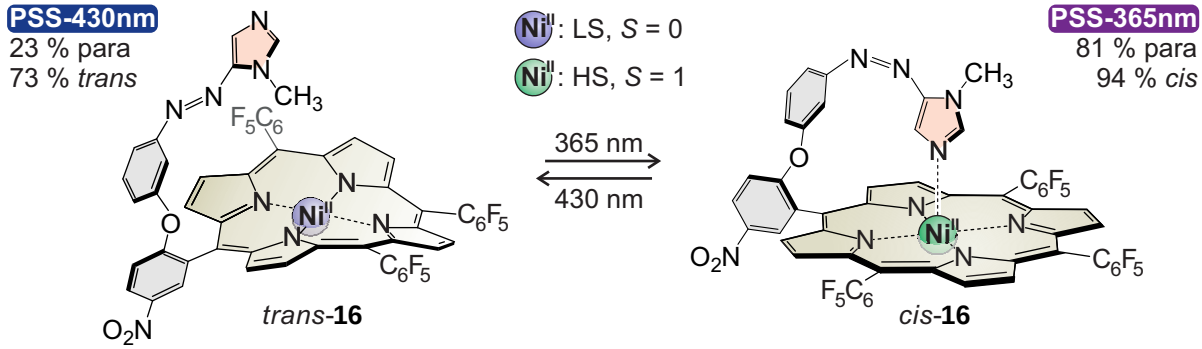

Abb. 4.3: Intramolekularer LD-CISSS mit Imidazol-Diphenylether-*Recordplayer* **16** in Toluol.

ChemPubSoc Europe

DOI: 10.1002/ejoc.201600548

EurJOC European Journal of Organic Chemistry

Full Paper

Spin Switching

Spin State Switching in Solution with an Azoimidazole-Functionalized Nickel(II)-Porphyrin

Gernot Heitmann,[a] Christian Schütt,[a] and Rainer Herges*[a]

Abstract: We herein report the synthesis and switching properties of an azo-1-methylimidazole-functionalized Ni^{2+} porphyrin. Upon irradiation and *cis*/*trans* isomerization of the azo unit, 1-methylimidazole is reversibly coordinated as an axial ligand to the Ni^{2+} porphyrin. Consequently, the Ni^{2+} is switched between a diamagnetic low-spin state (*trans*) and a paramagnetic high-spin state (*cis*) according to the light-driven coordination-induced spin state switching (LD-CISSS) principle. The spin state switching is operable in solution under ambient conditions. The paramagnetic *cis*-species is formed in exceptionally high amounts upon irradiation with UV light (365 nm), whereas an excess of the diamagnetic *trans*-species was obtained upon irradiation with blue light (430 nm).

Introduction

Several transition-metal ions such as Ni^{2+}, Fe^{2+}, Co^{2+}, Mn^{2+}, or Mn^{5+} undergo spin state switching in solution or on surfaces upon changing their coordination number.[1–6] Particularly, nickel has been extensively used for the so-called coordination-induced spin state switching (CISSS).[7–10] Ni^{2+} is diamagnetic (low spin, $S = 0$) in a square-planar coordination environment (coordination number 4) whereas square pyramidal and square bipyramidal Ni^{2+} complexes (coordination number 5 or 6) favor a paramagnetic spin state (high spin, $S = 1$).[11–16] We employed photoresponsive azopyridines to control the coordination and decoordination of axial ligands to Ni^{2+} porphyrins with light.[17,18] The concomitant change of spin state was coined light-driven coordination-induced spin state switching (LD-CISSS) and can be realized with free photodissociable ligands (PDLs) that strongly bind as *trans* isomers, whereas the *cis* isomers are prevented from binding to the Ni^{2+} because of their steric bulk.[17,19] As an alternative to this PDL mechanism, we developed an intramolecular approach in which the azopyridine is covalently tethered to the porphyrin framework ("record player" design). The systems are designed in such a way that the ligand coordinates only in the *cis* configuration.[18,20–22] The intramolecular LD-CISSS process with "record player" molecules proved to be fully reversible in homogeneous solution, under air and at ambient temperature with no side reactions or fatigue. A number of very promising applications for our light responsive spin switches are waiting to be explored, particularly in the fields of responsive ("smart") MRI contrast agents,[23–26] spin labeling and paramagnetic relaxation enhancement (PRE),[27] or magnetic levitation.[28,29] In previous studies, we introduced 1-methyl-5-phenylazoimidazoles as a new class of PDLs. They exhibit exceptionally high association constants to Ni^{2+} and provide excellent *trans*→*cis* photoconversions. Consequently, the carefully designed azoimidazole PDL molecules exhibit high switching efficiencies. The amount of paramagnetic Ni^{2+} species was reversibly changed upon irradiation with two different wavelengths of light (365 and 525 nm) by 70 % (between 20 and 90 %), which makes it the most efficient PDL to date.[30] To exploit their advantageous properties as LD-CISSS ligands within the "record player" concept as well, we now aim at tethering azoimidazole ligands covalently to the Ni^{2+} porphyrin. We recently presented a design study in which we optimized the molecular "record player" design for 1-methylimidazole as the photoresponsive axial ligand.[31] Simply replacing pyridine with 1-methylimidazole gave rise to a rather strained geometry of the coordinated *cis* species and consequently a somewhat lowered spin switching performance. However, an extension of the biphenyl tether (which connects the porphyrin with the switching unit) by a single atom is sufficient for obtaining a relaxed binding situation. A corresponding imidazole "record player" with biaryl thioether tether gave rise to high switching efficiencies, which could also be visualized in MRI. We now present another improved imidazole "record player": in imidazole "record player" **1** a biaryl ether unit tethers the porphyrin and the azo unit (see Figure 1, left). Calculations at the TPSSh/def2TZVP//TPSSh/SVP level of DFT (Turbomole 6.6[32]) predicted that an oxygen atom between the two phenyl groups in the tether would provide an almost perfect preorientation of the *cis* azoimidazole arm to bind to the Ni^{2+} ion. The calculated binding geometry (Ni–N bond length: 2.060 Å, deviation from orthogonal binding: 11.9°), and the high binding energy (ΔH_{calc} = –4.24 kcal/mol) provide evidence that the molecule should be a very efficient spin switch.

Encouraged by these results, we decided to synthesize biphenyl ether "record player" **1** by applying the synthetic strate-

[a] *Otto Diels-Institut für Organische Chemie, Christian-Albrechts-Universität zu Kiel,*
Otto-Hahn-Platz 4, 24098 Kiel, Germany
E-mail: rherges@oc.uni-kiel.de
http://www.otto-diels-institut.de/herges/

Supporting information for this article is available on the WWW under http://dx.doi.org/10.1002/ejoc.201600548.

ChemPubSoc Europe

EurJOC European Journal of Organic Chemistry
Full Paper

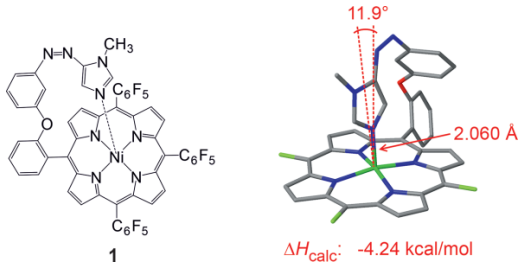

Figure 1. Left: molecular structure of the target "record player" structure **1**. Right: calculated geometry (TPSSh/SVP, for clarity, the pentafluorophenyl substituents are depicted as fluorine substituents) of the coordinated *cis*-conformer of target structure **1** with coordination parameter analysis and ligand binding energy (ΔH_{calc}, TPSSh/def2TZVP//TPSSh/SVP).

gies we developed for the previously reported "record player" derivatives and the azoimidazole-based PDLs.

Results and Discussion

Syntheses

So far, we mainly used mixed-aldehyde porphyrin syntheses to build up "record player" molecules[18,20,22,31] and we decided to pursue this strategy for the biphenyl ether "record player" as well. This so-called "tone arm" approach requires the synthesis of the biphenyl ether azoimidazole moiety as benzaldehyde derivative. We recently presented a convenient synthesis for hitherto unknown 1-methyl-5-phenylazoimidazoles.[30,33] The required 1,5-substitution pattern on the imidazole is obtained through a polar C–N bond formation of a regioselectively lithiated imidazole with an aryldiazonium species, followed by a deprotection–tritylation–methylation sequence. This synthetic route is also suitable for the biphenyl ether "tone arm", which leaves the formation of the biphenyl ether as the major synthetic challenge. We chose the nucleophilic aromatic substitution of a fluorinated or chlorinated benzaldehyde with an appropriate phenol derivative to prepare the ether moiety. In a first attempt, we synthesized the biaryl ether prior to the azo formation. Unfortunately, diazotization of the respective aniline was not successful, so we decided to perform the aryl etherification at a later stage. Diazotization of 3-hydroxyaniline (**2**) gave the respective diazonium salt **3**, which was then reacted with lithiated imidazole **5** prepared in situ, to obtain the double protected azoimidazole **6**. Remarkably, the lithium-mediated C–N bond formation is still feasible and gives good yields with a diazonium salt that bears an acidic group (-OH). Our general synthetic protocol proposes a silyl deprotection in situ with tetrabutylammonium fluoride (TBAF) as the next synthetic step;[30,33] however, because the double protected azoimidazole derivative **6** proved to be easier to handle with respect to purification and solubility, we decided to skip the silyl deprotection and used **6** for the following aryl etherification. The nucleophilic aromatic substitution of 2-fluorobenzaldehyde with **6** did not give the desired product because of insufficient reactivity. Therefore, we used the stronger electrophile, 2-chloro-5-nitrobenzaldehyde, and obtained aryl ether derivative **7** in fairly good yields. Our molecular design did not include a nitro group at the porphyrin's asymmetric *meso*-substituent; however, it should not adversely affect the spin state switching. With the

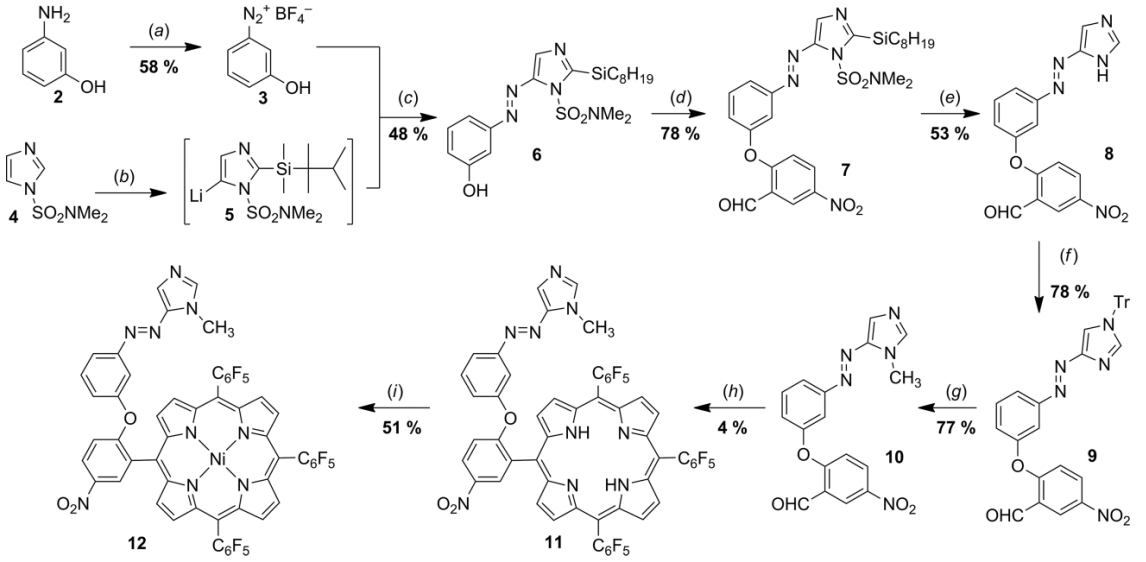

Scheme 1. Synthesis of biphenyl ether "record player" **12**. Reagents and conditions: (a) 1. isopentyl nitrite, HBF_4, EtOH, 0 °C, 20 min, 2. Et_2O, 0 °C, 10 min; (b) 1. *n*BuLi, THF, –78 °C, 45 min; 2. dimethylthexylchlorosilane, THF, –78 °C, 1 h, then room temp., 16 h; 3. *n*BuLi, THF, –78 °C, 40 min; (c) THF, –78 °C, 1 h, then room temp., 6 h; (d) 2-chloro-5-nitrobenzaldehyde, K_2CO_3, DMF, 90 °C, 5 h; (e) HCl/THF (1:5), 70 °C, 90 min; (f) trityl chloride, Et_3N, CH_2Cl_2, room temp., 16 h; (g) 1. MeOTf, CH_2Cl_2, room temp., 16 h; 2. acetone/H_2O (2:1), 40 °C, 4 h; (h) 1. Pentafluorophenyl dipyrromethane,[18] pentafluorobenzaldehyde, $BF_3{\cdot}OEt_2$, CH_3Cl, room temp., 7 h; 2. *p*-chloranil, CH_3Cl, 61 °C, 15 h; (i) $Ni^{II}(acac)_2$, toluene, 111 °C, 2 d.

ChemPubSoc Europe

EurJOC European Journal of Organic Chemistry
Full Paper

biaryl ether in hand, we again followed our general synthetic protocol for imidazole-based PDLs. Global deprotection of **7** gave the unsubstituted azoimidazole **8**, which was then regioselectively tritylated. Trityl-azoimidazole **9** was then methylated and trityl-deprotected in a one-pot procedure, giving the biaryl ether "record player tone arm" **10**. Mixed-aldehyde porphyrin synthesis under Lindsey conditions[34,35] with **10**, pentafluorobenzaldehyde, and pentafluorophenyl dipyrromethane[18] gave azoimidazole-functionalized porphyrin **11**. Subsequent refluxing of **11** with nickel(II)acetylacetonate yielded nitro-substituted biaryl ether "record player" **12** (see Scheme 1).

Switching Experiments

The UV/Vis spectra of diamagnetic and paramagnetic Ni^{2+} porphyrins are very characteristic, making UV/Vis spectroscopy a valuable tool for monitoring the LD-CISSS in "record player" molecules.[18,20] Diamagnetic species exhibit a Soret band at ca. 400 nm, which is bathochromically shifted by about 20 nm upon axial coordination and concomitantly switching to the paramagnetic species. Furthermore, the number of Q-bands (ca. 500–560 nm) is reduced from two to one (see Figure 2, left). UV/Vis switching experiments (see Figure 2, right) with **12** revealed that the paramagnetic *cis* species is formed most effectively upon irradiation with UV light (365–385 nm); however, also irradiation into the *trans* Q-band with green light (ca. 500 nm) gives an excess of the paramagnetic species. The diamagnetic *trans* species is obtained upon irradiation with blue light (ca. 430 nm). The thermal half-life of *cis*-**12** is very high ($t_{1/2}$ = 65.5 d, measured by ^{1}H NMR spectroscopic analysis in [D$_6$]DMSO). Thus, the thermodynamically disfavored *cis*-isomer is stabilized by intramolecular coordination to the Ni^{2+}, which is consistent with our computational studies.

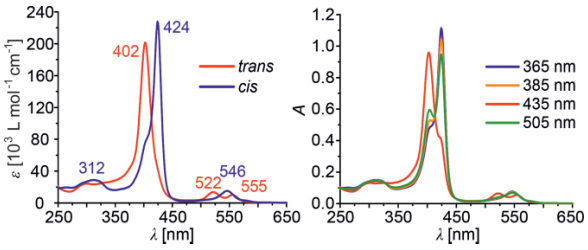

Figure 2. Left: UV/Vis spectra of *trans*-**12** and *cis*-**12** in acetonitrile. Right: UV/Vis switching experiments of **12** in acetonitrile. Irradiation was performed for ca. 1 min with LED light sources.

To quantify to what extent the *cis*-isomer is coordinated, we performed a series of ^{1}H NMR experiments. If completely diamagnetic (100 % *trans*) the pyrrole protons of "record player" **12** resonate at 9 ppm (δ_{dia}). In pure [D$_5$]pyridine, however, the solvent serves as axial ligand and completely converts the Ni^{2+} to the paramagnetic spin state. Consequently, the signal for the pyrrole protons is shifted to 53 ppm (δ_{para}). Given that the coordination and decoordination of the tethered ligand in *cis*-**12** is fast on the NMR timescale, only the time-averaged shift (δ_{cis}, see Figure 3) of the pyrrole protons is observed, which represents the equilibrium between both magnetic conformers. The amount of paramagnetic Ni^{2+} correlates linearly with δ_{cis}. Therefore, the percentage of paramagnetic *cis* isomer (cis_{para}) can be calculated by using Equation (1).[17,20]

$$cis_{para} = \frac{\delta_{cis} - \delta_{dia}}{\delta_{para} - \delta_{dia}} \times 100 = \frac{\delta_{cis} - 9}{53 - 9} \times 100 \quad (1)$$

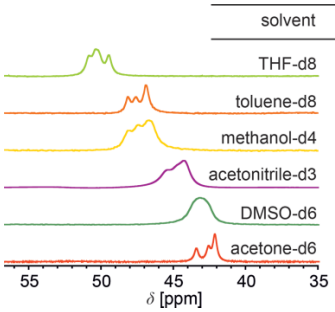

solvent	δ_{cis} / ppm	cis_{para} / %
THF-d8	50	93
toluene-d8	47	86
methanol-d4	47	86
acetonitrile-d3	45	82
DMSO-d6	43	77
acetone-d6	43	77

Figure 3. Solvent-dependent averaged chemical shifts (δ_{cis}) of the pyrrole protons of *cis* record player **12** and calculated amount of coordinated (paramagnetic) *cis* species [cis_{para}, calculated from Equation (1)].

Figure 3 shows the shifts of the pyrrole protons of *cis*-**12** in several solvents. The highest amount of coordinated *cis*-species was found in tetrahydrofuran (THF) (cis_{para} = 93 %), which is in good agreement with the results of the previously reported pyridine record player.[20] THF is a coordinating solvent and therefore stabilizes coordination of 1-methylimidazole by serving as a second axial ligand. The performance in toluene and methanol was also satisfactory (cis_{para} = 86 %); however, the relatively low amount of coordinated species in DMSO (cis_{para} = 77 %) is somewhat surprising. DMSO is also a coordinating solvent, which should stabilize the paramagnetic *cis*-species. The reason for this somewhat low performance in DMSO is not yet understood.

The overall performance of record player **12** can be quantified as switching efficiency (SE), which represents the difference in the amount of paramagnetic species in both switching states. The amount of paramagnetic species (%-para, see Table 1) is determined by the amount of *cis*-isomer (%-*cis*, see Table 1) and the amount of paramagnetic *cis*-species (cis_{para}, see Figure 3). The *cis*/*trans* ratios of the photostationary states at the most efficient irradiation wavelengths (365 nm, 430 nm) were determined by ^{1}H NMR spectroscopic analysis. Irradiation with UV light gives significantly higher amounts of *cis* isomer (ca. 90 %) in all solvents compared with the previously reported pyr-

Table 1. Amount of *cis* isomer (%-*cis*), amount of paramagnetic species (%-para) of record player **12** in both photostationary states (365 nm and 430 nm) and resulting switching efficiency (SE) in different solvents.

Solvent	%-cis_{365nm}	%-cis_{430nm}	%-$para_{365nm}$	%-$para_{430nm}$	SE [%]
THF	90	34	84	32	52
Toluene	94	27	81	23	58
Methanol	88	27	76	23	53
Acetonitrile	90	49	74	40	34
DMSO	90	49	69	38	31
Acetone	89	46	69	35	34

ChemPubSoc Europe

EurJOC European Journal of Organic Chemistry
Full Paper

idine[20] and imidazole[31] "record player" derivatives. Unfortunately, the back-isomerization by irradiation with blue light is somewhat impeded (27–49 % residual *cis*). The highest switching efficiency was found in toluene (SE = 58 %), closely followed by THF and methanol (SE = 52–53 %). The switching efficiencies in acetonitrile, DMSO, and acetone were not satisfactory.

Conclusions

We present a new single molecular spin switch that follows the intramolecular light-driven coordination-induced spin state switching (LD-CISSS) principle. 1-Methylimidazole biphenyl ether "record player" **12** was synthesized in 13 synthetic steps (eight pots) and its switching behavior in several solvents was investigated. In comparison with previously reported pyridine[20] and imidazole[31] derivatives, "record player" **12** provides exceptionally high *trans*→*cis* photoconversion in all solvents (up to 94 %). In toluene, the amount of *cis* species can be photochemically switched between 27 % (PSS at 435 nm) and 94 % (PSS at 365 nm). Consequently, the percentage of paramagnetic Ni^{2+} species switches between 23 and 81 % (switching efficiency 58 %). The switching efficiency of the parent pyridine "record player" in toluene is somewhat lower (<55 %).

Experimental Section

General Remarks: Commercially available solvents and starting materials were used as received. THF was distilled from benzophenone-Na. Dichloromethane was distilled from CaH_2. Column chromatography was carried out by using 0.04–0.063 mm mesh silica gel (Merck). R_f values were determined by thin-layer chromatography on Polygram Sil G/UV_{254} (Macherey–Nagel, 0.2 mm particle size). NMR spectra were measured in Schott Economic NMR tubes by using deuterated solvents (Deuterio). The degree of deuteration is given in parentheses. Chemical shifts are calibrated to residual protonated solvent signals [^{1}H: δ (CD_2Cl_2) = 5.32 ppm, δ (CD_3CN) = 1.94 ppm, δ ([D_6]acetone) = 2.05 ppm; ^{13}C: δ (CD_2Cl_2) = 53.84 ppm, δ (CD_3CN) = 1.32 ppm, δ ([D_6]acetone) = 29.84 ppm; deuteration grade 99.8 %]. Reference for ^{19}F NMR spectra was CCl_3F to which the spectrometer frequency was calibrated. The signal multiplicities are abbreviated as s (singlet), d (doublet), t (triplet), q (quartet), quint (quintet), sept (septet), m (multiplet) and br (broad signal). Measurements were performed with a Bruker DRX 500 (^{1}H NMR: 500 MHz, ^{13}C NMR: 125 MHz, ^{19}F NMR: 470 MHz) and a Bruker AV 600 (^{1}H NMR: 600 MHz, ^{13}C NMR: 150 MHz). The high-resolution (HR) mass spectra were measured with an APEX 3 FT-ICR with a 7.05 T magnet by co. Bruker Daltonics (ESI) or with an AccuTOF by co. Jeol (EI). Low-resolution mass spectra were measured with a MAT 8230 by co. Finnigan (EI/CI), an AccuTOF by co. Jeol (EI), an LCQ Classic by co. Thermo Finnigan (ESI) or an AutoflexSpeed by co. Bruker (MALDI-TOF). Infrared spectra were recorded with a Perkin–Elmer ATR spectrometer with a Golden-Gate-Diamond-ATR A531-G for neat samples. Signal intensities were abbreviated with w (weak), m (medium), s (strong) and vs. (very strong). Broad signals are additionally labeled with br. UV/Vis absorption spectra were recorded with a Perkin–Elmer Lambda-14 spectrophotometer with a Büchi thermostat using quartz cells of 1 cm path length. The amount of carbon, hydrogen, sulfur and nitrogen in a compound was determined with a CHNS-Elementaranalysator Euro EA 3000 Series by co. Euro Vector. Irradiation experiments were performed with LED light sources by co. Sahlmann Photochemical Solutions. Melting points were measured with a Melting Point B-540 by Büchi.

3-Hydroxybenzenediazonium Tetrafluoroborate (3): A solution of 3-hydroxyaniline (**2**) (10.3 g, 94.4 mmol) in ethanol (80 mL) was treated with aqueous fluoroboric acid (30 mL, 50 wt.-% in water) and cooled to 0 °C. Isopentylnitrite (15.1 mL, 112 mmol) was added dropwise over a period of 15 min under vigorous stirring. After another 5 min stirring, diethyl ether (200 mL) was added and the resulting mixture was stirred for 10 min. The deep-red precipitate was isolated, washed once with cold ethanol, three times with diethyl ether, and was dried in vacuo to obtain the desired product (11.3 g, 54.3 mmol, 58 %) which was thermally unstable and therefore used in the following step immediately after preparation. ^{1}H NMR (500 MHz, CD_3CN, 300 K): δ = 8.01 (ddd, ^3J = 8.06, ^4J = 1.99 Hz, ^4J = 0.96 Hz, 1 H, 6-H), 7.82 (t, ^4J = 2.28 Hz, 1 H, 2-H), 7.74 (t, ^3J = 8.30 Hz, 1 H, 5-H), 7.69 (ddd, ^3J = 8.51, ^4J = 2.49 Hz, ^4J = 0.94 Hz, 1 H, 4-H) ppm. ^{13}C NMR (125 MHz, CD_3CN, 300 K): δ = 159.4 (*C*-3), 158.5 (*C*-1), 134.0 (*C*-5), 131.2 (*C*-4), 125.4 (*C*-6), 117.8 (*C*-2) ppm. MS (EI, 70 eV): *m*/*z* (%) = 112.0 (100) [$C_6H_4OHF]^+$. MS (CI, isobutane): *m*/*z* (%) = 113.0 (100) [$C_6H_4OHF + H]^+$. Diazonium tetrafluoroborates undergo a Baltz Schiemann reaction during the vaporization process in EI-MS. Therefore, only the fluorinated derivative is found.

5-(3′-Hydroxyphenylazo)-1-(*N*,*N*-dimethylsulfamoyl)-2-(dimethylhexylsilyl)imidazole (6): 1-(*N*,*N*-Dimethylsulfamoyl)imidazole (**4**)[36] (2.00 g, 11.4 mmol) was dissolved in anhydrous THF (60 mL) and cooled to −78 °C. *n*-Butyllithium in *n*-hexane (4.60 mL, 11.5 mmol) was added dropwise over a period of 15 min. After 30 min stirring at −78 °C, dimethylhexylchlorosilane (2.46 mL, 12.5 mmol) was added. The reaction mixture was stirred at −78 °C for 60 min and at room temperature for 16 h. It was again cooled to −78 °C and *n*-butyllithium in *n*-hexane (5.00 mL, 12.5 mmol) was added dropwise over a period of 10 min. After 30 min stirring at −78 °C, 3-hydroxybenzenediazonium tetrafluoroborate (**3**) (1.66 g, 7.98 mmol) was added as a solid in one portion, and the reaction mixture immediately turned from light-yellow to deep-red. The mixture was stirred at −78 °C for 60 min and at room temperature for 6 h, then half saturated aqueous sodium hydrogen carbonate solution (60 mL) was added, the layers were separated and the aqueous layer was extracted with chloroform (2 × 40 mL). The combined organic layers were dried with magnesium sulfate and the solvents evaporated. The resulting crude product was purified by column chromatography on silica gel (dichloromethane/ethyl acetate, 5 vol.-%; R_f = 0.33). The desired product was obtained as a yellow solid (1.68 g, 3.84 mmol, 48 %), m.p. 123 °C. IR (ATR): $\tilde{\nu}$ = 2929 (w), 1591 (w), 1525 (w), 1462 (m), 1388 (s), 1255 (m), 1237 (m), 1165 (s), 1129 (s), 1105 (m), 985 (s), 850 (m), 814 (vs), 786 (vs), 728 (s), 588 (vs), 554 (vs), 514 (s), 473 (m), 411 (m) cm^{-1}. ^{1}H NMR (500 MHz, CD_2Cl_2, 300 K): δ = 7.52 (s, 1 H, 4-*H*), 7.41 (m, 1 H, 6′-*H*), 7.38 (m, 1 H, 5′-*H*), 7.26 (m, 1 H, 2′-*H*), 6.98 (ddd, ^3J = 7.60, ^4J = 2.55 Hz, ^4J = 1.40 Hz, 1 H, 4′-*H*), 6.14 (s, 1 H, O*H*), 2.90 [s, 6 H, N(CH_3)$_2$], 1.90 [sept, ^3J = 6.83 Hz, 1 H, $CH(CH_3)_2$], 0.98 [s, 6 H, SiC(CH_3)$_2$], 0.82 [d, ^3J = 6.85 Hz, 6 H, CH(CH_3)$_2$], 0.50 [s, 6 H, Si(CH_3)$_2$] ppm. ^{13}C NMR (125 MHz, CD_2Cl_2, 300 K): δ = 160.0 (*C*-2), 157.3 (*C*-3′), 154.8 (*C*-1′), 147.7 (*C*-5), 130.6 (*C*-5′), 119.3 (*C*-4), 119.0 (*C*-4′), 117.0 (*C*-6′), 108.8 (*C*-2′), 38.7 [N(CH_3)$_2$], 34.5 [CH(CH_3)$_2$], 25.9 [SiC(CH_3)$_2$], 22.1 [SiC(CH_3)$_2$], 18.7 [CH(CH_3)$_2$], −0.72 [Si(CH_3)$_2$] ppm. MS (EI): *m*/*z* (%) = 437.2 (5) $[M]^+$, 352.1 (100) $[M - C_6H_{13}]^+$, 330.2 (3) $[M - SO_2N(CH_3)_2 + H]^+$, 295.1 (16) $[M - C_8H_{19}Si + H]^+$, 188.1 (32) $[M - C_8H_{19}Si - SO_2N(CH_3)_2 + 2H]^+$. HRMS (EI): *m*/*z* calcd. for $C_{19}H_{31}N_5O_3SSi$ $[M]^{+\cdot}$ 437.1917; found 437.1902. [$C_{19}H_{31}N_5O_3SSi$ + 0.5Cy] (479.71): calcd. C 55.08, H 7.77, N 14.60, S 6.68; found C 55.38, H 7.90, N 14.70, S 6.67.

ChemPubSoc Europe

EurJOC European Journal of Organic Chemistry
Full Paper

5-[3′-(2′′-Formyl-4′′-nitrophenoxy)phenylazo]-1-(*N*,*N*-dimethylsulfamoyl)-2-(dimethylhexylsilyl)imidazole (7): A solution of **6** (1.51 g, 3.45 mmol) in DMF (35 mL) was treated with potassium carbonate (1.51 g, 10.9 mmol) and 2-chloro-5-nitrobenzaldehyde (832 mg, 4.49 mmol), and the reaction mixture was stirred for 5 h at 90 °C. After cooling to room temperature, the mixture was filtered through diatomaceous earth and washed thoroughly with DMF. The solvent was evaporated and the residue was diluted with ethyl acetate (50 mL). The organic layer was washed with water (3 × 40 mL), dried with magnesium sulfate and the solvents evaporated. Purification by column chromatography on silica gel (cyclohexane/ethyl acetate, 4:1, R_f = 0.13) gave a red solid (1.58 g, 2.70 mmol, 78 %), m.p. 70 °C. IR (ATR): $\tilde{\nu}$ = 3087 (w), 2954 (m), 2870 (w), 2363 (w), 2345 (w), 2325 (w), 1694 (s), 1614 (m), 1579 (m), 1525 (m), 1469 (s), 1419 (m), 1387 (s), 1342 (vs), 1254 (vs), 1240 (vs), 1199 (m), 1158 (vs), 1128 (s), 1104 (s), 978 (s), 960 (m), 941 (m), 920 (m), 876 (m), 843 (s), 815 (vs), 781 (s), 743 (s), 725 (vs), 685 (s), 637 (m), 594 (vs), 578 (s), 557 (s), 516 (s), 456 (s), 414 (s) cm^{-1}. ^{1}H NMR (500 MHz, CD_2Cl_2, 300 K): δ = 10.58 (s, 1 H, *CHO*), 8.76 (d, ^4J = 2.85 Hz, 1 H, 3′′-*H*), 8.34 (dd, ^3J = 9.18, ^4J = 2.88 Hz, 1 H, 5′′-*H*), 7.80 (ddd, ^3J = 8.00, ^4J = 1.75 Hz, ^4J = 0.95 Hz, 1 H, 6′-*H*), 7.65 (t, ^3J = 8.05 Hz, 1 H, 5′-*H*), 7.60 (m, 1 H, 2′-H), 7.56 (s, 1 H, 4-*H*), 7.30 (ddd, ^3J = 8.09, ^4J = 2.44 Hz, ^4J = 0.91 Hz, 1 H, 4′-*H*), 7.01 (d, ^3J = 9.20 Hz, 1 H, 6′′-*H*), 2.88 [s, 6 H, N(*CH*$_3$)$_2$], 1.90 [sept, ^3J = 6.85 Hz, 1 H, *CH*(CH$_3$)$_2$], 0.98 [s, 6 H, SiC(*CH*$_3$)$_2$], 0.82 [d, ^3J = 6.85 Hz, 1 H, CH(*CH*$_3$)$_2$], 0.49 [s, 6 H, Si(*CH*$_3$)$_2$] ppm. ^{13}C NMR (125 MHz, CD_2Cl_2, 300 K): δ = 187.4 (*CHO*), 164.3 (*C*-1′′), 160.9 (*C*-2), 155.5–155.3 (*C*-1′, *C*-3′), 147.7 (*C*-5), 143.6 (*C*-4′′), 131.7 (*C*-5′), 130.6 (*C*-5′′), 126.5 (*C*-2′′), 125.0 (*C*-3′′), 123.3 (*C*-4′), 121.4 (*C*-6′), 120.1 (*C*-4), 117.8 (*C*-6′′), 114.6 (*C*-2′), 38.6 [N(*CH*$_3$)$_2$], 34.6 [*CH*(CH$_3$)$_2$], 25.9 [SiC(*CH*$_3$)$_2$], 22.0 [SiC(*CH*$_3$)$_2$], 18.7 [*CH*(CH$_3$)$_2$], –0.78 [Si(*CH*$_3$)$_2$] ppm. MS (EI): *m*/*z* (%) = 571.2 (3) [M – CH_3]$^{+}$, 501.1 (100) [M – C_6H_{13}]$^{+}$, 444.1 (9) [M – SiC_8H_{19} + H]$^{+}$, 337.1 (22) [M – $SO_2N(CH_3)_2$-SiC_8H_{19} + 2H]$^{\cdot+}$, 108.0 (63) [$SO_2N(CH_3)_2$]$^{\cdot+}$. [$C_{26}H_{34}N_6O_6SSi$ + 0.2Cy] (603.57): calcd. C 54.13, H 6.08, N 13.92, S 5.31; found C 53.99, H 6.08, N 13.73, S 5.22.

4(5)-[3′-(2′′-Formyl-4′′-nitrophenoxy)phenylazo]imidazole (8): Azoimidazole **7** (1.32 g, 2.25 mmol) was dissolved in THF (60 mL) and hydrochloric acid (4 N, 60 mL) was added. The resulting mixture was stirred and heated to reflux for 90 min, then cooled to 0 °C and basified with saturated sodium hydrogen carbonate solution (ca. 260 mL). The mixture was extracted with dichloromethane (3 × 80 mL), and the combined organic layers were dried with magnesium sulfate and the solvents evaporated. The crude product was purified by column chromatography on silica gel (ethyl acetate, R_f = 0.28) to obtain the desired product as a yellow solid (400 mg, 1.19 mmol, 53 %), m.p. 139 °C. IR (ATR): $\tilde{\nu}$ = 3093 (w, br), 2364 (w), 2324 (w), 1691 (m), 1613 (m), 1579 (s), 1520 (m), 1470 (s), 1428 (m), 1398 (m), 1342 (vs), 1237 (vs), 1176 (m), 1108 (s), 1073 (s), 999 (m), 972 (m), 941 (s), 917 (m), 890 (m), 820 (s), 791 (s), 746 (s), 703 (s), 672 (s), 608 (s), 462 (s), 442 (s), 412 (m) cm^{-1}. ^{1}H NMR (600 MHz, CD_2Cl_2, 300 K): δ = 10.60 (s, 1 H, -*CHO*), 10.02 (br. s, 1 H, -N*H*), 8.76 (d, ^4J = 2.88 Hz, 1 H, 3′′-*H*), 8.33 (dd, ^3J = 9.18, ^4J = 2.88 Hz, 1 H, 5′′-*H*), 7.85 (d, ^3J = 7.68 Hz, 1 H, 6′-*H*), 7.84 [br. s, 1 H, 5(4)-*H*], 7.74 (s, 1 H, 2-*H*), 7.67–7.62 (m, 2 H, 2′-*H*, 5′-*H*), 7.29–7.26 (m, 1 H, 4′-*H*), 7.03 (d, ^3J = 9.18 Hz, 1 H, 6′′-*H*) ppm. ^{13}C NMR (150 MHz, CD_2Cl_2, 300 K): δ = 187.5 (-*CHO*), 164.5 (*C*-1′′), 155.4 (*C*-3′), 154.6 (*C*-1′, identified by HMBC), 143.5 (*C*-2′′), 136.9 (*C*-2, identified by HSQC), 131.5 (*C*-5′), 130.6 (*C*-5′′), 126.4 (*C*-4′′), 124.9 (*C*-3′′), 122.7 (*C*-4′), 122.1 (*C*-6′), 117.8 (*C*-6′′), 113.4 (*C*-2′) ppm. *C*-4 and *C*-5 could not be assigned due to their low signal intensity. MS (EI): *m*/*z* (%) = 337.1 (49) [M]$^{\cdot+}$, 196.1 (28) [PhOPhCHO]$^{\cdot+}$, 171.1 (9) [M – $OPhCHONO_2$]$^{\cdot+}$, 95.0 (100) [$C_3H_3N_4$]$^{\cdot+}$. HRMS (EI): *m*/*z* [M]$^{\cdot+}$ calcd. for $C_{16}H_{11}N_5O_4$, 337.0811; found 337.0800. [$C_{16}H_{11}N_5O_4$ + 0.1EtOAc] (346.10): calcd. C 56.91, H 3.44, N 20.23; found C 56.90, H 3.61, N 20.03.

4-[3′-(2′′-Formyl-4′′-nitrophenoxy)phenylazo]-1-(triphenylmethyl)imidazole (9): 4(5)-[3′-(2′′-Formyl-4′′-nitrophenoxy)phenylazo]imidazole (**8**) (417 mg, 1.24 mmol) was suspended in dichloromethane (20 mL). Triethylamine (223 µL, 1.61 mmol) and triphenylchloromethane (379 mg, 1.36 mmol) were added subsequently and the resulting mixture was stirred at room temperature overnight. The reaction mixture was washed with water (3 × 30 mL), and the organic layer was dried with magnesium sulfate and the solvents evaporated. The crude product was purified by column chromatography on silica gel (cylcohexane/ethyl acetate, 7:3, R_f = 0.19) to obtain the desired product as a yellow solid (558 mg, 963 µmol, 78 %), m.p. 102 °C. IR (ATR): $\tilde{\nu}$ = 3063 (w), 2925 (m), 2850 (w), 2324 (w), 2107 (w), 1732 (m), 1693 (m), 1613 (m), 1579 (m), 1525 (m), 1469 (m), 1446 (m), 1344 (s), 1237 (vs), 1074 (s), 1001 (m), 977 (m), 746 (s), 699 (s), 640 (m), 606 (m), 503 (m), 458 (m) cm^{-1}. ^{1}H NMR (600 MHz, [D_6]acetone, 300 K): δ = 10.60 (s, 1 H, -*CHO*), 8.65 (d, ^4J = 2.88 Hz, 1 H, 3′′-*H*), 8.44 (dd, ^3J = 9.18, ^4J = 2.88 Hz, 1 H, 5′′-*H*), 7.81 (d, ^3J = 8.16 Hz, 1 H, 6′-*H*), 7.71 (t, ^3J = 8.01 Hz, 1 H, 5′-*H*), 7.65 (t, ^4J = 2.01 Hz, 1 H, 2′-*H*), 7.59 (d, ^4J = 1.26 Hz, 1 H, 2-*H*), 7.55 (d, ^4J = 1.32 Hz, 1 H, 5-*H*), 7.49–7.39 (m, 10 H, *m*-Tr-*H*, *p*-Tr-*H*, 4′-*H*), 7.28–7.24 (m, 6 H, *o*-Tr-*H*), 7.20 (d, ^3J = 9.18 Hz, 1 H, 6′′-*H*) ppm. ^{13}C NMR (150 MHz, [D_6]acetone, 300 K): δ = 187.9 (-CHO), 165.1 (*C*-1′′), 156.3 (*C*-3′), 155.9 (*C*-1′), 154.6 (*C*-4), 144.0 (*C*-2′′), 142.9 (*C*-*i*-Tr), 140.2 (*C*-2), 132.1 (*C*-5′), 131.2 (*C*-5′′), 130.5 (*C*-*o*-Tr), 129.3 (*C*-*m*-Tr, *C*-*p*-Tr), 127.0 (*C*-4′′), 124.6 (*C*-3′′), 123.2 (*C*-4′), 122.3 (*C*-6′), 120.5 (*C*-5), 118.9 (*C*-6′′), 113.5 (*C*-2′), 77.0 (-CPh_3) ppm. MS (ESI-TOF, methanol): *m*/*z* (%) = 633.9 (41) [M + MeOH + Na]$^{+}$, 618.0 (6) [M + K]$^{+}$, 601.9 (56) [M + Na]$^{+}$, 243.1 (100) [CPh_3]$^{+}$. [$C_{35}H_{25}N_5O_4$ + 0.75Cy] (663.28): calcd. C 73.81, H 5.33, N 10.90; found C 74.15, H 5.52, N 11.22.

5-[3′-(2′′-Formyl-4′′-nitrophenoxy)phenylazo]-1-methylimidazole (10): The tritylated azoimidazole **9** (669 mg, 1.15 mmol) was dissolved in anhydrous dichloromethane (15 mL) and methyltriflate (196 µL, 1.73 mmol) was added. The resulting mixture was stirred at room temperature for 16 h. Acetone/water (2:1, 30 mL) was added and the mixture was stirred at 40 °C for 4 h. Saturated sodium hydrogen carbonate solution (5 mL) was added, the layers were separated and the aqueous layer was extracted with dichloromethane (2 × 20 mL). The combined organic layers were dried with magnesium sulfate and evaporated to dryness. Purification by column chromatography on silica gel (ethyl acetate, R_f = 0.14) gave an orange solid (311 mg, 886 µmol, 77 %), m.p. 160 °C. IR (ATR): $\tilde{\nu}$ = 3104 (w), 1677 (s), 1610 (m), 1578 (s), 1509 (s), 1467 (s), 1338 (vs), 1257 (vs), 1106 (s), 1071 (s), 941 (s), 924 (s), 834 (s), 797 (s), 747 (vs), 686 (s), 640 (s), 604 (s), 544 (m), 464 (s), 425 (s) cm^{-1}. ^{1}H NMR (600 MHz, [D_6]acetone, 298 K): δ = 10.61 (s, 1 H, -*CHO*), 8.66 (d, ^4J = 2.94 Hz, 1 H, 3′′-*H*), 8.46 (dd, ^3J = 9.18, ^4J = 2.94 Hz, 1 H, 5′′-*H*), 7.88–7.84 (m, 2 H, 2-*H*, 6′-*H*), 7.76 (t, ^4J = 2.10 Hz, 1 H, 2′-*H*), 7.74 (t, ^3J = 8.01 Hz, 1 H, 5′-*H*), 7.53 (s, 1 H, 4-*H*), 7.45 (ddd, ^3J = 8.04, ^4J = 2.34 Hz, ^4J = 0.66 Hz, 1 H, 4′-*H*), 7.22 (d, ^3J = 9.18 Hz, 1 H, 6′′-*H*), 4.00 (s, 3 H, -CH_3) ppm. ^{13}C NMR (150 MHz, [D_6]acetone, 298 K): δ = 188.0 (-CHO), 165.0 (*C*-1′′), 156.3 (*C*-3′), 156.0 (*C*-1′), 146.1 (*C*-5), 144.0 (*C*-2′′), 143.1 (*C*-2), 132.2 (*C*-5′), 131.3 (*C*-5′′), 127.0 (*C*-4′′), 125.1 (*C*-4), 124.6 (*C*-3′′), 123.3 (*C*-4′), 121.9 (*C*-6′), 118.8 (*C*-6′′), 113.9 (*C*-2′), 32.8 (-CH_3) ppm. MS (EI): *m*/*z* (%) = 351.1 (69) [M]$^{+}$, 196.1 (29) [PhOPhCHO]$^{+}$, 109.1 (100) [$C_4H_5N_4$]$^{+}$. HRMS (EI): *m*/*z* calcd. for $C_{17}H_{13}N_5O_4$ [M]$^{+}$ 351.0967; found 351.0958. UV/Vis (acetonitrile): λ_{max} (lg ε) = 235 (4.341), 363 (4.337) nm. [$C_{17}H_{13}N_5O_4$ + 0.2EtOAc] (368.94): calcd. C 57.95, H 3.99, N 18.98; found C 57.82, H 3.97, N 19.18.

ChemPubSoc Europe

EurJOC European Journal of Organic Chemistry
Full Paper

5-{4′-Nitrophenyl-2′-[phenoxy-3′′-(azo-*N*-methylimidazole)]}-10,15,20-tris(pentafluorophenyl)-porphyrin (11): To a solution of biphenyl ether "tone arm" **10** (535 mg, 1.52 mmol) and pentafluorobenzaldehyde (298 mg, 1.52 mmol) in chloroform (200 mL) was added borontrifluoride diethyl etherate (308 µL, 2.43 mmol) under an atmosphere of nitrogen. Pentafluorophenyl dipyrromethane[18] (949 mg, 3.04 mmol) in chloroform (20 mL) was added to the stirred solution over 1 h at room temperature. Stirring under nitrogen at room temperature was continued for an additional 6 h and the solution turned from dark-red to black. Chloranil (783 mg, 3.20 mmol) was then added and the solution was stirred and heated to reflux for 15 h. Triethylamine (1 mL) was added and stirring was continued for 45 min. The reaction mixture was filtered over diatomaceous earth and the solvents were evaporated in vacuo. The crude product was filtered over silica gel (dichloromethane). Subsequent column chromatography on silica gel (cyclohexane/ethyl acetate, 6:4 → 1:1, R_f = 0.19) gave a purple solid (77.0 mg, 68.2 µmol, 4 %) which was deep-red in solution, m.p. 226 °C. IR (ATR): $\tilde{\nu}$ = 3316 (w), 2923 (w), 2860 (w), 1729 (w), 1702 (w), 1650 (w), 1575 (w), 1517 (s), 1495 (vs), 1436 (m), 1403 (m), 1342 (s), 1316 (m), 1252 (m), 1143 (m), 1115 (m), 1075 (m), 1043 (m), 986 (vs), 936 (m), 917 (vs), 803 (s), 756 (s), 738 (s), 527 (m) cm^{-1}. ^{1}H NMR (600 MHz, [D$_6$]acetone, 300 K): δ = 9.80–8.85 (m, 9 H, pyrrole-*H*, 6′-*H*), 8.79 (dd, ^3J = 9.39, ^4J = 2.85 Hz, 1 H, 4′-*H*), 7.75 (s, 1 H, 2′′′-*H*), 7.63 (d, ^3J = 9.36 Hz, 1 H, 3′-*H*), 7.41–7.37 (m, 1 H, 4′′-*H*), 7.35 (s, 1 H, 4′′′-*H*), 7.34 (t, ^4J = 2.04 Hz, 1 H, 2′′-*H*), 7.27 (t, ^3J = 8.10 Hz, 1 H, 5′′-*H*), 7.07 (ddd, ^3J = 8.27, ^4J = 2.33 Hz, ^4J = 0.77 Hz, 1 H, 6′′-*H*), 3.79 (s, 3 H, C*H*$_3$), –2.86 (s, 2 H, N*H*) ppm. ^{19}F NMR (470 MHz, [D$_6$]acetone, 300 K): δ = –139.78 (dd, ^3J = 23.9, ^4J = 7.32 Hz, 2 F, A-*o*-*F*), –139.83 to –140.06 (m, 4 F, B-*o*-*F*, B-*o*′-*F*, A-*o*′-*F*), –155.51 to –155.70 (m, 3 F, A-*p*-F, B-*p*-F), –164.49 to –164.71 (m, 6 F, B-*m*-F, B-*m*′-F, A-*m*-F, A-*m*′-F) ppm. MS (MALDI-TOF): *m*/*z* (%) = 1152.7 (8) [M + Na]$^+$, 1130.7 (100) [M + H]$^+$, 1114.7 [M – CH$_3$]$^+$. Due to the small amount of substance and the large number of fluorine atoms, no elemental analysis was performed.

5-{4′-Nitrophenyl-2′-[phenoxy-3′′-(azo-*N*-methylimidazole)]}-10,15,20-tris(pentafluorophenyl)-nickel(II)porphyrin (12): The metal-free biphenyl ether record player **11** (50.0 mg, 44.3 µmol) was dissolved in toluene (55 mL) and nickel(II) acetylacetonate (114 mg, 443 µmol) was added. The resulting mixture was stirred and heated to reflux for 2 d, after which time no starting material was detectable by MALDI-TOF-MS. The reaction mixture was evaporated to dryness and the crude product was purified by column chromatography on silica gel [chloroform, R_f = 0.38 (*cis*) and 0.24 (*trans*)]. The product was obtained as a purple solid (27.0 mg, 22.8 µmol, 51 %) which was deep-red in solution, m.p. 230 °C. IR (ATR): $\tilde{\nu}$ = 2919 (w), 2852 (w), 1980 (w), 1720 (w), 1652 (w), 1575 (w), 1518 (s), 1490 (s), 1439 (m), 1341 (s), 1311 (m), 1253 (m), 1161 (m), 1142 (m), 1112 (m), 1073 (m), 1052 (m), 984 (vs), 959 (m), 937 (s), 918 (s), 848 (m), 800 (m), 758 (s), 750 (s), 706 (m), 685 (m), 529 (m), 408 (m) cm^{-1}. ^{1}H NMR (500 MHz, [D$_6$]acetone, 300 K): δ = 9.41 (br. s, 2 H, pyrrole-*H*), 9.37 (br. s, 6 H, pyrrole-*H*), 9.06 (d, ^4J = 2.80 Hz, 1 H, 6′-*H*), 8.72 (dd, ^3J = 9.28, ^4J = 2.83 Hz, 1 H, 4′-*H*), 7.94 (s, 1 H, 2′′′-*H*), 7.63 (s, 1 H, 4′′′-*H*), 7.55 (d, ^3J = 9.25 Hz, 1 H, 3′-*H*), 7.40 (ddd, ^3J = 7.91, ^4J = 1.73 Hz, ^4J = 1.03 Hz, 1 H, 4′′-*H*), 7.31–7.27 (m, 2 H, 2′′-*H*, 5′′-*H*), 7.06 (ddd, ^3J = 8.24, ^4J = 2.29 Hz, ^4J = 0.86 Hz, 1 H, 6′′-*H*), 3.78 (s, 3 H, C*H*$_3$) ppm. ^{19}F NMR (470 MHz, [D$_6$]acetone, 300 K): δ = –139.76 to –139.95 (m, 3 F, A-*o*-F, B-*o*-F), –139.96 to –140.12 (m, 3 F, B-*o*′-F, A-*o*′-F), –155.56 to –155.75 (m, 3 F, A-*p*-F, B-*p*-F), –164.34 to –164.60 (m, 6 F, B-*m*-F, B-*m*′-F, A-*m*-F, A-*m*′-F) ppm. HRMS (ESI, EtOH, 0.1 % HCOOH): *m*/*z* [M + H]$^+$ calcd. for [C$_{54}$H$_{20}$F$_{15}$N$_9$O$_3$Ni + H], 1186.087; found 1186.090. UV/Vis (acetonitrile): λ_{max} (lg ε) = 300 (4.369), 402 (5.304), 522 (4.112), 555 (3.990) nm. Due to the small amount of substance and the large number of fluorine atoms, no elemental analysis was performed.

Acknowledgments

The authors gratefully acknowledge financial support from the Deutsche Forschungsgemeinschaft (DFG) via the collaborative research center 677 (SFB677, Function by Switching).

Keywords: Spin crossover · Photochromism · Azo compounds · Porphyrinoids · Nickel · Ligand effects

[1] C. Wäckerlin, K. Tarafder, J. Girovsky, J. Nowakowski, T. Hählen, A. Shchyrba, D. Siewert, A. Kleibert, F. Nolting, P. M. Oppeneer, T. A. Jung, N. Ballav, *Angew. Chem. Int. Ed.* **2013**, *52*, 4568–4571; *Angew. Chem.* **2013**, *125*, 4666.
[2] C. Wäckerlin, K. Tarafder, J. Girovsky, J. Nowakowski, T. Hählen, A. Shchyrba, D. Siewert, A. Kleibert, F. Nolting, P. M. Oppeneer, T. A. Jung, N. Ballav, *Angew. Chem. Int. Ed.* **2013**, *52*, 4568; *Angew. Chem.* **2013**, *125*, 4666–4669.
[3] A. Petuker, K. Merz, C. Merten, U.-P. Apfel, *Inorg. Chem.* **2016**, *55*, 1183–1191.
[4] H. Kropp, A. Scheurer, F. W. Heinemann, J. Bendix, K. Meyer, *Inorg. Chem.* **2015**, *54*, 3562–3572.
[5] C. Wäckerlin, D. Chylarecka, A. Kleibert, K. Müller, C. Iacovita, F. Nolting, T. A. Jung, N. Ballav, *Nat. Commun.* **2010**, *1*, 61.
[6] C. Wäckerlin, K. Tarafder, D. Siewert, J. Girovsky, T. Hahlen, C. Iacovita, A. Kleibert, F. Nolting, T. A. Jung, P. M. Oppeneer, N. Ballav, *Chem. Sci.* **2012**, *3*, 3154–3160.
[7] C. Lochenie, K. G. Wagner, M. Karg, B. Weber, *J. Mater. Chem. C* **2015**, *3*, 7925–7935.
[8] M. Dommaschk, V. Thoms, C. Schütt, C. Näther, R. Puttreddy, K. Rissanen, R. Herges, *Inorg. Chem.* **2015**, *54*, 9390–9392.
[9] M. Dommaschk, F. Gutzeit, S. Boretius, R. Haag, R. Herges, *Chem. Commun.* **2014**, *50*, 12476–12478.
[10] S. Thies, C. Bornholdt, F. Köhler, F. D. Sönnichsen, C. Näther, F. Tuczek, R. Herges, *Chem. Eur. J.* **2010**, *16*, 10074–10083.
[11] W. S. Caughey, R. M. Deal, B. D. McLees, J. O. Alben, *J. Am. Chem. Soc.* **1962**, *84*, 1735–1736.
[12] W. S. Caughey, W. Y. Fujimoto, B. P. Johnson, *Biochemistry* **1966**, *5*, 3830–3843.
[13] S. J. Cole, G. C. Curthoys, E. A. Magnusson, J. N. Phillips, *Inorg. Chem.* **1972**, *11*, 1024–1028.
[14] D. Kim, Y. O. Su, T. G. Spiro, *Inorg. Chem.* **1986**, *25*, 3988–3993.
[15] B. D. McLees, W. S. Caughey, *Biochemistry* **1968**, *7*, 642–652.
[16] Y. Song, R. E. Haddad, S.-L. Jia, S. Hok, M. M. Olmstead, D. J. Nurco, N. E. Schore, J. Zhang, J.-G. Ma, K. M. Smith, S. Gazeau, J. Pécaut, J.-C. Marchon, C. J. Medforth, J. A. Shelnutt, *J. Am. Chem. Soc.* **2005**, *127*, 1179–1192.
[17] S. Thies, H. Sell, C. Schütt, C. Bornholdt, C. Näther, F. Tuczek, R. Herges, *J. Am. Chem. Soc.* **2011**, *133*, 16243–16250.
[18] S. Venkataramani, U. Jana, M. Dommaschk, F. D. Sönnichsen, F. Tuczek, R. Herges, *Science* **2011**, *331*, 445–448.
[19] S. Thies, H. Sell, C. Bornholdt, C. Schütt, F. Köhler, F. Tuczek, R. Herges, *Chem. Eur. J.* **2012**, *18*, 16358–16368.
[20] M. Dommaschk, C. Schütt, S. Venkataramani, U. Jana, C. Näther, F. D. Sönnichsen, R. Herges, *Dalton Trans.* **2014**, *43*, 17395–17405.
[21] M. Dommaschk, C. Näther, R. Herges, *J. Org. Chem.* **2015**, *80*, 8496–8500.
[22] M. Dommaschk, M. Peters, F. Gutzeit, C. Schütt, C. Näther, F. D. Sönnichsen, S. Tiwari, C. Riedel, S. Boretius, R. Herges, *J. Am. Chem. Soc.* **2015**, *137*, 7552–7555.
[23] R. Herges, O. Jansen, F. Tuczek, S. Venkatamarani, "Molecular Switch", Patent WO 2012022299 A1, Feb 23, **2012**.
[24] R. Herges, O. Jansen, F. Tuczek, S. Venkatamarani, "Photosensitive metal porphyrin complexes with pendant photoisomerizable chelate arm as photochromic molecular switches undergoing photoinduced spin transition", Patent DE 102010034 A1, Feb 16, **2012**.

ChemPubSoc Europe

EurJOC European Journal of Organic Chemistry
Full Paper

[25] R. Herges, *Nachr. Chem.* **2011**, *59*, 817–821.
[26] G.-L. Davies, I. Kramberger, J. J. Davis, *Chem. Commun.* **2013**, *49*, 9704–9721.
[27] G. E. Fanucci, D. S. Cafiso, *Curr. Opin. Struct. Biol.* **2006**, *16*, 644–653.
[28] K. A. Mirica, F. Ilievski, A. K. Ellerbee, S. S. Shevkoplyas, G. M. Whitesides, *Adv. Mater.* **2011**, *23*, 4134–4140.
[29] K. A. Mirica, S. S. Shevkoplyas, S. T. Phillips, M. Gupta, G. M. Whitesides, *J. Am. Chem. Soc.* **2009**, *131*, 10049–10058.
[30] C. Schütt, G. Heitmann, T. Wendler, B. Krahwinkel, R. Herges, *J. Org. Chem.* **2016**, *81*, 1206–1215.
[31] G. Heitmann, C Schütt, J. Gröbner, L. Huber, R. Herges, *Dalton Trans.* **2016**, DOI: 10.1039/C6DT01727D.
[32] TURBOMOLE V6.6 **2014**, a development of the University of Karlsruhe, Germany and Forschungszentrum Karlsruhe, GmbH, **1989**–**2007**, TURBOMOLE GmbH, since **2007**; available from http://www.turbomole.com.
[33] T. Wendler, C. Schütt, C. Näther, R. Herges, *J. Org. Chem.* **2012**, *77*, 3284–3287.
[34] J. S. Lindsey, R. W. Wagner, *J. Org. Chem.* **1989**, *54*, 828–836.
[35] J. S. Lindsey, I. C. Schreiman, H. C. Hsu, P. C. Kearney, A. M. Marguerettaz, *J. Org. Chem.* **1987**, *52*, 827–836.
[36] D. J. Chadwick, R. I. Ngochindo, *J. Chem. Soc. Perkin Trans. 1* **1984**, 481–486.

Received: May 2, 2016
Published Online: July 6, 2016

5 Syntheseoptimierung für *Recordplayer*-Moleküle

Porphyrine stellen mit ihren strukturellen, physikalischen und chemischen Eigenschaften äußerst begehrte chemische Strukturen dar, sind aber bei der Darstellung funktioneller Moleküle und Materialien gleichzeitig häufig ein synthetischer Flaschenhals. Während natürliche Porphyrinderivate ausschließlich in den β-Positionen funktionalisiert sind, findet man unter den synthetischen Derivaten häufiger die *meso*-substituierten Varianten, da sich diese direkt aus Pyrrol und den entsprechenden Aldehyden darstellen lassen. Seit den frühen Arbeiten von ROTHEMUND[160,161] haben sich einige effiziente Synthesemethoden zur Darstellung von *meso*-substituierten Porphyrinen etabliert. Symmetrisch funktionalisierte Tetraarylporphyrine können in guten Ausbeuten nach den Methoden von ADLER und LONGO[162] sowie von LINDSEY[163,164] erhalten werden. Deutlich schwieriger ist die Synthese von asymmetrisch funktionalisierten Derivaten mit zwei oder mehr unterschiedlichen *meso*-Substituenten, jedoch sind gerade diese Strukturen für neue Anwendungsgebiete, beispielsweise im Bereich der nicht-linearen Optik[165] oder der Photosensibilisierung,[166] hoch gefragt. Prinzipiell gibt es drei verschiedene Ansätze, die für die Darstellung asymmetrisch substituierter Porphyrine verfolgt werden können: (a) die gemischte Kondensation, (b) die Totalsynthese und (c) die Derivatisierung von zuvor aufgebauten Porphyrin-Vorstufen (siehe Abb. 5.1).[167]

Bisher wurden *Recordplayer*-Moleküle überwiegend in gemischten Kondensationsreaktionen hergestellt.[117,138,168,169] Bei diesem Ansatz werden die unterschiedlichen *meso*-Substituenten in Form ihrer Aldehyd-Derivate im statistischen Verhältnis mit Pyrrol zur Reaktion gebracht. Im Falle der *Recordplayer*-Moleküle werden die zuvor vollständig aufgebaute Schalteinheit und Pentafluorbenzaldehyd im Verhältnis 3:1 eingesetzt. Zwei Pentafluorbenzaldehyd-Einheiten werden als Dipyrromethan-Derivat verwendet, um die Zahl möglicher Produkte von sechs auf drei zu reduzieren. Dennoch ist dieser statistische Syntheseansatz leider sehr unökonomisch. Zum einen handelt es sich um eine nahezu vollständig lineare Synthesesequenz, welche eine sehr geringe Gesamtausbeute ergibt und für die Darstellung neuer Derivate meist komplett durchlaufen werden muss. Zum anderen wird durch die mit schlechten Ausbeuten verbundene Porphyrinsynthese als vorletztem Schritt sehr viel von zuvor aufwendig synthetisiertem Material vernichtet. Wenn *Recordplayer*-Moleküle zukünftig als MRT-Kontrastmittel medizinische Anwendung finden sollen, muss ihre Synthese hinsichtlich Zeit- und Kostenaufwand deutlich

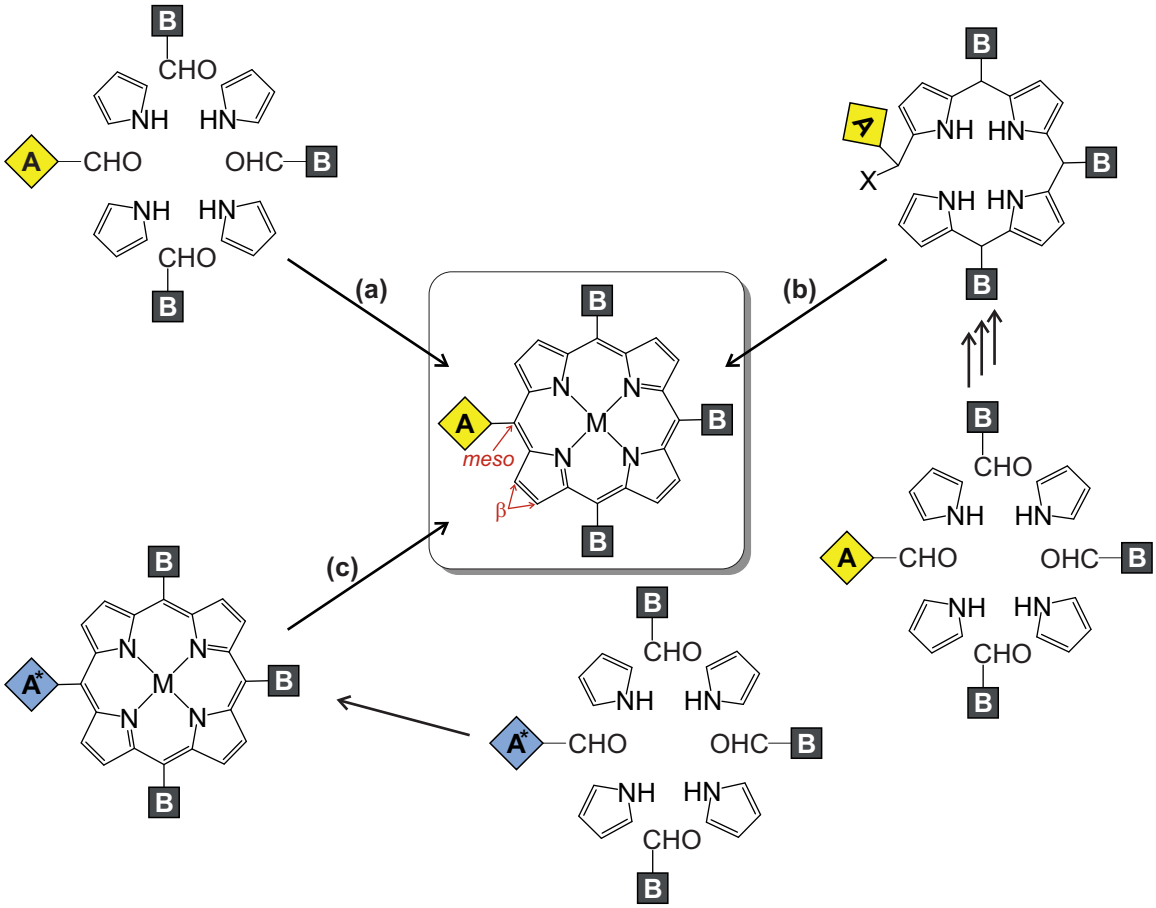

Abb. 5.1: Syntheseansätze für asymmetrisch funktionalisierte Porphyrine am Beispiel eines *meso*-AB_3-substituierten Porphyrins (z.B. *Recordplayer*-Moleküle). (a) Bei der gemischten Kondensation werden die substituierten Aldehyde im statistischen Verhältnis mit Pyrrol zur Reaktion gebracht. (b) Für den totalsynthetischen Ansatz wird der Makrozyklus über mehrere Schritte rational aufgebaut. (c) Der Precursor-Ansatz geht von einem leicht zugänglichen Vorläufer-Porphyrin aus, welches post-synthetisch mit der gewünschten Funktionalität versehen wird.

optimiert werden. Der totalsynthetische Ansatz, in dem der Makrozyklus über mehrere Syntheseschritte gezielt aufgebaut wird, ist für eine signifikante Verbesserung des synthetischen Zugangs nicht geeignet. Die Zahl der Nebenprodukte könnte gegenüber des statistischen Ansatzes zwar erheblich verringert und die Aufreinigung deutlich erleichtert werden. Allerdings ist aufgrund der erhöhten Zahl an Syntheseschritten ein synthetischer Mehraufwand zu verzeichnen und eine Verbesserung der Gesamtausbeute nicht zwangsläufig gegeben. Deutlich erfolgversprechender ist die Verwendung eines geeigneten Vorläufer-Porphyrins, welches idealerweise im letzten Syntheseschritt mit der gewünschten Schalteinheit versehen werden kann.

5.1 Modular Synthetic Route to Monofunctionalized Porphyrin Architectures.

Gernot Heitmann, Marcel Dommaschk, Roland Löw und Rainer Herges

Org. Lett. **2016**, *18*, 5228-5231.
http://dx.doi.org/10.1021/acs.orglett.6b02507

Zusammenfassung

In dieser Studie wird die effiziente Synthese des mono-borylierten Ni(II)porphyrins **20** und dessen Anwendung als modularer Baustein einer konvergenten Syntheseroute für *Recordplayer*-Moleküle beschrieben (siehe Abb 5.2). Porphyrin **20** konnte in drei Syntheseschritten in einer Gesamtausbeute von 22 % erhalten werden. Dabei wurde zunächst nach der Methode von LINDSEY das metallfreie Porphyrin **19** direkt aus den kommerziell erhältlichen Edukten Pyrrol, Pentafluorbenzaldehyd (**18**) und 2-Formylphenylboronsäurepinakolester (**17**) synthetisiert und dieses anschließend mit Ni(II)acetylacetonat metalliert. Porphyrin **20** konnte trotz der mit vielen Neben- und Zersetzungsprodukten verbundenen Porphyrinsynthese säulenchromatographisch exzellent aufgereinigt werden und ist bei Raumtemperatur und in Gegenwart von Sauerstoff sehr gut lagerfähig. Mittels Suzuki-Kreuzkupplungsreaktionen konnte **20** mit 10 verschiedenen halogenierten Azoverbindungen umgesetzt werden, wobei stets gute bis exzellente Ausbeuten erhalten wurden. Die Verwendung von bromierten Phenylazopyridinen und -imidazolen ergab 7 unterschiedliche *Recordplayer*-Moleküle, von denen vier (u.a. **21**-**23**, siehe Abb. 5.2) bisher unbekannt waren. Für die drei bereits bekannten Recordplayer-Derivate (u.a. **14**) wurden Gesamtausbeuten erhalten, welche mindestens eine Größenordnung über denen der konventionellen, linearen Route lagen. Die konvergente Synthese mit Porphyrin **20** als Schlüsselbaustein stellt unter den bislang bekannten Synthesewegen den mit Abstand effizientesten Zugang zu *Recordplayer*-Molekülen dar.

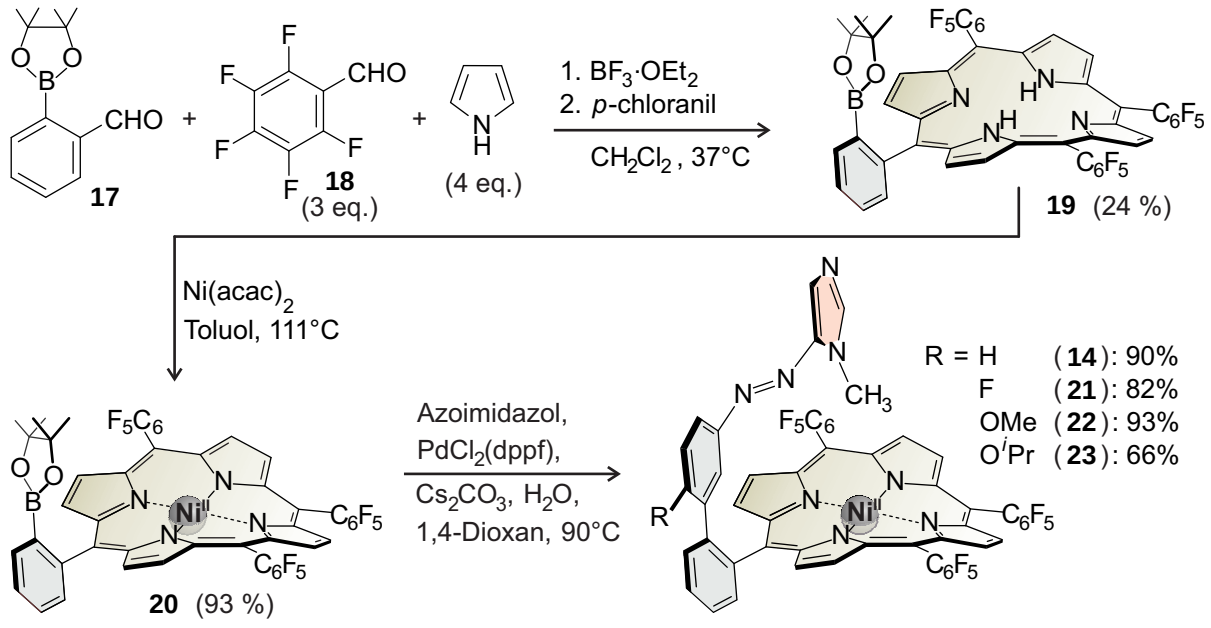

Abb. 5.2: Effiziente Synthese des borylierten Porphyrin-Precursors **20** und seine Anwendung in Suzuki-Kreuzkupplungsreaktionen, beispielhaft gezeigt mit Phenylazoimidazolen. Die Imidazol-*Recordplayer* **14** und **21**-**23** konnten in guten bis sehr guten Ausbeuten erhalten werden.

Organic LETTERS

Letter

pubs.acs.org/OrgLett

Modular Synthetic Route to Monofunctionalized Porphyrin Architectures

Gernot Heitmann, Marcel Dommaschk, Roland Löw, and Rainer Herges*

Otto Diels-Institute for Organic Chemistry, University of Kiel, Otto-Hahn-Platz 4, Kiel D-24119, Germany

Supporting Information

ABSTRACT: The synthesis of a borylated Ni^{2+} porphyrin and its application as a versatile precursor for building up functional *ortho*-substituted tetraaryl porphyrin architectures is reported. This precursor porphyrin provides the basis for efficient modular syntheses of porphyrin compounds with covalently attached axial ligands which are important as enzyme model complexes, electron transfer dyads, and many other applications. In the present study, the precursor porphyrin was used for the synthesis of molecular spin switches which previously showed high potential as photoresponsive contrast agents for magnetic resonance imaging.

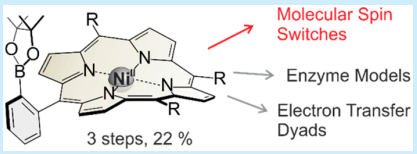

Porphyrins and metalloporphyrins are an important class of macrocyclic compounds and are extensively studied. These tetrapyrrolic macrocycles exhibit a high stability, a rigid structure, interesting photophysical properties, a rich coordination chemistry, and redox activity. They are ubiquitous in biological systems and have found technical applications in a large number of fields, e.g., catalysis,[1] solar energy harvesting,[2] sensors, tracers,[3] and triplet sensitizers in photodynamic therapy.[4−6] *meso*-Tetraarylporphyrins are the predominant molecular structures in synthetic porphyrin chemistry. A number of functionalized tetraaryl-substituted porphyrins are commercially available. Furthermore, they are relatively easy to synthesize, highly stable, and allow the introduction of a variety of functionalities by the proper choice of starting components or by postsynthetic derivatization of the *meso*-aryl substituents.[7,8] In particular, the *ortho* position of the *meso*-aryl groups is of great interest for the tethering of functional elements because it provides the closest connecting point with respect to the metal ion in the porphyrin center. Asymmetric tetraaryl porphyrins with only a single functional substituent connected in the *ortho*-position at one of the *meso*-aryl groups (see Figure 1) have been applied, e.g., for intramolecular axial coordination,[9,10] photoinduced electron transfer in porphyrin−fullerene dyads,[11,12] or enzyme model complexes.[13,14] We used this porphyrin architecture for the intramolecular light-driven coordination-induced spin-state switching (LD-CISSS)[15] of Ni^{2+} porphyrins.[16−21]

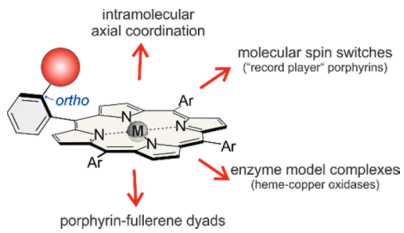

Figure 1. Asymmetric tetraaryl porphyrins with a functional substituent in the *ortho*-position at one of the aromatic *meso*-substituents are of interest for a number of applications.

The covalently bound functional substituent in this case is an azopyridine[16−19] or azoimidazole[20,21] that is reversibly coordinated to the Ni^{2+} porphyrin upon *cis*/*trans* isomerization of the azo function. The coordination and decoordination of the axial ligand gives rise to a spin transition between a diamagnetic ($S = 0$) state and a paramagnetic ($S = 1$) state. We coined the above-mentioned porphyrins "record player" molecules because the light-induced coordination of the switchable azo unit ("tone arm") to the metal center resembles the movement of a needle that is put down on a vinyl record. Light-driven spin transition in solution is highly promising for a number of applications such as light-controlled magnetic levitation,[22−25] photoactivatable paramagnetic relaxation enhancement,[26] and particularly responsive contrast agents for magnetic resonance imaging (MRI).[17,20,27−30] However, to date, the low-yielding, multistep syntheses of the spin switches (up to 14 individual steps)[20] are the major bottlenecks toward practical applications. Three key steps have to be performed during the synthesis of every derivative (see Figure 2): the formation of the switchable azo unit (yellow), the tethering of the switching unit to the porphyrin's *meso* substituent (blue), and the porphyrin synthesis including the Ni^{2+} insertion (red). Within the well-established linear approach (Figure 2a), these key steps are performed consecutively.[17−21] This route suffers from the disadvantage that even slight variations in the switching unit require each synthesis to be performed from scratch. Moreover, the "mixed aldehyde" porphyrin synthesis, though using cheap components, is known to give notoriously low yields and many side products. Therefore, it should preferentially be performed as the first step of the synthesis. In our previous procedure, the porphyrin synthesis in the final

Received: August 22, 2016
Published: October 7, 2016

DOI: 10.1021/acs.orglett.6b02507
Org. Lett. 2016, 18, 5228−5231

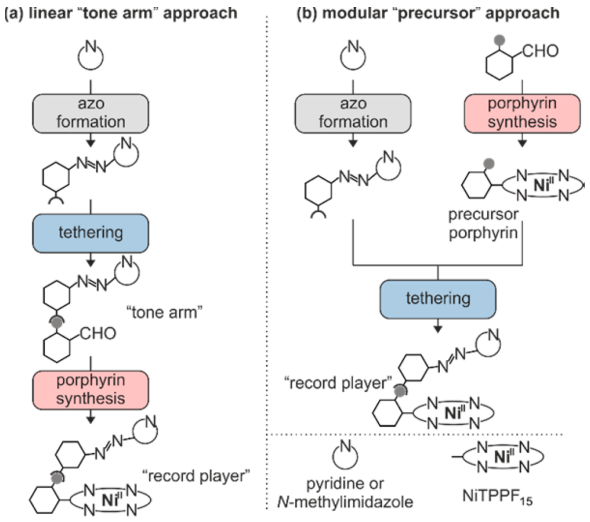

Figure 2. Schematic depiction of possible synthetic routes toward "record player" molecules. Key steps are the formation of the switchable azo unit (gray), tethering the switching unit to the porphyrin's *meso* substituent (blue), and the synthesis of the Ni^{2+} porphyrin (red). The key steps might be carried out (a) in a linear fashion via the well-established "tone arm" approach or (b) in a convergent fashion via a modular approach which requires the synthesis of a suitable precursor porphyrin.

step gives rise to a significant loss of the valuable azo compound. A modular approach with an appropriate precursor porphyrin (Figure 2b) would certainly be much more efficient.

We previously reported a monoiodinated derivative of the widely used Ni^{2+} porphyrin Ni–$TPPF_{20}$ as a precursor porphyrin. The porphyrin was obtained in nine synthetic steps (five pots) and was coupled with borylated azopyridine to give the perfluorinated "record player" derivative.[16] To provide an even more straightforward access to the porphyrin key intermediate, we use the commercially available 2-formylphenylboronic acid pinacol ester (**1**) pentafluorobenzaldehyde (**2**), and pyrrole (**3**) for the porphyrin synthesis via the Lindsey method (see Scheme 1).[31,32] The monoborylated metal-free

Scheme 1. Synthesis of Precursor 5

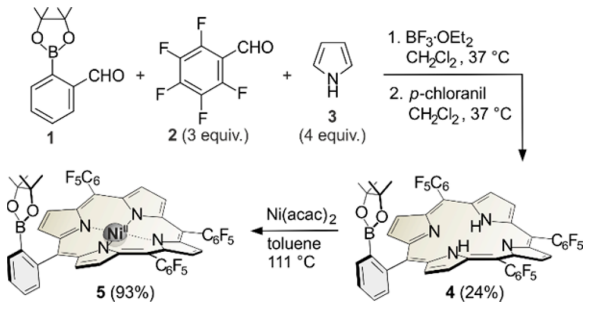

porphyrin **4** was obtained in a fairly high yield, and the following metalation with nickel(II) acetylacetonate gave almost quantitative yields of the desired precursor porphyrin **5**. The synthesis of a similar Zn(II)porphyrin has been described previously.[33] However, this porphyrin did not contain the *meso*-pentafluorophenyl substituents that are required for efficient spin switching, and it was obtained in only very poor yields. Porphyrin **5** is easily accessible in high purity, exhibits a high thermal stability, and can be stored at ambient conditions for several months without any sign of degradation. Therefore, it meets all requirements for an efficient precursor for monosubstituted porphyrins.

With the key intermediate **5** in hand, we set out to evaluate its scope in Suzuki cross-coupling reactions,[34,35] particularly with photoisomerizable azo compounds (see Scheme 2). For this purpose, we synthesized the iodinated azobenzenes **6**[36] with the azo substituent in the *ortho* (**6a**), *meta* (**6b**), and *para* (**6c**) position with regard to the iodo substituent (for details, see the Supporting Information). The azobenzenes **6** were reacted with precursor **5** by applying a standard Suzuki cross-coupling protocol we already used for the former linear approach.[17,19] By using tetrakis(triphenylphospine)-palladium(0) as catalyst, potassium carbonate as the base, and a toluene–ethanol–water solvent mixture, all azobenzenes **6** were coupled to precursor **5**, giving the respective azo-functionalized Ni^{2+} porphyrins **7** in excellent isolated yields (**7a**, 94%; **7b**, 97%; **7c**, 93%, see Scheme 2, middle). Cross coupling of **5** is also feasible with (3′-bromophenylazo)-pyridines **8** and (3′-bromophenylazo)-*N*-methylimidazoles **9**, which provide a photoresponsive coordinating unit and therefore are suitable ligands for molecular spin switches. The azo heterocycles **8** and **9** were synthesized according to convenient synthetic routes (for details, see the SI).[37−39] The Suzuki cross-coupling reactions of **5** with azopyridines **8** were performed by applying the same synthetic protocol we used for azobenzenes **6**. The respective azopyridine-functionalized porphyrins **10** were obtained in very high yields (**10a**, >99%; **10b**, 95%; **10c**, 90%; see Scheme 2, right). For the coupling reactions with azoimidazoles **9**, we had to adjust the synthetic protocol and used [1,1′-bis(diphenylphosphino)ferrocene]-dichloropalladium(II) as catalyst, cesium carbonate as base, and a 1,4-dioxane–water solvent mixture, giving the derivatives **11** in satisfying yields as well (**11a**, 90%; **11b**, 82%; **11c**, 93%; **11d**, 66%; see Scheme 2, left).

Table 1 compares the yields of spin switches **10a**,[19] **10b**,[17] and **11a**[20] obtained from both the linear and the convergent synthesis. The formation and derivatization of the azo unit (Figure 2, gray) is identical for both synthetic approaches. Therefore, we only considered the respective linear sequence which includes the Ni^{2+} porphyrin synthesis (Figure 2, red) and the tethering of the switching unit to the porphyrin's *meso*-substituent (Figure 2, blue). The yields for the tethering step via Suzuki cross-coupling reactions are almost identical (90% or higher). However, the synthesis of the Ni^{2+} porphyrin is much more efficient for the convergent route. Precursor porphyrin **5** was obtained in 22% yield, whereas the linear approach provided only 2–5% yield for the porphyrin synthesis and metalation. Consequently, the modular (convergent) route improves the overall yields strikingly by a factor of 4–11. Furthermore, porphyrin **5** is accessible from commercially available starting materials. In the linear route, more than 95% of the compounds synthesized in previous steps are lost because the last step (porphyrin synthesis) proceeds only in 2–5% yield.

In summary, we present the synthesis of the boronic acid pinacol ester functionalized Ni^{2+}porphyrin **5** and its applications as a building block for the convergent syntheses of functionalized porphyrins. The Ni^{2+}porphyrin **5** is accessible in pure form from commercially available compounds in only

DOI: 10.1021/acs.orglett.6b02507
Org. Lett. 2016, 18, 5228–5231

Scheme 2. Suzuki Cross-Coupling Reactions of Precursor 5 with Azobenzenes 6, Azopyridines 8, and Azoimidazoles 9

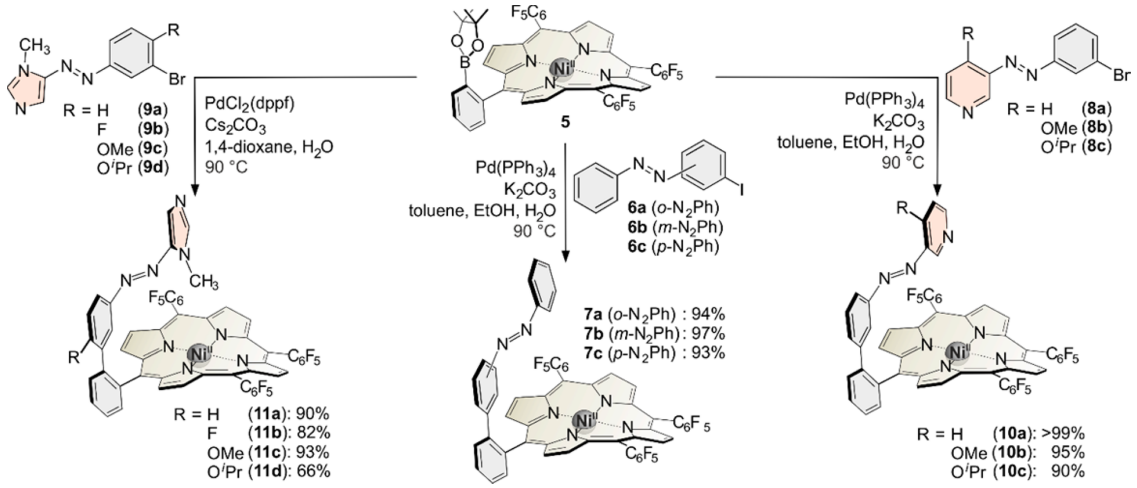

Table 1. Yields (Suzuki Coupling and Porphyrin Synthesis) for Spin Switches 10a, 10b, and 11a via the Linear Approach and the New Modular Approach

	overall yield (%)	
derivative	linear approach	modular approach
10a	5.0[19]	22
10b	1.9[17]	21
11a	3.3[20]	20

three synthetic steps (two pots) and can be stored for several months at ambient conditions without degradation. Subsequent Suzuki cross-coupling reactions of **5** were successfully demonstrated. Porphyrin **5** was coupled with 10 different halogenated azo compounds in high isolated yields. The reaction with photoswitchable azopyridines or azoimidazoles provides efficient access to molecular spin switches that exhibit intramolecular light-driven coordination-induced spin-state switching (LD-CISSS). The modular synthetic approach via the novel precursor porphyrin **5** is a considerable improvement to previously applied routes. Our new synthetic concept certainly will help us to further develop and optimize our spin switches toward applications as smart MRI contrast agents. The new precursor porphyrin should also be a versatile key intermediate for other functional porphyrins. *Ortho*-substitution in asymmetric tetraaryl porphyrins is a recurring structural element and is found in many studies regarding different applications. The pentafluorophenyl substituents at the porphyrin's *meso*-positions further increase the possibilities for functionalization since they are highly reactive in nucleophilic aromatic substitution reactions[40−42] and allow, for example, the introduction of solubilizing substituents.[43]

■ ASSOCIATED CONTENT

Supporting Information

The Supporting Information is available free of charge on the ACS Publications website at DOI: 10.1021/acs.orglett.6b02507.

Syntheses of azo compounds **6**, **8**, and **9**, experimental procedures, characterization data, and NMR spectra (PDF)

■ AUTHOR INFORMATION

Corresponding Author

*E-mail: rherges@oc.uni-kiel.de.

Notes

The authors declare no competing financial interest.

■ ACKNOWLEDGMENTS

Financial support from the "Deutsche Forschungsgemeinschaft" (DFG) via CRC677 "Function by Switching" is gratefully acknowledged.

■ REFERENCES

(1) Che, C.-M.; Huang, J.-S. *Chem. Commun.* **2009**, 3996−4015.
(2) Li, L.-L.; Diau, E. W.-G. *Chem. Soc. Rev.* **2013**, *42*, 291−304.
(3) Biesaga, M.; Pyrzynska, K.; Trojanowicz, M. *Talanta* **2000**, *51*, 209−224.
(4) Josefsen, L. B.; Boyle, R. W. *Theranostics* **2012**, *2*, 916−966.
(5) Sternberg, E. D.; Dolphin, D.; Brückner, C. *Tetrahedron* **1998**, *54*, 4151−4202.
(6) Ethirajan, M.; Chen, Y.; Joshi, P.; Pandey, R. K. *Chem. Soc. Rev.* **2011**, *40*, 340−362.
(7) Rao, P. D.; Dhanalekshmi, S.; Littler, B. J.; Lindsey, J. S. *J. Org. Chem.* **2000**, *65*, 7323−7344.
(8) Senge, M. O. *Chem. Commun.* **2011**, *47*, 1943.
(9) Liu, H.; Tu, J.-Q.; Zhang, C.-H.; Xiao, Q.-T.; Wang, T.-H.; Ju, X.-L. *New J. Chem.* **2016**, *40*, 5679.
(10) Li, Y.; Sharma, S. K.; Karlin, K. D. *Polyhedron* **2013**, *58*, 190−196.
(11) D'Souza, F.; Gadde, S.; Zandler, M. E.; Arkady, K.; El-Khouly, M. E.; Fujitsuka, M.; Ito, O. *J. Phys. Chem. A* **2002**, *106*, 12393−12404.
(12) D'Souza, F.; Chitta, R.; Gadde, S.; Zandler, M. E.; McCarty, A. L.; Sandanayaka, A. S. D.; Araki, Y.; Ito, O. *Chem. - Eur. J.* **2005**, *11*, 4416−4428.
(13) Ghiladi, R. A.; Ju, T. D.; Lee, D.-H.; Moënne-Loccoz, P.; Kaderli, S.; Neuhold, Y.-M.; Zuberbühler, A. D.; Woods, A. S.; Cotter, R. J.; Karlin, K. D. *J. Am. Chem. Soc.* **1999**, *121*, 9885−9886.
(14) Liu, J.-G.; Naruta, Y.; Tani, F. *Chem. - Eur. J.* **2007**, *13*, 6365−6378.
(15) Thies, S.; Sell, H.; Schütt, C.; Bornholdt, C.; Näther, C.; Tuczek, F.; Herges, R. *J. Am. Chem. Soc.* **2011**, *133*, 16243−16250.
(16) Dommaschk, M.; Näther, C.; Herges, R. *J. Org. Chem.* **2015**, *80*, 8496−8500.

DOI: 10.1021/acs.orglett.6b02507
Org. Lett. 2016, 18, 5228−5231

(17) Dommaschk, M.; Peters, M.; Gutzeit, F.; Schütt, C.; Näther, C.; Sönnichsen, F. D.; Tiwari, S.; Riedel, C.; Boretius, S.; Herges, R. *J. Am. Chem. Soc.* **2015**, *137*, 7552−7555.
(18) Dommaschk, M.; Schütt, C.; Venkataramani, S.; Jana, U.; Näther, C.; Sönnichsen, F. D.; Herges, R. *Dalton T.* **2014**, *43*, 17395−17405.
(19) Venkataramani, S.; Jana, U.; Dommaschk, M.; Sönnichsen, F. D.; Tuczek, F.; Herges, R. *Science* **2011**, *331*, 445−448.
(20) Heitmann, G.; Schütt, C.; Gröbner, J.; Huber, L. M.; Herges, R. *Dalton T.* **2016**, *45*, 11407−11412.
(21) Heitmann, G.; Schütt, C.; Herges, R. *Eur. J. Org. Chem.* **2016**, *2016*, 3817−3823.
(22) Mirica, K. A.; Phillips, S. T.; Shevkoplyas, S. S.; Whitesides, G. M. *J. Am. Chem. Soc.* **2008**, *130*, 17678−17680.
(23) Mirica, K. A.; Shevkoplyas, S. S.; Phillips, S. T.; Gupta, M.; Whitesides, G. M. *J. Am. Chem. Soc.* **2009**, *131*, 10049−10058.
(24) Mirica, K. A.; Phillips, S. T.; Mace, C. R.; Whitesides, G. M. *J. Agric. Food Chem.* **2010**, *58*, 6565−6569.
(25) Mirica, K. A.; Ilievski, F.; Ellerbee, A. K.; Shevkoplyas, S. S.; Whitesides, G. M. *Adv. Mater.* **2011**, *23*, 4134−4140.
(26) Fanucci, G. E.; Cafiso, D. S. *Curr. Opin. Struct. Biol.* **2006**, *16*, 644−653.
(27) Herges, R.; Jansen, O.; Tuczek, F.; Venkatamarani, S. Transition metal complexes with photosensitive tethered ligands as visible light-induced spin-crossover magnetic molecular switches. Patent WO 2012022299 A1, Feb 23, 2012.
(28) Herges, R.; Jansen, O.; Tuczek, F.; Venkatamarani, S. Photosensitive metal porphyrin complexes with pendant photo-isomerizable chelate arm as photochromic molecular switches undergoing photoinduced spin transition. Patent DE 102010034496 A1, Feb 16, 2012.
(29) Herges, R. *Nachr. Chem.* **2011**, *59*, 817−821.
(30) Davies, G.-L.; Kramberger, I.; Davis, J. J. *Chem. Commun.* **2013**, *49*, 9704−9721.
(31) Lindsey, J. S.; Schreiman, I. C.; Hsu, H. C.; Kearney, P. C.; Marguerettaz, A. M. *J. Org. Chem.* **1987**, *52*, 827−836.
(32) Lindsey, J. S.; Wagner, R. W. *J. Org. Chem.* **1989**, *54*, 828−836.
(33) Imada, T.; Kijima, H.; Takeuchi, M.; Shinkai, S. *Tetrahedron Lett.* **1995**, *36*, 2093−2096.
(34) Miyaura, N.; Suzuki, A. *J. Chem. Soc., Chem. Commun.* **1979**, 866−867.
(35) Miyaura, N.; Yamada, K.; Suzuki, A. *Tetrahedron Lett.* **1979**, *20*, 3437−3440.
(36) Strueben, J.; Lipfert, M.; Springer, J.-O.; Gould, C. A.; Gates, P. J.; Sönnichsen, F. D.; Staubitz, A. *Chem. - Eur. J.* **2015**, *21*, 11165−11173.
(37) Schütt, C.; Heitmann, G.; Wendler, T.; Krahwinkel, B.; Herges, R. *J. Org. Chem.* **2016**, *81*, 1206−1215.
(38) Thies, S.; Sell, H.; Bornholdt, C.; Schütt, C.; Köhler, F.; Tuczek, F.; Herges, R. *Chem. - Eur. J.* **2012**, *18*, 16358−16368.
(39) Wendler, T.; Schütt, C.; Näther, C.; Herges, R. *J. Org. Chem.* **2012**, *77*, 3284−3287.
(40) Samaroo, D.; Vinodu, M.; Chen, X.; Drain, C. M. *J. Comb. Chem.* **2007**, *9*, 998−1011.
(41) Samaroo, D.; Soll, C. E.; Todaro, L. J.; Drain, C. M. *Org. Lett.* **2006**, *8*, 4985−4988.
(42) Singh, S.; Aggarwal, A.; Thompson, S.; Tome, J. P. C.; Zhu, X.; Samaroo, D.; Vinodu, M.; Gao, R.; Drain, C. M. *Bioconjugate Chem.* **2010**, *21*, 2136−2146.
(43) Dommaschk, M.; Gutzeit, F.; Boretius, S.; Haag, R.; Herges, R. *Chem. Commun.* **2014**, *50*, 12476−12478.

DOI: 10.1021/acs.orglett.6b02507
Org. Lett. 2016, 18, 5228−5231

6 Zusammenfassung

Bis vor kurzem war magnetische Bistabilität im Wesentlichen auf Festkörper beziehungsweise in Einzelmolekülen auf sehr tiefe Temperaturen beschränkt. Der 2011 von HERGES *et al.* vorgestellte und anhand von Ni(II)-Komplexen untersuchte *Light-Driven Coordination-Induced Spin State Switch* (LD-CISSS) ist der erste erfolgreiche Ansatz für eine effiziente und reversible Spinschaltung von isolierten Einzelmolekülen in homogener Lösung bei Raumtemperatur.[116,117] Ni(II) (Elektronenkonfiguration $3d^8$) ist kein klassisches Spin Crossover Element, allerdings kann ein Spinübergang durch eine Änderung der Ligandenfeldgeometrie erreicht werden. Im quadratisch-planaren Ligandenfeld ist Ni(II) diamagnetisch (Gesamtelektronenspin $S = 0$), während eine quadratisch-pyramidale oder oktaedrische Koordinationssphäre zu einem paramagnetischen ($S = 1$) Spinzustand führt. Als quadratisch-planare Basiskomplexe haben sich elektronenarme Ni(II)porphyrine bewährt.[118–120] An diesen kann der LD-CISSS durch eine lichtgetriebene Assoziation, bzw. Dissoziation eines photoschaltbaren, axialen Liganden hervorgerufen werden (siehe Abb. 6.1). Beim intermolekularen Ansatz wird ein freier, photodissoziierbarer Ligand (PDL) verwendet, der als *trans*-Isomer gut und als *cis*-Isomer möglichst schlecht koordiniert.[116,135] Der intramolekulare *Recordplayer*-Ansatz basiert auf einer kova-

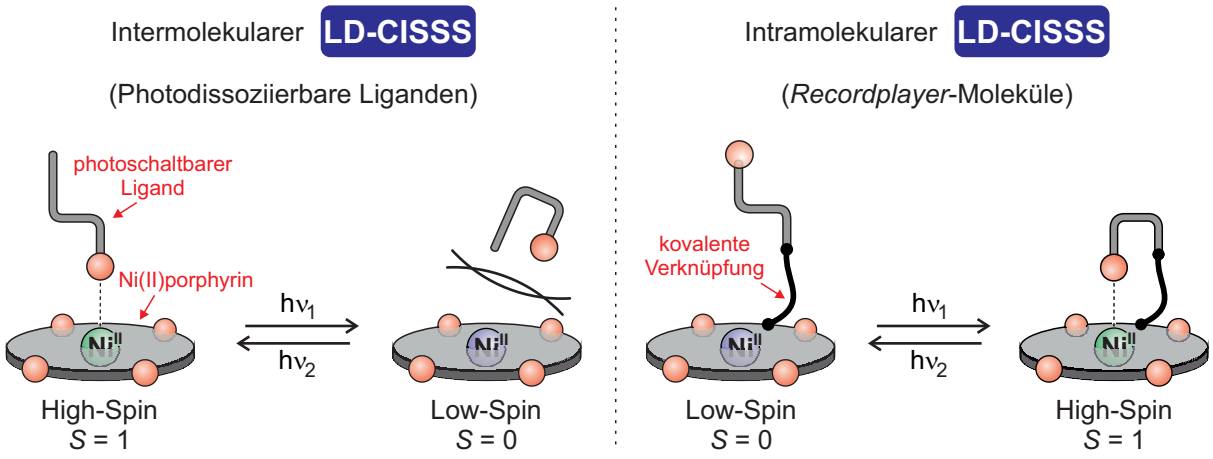

Abb. 6.1: *Light-Driven Coordination-Induced Spin State Switch* in Ni(II)-Komplexen. Der intermolekulare Ansatz mit photodissoziierbaren Liganden (PDLs) basiert auf einer unterschiedlichen Koordinationsfähigkeit der Photoisomere des Liganden. Beim intramolekularen *Recordplayer*-Ansatz erfolgt eine kovalente Anbindung des schaltbaren Liganden, sodass dessen intramolekulare Koordination ausschließlich in einem der beiden Photoisomere möglich ist. Für beide Konzepte wurden im Rahmen dieser Arbeit neue, photoresponsive Phenylazoimidazol-Liganden realisiert.

lenten Anbindung des Liganden an das Porphyrin, welche eine intramolekulare Koordination ausschließlich für das *cis*-Isomer erlaubt.[117,138–140]

Die durch das LD-CISSS-Prinzip beschriebene Spinschaltung ist äußerst vielversprechend für eine ganze Reihe an Anwendungen. Hervorzuheben ist dabei die Realisierung photoschaltbarer Kontrastmittel für die Magnetresonanztomographie (MRT), die insbesondere für neue MR-angiographische Methoden in der interventionellen Radiologie gefragt sind. Um die Entwicklung des LD-CISSS-Konzeptes hinsichtlich einer zukünftigen medizinischen Anwendung weiter voranzutreiben, wurden in dieser Arbeit die bislang verwendeten Pyridin-Liganden durch *N*-Methylimidazol-Derivate ersetzt. *N*-Methylimidazol ist ein sehr starker Ligand für Ni(II)porphyrine und weist darüber hinaus im Vergleich zu Pyridin-Derivaten ein deutlich günstigeres Verhältnis zwischen Ligandenstärke und Basizität auf. Dies ist für die angestrebte Anwendung als photoschaltbares MRT-Kontrastmittel von sehr hoher Bedeutung, da unter physiologischen Bedingungen die Donorstärke basischer Liganden durch Wasserstoffbrückenbindungen oder Protonierung drastisch reduziert werden kann. Auf Basis des bereits bekannten Phenylazoimidazol-Stammsystems **11**[142] (siehe Abb. 6.2) wurden sowohl effiziente photodissoziierbare Liganden (PDLs) als auch *Recordplayer*-Moleküle entwickelt, synthetisiert und hinsichtlich ihrer Effektivität für die Spinschaltung von Ni(II) ausführlich untersucht.

Für die Realisierung eines von **11** abgeleiteten PDLs wurden umfassende theoretische Studien auf dichtefunktionalem Niveau (B3LYP/def2TZVP//PBE/SVP) in Kombination mit experimentellen Untersuchungen durchgeführt. Photophysikalisches und sterisches Design ergab das Derivat **12** als vielversprechensten Kandidaten (siehe Abb. 6.2). Azoimidazol **12** konnte unter Anwendung der für das Stammsystem **11** entwickelten Syntheseroute[142] erhalten und hinsichtlich seiner Eignung als PDL untersucht werden. Anhand von Titrationsreihen wurden mittels einer in frü-

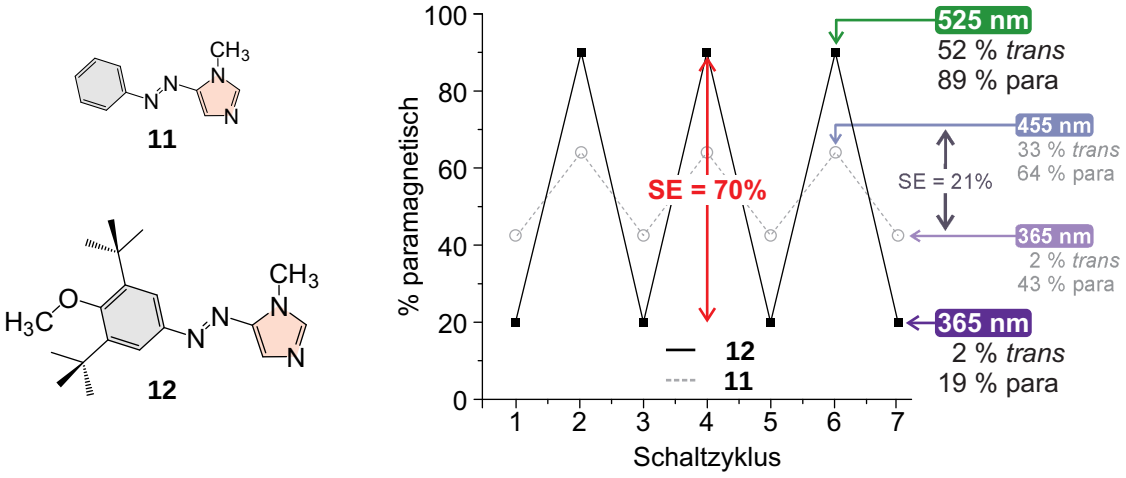

Abb. 6.2: Vollständig reversibler und ermüdungsfreier intermolekularer LD-CISSS von $NiTPPF_{20}$ mit dem Azoimidazol-Stammsystem **11** und dem daraus entwickelten volloptimierten PDL **12**. Die Schalteffizenz (SE), bezogen auf den magnetischen Zustand des Ni(II)porphyrins, konnte von 21 % (**11**) auf 70 % (**12**) verbessert werden. Azoimidazol **12** ist der bisher effektivste PDL für den LD-CISSS von Ni(II).

heren Arbeiten entwickelten NMR-Methode[116,135] die Assoziationskonstanten (K_{1S}, K_2) bei verschiedenen Temperaturen sowie die thermodynamischen Parameter (ΔH, ΔS) für die Koordination beider Photosisomere an *meso*-Tetrakis(pentafluorphenyl)nickel(II)porphyrin ($NiTPPF_{20}$) bestimmt. Dabei wurden sehr gute Übereinstimmungen zwischen den theoretischen und den experimentell bestimmten Differenzen der Komplexbildungsenergien erhalten. Es kann folglich davon ausgegangen werden, dass die verwendete theoretische Methode das LD-CISSS-System adäquat beschreibt. In Schaltexperimenten zeigte **12** herausragend gute Eigenschaften. Der Anteil der paramagnetischen Spezies von $NiTPPF_{20}$ konnte mit **12** zwischen 19 % (Belichtung mit 365 nm, 98 % *cis*) und 89 % (Belichtung mit 525 nm, 49 % *cis*) vollständig reversibel über mehrere Zyklen geschaltet werden. Die auf den magnetischen Zustand bezogene Schalteffizienz von 70 % ist für den intermolekularen LD-CISSS mit photodissoziierbaren Liganden absoluter Rekord und stellt eine Verbesserung um 20 % zum bisher effektivsten Pyridin-System dar.[116] Darüber hinaus konnte aufgrund der stark verbesserten Koordination des *trans*-Isomers die für die maximale Schalteffizienz benötigte optimale Ligandenkonzentration deutlich reduziert werden. Azoimidazol **12** ist unter den bislang bekannten PDLs für den intermolekularen LD-CISSS von Ni(II) der mit Abstand effizienteste Ligand.

Um die höchst vorteilhaften Eigenschaften der Phenylazoimidazole auch für den intramolekularen LD-CISSS und somit perspektivisch für die Entwicklung eines photoschaltbaren MRT-Kontrastmittels nutzen zu können, wurde im Folgenden die Synthese mehrerer *Recordplayer*-Moleküle mit *N*-Methylimidazol als photoresponsivem axialem Liganden verfolgt. Die Schalteffizienz eines Recordplayer-Moleküls ist entscheidend von der Geometrie des bindenden Zustands abhängig.[140] Aus diesem Grund wurde zunächst basierend auf DFT-Rechnungen (Theorielevel: TPSSh/def2TZVP//TPSSh/SVP) eine Überprüfung und Optimierung des molekularen Designs vorgenommen. Aus den quantenchemischen Rechnungen gingen drei Zielstrukturen hervor, welche als Biphenyl- (**14**), Diphenylether- (**16**) und Diphenylthioether-*Recordplayer* (**15**) bezeichnet wurden (siehe Abb. 6.3). Für alle ist eine Koordination der Imidazol-Einheit im jeweiligen *cis*-Isomer vorgesehen. Das Thioether-Derivat **15** stellt bezogen auf die Geometrie des bindenden *cis*-Konformers eines der bislang besten *Recordplayer*-Designs dar.

Alle drei Imidazol-Recordplayer-Derivate konnten durch Kombination der für die Imidazol-PDLs entwickelten Synthesestrategie und des bereits für die Pyridin-*Recordplayer* verfolgten Schaltarm-Ansatzes erfolgreich synthetisiert werden. Ihre Schalteigenschaften wurden ausführlich mit UV/Vis- sowie NMR-Spektroskopie untersucht. Der effizienteste Imidazol-*Recordplayer* ist das Thioether-Derivat **15**, welches bereits aus der theoretischen Studie als vielversprechendster Kandidat hervorging. Der Anteil der paramagnetischen Spezies von **15** konnte in Acetonitril zwischen 10 % (Belichtung mit 435 nm, 87 % *trans*) und 65 % (Belichtung mit 365 nm, 85 % *cis*) geschaltet werden (siehe Abb. 6.4). Die Schalteffizienz (SE) von 55 % stellt eine leichte Verbesserung zum Biphenyl-Derivat **14** (SE = 51 %) sowie zum ursprünglichen Pyridin-*Recordplayer* (SE = 52 %)[140] dar, allerdings fiel die Steigerung der SE geringer aus als erwartet. Als mögliche

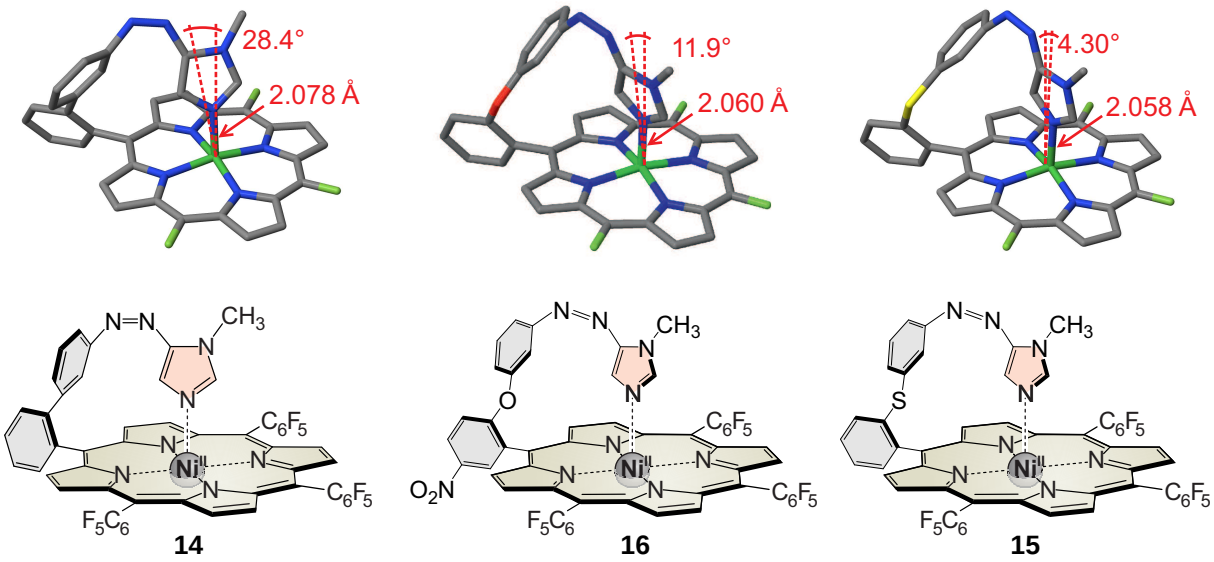

Abb. 6.3: Mithilfe quantenchemischer Rechnungen auf dichtefunktionalem Niveau (TPSSh/def2TZVP//TPSSh/SVP) wurden drei vielversprechende molekulare *Recordplayer*-Strukturen für *N*-Methylimidazol als photoresponsivem Liganden entwickelt und anschließend synthetisiert.

Ursache wurde die höhere Flexibilität des Schaltarms von **15** identifiziert, welche die Koordination entropisch benachteiligen könnte. Diese Annahme konnte mittels temperaturabhängiger NMR-Messungen bestätigt werden. Auch das Diphenylether-Derivat **16** ist von diesem Problem betroffen. Des Weiteren wird bei *Recordplayer* **16** eine hohe Schalteffizienz durch eine unvollständige *cis*→*trans* Isomerisierung verhindert.

Die Implementierung von *N*-Methylimidazol als photoresponsiver Ligand für das *Recordplayer*-Konzept konnte erfolgreich durchgeführt werden. Die erhaltenen Derivate zeigen bisher noch nicht gänzlich zufriedenstellende Schalteigenschaften, sind aber dennoch eine wichtige Ergänzung zu den bereits bekannten Pyridin-Systemen. Insbesondere dem Thioether-Derivat **15** konnte durch erfolgreiche Schaltversuche in Gegenwart von Wasser und MRT-Schaltexperimente ein

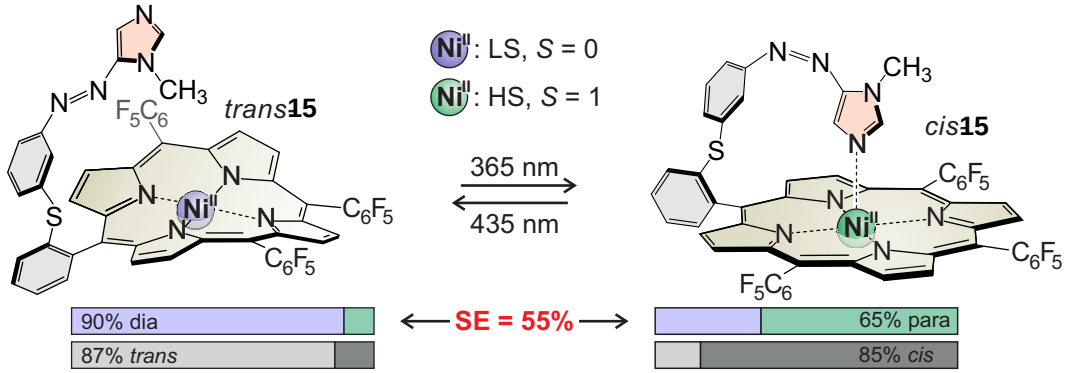

Abb. 6.4: Das Thioether-Derivat **15** zeigt von den in dieser Arbeit vorgestellten Imidazol-*Recordplayer*n in Acetonitril die besten Schalteigenschaften.

hohes Potential für die Entwicklung photoresponsiver Kontrastmittel attestiert werden. Die Möglichkeit, Imidazol-*Recordplayer* mittels UV-Licht (365 nm) in das paramagnetische Isomer zu überführen, könnte zudem für weitere zukünftige Anwendungen interessant sein. Pyridin-*Recordplayer* können ausschließlich durch eine Anregung des Porphyrins mit grünem Licht (ca. 500 nm) ins paramagnetische *cis*-Isomer geschaltet werden.[117,138–140] Dies ist für die Isomerisierung einer Azoverbindung eine sehr ungewöhnliche Wellenlänge und die Photoschaltung vermutlich nicht sehr effizient. Der zugrundeliegende Mechanismus ist Gegenstand aktueller Diskussionen und Untersuchungen.[170,171] Wahrscheinlich ist die Koordination des Liganden in den Isomerisierungsschritt involviert. Die bei den Imidazol-Derivaten festgestellte *trans*→*cis*-Isomerisierung mittels direkter Anregung der $\pi - \pi^*$-Bande der Azofunktion durch UV-Licht sollte mit einer deutlich größeren Quantenausbeute verbunden sein. Folglich sind die Imidazol-*Recordplayer* sehr gut für Anwendungszwecke geeignet, in denen es auf eine möglichst zeiteffiziente Photoisomerisierung der Spinschalter ankommt.

Der Komplexität dieser Verbindungen entsprechend erfordert die Darstellung von *Recordplayer*-Molekülen in der Regel eine hohe Zahl an Syntheseschritten. Beispielsweise war für die erstmalige Darstellung des Imidazol-*Recordplayer*s **14** eine lineare Synthesesequenz bestehend aus 13 individuellen Schritten und 6 isolierten Zwischenprodukten erforderlich (siehe Abb. 6.5).[168] Insbesondere die Porphyrinsynthese als vorletzter Schritt ist sehr ungünstig, da aufgrund der geringen Ausbeuten von meist deutlich unter 10 % bei dieser Reaktion ein Großteil der zuvor aufwendig synthetisierten Azoverbindung verloren geht. Um *Recordplayer*-Moleküle zukünftig einfacher und in höheren Ausbeuten herstellen zu können, wurde die Identifizierung und Synthese eines geeigneten, leicht zugänglichen Vorläufer-Porphyrins verfolgt, welches sich post-synthetisch mit der gewünschten Schalteinheit kuppeln lassen sollte. Das borylierte Ni(II)porphyrin **20** erfüllt diese Anforderungen annähernd perfekt. Es konnte in lediglich drei

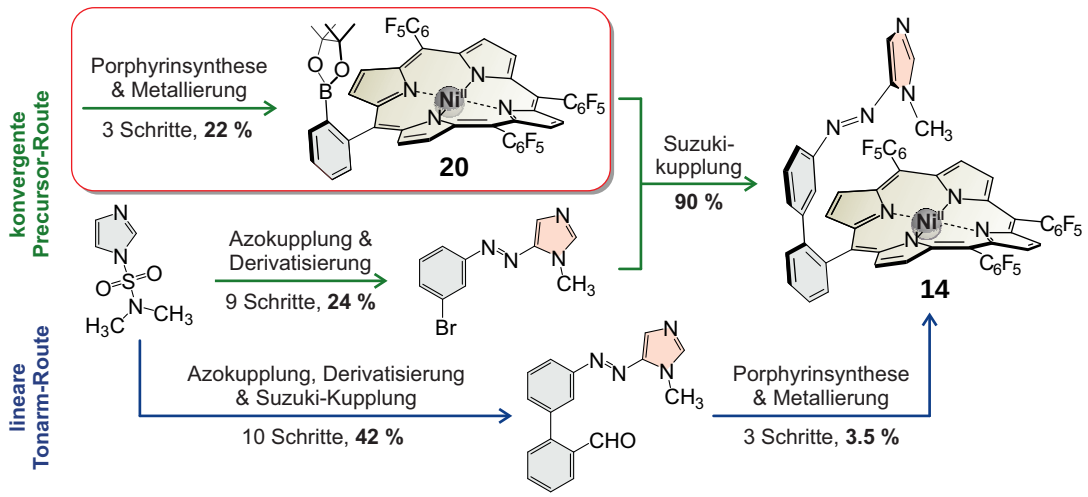

Abb. 6.5: Vergleich der neuen, konvergenten *Recordplayer*-Synthese über Porphyrin-Precursor **20** mit der zuvor angewandten, linearen Synthese am Beispiel des Imidazol-*Recordplayer*s **14**.

Syntheseschritten mit einer bemerkenswerten Gesamtausbeute von 22 % direkt aus kommerziell erhältlichen Substanzen erhalten werden (siehe Abb. 6.5). Suzuki-Kreuzkupplungsreaktionen von **20** mit zehn unterschiedlicher Azoverbindungen ergab durchgängig gute bis exzellente Ausbeuten der jeweils gewünschten Zielverbindung. Drei bereits bekannte *Recordplayer*-Derivate wurden durch die Verwendung des Porphyrin-Precursors **20** in Ausbeuten erhalten, die mindestens eine Größenordnung über denen der zuvor angewandten linearen Syntheseroute lagen. So wurde für den Imidazol-*Recordplayer* **14** eine Verbesserung der Gesamtausbeute von 1.4 % auf 15 % erzielt. Die längste lineare Synthesesequenz der modularen Route umfasste dabei zehn Einzelschritte und vier isolierte Zwischenprodukte (siehe Abb. 6.5). Des Weiteren konnten vier bisher unbekannte *Recordplayer*-Derivate erhalten und so der Nachweis erbracht werden, dass sich die neue, konvergente Syntheseroute sehr gut für ein zielgerichtetes Screening neuer Schalteinheiten eignet. Nachteilig bei der Verwendung von Precursor **20** ist, dass seine Anwendung auf das für die Pyridin-*Recordplayer* und das Imidazol-Derivat **14** verwendete Biphenyl-Design beschränkt ist. Trotzdem bleibt festzuhalten, dass die neue konvergente Syntheseroute über das Precursor-Porphyrin **20** die Vorteile einer unkomplizierten Porphyrinsynthese nach der Methode von LINDSEY nahezu ideal mit der Möglichkeit verbindet, Recordplayer-Moleküle nach dem Baukastenprinzip herzustellen und zu derivatisieren.

Die Ergebnisse dieser Arbeit haben die Studien zur Spinschaltung von Ni(II) mittels des *Light-Driven Coordination-Induced Spin State Switch* (LD-CISSS) entscheidend vorangebracht. Es gelang, das im Vergleich zu bisher verwendeten Pyridin-Derivaten deutlich stärker koordinierende *N*-Methylimidazol als photoresponsiven Liganden sowohl für den intermolekularen PDL-Ansatz als auch für den intramolekularen *Recordplayer*-Ansatz zu etablieren. Insbesondere die erreichbaren Schalteffizienzen mit den freien, photodissoziierbaren Liganden (PDLs) sind äußerst beeindruckend und im Vergleich zu den bisher verwendeten Azopyridinen stark verbessert.[159] Die *Recordplayer*-Moleküle zeigen nicht gänzlich zufriedenstellende Schalteigenschaften, allerdings wurden viele wichtige Erkenntnisse gewonnen, die weiterführende Arbeiten auf dem Weg zu effizienten, wasserlöslichen Spinschaltern maßgeblich beeinflussen und erleichtern werden.[168,169] Die in dieser Arbeit entwickelte, modulare Syntheseroute für *Recordplayer*-Moleküle stellt zudem eine enorme Verbesserung zu den bisher angewandten Syntheseprotokollen dar[172] und ist aus aktuellen Studien zur Entwicklung von pH- und temperatur-responsiven,[173,174] sowie wasserlöslichen[175,176] Spinschaltern nicht mehr wegzudenken.

7 Ausblick

Die Parameter, welche die Effizienz der durch den LD-CISSS beschriebenen Spinschaltung bestimmen, sind nicht zuletzt dank der Ergebnisse dieser Arbeit inzwischen sehr gut verstanden. In Hinblick auf die vielseitigen interessanten Anwendungsmöglichkeiten, insbesondere im Bereich der responsiven MRT-Kontrastmittel, sollte somit die Entwicklung effektiver wasserlöslicher Spinschalter im Fokus zukünftiger Studien stehen.

Für den intermolekularen LD-CISSS in Wasser ließe sich ein photodissoziierbarer Ligand (PDL) auf Basis des in dieser Arbeit beschriebenen Azoimidazols beispielsweise durch die Substitution mit Glycerin-Dendrimeren erhalten (siehe Abb. 7.1). Die Dendronisierung als Strategie zur Löslichkeitsvermittlung hat sich bereits bei der Konzeption

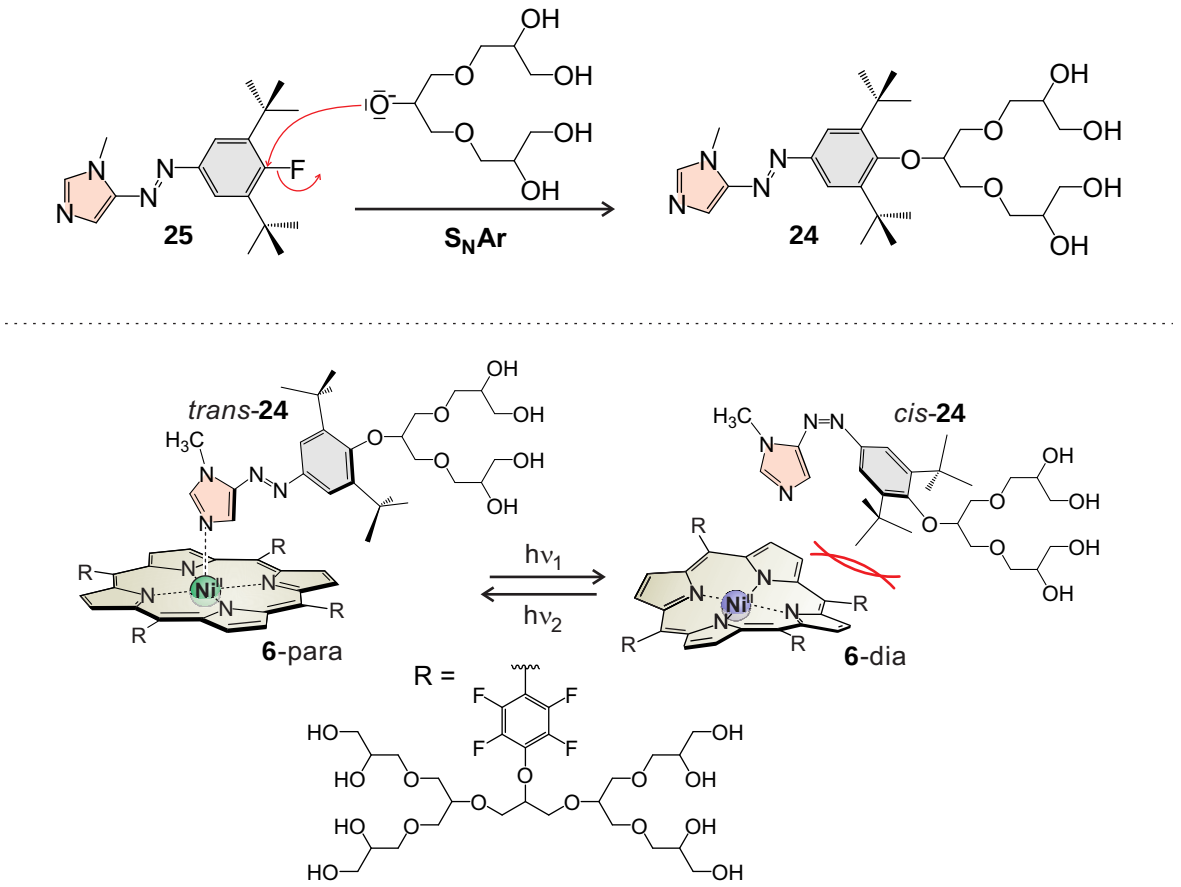

Abb. 7.1: Vorschlag für die Synthese des wasserlöslichen photodissoziierbaren Liganden (PDL) **24** und dessen Anwendung für den intermolekularen LD-CISSS von Porphyrin **6** in Wasser.

des wasserlöslichen Ni(II)porphyrins **6** bewährt.[119] Mit dem hypothetischen Azoimidazol **24**, welches sich z.B. aus dem Fluor-Derivat **25** mittels nukleophiler Aromatensubstitution durch ein geeignetes Glycerin-Dendrimer herstellen lassen sollte, könnte der LD-CISSS von **6** im wässrigen Medium realisiert werden. Als MRT-Kontrastmittel ist der intermolekulare LD-CISSS Ansatz aufgrund der starken Abhängigkeit von der Ligandenkonzentration kaum geeignet. Wasserlösliche PDLs könnten aber als Modellsysteme für Photopharmazeutika oder für die Realisierung einer lichtgesteuerten magnetischen Levitation in wässriger Lösung Anwendung finden.

Eine Derivatisierung der in dieser Arbeit vorgestellten Imidazol-*Recordplayer* für die Darstellung wasserlöslicher Spinschalter erscheint wenig erfolgversprechend, da die Schalteffizienzen in organischen Lösungsmitteln bislang noch nicht optimal sind. Ein Problem, welches insbesondere die *Recordplayer* **15** und **16** betrifft, ist die hohe Flexibilität der Schalteinheit und die daraus folgende entropische Benachteiligung der koordinierten *cis*-Spezies. Um die Rotation des axialen Liganden aus der Porphyrinebene zu verhindern, könnte ein Ether- oder Thioether-*Recordplayer*-Derivat synthetisiert werden, in dem die Phenylringe über eine zusätzliche kovalente Verbindung zweifach verbrückt sind. Die Struktur des koordinierten *cis*-Konformers dieses *Recordplayer*-Designs wurde bereits an einem vereinfachten Modellsystem überprüft (siehe Abb. 7.2).[177] Die zusätzliche kovalente Verbindung der Phenylringe hat keinen negativen Einfluss auf die sehr gute Geometrie der paramagnetischen *cis*-Spezies. Der hypothetische *Recordplayer* **26** (siehe Abb. 7.2) ist ein sehr vielversprechender Kandidat für eine effiziente Spinschaltung im wässrigen Medium. Die Flexibilität des Schaltarms ist wie beschrieben weitestgehend eingeschränkt. Die Einführung von Glycerin-Dendrimeren an den *meso*-Substituenten des Porphyrins vermittelt die gewünschte Wasserlöslichkeit und verhindert gleichzeitig eine unerwünschte Spinschaltung durch die Koordination von Wasser.[119] Des Weiteren kann durch Substitution mehrerer β-Positionen des Porphyrins unter Ausbildung eines Isobakteriochlorins eine wesentlich stärkere Koordination des Donorliganden *N*-Methylimidazol erreicht werden.[120] Voraussetzung für die Realisierung des wasserlöslichen Imidazol-Recordplayers **26** ist die Synthetisierbarkeit des zweifach verbrückten Schaltarms. Dies gilt es in kommenden Arbeiten zu überprüfen.

Das (LD-)CISSS Konzept ist nicht grundsätzlich auf Ni(II) beschränkt. Kürzlich wurde über einen Mn(V)-Komplex berichtet, der einen temperaturabhängigen CISSS zeigt.[178] Weitere Metallionen, deren Spinzustand durch die Koordination, bzw. Dissoziation photochromer Liganden beeinflusst werden kann, sind beispielsweise Fe(II), Fe(III) oder Mn(II). Insbesondere Fe(II) ist interessant, da es analog zu Ni(II) einen diamagnetischen Low-Spin-Zustand besitzt und somit bei einer möglichen Anwendung als schaltbares MRT-Kontrastmittel ebenfalls einen vollständig MR-inaktiven Zustand aufweisen würde. Der Spinwechsel von Low-Spin ($S = 0$) zu High-Spin ($S = 2$) findet in oktaedrischen Fe(II)-Komplexen durch die Dissoziation eines Liganden unter Ausbildung des quadratisch-pyramidalen Komplexes statt. Fünffach koordinierte Fe(II)-Spezies sind allerdings wenig beständig, sodass der Komplex durch die Assoziation

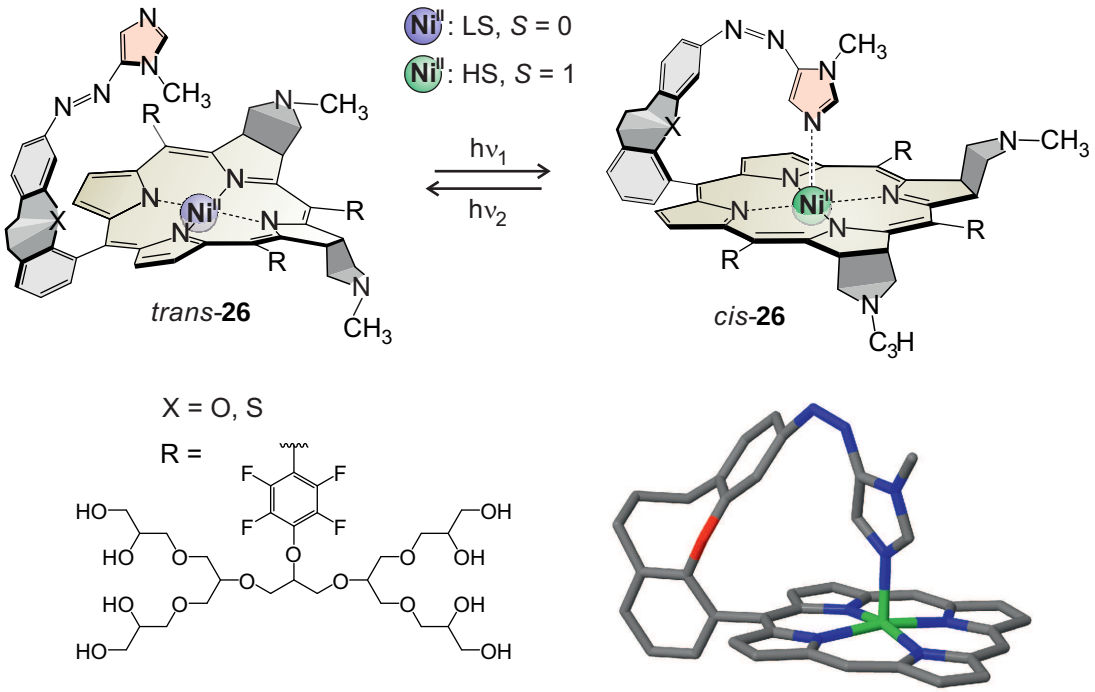

Abb. 7.2: Strukturvorschlag für einen effizienten, wasserlöslichen Imidazol-*Recordplayer*. Die zweite Verbrückung der Phenylringe in der Schalteinheit verhindert das Herausdrehen des axialen Liganden aus der Porphyrinebene. Die Glycerol-Dendrimere an den fluorierten meso-Substituenten sorgen für die gewünschte Wasserlöslichkeit und die Funktionalisierung zweier β-Positionen unter Ausbildung eines Isobakteriochlorin-Derivats verstärkt die Koordination des axialen Liganden. Die Struktur der koordinierten *cis*-Spezies wurde quantenchemisch auf dichtefunktionalem Niveau (PBE/SVP) anhand eines vereinfachten Modellsystems überprüft.

eines schwachen Liganden in der Umgebung, beispielsweise eines Lösungsmittelmoleküls, stabilisiert wird. Aufgrund des deutlich geschwächten (verzerrt) oktaedrischen Ligandenfeldes befindet sich der Komplex anschließend im HS-Zustand. Strenggenommen handelt es sich bei dieser Art von Spinschaltung nicht um einen LD-CISSS. Statt als Folge einer Änderung der Koordinationszahl findet der Spinwechsel aufgrund eines Ligandenaustausches statt. In Analogie zu den bislang entwickelten Konzepten könnte dieser Effekt als *Light-Driven Ligand Exchange-Induced Spin Change* (LD-LEISC) bezeichnet werden (siehe Abb. 7.3) Die größte Schwierigkeit bei der Realisierung eines LD-LEISC mit Fe(II) ist die Identifizierung und Darstellung des quadratisch-pyramidalen Basiskomplexes. Dieser muss ausreichend rigide sein, um stabile Konformationen in beiden Schaltzuständen zu gewährleisten. Prinzipiell wären hierfür erneut die in dieser Arbeit verwendeten Porphyrine geeignet, die zusätzlich mit einem kovalent gebundenen axialen Liganden versehen werden könnten. Leider sind Fe(II)porphyrine sehr oxidationsempfindlich und somit für *in vivo* Anwendungen nicht geeignet.[179,180] Allerdings sind bereits einige Chelatliganden auf Basis von 1,4,7-Triazacyclononan für Fe(II) entwickelt worden, die vielversprechende Eigenschaften für die angestrebte Spinschaltung aufweisen.[181–184] Entsprechende Fe(II)-Komplexe weisen unter physiologischen Bedingungen eine hohe Stabilität

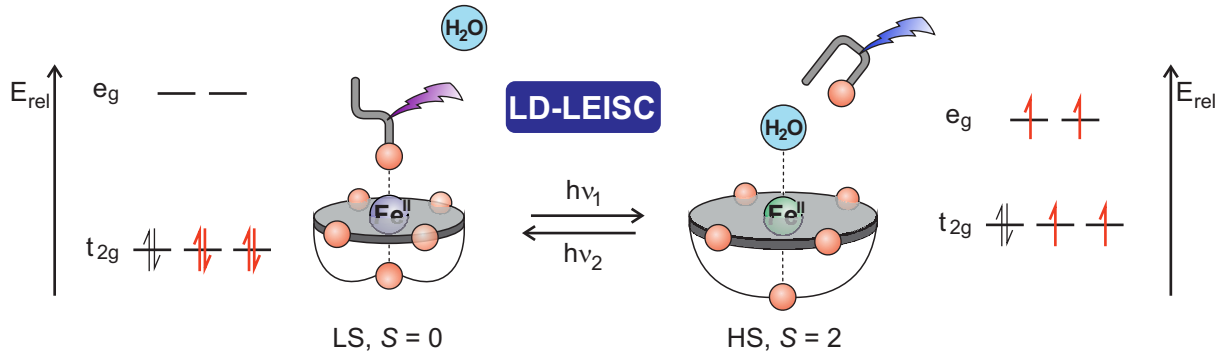

Abb. 7.3: Vorschlag für eine lichtinduzierte Spinschaltung von Fe(II) durch eine Ligandenaustauschreaktion mittels photochromer Liganden (*engl. Light-Driven Ligand Exchange-Induced Spin Change*, LD-LEISC) in Wasser. Im oktaedrischen Komplex ist Fe(II), ausreichend starke Liganden vorrausgesetzt, diamagnetisch (LS, $S = 0$). Die Dissoziation eines photoschaltbaren Liganden führt zum quadratisch-pyramidalen Komplex. Dieser wird durch die Koordination eines Lösungsmittelmoleküls stabilisiert. Der oktaedrische Komplex befindet sich anschließend aufgrund des schwächeren Ligandenfeldes im HS-Zustand ($S = 2$). Für den LD-LEISC von Fe(II) wird ein quadratisch-pyramidal koordinierender, rigider Chelatligand benötigt.

auf und können bezüglich ihres magnetischen Zustands gut eingestellt werden.[185,186] Einige Systeme zeigen bereits eine auf Ligandenaustausch-Reaktionen beruhende Spinschaltung im wässrigen Medium, allerdings ist der Spinübergang irreversibel[46,187] bzw. nur unter sehr harschen Bedingungen durchführbar.[188] Ein mit Licht schaltbares System ist bisher noch nicht bekannt, vermutlich aufgrund der deutlich höheren Flexibilität dieser Systeme und der damit verbundenen erschwerten Realisierung stabiler Schaltzustände.

In dieser Arbeit wurden auf Basis des Stammsystems **11** 5-Phenylazoimidazole für die lichtgetriebene Spinschaltung von Ni(II) verwendet. Azoimidazole sind aber auch darüber hinaus als Photoschalter interessant und könnten in zukünftigen Arbeiten bezüglich ihrer photochromen Eigenschaften weiterentwickelt werden. Die Kombination aus schaltbarer Azofunktion und zur Koordination befähigtem Heterozyklus ist bisher noch relativ selten zu finden,[145–148,189,190] sodass es in diesem Bereich ein großes Entwicklungspotential gibt. Ein sehr vielversprechender Kandidat für einen neuartigen Photoschalter ist in Abb. 7.4 gezeigt. In Azoimidazol **28** sind Phenylring und Heterozyklus nicht nur über die Azofunktion, sondern zusätzlich über eine Ethylenbrücke verbunden. Das entsprechende Azobenzol-Derivat **27** ist bereits bekannt und zeigt sehr ungewöhnliche photochrome Eigenschaften.[191] Im Gegensatz zum unverbrückten Stammsystem ist in **27** nicht das *trans*- sondern das *cis*-Isomer die thermodynamisch stabile Konfiguration. Des Weiteren sind die Wellenlängen für die *cis*/*trans*-Photoisomerisierung stark verschoben. Die Integration des Donorliganden Imidazol in diese als Diazocine bezeichneten Photoschalter wäre äußerst interessant. Das *cis*-Isomer von **28** könnte in Analogie zu den in dieser Arbeit entwickelten PDLs durch geeignete Substituenten an der Koordination an Metallkomplexe gehindert werden, während die Assoziation des *trans*-Isomers unbeeinflusst

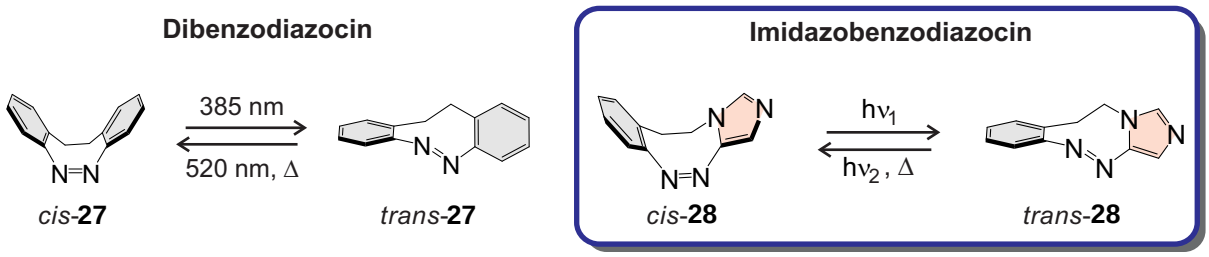

Abb. 7.4: Vorschlag für einen neuartigen Azoimdiazol-Photoschalter. Wie an dem bereits bekannten Dibenzodiazocin **27** gezeigt werden konnte bedingt die zusätzliche Verbrückung der aromatischen Systeme tiefgreifende Änderungen der photochromen Eigenschaften. In Diazocin-Derivaten ist die *cis*-Konfiguration thermodynamisch bevorzugt und die jeweiligen Wellenlängen für die *cis*/*trans*-Photoisomerisierung stark verschoben. Imidazol-Diazocin **28** könnte für die Realisierung von photoassoziativen Liganden (PALs) und von konformativ stark eingeschränkten *Recordplayer*-Molekülen verwendet werden.

bleibt. Da der Ligand bevorzugt im nicht-bindenden Zustand vorläge, würde es sich bei diesem System um einen photoassoziierbaren Liganden (PAL) handeln. PALs wären für den in dieser Arbeit behandelten LD-CISSS, insbesondere aber auch für die Entwicklung photoaktivierbarer medizinischer Wirkstoffe für die Photopharmakologie hochinteressant.[150] Des Weiteren könnten neue *Recordplayer*-Designs konzipiert werden, in denen die Flexibilität der Schalteinheit durch die Verwendung von **28** maximal eingeschränkt ist.

8 Begleitmaterial (*Supporting Information*) zu den Publikationen

8.1 Design and Synthesis of Photodissociable Ligands Based on Azoimidazoles for Light-Driven Coordination-Induced Spin State Switching in Homogeneous Solution

Christian Schütt, Gernot Heitmann, Thore Wendler, Bahne Krahwinkel und Rainer Herges

Supporting Information
J. Org. Chem. **2016**, *81*, 1206-1215.
http://dx.doi.org/10.1021/acs.joc.5b02817

Design and Synthesis of Photodissociable Ligands (PDL) Based on Azoimidazoles for Light-Driven Coordination-Induced Spin State Switching (LD-CISSS) in Homogeneous Solution.

Christian Schütt, Gernot Heitmann, Thore Wendler,
Bahne Krahwinkel and Rainer Herges*

Table of Contents

I. Computational Details

I.1 1-Substituted 5-phenylazoimidazoles

The calculations have been performed using Turbomole 6.3.[1] The geometry optimizations have been carried out at the PBE/SVP level of theory.

Table S1. Calculated (PBE/SVP) relative energies of the *cis*- and *trans*-isomers of 1-substituted-5-phenylazoimidazoles and their respective conformers, relative to the *trans* β isomer.

Ligand	Isomer	E_{abs} [Hartree]	E_{rel} [kcal/mol]
1	*cis*-α	-565.61636046	14.78
	cis-β	-565.61656729	14.65
	trans-α	-565.63559816	2.71
	trans-β	-565.63991806	0.00
2	*cis*-α	-604.84043867	12.21
	cis-β	-604.83179640	17.63
	trans-α	-604.85951027	0.24
	trans-β	-604.85989322	0.00
3	*cis*-α	-683.29354830	10.81
	cis-β	-683.28233428	17.85
	trans-α	-683.31235786	-0.99
	trans-β	-683.31100720	0.00
4	*cis*-α	-973.79344593	12.17
	cis-β	-973.77805887	21.83
	trans-α	-973.81151982	0.83
	trans-β	-973.81284143	0.00
5	*cis*-α	-722.51420713	10.36
	cis-β	-722.49616539	21.68
	trans-α	-722.53368385	-1.86
	trans-β	-722.53072157	0.00

	R^1	*trans*-α	*trans*-β	*cis*-α	*cis*-β
1	H	0.00	-2.71	0.00	-0.13
2	Me	0.00	-0.24	0.00	5.42
3	^{i}Pr	0.00	0.99	0.00	7.04
4	$SiMe_3$	0.00	0.30	0.00	9.65
5	^{t}Bu	0.00	1.86	0.00	11.32

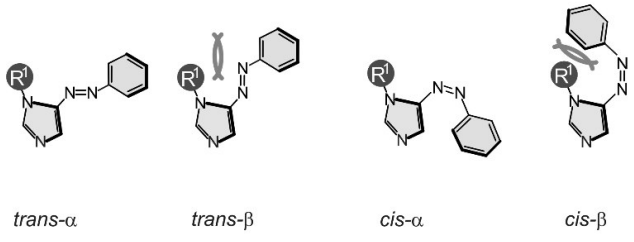

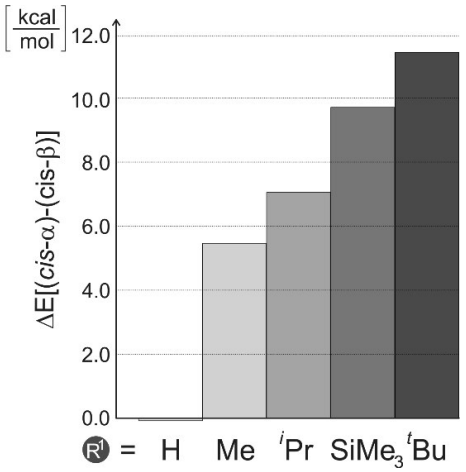

Figure S1. Energy differences (Δ*E*) of the α and β conformer of the *trans* and *cis* isomer relative to the respective α conformation (left). Bar diagram of the energy difference of the two *cis* conformers in kcal·mol^{-1} (Δ*E*) (right). Intramolecular sterical hindrance is indicated by blue arcs.

I.2 Calculated UV Spectra

The TD-DFT calculations of the 1-methyl-5-phenylazoimidazole (**2**) and its corresponding derivatives **2a-c** and **2e** were performed at the B3LYP/6-31G* level of theory using Gaussian 09.D01.[2] The calculated wavelengths of the transitions predicted by the TD-DFT calculations deviate systematically by 10-30 nm with respect to our experimental UV-VIS spectra.[3]

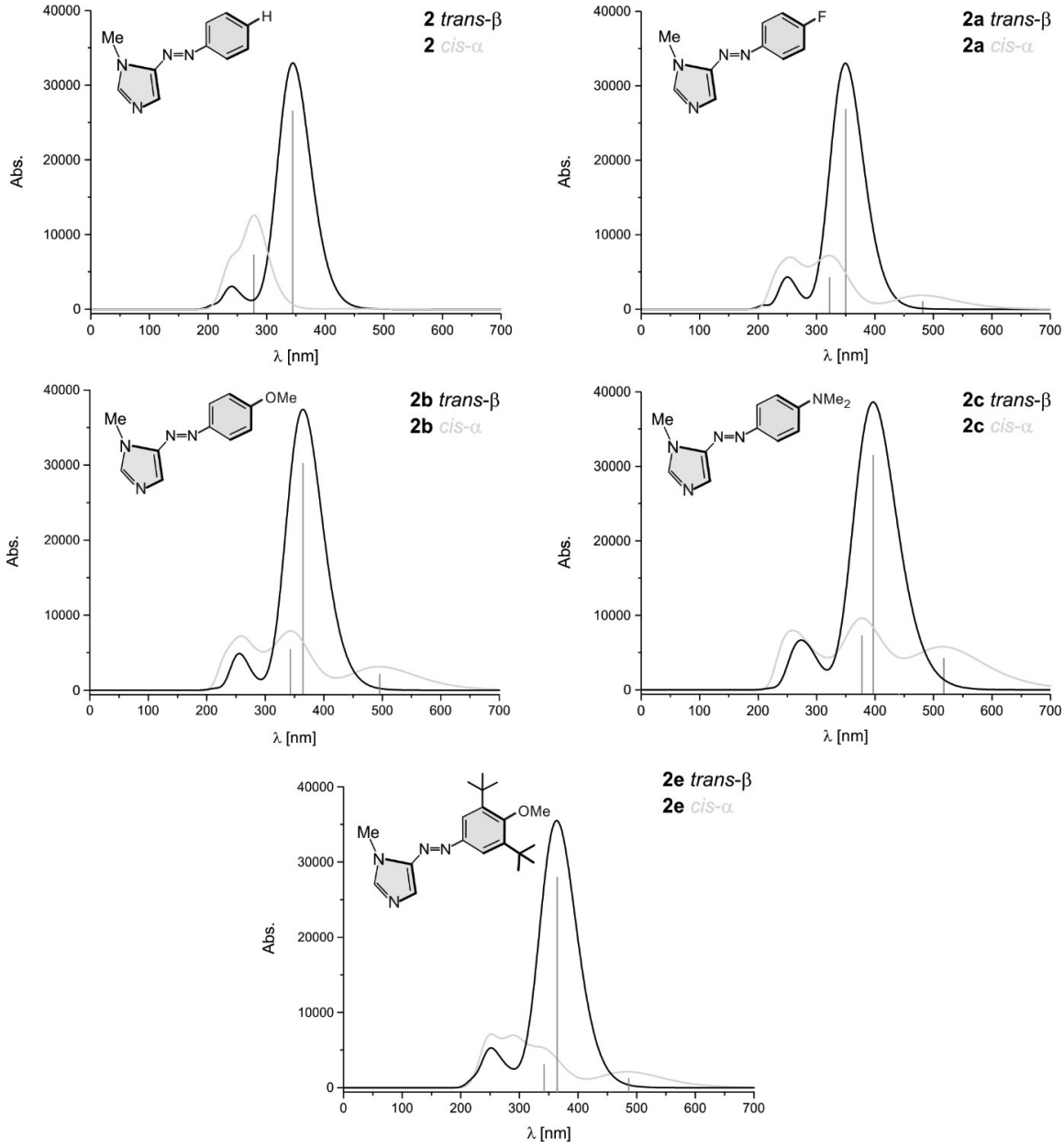

Figure S2. Calculated (TD-B3LYP/6-31G*) UV spectra of the most stable conformation of the *trans* (black) and *cis* (green) isomer of the parent system **2** (top left) and its corresponding derivatives **2a** (top right), **2b** (middle left), **2c** (middle right) and **2e** (bottom). The orange (*trans* isomer) and cyan (*cis* isomer) bars represent the π-π* and n-π* transitions, the height of the bars is proportional to the oscillator strength. The UV spectra are simulated by an overlay of Gaussian functions with a half-width of 0.333 eV.

According to the calculations the photochemical isomerization from *trans* to *cis* should be efficient in **2**, **2a** and **2b**, because there is little overlap of the π-π* transition of the *trans* with transitions of the *cis* form. In **2c**, however, the π-π* bands of *trans* and *cis* exhibit considerable overlap, therefore an inefficient *trans*→*cis* switching is predicted. The calculations predict a very low oscillator strength for the n-π* transition of the parent system in *trans* as well as in *cis* configuration. Hence, back-switching (*cis*→*trans*) should be hampered in the parent system, which leaves the fluoro- and methoxy substituted systems **2a** and **2b** as viable candidates. The methoxy substituted system **2b** is superior because it combines a good separation between the π-π* transition of the *trans* form and the n-π* transition of the *cis* configuration with a high oscillator strength of the n-π* transition in the *cis* form (for details see Table S2). Introduction of two *t*-butyl groups at the phenyl ring (**2e**) leads to small hypsochromic shift of the vital transitions of the PDL in comparison to **2b**. Nevertheless, **2e** exhibits a good separation between the π-π* transition of the *trans* form and the n-π* transition of the *cis* isomer maintaining a high oscillator strength of the n-π* transition in the *cis* configuration.

Table S2. Calculated (TD-B3LYP/6-31G*) transitions of the most stable *cis*- and *trans*-isomers of 1-methyl-5-phenylazoimidazole (**2**) and its derivatives **2a**, **2b**, **2c** and **2e**.

#	Isomer	λ [nm]	*f*	Transition [a)]
2	*trans*-β	345	0.809	π-π*
		456	0.000	n-π*
	cis-α	279	0.248	π-π*
		451	0.001	n-π*
2a	*trans*-β	350	0.815	π-π*
		449	0.000	n-π*
	cis-α	331	0.101	n-π* (π-π*)
		470	0.033	n-π* (π-π*)
2b	*trans*-β	364	0.924	π-π*
		444	0.000	n-π*
	cis-α	349	0.177	n-π* (π-π*)
		495	0.077	n-π* (π-π*)
2c	*trans*-β	397	0.954	π-π*
		442	0.001	n-π*
	cis-α	378	0.235	n-π* (π-π*)
		519	0.142	n-π* (π-π*)
2e	*trans*-β	364	0.865	π-π*
		452	0.000	n-π*
	cis-α	345	0.109	n-π* (π-π*)
		484	0.052	n-π* (π-π*)

a) An unequivocal assignment of excitations to π-π* or n-π* is not possible because π and n orbitals are not exactly orthogonal in the *cis* configurations. The major contributions are given in the Table and the minor contributions are given in parentheses.

I.3 Calculated Complex Formation Energy of 1-Methylimidazole with $NiTPPF_{20}$

The geometry optimizations of the five and six coordinated $NiTPPF_{20}$ complexes with 1-methylimidazole (1-MeIm) were performed at the PBE/SVP level of density functional theory. Single point energies were calculated at the optimized geometries applying several functionals and basis sets using Gaussian 09. The data (Table S3 and Figure S3) confirm that the B3LYP/def2TZVP//PBE/SVP level of theory is a good compromise between computational costs and accuracy. The calculated complex formation energies (ΔE_f) of the five and six coordinated complex with $NiTPPF_{20}$ are compared with the corresponding experimentally determined ($\Delta H_{exptl.}$) values (see section II.5).

Table S3. Calculated energies for the formation of the five coordinate (ΔE_f one axial ligand) and six coordinate (ΔE_f two axial ligands) complexes of $NiTPPF_{20}$ with 1-methylimidazole, according to the following equations: : ΔE_f(5-coord.) : $NiTPPF_{20}$(singlet) + MeIm $\rightarrow$ $NiTPPF_{20}$·MeIm(triplet)
ΔE_f(6-coord.) : $NiTPPF_{20}$(singlet) + 2 MeIm $\rightarrow$ $NiTPPF_{20}$·2 MeIm(triplet)

Functional	Basis set	E_{abs} 1-MeIm [a.u.]	E_{abs} $NiTPPF_{20}$ (singlet) [a.u.]	E_{abs} $NiTPPF_{20}$ · MeIm (triplet) [a.u.]	E_{abs} $NiTPPF_{20}$ · 2 MeIm (triplet) [a.u.]	ΔE_f 5-coord. [kcal/mol]	ΔE_f 6-coord. [kcal/mol]
PBE	**SVP**	-265.0101862	-5398.2568650	-5663.2798821	-5928.3148331	**-8.05**	**-23.59**
PBE	**def2TZVP**	-265.2980412	-5402.8891357	-5668.1864973	-5933.5000643	**0.43**	**-9.32**
PBE	**6-31G***	-265.1983126	-5401.0648635	-5666.2697842	-5931.4909873	**-4.15**	**-18.51**
PBE	**6-31+G***	-265.2104974	-5401.3237703	-5666.5373792	-5931.7677293	**-1.95**	**-14.41**
PBE	**6-311G***	-265.2547987	-5402.2047107	-5667.4679998	-5932.7473535	**-5.33**	**-20.74**
PBE0	**SVP**	-265.0286380	-5398.2512105	-5663.3211890	-5928.3745799	**-25.74**	**-41.47**
PBE0	**def2TZVP**	-265.3129806	-5402.8745546	-5668.2155754	-5933.5449613	**-17.60**	**-27.89**
PBE0	**6-31G***	-265.2166579	-5401.1095675	-5666.3622832	-5931.6012891	**-22.63**	**-36.65**
PBE0	**6-31+G***	-265.2264723	-5401.3212005	-5666.5786260	-5931.8259368	**-19.42**	**-32.50**
PBE0	**6-311G***	-265.2693873	-5402.1828943	-5667.4903560	-5932.7840898	**-23.89**	**-39.17**
B3LYP	**SVP**	-265.3355052	-5402.5025914	-5667.8676603	-5933.2218140	**-18.55**	**-30.25**
B3LYP	**def2TZVP**	-265.6288445	-5407.1843308	-5672.8291203	-5938.4677819	**-10.10**	**-16.17**
B3LYP	**6-31G***	-265.5259460	-5405.3375140	-5670.8881057	-5936.4306552	**-15.47**	**-25.88**
B3LYP	**6-31+G***	-265.5380757	-5405.5828883	-5671.1393098	-5936.6907076	**-11.51**	**-19.87**
B3LYP	**6-311G***	-265.5849436	-5406.4938291	-5672.1047572	-5937.7076955	**-16.31**	**-27.60**
MN12L	**SVP**	-265.0581622	-5399.3187902	-5664.3876208	-5929.4844044	**-6.69**	**-30.93**
MN12L	**def2TZVP**	-265.3522601	-5404.0980455	-5669.4416754	-5934.8212210	**5.42**	**-11.71**
MN12L	**6-31G***	-265.2584960	-5402.3841366	-5667.6458856	-5932.9405982	**-2.04**	**-24.77**
MN12L	**6-31+G***	-265.2669770	-5402.5875865	-5667.8549774	-5933.1563276	**-0.26**	**-21.83**
MN12L	**6-311G***	-265.3031440	-5403.4217338	-5668.7257112	-5934.0670213	**-0.52**	**-24.47**
MN12SX	**SVP**	-265.0822315	-5399.4116786	-5664.5207329	-5929.6377437	**-16.83**	**-38.66**
MN12SX	**def2TZVP**	-265.4050773	-5404.5373742	-5669.9538100	-5935.3840315	**-7.13**	**-22.91**
MN12SX	**6-31G***	-265.3060581	-5402.7451774	-5668.0732325	-5933.4114938	**-13.80**	**-34.01**
MN12SX	**6-31+G***	-265.3161113	-5402.9504155	-5668.2842261	-5933.6298726	**-11.11**	**-29.64**
MN12SX	**6-311G***	-265.3562694	-5403.8129199	-5669.1898686	-5934.5809836	**-12.98**	**-34.84**
TPSSh	**SVP**	-265.3591214	-5402.6125677	-5667.9997498	-5933.3819689	**-17.61**	**-38.10**
TPSSh	**def2TZVP**	-265.6431682	-5407.2468389	-5672.9048322	-5938.5625278	**-9.30**	**-18.42**
TPSSh	**6-31G***	-265.5449205	-5405.4465224	-5671.0143717	-5936.5803601	**-14.39**	**-27.61**
TPSSh	**6-31+G***	-265.5547181	-5405.6636485	-5671.2369181	-5936.8106801	**-11.64**	**-23.59**
TPSSh	**6-311G***	-265.6006346	-5406.5601912	-5672.1852690	-5937.8088192	**-15.34**	**-29.72**
Experiment ($\Delta H_{exptl.}$)						**-7.27 (± 0.37)**	**-13.86 (± 0.67)**

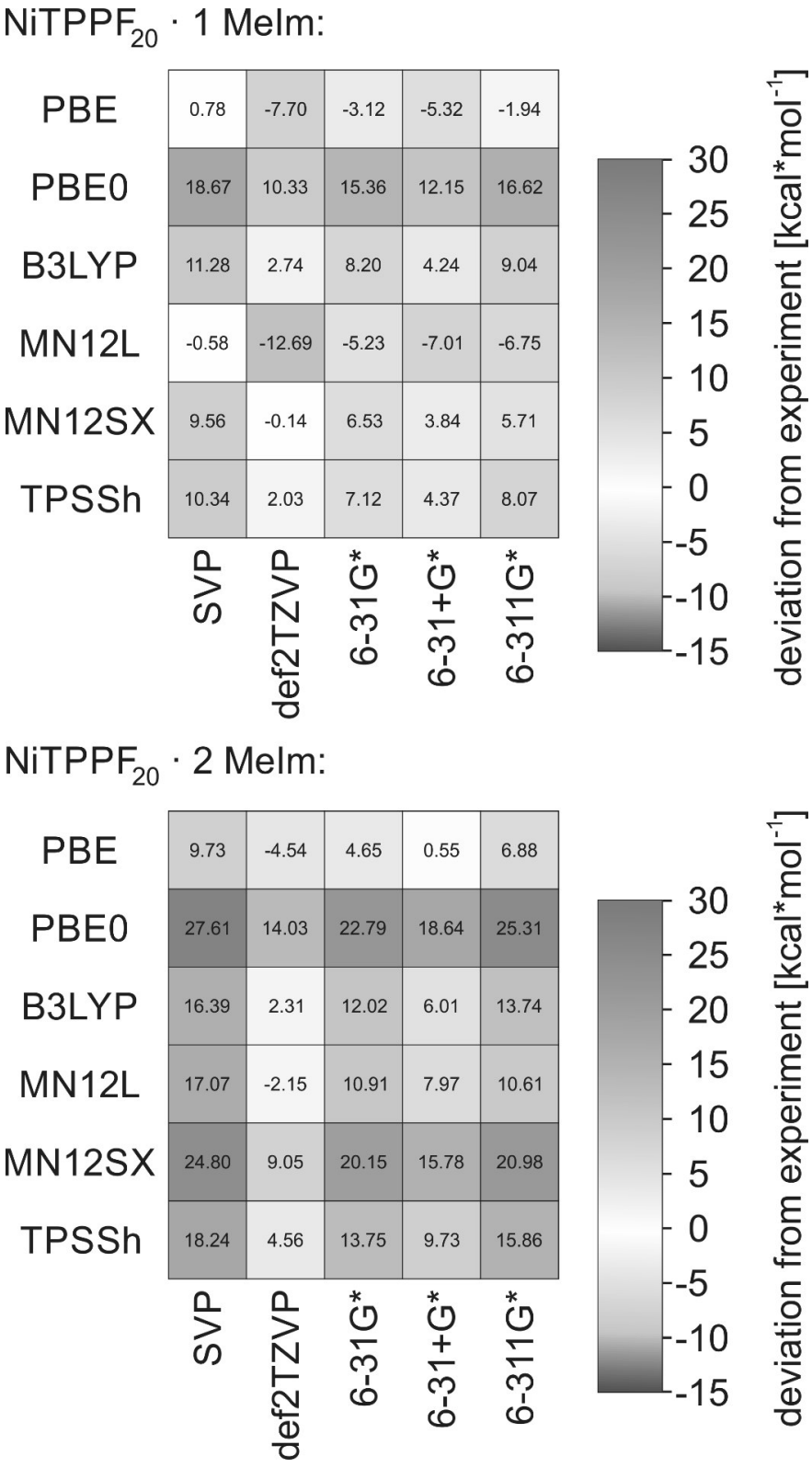

Figure S3. Color coded representation of the deviation of theoretically calculated and experimentally determined values for the formation of the five- (top) and six coordinate (bottom) complex of $NiTPPF_{20}$ with on and two methylimidazole molecules at different levels of theory. The exact values are given in $kcal*mol^{-1}$.

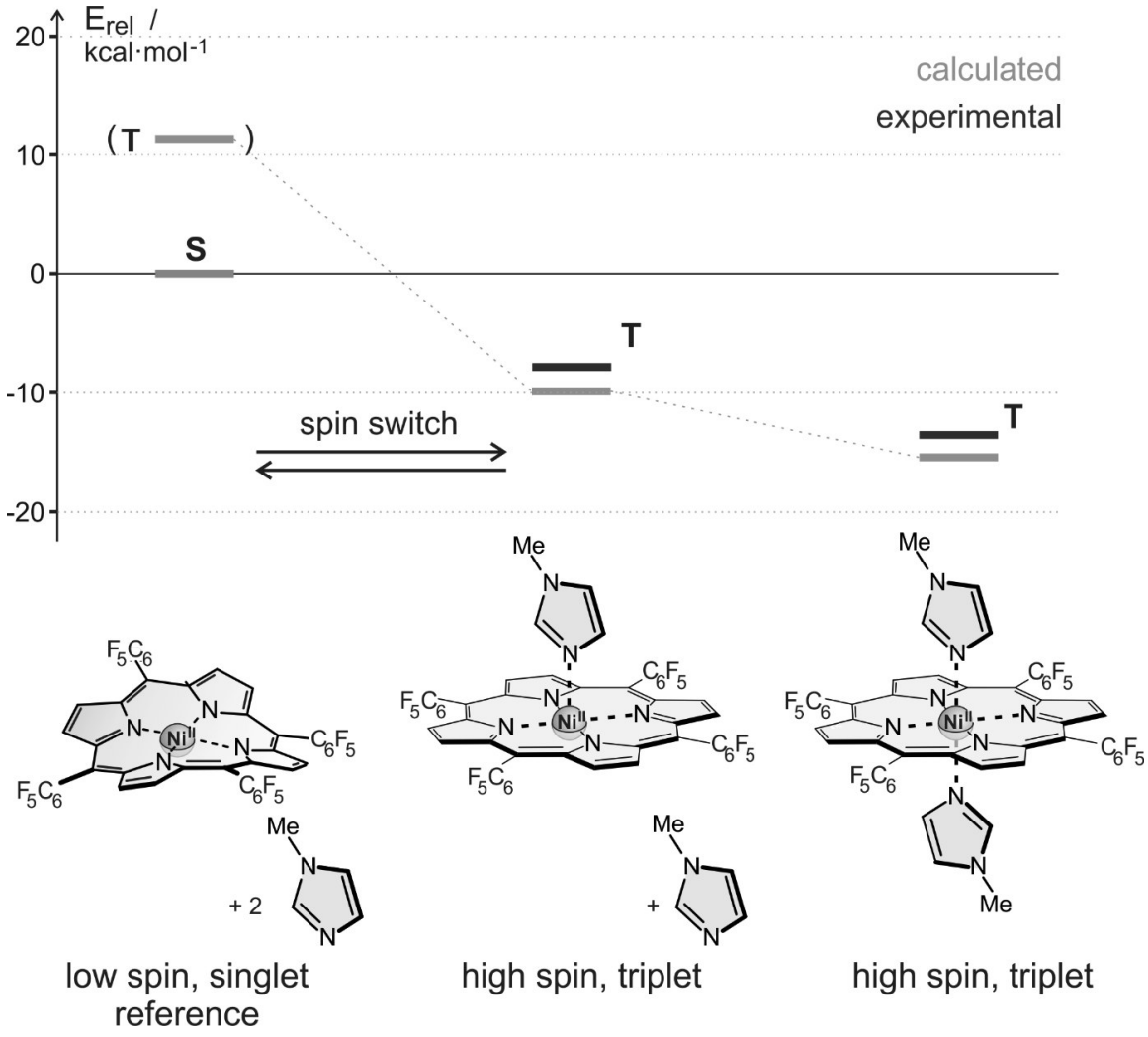

Figure S4. Calculated (B3LYP/def2TZVP//PBE/SVP) complex formation energies (kcal mol^{-1}) of 1-methyl imidazole to $NiTPPF_{20}$ (orange). The energies are relative to the corresponding porphyrin in its low-spin singlet state including two unbound imidazole molecules. The experimental derived association energies for the $NiTPPF_{20}$ for the 1:1 and 1:2 complexes with imidazole are given as blue bars. Note that the experimental and calculated association energies agree quite well.

I.4 Effect of Substituents at the Phenyl Ring on the Complex Formation Energies

The geometry optimizations of the $NiTPPF_{20}$ complexes were performed at the PBE/SVP level of density functional theory. Single point energies at the B3LYP/def2TZVP level of theory were performed on the optimized geometries. The complex formation energies (ΔE_f) are compared to the corresponding experimentally determined ($\Delta H_{exptl.}$) values (see section II.5).

Table S4. Calculated (B3LYP/def2TZVP//PBE/SVP) complex formation energies (ΔE_f) for the formation of the 5-coordinate complex of $NiTPPF_{20}$ with the investigated azoimidazole compounds **2**, **2b**, **2d** and **2e** relative to the most stable conformer of the regarding isomer.

#	Isomer	E_{abs} ligand [a.u.]	E_{abs} $NiTPPF_{20}$ (singlet) [a.u.]	E_{abs} $NiTPPF_{20}$ · 1 ligand (triplet) [a.u.]	ΔE_f 1 ligand [kcal/mol]	$\Delta H_{exptl.}$ 1 ligand [kcal/mol]
2	*cis*-α	-605.88279113	-5405.27432658	-6011.16545150	**-5.23**	-4.67 (± 0.11)
	cis-β	-605.87234860	-5405.27432658	-6011.15820404	-0.68	
	trans-α	-605.90308634	-5405.27432658	-6011.18974554	-7.73	-6.84 (± 0.20)
	trans-β	-605.90310315	-5405.27432658	-6011.19035464	**-8.11**	
2b	*cis*-α	-720.39117482	-5405.27432658	-6125.67575539	**-6.43**	-4.97 (± 0.16)
	cis-β	-720.38296164	-5405.27432658	-6125.67030373	-3.01	
	trans-α	-720.41471798	-5405.27432658	-6125.70161616	-7.89	-6.63 (± 0.26)
	trans-β	-720.41437364	-5405.27432658	-6125.70209407	**-8.19**	
2d	*cis*-α	-798.98877206	-5405.27432658	-6204.27420688	**-6.97**	no exp. value
	cis-β	-798.98002447	-5405.27432658	-6204.26644469	-2.10	
	trans-α	-799.01086793	-5405.27432658	-6204.29664414	-7.18	
	trans-β	-799.01080266	-5405.27432658	-6204.29871214	**-8.48**	
2e	*cis*-α	-1034.74897618	-5405.27432658	-6440.03014528	**-4.29**	-3.01 (± 0.11)
	cis-β	-1034.73891633	-5405.27432658	-6440.02461737	**-0.82**	
	trans-α	-1034.77084972	-5405.27432658	-6440.05829011	**-8.23**	-7.10 (± 0.15)
	trans-β	-1034.77059313	-5405.27432658	-6440.05866446	**-8.46**	

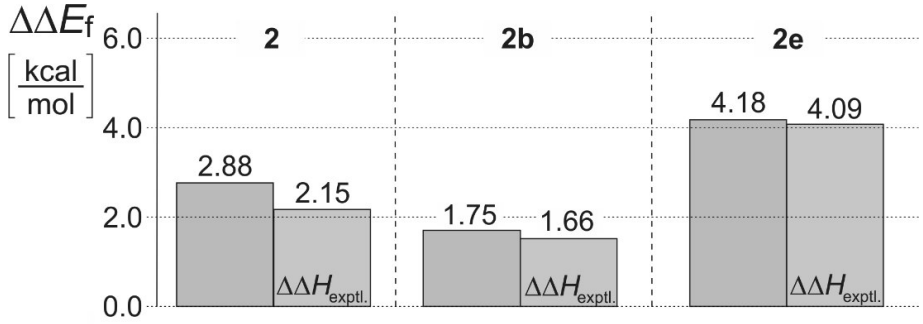

Figure S5. Comparison of calculated ($\Delta\Delta E_f$, B3LYP/def2TZVP//PBE/SVP, grey columns) and experimentally derived ($\Delta\Delta H_{exptl.}$) energy differences (orange columns) of **2**, **2b** and **2e** in kcal mol^{-1}.

The calculated (ΔE_f, B3LYP/def2TZVP//PBE/SVP) and the experimentally determined association enthalpies ($\Delta H_{exptl.}$) as well as the energy differences of the most stable complexes ($\Delta\Delta E_f$ and $\Delta\Delta H_{exptl.}$, Figure S05) are in good agreement. Note that a large $\Delta\Delta E_f$ ($\Delta\Delta H$) is a prerequisite for an efficient PDL.

I.5 XYZ Coordinates of the PBE/SVP optimized Ligands

I.5.1 Phenylazoimidazole (1)

***cis*-α**

$E_{PBE/SVP}$ = -565.6163604558 Hartree

NImag = 0

C	1.004710	-0.000299	0.936070
C	1.558280	-1.178440	0.391220
C	2.481950	-1.092230	-0.661010
C	2.869580	0.159440	-1.169190
C	2.331520	1.331420	-0.610230
C	1.405210	1.259030	0.440460
N	0.136890	-0.079320	2.063720
N	-1.120540	-0.114940	1.942250
C	-1.795870	-0.095720	0.727630
C	-1.566360	-0.054450	-0.668150
N	-3.185400	-0.139670	0.834490
N	-2.745040	-0.072300	-1.348670
C	-3.700950	-0.123150	-0.418230
H	1.256850	-2.155070	0.802160
H	2.906440	-2.016850	-1.086450
H	3.598130	0.222160	-1.993540
H	2.637810	2.318320	-0.995340
H	0.985040	2.173450	0.888850
H	-0.603820	-0.013860	-1.191840
H	-4.781990	-0.148960	-0.618540
H	-3.672450	-0.178560	1.734340

***cis*-β**

$E_{PBE/SVP}$ = -565.6165672927 Hartree

NImag = 0

C	0.678780	-0.011640	1.152770
C	0.009740	1.164110	1.564640
C	-1.266020	1.078500	2.142700
C	-1.885200	-0.170160	2.328420
C	-1.213690	-1.340330	1.932970
C	0.060860	-1.269090	1.349910
N	2.017270	0.061250	0.673360
N	2.323210	0.100060	-0.554050
C	1.431770	0.107080	-1.606970
C	1.806680	0.153490	-2.961820
N	0.027600	0.089480	-1.646080
N	0.720530	0.162360	-3.778450
C	-0.329870	0.123800	-2.957740
H	0.506480	2.138200	1.429630
H	-1.780680	2.001960	2.456480
H	-2.883730	-0.231530	2.789940
H	-1.685640	-2.325660	2.083000
H	0.597000	-2.183520	1.049010
H	2.837940	0.180990	-3.339590
H	-1.382900	0.119790	-3.277530
H	-0.590130	0.050870	-0.830580

***trans*-α**

$E_{PBE/SVP}$ = -565.6355981556 Hartree

NImag = 0

C	-1.023780	-0.581900	0.000083
C	-2.428120	-0.419820	0.000070
C	-3.270890	-1.539100	-0.000014
C	-2.719710	-2.831790	-0.000081
C	-1.319870	-2.999840	-0.000028
C	-0.473240	-1.887940	0.000062
N	-0.272080	0.610390	0.000077
N	0.994620	0.449340	0.000078
C	1.728080	1.608950	0.000023
C	1.469210	2.993270	-0.000049
N	3.115930	1.518220	0.000019
N	2.633660	3.699610	-0.000095
C	3.607620	2.787380	-0.000052
H	-2.825630	0.607630	0.000131
H	-4.365060	-1.404150	-0.000024
H	-3.380320	-3.714410	-0.000181
H	-0.890670	-4.015990	-0.000059
H	0.622130	-1.993910	0.000123
H	0.482930	3.474680	-0.000074
H	4.685390	3.005700	-0.000070
H	3.629800	0.633680	0.000061

***trans*-β**

$E_{PBE/SVP}$ = -565.6399180617 Hartree

NImag = 0

C	-0.249930	-1.071480	-0.000141
C	0.521720	-2.255720	-0.000301
C	-0.104240	-3.509080	-0.000264
C	-1.507050	-3.591760	0.000104
C	-2.281280	-2.413680	0.000308
C	-1.664100	-1.159750	0.000200
N	0.473900	0.137430	-0.000307
N	-0.238140	1.201440	-0.000448
C	0.494170	2.358620	-0.000225
C	0.068670	3.697620	-0.000460
N	1.882360	2.430880	0.000383
N	1.139000	4.542500	-0.000249
C	2.212650	3.751430	0.000271
H	1.618990	-2.156690	-0.000352
H	0.504020	-4.428410	-0.000563
H	-2.002690	-4.576620	0.000238
H	-3.382100	-2.482310	0.000551
H	-2.246070	-0.225840	0.000495
H	-0.969600	4.056160	-0.000699
H	3.255990	4.100730	0.000569
H	2.473730	1.594530	0.000888

I.5.2 1-Methyl-phenylazoimidazole (2)

***cis*-α**

$E_{PBE/SVP}$ = -604.8404386679 Hartree

NImag = 0

C	1.023350	0.007910	0.924790
C	1.567660	-1.172710	0.375290
C	2.489280	-1.090740	-0.679010
C	2.884080	0.159200	-1.185980
C	2.355000	1.333540	-0.623440
C	1.431380	1.265260	0.429870
N	0.164330	-0.066710	2.058900
N	-1.095080	-0.108010	1.949660
C	-1.795540	-0.096390	0.757030
C	-1.559510	-0.055470	-0.638720
N	-3.197260	-0.146260	0.870150
N	-2.730610	-0.078110	-1.324330
C	-3.687930	-0.132090	-0.394230
H	1.260680	-2.148290	0.784740
H	2.906480	-2.017420	-1.107290
H	3.611250	0.218640	-2.011800
H	2.666700	2.319150	-1.007570
H	1.018450	2.181630	0.881000
H	-4.768440	-0.162940	-0.600430
C	-3.951370	-0.200530	2.113700
H	-4.568670	-1.123170	2.154050
H	-3.217930	-0.207650	2.944500
H	-4.611480	0.688020	2.208140
H	-0.593120	-0.012160	-1.155010

***cis*-β**

$E_{PBE/SVP}$ = -604.8317963959 Hartree

NImag = 0

C	0.523940	0.423140	1.207770
C	-0.176360	1.229490	2.137280
C	-1.212380	0.686110	2.905690
C	-1.531880	-0.680640	2.800200
C	-0.805650	-1.497820	1.914830
C	0.207360	-0.956150	1.112050
N	1.644740	0.996130	0.564120
N	2.019520	0.728730	-0.616230
C	1.287650	0.102650	-1.608740
C	1.853680	-0.658260	-2.649160
N	-0.088500	0.142030	-1.906640
N	0.899600	-1.105490	-3.508650
C	-0.237220	-0.586320	-3.058360
H	0.115550	2.287510	2.234070
H	-1.765060	1.328750	3.611000
H	-2.332760	-1.112950	3.421700
H	-1.031110	-2.575400	1.849250
H	0.780040	-1.603100	0.428520
H	2.917850	-0.911160	-2.751910
C	-1.213220	-0.657680	-3.563250
H	-1.132660	0.951740	-1.297490
H	-1.576310	0.450110	-0.411970
H	-0.716320	1.928360	-0.977330
H	-1.923320	1.135630	-2.054260

***trans*-α**

$E_{PBE/SVP}$ = -604.8595102651 Hartree

NImag = 0

C	-1.03014	-0.58508	3.71E-04
C	-2.43398	-0.41662	0.00334
C	-3.28278	-1.53128	0.00298
C	-2.7389	-2.82707	-5.03E-04
C	-1.33997	-3.00201	-0.0036
C	-0.48737	-1.89452	-0.00312
N	-0.27424	0.60411	4.81E-04
N	0.99316	0.44013	4.09E-04
C	1.72999	1.59555	-7.00E-04
C	1.45924	2.97879	-0.00364
N	3.12403	1.50213	9.29E-04
N	2.61566	3.6925	-0.00357
C	3.59223	2.78246	-7.87E-04
H	-2.82609	0.6129	0.00562
H	-4.37622	-1.3902	0.00539
H	-3.40416	-3.70622	-6.71E-04
H	-0.91593	-4.02039	-0.00673
H	0.60727	-2.00807	-0.00561
H	4.6699	3.00539	-1.33E-04
C	3.89695	0.27268	0.00349
H	3.66355	-0.33325	0.90396
H	3.66474	-0.33616	-0.89531
H	4.97504	0.53217	0.00379
H	0.46783	3.45006	-0.00598

***trans*-β**

$E_{PBE/SVP}$ = -604.8598932150 Hartree

NImag = 0

C	-0.653950	-1.269240	0.000000
C	0.050690	-2.494520	0.000000
C	-0.642960	-3.711980	0.000000
C	-2.048130	-3.718720	0.000000
C	-2.756060	-2.499900	0.000000
C	-2.070660	-1.281580	0.000000
N	0.137180	-0.099780	0.000000
N	-0.526440	0.994130	0.000000
C	0.184930	2.158830	0.000000
C	-0.364860	3.455040	0.000000
N	1.577740	2.362490	0.000000
N	0.607400	4.402910	0.000000
C	1.749620	3.717120	0.000000
H	1.151970	-2.458660	0.000000
H	-0.085240	-4.662990	0.000000
H	-2.596650	-4.675120	0.000000
H	-3.859040	-2.507470	0.000000
H	-2.600660	-0.317120	0.000000
H	-1.436620	3.697370	0.000000
C	2.756570	4.163990	0.000000
H	2.647420	1.376070	0.000000
H	2.580810	0.724880	0.894220
H	2.580810	0.724880	-0.894220
H	3.616130	1.919400	0.000000

I.5.3 1-*iso*-propyl-phenylazoimidazole (3)

***cis*-α**

$E_{PBE/SVP}$ = -683.2935482972 Hartree

NImag = 0

C	1.026700	0.012480	0.914580
C	1.567400	-1.168890	0.363000
C	2.490790	-1.088230	-0.689800
C	2.890950	0.161260	-1.193730
C	2.365630	1.336360	-0.629200
C	1.440600	1.269210	0.422960
N	0.166370	-0.061070	2.047490
N	-1.092950	-0.105520	1.937300
C	-1.794090	-0.096380	0.745470
C	-1.552930	-0.053400	-0.649610
N	-3.196500	-0.150490	0.856010
N	-2.721240	-0.078920	-1.338850
C	-3.681870	-0.136270	-0.410670
H	1.256060	-2.144190	0.769780
H	2.905060	-2.015580	-1.119490
H	3.619140	0.219700	-2.018760
H	2.681440	2.321650	-1.010910
H	1.030840	2.186140	0.875880
H	-4.759280	-0.169150	-0.628830
C	-3.962420	-0.206040	2.116740
H	-3.175760	-0.211420	2.900190
H	-0.585110	-0.006520	-1.163110
C	-4.769030	-1.507510	2.208580
H	-5.262650	-1.575030	3.202100
H	-5.564360	-1.557190	1.431250
H	-4.109260	-2.393470	2.090070
C	-4.826590	1.050400	2.284920
H	-5.622140	1.111260	1.508600
H	-5.323390	1.036110	3.279140
H	-4.206780	1.970410	2.222480

***cis*-β**

$E_{PBE/SVP}$ = -683.2823342773 Hartree

NImag = 0

C	0.526860	0.527450	1.402520
C	-0.282140	1.166030	2.374640
C	-1.024560	0.407410	3.287320
C	-0.932410	-0.996800	3.281380
C	-0.091090	-1.634520	2.351280
C	0.626820	-0.887880	1.407840
N	1.348890	1.355070	0.603750
N	1.680330	1.112360	-0.595120
C	1.117740	0.196410	-1.468130
C	1.855260	-0.463930	-2.467510
N	-0.211400	-0.243620	-1.650100
N	1.065600	-1.299500	-3.192490
C	-0.159580	-1.116110	-2.709200
H	-0.307560	2.267390	2.387550
H	-1.666350	0.915700	4.025920
H	-1.500110	-1.592990	4.014130
H	0.008380	-2.732830	2.361960
H	1.291720	-1.393320	0.690120
H	2.939850	-0.379970	-2.622700
C	-1.065300	-1.573400	-3.128950
H	-1.441140	0.369740	-1.097000
H	-1.308590	0.400880	0.003060
C	-2.677280	-0.486900	-1.384560
H	-2.536180	-1.535290	-1.044960
H	-3.540350	-0.062960	-0.828820
H	-2.947220	-0.491310	-2.463290
C	-1.597460	1.807880	-1.612910
H	-2.490610	2.281000	-1.149880
H	-0.711580	2.428130	-1.359120
H	-1.728240	1.818790	-2.717910

***trans*-α**

$E_{PBE/SVP}$ = -683.3123578560 Hartree

NImag = 0

C	-1.030710	-0.584580	-0.001420
C	-2.433670	-0.406630	-0.006270
C	-3.290930	-1.514640	-0.004980
C	-2.757010	-2.814540	0.001390
C	-1.359560	-2.999430	0.006300
C	-0.498390	-1.898320	0.004810
N	-0.270010	0.601310	-0.003110
N	0.997300	0.437660	0.000358
C	1.735140	1.591600	0.000149
C	1.445560	2.970610	-0.000940
N	3.133830	1.515040	0.002270
N	2.591020	3.699620	0.000331
C	3.581810	2.802230	0.001950
H	-2.818080	0.625770	-0.010970
H	-4.383240	-1.365090	-0.008990
H	-3.428690	-3.688760	0.002560
H	-0.942840	-4.020770	0.011450
H	0.594900	-2.024490	0.008400
H	4.652800	3.051310	0.002640
C	3.932960	0.276450	0.002230
H	3.170850	-0.531540	0.006960
H	0.447200	3.427020	-0.002280
C	4.777580	0.169280	1.278780
H	5.302660	-0.810140	1.304640
H	5.549710	0.969410	1.328890
H	4.139150	0.244550	2.184940
C	4.767630	0.163410	-1.280460
H	5.538910	0.963680	-1.340060
H	5.292670	-0.816050	-1.306200
H	4.122040	0.234610	-2.181860

***trans*-β**

$E_{PBE/SVP}$ = -683.3110071957 Hartree

NImag = 0

C	-0.372390	-1.268340	0.000024
C	0.275370	-2.524420	0.000338
C	-0.473870	-3.708630	-0.002000
C	-1.877820	-3.651560	-0.004880
C	-2.528750	-2.401520	-0.005170
C	-1.788060	-1.215990	-0.002610
N	0.468870	-0.134040	0.001800
N	-0.145510	0.987130	0.001840
C	0.581080	2.144610	0.002480
C	0.003810	3.430150	-0.000398
N	1.970000	2.379310	0.004490
N	0.952130	4.400340	-0.000815
C	2.110560	3.738050	0.002210
H	1.377140	-2.542430	0.002230
H	0.040020	-4.684080	-0.001690
H	-2.469330	-4.581900	-0.006990
H	-3.630920	-2.357860	-0.007600
H	-2.273330	-0.228320	-0.002810
H	-1.073730	3.646330	-0.002410
C	3.100860	4.218230	0.003330
H	3.082920	1.398370	0.007510
H	2.574330	0.415080	0.018320
C	3.925160	1.540190	1.281810
H	4.698540	0.741830	1.312660
H	4.449330	2.520860	1.328070
H	3.292200	1.440100	2.189630
C	3.911350	1.517550	-1.278090
H	4.431460	2.498950	-1.348620
H	4.686960	0.721070	-1.301810
H	3.269000	1.398030	-2.176870

I.5.4 1-Trimethylsilyl-phenylazoimidazole (4)

***cis*-α**

$E_{PBE/SVP}$ = -973.7934459327 Hartree

NImag = 0

C	-3.513620	2.007580	-2.066790
C	-2.186160	1.556630	-2.034840
C	-1.291770	2.073450	-1.072350
C	-1.733470	3.058550	-0.163640
C	-3.065630	3.496470	-0.201500
C	-3.962010	2.973050	-1.148860
H	-4.206680	1.598610	-2.820890
H	-1.827620	0.804050	-2.755250
H	-1.021280	3.472880	0.567710
H	-3.404910	4.261150	0.517090
H	-5.005970	3.324530	-1.178550
N	0.082750	1.700810	-1.100310
N	0.512510	0.666670	-0.511190
C	-1.584800	-0.357750	0.703570
C	-0.463640	-1.994580	1.508920
H	-0.200960	-2.912660	2.053950
N	-1.691550	-1.467910	1.479840
N	0.454750	-1.287780	0.793020
C	-0.254350	-0.203570	0.248810
H	-2.449160	0.285930	0.500000
C	2.584280	-1.873860	-1.277640
H	2.384800	-0.938000	-1.841550
H	3.646950	-2.164600	-1.439510
H	1.941710	-2.680820	-1.694330
C	3.227040	-0.192300	1.306780
H	4.319790	-0.397270	1.245270
H	3.013110	0.749910	0.759170
H	2.965710	-0.045850	2.378170
C	2.556030	-3.218540	1.521800
H	3.630330	-3.497730	1.433360
H	2.332360	-3.108340	2.606060
H	1.959730	-4.069770	1.125070
Si	2.251710	-1.618940	0.558580

***cis*-β**

$E_{PBE/SVP}$ = -973.7780588708 Hartree

NImag = 0

C	0.560340	0.884610	3.411330
C	1.437120	0.481500	2.397740
C	1.126640	-0.628470	1.573190
C	-0.059710	-1.363730	1.830910
C	-0.907600	-0.979280	2.877700
C	-0.616160	0.153290	3.659600
H	0.806490	1.762180	4.031820
H	2.391470	1.005760	2.227480
H	-0.296130	-2.256190	1.231320
H	-1.814520	-1.571870	3.083740
H	-1.296630	0.454770	4.472460
N	2.157490	-1.066260	0.701130
N	1.978930	-1.707530	-0.375980
C	0.372250	-3.050500	-1.668850
C	-1.172650	-1.633500	-2.042370
H	0.915680	-4.005120	-1.651700
N	-2.065060	-1.150460	-2.467000
N	-0.862930	-2.909160	-2.229060
C	-0.231730	-0.911590	-1.330390
H	0.784230	-1.852980	-1.063800
C	-1.303070	1.591610	0.046220
H	-2.323000	1.151250	-0.009840
H	-0.888070	1.374870	1.052480
H	-1.405500	2.695810	-0.057440
C	1.562470	1.530900	-1.307260
H	2.146980	1.083490	-2.141210
H	1.565670	2.636260	-1.443890
H	2.090950	1.302560	-0.358990
C	-0.990140	1.419410	-3.011800
H	-0.906810	2.522800	-3.139630
H	-0.462960	0.938320	-3.865000
H	-2.070260	1.163200	-3.082870
Si	-0.223780	0.934050	-1.350030

***trans*-α**

$E_{PBE/SVP}$ = -973.8115198197 Hartree

NImag = 0

C	-1.569040	2.279010	-4.285690
C	-1.009420	2.540820	-3.028520
C	-0.701750	1.481140	-2.143820
C	-0.961780	0.146530	-2.546050
C	-1.517790	-0.107810	-3.803420
C	-1.825010	0.954020	-4.677740
H	-1.806930	3.112730	-4.966680
H	-0.794460	3.566930	-2.690330
H	-0.716080	-0.673880	-1.854640
H	-1.716650	-1.147410	-4.114090
H	-2.263270	0.744270	-5.667410
N	-0.142990	1.867020	-0.909610
N	0.089710	0.913900	-0.090990
C	1.057990	2.513250	1.675790
C	1.453660	0.990550	3.124890
H	1.004440	3.506480	1.211460
N	1.768580	0.480330	4.046490
N	1.556220	2.306660	2.924090
C	0.911240	0.309900	2.067370
H	0.644690	1.294360	1.106100
C	-1.258760	-1.742170	1.655430
H	-1.497810	-2.827470	1.588730
H	-1.838480	-1.313860	2.502790
H	-1.597050	-1.248110	0.719370
C	1.157500	-2.231820	3.550310
H	0.989290	-3.332340	3.530720
H	2.241410	-2.064920	3.736340
H	0.586680	-1.824880	4.414100
C	1.629030	-2.147070	0.477860
H	1.344200	-1.647090	-0.472650
H	2.712450	-1.966190	0.654070
H	1.478710	-3.243880	0.358760
Si	0.591480	-1.488990	1.906970

***trans*-β**

$E_{PBE/SVP}$ = -973.8128414290 Hartree

NImag = 0

C	-3.880560	-1.659700	0.002040
C	-2.540440	-1.248460	-0.000262
C	-2.214160	0.127640	0.001010
C	-3.256090	1.087890	0.004750
C	-4.589910	0.669470	0.007050
C	-4.909670	-0.703290	0.005680
H	-4.124460	-2.734830	0.001030
H	-1.720630	-1.984920	-0.003000
H	-2.982600	2.153600	0.005850
H	-5.398240	1.420060	0.009820
H	-5.964160	-1.024550	0.007300
N	-0.838320	0.449420	-0.001120
N	-0.576280	1.700250	-0.001450
C	1.233740	3.362300	-0.004870
C	2.933980	2.084250	-0.006070
H	0.627510	4.278930	-0.004740
N	3.975200	1.732690	-0.006900
N	2.591800	3.372510	-0.006590
C	1.876130	1.206640	-0.004160
H	0.741890	2.045540	-0.003330
C	1.359330	-1.357740	-1.600940
H	1.847210	-0.885100	-2.482530
H	1.580400	-2.448890	-1.637720
H	0.263060	-1.212760	-1.683270
C	1.359110	-1.353090	1.600380
H	1.595620	-2.440550	1.648340
H	1.834900	-0.865740	2.480600
H	0.260490	-1.222750	1.675380
C	3.921540	-0.913110	-0.000384
H	4.421390	-0.497620	-0.903150
H	4.420680	-0.496370	0.902190
H	4.107660	-2.011250	0.000355
Si	2.043850	-0.630470	-0.001300

I.5.5 1-*tert*-Butyl-phenylazoimidazole (5)

***cis*-α**

$E_{PBE/SVP}$ = -722.5142071297 Hartree

NImag = 0

C	-3.313470	2.638080	-1.968800
C	-1.964100	2.254830	-1.996030
C	-1.230160	2.177200	-0.792860
C	-1.849940	2.527040	0.428180
C	-3.193900	2.925130	0.440170
C	-3.935090	2.973870	-0.753820
H	-3.883400	2.682330	-2.911780
H	-1.463450	2.007260	-2.945560
H	-1.264770	2.490180	1.361180
H	-3.668810	3.200310	1.396690
H	-4.992180	3.284370	-0.738150
N	0.163350	1.893690	-0.837770
N	0.658610	0.788450	-0.468800
C	-1.424480	-0.732520	-0.071560
C	-0.288670	-2.412820	0.606730
H	-0.032640	-3.410690	0.982700
N	-1.536630	-2.016530	0.345110
N	0.647900	-1.454100	0.370110
C	-0.069940	-0.322470	-0.076400
H	-2.302600	-0.145960	-0.366600
C	2.132460	-1.582240	0.544620
C	2.616620	-0.512700	1.544940
H	3.711310	-0.622460	1.704750
H	2.416290	0.506730	1.157370
H	2.108190	-0.633480	2.526780
C	2.816560	-1.411160	-0.827520
H	3.914730	-1.540670	-0.713330
H	2.449110	-2.176000	-1.546520
H	2.616080	-0.401460	-1.240260
C	2.459750	-2.978330	1.103590
H	3.559660	-3.051780	1.236950
H	1.990100	-3.153210	2.096250
H	2.153520	-3.790860	0.409670

***cis*-β**

$E_{PBE/SVP}$ = -722.4961653889 Hartree

NImag = 0

C	2.358180	1.713470	2.130050
C	2.560990	0.845270	1.050650
C	1.796780	-0.340730	0.927550
C	0.871440	-0.674570	1.949660
C	0.713850	0.176260	3.052420
C	1.435180	1.380810	3.138940
H	2.942140	2.645930	2.200110
H	3.317150	1.059310	0.278260
H	0.299080	-1.612730	1.893290
H	0.009220	-0.102510	3.853380
H	1.291320	2.051090	4.001820
N	2.168420	-1.218000	-0.125540
N	1.378640	-1.995210	-0.734300
C	-0.735620	-3.161090	-0.312590
C	-2.168960	-1.585730	-0.398390
H	-0.307200	-4.158650	-0.145070
N	-3.124340	-1.046670	-0.444640
N	-2.055640	-2.876550	-0.123960
C	-0.973110	-0.971370	-0.711950
H	-0.014200	-2.000760	-0.627580
C	-0.906860	0.397710	-1.342060
C	0.414370	0.589360	-2.106290
H	0.585190	-0.230530	-2.836280
H	0.355980	1.545150	-2.669070
H	1.293010	0.654660	-1.436980
C	-1.068740	1.470540	-0.248260
H	-0.240080	1.428490	0.488460
H	-1.074340	2.481370	-0.711200
H	-2.027490	1.337290	0.298730
C	-2.057700	0.516870	-2.369370
H	-2.011740	-0.306070	-3.115310
H	-3.060610	0.505140	-1.893500
H	-1.964290	1.482470	-2.910990

***trans*-α**

$E_{PBE/SVP}$ = -722.5336838549 Hartree

NImag = 0

C	-3.787420	3.389880	-0.318900
C	-2.415440	3.225880	-0.089280
C	-1.817900	1.947980	-0.189740
C	-2.622690	0.832310	-0.533320
C	-3.990640	1.004150	-0.764800
C	-4.579820	2.279930	-0.657730
H	-4.243560	4.390110	-0.235530
H	-1.765050	4.074540	0.175590
H	-2.150740	-0.158450	-0.616540
H	-4.613340	0.134860	-1.035390
H	-5.659340	2.406230	-0.842830
N	-0.432680	1.907430	0.061760
N	0.092460	0.742220	0.044170
C	2.411460	1.728110	0.472200
C	3.460040	-0.132880	0.553950
H	2.224040	2.809550	0.488350
N	4.265100	-0.871200	0.652230
N	3.642700	1.186970	0.643890
C	2.160060	-0.489150	0.326290
H	1.447410	0.721600	0.269870
C	1.611390	-1.873110	0.177670
C	0.559100	-2.114340	1.279770
H	1.014730	-2.001470	2.287840
H	-0.279630	-1.393950	1.185370
H	0.155560	-3.146660	1.193520
C	2.749910	-2.896440	0.330040
H	2.323960	-3.915820	0.216720
H	3.531070	-2.770920	-0.450930
H	3.229340	-2.842410	1.331380
C	0.986490	-2.013420	-1.225660
H	1.750290	-1.838250	-2.014600
H	0.580570	-3.040400	-1.354950
H	0.162570	-1.282870	-1.360410

***trans*-β**

$E_{PBE/SVP}$ = -722.5307215653 Hartree

NImag = 0

C	-4.177770	-1.665900	0.002020
C	-2.803630	-1.390200	0.001480
C	-2.342780	-0.054240	0.000436
C	-3.282180	1.005730	-0.000250
C	-4.651400	0.722860	0.000343
C	-5.106170	-0.611110	0.001510
H	-4.528240	-2.711110	0.002830
H	-2.056820	-2.200440	0.001940
H	-2.903050	2.038590	-0.001070
H	-5.380950	1.550260	-0.000236
H	-6.187620	-0.825690	0.001810
N	-0.938420	0.119580	0.000415
N	-0.556300	1.336540	0.001030
C	1.142160	3.041970	0.003310
C	2.958990	1.946790	0.002130
H	0.440260	3.887940	0.004410
N	4.029880	1.709850	0.002020
N	2.484920	3.193730	0.003840
C	1.998920	0.971750	0.000611
H	0.763560	1.683160	0.001340
C	2.273550	-0.504650	-0.001470
C	1.670670	-1.126020	1.273440
H	1.883010	-2.217350	1.291270
H	2.119930	-0.668420	2.182090
H	0.570120	-0.983890	1.290920
C	3.794470	-0.750070	-0.002210
H	4.289040	-0.335910	-0.907440
H	4.289480	-0.338430	0.903940
H	3.965690	-1.847150	-0.003710
C	1.669990	-1.122380	-1.277870
H	1.883110	-2.213480	-1.299440
H	0.569350	-0.980790	-1.294080
H	2.118260	-0.661520	-2.185380

I.5.6 1-Methyl-4'-fluorophenylazoimidazole (2a)

***cis*-α**

$E_{PBE/SVP}$ = -703.9186171982 Hartree

NImag = 0

C	1.524870	-0.212140	0.549310
C	2.384140	-1.239080	0.102030
C	3.329840	-0.987680	-0.900740
C	3.443900	0.308050	-1.421930
C	2.629430	1.354030	-0.963570
C	1.664140	1.090320	0.016230
N	0.654260	-0.478590	1.642290
N	-0.604250	-0.374820	1.559040
C	-1.325020	-0.159710	0.397620
C	-1.139560	-0.182390	-1.005860
N	-2.715420	-0.025490	0.559500
N	-2.328330	-0.069950	-1.650460
C	-3.248070	0.033030	-0.687560
H	2.293740	-2.241780	0.548220
H	3.994890	-1.780800	-1.276220
F	4.364680	0.556270	-2.370890
H	2.762090	2.364620	-1.380640
H	1.016950	1.902060	0.384340
H	-4.328720	0.155760	-0.854790
C	-3.416420	0.056490	1.831120
H	-4.375970	-0.496100	1.764660
H	-2.765260	-0.395010	2.606140
H	-3.619380	1.114540	2.107590
H	-0.196530	-0.291630	-1.555420

***cis*-β**

$E_{PBE/SVP}$ = -703.9101367469 Hartree

NImag = 0

C	0.656190	0.448980	1.198990
C	-0.023750	1.233940	2.162690
C	-1.037730	0.682820	2.951790
C	-1.337110	-0.681740	2.817230
C	-0.647150	-1.496240	1.906480
C	0.338170	-0.929880	1.088980
N	1.760240	1.047890	0.549150
N	2.147600	0.770530	-0.626100
C	1.433920	0.105230	-1.606540
C	2.006180	-0.686200	-2.619760
N	0.060690	0.139580	-1.915050
N	1.056110	-1.154880	-3.473350
C	-0.082510	-0.620690	-3.047790
H	0.267560	2.290470	2.273830
H	-1.586810	1.285290	3.692050
F	-2.291860	-1.224580	3.591830
H	-0.889670	-2.569230	1.852970
H	0.890340	-1.567550	0.380830
H	3.069850	-0.946280	-2.707690
H	-1.054520	-0.702210	-3.558580
C	-0.980100	0.973930	-1.334890
H	-1.444100	0.493940	-0.447510
H	-0.553380	1.949500	-1.024870
H	-1.758140	1.157360	-2.104700

***trans*-α**

$E_{PBE/SVP}$ = -703.9390150324 Hartree

NImag = 0

C	-1.026100	-0.569050	-0.000487
C	-2.431440	-0.406640	-0.000346
C	-3.282400	-1.517250	0.000092
C	-2.715280	-2.799040	0.000599
C	-1.322450	-2.992330	-0.000071
C	-0.481500	-1.878930	-0.000557
N	-0.271780	0.617700	-0.000573
N	0.995920	0.452120	-0.000067
C	1.735950	1.605120	-0.000014
C	1.470240	2.989280	0.000192
N	3.129430	1.506260	0.000108
N	2.629560	3.698470	0.000352
C	3.602650	2.784980	0.000171
H	-2.830000	0.620110	-0.000405
H	-4.378150	-1.410250	0.000167
F	-3.519910	-3.874790	0.000855
H	-0.925970	-4.020130	0.000028
H	0.613120	-1.990780	-0.001040
H	4.681220	3.003290	0.000076
C	3.896910	0.273480	0.000278
H	3.662080	-0.332490	0.900420
H	3.660940	-0.333290	-0.899020
H	4.976170	0.527800	-0.000526
H	0.480610	3.464350	0.000165

***trans*-β**

$E_{PBE/SVP}$ = -703.9392923658 Hartree

NImag = 0

C	-0.641910	-1.262940	-0.000925
C	0.055900	-2.492770	-0.006450
C	-0.635010	-3.709950	-0.006070
C	-2.036500	-3.688430	0.000400
C	-2.756840	-2.481150	0.006450
C	-2.059760	-1.272180	0.005710
N	0.148910	-0.096380	-0.002070
N	-0.515690	0.997550	-0.003160
C	0.191580	2.164310	-0.003120
C	-0.363620	3.458200	-0.006810
N	1.583370	2.373670	0.000643
N	0.604750	4.410080	-0.005400
C	1.749750	3.729360	-0.000869
H	1.157110	-2.465690	-0.011480
H	-0.108620	-4.676920	-0.010490
F	-2.712690	-4.849810	0.000991
H	-3.857820	-2.515780	0.011710
H	-2.586910	-0.306360	0.010270
H	-1.436420	3.695770	-0.010520
H	2.754880	4.180210	0.001710
C	2.656590	1.391200	0.006230
H	2.589070	0.741180	0.901390
H	2.596500	0.738890	-0.887780
H	3.623390	1.937940	0.009630

I.5.7 1-Methyl-4'-methoxyphenylazoimidazole (2b)

***cis*-α**

$E_{PBE/SVP}$ = -719.1478560887 Hartree

NImag = 0

C	0.664690	-0.343780	0.918110
C	1.690920	-1.243560	0.564330
C	2.711460	-0.870100	-0.322370
C	2.754280	0.448060	-0.826220
C	1.758270	1.373320	-0.429440
C	0.723390	0.982340	0.417320
N	-0.272070	-0.756770	1.898230
N	-1.522850	-0.585360	1.789330
C	-2.201440	-0.204170	0.643510
C	-1.998720	-0.167420	-0.756120
N	-3.581690	0.012770	0.796190
N	-3.169370	0.054820	-1.408900
C	-4.093140	0.172940	-0.453080
H	1.668240	-2.258780	0.991270
H	-0.043780	1.713870	0.716340
H	-5.159690	0.383630	-0.623480
C	-4.289870	0.069970	2.063510
H	-5.314530	-0.335030	1.934530
H	-3.723410	-0.538490	2.797400
H	-4.352890	1.114090	2.442260
H	-1.056010	-0.313650	-1.298200
O	3.706850	0.926190	-1.671130
C	4.735680	0.055160	-2.099450
H	4.329990	-0.821270	-2.659210
H	5.382010	0.649650	-2.776450
H	5.348460	-0.315020	-1.243010
H	1.826910	2.405480	-0.807600
H	3.478300	-1.608880	-0.597670

***cis*-β**

$E_{PBE/SVP}$ = -719.1400392556 Hartree

NImag = 0

C	1.023860	1.016290	0.468100
C	0.367860	1.867190	1.395650
C	-0.532230	1.356300	2.326290
C	-0.763380	-0.038950	2.404830
C	-0.074370	-0.903830	1.523980
C	0.794780	-0.378400	0.558120
N	2.013380	1.608340	-0.348040
N	2.347970	1.190800	-1.499570
C	1.633470	0.314280	-2.301660
C	2.190240	-0.606660	-3.206120
N	0.246140	0.226750	-2.512780
N	1.218350	-1.261460	-3.901360
C	0.077770	-0.723010	-3.489940
H	0.588380	2.945900	1.355240
H	1.330370	-1.067720	-0.113360
H	3.260110	-0.824310	-3.326800
C	-0.917930	-0.939460	-3.907270
H	-0.802920	1.088750	-1.993030
H	-1.639370	1.111690	-2.722540
H	-1.177760	0.732440	-1.010090
H	-0.415690	2.120500	-1.867640
O	-1.639790	-0.444750	3.359610
C	-1.902720	-1.828310	3.505410
H	-2.635820	-1.917050	4.332330
H	-2.343640	-2.265320	2.578140
H	-0.981370	-2.398240	3.772670
H	-1.061040	2.012830	3.034970
H	-0.204640	-1.994600	1.584870

***trans*-α**

$E_{PBE/SVP}$ = -719.1690336034 Hartree

NImag = 0

C	-0.715650	-0.033930	-0.108390
C	-2.109820	0.056190	-0.313230
C	-2.912310	-1.089050	-0.389250
C	-2.317800	-2.363610	-0.259390
C	-0.916800	-2.465100	-0.053380
C	-0.129370	-1.322720	0.020970
N	-0.020550	1.182370	-0.051580
N	1.240290	1.082720	0.144570
C	1.915720	2.275890	0.192860
C	1.589180	3.640480	0.068410
N	3.294690	2.255670	0.413670
N	2.700650	4.413530	0.204400
C	3.702430	3.558090	0.410070
H	-2.547900	1.062230	-0.411470
H	0.957660	-1.388660	0.179470
H	4.756310	3.834760	0.564200
C	4.108540	1.070520	0.611390
H	3.770370	0.507710	1.507090
H	4.037350	0.397020	-0.268390
H	5.163340	1.383360	0.750940
H	0.591060	4.058540	-0.114700
O	-2.991770	-3.540960	-0.317230
C	-4.391700	-3.518590	-0.527120
H	-4.655300	-3.041680	-1.500890
H	-4.718360	-4.577920	-0.541730
H	-4.923890	-2.983620	0.294930
H	-0.481430	-3.472740	0.043240
H	-3.994960	-0.980470	-0.549450

***trans*-β**

$E_{PBE/SVP}$ = -719.1691145475 Hartree

NImag = 0

C	-0.053040	0.240370	-0.067210
C	0.566640	-1.001690	-0.322150
C	-0.180400	-2.182480	-0.425820
C	-1.583450	-2.132620	-0.272400
C	-2.215310	-0.887630	-0.017320
C	-1.465620	0.278050	0.083670
N	0.793160	1.358770	0.021630
N	0.196050	2.468240	0.254240
C	0.972230	3.587590	0.357160
C	0.504070	4.889960	0.611810
N	2.368400	3.726790	0.248090
N	1.528110	5.782470	0.660360
C	2.621570	5.056420	0.439690
H	1.662350	-1.019530	-0.437450
H	-1.941360	1.250280	0.282150
H	-0.546530	5.176790	0.757420
C	3.649700	5.450520	0.407080
H	3.372130	2.706570	-0.012200
H	3.348750	1.922400	0.770920
H	3.186470	2.211210	-0.986350
H	4.367890	3.198980	-0.023550
O	-2.408800	-3.208520	-0.349460
C	-1.849030	-4.483990	-0.600980
H	-2.698990	-5.195930	-0.618480
H	-1.324130	-4.518100	-1.585160
H	-1.135370	-4.787430	0.201560
H	0.335850	-3.133020	-0.624460
H	-3.311060	-0.878690	0.097390

I.5.8 1-Methyl-4'-*N*,*N*-dimethylaminophenylazoimidazole (2c)

***cis*-α**

$E_{PBE/SVP}$ = -738.5302993690 Hartree

NImag = 0

C	0.930420	-0.689150	0.785620
C	1.959600	-1.627250	0.531390
C	3.017010	-1.340340	-0.330840
C	3.136860	-0.057640	-0.943420
C	2.135660	0.910410	-0.625120
C	1.057350	0.595290	0.200260
N	-0.031350	-1.045420	1.753420
N	-1.255570	-0.709840	1.717330
C	-1.945610	-0.187910	0.634730
C	-1.844190	-0.143550	-0.775040
N	-3.269110	0.209010	0.893150
N	-3.019610	0.249720	-1.335650
C	-3.845750	0.468020	-0.312260
H	1.897290	-2.608500	1.028660
H	3.770920	-2.118670	-0.514470
H	2.204030	1.931950	-1.025230
H	0.309560	1.372900	0.419970
H	-4.882120	0.827950	-0.396290
C	-3.866930	0.322990	2.210950
H	-4.951590	0.099090	2.146650
H	-3.359770	-0.403530	2.878510
H	-3.728420	1.344130	2.631370
H	-0.971490	-0.401740	-1.388190
N	4.186790	0.243840	-1.792310
C	5.216780	-0.744190	-2.050260
H	4.796880	-1.673080	-2.504140
H	5.957410	-0.325890	-2.760290
H	5.762100	-1.039360	-1.120800
C	4.293300	1.567420	-2.375680
H	5.172650	1.602250	-3.048960
H	3.392580	1.827490	-2.980770
H	4.423290	2.363520	-1.602380

***cis*-β**

$E_{PBE/SVP}$ = -738.5231243924 Hartree

NImag = 0

C	0.930420	-0.689150	0.785620
C	1.959600	-1.627250	0.531390
C	3.017010	-1.340340	-0.330840
C	3.136860	-0.057640	-0.943420
C	2.135660	0.910410	-0.625120
C	1.057350	0.595290	0.200260
N	-0.031350	-1.045420	1.753420
N	-1.255570	-0.709840	1.717330
C	-1.945610	-0.187910	0.634730
C	-1.844190	-0.143550	-0.775040
N	-3.269110	0.209010	0.893150
N	-3.019610	0.249720	-1.335650
C	-3.845750	0.468020	-0.312260
H	1.897290	-2.608500	1.028660
H	3.770920	-2.118670	-0.514470
H	2.204030	1.931950	-1.025230
H	0.309560	1.372900	0.419970
H	-4.882120	0.827950	-0.396290
C	-3.866930	0.322990	2.210950
H	-4.951590	0.099090	2.146650
H	-3.359770	-0.403530	2.878510
H	-3.728420	1.344130	2.631370
H	-0.971490	-0.401740	-1.388190
N	4.186790	0.243840	-1.792310
C	5.216780	-0.744190	-2.050260
H	4.796880	-1.673080	-2.504140
H	5.957410	-0.325890	-2.760290
H	5.762100	-1.039360	-1.120800
C	4.293300	1.567420	-2.375680
H	5.172650	1.602250	-3.048960
H	3.392580	1.827490	-2.980770
H	4.423290	2.363520	-1.602380

***trans*-α**

$E_{PBE/SVP}$ = -738.5517782074 Hartree

NImag = 0

C	-0.297400	0.587150	-0.277810
C	-1.636860	0.752200	-0.703390
C	-2.566680	-0.281620	-0.609940
C	-2.195580	-1.552270	-0.077340
C	-0.840480	-1.713470	0.355060
C	0.077290	-0.673680	0.255150
N	0.544510	1.692870	-0.419560
N	1.755430	1.516640	-0.036460
C	2.570010	2.612460	-0.177690
C	2.433750	3.935370	-0.640460
N	3.907670	2.504900	0.208990
N	3.617750	4.602580	-0.544400
C	4.477970	3.722430	-0.034080
H	-1.924300	1.733190	-1.114620
H	-3.594320	-0.100230	-0.954320
H	-0.505480	-2.672240	0.776530
H	1.117290	-0.807310	0.590260
H	5.539410	3.917260	0.182020
C	4.541370	1.321550	0.758910
H	4.046080	1.014860	1.704450
H	4.475700	0.474050	0.044240
H	5.607770	1.550760	0.960270
H	1.518490	4.399300	-1.029870
N	-3.106420	-2.587450	0.019010
C	-4.476190	-2.391130	-0.417290
H	-5.045970	-3.330190	-0.273660
H	-4.990200	-1.586170	0.161400
H	-4.533860	-2.118990	-1.498150
C	-2.705780	-3.863060	0.582660
H	-3.569000	-4.557370	0.568050
H	-1.878920	-4.335980	0.001070
H	-2.363040	-3.766410	1.640950

***trans*-β**

$E_{PBE/SVP}$ = -738.5519143641 Hartree

NImag = 0

C	0.139140	0.188940	0.020820
C	0.799530	-0.957120	0.520810
C	0.190660	-2.211340	0.518350
C	-1.130490	-2.381490	0.007480
C	-1.794350	-1.217680	-0.495280
C	-1.175090	0.027320	-0.487690
N	0.840620	1.399850	0.069060
N	0.208660	2.412840	-0.401340
C	0.853140	3.617930	-0.373860
C	0.333550	4.838450	-0.842180
N	2.136860	3.940000	0.104530
N	1.223060	5.853920	-0.671890
C	2.283510	5.283960	-0.106520
H	1.820710	-0.833620	0.916780
H	0.749190	-3.069240	0.918350
H	-2.814660	-1.293680	-0.898490
H	-1.692080	0.917880	-0.876780
H	-0.658570	4.982240	-1.291970
H	3.209820	5.806880	0.179950
C	3.135110	3.069520	0.704560
H	2.739250	2.588960	1.621530
H	3.426190	2.261400	0.003870
H	4.023490	3.687900	0.956520
N	-1.746420	-3.618940	-0.002670
C	-1.047020	-4.780730	0.511960
H	-1.697640	-5.672630	0.419440
H	-0.104340	-4.985370	-0.050690
H	-0.777940	-4.664190	1.589270
C	-3.089680	-3.761400	-0.532240
H	-3.402250	-4.821900	-0.459090
H	-3.830940	-3.147350	0.033110
H	-3.151030	-3.461320	-1.605670

I.5.9 1-Methyl-2',5'-dimethyl-4'-methoxyphenylazoimidazole (2d)

***cis*-α**

$E_{PBE/SVP}$ = -797.5971301712 Hartree

NImag = 0

C	0.983500	-0.442980	0.833740
C	1.765600	-1.489730	0.309960
C	2.723460	-1.249700	-0.692500
C	2.923320	0.084270	-1.123430
C	2.161830	1.158430	-0.595850
C	1.189660	0.877010	0.376420
N	0.102380	-0.719920	1.915550
N	-1.143850	-0.507510	1.858260
C	-1.853420	-0.166970	0.718440
C	-1.690640	-0.172490	-0.686960
N	-3.219330	0.104200	0.907190
N	-2.871590	0.077010	-1.309590
C	-3.761470	0.250950	-0.329680
H	1.600400	-2.513270	0.684180
H	0.584300	1.697220	0.795780
H	-4.825280	0.492580	-0.474560
C	-3.885970	0.229740	2.192570
H	-4.921240	-0.160820	2.113890
H	-3.307870	-0.356160	2.935160
H	-3.918100	1.290730	2.525240
H	-0.770420	-0.366360	-1.251850
C	3.517350	-2.382430	-1.297790
H	3.775850	-2.162700	-2.355160
H	4.474640	-2.554370	-0.752510
H	2.946680	-3.334530	-1.260200
C	2.388610	2.562720	-1.101380
H	3.385810	2.955240	-0.797840
H	2.361010	2.596050	-2.212260
H	1.619230	3.258950	-0.706680
O	3.834740	0.356880	-2.126780
C	5.181660	0.519160	-1.704580
H	5.593490	-0.412290	-1.247480
H	5.773120	0.765190	-2.611310
H	5.287440	1.350110	-0.966100

***cis*-β**

$E_{PBE/SVP}$ = -797.5892489900 Hartree

NImag = 0

C	0.544920	0.458670	1.190080
C	-0.127270	1.266640	2.136070
C	-1.149660	0.748550	2.942730
C	-1.456030	-0.633220	2.835680
C	-0.780260	-1.476510	1.916870
C	0.208490	-0.912260	1.092560
N	1.647920	1.040200	0.521120
N	2.021920	0.745670	-0.654330
C	1.291820	0.068410	-1.616900
C	1.842320	-0.752680	-2.617570
N	-0.081790	0.120780	-1.915810
N	0.877020	-1.222750	-3.454700
C	-0.248780	-0.661120	-3.030730
H	0.169170	2.325190	2.219260
H	0.742290	-1.557290	0.375930
H	2.900620	-1.032450	-2.709100
C	-1.226960	-0.737050	-3.530510
H	-1.104820	0.975650	-1.335000
H	-1.889830	1.158240	-2.098040
H	-1.561420	0.513600	-0.434230
H	-0.661950	1.949510	-1.042830
C	-1.135850	-2.940340	1.810760
H	-0.564330	-3.558150	2.541550
H	-2.215000	-3.102310	2.017250
H	-0.901980	-3.335200	0.799360
C	-1.915500	1.617370	3.910920
H	-3.011330	1.540380	3.737950
H	-1.742120	1.311230	4.967260
H	-1.615470	2.681780	3.815100
O	-2.480680	-1.136620	3.611150
C	-2.088010	-1.783480	4.815470
H	-3.021830	-2.091100	5.330480
H	-1.467470	-2.690280	4.621740
H	-1.513030	-1.097930	5.482840

***trans*-α**

$E_{PBE/SVP}$ = -797.6172430495 Hartree

NImag = 0

C	-0.991190	-0.585320	-0.063510
C	-2.392290	-0.417770	-0.070260
C	-3.265430	-1.517670	-0.069300
C	-2.694900	-2.814270	-0.071760
C	-1.286670	-3.015230	-0.042210
C	-0.450390	-1.893920	-0.040790
N	-0.236680	0.601480	-0.068960
N	1.031130	0.441790	-0.021030
C	1.762910	1.601730	-0.041790
C	1.488060	2.980390	-0.133560
N	3.155070	1.517260	0.033320
N	2.641520	3.700920	-0.115930
C	3.619230	2.799300	-0.014150
H	-2.782250	0.613200	-0.062270
H	0.644600	-2.007600	-0.020360
H	4.694880	3.027430	0.030190
C	3.930220	0.295290	0.148330
H	3.659810	-0.254100	1.074720
H	3.738760	-0.371160	-0.718610
H	5.006740	0.559850	0.178960
H	0.496440	3.444180	-0.213640
C	-0.735740	-4.419930	0.008040
H	-1.018860	-5.009600	-0.892920
H	0.372450	-4.409190	0.073210
H	-1.135460	-4.976640	0.884280
C	-4.763220	-1.328780	-0.036000
H	-5.030150	-0.371100	0.459270
H	-5.202740	-1.298540	-1.060050
H	-5.256040	-2.160760	0.510370
O	-3.504220	-3.930100	-0.024400
C	-4.062220	-4.348700	-1.262880
H	-3.268720	-4.595130	-2.008560
H	-4.656500	-5.262080	-1.051550
H	-4.734350	-3.575820	-1.705370

***trans*-β**

$E_{PBE/SVP}$ = -797.6175565840 Hartree

NImag = 0

C	0.093480	0.116290	0.155110
C	0.796880	-1.105870	0.119110
C	0.126190	-2.340070	0.105410
C	-1.290100	-2.323350	0.125050
C	-2.025720	-1.107650	0.187560
C	-1.320950	0.101060	0.197770
N	0.881410	1.285050	0.162580
N	0.218070	2.379560	0.188770
C	0.931630	3.544120	0.196840
C	0.384940	4.840760	0.219580
N	2.324570	3.745560	0.183670
N	1.359500	5.787750	0.220370
C	2.499740	5.100630	0.198930
H	1.898770	-1.067200	0.113320
H	-1.850250	1.065450	0.244530
H	-0.686240	5.084900	0.234560
C	3.507930	5.544690	0.193590
H	3.392250	2.757640	0.161430
H	3.333450	2.095600	1.048380
H	3.316330	2.116950	-0.739680
H	4.361990	3.299550	0.158900
C	0.884850	-3.645810	0.098870
H	1.046370	-4.028680	-0.935850
H	1.887830	-3.524600	0.560240
H	0.329360	-4.429700	0.656230
C	-3.532710	-1.149300	0.263980
H	-3.950570	-0.130260	0.400430
H	-3.982390	-1.580710	-0.658860
H	-3.873190	-1.789030	1.107540
O	-1.995240	-3.509020	0.165680
C	-2.214230	-4.144840	-1.086630
H	-2.815760	-5.054710	-0.880860
H	-2.779380	-3.486670	-1.789150
H	-1.258800	-4.448120	-1.577370

I.5.10 1-Methyl-2',5'-di-tert-butyl-4'-methoxyphenylazoimidazole (2e)

***cis*-α**

$E_{PBE/SVP}$ = -1032.917950750 Hartree

NImag = 0

C	1.153400	-0.373980	0.846120
C	1.882430	-1.431930	0.287070
C	2.787170	-1.236790	-0.778180
C	3.049850	0.113080	-1.156030
C	2.260470	1.207010	-0.668960
C	1.320350	0.929040	0.335210
N	0.348480	-0.630320	1.989590
N	-0.889240	-0.369910	2.037170
C	-1.682320	0.001510	0.963320
C	-1.646970	-0.013500	-0.450900
N	-3.015500	0.321230	1.271450
N	-2.869580	0.276090	-0.967210
C	-3.661180	0.484310	0.087200
H	1.700790	-2.438620	0.693530
H	0.704310	1.731710	0.761470
H	-4.724070	0.764330	0.037060
C	-3.560130	0.469410	2.610550
H	-4.609330	0.109390	2.627390
H	-2.934410	-0.131910	3.300360
H	-3.531660	1.531610	2.939780
H	-0.788280	-0.242280	-1.094350
C	3.366180	-2.514540	-1.454720
C	2.350380	2.631880	-1.278780
O	4.080590	0.406210	-2.032360
C	5.377570	0.384660	-1.447550
H	5.652230	-0.626440	-1.067200
H	6.090830	0.674210	-2.247340
H	5.459070	1.108470	-0.603480
C	2.187080	-3.487920	-1.738640
H	1.667070	-3.821840	-0.816570
H	1.431730	-3.013690	-2.403670
H	2.570000	-4.399590	-2.248490
C	4.049720	-2.285210	-2.823800
H	5.027720	-1.771670	-2.751760
H	4.238640	-3.277520	-3.291490
H	3.405780	-1.700180	-3.513010
C	4.360980	-3.217140	-0.498060
H	5.242580	-2.575330	-0.279190
H	3.883220	-3.472200	0.473460
H	4.733360	-4.162350	-0.953760
C	3.727570	3.297380	-1.036950
H	4.531230	2.816650	-1.627730
H	3.685280	4.366310	-1.345050
H	4.007590	3.267430	0.039490
C	2.078010	2.541980	-2.802460
H	2.129840	3.556100	-3.259680
H	2.823290	1.893020	-3.305930
H	1.062250	2.132110	-2.997970
C	1.283770	3.572960	-0.675220
H	0.251480	3.186950	-0.822350
H	1.442500	3.748320	0.411860
H	1.343160	4.561210	-1.181230

***cis*-β**

$E_{PBE/SVP}$ = -1032.909522557 Hartree

NImag = 0

C	1.599780	0.940390	-0.452540
C	0.881550	1.762000	0.438070
C	-0.174150	1.267180	1.217060
C	-0.442880	-0.141470	1.149640
C	0.214310	-0.992430	0.202020
C	1.241910	-0.416390	-0.570640
N	2.745620	1.503840	-1.063100
N	3.184540	1.195560	-2.212320
C	2.503720	0.517470	-3.211190
C	3.098430	-0.324490	-4.167990
N	1.153290	0.595210	-3.596200
N	2.177650	-0.782030	-5.060960
C	1.039780	-0.193670	-4.713820
H	1.190500	2.814570	0.493180
H	1.803040	-1.038770	-1.279630
H	4.154440	-0.626010	-4.191610
C	0.093860	-0.252670	-5.274270
H	0.114040	1.473320	-3.083550
H	-0.618810	1.667710	-3.894130
H	-0.406200	1.025270	-2.210290
H	0.557860	2.439590	-2.768320
C	-0.137740	-2.486750	-0.061240
C	-1.016140	2.241470	2.083940
O	-1.415340	-0.627160	2.002220
C	-1.021240	-1.375910	3.145780
H	-1.716400	-1.114870	3.973560
H	-1.102940	-2.472510	2.963840
H	0.019630	-1.134330	3.456440
C	0.689730	-3.402910	0.876610
H	0.483180	-3.219300	1.950470
H	0.463890	-4.472920	0.665470
H	1.778990	-3.245250	0.714210
C	0.228510	-2.888820	-1.515270
H	-0.237060	-2.207730	-2.261220
H	1.323150	-2.908530	-1.701980
H	-0.145040	-3.916910	-1.714250
C	-1.653070	-2.775110	0.078120
H	-1.852960	-3.833380	-0.201340
H	-2.047960	-2.607910	1.096820
H	-2.239400	-2.127530	-0.610850
C	-0.604590	3.711800	1.843750
H	0.437910	3.920790	2.169520
H	-0.701620	4.004530	0.775590
H	-1.272880	4.376360	2.433700
C	-0.828470	1.968990	3.596890
H	-1.259620	0.999370	3.910040
H	0.249130	1.981440	3.872970
H	-1.338450	2.763010	4.187780
C	-2.513470	2.119390	1.702580
H	-2.890910	1.089670	1.863510
H	-3.121150	2.819570	2.319300
H	-2.669950	2.387250	0.633640

***trans*-α**

$E_{PBE/SVP}$ = -1032.937999150 Hartree

NImag = 0

C	-1.034030	-0.634860	-0.148690
C	-2.431340	-0.490610	-0.141530
C	-3.308430	-1.590700	-0.101320
C	-2.706320	-2.887630	-0.142820
C	-1.282840	-3.070710	-0.035640
C	-0.476150	-1.927110	-0.054990
N	-0.297780	0.561680	-0.209960
N	0.972360	0.423170	-0.164090
C	1.687690	1.591290	-0.238410
C	1.392410	2.961040	-0.383660
N	3.081370	1.529690	-0.169370
N	2.535480	3.698150	-0.402430
C	3.526640	2.815380	-0.271370
H	-2.806120	0.541900	-0.154600
H	0.617890	-1.991040	-0.003570
H	4.599170	3.060250	-0.243530
C	3.875390	0.324940	-0.010530
H	3.619360	-0.190700	0.939100
H	3.688550	-0.378930	-0.848460
H	4.948040	0.606330	0.001950
H	0.393770	3.407240	-0.475240
C	-0.636300	-4.471060	0.140900
C	-4.833560	-1.305010	0.014720
O	-3.469320	-4.036040	-0.217880
C	-4.066720	-4.383180	-1.461140
H	-4.049680	-5.492230	-1.541690
H	-5.129610	-4.052070	-1.512780
H	-3.507820	-3.948910	-2.320100
C	-1.242990	-5.179770	1.378290
H	-2.338020	-5.313920	1.273550
H	-0.775170	-6.182020	1.509510
H	-1.048990	-4.590330	2.301820
C	-0.825690	-5.348890	-1.121060
H	-0.244010	-6.292220	-1.014850
H	-1.883180	-5.631130	-1.284480
H	-0.456240	-4.824730	-2.030570
C	0.886410	-4.361400	0.381530
H	1.422540	-3.933030	-0.493330
H	1.124710	-3.743480	1.274500
H	1.300730	-5.378360	0.558760
C	-5.579620	-2.368510	0.856800
H	-6.642640	-2.061910	0.976330
H	-5.563050	-3.381340	0.414630
H	-5.133130	-2.445990	1.872620
C	-5.465160	-1.171820	-1.394520
H	-4.973760	-0.353560	-1.965490
H	-5.374270	-2.098670	-1.996380
H	-6.548220	-0.927190	-1.308800
C	-5.072980	0.044890	0.742780
H	-4.551750	0.077750	1.724230
H	-4.744850	0.922530	0.146540
H	-6.162270	0.172340	0.927420

***trans*-β**

$E_{PBE/SVP}$ = -1032.938097054 Hartree

NImag = 0

C	0.623010	0.984970	0.026620
C	1.340320	-0.222930	0.101470
C	0.696000	-1.469710	0.100100
C	-0.732750	-1.470360	-0.011870
C	-1.500590	-0.257940	0.047400
C	-0.783600	0.949400	0.032440
N	1.392340	2.166210	-0.003610
N	0.712110	3.248500	-0.064830
C	1.403690	4.425700	-0.099870
C	0.832480	5.710390	-0.162220
N	2.792270	4.654150	-0.085710
N	1.788770	6.675640	-0.185330
C	2.941790	6.011510	-0.138910
H	2.434050	-0.139570	0.155290
H	-1.295300	1.920650	0.041360
H	-0.243080	5.933610	-0.188940
C	3.941320	6.474750	-0.141870
H	3.878280	3.687730	-0.031620
H	3.811670	3.071960	0.887430
H	3.835430	2.999500	-0.899440
H	4.837610	4.247760	-0.041950
C	1.524780	-2.772030	0.260150
C	-3.051380	-0.182770	0.157910
O	-1.343700	-2.705940	-0.103030
C	-1.882600	-3.117360	-1.353180
H	-1.709940	-4.212000	-1.448760
H	-2.981600	-2.938130	-1.404350
H	-1.388660	-2.597770	-2.204300
C	-3.651020	-1.343370	0.988840
H	-4.745970	-1.183650	1.105660
H	-3.496520	-2.341300	0.539440
H	-3.201870	-1.367990	2.006090
C	-3.476660	1.117520	0.890720
H	-2.971410	1.214780	1.876510
H	-3.266810	2.035150	0.301580
H	-4.574120	1.093970	1.068340
C	-3.686680	-0.127080	-1.255200
H	-3.309710	0.756160	-1.816440
H	-3.466130	-1.027630	-1.863180
H	-4.793560	-0.035000	-1.175120
C	3.018400	-2.463880	0.510350
H	3.496210	-1.955650	-0.355480
H	3.170670	-1.833490	1.413560
H	3.563630	-3.419100	0.674820
C	1.013900	-3.572380	1.485150
H	-0.052900	-3.851180	1.372330
H	1.611870	-4.503940	1.606840
H	1.122210	-2.973970	2.417020
C	1.458500	-3.649530	-1.013890
H	0.447300	-4.063280	-1.188960
H	1.761630	-3.069480	-1.913960
H	2.156320	-4.511600	-0.915400

I.6 XYZ Coordinates of the PBE/SVP optimized Complexes

I.6.1 Ni-tetrakis(pentafluorophenyl)porphyrin ($NiTPPF_{20}$)

$NiTPPF_{20}$

$E_{PBE/SVP}$ = -5398.245789419 Hartree

NImag = 0

C	-1.039060	-0.362540	2.768340
N	0.000000	0.000000	1.929800
C	-0.635480	-0.254800	4.152410
C	0.635480	0.254800	4.152410
C	1.039060	0.362540	2.768340
C	-2.349800	-0.635580	2.350540
C	-2.762280	-0.365800	1.037210
C	-4.146820	-0.251040	0.637610
C	-4.146820	0.251040	-0.637610
C	-2.762280	0.365800	-1.037210
N	-1.924810	0.000000	0.000000
Ni	0.000000	0.000000	0.000000
N	1.924810	0.000000	0.000000
C	2.762280	-0.365800	-1.037210
C	4.146820	-0.251040	-0.637610
C	4.146820	0.251040	0.637610
C	2.762280	0.365800	1.037210
C	-2.349800	0.635580	-2.350540
C	-1.039060	0.362540	-2.768340
C	-0.635480	0.254800	-4.152410
C	0.635480	-0.254800	-4.152410
C	1.039060	-0.362540	-2.768340
N	0.000000	0.000000	-1.929800
C	2.349800	-0.635580	-2.350540
C	2.349800	0.635580	2.350540
H	-5.006740	0.487190	-1.275960
H	-5.006740	-0.487190	1.275960
H	-1.264900	0.501130	-5.015460
H	1.264900	-0.501130	-5.015460
H	5.006740	0.487190	1.275960
H	5.006740	-0.487190	-1.275960
H	-1.264900	-0.501130	5.015460
H	1.264900	0.501130	5.015460
C	-3.362670	-1.098680	3.342960
C	3.362670	1.098680	3.342960
C	-3.362670	1.098680	-3.342960
C	3.362670	-1.098680	-3.342960
C	3.795070	-2.439320	-3.342850
C	4.744150	-2.908990	-4.265610
C	5.284020	-2.023030	-5.213200
C	4.876940	-0.677700	-5.230750
C	3.925960	-0.231340	-4.298080
F	3.294950	-3.302250	-2.454020
F	5.130880	-4.185950	-4.252360
F	6.182370	-2.460390	-6.094600
F	5.395120	0.164920	-6.126810
F	3.559020	1.054240	-4.333320
C	3.925960	0.231340	4.298080
C	4.876940	0.677700	5.230750
C	5.284020	2.023030	5.213200
C	4.744150	2.908990	4.265610

C	3.795070	2.439320	3.342850
F	3.559020	-1.054240	4.333320
F	5.395120	-0.164920	6.126810
F	6.182370	2.460390	6.094600
F	5.130880	4.185950	4.252360
F	3.294950	3.302250	2.454020
C	-3.925960	0.231340	-4.298080
C	-4.876940	0.677700	-5.230750
C	-5.284020	2.023030	-5.213200
C	-4.744150	2.908990	-4.265610
C	-3.795070	2.439320	-3.342850
F	-3.559020	-1.054240	-4.333320
F	-5.395120	-0.164920	-6.126810
F	-6.182370	2.460390	-6.094600
F	-5.130880	4.185950	-4.252360
F	-3.294950	3.302250	-2.454020
C	-3.925960	-0.231340	4.298080
C	-4.876940	-0.677700	5.230750
C	-5.284020	-2.023030	5.213200
C	-4.744150	-2.908990	4.265610
C	-3.795070	-2.439320	3.342850
F	-3.559020	1.054240	4.333320
F	-5.395120	0.164920	6.126810
F	-6.182370	-2.460390	6.094600
F	-5.130880	-4.185950	4.252360
F	-3.294950	-3.302250	2.454020

I.6.2 5-Phenylazoimidazole · $NiTPPF_{20}$

***cis*-α**

$E_{PBE/SVP}$ = -5963.873770674 Hartree

NImag = 0

C	2.635940	-2.589100	3.550880
C	2.524650	-3.991500	3.433470
C	3.406980	-4.696020	2.603330
C	4.442800	-4.021010	1.934840
C	4.581110	-2.629390	2.085750
C	3.676600	-1.908310	2.875290
N	1.803890	-1.923640	4.489570
N	1.081080	-0.929250	4.208350
C	0.823680	-0.452850	2.923100
C	0.887110	-0.867120	1.581100
N	0.131030	0.755790	2.879860
N	0.264080	0.061740	0.792940
C	-0.174370	1.040370	1.597830
H	1.726940	-4.510470	3.987420
H	3.280470	-5.783900	2.478610
H	5.150470	-4.580970	1.302330
H	5.398720	-2.089540	1.582060
H	3.786800	-0.817960	2.988400
H	1.326010	-1.777810	1.159950
H	-0.681170	1.956350	1.268350
H	-0.095070	1.299170	3.718020
C	1.360320	2.901510	-1.348620
N	1.538650	1.543740	-1.481940
C	2.645450	3.581030	-1.334160
C	3.602130	2.610980	-1.480550
C	2.897240	1.343420	-1.564270
C	0.110110	3.554650	-1.264530
C	-1.146440	2.907540	-1.315460
C	-2.421330	3.603540	-1.321900
C	-3.394990	2.639100	-1.348900
C	-2.711740	1.358090	-1.363510
N	-1.346270	1.544780	-1.354240
Ni	0.099910	0.087640	-1.244480
N	1.512900	-1.343550	-1.647880
C	1.313180	-2.704330	-1.704130
C	2.574030	-3.391850	-1.920570
C	3.542570	-2.424000	-1.978980
C	2.868520	-1.150610	-1.796230
C	-3.370650	0.108870	-1.359680
C	-2.724790	-1.146490	-1.383740
C	-3.421500	-2.422420	-1.377110
C	-2.457480	-3.394970	-1.413980
C	-1.178760	-2.707320	-1.466570
N	-1.364420	-1.343880	-1.440660
C	0.068230	-3.358750	-1.570950
C	3.530760	0.094390	-1.734250
H	-4.481920	2.785170	-1.361140
H	-2.556710	4.692010	-1.323720
H	-4.509810	-2.557430	-1.358000
H	-2.600420	-4.482480	-1.422560
H	4.619510	-2.561650	-2.134810
H	2.700650	-4.476070	-2.028220
H	2.798650	4.662460	-1.234780

***cis*-β**

$E_{PBE/SVP}$ = -5963.871248498 Hartree

NImag = 0

C	0.105230	-0.163330	5.856110
C	-0.637950	0.959990	6.284140
C	-1.920760	0.782700	6.824390
C	-2.468520	-0.505190	6.959120
C	-1.719510	-1.622910	6.551910
C	-0.437720	-1.461130	6.003470
N	1.445440	0.005010	5.401660
N	1.767350	0.057290	4.181600
C	0.888250	0.002370	3.113580
C	1.291260	0.072150	1.774470
N	-0.512800	-0.099880	3.054210
N	0.200130	0.012800	0.958440
C	-0.874700	-0.089810	1.752700
H	-0.195700	1.964570	6.189910
H	-2.497370	1.664690	7.148900
H	-3.473370	-0.638040	7.390770
H	-2.135360	-2.637880	6.664280
H	0.158930	-2.333770	5.692700
H	2.317500	0.166960	1.398650
H	-1.915210	-0.162090	1.405530
H	-1.136390	-0.181130	3.863030
C	1.411800	2.860110	-1.318930
N	1.600200	1.496020	-1.319180
C	2.691640	3.546540	-1.360850
C	3.656850	2.575030	-1.389450
C	2.962370	1.299430	-1.356310
C	0.161900	3.516260	-1.284630
C	-1.092070	2.866970	-1.259070
C	-2.367770	3.562030	-1.254870
C	-3.340320	2.597420	-1.222450
C	-2.653740	1.317280	-1.225910
N	-1.289660	1.504510	-1.249160
Ni	0.159470	0.052890	-1.078010
N	1.593360	-1.392840	-1.355040
C	1.395010	-2.754810	-1.382030
C	2.669450	-3.450060	-1.441290
C	3.642460	-2.486010	-1.431680
C	2.956830	-1.205850	-1.383260
C	-3.307560	0.065460	-1.212420
C	-2.659920	-1.189240	-1.263140
C	-3.355190	-2.463990	-1.300410
C	-2.388860	-3.435050	-1.342360
C	-1.108920	-2.748630	-1.336420
N	-1.297240	-1.385170	-1.292000
C	0.141450	-3.403790	-1.369430
C	3.611750	0.045270	-1.369990
H	-4.427450	2.742170	-1.209540
H	-2.503930	4.649960	-1.284460
H	-4.443730	-2.599370	-1.309600
H	-2.531980	-4.521840	-1.379270
H	4.729200	-2.630170	-1.461720
H	2.803390	-4.537460	-1.492520
H	2.835490	4.633730	-1.369680

H	4.690060	2.741950	-1.534100	H	4.744080	2.710390	-1.440740
C	0.101240	5.037410	-1.085940	C	0.163620	5.010920	-1.275560
C	5.021210	0.073620	-1.851670	C	5.105740	0.045150	-1.348380
C	-4.865370	0.115810	-1.329710	C	-4.799020	0.063770	-1.120620
C	0.100470	-4.850670	-1.490150	C	0.139850	-4.898670	-1.389720
C	0.570690	-5.474110	-0.318560	C	0.504680	-5.641840	-0.250720
C	0.679360	-6.868620	-0.207170	C	0.510790	-7.046770	-0.253710
C	0.288050	-7.676800	-1.288460	C	0.146440	-7.736700	-1.422480
C	-0.199480	-7.083920	-2.466460	C	-0.221870	-7.021650	-2.574770
C	-0.291960	-5.683590	-2.554160	C	-0.221770	-5.616430	-2.546060
F	0.940230	-4.727010	0.730240	F	0.855050	-5.008730	0.875380
F	1.147490	-7.426490	0.914800	F	0.854510	-7.730210	0.841040
F	0.381550	-9.003410	-1.198910	F	0.149230	-9.069820	-1.437490
F	-0.565420	-7.852540	-3.494550	F	-0.563480	-7.681670	-3.683900
F	-0.753300	-5.150790	-3.689630	F	-0.575740	-4.959320	-3.655150
C	-5.574350	-0.236390	-0.165270	C	-5.444890	-0.295610	0.077200
C	-6.978850	-0.238490	-0.124770	C	-6.843970	-0.310900	0.194490
C	-7.703180	0.120960	-1.274050	C	-7.630140	0.042840	-0.915880
C	-7.022610	0.478030	-2.450570	C	-7.014290	0.409240	-2.125050
C	-5.617350	0.472550	-2.465770	C	-5.611650	0.416540	-2.214810
F	-4.907380	-0.580900	0.942790	F	-4.716410	-0.630660	1.155130
F	-7.629330	-0.572790	0.992780	F	-7.430140	-0.651460	1.345660
F	-9.036070	0.123390	-1.248080	F	-8.959610	0.033230	-0.820580
F	-7.714820	0.815560	-3.540930	F	-7.763090	0.743100	-3.177690
F	-4.994220	0.816610	-3.597690	F	-5.053860	0.770240	-3.376530
C	5.845370	0.159990	-0.715210	C	5.806790	0.392790	-0.177700
C	7.244110	0.074750	-0.802710	C	7.210590	0.400470	-0.127910
C	7.847850	-0.078650	-2.062400	C	7.941610	0.053080	-1.277170
C	7.050740	-0.155410	-3.217550	C	7.269070	-0.300020	-2.459600
C	5.652210	-0.080760	-3.100520	C	5.863890	-0.299490	-2.483450
F	5.297680	0.296210	0.502320	F	5.130070	0.721910	0.931330
F	7.997720	0.122770	0.299080	F	7.854200	0.728970	0.994480
F	9.174840	-0.156470	-2.161040	F	9.274240	0.056210	-1.244560
F	7.625150	-0.301020	-4.413400	F	7.968670	-0.627740	-3.548120
F	4.917690	-0.167220	-4.213250	F	5.247900	-0.637700	-3.621030
C	0.499790	5.919120	-2.109720	C	0.515990	5.751390	-2.420790
C	0.465290	7.313960	-1.941220	C	0.517960	7.156770	-2.421830
C	0.024670	7.854700	-0.721040	C	0.159550	7.850060	-1.253270
C	-0.377090	7.000000	0.320200	C	-0.197270	7.137900	-0.095640
C	-0.328360	5.610580	0.127110	C	-0.191220	5.733190	-0.119650
F	0.917700	5.437850	-3.284290	F	0.858470	5.116890	-3.546790
F	0.841620	8.125460	-2.931720	F	0.851840	7.837330	-3.520670
F	-0.013710	9.176080	-0.551260	F	0.157670	9.183160	-1.242790
F	-0.794040	7.510940	1.481380	F	-0.533400	7.800320	1.014440
F	-0.708650	4.822110	1.146140	F	-0.533670	5.079370	0.997170

***trans*-α**

$E_{PBE/SVP}$ = -5963.893533912 Hartree

NImag = 0

C	-3.078050	-0.335400	5.183830
C	-4.468830	-0.464180	4.955840
C	-5.350110	-0.573550	6.039240
C	-4.851750	-0.555670	7.353380
C	-3.466350	-0.426440	7.584160
C	-2.579310	-0.316710	6.510550
N	-2.288580	-0.238000	4.025990
N	-1.031350	-0.121510	4.211640
C	-0.314990	-0.039610	3.038790
C	-0.640360	-0.060580	1.678920
N	1.068640	0.091050	3.077740
N	0.504550	0.051440	0.942060
C	1.527540	0.142790	1.802910
H	-4.823010	-0.475320	3.912320
H	-6.432940	-0.674450	5.859670
H	-5.544270	-0.643020	8.206790
H	-3.082440	-0.412910	8.617890
H	-1.494020	-0.216080	6.663220
H	-1.636330	-0.153550	1.233370
H	2.585920	0.246810	1.528790
H	1.618830	0.136880	3.939050
C	1.825380	2.862410	-1.327860
N	2.015660	1.499110	-1.295950
C	3.104700	3.550510	-1.331690
C	4.072170	2.580120	-1.302400
C	3.378150	1.304200	-1.275630
C	0.573770	3.515990	-1.350760
C	-0.679100	2.865320	-1.355870
C	-1.955400	3.559400	-1.384070
C	-2.926870	2.594270	-1.349850
C	-2.238550	1.314760	-1.323500
N	-0.875190	1.503130	-1.333130
Ni	0.567550	0.056450	-1.090140
N	2.010790	-1.391130	-1.300670
C	1.814100	-2.753080	-1.334940
C	3.090620	-3.446830	-1.353020
C	4.062350	-2.482000	-1.308490
C	3.374390	-1.202600	-1.282250
C	-2.891390	0.062480	-1.290340
C	-2.242480	-1.190890	-1.323340
C	-2.937640	-2.466120	-1.346620
C	-1.971030	-3.436890	-1.370760
C	-0.690770	-2.749130	-1.362050
N	-0.879810	-1.385800	-1.340840
C	0.560640	-3.403580	-1.357930
C	4.026770	0.049580	-1.249130
H	-4.014120	2.737800	-1.352770
H	-2.091910	4.646750	-1.429650
H	-4.026450	-2.600040	-1.356420
H	-2.113540	-4.524190	-1.390240
H	5.149620	-2.626050	-1.304530
H	3.227710	-4.533840	-1.404440
H	3.246450	4.637820	-1.358380
H	5.160590	2.716660	-1.313710
C	0.573530	5.011000	-1.360660

***trans*-β**

$E_{PBE/SVP}$ = -5963.895992443 Hartree

NImag = 0

C	-1.153990	-0.161760	6.377810
C	-0.367390	-0.119130	7.551560
C	-0.975260	-0.189470	8.811530
C	-2.372670	-0.302020	8.908590
C	-3.161220	-0.344390	7.740380
C	-2.562870	-0.275460	6.479740
N	-0.448410	-0.084880	5.161710
N	-1.165360	-0.132900	4.104680
C	-0.433740	-0.053790	2.945810
C	-0.863990	-0.080650	1.616080
N	0.950060	0.073280	2.881170
N	0.225090	0.025900	0.792720
C	1.307300	0.117850	1.577940
H	0.724970	-0.030340	7.440000
H	-0.357990	-0.156060	9.723940
H	-2.854110	-0.356970	9.898880
H	-4.257320	-0.432480	7.822590
H	-3.155870	-0.307040	5.553380
H	-1.889460	-0.173660	1.238910
H	2.342340	0.218210	1.222850
H	1.533960	0.118170	3.722150
C	1.507980	2.840180	-1.468710
N	1.695890	1.476180	-1.450240
C	2.788370	3.526180	-1.475770
C	3.754400	2.554130	-1.462270
C	3.058560	1.279220	-1.440500
C	0.257600	3.496240	-1.479380
C	-0.996340	2.847580	-1.491390
C	-2.271040	3.543880	-1.533100
C	-3.244200	2.579880	-1.531490
C	-2.558370	1.299150	-1.505220
N	-1.194830	1.485530	-1.482230
Ni	0.241370	0.034950	-1.242700
N	1.687040	-1.414010	-1.458890
C	1.488760	-2.775980	-1.484360
C	2.764050	-3.471740	-1.502470
C	3.737260	-2.508010	-1.468080
C	3.051110	-1.227590	-1.446990
C	-3.213520	0.048210	-1.506680
C	-2.565360	-1.206560	-1.518640
C	-3.260940	-2.481220	-1.565300
C	-2.295810	-3.453460	-1.560000
C	-1.015450	-2.767930	-1.518950
N	-1.203250	-1.404100	-1.496870
C	0.234520	-3.424570	-1.505530
C	3.705760	0.023680	-1.420310
H	-4.331120	2.724550	-1.554030
H	-2.405010	4.631910	-1.568720
H	-4.348700	-2.615330	-1.609420
H	-2.439790	-4.540410	-1.584740
H	4.824340	-2.653460	-1.467670
H	2.899250	-4.559280	-1.546960
H	2.931940	4.613400	-1.493370
H	4.842900	2.689020	-1.480610
C	0.259680	4.991180	-1.479960

C	5.518520	0.050440	-1.165410	C	5.198040	0.021450	-1.345290
C	-4.381000	0.069810	-1.162530	C	-4.707440	0.048500	-1.474320
C	0.560810	-4.898170	-1.367660	C	0.233030	-4.919280	-1.514560
C	0.927280	-5.634350	-0.224210	C	0.592200	-5.654840	-0.368460
C	0.933620	-7.039260	-0.217820	C	0.599190	-7.059780	-0.361600
C	0.567800	-7.737190	-1.381250	C	0.240010	-7.758260	-1.526790
C	0.197970	-7.029800	-2.537670	C	-0.122400	-7.051410	-2.685900
C	0.198280	-5.624490	-2.518690	C	-0.122000	-5.646110	-2.667580
F	1.278920	-4.994720	0.897670	F	0.937690	-5.014440	0.754850
F	1.279070	-7.715430	0.881090	F	0.938840	-7.735410	0.739360
F	0.571070	-9.070560	-1.387420	F	0.243290	-9.091570	-1.532360
F	-0.143920	-7.697330	-3.642380	F	-0.458310	-7.719330	-3.792160
F	-0.155500	-4.975930	-3.633050	F	-0.468620	-4.998060	-3.784550
C	-4.994020	-0.208660	0.074050	C	-5.400690	-0.304800	-0.300940
C	-6.386590	-0.158630	0.242740	C	-6.804000	-0.313520	-0.241490
C	-7.202360	0.163680	-0.855390	C	-7.543250	0.039160	-1.383710
C	-6.619810	0.437700	-2.105190	C	-6.878740	0.397630	-2.569020
C	-5.222080	0.387530	-2.245210	C	-5.473650	0.398700	-2.602210
F	-4.242220	-0.514800	1.141570	F	-4.717080	-0.639750	0.802790
F	-6.936070	-0.406160	1.436860	F	-7.439590	-0.647330	0.884750
F	-8.526900	0.213440	-0.711400	F	-8.875810	0.035230	-1.341800
F	-7.395110	0.743940	-3.147700	F	-7.585680	0.729750	-3.651420
F	-4.695510	0.659840	-3.443140	F	-4.866190	0.743270	-3.742180
C	6.170690	0.386330	0.035880	C	5.858280	0.358920	-0.148910
C	7.570510	0.393140	0.146750	C	7.258590	0.360630	-0.045220
C	8.350160	0.052180	-0.972140	C	8.030880	0.016550	-1.168230
C	7.727650	-0.288520	-2.185330	C	7.400470	-0.326190	-2.376750
C	6.324700	-0.287040	-2.269070	C	5.997040	-0.319800	-2.453040
F	5.448450	0.708550	1.121370	F	5.142880	0.684040	0.940530
F	8.163890	0.710410	1.300940	F	7.859310	0.678330	1.104920
F	9.680200	0.052190	-0.881980	F	9.361330	0.012900	-1.085620
F	8.470700	-0.610220	-3.246060	F	8.136870	-0.651560	-3.440910
F	5.759750	-0.616040	-3.434790	F	5.424450	-0.650120	-3.614590
C	0.930510	5.736730	-2.513500	C	0.621280	5.723540	-2.627220
C	0.930060	7.142090	-2.532780	C	0.621440	7.128930	-2.638210
C	0.564150	7.849360	-1.375000	C	0.253830	7.829600	-1.476950
C	0.204060	7.151590	-0.209660	C	-0.110880	7.125210	-0.317030
C	0.211610	5.746590	-0.215630	C	-0.104690	5.720230	-0.331510
F	1.281580	5.087470	-3.628280	F	0.974510	5.080860	-3.745210
F	1.267940	7.809710	-3.638690	F	0.962730	7.802760	-3.739220
F	0.560020	9.182750	-1.381460	F	0.251220	9.162960	-1.475430
F	-0.137660	7.827940	0.890270	F	-0.454420	7.795310	0.786110
F	-0.134710	5.106290	0.907220	F	-0.455100	5.073290	0.786220

I.6.3 1-Methyl-5-phenylazoimidazole · $NiTPPF_{20}$ (2)

***cis*-α**

$E_{PBE/SVP}$ = -6003.099149714 Hartree

NImag = 0

C	2.066860	-2.320350	3.993330
C	1.967540	-3.727410	3.927060
C	2.853570	-4.455910	3.122110
C	3.883760	-3.798100	2.428430
C	4.012820	-2.400740	2.529600
C	3.104060	-1.658230	3.293090
N	1.226880	-1.636270	4.910680
N	0.550060	-0.611830	4.617520
C	0.324490	-0.126050	3.334540
C	0.300980	-0.611480	2.014390
N	-0.257210	1.147620	3.263960
N	-0.260260	0.329750	1.200640
C	-0.572060	1.381660	1.971950
H	1.174470	-4.230430	4.502120
H	2.735960	-5.548620	3.037470
H	4.594830	-4.375220	1.815330
H	4.826550	-1.873990	2.006140
H	3.207980	-0.563860	3.365150
H	0.635270	-1.582940	1.633490
H	-1.003880	2.325530	1.614530
C	0.805800	3.158480	-0.898590
N	0.990380	1.805960	-1.070970
C	2.088250	3.842990	-0.865940
C	3.048580	2.882910	-1.049280
C	2.349720	1.614430	-1.161160
C	-0.449960	3.800510	-0.795220
C	-1.701520	3.147330	-0.885540
C	-2.980170	3.836180	-0.904650
C	-3.946310	2.866990	-0.980910
C	-3.254340	1.590340	-1.002830
N	-1.891110	1.785040	-0.959470
Ni	-0.437900	0.336360	-0.834550
N	0.988390	-1.085260	-1.218040
C	0.801670	-2.448190	-1.249680
C	2.069850	-3.127920	-1.449600
C	3.028380	-2.151630	-1.530220
C	2.341640	-0.881920	-1.369700
C	-3.905000	0.337050	-1.024940
C	-3.251010	-0.914490	-1.028230
C	-3.939870	-2.194720	-1.032070
C	-2.969460	-3.161560	-1.028810
C	-1.693800	-2.466550	-1.052440
N	-1.888560	-1.104160	-1.043700
C	-0.440130	-3.110240	-1.121610
C	2.991580	0.370260	-1.332660
H	-5.033570	3.006490	-1.017510
H	-3.121470	4.923880	-0.885610
H	-5.027410	-2.336590	-1.044130
H	-3.106280	-4.249830	-1.030120
H	4.106460	-2.280340	-1.686510
H	2.207070	-4.212730	-1.536240
H	2.239310	4.921010	-0.733630
H	4.135750	3.020450	-1.102480

***cis*-β**

$E_{PBE/SVP}$ = -6003.091275671 Hartree

NImag = 0

C	0.553210	-1.459150	5.364500
C	-0.020030	-1.737060	6.629110
C	-0.609880	-2.981110	6.878670
C	-0.581350	-3.986560	5.894200
C	0.032500	-3.734230	4.654100
C	0.583300	-2.475380	4.375600
N	1.244450	-0.230280	5.238940
N	1.345120	0.445340	4.175020
C	0.578250	0.302050	3.024040
C	1.038620	0.545490	1.724370
N	-0.801630	0.058560	2.889910
N	0.006960	0.401910	0.840000
C	-1.085890	0.143300	1.562000
H	0.013250	-0.951190	7.400500
H	-1.073960	-3.180030	7.858690
H	-1.020280	-4.976230	6.100500
H	0.090260	-4.526760	3.890900
H	1.070080	-2.294300	3.404360
H	2.066120	0.772580	1.415280
H	-2.106110	0.052940	1.163880
C	1.306740	3.174770	-1.640080
N	1.511490	1.822020	-1.486680
C	2.578020	3.877820	-1.669240
C	3.554890	2.927460	-1.536570
C	2.875790	1.648060	-1.423870
C	0.049470	3.808160	-1.758630
C	-1.196050	3.142930	-1.720450
C	-2.479970	3.811600	-1.843350
C	-3.440030	2.840960	-1.735610
C	-2.737250	1.578700	-1.580230
N	-1.376010	1.786160	-1.570250
Ni	0.079220	0.381190	-1.197670
N	1.548020	-1.057160	-1.287360
C	1.366060	-2.415370	-1.168060
C	2.649080	-3.091890	-1.074650
C	3.609760	-2.115880	-1.119950
C	2.907870	-0.850040	-1.246180
C	-3.375600	0.322540	-1.474930
C	-2.711890	-0.922340	-1.407760
C	-3.388790	-2.205620	-1.337400
C	-2.408660	-3.158990	-1.235720
C	-1.139520	-2.452650	-1.254010
N	-1.346990	-1.097260	-1.376030
C	0.120190	-3.078260	-1.131380
C	3.543000	0.410000	-1.292300
H	-4.528180	2.970230	-1.776610
H	-2.630600	4.886740	-1.998320
H	-4.474590	-2.358750	-1.374040
H	-2.535830	-4.246210	-1.164330
H	4.698260	-2.242650	-1.074160
H	2.796540	-4.176320	-0.997910
H	2.708590	4.961400	-1.775640
H	4.641270	3.078120	-1.531430

C	-0.465400	5.270980	-0.536660	C	0.040340	5.289000	-1.961940
C	4.482100	0.360910	-1.456090	C	5.030990	0.448530	-1.160210
C	-5.400000	0.335410	-1.031910	C	-4.867020	0.317460	-1.380290
C	-0.399680	-4.600990	-1.027790	C	0.139020	-4.544430	-0.839480
C	0.066270	-5.213740	0.151050	C	0.388530	-4.985770	0.473260
C	0.179560	-6.607010	0.273580	C	0.406710	-6.345740	0.815450
C	-0.202980	-7.424970	-0.803480	C	0.177690	-7.307600	-0.183030
C	-0.685310	-6.842990	-1.988990	C	-0.067670	-6.898960	-1.505630
C	-0.781790	-5.443850	-2.087930	C	-0.091850	-5.527750	-1.818730
F	0.426540	-4.457850	1.196810	F	0.605360	-4.086850	1.446240
F	0.642150	-7.154800	1.402640	F	0.627280	-6.727110	2.079440
F	-0.105730	-8.750570	-0.702860	F	0.193100	-8.604620	0.122990
F	-1.043390	-7.620470	-3.013270	F	-0.276650	-7.815320	-2.453000
F	-1.237830	-4.921790	-3.230560	F	-0.341980	-5.171180	-3.081690
C	-6.135590	-0.024660	0.113560	C	-5.505050	0.071720	-0.149750
C	-7.540640	-0.031010	0.119580	C	-6.901530	0.108790	-0.012900
C	-8.238240	0.330430	-1.045520	C	-7.695370	0.394480	-1.137340
C	-7.530780	0.694770	-2.203720	C	-7.088700	0.638260	-2.381330
C	-6.125500	0.694000	-2.184470	C	-5.688140	0.591830	-2.490360
F	-5.495150	-0.370860	1.236460	F	-4.771950	-0.195370	0.946210
F	-8.217050	-0.371510	1.219610	F	-7.477350	-0.114560	1.171470
F	-9.571460	0.327980	-1.051750	F	-9.022560	0.436920	-1.022010
F	-8.198000	1.033790	-3.309370	F	-7.843520	0.912300	-3.446960
F	-5.475690	1.045100	-3.298980	F	-5.139090	0.828100	-3.685480
C	5.310590	0.406330	-0.320670	C	5.630920	0.908720	0.027890
C	6.709210	0.331260	-0.418210	C	7.025400	0.982000	0.176000
C	7.307450	0.229550	-1.685800	C	7.852790	0.582010	-0.887770
C	6.505390	0.191520	-2.839380	C	7.282660	0.112790	-2.083740
C	5.107350	0.262660	-2.713100	C	5.884200	0.047990	-2.205860
F	4.768090	0.497220	0.903640	F	4.865900	1.291170	1.059510
F	7.468670	0.349270	0.680370	F	7.566520	1.423480	1.313540
F	8.634350	0.160650	-1.793210	F	9.178330	0.647410	-0.761980
F	7.074660	0.088600	-4.042230	F	8.069800	-0.262210	-3.094790
F	4.367160	0.217100	-3.824070	F	5.370860	-0.402190	-3.355120
C	-0.022110	6.209370	-1.489510	C	0.500870	5.855720	-3.167390
C	-0.020320	7.589820	-1.225290	C	0.506920	7.244100	-3.380310
C	-0.484580	8.059580	0.015090	C	0.034990	8.100870	-2.371450
C	-0.941180	7.148800	0.983460	C	-0.435460	7.565040	-1.160540
C	-0.921810	5.775060	0.697660	C	-0.425490	6.173110	-0.969030
F	0.414530	5.796160	-2.682980	F	0.948260	5.066700	-4.149870
F	0.413570	8.455990	-2.142960	F	0.951100	7.751650	-4.532380
F	-0.490500	9.366570	0.275190	F	0.032510	9.420390	-2.562700
F	-1.378220	7.594070	2.163980	F	-0.882600	8.380560	-0.201820
F	-1.348750	4.930250	1.654300	F	-0.875260	5.695390	0.196990
C	-0.450720	2.052700	4.387440	C	-1.805670	-0.089660	3.935070
H	-0.953020	1.510930	5.214030	H	-1.847230	-1.135010	4.306050
H	0.525860	2.428970	4.758590	H	-1.565600	0.582230	4.783860
H	-1.069640	2.907590	4.049210	H	-2.792600	0.196290	3.517160

***trans*-α**

$E_{PBE/SVP}$ = -6003.118228453 Hartree

NImag = 0

C	-3.102740	-0.330900	5.057310
C	-4.495710	-0.447650	4.835260
C	-5.373610	-0.555830	5.921500
C	-4.870290	-0.549200	7.233840
C	-3.482930	-0.432810	7.459130
C	-2.599350	-0.323850	6.382410
N	-2.318900	-0.233490	3.895760
N	-1.059400	-0.120410	4.073430
C	-0.348910	-0.040600	2.898220
C	-0.695060	-0.068630	1.542590
N	1.040870	0.092940	2.930970
N	0.437090	0.041640	0.791500
C	1.467880	0.138550	1.643740
H	-4.854130	-0.450990	3.793120
H	-6.457890	-0.647330	5.745430
H	-5.560010	-0.635660	8.089600
H	-3.094480	-0.428770	8.491310
H	-1.512800	-0.233230	6.532470
H	-1.697890	-0.165560	1.113150
H	2.523260	0.244080	1.357150
C	1.749710	2.854070	-1.474900
N	1.940370	1.491010	-1.441420
C	3.028790	3.542740	-1.469930
C	3.996410	2.572730	-1.430920
C	3.302530	1.296560	-1.409440
C	0.497830	3.507100	-1.502160
C	-0.754930	2.856010	-1.505410
C	-2.031650	3.549550	-1.533000
C	-3.002660	2.584150	-1.493460
C	-2.313680	1.304980	-1.465270
N	-0.950520	1.493860	-1.478890
Ni	0.491910	0.047270	-1.238700
N	1.936320	-1.399240	-1.452240
C	1.740030	-2.760960	-1.493950
C	3.016840	-3.454390	-1.509050
C	3.988030	-2.489700	-1.452160
C	3.299580	-1.210500	-1.423540
C	-2.965910	0.052500	-1.428600
C	-2.316980	-1.200580	-1.465680
C	-3.011930	-2.475970	-1.489550
C	-2.045040	-3.446260	-1.522870
C	-0.764990	-2.757860	-1.517590
N	-0.954470	-1.394880	-1.490190
C	0.486780	-3.411680	-1.520800
C	3.951060	0.041890	-1.378490
H	-4.090010	2.727090	-1.494080
H	-2.168750	4.636710	-1.581770
H	-4.100770	-2.610090	-1.493670
H	-2.187100	-4.533570	-1.546010
H	5.075240	-2.633860	-1.442050
H	3.154460	-4.541080	-1.565690
H	3.170330	4.630100	-1.496590
H	5.084850	2.709740	-1.433510
C	0.497050	5.002090	-1.514180
C	5.441590	0.042570	-1.275920

***trans*-β**

$E_{PBE/SVP}$ = -6003.116744246 Hartree

NImag = 0

C	-1.270620	-0.203560	6.243670
C	-0.608360	-0.183760	7.492110
C	-1.341340	-0.271140	8.682910
C	-2.741700	-0.378390	8.637000
C	-3.406810	-0.398210	7.394160
C	-2.682680	-0.312010	6.202010
N	-0.442600	-0.110230	5.104760
N	-1.062150	-0.136850	3.987970
C	-0.302180	-0.049120	2.854100
C	-0.804950	-0.067280	1.545840
N	1.095200	0.073450	2.714470
N	0.224110	0.037950	0.658780
C	1.346660	0.120800	1.383810
H	0.490070	-0.098670	7.496610
H	-0.818940	-0.255720	9.653460
H	-3.320960	-0.447100	9.572440
H	-4.505880	-0.482470	7.362160
H	-3.178890	-0.325600	5.219870
H	-1.854830	-0.155110	1.240560
H	2.360660	0.217310	0.970540
C	2.121720	0.138780	3.748850
C	1.439520	2.850170	-1.633240
N	1.626800	1.486490	-1.611900
C	2.720510	3.535790	-1.640070
C	3.686310	2.563380	-1.617540
C	2.989320	1.289270	-1.596740
C	0.188780	3.506140	-1.637160
C	-1.065210	2.857180	-1.622900
C	-2.340730	3.553070	-1.647890
C	-3.313550	2.589510	-1.613660
C	-2.627390	1.308890	-1.586940
N	-1.263700	1.495390	-1.593920
Ni	0.174340	0.045530	-1.375050
N	1.616930	-1.404260	-1.613930
C	1.418640	-2.766070	-1.641380
C	2.693730	-3.461750	-1.671880
C	3.667200	-2.498080	-1.637160
C	2.980780	-1.217850	-1.606270
C	-3.282520	0.058130	-1.565090
C	-2.635000	-1.196890	-1.588430
C	-3.331490	-2.471610	-1.623530
C	-2.366400	-3.443730	-1.644700
C	-1.085600	-2.757950	-1.629190
N	-1.273060	-1.394340	-1.597470
C	0.164280	-3.414490	-1.643940
C	3.634960	0.033700	-1.571900
H	-4.400640	2.734460	-1.614960
H	-2.475860	4.640510	-1.694680
H	-4.419950	-2.605790	-1.643460
H	-2.510360	-4.530680	-1.671630
H	4.754290	-2.643500	-1.644730
H	2.828510	-4.549110	-1.722360
H	2.864370	4.622970	-1.660250
H	4.775280	2.696480	-1.629960
C	0.190990	5.000820	-1.651850

C	-4.455220	0.060400	-1.296720	C	5.125770	0.023950	-1.467950
C	0.487120	-4.906250	-1.536830	C	-4.775360	0.058390	-1.500820
C	0.850920	-5.647250	-0.395680	C	0.162790	-4.909340	-1.655410
C	0.856610	-7.052130	-0.395060	C	0.528290	-5.646200	-0.512240
C	0.491900	-7.745210	-1.561730	C	0.535280	-7.051140	-0.507270
C	0.125000	-7.032970	-2.716090	C	0.170530	-7.747950	-1.671730
C	0.125720	-5.627710	-2.691250	C	-0.197980	-7.039600	-2.828010
F	1.201440	-5.012560	0.729410	C	-0.198540	-5.634270	-2.807480
F	1.199870	-7.732860	0.701780	F	0.880000	-5.007100	0.609880
F	0.494380	-9.078590	-1.573170	F	0.880360	-7.728320	0.591080
F	-0.215700	-7.695920	-3.823990	F	0.174510	-9.081290	-1.679330
F	-0.226090	-4.974370	-3.803380	F	-0.538950	-7.706180	-3.933560
C	-5.065180	-0.206620	-0.056210	F	-0.551820	-4.984290	-3.921140
C	-6.457270	-0.152090	0.115540	C	-5.443820	-0.294050	-0.312760
C	-7.275370	0.161160	-0.983510	C	-6.845600	-0.303720	-0.224100
C	-6.695800	0.422720	-2.237310	C	-7.608980	0.047010	-1.350950
C	-5.298600	0.367980	-2.380490	C	-6.969440	0.404470	-2.550270
F	-4.311130	-0.504670	1.011910	C	-5.565490	0.406500	-2.612780
F	-7.004240	-0.388040	1.313000	F	-4.737830	-0.627880	0.776740
F	-8.599490	0.214540	-0.836440	F	-7.456650	-0.636490	0.916140
F	-7.473320	0.721470	-3.280440	F	-8.940420	0.042040	-1.281290
F	-4.774360	0.628120	-3.582110	F	-7.698020	0.734920	-3.618730
C	6.079070	0.376530	-0.066170	F	-4.983250	0.749960	-3.766320
C	7.477220	0.380260	0.063130	C	5.762440	0.297130	-0.243120
C	8.271050	0.042190	-1.046690	C	7.158700	0.257080	-0.103390
C	7.663630	-0.296780	-2.267980	C	7.951950	-0.058000	-1.220490
C	6.261910	-0.292230	-2.369970	C	7.345660	-0.331000	-2.458710
F	5.344020	0.696850	1.012080	C	5.945270	-0.284780	-2.569820
F	8.055610	0.694210	1.225970	F	5.027080	0.595090	0.843350
F	9.599850	0.040570	-0.939300	F	7.735180	0.506770	1.075440
F	8.419270	-0.616990	-3.320220	F	9.279030	-0.101280	-1.103490
F	5.712220	-0.618540	-3.543640	F	8.100780	-0.631650	-3.516840
C	0.856720	5.726460	-2.667050	F	5.394880	-0.551310	-3.757710
C	0.854060	7.131800	-2.688750	C	0.551070	5.721500	-2.807130
C	0.486250	7.840520	-1.532480	C	0.551810	7.126690	-2.832800
C	0.124240	7.144180	-0.366910	C	0.186260	7.839430	-1.678290
C	0.133010	5.739190	-0.370750	C	-0.176700	7.147050	-0.510610
F	1.210580	5.075910	-3.780180	C	-0.170850	5.742030	-0.510290
F	1.193040	7.798110	-3.795160	F	0.901580	5.067240	-3.919170
F	0.480860	9.173940	-1.540970	F	0.891540	7.788980	-3.941350
F	-0.219140	7.821880	0.731740	F	0.184030	9.172740	-1.690440
F	-0.214830	5.100460	0.752570	F	-0.518290	7.828460	0.586140
C	1.863600	0.171530	4.128440	F	-0.518950	5.107470	0.615300
H	1.565750	1.046340	4.742640	H	3.107010	0.230630	3.245750
H	1.741700	-0.746620	4.739260	H	2.096890	-0.774400	4.375120
H	2.923770	0.276670	3.822970	H	1.948670	1.009870	4.410560

I.6.4 1-*iso*-Propyl-5-phenylazoimidazole · $NiTPPF_{20}$ (3)

***cis*-α**

$E_{PBE/SVP}$ = -6081.554115667 Hartree

NImag = 0

C	1.495320	-2.269810	4.089220
C	0.726750	-3.449830	4.172330
C	1.109710	-4.583900	3.441120
C	2.279040	-4.565790	2.662210
C	3.068730	-3.402410	2.614250
C	2.680080	-2.255100	3.317000
N	1.137390	-1.154500	4.895970
N	0.875790	-0.018870	4.407730
C	0.709740	0.248910	3.055080
C	0.414740	-0.467780	1.880230
N	0.615480	1.602690	2.692110
N	0.167310	0.412560	0.870760
C	0.313570	1.646400	1.378980
H	-0.179470	-3.455870	4.798050
H	0.483030	-5.489410	3.480870
H	2.581610	-5.462580	2.097930
H	3.990610	-3.378150	2.010730
H	3.294550	-1.341390	3.279940
H	0.346810	-1.550560	1.730210
H	0.217400	2.572920	0.802440
C	-2.097730	2.626640	-1.128820
N	-0.908440	2.003920	-1.435410
C	-2.003450	4.051800	-1.387540
C	-0.729180	4.284450	-1.839210
C	-0.050990	3.000130	-1.845880
C	-3.237560	1.991110	-0.590460
C	-3.354100	0.606870	-0.341250
C	-4.552240	-0.025020	0.184710
C	-4.284160	-1.365620	0.261840
C	-2.925950	-1.546180	-0.223440
N	-2.380360	-0.335330	-0.580260
Ni	-0.413720	0.040850	-1.045340
N	1.422410	0.361740	-1.911310
C	2.413500	-0.572010	-2.104850
C	3.631730	0.072130	-2.567150
C	3.365840	1.414570	-2.628130
C	1.979770	1.580580	-2.224930
C	-2.275930	-2.797440	-0.318200
C	-0.948560	-2.986600	-0.763270
C	-0.314760	-4.285300	-0.909890
C	0.963500	-4.051410	-1.342330
C	1.100560	-2.611590	-1.474920
N	-0.073230	-1.984420	-1.119630
C	2.276720	-1.965020	-1.913010
C	1.309030	2.822280	-2.183530
H	-4.948660	-2.161400	0.618940
H	-5.483890	0.489620	0.449540
H	-0.789550	-5.254970	-0.717740
H	1.742700	-4.791690	-1.560050
H	4.045190	2.219010	-2.935310
H	4.569150	-0.437290	-2.821310
H	-2.810150	4.781770	-1.247820
H	-0.291590	5.241020	-2.150850

***cis*-β**

$E_{PBE/SVP}$ = -6081.544586755 Hartree

NImag = 0

C	-0.915390	-2.922320	4.444150
C	-1.680060	-3.143900	5.615190
C	-2.949490	-3.726500	5.531410
C	-3.447320	-4.156750	4.287390
C	-2.672690	-3.984320	3.126210
C	-1.422810	-3.351380	3.191350
N	0.415100	-2.468740	4.641200
N	1.060470	-1.730170	3.844490
C	0.521770	-1.003140	2.782480
C	1.117210	-0.847710	1.527380
N	-0.624880	-0.191730	2.763270
N	0.342010	-0.021950	0.759960
C	-0.670790	0.383060	1.529320
H	-1.244950	-2.851970	6.584410
H	-3.544970	-3.875190	6.447160
H	-4.432960	-4.645980	4.225350
H	-3.041520	-4.346450	2.153220
H	-0.825860	-3.226990	2.274490
H	2.023100	-1.338020	1.150650
H	-1.424960	1.124530	1.236130
C	3.407690	1.610180	-1.059510
N	2.601290	0.523380	-1.310520
C	4.806450	1.217950	-1.081310
C	4.833090	-0.122860	-1.359360
C	3.450110	-0.543180	-1.501830
C	2.958380	2.929060	-0.827230
C	1.604160	3.329290	-0.802480
C	1.163840	4.695800	-0.580530
C	-0.204990	4.678080	-0.620300
C	-0.592980	3.304330	-0.891160
N	0.520920	2.502690	-0.996410
Ni	0.550670	0.456080	-1.206780
N	0.606450	-1.486390	-1.879220
C	-0.474240	-2.302200	-2.121020
C	-0.029710	-3.646920	-2.446920
C	1.338290	-3.634970	-2.376170
C	1.721800	-2.280860	-2.016600
C	-1.930070	2.871870	-1.033840
C	-2.330790	1.555360	-1.352460
C	-3.713090	1.135640	-1.501540
C	-3.685480	-0.206720	-1.777090
C	-2.286190	-0.595700	-1.810900
N	-1.481800	0.491080	-1.554490
C	-1.829430	-1.907820	-2.068300
C	3.054830	-1.859540	-1.822590
H	-0.889370	5.525230	-0.490710
H	1.817820	5.561660	-0.422170
H	-4.592810	1.785400	-1.416890
H	-4.541140	-0.870620	-1.948820
H	2.027720	-4.468510	-2.556900
H	-0.679670	-4.490220	-2.710600
H	5.660380	1.883260	-0.906140
H	5.712140	-0.769080	-1.471970

C	-4.404370	2.851220	-0.225530	C	3.996420	3.985000	-0.624560
C	2.104580	4.055980	-2.462730	C	4.130890	-2.890340	-1.944070
C	-3.056230	-4.010190	0.066950	C	-3.006350	3.886950	-0.824980
C	3.461950	-2.821180	-2.223670	C	-2.860270	-2.969970	-2.265280
C	4.594300	-2.842500	-1.388080	C	-3.060720	-3.965980	-1.291270
C	5.719810	-3.629890	-1.680830	C	-4.038530	-4.962290	-1.430980
C	5.724680	-4.422000	-2.841490	C	-4.841590	-4.981770	-2.584040
C	4.605030	-4.429340	-3.690370	C	-4.661720	-4.005180	-3.578680
C	3.493070	-3.630470	-3.375840	C	-3.677420	-3.016390	-3.410880
F	4.617000	-2.101530	-0.270530	F	-2.312640	-3.971670	-0.176280
F	6.779960	-3.631590	-0.868220	F	-4.214100	-5.879510	-0.474080
F	6.788510	-5.169280	-3.135480	F	-5.773420	-5.922430	-2.734350
F	4.609770	-5.185720	-4.789910	F	-5.422810	-4.025590	-4.674510
F	2.443830	-3.653050	-4.203650	F	-3.530570	-2.101440	-4.373560
C	-2.725200	-4.769100	1.205780	C	-3.791930	3.890260	0.342090
C	-3.452390	-5.911900	1.574680	C	-4.802010	4.841700	0.556620
C	-4.553370	-6.310650	0.798210	C	-5.036140	5.827400	-0.418450
C	-4.911260	-5.571790	-0.341870	C	-4.264980	5.852610	-1.592990
C	-4.160810	-4.438810	-0.695320	C	-3.265210	4.884260	-1.784440
F	-1.690550	-4.405240	1.976810	F	-3.577150	2.967240	1.298680
F	-3.111310	-6.614160	2.659050	F	-5.532990	4.824550	1.674050
F	-5.257740	-7.388700	1.141800	F	-5.987700	6.740350	-0.226980
F	-5.955480	-5.952060	-1.081200	F	-4.487310	6.790170	-2.515650
F	-4.520050	-3.761870	-1.790570	F	-2.546920	4.928910	-2.909540
C	2.483030	4.912980	-1.411490	C	4.731840	-3.435870	-0.793980
C	3.226830	6.082380	-1.634220	C	5.740070	-4.410650	-0.876060
C	3.604750	6.417220	-2.946560	C	6.166340	-4.854380	-2.140050
C	3.241190	5.582240	-4.016860	C	5.585580	-4.325460	-3.305290
C	2.500110	4.414880	-3.764930	C	4.576590	-3.353620	-3.196070
F	2.133750	4.618240	-0.146060	F	4.339480	-3.029750	0.421260
F	3.575710	6.872330	-0.615430	F	6.289130	-4.918410	0.229760
F	4.307610	7.526110	-3.176770	F	7.122250	-5.778610	-2.236880
F	3.596590	5.905080	-5.261900	F	5.997390	-4.748640	-4.502610
F	2.168820	3.640600	-4.802140	F	4.039280	-2.868440	-4.319750
C	-5.282710	3.358330	-1.201590	C	4.812770	4.409710	-1.691710
C	-6.396110	4.143370	-0.855910	C	5.795760	5.399000	-1.525780
C	-6.641430	4.437640	0.496070	C	5.974130	5.990830	-0.263950
C	-5.776210	3.951330	1.491440	C	5.172170	5.590590	0.818290
C	-4.669490	3.170430	1.119880	C	4.197520	4.597040	0.627560
F	-5.069870	3.092320	-2.494050	F	4.662210	3.869210	-2.905010
F	-7.221660	4.607960	-1.796360	F	6.554180	5.781600	-2.555800
F	-7.696400	5.178320	0.834930	F	6.903460	6.930820	-0.093000
F	-6.010750	4.237600	2.774640	F	5.344030	6.152070	2.017740
F	-3.855640	2.722050	2.087160	F	3.451600	4.236850	1.678260
C	0.842530	2.758480	3.587040	C	-1.463870	0.235260	3.910600
C	2.297190	3.237420	3.485520	C	-2.949010	-0.020910	3.630000
H	2.474170	4.060870	4.210760	H	-3.543810	0.227540	4.534960
H	3.006700	2.415490	3.721270	H	-3.319020	0.617100	2.797240
H	2.521150	3.619980	2.464570	H	-3.132100	-1.085910	3.375740
C	-0.170200	3.873160	3.300800	C	-1.173100	1.700150	4.270040
H	-0.099670	4.644890	4.096880	H	-1.522150	2.388540	3.469210
H	0.034660	4.378330	2.330770	H	-1.709880	1.968820	5.205490
H	-1.211940	3.486050	3.282330	H	-0.086870	1.867440	4.433830
H	0.669470	2.343020	4.601820	H	-1.146060	-0.403900	4.757670

***trans*-α**

$E_{PBE/SVP}$ = -6081.569156201 Hartree

NImag = 0

C	-2.856990	1.587200	4.953370
C	-4.271200	1.584940	4.946050
C	-4.985740	1.936010	6.098530
C	-4.294620	2.290140	7.269780
C	-2.884560	2.292830	7.283770
C	-2.164880	1.945310	6.137540
N	-2.247530	1.211420	3.741120
N	-0.972260	1.240930	3.734650
C	-0.392760	0.853330	2.551360
C	-0.874740	0.402790	1.313430
N	1.002190	0.852820	2.436400
N	0.182850	0.142750	0.493410
C	1.296570	0.418910	1.190130
H	-4.778290	1.300560	4.010550
H	-6.087810	1.932780	6.085850
H	-4.853830	2.564440	8.179450
H	-2.347040	2.569240	8.206280
H	-1.064490	1.938810	6.130280
H	-1.917100	0.272630	1.003470
H	2.315950	0.307180	0.803390
C	3.025390	0.573430	-1.981950
N	2.229250	-0.500150	-1.647930
C	4.427830	0.218240	-1.861230
C	4.466590	-1.085450	-1.437250
C	3.087630	-1.517180	-1.294420
C	2.559010	1.855630	-2.346540
C	1.201560	2.219980	-2.475330
C	0.747390	3.542860	-2.869840
C	-0.621880	3.501070	-2.871170
C	-0.995200	2.149480	-2.488910
N	0.127240	1.388810	-2.259160
Ni	0.179260	-0.498140	-1.439580
N	0.247680	-2.515510	-1.043310
C	-0.826330	-3.351440	-0.843250
C	-0.372820	-4.661170	-0.405890
C	0.992910	-4.596000	-0.325920
C	1.368290	-3.253730	-0.737670
C	-2.327650	1.696010	-2.378490
C	-2.710320	0.381090	-2.036950
C	-4.085760	-0.083670	-2.009320
C	-4.045440	-1.404460	-1.645670
C	-2.645020	-1.739570	-1.452460
N	-1.851850	-0.641720	-1.701030
C	-2.181870	-3.009010	-1.042020
C	2.700540	-2.795890	-0.834460
H	-1.318210	4.312140	-3.116230
H	1.393830	4.392150	-3.123100
H	-4.968420	0.521430	-2.250020
H	-4.890850	-2.091420	-1.518130
H	1.684970	-5.392340	-0.026540
H	-1.016650	-5.523320	-0.193830
H	5.276680	0.877490	-2.079210
H	5.353350	-1.704150	-1.253120

***trans*-β**

$E_{PBE/SVP}$ = -6081.569660356 Hartree

NImag = 0

C	1.271090	-5.652030	2.156170
C	1.913160	-6.287890	3.242750
C	1.972460	-7.686200	3.308940
C	1.391850	-8.461130	2.290740
C	0.750500	-7.831090	1.204940
C	0.686830	-6.436940	1.131670
N	1.265550	-4.240660	2.181160
N	0.674910	-3.688240	1.194160
C	0.623560	-2.320450	1.136050
C	-0.011350	-1.621560	0.098100
N	1.130850	-1.325650	1.997550
N	0.100000	-0.281790	0.310910
C	0.787160	-0.133940	1.451840
H	2.360010	-5.656200	4.027190
H	2.474570	-8.175940	4.159320
H	1.437840	-9.561470	2.340010
H	0.296160	-8.442410	0.407390
H	0.192360	-5.922260	0.294100
H	-0.522880	-2.051560	-0.771800
H	1.053490	0.834070	1.895900
C	-2.530480	2.340350	1.216820
N	-1.273130	2.426590	0.664260
C	-2.617600	3.169500	2.406990
C	-1.389420	3.756050	2.567530
C	-0.559010	3.279830	1.475400
C	-3.593090	1.554100	0.717070
C	-3.527790	0.745280	-0.438580
C	-4.650260	-0.013280	-0.964080
C	-4.196080	-0.660060	-2.082720
C	-2.800980	-0.285640	-2.240500
N	-2.417890	0.570530	-1.233420
Ni	-0.520810	1.260040	-0.859210
N	1.253140	2.298900	-0.737410
C	2.365350	2.120380	-1.527350
C	3.461910	2.945610	-1.049700
C	3.000270	3.609180	0.057350
C	1.622030	3.191290	0.243660
C	-1.966640	-0.752470	-3.279940
C	-0.611360	-0.395310	-3.455880
C	0.225640	-0.881840	-4.539360
C	1.465940	-0.331860	-4.352730
C	1.375940	0.504540	-3.168000
N	0.105180	0.450510	-2.640660
C	2.446650	1.267570	-2.651140
C	0.794670	3.637330	1.296680
H	-4.758050	-1.330490	-2.744020
H	-5.660600	-0.038460	-0.537780
H	-0.095500	-1.552860	-5.345250
H	2.361200	-0.476790	-4.969110
H	3.537970	4.334250	0.680860
H	4.453230	3.021880	-1.512960
H	-3.504100	3.288160	3.041500
H	-1.074840	4.454560	3.352840

C	3.583560	2.921880	-2.562770	C	-4.875940	1.565020	1.483630
C	3.794260	-3.714960	-0.396440	C	1.424080	4.497610	2.346670
C	-3.416100	2.690110	-2.628110	C	-2.557360	-1.709260	-4.263690
C	-3.206780	-4.069200	-0.794010	C	3.772200	1.155770	-3.331590
C	-3.543800	-4.465920	0.514080	C	4.849430	0.495750	-2.708400
C	-4.510350	-5.455020	0.762180	C	6.103850	0.375000	-3.327360
C	-5.158720	-6.073580	-0.320370	C	6.299420	0.922930	-4.606240
C	-4.840370	-5.699910	-1.636890	C	5.244310	1.589350	-5.252130
C	-3.873630	-4.704880	-1.859000	C	3.998950	1.698600	-4.610830
F	-2.942190	-3.891540	1.561830	F	4.692800	-0.042040	-1.492700
F	-4.818590	-5.806820	2.013370	F	7.106170	-0.259410	-2.713820
F	-6.077240	-7.014630	-0.100750	F	7.485600	0.809860	-5.204440
F	-5.454900	-6.294440	-2.662340	F	5.431540	2.116470	-6.464450
F	-3.591100	-4.368410	-3.121480	F	3.015300	2.340030	-5.249670
C	-4.128050	3.259780	-1.554910	C	-2.200280	-3.071150	-4.258100
C	-5.132880	4.219480	-1.761100	C	-2.736500	-3.981570	-5.182970
C	-5.450710	4.615030	-3.071620	C	-3.658790	-3.528470	-6.141710
C	-4.763640	4.055290	-4.162530	C	-4.037920	-2.175510	-6.168570
C	-3.755640	3.103880	-3.929890	C	-3.485680	-1.284590	-5.233280
F	-3.842360	2.901120	-0.297810	F	-1.327140	-3.531460	-3.351440
F	-5.782970	4.760630	-0.727280	F	-2.382620	-5.269070	-5.157060
F	-6.403380	5.524540	-3.278140	F	-4.173600	-4.384320	-7.024650
F	-5.073750	4.427960	-5.406820	F	-4.912780	-1.745380	-7.080710
F	-3.111670	2.591650	-4.983650	F	-3.861860	-0.002880	-5.282150
C	4.505550	-3.464460	0.792770	C	2.112530	3.909220	3.422330
C	5.553610	-4.293120	1.222910	C	2.716370	4.672920	4.432450
C	5.907930	-5.411560	0.449290	C	2.636380	6.075260	4.370090
C	5.214990	-5.689750	-0.741000	C	1.954130	6.694050	3.308380
C	4.171660	-4.841960	-1.150500	C	1.356500	5.902350	2.311280
F	4.188450	-2.403020	1.550870	F	2.200580	2.567270	3.507360
F	6.211390	-4.029390	2.355520	F	3.359390	4.082810	5.442920
F	6.902550	-6.206820	0.844000	F	3.206380	6.816810	5.319770
F	5.554850	-6.751750	-1.474500	F	1.879530	8.025240	3.253280
F	3.532480	-5.129970	-2.288580	F	0.714420	6.516550	1.314790
C	4.381820	2.960280	-3.720980	C	-5.716710	2.694340	1.502300
C	5.356450	3.954020	-3.913930	C	-6.906970	2.719000	2.248620
C	5.543300	4.939870	-2.930250	C	-7.276920	1.589570	2.998430
C	4.759850	4.926490	-1.763490	C	-6.461390	0.445380	2.992340
C	3.795460	3.920450	-1.593320	C	-5.277190	0.444830	2.237400
F	4.226150	2.032200	-4.669760	F	-5.388190	3.784110	0.801270
F	6.103650	3.968390	-5.019770	F	-7.685270	3.803680	2.250650
F	6.465600	5.886680	-3.102430	F	-8.399940	1.602790	3.716720
F	4.942880	5.861080	-0.827030	F	-6.811510	-0.625890	3.708870
F	3.073010	3.919630	-0.463450	F	-4.517380	-0.655710	2.256230
C	1.971320	1.279960	3.468230	C	1.925060	-1.478320	3.247330
C	2.877340	0.111340	3.875320	C	1.179740	-0.859920	4.436300
H	3.565310	0.434890	4.685710	H	1.096370	0.245220	4.343060
H	2.276950	-0.744110	4.252640	H	0.158890	-1.287450	4.536060
H	3.496660	-0.250890	3.025830	H	1.736350	-1.076470	5.373560
C	2.743020	2.518800	2.994480	C	3.334080	-0.902250	3.056460
H	3.359320	2.303790	2.093670	H	3.950550	-1.125840	3.953780
H	2.048310	3.348230	2.742130	H	3.835360	-1.353080	2.173160
H	3.423910	2.868410	3.800020	H	3.313840	0.202330	2.926770
H	1.332400	1.559770	4.331150	H	1.992190	-2.574110	3.385490

I.6.4 1-Trimethylsilyl-5-phenylazoimidazole · $NiTPPF_{20}$ (4)

***cis*-α**

$E_{PBE/SVP}$ = -6372.055197751 Hartree

NImag = 0

C	1.817430	-2.612400	3.619650
C	1.592220	-3.978390	3.346980
C	2.516150	-4.699240	2.577480
C	3.690010	-4.081180	2.114740
C	3.932720	-2.729270	2.417470
C	3.000510	-1.990220	3.157740
N	0.925590	-1.934480	4.495590
N	0.259440	-0.916580	4.158080
C	0.158900	-0.395380	2.871170
C	0.468660	-0.765190	1.549660
N	-0.570020	0.800890	2.779170
N	-0.048200	0.168760	0.699210
C	-0.649670	1.095270	1.463290
H	0.678830	-4.457010	3.733480
H	2.310660	-5.755190	2.337610
H	4.422300	-4.655440	1.524450
H	4.852640	-2.236800	2.064120
H	3.188910	-0.930630	3.394130
H	1.009630	-1.642730	1.180390
H	-1.142890	1.989120	1.065650
C	1.489540	2.772180	-1.664970
N	1.480670	1.396420	-1.697390
C	2.851350	3.272140	-1.752520
C	3.665010	2.173850	-1.846770
C	2.796050	1.009930	-1.803840
C	0.346480	3.595090	-1.565250
C	-0.985210	3.128000	-1.500880
C	-2.149940	3.990880	-1.412220
C	-3.238930	3.166880	-1.281040
C	-2.733090	1.806380	-1.305120
N	-1.365450	1.805220	-1.462810
Ni	-0.125700	0.163390	-1.339970
N	1.063980	-1.468230	-1.705970
C	0.675430	-2.788790	-1.743190
C	1.828410	-3.648370	-1.948900
C	2.922940	-2.826790	-2.018590
C	2.431910	-1.468510	-1.865430
C	-3.539140	0.658540	-1.148830
C	-3.083290	-0.673910	-1.225840
C	-3.945680	-1.837300	-1.109890
C	-3.138420	-2.935500	-1.249620
C	-1.787070	-2.435530	-1.443780
N	-1.779260	-1.060570	-1.433630
C	-0.648880	-3.258860	-1.597680
C	3.254930	-0.322300	-1.883730
H	-4.293850	3.454570	-1.193430
H	-2.138520	5.086900	-1.455660
H	-5.031190	-1.815030	-0.952320
H	-3.432070	-3.991640	-1.217660
H	3.970780	-3.113160	-2.170790
H	1.801780	-4.741000	-2.041030
H	3.146900	4.328340	-1.751520
H	4.757500	2.152340	-1.943790

***cis*-β**

$E_{PBE/SVP}$ = -6372.040582192 Hartree

NImag = 0

C	1.868980	-0.227900	4.824040
C	1.880260	-0.739650	6.145270
C	2.402990	-2.009910	6.411550
C	2.987520	-2.761370	5.375150
C	3.032500	-2.236590	4.071000
C	2.458990	-0.990390	3.783230
N	1.470430	1.129820	4.694130
N	0.958670	1.650140	3.663370
C	0.440930	0.956430	2.569560
C	0.652860	1.317250	1.238020
N	-0.427830	-0.152900	2.557290
N	0.003570	0.424860	0.426090
C	-0.647990	-0.414020	1.230990
H	1.480920	-0.105800	6.953360
H	2.385140	-2.405840	7.440310
H	3.429380	-3.748410	5.588070
H	3.527330	-2.798140	3.263080
H	2.508570	-0.593550	2.757780
H	1.267490	2.140280	0.854080
H	-1.330380	-1.197970	0.876890
C	2.655730	1.817770	-1.932870
N	1.980490	0.621000	-1.866120
C	4.091160	1.591580	-1.901380
C	4.271240	0.237020	-1.800590
C	2.945040	-0.355790	-1.771950
C	2.051730	3.093900	-1.979950
C	0.658830	3.331800	-1.976200
C	0.059470	4.654960	-2.026140
C	-1.295930	4.473340	-1.964120
C	-1.520730	3.039070	-1.899500
N	-0.319650	2.366270	-1.909910
Ni	-0.039620	0.356200	-1.603230
N	0.228560	-1.681550	-1.744850
C	-0.747070	-2.651660	-1.719860
C	-0.146990	-3.973290	-1.657100
C	1.210490	-3.783960	-1.621810
C	1.429480	-2.349000	-1.675810
C	-2.797080	2.436500	-1.849020
C	-3.034910	1.043220	-1.835920
C	-4.358120	0.443290	-1.871520
C	-4.174800	-0.914290	-1.840370
C	-2.740320	-1.136200	-1.796640
N	-2.067490	0.065500	-1.804540
C	-2.138260	-2.411220	-1.736100
C	2.702410	-1.740780	-1.660150
H	-2.073750	5.246150	-1.968180
H	0.604810	5.603080	-2.107420
H	-5.307630	0.989190	-1.931630
H	-4.943540	-1.696610	-1.859210
H	1.995260	-4.549380	-1.578860
H	-0.693860	-4.924560	-1.651920
H	4.863510	2.368820	-1.947070
H	5.218990	-0.314300	-1.758460

C	0.553570	5.070930	-1.454060	C	2.947530	4.289100	-1.969970
C	4.731670	-0.534410	-1.998840	C	3.884660	-2.626640	-1.425880
C	-4.976910	0.879940	-0.799270	C	-3.993220	3.329850	-1.804510
C	-0.857770	-4.738040	-1.565330	C	-3.040570	-3.599560	-1.636270
C	-0.442930	-5.499910	-0.456320	C	-3.272150	-4.224200	-0.397510
C	-0.639380	-6.888480	-0.391080	C	-4.104860	-5.347240	-0.271650
C	-1.273690	-7.545530	-1.459050	C	-4.726480	-5.872470	-1.418370
C	-1.701680	-6.811700	-2.578930	C	-4.517910	-5.268430	-2.670050
C	-1.488620	-5.423030	-2.621480	C	-3.682000	-4.142130	-2.765560
F	0.153450	-4.897730	0.581130	F	-2.693610	-3.738070	0.717390
F	-0.236870	-7.583310	0.677720	F	-4.307080	-5.917010	0.919200
F	-1.469950	-8.863240	-1.410380	F	-5.516700	-6.941320	-1.319090
F	-2.303950	-7.438180	-3.592120	F	-5.108160	-5.770990	-3.756370
F	-1.902420	-4.751830	-3.700780	F	-3.503480	-3.586260	-3.966630
C	-5.367990	0.949330	0.550520	C	-4.801990	3.397030	-0.652620
C	-6.701550	1.167270	0.930060	C	-5.947860	4.206810	-0.595160
C	-7.679790	1.327510	-0.066890	C	-6.300910	4.984170	-1.711330
C	-7.318440	1.266840	-1.423800	C	-5.510690	4.943000	-2.872270
C	-5.975520	1.042640	-1.775760	C	-4.372750	4.119990	-2.907200
F	-4.444970	0.816180	1.519440	F	-4.488750	2.672470	0.429520
F	-7.044330	1.226960	2.219600	F	-6.698110	4.245610	0.509070
F	-8.950430	1.541530	0.274360	F	-7.385680	5.757840	-1.671160
F	-8.250620	1.424150	-2.365590	F	-5.849730	5.678260	-3.933650
F	-5.657900	0.994240	-3.072300	F	-3.648280	4.096020	-4.030590
C	5.554930	-0.532470	-0.858570	C	4.379770	-2.789670	-0.119780
C	6.941640	-0.736350	-0.943050	C	5.477710	-3.614390	0.166850
C	7.533730	-0.932920	-2.202350	C	6.115360	-4.295240	-0.884300
C	6.736670	-0.935350	-3.360080	C	5.646240	-4.149470	-2.201760
C	5.349540	-0.738200	-3.246580	C	4.536790	-3.323280	-2.458750
F	5.017370	-0.342450	0.354750	F	3.784760	-2.150360	0.899360
F	7.695780	-0.743490	0.159450	F	5.912670	-3.758410	1.423470
F	8.850130	-1.120190	-2.298430	F	7.163210	-5.079260	-0.630810
F	7.301150	-1.120440	-4.555470	F	6.256490	-4.795480	-3.197420
F	4.613500	-0.749730	-4.361240	F	4.106020	-3.211540	-3.718400
C	0.922480	5.862780	-2.557400	C	3.730160	4.647200	-3.084020
C	1.103340	7.251890	-2.442040	C	4.551550	5.787160	-3.072930
C	0.918090	7.874190	-1.195820	C	4.601280	6.594730	-1.924140
C	0.552310	7.108030	-0.075570	C	3.836430	6.257880	-0.794100
C	0.377040	5.722920	-0.218730	C	3.027130	5.111280	-0.829290
F	1.104630	5.298450	-3.754780	F	3.701420	3.899390	-4.191710
F	1.445920	7.982510	-3.504860	F	5.279210	6.111110	-4.144310
F	1.087920	9.190850	-1.075870	F	5.374530	7.680300	-1.906760
F	0.381570	7.697750	1.110570	F	3.887360	7.022510	0.298710
F	0.033800	5.013530	0.868320	F	2.316830	4.805540	0.264820
C	-0.065970	2.199770	5.414670	C	-3.249010	-0.969640	2.989330
H	-0.511500	2.820410	6.224690	H	-4.025270	-1.223160	3.746560
H	0.389150	1.296580	5.873650	H	-3.538780	-0.004200	2.517930
H	0.738630	2.797290	4.931630	H	-3.277370	-1.763210	2.210870
C	-2.153180	3.222350	3.328190	C	-1.678760	0.366860	5.274370
H	-2.636770	3.860500	4.102150	H	-1.950020	1.381730	4.908930
H	-1.404570	3.849830	2.796460	H	-2.490760	0.025470	5.955930
H	-2.942860	2.925810	2.602770	H	-0.747240	0.453480	5.869500
C	-2.732870	0.589270	4.860760	C	-0.945570	-2.570270	4.306930
H	-3.278010	1.105280	5.683190	H	-0.941850	-3.228460	3.409800
H	-3.471200	0.335220	4.068260	H	0.078830	-2.552090	4.735230
H	-2.295470	-0.349150	5.262650	H	-1.628560	-3.028690	5.057670
Si	-1.391730	1.713950	4.171840	Si	-1.569530	-0.856100	3.848040

***trans*-α**

$E_{PBE/SVP}$ = -6372.072215141 Hartree

NImag = 0

C	-3.350980	-0.520260	4.595750
C	-4.718280	-0.785340	4.343150
C	-5.617770	-0.924050	5.408030
C	-5.163160	-0.800510	6.732060
C	-3.802380	-0.535870	6.989000
C	-2.897410	-0.395790	5.933240
N	-2.545750	-0.402980	3.449770
N	-1.307970	-0.163590	3.647800
C	-0.572660	-0.063030	2.485940
C	-0.898240	-0.176310	1.131270
N	0.799990	0.206170	2.550310
N	0.231090	0.016290	0.391010
C	1.229290	0.242450	1.258950
H	-5.041380	-0.877870	3.293830
H	-6.681380	-1.130870	5.205370
H	-5.869610	-0.910750	7.571270
H	-3.450400	-0.439450	8.029700
H	-1.831830	-0.189970	6.117700
H	-1.879850	-0.384310	0.692980
H	2.269130	0.436800	0.965980
C	1.441370	2.854730	-1.923920
N	1.688960	1.501630	-1.862270
C	2.690630	3.595060	-1.952000
C	3.697920	2.667090	-1.901060
C	3.058370	1.364040	-1.839820
C	0.163810	3.457040	-1.940030
C	-1.062750	2.758530	-1.907840
C	-2.366170	3.401580	-1.897640
C	-3.296870	2.398670	-1.833690
C	-2.558140	1.147280	-1.835540
N	-1.204120	1.390010	-1.880200
Ni	0.301310	0.003430	-1.639280
N	1.806790	-1.383120	-1.851710
C	1.665600	-2.751220	-1.896280
C	2.968990	-3.393810	-1.887730
C	3.899940	-2.391160	-1.817240
C	3.161060	-1.140210	-1.808040
C	-3.157100	-0.132190	-1.809720
C	-2.453620	-1.355920	-1.882550
C	-3.093760	-2.658570	-1.947710
C	-2.087270	-3.586450	-1.997940
C	-0.837450	-2.846380	-1.960790
N	-1.084100	-1.493160	-1.903390
C	0.439460	-3.449710	-1.954800
C	3.760530	0.138490	-1.782130
H	-4.388270	2.500050	-1.801060
H	-2.547520	4.482610	-1.936960
H	-4.175440	-2.839490	-1.969530
H	-2.184500	-4.677500	-2.051520
H	4.991610	-2.492440	-1.788340
H	3.150600	-4.474310	-1.938630
H	2.787550	4.686150	-2.006920
H	4.779330	2.849790	-1.922270

***trans*-β**

$E_{PBE/SVP}$ = -6372.072244543 Hartree

NImag = 0

C	-3.273500	-0.533720	4.970820
C	-3.075930	-0.356960	6.359610
C	-4.137270	-0.549840	7.254370
C	-5.403560	-0.921150	6.772180
C	-5.605000	-1.097980	5.388290
C	-4.552490	-0.907010	4.488900
N	-2.145850	-0.324850	4.145860
N	-2.354710	-0.471940	2.896470
C	-1.275930	-0.287900	2.077990
C	-1.307560	-0.416090	0.684990
N	0.051930	0.043110	2.424500
N	-0.061110	-0.182940	0.184580
C	0.720800	0.083590	1.240130
H	-2.075530	-0.065740	6.717710
H	-3.976190	-0.410810	8.335970
H	-6.239020	-1.074780	7.474750
H	-6.599660	-1.389850	5.012030
H	-4.685040	-1.040240	3.404720
H	-2.174570	-0.648510	0.054940
H	1.789480	0.314170	1.156080
C	2.109950	2.527490	-1.033610
N	2.132060	1.189490	-1.352080
C	3.438850	2.980960	-0.663310
C	4.264430	1.889190	-0.754320
C	3.430930	0.773110	-1.163550
C	0.967890	3.359750	-1.061370
C	-0.302580	2.979600	-1.545960
C	-1.452410	3.865210	-1.616050
C	-2.482600	3.126950	-2.135570
C	-1.961430	1.789160	-2.362970
N	-0.633230	1.727520	-2.012370
Ni	0.493180	0.017280	-1.767090
N	1.743970	-1.601810	-1.964470
C	1.368330	-2.890390	-2.264070
C	2.510180	-3.784670	-2.172730
C	3.582430	-3.014380	-1.807430
C	3.089890	-1.654150	-1.678960
C	-2.739050	0.701720	-2.821460
C	-2.278830	-0.627920	-2.950950
C	-3.099940	-1.732140	-3.416580
C	-2.323880	-2.858110	-3.338830
C	-1.023610	-2.433580	-2.850190
N	-1.017140	-1.074460	-2.626160
C	0.072600	-3.301320	-2.649960
C	3.890750	-0.555060	-1.301260
H	-3.510090	3.456570	-2.331100
H	-1.472270	4.917920	-1.309250
H	-4.136490	-1.655490	-3.766890
H	-2.606430	-3.884880	-3.599820
H	4.617990	-3.337850	-1.646350
H	2.497810	-4.861180	-2.382300
H	3.712380	4.009910	-0.398780
H	5.345260	1.846650	-0.571780

C	0.109320	4.950690	-1.981720	C	1.115750	4.724750	-0.473350
C	5.249190	0.211240	-1.677260	C	5.321640	-0.823210	-0.960630
C	-4.641570	-0.206270	-1.651240	C	-4.179170	0.964110	-3.119680
C	0.495120	-4.942860	-1.999740	C	-0.144780	-4.766910	-2.847420
C	0.862570	-5.695670	-0.867700	C	-0.160170	-5.637520	-1.739690
C	0.907630	-7.099660	-0.894520	C	-0.345650	-7.021740	-1.885590
C	0.580230	-7.779700	-2.079770	C	-0.522450	-7.562980	-3.170170
C	0.210820	-7.055350	-3.225710	C	-0.513030	-6.719410	-4.293990
C	0.173580	-5.651450	-3.173860	C	-0.325160	-5.337270	-4.121990
F	1.176130	-5.074570	0.275680	F	0.005080	-5.150140	-0.505180
F	1.252890	-7.791930	0.194470	F	-0.357810	-7.821840	-0.816550
F	0.619650	-9.112140	-2.116520	F	-0.698490	-8.875860	-3.323000
F	-0.096730	-7.705030	-4.351250	F	-0.676180	-7.236940	-5.514120
F	-0.180590	-4.986540	-4.278370	F	-0.316830	-4.561760	-5.211100
C	-5.207390	-0.649420	-0.439410	C	-5.191540	0.474300	-2.271210
C	-6.595300	-0.729910	-0.248790	C	-6.551660	0.722070	-2.516450
C	-7.457960	-0.364060	-1.296040	C	-6.922400	1.481480	-3.639700
C	-6.924520	0.082070	-2.517800	C	-5.934920	1.984580	-4.503770
C	-5.530410	0.155860	-2.681590	C	-4.580710	1.722000	-4.236640
F	-4.415450	-0.997810	0.585060	F	-4.868390	-0.243720	-1.186620
F	-7.095140	-1.145770	0.920130	F	-7.488880	0.249800	-1.690430
F	-8.778970	-0.436910	-1.130860	F	-8.209860	1.725690	-3.885070
F	-7.742730	0.426990	-3.514960	F	-6.288690	2.703910	-5.571160
F	-5.056590	0.585030	-3.855380	F	-3.665450	2.214470	-5.076730
C	5.862990	0.655570	-0.490730	C	5.741280	-0.862640	0.382150
C	7.256820	0.757320	-0.361450	C	7.076590	-1.108600	0.738870
C	8.075390	0.400260	-1.446840	C	8.028190	-1.326290	-0.272320
C	7.494200	-0.052910	-2.643550	C	7.639800	-1.292580	-1.622460
C	6.095250	-0.142160	-2.746290	C	6.295440	-1.046860	-1.951760
F	5.107280	0.993170	0.568080	F	4.849140	-0.665950	1.365280
F	7.805730	1.183750	0.779410	F	7.445660	-1.142240	2.021970
F	9.401170	0.489980	-1.340220	F	9.299860	-1.564570	0.048790
F	8.271400	-0.389090	-3.675120	F	8.549210	-1.492020	-2.578840
F	5.576090	-0.572810	-3.899730	F	5.952670	-1.026800	-3.242960
C	0.429190	5.660400	-3.155410	C	1.116980	5.895290	-1.255060
C	0.392920	7.064450	-3.205210	C	1.260200	7.168770	-0.677360
C	0.025870	7.787360	-2.057580	C	1.405580	7.287630	0.715430
C	-0.299480	7.105950	-0.872520	C	1.404100	6.136740	1.522350
C	-0.254410	5.701840	-0.847610	C	1.261270	4.878220	0.919230
F	0.781970	4.996440	-4.260830	F	0.984190	5.814530	-2.582310
F	0.699930	7.715600	-4.330000	F	1.264240	8.263570	-1.440120
F	-0.012600	9.119890	-2.092360	F	1.544360	8.491270	1.270860
F	-0.642190	7.797050	0.218070	F	1.531730	6.247380	2.847550
F	-0.564150	5.078850	0.295880	F	1.256870	3.795260	1.716430
C	1.702720	-1.111180	5.095650	C	0.887020	-1.027790	5.169720
H	2.303450	-1.013240	6.027690	H	-0.128940	-1.371040	5.451330
H	0.650650	-1.333300	5.376440	H	1.418510	-1.864330	4.663970
H	2.100680	-1.976720	4.521370	H	1.451930	-0.783400	6.098140
C	1.070760	1.969650	4.968280	C	0.024210	2.042730	4.732180
H	1.651570	2.191920	5.891930	H	0.536900	2.342510	5.674580
H	1.102390	2.872410	4.319140	H	0.143080	2.876700	4.005120
H	0.013360	1.782640	5.254280	H	-1.053520	1.897710	4.947930
C	3.547000	0.812170	3.474850	C	2.618380	0.940430	3.580340
H	3.972620	-0.038390	2.899500	H	3.188320	0.106820	3.116290
H	3.607430	1.721250	2.837700	H	2.662280	1.820110	2.900990
H	4.207580	0.979990	4.355470	H	3.154270	1.222350	4.515650
Si	1.795510	0.473780	4.084320	Si	0.841750	0.487540	4.050990

I.6.5 1-*tert*-Butyl-5-phenylazoimidazole · $NiTPPF_{20}$ (5)

***cis*-α**

$E_{PBE/SVP}$ = -6120.773007405 Hartree

NImag = 0

C	1.981090	-2.701110	3.287340
C	2.096110	-3.985150	2.711460
C	3.241030	-4.314730	1.971740
C	4.293480	-3.392510	1.836780
C	4.193480	-2.126560	2.441320
C	3.041720	-1.774020	3.156530
N	0.871820	-2.424370	4.132600
N	0.069360	-1.467240	3.942800
C	0.017000	-0.692690	2.787970
C	0.405830	-0.875820	1.449780
N	-0.782550	0.468170	2.790630
N	-0.131110	0.114230	0.686660
C	-0.820660	0.911780	1.513690
H	1.271190	-4.704090	2.833870
H	3.317140	-5.311240	1.506080
H	5.197940	-3.664670	1.269060
H	5.015860	-1.399070	2.346940
H	2.960900	-0.783290	3.631900
H	1.002090	-1.683490	1.012940
H	-1.337620	1.819330	1.189280
C	1.139120	3.068280	-1.471410
N	1.297620	1.703090	-1.540770
C	2.432480	3.730420	-1.515060
C	3.375970	2.739880	-1.590260
C	2.653180	1.479290	-1.603160
C	-0.094660	3.747370	-1.368450
C	-1.362250	3.125340	-1.337310
C	-2.614920	3.838500	-1.164090
C	-3.602550	2.888290	-1.108050
C	-2.949450	1.600150	-1.261590
N	-1.589330	1.768010	-1.404590
Ni	-0.162810	0.277760	-1.344020
N	1.226760	-1.178190	-1.761810
C	0.999610	-2.534130	-1.845860
C	2.256240	-3.251250	-1.966860
C	3.249600	-2.307650	-1.933170
C	2.593670	-1.017900	-1.799900
C	-3.622550	0.357750	-1.234800
C	-3.005830	-0.902280	-1.400530
C	-3.727530	-2.163780	-1.437570
C	-2.786720	-3.147800	-1.589300
C	-1.496490	-2.481200	-1.644590
N	-1.655870	-1.118570	-1.549030
C	-0.263840	-3.157250	-1.769240
C	3.274440	0.215340	-1.697430
H	-4.679340	3.051510	-0.979110
H	-2.726660	4.926880	-1.085370
H	-4.816540	-2.280130	-1.375820
H	-2.951020	-4.229280	-1.672260
H	4.331880	-2.473980	-1.990520
H	2.365510	-4.338660	-2.060080
H	2.596280	4.815070	-1.506100
H	4.465310	2.851900	-1.656580

***cis*-β**

$E_{PBE/SVP}$ = -6120.758361326 Hartree

NImag = 0

C	-1.463540	-0.914240	4.889300
C	-1.770740	-0.525130	6.215920
C	-2.905180	0.248960	6.483010
C	-3.788050	0.584410	5.440140
C	-3.521510	0.149820	4.129520
C	-2.356810	-0.576100	3.841170
N	-0.355110	-1.792540	4.754900
N	0.417550	-1.852100	3.760920
C	0.427120	-0.959760	2.673790
C	0.309540	-1.386950	1.351600
N	0.580650	0.440170	2.621740
N	0.306680	-0.296520	0.523930
C	0.491020	0.770210	1.296870
H	-1.095700	-0.851640	7.023180
H	-3.120550	0.568480	7.515840
H	-4.698620	1.167910	5.652520
H	-4.228840	0.375620	3.315890
H	-2.165820	-0.909800	2.809860
H	0.179780	-2.414920	0.993020
H	0.609690	1.791670	0.919130
C	1.740890	2.405900	-1.759490
N	1.762090	1.029630	-1.802570
C	3.088480	2.936690	-1.869130
C	3.924020	1.857360	-1.986120
C	3.085340	0.672410	-1.926130
C	0.582500	3.202710	-1.622710
C	-0.740390	2.710340	-1.566300
C	-1.921230	3.551580	-1.478510
C	-2.999740	2.706730	-1.436380
C	-2.470340	1.355590	-1.501880
N	-1.097410	1.381770	-1.589600
Ni	0.168320	-0.242040	-1.502830
N	1.403990	-1.840250	-1.876950
C	1.043730	-3.168490	-1.905650
C	2.221560	-4.009230	-2.033750
C	3.301030	-3.167480	-2.066360
C	2.777040	-1.814940	-1.974270
C	-3.266470	0.190530	-1.468790
C	-2.779110	-1.131020	-1.551120
C	-3.625400	-2.311580	-1.542580
C	-2.789100	-3.392170	-1.641780
C	-1.437220	-2.864430	-1.719540
N	-1.455610	-1.489980	-1.664400
C	-0.276750	-3.663470	-1.826470
C	3.577760	-0.650700	-1.992770
H	-4.061200	2.975810	-1.373280
H	-1.926440	4.648490	-1.467680
H	-4.720440	-2.313170	-1.477370
H	-3.064670	-4.453350	-1.662450
H	4.359730	-3.440690	-2.148540
H	2.222290	-5.104000	-2.098780
H	3.361360	3.998890	-1.872230
H	5.013010	1.865530	-2.114870

C	-0.052480	5.235080	-1.230940	C	0.767600	4.679620	-1.487950
C	4.766120	0.168390	-1.628430	C	5.059050	-0.825410	-2.090220
C	-5.091580	0.370240	-0.964170	C	-4.741700	0.371920	-1.307340
C	-0.296600	-4.651060	-1.711820	C	-0.462860	-5.146340	-1.841130
C	-0.201560	-5.456690	-2.861040	C	-0.108790	-5.934560	-0.729430
C	-0.251430	-6.859890	-2.783730	C	-0.290110	-7.327510	-0.721700
C	-0.387480	-7.480970	-1.530270	C	-0.840050	-7.958890	-1.850900
C	-0.473330	-6.699900	-0.364630	C	-1.205000	-7.197510	-2.974290
C	-0.430740	-5.300860	-0.470320	C	-1.009850	-5.806150	-2.958460
F	-0.063380	-4.892620	-4.064720	F	0.407860	-5.357220	0.363860
F	-0.176690	-7.604680	-3.889060	F	0.048460	-8.053060	0.346340
F	-0.431880	-8.810780	-1.446620	F	-1.018600	-9.280120	-1.854160
F	-0.593960	-7.288000	0.828900	F	-1.729110	-7.798720	-4.045200
F	-0.511210	-4.578110	0.655950	F	-1.362870	-5.105220	-4.040580
C	-5.595430	-0.094530	0.266780	C	-5.357200	0.181090	-0.057800
C	-6.969010	-0.093890	0.556710	C	-6.735170	0.367470	0.131610
C	-7.875380	0.389380	-0.402720	C	-7.534530	0.741150	-0.962460
C	-7.403010	0.865180	-1.637790	C	-6.949520	0.932370	-2.226160
C	-6.023440	0.847660	-1.905650	C	-5.565060	0.748060	-2.384530
F	-4.751710	-0.548990	1.206160	F	-4.615890	-0.178690	1.002280
F	-7.418400	-0.540030	1.732250	F	-7.285870	0.194780	1.336790
F	-9.182030	0.398790	-0.139110	F	-8.846100	0.916830	-0.800890
F	-8.266090	1.325770	-2.545780	F	-7.710150	1.284040	-3.264760
F	-5.603570	1.302230	-3.090360	F	-5.034100	0.942530	-3.594660
C	5.424170	0.381980	-0.402300	C	5.905220	-0.503210	-1.010480
C	6.817430	0.271710	-0.276040	C	7.299860	-0.648430	-1.090530
C	7.591050	-0.036010	-1.408000	C	7.878780	-1.132760	-2.275980
C	6.964060	-0.238770	-2.649510	C	7.060960	-1.465590	-3.369080
C	5.565640	-0.132960	-2.746860	C	5.668880	-1.306240	-3.265980
F	4.714990	0.670560	0.697180	F	5.387800	-0.042470	0.135380
F	7.403510	0.442370	0.913340	F	8.075040	-0.333870	-0.049330
F	8.915880	-0.141120	-1.303890	F	9.201430	-1.275620	-2.363020
F	7.698800	-0.532990	-3.724390	F	7.608700	-1.923070	-4.497510
F	4.997880	-0.341660	-3.938890	F	4.921010	-1.623760	-4.327590
C	-0.421030	6.087280	-2.289240	C	1.106640	5.494650	-2.584140
C	-0.365990	7.486120	-2.165100	C	1.278150	6.883040	-2.447630
C	0.060940	8.058090	-0.954270	C	1.104920	7.483080	-1.188780
C	0.426030	7.231590	0.122580	C	0.768740	6.693940	-0.075070
C	0.360890	5.836770	-0.026670	C	0.605480	5.310220	-0.240770
F	-0.834750	5.572680	-3.451070	F	1.275910	4.952490	-3.793070
F	-0.712200	8.271430	-3.187380	F	1.599200	7.633560	-3.502910
F	0.117490	9.383850	-0.825970	F	1.263400	8.799080	-1.049100
F	0.825220	7.774620	1.275990	F	0.612300	7.261540	1.123600
F	0.699110	5.072660	1.021400	F	0.297390	4.576490	0.845450
C	-1.501090	1.090250	3.955920	C	1.055620	1.438030	3.656880
C	-2.102610	2.436730	3.514830	C	2.196310	2.273520	3.028930
H	-2.594030	2.902560	4.394550	H	2.637200	2.925850	3.812650
H	-1.325530	3.143530	3.148740	H	3.000740	1.619190	2.628580
H	-2.877890	2.311750	2.728480	H	1.839140	2.939930	2.216750
C	-0.493770	1.333480	5.096740	C	1.623130	0.716280	4.890160
H	-1.012320	1.833640	5.942730	H	2.393370	-0.033370	4.609590
H	-0.068480	0.377100	5.463950	H	2.105800	1.475270	5.541350
H	0.333940	1.994680	4.758600	H	0.842320	0.215140	5.493100
C	-2.630620	0.133980	4.391060	C	-0.118480	2.357560	4.041920
H	-3.344810	-0.033500	3.554920	H	-0.498200	2.906560	3.153160
H	-2.213220	-0.842190	4.711830	H	-0.956870	1.783930	4.488530
H	-3.187830	0.581790	5.242520	H	0.226510	3.108080	4.785720

***trans*-α**

$E_{PBE/SVP}$ = -6120.794544253 Hartree

NImag = 0

C	-3.337320	-0.399320	4.615840
C	-4.720450	-0.525230	4.341640
C	-5.638830	-0.648090	5.392240
C	-5.187270	-0.649170	6.723110
C	-3.810540	-0.525240	7.001400
C	-2.886710	-0.400570	5.960290
N	-2.513340	-0.287200	3.482840
N	-1.263990	-0.146910	3.704100
C	-0.514540	-0.054970	2.549160
C	-0.873710	-0.106470	1.197730
N	0.879660	0.117450	2.572760
N	0.243300	0.026460	0.433190
C	1.279260	0.159330	1.274710
H	-5.041150	-0.522580	3.287650
H	-6.714670	-0.745390	5.172900
H	-5.908520	-0.748340	7.551080
H	-3.461170	-0.528090	8.047370
H	-1.808900	-0.304820	6.161840
H	-1.880030	-0.232770	0.784390
H	2.318250	0.287750	0.952920
C	1.572700	2.829070	-1.834030
N	1.758650	1.465440	-1.799590
C	2.854120	3.513480	-1.830780
C	3.818600	2.540130	-1.792960
C	3.120310	1.266410	-1.770670
C	0.323020	3.486360	-1.862360
C	-0.932040	2.839750	-1.866840
C	-2.206310	3.537910	-1.895810
C	-3.180700	2.575860	-1.859580
C	-2.496150	1.294160	-1.832230
N	-1.132470	1.478390	-1.842360
Ni	0.302420	0.026430	-1.595190
N	1.744180	-1.424780	-1.809370
C	1.543640	-2.785690	-1.853230
C	2.818150	-3.483370	-1.871500
C	3.792550	-2.521850	-1.815840
C	3.108080	-1.240500	-1.784430
C	-3.152710	0.043870	-1.800890
C	-2.508030	-1.211570	-1.835340
C	-3.207260	-2.484600	-1.864540
C	-2.243640	-3.458180	-1.894610
C	-0.961260	-2.774210	-1.882510
N	-1.146260	-1.410640	-1.853540
C	0.288280	-3.432280	-1.883580
C	3.764420	0.009460	-1.742880
H	-4.267530	2.722740	-1.861920
H	-2.339610	4.625620	-1.942740
H	-4.296470	-2.615310	-1.874720
H	-2.389440	-4.544950	-1.919790
H	4.879390	-2.669310	-1.808920
H	2.952230	-4.570400	-1.930000
H	2.999340	4.600350	-1.858300
H	4.907530	2.673270	-1.797500

***trans*-β**

$E_{PBE/SVP}$ = -6120.788005657 Hartree

NImag = 0

C	-3.473640	-0.972920	4.773430
C	-3.486630	-1.040060	6.184980
C	-4.675670	-1.330100	6.867440
C	-5.861210	-1.553230	6.147000
C	-5.853030	-1.484020	4.739050
C	-4.671080	-1.196380	4.050560
N	-2.223690	-0.680230	4.179520
N	-2.233450	-0.662670	2.906900
C	-1.103880	-0.403650	2.179840
C	-1.159010	-0.433420	0.777730
N	0.255390	-0.097710	2.490550
N	0.064450	-0.174220	0.252660
C	0.884620	0.019160	1.294170
H	-2.543720	-0.861850	6.726480
H	-4.678960	-1.383120	7.968410
H	-6.797880	-1.781460	6.681740
H	-6.785500	-1.657770	4.176410
H	-4.640300	-1.137180	2.952120
H	-2.050350	-0.624480	0.167690
H	1.949140	0.250410	1.184250
C	2.035650	2.739870	-0.881760
N	2.127330	1.420200	-1.264370
C	3.336230	3.236760	-0.468290
C	4.217190	2.195980	-0.613020
C	3.444690	1.061240	-1.086280
C	0.850590	3.509410	-0.877700
C	-0.403880	3.069800	-1.353270
C	-1.587250	3.909910	-1.421210
C	-2.589200	3.131830	-1.938640
C	-2.013220	1.818770	-2.178150
N	-0.682600	1.809820	-1.830430
Ni	0.547740	0.167740	-1.694590
N	1.881300	-1.368020	-1.972520
C	1.566640	-2.666860	-2.298350
C	2.752580	-3.504360	-2.240380
C	3.788380	-2.690800	-1.863890
C	3.229880	-1.360190	-1.695950
C	-2.741850	0.706030	-2.655620
C	-2.215830	-0.592860	-2.832120
C	-2.987570	-1.727480	-3.308850
C	-2.148410	-2.810160	-3.285000
C	-0.860710	-2.327210	-2.817120
N	-0.923160	-0.977250	-2.553450
C	0.286760	-3.137250	-2.667200
C	3.973550	-0.234720	-1.278140
H	-3.628650	3.421040	-2.134930
H	-1.639620	4.965000	-1.125500
H	-4.036580	-1.698770	-3.627940
H	-2.380130	-3.843290	-3.570410
H	4.839230	-2.967950	-1.716930
H	2.790660	-4.575320	-2.474350
H	3.555840	4.255720	-0.127600
H	5.296960	2.199820	-0.420150

C	0.327330	4.981340	-1.875800	C	0.920870	4.876120	-0.276160
C	5.256160	0.003490	-1.656530	C	5.413950	-0.444010	-0.937940
C	-4.642670	0.055210	-1.679350	C	-4.195430	0.908110	-2.936610
C	0.284080	-4.926770	-1.905010	C	0.136830	-4.608930	-2.883470
C	0.647950	-5.673650	-0.767700	C	0.152750	-5.489450	-1.783780
C	0.650400	-7.078560	-0.773420	C	0.010280	-6.877330	-1.942060
C	0.284760	-7.765760	-1.943260	C	-0.149290	-7.411800	-3.231730
C	-0.082700	-7.047630	-3.093750	C	-0.166890	-6.558250	-4.348000
C	-0.079060	-5.642530	-3.062490	C	-0.023440	-5.172240	-4.163430
F	1.000610	-5.045120	0.360200	F	0.303040	-5.007550	-0.545170
F	0.993680	-7.764820	0.319980	F	0.021680	-7.686940	-0.880160
F	0.285300	-9.099130	-1.960870	F	-0.284560	-8.728050	-3.396420
F	-0.425050	-7.704840	-4.204640	F	-0.315380	-7.069750	-5.572520
F	-0.430240	-4.983620	-4.171500	F	-0.041970	-4.385920	-5.244540
C	-5.261190	-0.225830	-0.446380	C	-5.179820	0.383930	-2.076480
C	-6.654210	-0.173270	-0.282540	C	-6.550130	0.588410	-2.305510
C	-7.465000	0.153920	-1.382870	C	-6.959590	1.334070	-3.424660
C	-6.877040	0.429530	-2.629770	C	-5.999970	1.867320	-4.302050
C	-5.478900	0.376570	-2.764730	C	-4.635080	1.648550	-4.050600
F	-4.513260	-0.537670	0.622150	F	-4.820400	-0.324670	-0.996850
F	-7.208820	-0.423340	0.908710	F	-7.461760	0.087820	-1.467660
F	-8.790020	0.206490	-1.243810	F	-8.257540	1.536460	-3.652430
F	-7.647880	0.739530	-3.674540	F	-6.388500	2.574120	-5.365800
F	-4.947370	0.650220	-3.960160	F	-3.745220	2.168680	-4.901300
C	5.910650	0.323800	-0.452590	C	5.837400	-0.458100	0.404550
C	7.310070	0.316390	-0.339070	C	7.179800	-0.659250	0.762040
C	8.088300	-0.019280	-1.460530	C	8.137390	-0.855410	-0.247930
C	7.464130	-0.343110	-2.677440	C	7.746320	-0.845640	-1.597690
C	6.061320	-0.327300	-2.763100	C	6.394920	-0.642970	-1.927720
F	5.189450	0.640070	0.636970	F	4.941820	-0.278930	1.389890
F	7.904290	0.616450	0.819400	F	7.550130	-0.670850	2.045130
F	9.418180	-0.032210	-1.368660	F	9.416120	-1.050660	0.074060
F	8.205630	-0.660710	-3.740420	F	8.659960	-1.026260	-2.553490
F	5.495330	-0.639040	-3.932820	F	6.051960	-0.642600	-3.218960
C	0.688610	5.702920	-3.029930	C	1.551260	5.954620	-0.924000
C	0.690170	7.108230	-3.053920	C	1.642920	7.223760	-0.327560
C	0.325390	7.819840	-1.898490	C	1.090240	7.432200	0.947390
C	-0.038800	7.126320	-0.731900	C	0.450020	6.374810	1.616400
C	-0.033580	5.721300	-0.733280	C	0.374850	5.115770	0.999830
F	1.039550	5.049580	-4.142320	F	2.092630	5.784900	-2.134340
F	1.031070	7.771780	-4.161450	F	2.250870	8.229390	-0.960560
F	0.324010	9.153290	-1.909000	F	1.177020	8.631820	1.522580
F	-0.380000	7.806710	0.365820	F	-0.071540	6.569990	2.830340
F	-0.382570	5.085530	0.391460	F	-0.227310	4.120320	1.667320
C	1.762050	0.233620	3.781400	C	0.922340	0.166050	3.816910
C	1.640870	-1.066060	4.602500	C	0.865960	-1.115060	4.669100
H	2.298560	-1.004130	5.496220	H	1.357740	-0.927720	5.648320
H	0.595460	-1.222090	4.939680	H	-0.185930	-1.413410	4.856250
H	1.956940	-1.944000	3.997810	H	1.405800	-1.945150	4.163000
C	1.310960	1.458790	4.602040	C	0.197220	1.348740	4.488220
H	1.955060	1.558780	5.502150	H	0.227920	2.247480	3.833360
H	1.404300	2.390090	4.001750	H	-0.858430	1.088500	4.709750
H	0.256540	1.348610	4.929360	H	0.702440	1.595770	5.447190
C	3.220370	0.425590	3.333920	C	2.395890	0.549840	3.587330
H	3.599040	-0.436110	2.743630	H	2.980040	-0.261270	3.103270
H	3.360650	1.353500	2.738770	H	2.504750	1.479570	2.988170
H	3.854100	0.512210	4.241500	H	2.854910	0.739510	4.580320

I.6.6 1-Methyl-4'-methoxy-5-phenylazoimidazole · $NiTPPF_{20}$ (2b)

***cis*-α**

$E_{PBE/SVP}$ = -6117.410019923 Hartree

NImag = 0

C	1.369900	-2.073120	3.994380
C	1.270540	-3.468890	4.232650
C	2.065060	-4.372650	3.534650
C	3.033600	-3.902950	2.616340
C	3.199820	-2.510610	2.430510
C	2.364590	-1.611200	3.100870
N	0.577490	-1.242230	4.814390
N	0.057070	-0.145630	4.454740
C	-0.072820	0.338330	3.157780
C	-0.138600	-0.160240	1.843810
N	-0.512030	1.668390	3.057910
N	-0.586320	0.823720	1.008510
C	-0.790370	1.915400	1.758420
H	0.532050	-3.816440	4.972310
H	2.508820	-0.532400	2.935560
H	0.100030	-1.165090	1.478320
H	-1.120910	2.893360	1.384030
C	0.385620	3.637050	-1.226610
N	0.616730	2.284510	-1.334280
C	1.642220	4.366660	-1.223550
C	2.636550	3.432170	-1.345970
C	1.982580	2.136100	-1.410890
C	-0.888080	4.242860	-1.138380
C	-2.119020	3.547150	-1.154710
C	-3.419970	4.194000	-1.148930
C	-4.354750	3.192410	-1.147070
C	-3.621450	1.938550	-1.154430
N	-2.265120	2.177970	-1.169580
Ni	-0.763080	0.781060	-1.021920
N	0.711830	-0.606590	-1.371930
C	0.561070	-1.973470	-1.411770
C	1.843040	-2.617240	-1.639490
C	2.773520	-1.613770	-1.728290
C	2.056310	-0.364860	-1.540700
C	-4.231350	0.664930	-1.127260
C	-3.536530	-0.564690	-1.132420
C	-4.183790	-1.866310	-1.112600
C	-3.183320	-2.801570	-1.129700
C	-1.931420	-2.066330	-1.185010
N	-2.169330	-0.710630	-1.179020
C	-0.659720	-2.671270	-1.272760
C	2.668960	0.907480	-1.530490
H	-5.446450	3.296190	-1.140560
H	-3.597540	5.276310	-1.163490
H	-5.266160	-2.042960	-1.098240
H	-3.285410	-3.893550	-1.122110
H	3.848140	-1.708910	-1.929010
H	2.003680	-3.697000	-1.749770
H	1.753060	5.454620	-1.140560
H	3.718990	3.606630	-1.379200
C	-0.947790	5.727800	-0.988670
C	4.157520	0.956190	-1.648460
C	-5.725000	0.617260	-1.085980

***cis*-β**

$E_{PBE/SVP}$ = -6117.400704494 Hartree

NImag = 0

C	0.734390	-0.898420	4.735050
C	0.292320	-1.234940	6.036260
C	-0.219750	-2.502250	6.330230
C	-0.235420	-3.497530	5.325160
C	0.258580	-3.190070	4.032500
C	0.717680	-1.909830	3.732610
N	1.326900	0.374950	4.604060
N	1.411350	1.039030	3.527040
C	0.687800	0.804580	2.360220
C	1.149530	0.982530	1.052210
N	-0.688710	0.546810	2.237280
N	0.115850	0.791330	0.175000
C	-0.975570	0.559740	0.905160
H	0.360070	-0.461150	6.817560
H	1.105950	-1.706250	2.722610
H	2.174310	1.201200	0.729360
H	-1.994350	0.438270	0.512000
C	1.378680	3.571870	-2.239950
N	1.598070	2.215860	-2.147320
C	2.642640	4.285740	-2.301060
C	3.630300	3.338330	-2.246960
C	2.964770	2.050950	-2.141350
C	0.113580	4.197770	-2.273650
C	-1.125040	3.520320	-2.258670
C	-2.414820	4.184780	-2.335430
C	-3.365760	3.199220	-2.301480
C	-2.651000	1.936500	-2.219960
N	-1.292250	2.155810	-2.194580
Ni	0.179920	0.759460	-1.858540
N	1.660040	-0.663350	-1.970870
C	1.490050	-2.020290	-1.826850
C	2.779250	-2.687050	-1.748860
C	3.732080	-1.706200	-1.837050
C	3.018840	-0.446880	-1.966150
C	-3.277150	0.670860	-2.170080
C	-2.600410	-0.567730	-2.107450
C	-3.263660	-1.859340	-2.054930
C	-2.276110	-2.800810	-1.922120
C	-1.014990	-2.080260	-1.913920
N	-1.234720	-0.727740	-2.044530
C	0.249550	-2.691960	-1.772020
C	3.644160	0.816670	-2.040510
H	-4.455230	3.319450	-2.338650
H	-2.573150	5.267170	-2.416130
H	-4.346000	-2.026340	-2.120220
H	-2.393300	-3.888990	-1.849080
H	4.822260	-1.825280	-1.816530
H	2.935530	-3.769030	-1.656270
H	2.761100	5.373180	-2.379300
H	4.714980	3.496530	-2.286250
C	0.081160	5.691450	-2.328120
C	5.135160	0.863060	-1.951270
C	-4.770240	0.643560	-2.123150

C	-0.578510	-4.160410	-1.179700	C	0.281670	-4.151970	-1.453020
C	-0.092040	-4.759620	-0.002210	C	0.540540	-4.566720	-0.133330
C	0.034170	-6.151140	0.130410	C	0.574120	-5.920060	0.233540
C	-0.346460	-6.978820	-0.940350	C	0.349050	-6.902170	-0.745990
C	-0.842190	-6.410210	-2.126850	C	0.094140	-6.520270	-2.074670
C	-0.956440	-5.013140	-2.233250	C	0.056670	-5.155550	-2.412650
F	0.267570	-3.990460	1.033870	F	0.752290	-3.648910	0.823000
F	0.501730	-6.689010	1.260190	F	0.806270	-6.275300	1.502420
F	-0.236100	-8.302940	-0.831890	F	0.377210	-8.193450	-0.416360
F	-1.197780	-7.198310	-3.144220	F	-0.110890	-7.455240	-3.004890
F	-1.428690	-4.502410	-3.374600	F	-0.201450	-4.824850	-3.681270
C	-6.411670	0.230060	0.081340	C	-5.446210	0.325300	-0.929670
C	-7.815090	0.188960	0.137260	C	-6.847710	0.312870	-0.846820
C	-8.562190	0.541560	-0.999420	C	-7.606540	0.628820	-1.987080
C	-7.904670	0.931620	-2.178530	C	-6.961170	0.952860	-3.192710
C	-6.500210	0.964760	-2.209560	C	-5.556670	0.953340	-3.249230
F	-5.724790	-0.106970	1.178620	F	-4.746110	0.031190	0.179690
F	-8.442950	-0.175230	1.258520	F	-7.462730	0.013120	0.300920
F	-9.894390	0.506980	-0.958920	F	-8.938120	0.623820	-1.923300
F	-8.617230	1.263510	-3.257590	F	-7.684770	1.254630	-4.272580
F	-5.901910	1.340820	-3.345060	F	-4.970320	1.264170	-4.409290
C	4.993490	0.535200	-0.596610	C	5.765290	1.316270	-0.776050
C	6.393530	0.581650	-0.692420	C	7.163120	1.391390	-0.663850
C	6.988880	1.066860	-1.869740	C	7.962720	1.000850	-1.751980
C	6.182090	1.493070	-2.938700	C	7.362140	0.538760	-2.935680
C	4.783280	1.434090	-2.816990	C	5.961020	0.470480	-3.021440
F	4.458710	0.073390	0.545810	F	5.026510	1.688800	0.277550
F	7.158490	0.180530	0.326980	F	7.733890	1.825190	0.462500
F	8.316800	1.119290	-1.972720	F	9.291200	1.068300	-1.660900
F	6.746450	1.947870	-4.059340	F	8.123750	0.172970	-3.969500
F	4.043450	1.840390	-3.852370	F	5.418840	0.024590	-4.159190
C	-0.595950	6.600090	-2.037400	C	0.423440	6.392950	-3.500190
C	-0.671780	7.996320	-1.896680	C	0.400300	7.797090	-3.555970
C	-1.109000	8.548590	-0.680470	C	0.025900	8.527940	-2.415720
C	-1.463540	7.703920	0.385810	C	-0.322050	7.854550	-1.232480
C	-1.374280	6.313100	0.219550	C	-0.292640	6.450200	-1.202110
F	-0.181740	6.108090	-3.208580	F	0.782670	5.720980	-4.598920
F	-0.338200	8.797720	-2.910240	F	0.725890	8.441100	-4.679740
F	-1.186590	9.871370	-0.537230	F	0.000552	9.860550	-2.456320
F	-1.874870	8.225640	1.544320	F	-0.672720	8.552960	-0.149510
F	-1.708410	5.534700	1.263570	F	-0.629090	5.834200	-0.063060
C	-0.622960	2.602510	4.167500	C	-1.680660	0.440370	3.297220
H	-1.068600	2.074790	5.034530	H	-1.716760	-0.589030	3.712260
H	0.378140	2.981260	4.466140	H	-1.430220	1.146490	4.114810
H	-1.260880	3.453710	3.855690	H	-2.673360	0.708230	2.881020
O	3.758460	-4.853580	1.975370	O	-0.679170	-4.764830	5.502190
C	4.752570	-4.447620	1.050220	C	-1.166320	-5.153030	6.775450
H	5.551100	-3.843030	1.541740	H	-2.055160	-4.550020	7.077460
H	5.198460	-5.380420	0.649960	H	-1.464250	-6.216160	6.679060
H	4.314370	-3.857110	0.210630	H	-0.380140	-5.063070	7.561510
H	3.971330	-2.112710	1.756150	H	0.280020	-3.989020	3.275660
H	1.959960	-5.459500	3.673330	H	-0.575920	-2.716520	7.348570

***trans*-α**

$E_{PBE/SVP}$ = -6117.428319313 Hartree

NImag = 0

C	-2.701870	-0.188400	4.253120
C	-4.091290	-0.356390	4.014160
C	-4.988790	-0.440290	5.074300
C	-4.522240	-0.356430	6.408630
C	-3.136260	-0.187170	6.658800
C	-2.242080	-0.104390	5.590250
N	-1.894520	-0.124860	3.115420
N	-0.638850	0.023530	3.312750
C	0.089050	0.071080	2.145790
C	-0.234760	-0.006180	0.787210
N	1.475680	0.227050	2.194610
N	0.908440	0.098320	0.049230
C	1.923620	0.238260	0.912210
H	-4.431950	-0.417390	2.967940
H	-1.163070	0.025510	5.765190
H	-1.229030	-0.131000	0.346050
H	2.982160	0.348540	0.639910
C	2.268090	2.856940	-2.258630
N	2.449810	1.494300	-2.190130
C	3.550770	3.538980	-2.237250
C	4.511520	2.564990	-2.150440
C	3.809680	1.293420	-2.121370
C	1.020550	3.515740	-2.326660
C	-0.236060	2.872400	-2.329060
C	-1.507910	3.573430	-2.383400
C	-2.485500	2.615880	-2.325320
C	-1.805400	1.332920	-2.263900
N	-0.441040	1.512620	-2.272410
Ni	0.989860	0.062790	-1.979330
N	2.428720	-1.395410	-2.149120
C	2.225930	-2.756150	-2.181400
C	3.499240	-3.456320	-2.171200
C	4.474420	-2.496170	-2.105570
C	3.792020	-1.213370	-2.098900
C	-2.465520	0.085220	-2.205870
C	-1.822700	-1.172350	-2.218090
C	-2.524120	-2.444440	-2.237690
C	-1.562400	-3.420180	-2.251020
C	-0.278750	-2.738790	-2.237350
N	-0.461320	-1.374520	-2.225210
C	0.969130	-3.399840	-2.218710
C	4.449420	0.035980	-2.056030
H	-3.571660	2.766680	-2.335060
H	-1.637550	4.659970	-2.458850
H	-3.613300	-2.574170	-2.254880
H	-1.710660	-4.506810	-2.265820
H	5.560640	-2.645570	-2.076890
H	3.632320	-4.544090	-2.216980
H	3.698880	4.624850	-2.283780
H	5.600620	2.695200	-2.126230
C	1.029720	5.009940	-2.379020
C	5.937970	0.025440	-1.924520
C	-3.955410	0.098770	-2.086430
C	0.961250	-4.894460	-2.221110
C	1.318390	-5.627440	-1.072450

***trans*-β**

$E_{PBE/SVP}$ = -6117.426950607 Hartree

NImag = 0

C	-1.114090	0.006710	5.329630
C	-0.477720	0.064040	6.588580
C	-1.213780	0.023470	7.778660
C	-2.622140	-0.075580	7.720540
C	-3.270060	-0.133980	6.458000
C	-2.531400	-0.093870	5.282880
N	-0.277980	0.055880	4.204550
N	-0.881500	-0.004660	3.077400
C	-0.099600	0.042710	1.955040
C	-0.574970	-0.016720	0.638380
N	1.300490	0.157190	1.839370
N	0.473660	0.056870	-0.231340
C	1.580570	0.160440	0.512380
H	0.621110	0.141240	6.611330
H	-3.020050	-0.138000	4.297840
H	-1.618370	-0.111990	0.314440
H	2.603030	0.244430	0.118410
C	2.306600	0.256940	2.890150
C	1.745780	2.807290	-2.570360
N	1.929180	1.444180	-2.506130
C	3.028210	3.489440	-2.579000
C	3.990640	2.516170	-2.509800
C	3.290370	1.244260	-2.459020
C	0.497640	3.466980	-2.604940
C	-0.758870	2.823360	-2.590750
C	-2.031400	3.523360	-2.639660
C	-3.007920	2.563780	-2.598800
C	-2.326310	1.281440	-2.544780
N	-0.962270	1.463190	-2.540770
Ni	0.467820	0.013680	-2.264610
N	1.913210	-1.444470	-2.445300
C	1.710440	-2.805740	-2.458750
C	2.983580	-3.505970	-2.439490
C	3.959010	-2.545320	-2.385850
C	3.277070	-1.262470	-2.399540
C	-2.984960	0.032690	-2.512600
C	-2.340070	-1.223790	-2.509900
C	-3.039480	-2.496870	-2.542130
C	-2.076950	-3.471620	-2.537550
C	-0.794380	-2.789110	-2.507380
N	-0.978620	-1.424970	-2.493850
C	0.453790	-3.449620	-2.488670
C	3.933610	-0.011880	-2.377090
H	-4.094400	2.712540	-2.612710
H	-2.162070	4.610400	-2.705290
H	-4.127890	-2.628290	-2.578000
H	-2.224160	-4.558310	-2.554040
H	5.045120	-2.694850	-2.355320
H	3.116380	-4.594280	-2.470270
H	3.175610	4.575010	-2.632190
H	5.079670	2.648190	-2.511420
C	0.505150	4.961380	-2.645680
C	5.420540	-0.005590	-2.228250
C	-4.478420	0.038320	-2.467410
C	0.445350	-4.944400	-2.492850

C	1.318080	-7.032330	-1.059740	C	0.795870	-5.680080	-1.344120
C	0.957410	-7.733970	-2.222460	C	0.795160	-7.085070	-1.334970
C	0.595500	-7.030050	-3.383400	C	0.433500	-7.783710	-2.499210
C	0.602930	-5.624670	-3.371000	C	0.079250	-7.076880	-3.660770
F	1.665650	-4.985130	0.049090	C	0.087980	-5.671610	-3.645010
F	1.656270	-7.705200	0.043740	F	1.141680	-5.040280	-0.220660
F	0.955370	-9.067570	-2.222850	F	1.128280	-7.760690	-0.231780
F	0.256510	-7.701030	-4.487110	F	0.428460	-9.117220	-2.502130
F	0.257710	-4.980030	-4.490370	F	-0.258490	-7.744950	-4.766570
C	-4.577100	-0.203280	-0.859240	F	-0.252210	-5.023940	-4.764180
C	-5.970760	-0.156390	-0.698170	C	-5.163030	-0.298760	-1.284020
C	-6.780230	0.182130	-1.795940	C	-6.565890	-0.300070	-1.212380
C	-6.189540	0.479980	-3.036350	C	-7.313690	0.048840	-2.350100
C	-4.791010	0.433140	-3.168670	C	-6.658000	0.389330	-3.545540
F	-3.833070	-0.526200	0.208290	C	-5.253400	0.382280	-3.591360
F	-6.527080	-0.425030	0.488350	F	-4.472100	-0.627400	-0.183560
F	-8.105960	0.227620	-1.659900	F	-7.192880	-0.618950	-0.076820
F	-6.958530	0.800230	-4.079600	F	-8.645990	0.054320	-2.295680
F	-4.259200	0.723880	-4.360320	F	-7.372630	0.716380	-4.624650
C	6.555880	0.331970	-0.697850	F	-4.655310	0.710780	-4.741190
C	7.951000	0.306750	-0.540360	C	6.017330	0.392410	-1.016630
C	8.761480	-0.024260	-1.640170	C	7.410120	0.437250	-0.848620
C	8.173510	-0.332620	-2.878950	C	8.243490	0.064210	-1.917520
C	6.774460	-0.301840	-3.008430	C	7.678620	-0.345610	-3.137520
F	5.805450	0.647580	0.371030	C	6.280560	-0.378470	-3.278890
F	8.510870	0.589230	0.639570	F	5.246780	0.745070	0.027920
F	10.087740	-0.051370	-1.505760	F	7.944620	0.823480	0.313170
F	8.944650	-0.646870	-3.921930	F	9.568320	0.099700	-1.773500
F	6.242460	-0.601240	-4.197210	F	8.470320	-0.696500	-4.153020
C	1.404980	5.699160	-3.548410	F	5.775150	-0.772780	-4.451270
C	1.414420	7.103310	-3.609890	C	0.871030	5.661880	-3.811350
C	1.041540	7.846980	-2.477500	C	0.876870	7.066520	-3.860150
C	0.664020	7.186110	-1.296250	C	0.512140	7.799240	-2.718000
C	0.660080	5.781610	-1.260580	C	0.142970	7.127100	-1.540500
F	1.762750	5.015070	-4.639670	C	0.143480	5.722310	-1.517130
F	1.768430	7.735220	-4.732050	F	1.222290	4.988360	-4.911480
F	1.046970	9.179840	-2.523060	F	1.221930	7.709430	-4.978740
F	0.316110	7.896280	-0.219710	F	0.515160	9.132370	-2.751570
F	0.296220	5.179000	-0.122440	F	-0.198590	7.827100	-0.455460
C	2.277740	0.353450	3.401020	F	-0.210510	5.108190	-0.382170
H	1.942830	1.229090	3.994800	H	3.301140	0.336360	2.403050
H	2.177170	-0.556460	4.028340	H	2.272690	-0.636350	3.544200
H	3.338580	0.487150	3.108920	H	2.119850	1.147370	3.521710
O	-5.468100	-0.450610	7.374120	O	-3.437120	-0.122170	8.802110
C	-5.082420	-0.354580	8.734570	C	-2.866840	-0.057360	10.097850
H	-4.586750	0.620110	8.954910	H	-2.305450	0.894030	10.253040
H	-6.018050	-0.427470	9.324440	H	-3.715760	-0.098940	10.809590
H	-4.399910	-1.186670	9.028490	H	-2.185160	-0.918950	10.290760
H	-6.069080	-0.571720	4.907330	H	-0.686790	0.068510	8.742670
H	-2.754490	-0.122160	7.688630	H	-4.368900	-0.211010	6.444670

I.6.7 1-Methyl-3',5'-dimethyl-4'-methoxy-5-phenylazoimidazole · $NiTPPF_{20}$ (2f)

***cis*-α**

$E_{PBE/SVP}$ = -6195.859320536 Hartree

NImag = 0

C	1.342090	-1.982400	4.012460
C	1.089260	-3.363590	4.153090
C	1.837470	-4.314520	3.443240
C	2.905770	-3.855780	2.632950
C	3.216520	-2.475920	2.514840
C	2.413540	-1.550300	3.199180
N	0.599970	-1.106640	4.842040
N	0.098880	-0.012250	4.457610
C	-0.036200	0.424190	3.144110
C	-0.089780	-0.110070	1.842310
N	-0.472330	1.750800	3.006290
N	-0.531950	0.851010	0.979370
C	-0.741060	1.962070	1.700730
H	0.273970	-3.681170	4.823070
H	2.638230	-0.475250	3.109860
H	0.152560	-1.123900	1.504500
H	-1.069860	2.929690	1.299250
C	0.355300	3.682800	-1.282300
N	0.604160	2.331660	-1.366310
C	1.600250	4.430350	-1.338320
C	2.604510	3.507990	-1.470380
C	1.969820	2.200920	-1.476120
C	-0.923580	4.272640	-1.158660
C	-2.144750	3.561010	-1.112970
C	-3.451630	4.189470	-1.023960
C	-4.370210	3.174940	-0.959360
C	-3.622480	1.931550	-1.022380
N	-2.272950	2.189650	-1.122900
Ni	-0.746570	0.805880	-1.050650
N	0.733120	-0.556590	-1.478540
C	0.597940	-1.923690	-1.565820
C	1.891690	-2.549390	-1.778130
C	2.813780	-1.536070	-1.810170
C	2.077300	-0.297870	-1.623230
C	-4.212220	0.648710	-0.985250
C	-3.504290	-0.569880	-1.085520
C	-4.139100	-1.876910	-1.130930
C	-3.133380	-2.796040	-1.272120
C	-1.890750	-2.045110	-1.317530
N	-2.139180	-0.696330	-1.200500
C	-0.618830	-2.633520	-1.481030
C	2.671610	0.981950	-1.601300
H	-5.460400	3.263720	-0.880730
H	-3.644890	5.269180	-1.025910
H	-5.218250	-2.066210	-1.081360
H	-3.224220	-3.886530	-1.349160
H	3.897730	-1.619910	-1.955150
H	2.070830	-3.625520	-1.892600
H	1.697230	5.521650	-1.291860
H	3.680710	3.697980	-1.563960
C	-0.991190	5.758920	-1.023180
C	4.159370	1.057980	-1.727440
C	-5.698090	0.568310	-0.843220

***cis*-β**

$E_{PBE/SVP}$ = -6195.848580914 Hartree

NImag = 0

C	0.409850	-0.762970	4.973620
C	-0.190550	-0.894170	6.247170
C	-0.888190	-2.054610	6.608030
C	-0.916820	-3.133390	5.685670
C	-0.294590	-3.046020	4.412480
C	0.353270	-1.847750	4.065220
N	1.179680	0.404640	4.765580
N	1.354120	0.979090	3.651610
C	0.619550	0.785080	2.486620
C	1.135990	0.911260	1.191410
N	-0.767600	0.611780	2.316820
N	0.127300	0.768160	0.279960
C	-1.001680	0.619840	0.975990
H	-0.103200	-0.049670	6.949990
H	0.844510	-1.772560	3.081440
H	2.183530	1.067460	0.906970
H	-2.011250	0.556590	0.547260
C	-1.816040	0.601480	3.328210
C	1.422760	3.565520	-2.135510
N	1.647380	2.215570	-1.987950
C	2.681230	4.291580	-2.117940
C	3.670350	3.357890	-1.959540
C	3.011270	2.065040	-1.884530
C	0.158660	4.178250	-2.285750
C	-1.077350	3.494540	-2.263010
C	-2.371230	4.143120	-2.391110
C	-3.316860	3.158600	-2.277680
C	-2.594710	1.907990	-2.118930
N	-1.236950	2.135500	-2.111460
Ni	0.238270	0.743210	-1.753490
N	1.728890	-0.667530	-1.876590
C	1.573410	-2.034810	-1.886460
C	2.870230	-2.690000	-1.840740
C	3.809650	-1.695740	-1.770660
C	3.084040	-0.437570	-1.801600
C	-3.212300	0.641570	-2.015100
C	-2.529160	-0.593990	-1.981720
C	-3.187000	-1.888540	-1.956700
C	-2.191680	-2.831170	-1.944660
C	-0.932020	-2.106780	-1.958170
N	-1.161490	-0.750230	-1.986830
C	0.339660	-2.722020	-1.921520
C	3.696520	0.834600	-1.770850
H	-4.407040	3.270170	-2.320060
H	-2.538340	5.215190	-2.550520
H	-4.271360	-2.055430	-1.965620
H	-2.304280	-3.922050	-1.927040
H	4.899220	-1.806380	-1.714230
H	3.042830	-3.772870	-1.866290
H	2.794870	5.378330	-2.211570
H	4.752890	3.528450	-1.916760
C	0.133060	5.655930	-2.508440
C	5.181060	0.895460	-1.611610

C	-0.551530	-4.123220	-1.595090	C	-4.703290	0.611550	-1.910310
C	-0.187220	-4.921850	-0.495560	C	0.379260	-4.214760	-1.872170
C	-0.111360	-6.320810	-0.595910	C	0.770110	-4.889860	-0.700280
C	-0.395840	-6.945550	-1.822040	C	0.794350	-6.290740	-0.615420
C	-0.762210	-6.171670	-2.935990	C	0.433740	-7.053310	-1.739480
C	-0.838490	-4.774040	-2.809800	C	0.043510	-6.409990	-2.926670
F	0.094670	-4.348440	0.682200	C	0.020450	-5.005500	-2.981280
F	0.230080	-7.068940	0.459620	F	1.118180	-4.186860	0.388920
F	-0.320430	-8.272420	-1.926120	F	1.153530	-6.899410	0.519220
F	-1.029150	-6.766830	-4.100960	F	0.456680	-8.384920	-1.678330
F	-1.189820	-4.059130	-3.882200	F	-0.295760	-7.136280	-3.993690
C	-6.289700	0.101700	0.347180	F	-0.358200	-4.424980	-4.124100
C	-7.682980	0.000272	0.493670	C	-5.329450	0.381750	-0.671080
C	-8.519620	0.376660	-0.570810	C	-6.725940	0.386920	-0.528840
C	-7.958670	0.848990	-1.769680	C	-7.531230	0.622820	-1.656800
C	-6.561970	0.939470	-1.892160	C	-6.936260	0.851570	-2.909310
F	-5.520830	-0.260370	1.380140	C	-5.535200	0.838660	-3.023050
F	-8.214030	-0.446100	1.634850	F	-4.584750	0.161090	0.428120
F	-9.843670	0.285690	-0.443600	F	-7.291470	0.178510	0.663090
F	-8.752270	1.201850	-2.783870	F	-8.858720	0.633070	-1.536470
F	-6.060430	1.389100	-3.047210	F	-7.702680	1.079260	-3.977900
C	4.970350	1.354250	-0.616550	F	-4.996140	1.059810	-4.225350
C	6.366860	1.455450	-0.718580	C	5.754840	1.349930	-0.408260
C	6.982150	1.256420	-1.966290	C	7.145480	1.447180	-0.238460
C	6.200060	0.950560	-3.093070	C	7.996560	1.077120	-1.294190
C	4.804050	0.855000	-2.962500	C	7.453330	0.614380	-2.504990
F	4.411870	1.535070	0.590370	C	6.058430	0.528680	-2.650030
F	7.109260	1.738800	0.354800	F	4.968780	1.704600	0.617190
F	8.307040	1.352610	-2.079600	F	7.661030	1.883700	0.912790
F	6.785400	0.761590	-4.277780	F	9.318720	1.164160	-1.146480
F	4.086400	0.561480	-4.050820	F	8.261970	0.266670	-3.509040
C	-0.680740	6.620220	-2.093900	F	5.571840	0.089790	-3.815440
C	-0.739540	8.018050	-1.961290	C	0.609480	6.208080	-3.714590
C	-1.122360	8.583260	-0.732770	C	0.596810	7.592030	-3.953700
C	-1.438270	7.749960	0.354460	C	0.092250	8.459080	-2.969850
C	-1.365500	6.357100	0.196080	C	-0.391900	7.937990	-1.758000
F	-0.316580	6.115700	-3.276680	C	-0.363820	6.550090	-1.540230
F	-0.439330	8.809080	-2.993220	F	1.089350	5.407980	-4.672300
F	-1.183900	9.907730	-0.597240	F	1.053510	8.086140	-5.106700
F	-1.796440	8.285160	1.524740	F	0.072050	9.774710	-3.185750
F	-1.661560	5.588960	1.259760	F	-0.869140	8.764480	-0.823460
C	-0.593900	2.717240	4.087610	F	-0.826670	6.086090	-0.373750
H	-1.165260	2.264060	4.922560	H	-2.775410	0.869250	2.840260
H	0.408470	3.006540	4.467890	H	-1.587760	1.350160	4.113730
H	-1.114910	3.615650	3.700180	H	-1.906210	-0.398020	3.802270
C	4.363880	-2.019050	1.646860	C	-0.359400	-4.205780	3.448760
H	5.350400	-2.220940	2.124090	H	-1.350870	-4.704560	3.499630
H	4.356210	-2.555300	0.673950	H	-0.171340	-3.875490	2.407340
H	4.306510	-0.927610	1.453360	H	0.407010	-4.980940	3.679970
C	1.513770	-5.785990	3.516280	C	-1.587910	-2.182230	7.939070
H	0.663120	-5.970180	4.205090	H	-2.648100	-2.489360	7.805810
H	1.240860	-6.178650	2.513340	H	-1.114150	-2.959370	8.580570
H	2.377980	-6.388180	3.874490	H	-1.562140	-1.223360	8.497050
O	3.619070	-4.778650	1.895540	O	-1.625260	-4.263090	6.029240
C	4.810560	-5.273690	2.494090	C	-0.868430	-5.345830	6.559980
H	4.605650	-5.781810	3.466560	H	-0.309830	-5.045230	7.478140
H	5.239110	-6.012420	1.785150	H	-1.595850	-6.141440	6.822100
H	5.559260	-4.465520	2.670460	H	-0.140350	-5.751570	5.819090

***trans*-α**

$E_{PBE/SVP}$ = -6195.877350018 Hartree

NImag = 0

C	-2.588610	-0.271240	4.293390
C	-3.964260	-0.460350	4.026410
C	-4.907020	-0.502480	5.062100
C	-4.440850	-0.343560	6.391810
C	-3.058890	-0.177080	6.693430
C	-2.146810	-0.141250	5.631290
N	-1.768610	-0.239640	3.159440
N	-0.515240	-0.083210	3.356460
C	0.204690	-0.046870	2.182490
C	-0.139950	-0.122870	0.829400
N	1.590920	0.113240	2.210370
N	0.989640	-0.010960	0.073140
C	2.018360	0.128610	0.920800
H	-4.271500	-0.579560	2.975130
H	-1.068020	-0.022090	5.818720
H	-1.140740	-0.250150	0.404760
H	3.071920	0.244920	0.632140
C	2.250230	2.832510	-2.183250
N	2.446420	1.470440	-2.161600
C	3.527010	3.526100	-2.181260
C	4.498600	2.559630	-2.149810
C	3.809520	1.281000	-2.135820
C	0.995140	3.481030	-2.182760
C	-0.255790	2.826580	-2.152990
C	-1.533700	3.517190	-2.109570
C	-2.499980	2.549370	-2.039130
C	-1.809970	1.270760	-2.076430
N	-0.448610	1.463600	-2.145420
Ni	1.007790	0.018010	-1.959070
N	2.453790	-1.417130	-2.224720
C	2.261900	-2.777190	-2.305400
C	3.540650	-3.466550	-2.335110
C	4.508700	-2.501040	-2.246890
C	3.816050	-1.225040	-2.187780
C	-2.456260	0.013440	-2.056810
C	-1.800490	-1.233320	-2.174780
C	-2.489920	-2.509490	-2.258320
C	-1.520160	-3.472250	-2.353740
C	-0.243160	-2.779670	-2.324210
N	-0.438030	-1.419880	-2.229510
C	1.010140	-3.429280	-2.356450
C	4.462710	0.028940	-2.119320
H	-3.585290	2.693680	-1.981410
H	-1.675970	4.604480	-2.130620
H	-3.577910	-2.649530	-2.262660
H	-1.658610	-4.557260	-2.434050
H	5.596260	-2.642570	-2.236880
H	3.681790	-4.550880	-2.420970
H	3.664610	4.614110	-2.200750
H	5.586710	2.700020	-2.153020
C	0.992660	4.976030	-2.193790
C	5.952790	0.028760	-2.009510
C	-3.934380	-0.007200	-1.835370

***trans*-β**

$E_{PBE/SVP}$ = -6195.875085082 Hartree

NImag = 0

C	-0.981650	-0.177450	5.377800
C	-0.318400	-0.143580	6.622830
C	-1.027280	-0.209510	7.832860
C	-2.439700	-0.307240	7.766670
C	-3.133180	-0.370150	6.525510
C	-2.391290	-0.299690	5.341690
N	-0.158200	-0.099630	4.238740
N	-0.777720	-0.135480	3.120950
C	-0.014120	-0.059560	1.987600
C	-0.512250	-0.084140	0.678260
N	1.383910	0.058010	1.851230
N	0.520710	0.013280	-0.206910
C	1.640700	0.096840	0.520450
H	0.781820	-0.074560	6.621590
H	-2.887270	-0.342750	4.359680
H	-1.561210	-0.170420	0.369920
H	2.656460	0.188440	0.110700
C	2.407660	0.125870	2.887740
C	1.736790	2.827450	-2.491620
N	1.925730	1.464020	-2.474680
C	3.016910	3.514770	-2.496460
C	3.983880	2.543470	-2.477490
C	3.288370	1.268410	-2.460110
C	0.485230	3.481820	-2.493770
C	-0.768060	2.831470	-2.484030
C	-2.044300	3.526080	-2.509860
C	-3.016090	2.561200	-2.482720
C	-2.328380	1.281330	-2.458450
N	-0.965020	1.469450	-2.460730
Ni	0.474510	0.020760	-2.240250
N	1.919350	-1.426800	-2.480960
C	1.722680	-2.788740	-2.509510
C	2.998620	-3.483000	-2.539730
C	3.970910	-2.518210	-2.504270
C	3.282910	-1.238780	-2.472930
C	-2.982030	0.029720	-2.442160
C	-2.333000	-1.224500	-2.464590
C	-3.027930	-2.500020	-2.503390
C	-2.061640	-3.470960	-2.522030
C	-0.781700	-2.783580	-2.501810
N	-0.970880	-1.420320	-2.469100
C	0.469050	-3.438590	-2.514620
C	3.935590	0.013540	-2.437760
H	-4.103380	2.704740	-2.486840
H	-2.180510	4.613570	-2.552590
H	-4.116150	-2.635580	-2.527030
H	-2.204310	-4.558050	-2.550130
H	5.058180	-2.662410	-2.511280
H	3.134750	-4.570190	-2.590480
H	3.159500	4.602180	-2.513210
H	5.072660	2.678060	-2.489810
C	0.485670	4.976580	-2.500470
C	5.426550	0.005850	-2.336270

C	1.014870	-4.922650	-2.423430	C	-4.475220	0.028230	-2.386570
C	1.375280	-5.700190	-1.305730	C	0.469200	-4.933420	-2.528530
C	1.385850	-7.104200	-1.352530	C	0.835200	-5.671960	-1.386570
C	1.030010	-7.759330	-2.543660	C	0.842950	-7.076930	-1.384000
C	0.666220	-7.010050	-3.675300	C	0.479110	-7.772080	-2.549700
C	0.662210	-5.606440	-3.603060	C	0.110250	-7.062070	-3.704800
F	1.718220	-5.103710	-0.157800	C	0.108930	-5.656790	-3.681940
F	1.726410	-7.819060	-0.276920	F	1.186430	-5.034740	-0.263380
F	1.037850	-9.091690	-2.599740	F	1.188360	-7.755770	-0.286720
F	0.333200	-7.636070	-4.807160	F	0.483810	-9.105500	-2.559450
F	0.313190	-4.917640	-4.694350	F	-0.230000	-7.727090	-4.811650
C	-4.459920	-0.478170	-0.615140	F	-0.244430	-5.005350	-4.794780
C	-5.837190	-0.482300	-0.347100	C	-5.150940	-0.327230	-1.203540
C	-6.732320	-0.013210	-1.322940	C	-6.553350	-0.339270	-1.124520
C	-6.240480	0.457310	-2.552730	C	-7.309750	0.011890	-2.255870
C	-4.855960	0.449670	-2.797230	C	-6.662840	0.372590	-3.450210
F	-3.634900	-0.918060	0.345410	C	-5.258500	0.377030	-3.503190
F	-6.299650	-0.921490	0.830440	F	-4.451790	-0.661630	-0.110040
F	-8.043600	-0.010440	-1.081780	F	-7.171950	-0.675050	0.010920
F	-7.091500	0.903320	-3.479830	F	-8.641760	0.004520	-2.195160
F	-4.422550	0.901550	-3.978120	F	-7.385160	0.703480	-4.522920
C	6.584060	0.322420	-0.786300	F	-4.668980	0.723300	-4.652160
C	7.980770	0.298560	-0.644390	C	6.065490	0.284120	-1.113680
C	8.779650	-0.021210	-1.755930	C	7.462260	0.248090	-0.977350
C	8.178650	-0.314280	-2.992120	C	8.253630	-0.068610	-2.095260
C	6.778250	-0.283850	-3.106210	C	7.645030	-0.347030	-3.331120
F	5.844980	0.624840	0.294470	C	6.244300	-0.304600	-3.439020
F	8.552790	0.567840	0.532690	F	5.332300	0.583570	-0.026530
F	10.107170	-0.049340	-1.635930	F	8.041150	0.503120	0.199290
F	8.938900	-0.617790	-4.046120	F	9.581230	-0.108120	-1.981380
F	6.234110	-0.567360	-4.293450	F	8.398470	-0.649070	-4.390190
C	1.344340	5.698010	-3.350940	F	5.691950	-0.575970	-4.624980
C	1.345630	7.103230	-3.375460	C	0.844710	5.704740	-3.651310
C	0.987540	7.815230	-2.218260	C	0.844040	7.110090	-3.668150
C	0.633090	7.121780	-1.048700	C	0.478100	7.815360	-2.509210
C	0.640400	5.716750	-1.048960	C	0.116130	7.115430	-1.345800
F	1.688210	5.045020	-4.465730	C	0.123410	5.710450	-1.354260
F	1.678730	7.766310	-4.485690	F	1.195800	5.058000	-4.767610
F	0.984530	9.148760	-2.229510	F	1.182900	7.779680	-4.772650
F	0.298140	7.802430	0.050960	F	0.474480	9.148870	-2.513140
F	0.302460	5.082190	0.079940	F	-0.225720	7.789900	-0.244610
C	2.410880	0.240870	3.404810	F	-0.223560	5.068620	-0.232590
H	2.078250	1.111830	4.006590	H	3.394560	0.213130	2.386720
H	2.326440	-0.672010	4.030200	H	2.379570	-0.784120	3.518570
H	3.466090	0.383350	3.097020	H	2.235060	1.000100	3.545360
C	-2.597780	-0.072260	8.127380	C	-4.633690	-0.531310	6.515150
H	-1.535230	-0.379180	8.225620	H	-5.147740	0.356910	6.947360
H	-2.673250	0.971080	8.512830	H	-5.010390	-0.670890	5.480720
H	-3.217740	-0.711060	8.791580	H	-4.945870	-1.404590	7.128650
C	-6.373540	-0.731750	4.788640	C	-0.314830	-0.208370	9.163850
H	-6.999230	0.118850	5.140640	H	0.737890	-0.542660	9.050800
H	-6.555280	-0.860890	3.701280	H	-0.288340	0.807550	9.621740
H	-6.744340	-1.635910	5.320160	H	-0.826400	-0.878140	9.887660
O	-5.357870	-0.436050	7.415040	O	-3.175370	-0.428890	8.924850
C	-5.833140	0.794900	7.947130	C	-3.497490	0.784270	9.594480
H	-6.329040	1.416390	7.163570	H	-4.093100	1.467060	8.943050
H	-6.577390	0.536270	8.728320	H	-4.106360	0.505780	10.479380
H	-5.015760	1.396040	8.411420	H	-2.586650	1.328370	9.939810

I.6.8 1-Methyl-3',5'-di-*tert*-butyl-4'-methoxy-5-phenylazoimidazole · $NiTPPF_{20}$ (2g)

***cis*-α**

$E_{PBE/SVP}$ = -6431.179007152 Hartree

NImag = 0

C	0.582160	-1.767290	3.593890
C	0.467340	-3.164360	3.483930
C	1.511380	-3.950880	2.972150
C	2.745880	-3.291400	2.656520
C	2.876600	-1.863700	2.704000
C	1.770620	-1.137730	3.182160
N	-0.442120	-1.074440	4.284680
N	-0.896630	0.052630	3.943810
C	-0.732790	0.663830	2.704270
C	-0.673770	0.246710	1.362890
N	-1.015090	2.034910	2.647100
N	-0.910760	1.319740	0.549230
C	-1.086700	2.384650	1.342160
H	-0.478660	-3.614390	3.811720
H	1.833390	-0.045780	3.272460
H	-0.523170	-0.764530	0.967120
H	-1.261890	3.413700	1.001100
C	-0.144510	4.285790	-1.754560
N	0.114640	2.936850	-1.852770
C	1.063160	5.053270	-2.003430
C	2.054740	4.145520	-2.265050
C	1.455260	2.826970	-2.146280
C	-1.402600	4.859900	-1.469210
C	-2.610000	4.140840	-1.321380
C	-3.909780	4.761180	-1.130510
C	-4.824410	3.741540	-1.080720
C	-4.077000	2.505470	-1.229510
N	-2.734300	2.771430	-1.377300
Ni	-1.197510	1.396060	-1.472850
N	0.256530	0.054640	-2.029580
C	0.135700	-1.316670	-2.059500
C	1.435960	-1.935580	-2.247070
C	2.342980	-0.913720	-2.348210
C	1.592190	0.324830	-2.221140
C	-4.665200	1.222720	-1.256860
C	-3.959690	0.013890	-1.442970
C	-4.591740	-1.292630	-1.504110
C	-3.589650	-2.203030	-1.707210
C	-2.348110	-1.449600	-1.756210
N	-2.596800	-0.105210	-1.600520
C	-1.075480	-2.033570	-1.949010
C	2.164550	1.615090	-2.308080
H	-5.913080	3.821320	-0.973110
H	-4.102430	5.839600	-1.073930
H	-5.665970	-1.490150	-1.407210
H	-3.686660	-3.288730	-1.826440
H	3.427220	-0.995330	-2.490800
H	1.631750	-3.014130	-2.288700
H	1.140110	6.147380	-1.995630
H	3.099590	4.353780	-2.525040
C	-1.476730	6.344320	-1.313060

***cis*-β**

$E_{PBE/SVP}$ = -6431.168756492 Hartree

NImag = 0

C	0.282370	0.086750	4.212670
C	-0.455940	-0.187160	5.377430
C	-0.776870	-1.497910	5.774050
C	-0.173010	-2.562650	5.026290
C	0.560200	-2.320150	3.815620
C	0.752500	-0.985800	3.425560
N	0.651940	1.431540	3.980160
N	0.788350	1.954320	2.835690
C	0.285750	1.446540	1.637370
C	0.874780	1.577060	0.374680
N	-0.997450	0.925640	1.395770
N	0.008440	1.122810	-0.583120
C	-1.111260	0.766090	0.048020
H	-0.804110	0.680450	5.954770
H	1.328750	-0.753740	2.521470
H	1.880680	1.946440	0.142470
H	-2.042180	0.444770	-0.437830
C	1.546330	3.915530	-2.824790
N	1.700920	2.551660	-2.714780
C	2.839030	4.575580	-2.761940
C	3.775280	3.589200	-2.597410
C	3.050900	2.330070	-2.564500
C	0.314910	4.596260	-2.947740
C	-0.952590	3.974850	-2.982100
C	-2.212480	4.694540	-3.063960
C	-3.204960	3.750000	-3.050120
C	-2.543780	2.456990	-2.994050
N	-1.177950	2.618090	-2.947370
Ni	0.218610	1.140300	-2.613060
N	1.648250	-0.331930	-2.735580
C	1.430470	-1.687300	-2.828390
C	2.678250	-2.412450	-2.659380
C	3.650230	-1.471880	-2.440880
C	2.996630	-0.175060	-2.512900
C	-3.217260	1.216510	-3.029710
C	-2.585540	-0.045750	-3.095140
C	-3.291790	-1.302240	-3.273370
C	-2.336620	-2.285570	-3.308940
C	-1.054570	-1.625350	-3.135950
N	-1.228230	-0.264430	-3.021350
C	0.180600	-2.303540	-3.051650
C	3.666460	1.065950	-2.414790
H	-4.288360	3.915610	-3.094910
H	-2.324490	5.783730	-3.128250
H	-4.377530	-1.415950	-3.382860
H	-2.488180	-3.364130	-3.439870
H	4.718080	-1.644410	-2.260980
H	2.795310	-3.502460	-2.702020
H	3.009750	5.656740	-2.830830
H	4.863630	3.703490	-2.523360
C	0.361360	6.087720	-3.044270

C	3.626980	1.696430	-2.601030	C	5.132260	1.051380	-2.130480
C	-6.149530	1.135960	-1.103340	C	-4.710820	1.227460	-2.987810
C	-1.028250	-3.521600	-2.071230	C	0.146090	-3.793810	-3.175520
C	-1.298990	-4.350900	-0.966600	C	0.185720	-4.620950	-2.039310
C	-1.336480	-5.749560	-1.076610	C	0.118840	-6.020030	-2.131370
C	-1.078030	-6.351230	-2.319680	C	0.009150	-6.620970	-3.396880
C	-0.792400	-5.551250	-3.439060	C	-0.034230	-5.820670	-4.551860
C	-0.765930	-4.152610	-3.303340	C	0.038750	-4.422080	-4.430360
F	-1.521340	-3.803300	0.238740	F	0.282560	-4.072380	-0.820200
F	-1.592530	-6.512560	-0.009070	F	0.152270	-6.776930	-1.029880
F	-1.103120	-7.678950	-2.436050	F	-0.057470	-7.948390	-3.502150
F	-0.556650	-6.123250	-4.621970	F	-0.143010	-6.393100	-5.752970
F	-0.498740	-3.419590	-4.388090	F	-0.006230	-3.685880	-5.543910
C	-6.774970	1.359240	0.138030	C	-5.393790	0.859380	-1.813110
C	-8.167040	1.254540	0.295670	C	-6.795550	0.846830	-1.737140
C	-8.966020	0.924970	-0.812300	C	-7.547180	1.216050	-2.866100
C	-8.370370	0.703530	-2.065550	C	-6.894770	1.588880	-4.053750
C	-6.976290	0.814200	-2.197260	C	-5.489770	1.593970	-4.101590
F	-6.040120	1.674970	1.210650	F	-4.699280	0.503800	-0.716800
F	-8.733660	1.459470	1.487640	F	-7.417330	0.496750	-0.607700
F	-10.288140	0.821920	-0.674260	F	-8.878960	1.210100	-2.810220
F	-9.129500	0.393120	-3.118920	F	-7.612700	1.932780	-5.124580
F	-6.437620	0.600930	-3.402230	F	-4.896130	1.953490	-5.243500
C	4.546500	2.196900	-1.658460	C	5.626690	1.527740	-0.899630
C	5.926060	2.246440	-1.915430	C	6.998130	1.526200	-0.598260
C	6.415720	1.797420	-3.153530	C	7.911740	1.032840	-1.545320
C	5.523930	1.300010	-4.118880	C	7.449560	0.551060	-2.781710
C	4.148170	1.261380	-3.837030	C	6.072920	0.570770	-3.062390
F	4.117330	2.629040	-0.464500	F	4.779380	1.995490	0.027360
F	6.772240	2.711410	-0.991630	F	7.439050	1.979980	0.577140
F	7.723300	1.839060	-3.410270	F	9.216080	1.021780	-1.269590
F	5.987640	0.875660	-5.296330	F	8.319990	0.085330	-3.680620
F	3.327580	0.790010	-4.780790	F	5.665740	0.117590	-4.252680
C	-1.438060	7.209230	-2.422730	C	0.806400	6.723140	-4.219990
C	-1.545570	8.602820	-2.277230	C	0.873730	8.122370	-4.327070
C	-1.687760	9.155800	-0.993090	C	0.488050	8.917840	-3.234740
C	-1.724520	8.316370	0.133990	C	0.035870	8.311650	-2.050180
C	-1.616500	6.927480	-0.040250	C	-0.024070	6.910240	-1.968350
F	-1.304280	6.708940	-3.654340	F	1.180100	5.990790	-5.274050
F	-1.517730	9.401050	-3.346170	F	1.299190	8.698220	-5.454480
F	-1.789330	10.476370	-0.842910	F	0.548870	10.247010	-3.322560
F	-1.857510	8.843730	1.353740	F	-0.326640	9.068540	-1.011350
F	-1.650770	6.148510	1.054480	F	-0.459850	6.363610	-0.827900
C	-1.184260	2.905520	3.799510	C	-2.091780	0.739360	2.338020
H	-1.761880	2.356620	4.571290	H	-2.000720	-0.229100	2.873590
H	-0.200350	3.192090	4.230080	H	-2.086720	1.559720	3.084870
H	-1.726660	3.819100	3.483610	H	-3.047700	0.770790	1.775830
C	4.131400	-1.060490	2.254690	C	-1.760570	-1.678300	6.966900
C	1.285740	-5.470650	2.746080	C	1.094630	-3.465050	2.913300
O	3.784610	-4.094880	2.230090	O	-0.318110	-3.878820	5.407370
C	4.870570	-4.380440	3.102690	C	0.409440	-4.361010	6.533220
H	4.592530	-4.231080	4.169760	H	-0.243040	-4.437200	7.432910
H	5.156020	-5.444620	2.949960	H	0.776260	-5.381700	6.288550
H	5.758860	-3.751670	2.862640	H	1.281550	-3.710880	6.766510
C	4.782270	-1.655500	0.981420	C	-0.100640	-4.314310	2.410120
H	4.051840	-1.657820	0.141430	H	-0.803300	-3.689480	1.816180
H	5.647290	-1.023280	0.679690	H	0.258160	-5.130070	1.743600
H	5.137850	-2.694400	1.108790	H	-0.656890	-4.765090	3.257500

C	3.755240	0.397540	1.886170	C	1.838670	-2.909980	1.677600
H	4.639350	0.904080	1.444060	H	2.181290	-3.758210	1.048420
H	2.934850	0.440730	1.136350	H	1.191220	-2.277570	1.033750
H	3.454580	1.002730	2.769090	H	2.738130	-2.320380	1.962340
C	5.153090	-0.968080	3.417380	C	2.104220	-4.369530	3.663460
H	4.690040	-0.479550	4.303010	H	2.893350	-3.766370	4.164910
H	5.533630	-1.955920	3.743920	H	1.614630	-5.010990	4.419760
H	6.028270	-0.353450	3.107080	H	2.608400	-5.045010	2.936890
C	1.582530	-5.822120	1.266340	C	-2.670970	-2.920260	6.802470
H	0.928490	-5.226320	0.592990	H	-2.124840	-3.880940	6.815070
H	2.637680	-5.612090	1.001270	H	-3.418200	-2.939390	7.626970
H	1.371950	-6.899130	1.079700	H	-3.228830	-2.872810	5.841320
C	-0.180300	-5.871720	3.028650	C	-2.725200	-0.465510	7.056520
H	-0.312870	-6.950380	2.793780	H	-3.493770	-0.667760	7.833800
H	-0.457820	-5.729280	4.095890	H	-2.214290	0.475750	7.350440
H	-0.897080	-5.306920	2.396390	H	-3.254150	-0.289980	6.093330
C	2.169520	-6.326550	3.686140	C	-0.984170	-1.731870	8.307380
H	1.892380	-7.399930	3.585050	H	-0.283030	-2.588360	8.365070
H	3.247480	-6.242980	3.451310	H	-0.390070	-0.802860	8.452570
H	2.016950	-6.036950	4.749690	H	-1.695920	-1.820100	9.159100

***trans*-α**

$E_{PBE/SVP}$ = -6431.198221422 Hartree

NImag = 0

C	-1.967860	-0.274390	3.414740
C	-3.337120	-0.531850	3.208270
C	-4.243910	-0.605150	4.275260
C	-3.728440	-0.358010	5.590580
C	-2.319180	-0.224020	5.847250
C	-1.474330	-0.157910	4.728810
N	-1.191970	-0.198730	2.250670
N	0.061460	-0.011420	2.414290
C	0.760310	0.065750	1.231390
C	0.407450	0.023450	-0.122170
N	2.146560	0.230790	1.255370
N	1.534640	0.156010	-0.879860
C	2.567040	0.277670	-0.034400
H	-3.652460	-0.664630	2.164510
H	-0.390130	-0.026540	4.839010
H	-0.595450	-0.092310	-0.547280
H	3.619380	0.398250	-0.325700
C	2.897820	2.974070	-3.097580
N	3.073620	1.609080	-3.077050
C	4.183810	3.649420	-3.062190
C	5.140670	2.668810	-3.016290
C	4.433030	1.400300	-3.023550
C	1.653020	3.639860	-3.137730
C	0.393780	3.001980	-3.166430
C	-0.874830	3.709570	-3.211470
C	-1.856420	2.754160	-3.206620
C	-1.181660	1.467280	-3.179680
N	0.183240	1.641860	-3.158620
Ni	1.605910	0.177750	-2.907850
N	3.039270	-1.281480	-3.113160
C	2.830730	-2.640700	-3.167560
C	4.100870	-3.346440	-3.172050
C	5.080390	-2.391680	-3.094940
C	4.403500	-1.106250	-3.063860
C	-1.847490	0.221630	-3.179820
C	-1.210110	-1.038380	-3.208190
C	-1.916650	-2.306650	-3.265180
C	-0.959440	-3.286670	-3.276990
C	0.326780	-2.611850	-3.231380
N	0.150250	-1.247140	-3.195260
C	1.571540	-3.278670	-3.216870
C	5.066920	0.138870	-2.996420
H	-2.942040	2.908580	-3.228030
H	-0.999310	4.798730	-3.247980
H	-3.005790	-2.431240	-3.304280
H	-1.112450	-4.372110	-3.312850
H	6.166010	-2.546220	-3.072770
H	4.229010	-4.433860	-3.236090
H	4.336620	4.735590	-3.073300
H	6.230560	2.793030	-2.995500
C	1.668380	5.134880	-3.142140
C	6.555520	0.115160	-2.868710
C	-3.341560	0.234750	-3.131840

***trans*-β**

$E_{PBE/SVP}$ = -6431.195810712 Hartree

NImag = 0

C	-0.646760	-0.127610	4.250850
C	-0.010610	-0.031820	5.499610
C	-0.714670	-0.110130	6.715680
C	-2.137980	-0.234900	6.621310
C	-2.803320	-0.458110	5.364010
C	-2.033510	-0.378570	4.198500
N	0.184870	-0.008450	3.121450
N	-0.421350	-0.075120	1.997900
C	0.346040	0.027520	0.869380
C	-0.145780	-0.001680	-0.442000
N	1.741510	0.176840	0.739730
N	0.888490	0.123130	-1.322310
C	2.003370	0.227000	-0.589980
H	1.079840	0.099270	5.481580
H	-2.476780	-0.505100	3.203010
H	-1.191600	-0.107300	-0.754840
H	3.019160	0.337490	-0.994930
C	2.758850	0.256910	1.781430
C	2.131290	2.918670	-3.623170
N	2.308040	1.553760	-3.596930
C	3.417530	3.594480	-3.630470
C	4.375780	2.614670	-3.603340
C	3.668870	1.346070	-3.579220
C	0.885500	3.583990	-3.631080
C	-0.373400	2.944560	-3.616290
C	-1.643610	3.650030	-3.644960
C	-2.623690	2.693970	-3.607680
C	-1.947060	1.408310	-3.575400
N	-0.582150	1.584520	-3.582730
Ni	0.844610	0.124420	-3.355130
N	2.275990	-1.337170	-3.588780
C	2.067470	-2.697390	-3.611660
C	3.337360	-3.402860	-3.638280
C	4.317980	-2.446440	-3.605710
C	3.641010	-1.160960	-3.579850
C	-2.611650	0.162620	-3.548110
C	-1.974040	-1.097430	-3.566670
C	-2.680470	-2.366810	-3.596080
C	-1.722880	-3.346440	-3.613860
C	-0.436780	-2.670380	-3.601620
N	-0.613740	-1.305370	-3.575550
C	0.808190	-3.336330	-3.613180
C	4.304620	0.085600	-3.549190
H	-3.709660	2.847070	-3.610300
H	-1.770530	4.738280	-3.696070
H	-3.769990	-2.492490	-3.614650
H	-1.875210	-4.432370	-3.635990
H	5.403990	-2.599980	-3.611350
H	3.464070	-4.491370	-3.684720
H	3.569810	4.680460	-3.654110
H	5.465760	2.739340	-3.614520
C	0.898480	5.078590	-3.650430
C	5.795250	0.065270	-3.444150

C	1.558770	-4.773010	-3.243100	C	-4.104390	0.175420	-3.482160
C	1.911180	-5.524590	-2.105090	C	0.795710	-4.831150	-3.619820
C	1.909990	-6.929460	-2.115140	C	1.157140	-5.567320	-2.474860
C	1.547980	-7.612220	-3.288660	C	1.155870	-6.972290	-2.466470
C	1.191210	-6.889540	-4.439640	C	0.786370	-7.669890	-3.628920
C	1.200250	-5.484560	-4.404640	C	0.421460	-6.962280	-4.786750
F	2.258440	-4.900930	-0.972970	C	0.429070	-5.556930	-4.769690
F	2.244740	-7.619750	-1.021650	F	1.513480	-4.927770	-1.354620
F	1.543500	-8.945590	-3.309860	F	1.497780	-7.648840	-1.366630
F	0.852810	-7.542430	-5.554410	F	0.782490	-9.003360	-3.633170
F	0.859400	-4.821750	-5.514650	F	0.076340	-7.629690	-5.890630
C	-4.031460	-0.102940	-1.951070	F	0.079030	-4.907840	-5.884930
C	-5.434270	-0.093760	-1.884820	C	-4.774730	-0.160180	-2.290270
C	-6.178210	0.262110	-3.022580	C	-6.176450	-0.153420	-2.199650
C	-5.517160	0.602490	-4.214880	C	-6.937670	0.196250	-3.328240
C	-4.112360	0.586350	-4.256360	C	-6.296170	0.535980	-4.531620
F	-3.347020	-0.440030	-0.848330	C	-4.892390	0.521930	-4.596080
F	-6.070020	-0.410610	-0.750940	F	-4.071320	-0.492770	-1.198910
F	-7.510440	0.275560	-2.970500	F	-6.789470	-0.469560	-1.055600
F	-6.226770	0.936020	-5.295170	F	-8.269130	0.207210	-3.256410
F	-3.509100	0.915780	-5.402820	F	-7.022910	0.865380	-5.601810
C	7.177010	0.374710	-1.633250	F	-4.307990	0.848940	-5.753320
C	8.571160	0.320060	-1.475870	C	6.433110	0.335130	-2.219210
C	9.376890	0.005020	-2.583860	C	7.829100	0.286410	-2.079160
C	8.785410	-0.252970	-3.832330	C	8.620730	-0.034420	-3.195690
C	7.387320	-0.192880	-3.961610	C	8.013190	-0.303930	-4.434020
F	6.430830	0.672780	-0.556100	C	6.613150	-0.249480	-4.545460
F	9.134240	0.555790	-0.287490	F	5.699750	0.639200	-1.133500
F	10.702040	-0.051800	-2.448740	F	8.406860	0.533330	-0.900260
F	9.552020	-0.552630	-4.882850	F	9.947610	-0.085860	-3.078250
F	6.850910	-0.444630	-5.159200	F	8.766930	-0.609210	-5.491950
C	2.043050	5.859220	-4.290250	F	6.061560	-0.513120	-5.733450
C	2.054570	7.264570	-4.307570	C	1.264530	5.793250	-4.807590
C	1.687130	7.973170	-3.151140	C	1.273330	7.198340	-4.838360
C	1.310850	7.276760	-1.990160	C	0.910320	7.917260	-3.686920
C	1.304870	5.871710	-1.998540	C	0.541800	7.231010	-2.517420
F	2.397120	5.208640	-5.403170	C	0.539610	5.826010	-2.511950
F	2.406430	7.931070	-5.409940	F	1.612730	5.133240	-5.916910
F	1.695510	9.306750	-3.155180	F	1.618000	7.854820	-5.949010
F	0.967530	7.954620	-0.891360	F	0.915530	9.250660	-3.703780
F	0.943180	5.233030	-0.879620	F	0.202390	7.918230	-1.423450
C	2.974400	0.330650	2.447120	F	0.186120	5.197970	-1.384420
H	2.656620	1.196550	3.064070	H	3.748130	0.347260	1.285720
H	2.882330	-0.590520	3.058830	H	2.732990	-0.650340	2.416310
H	4.029350	0.464710	2.134480	H	2.577480	1.133320	2.433900
C	-1.667750	-0.179660	7.260150	C	-4.310450	-0.816480	5.270560
C	-5.726340	-0.975330	4.007130	C	0.103710	-0.087730	8.039060
O	-4.647870	-0.330510	6.616440	O	-2.937720	-0.224430	7.743540
C	-4.996790	0.916080	7.207220	C	-3.197770	1.008780	8.403600
H	-6.082150	0.880780	7.445090	H	-4.250850	0.982080	8.759330
H	-4.441850	1.086080	8.158840	H	-2.538730	1.142820	9.292010
H	-4.805370	1.765570	6.514830	H	-3.068920	1.875440	7.718200
C	-0.217730	-0.729590	7.201980	C	-4.719760	-1.152940	3.818580
H	-0.182650	-1.742420	6.744600	H	-4.614410	-0.282990	3.134420
H	0.472530	-0.068380	6.636370	H	-4.129110	-1.997200	3.401240
H	0.185970	-0.805140	8.235360	H	-5.789560	-1.455670	3.805000
C	-2.408930	-1.067080	8.290250	C	-4.608160	-2.071150	6.130410
H	-1.842410	-1.068550	9.247750	H	-4.363370	-1.902780	7.198200

H	-3.441150	-0.735040	8.504120	H	-5.686860	-2.335660	6.053350
H	-2.469000	-2.117600	7.930040	H	-4.018760	-2.942740	5.768400
C	-1.570160	1.284850	7.759630	C	-5.202310	0.365670	5.723920
H	-0.968850	1.898300	7.052810	H	-5.101610	0.583180	6.804380
H	-2.560550	1.772200	7.863060	H	-4.959510	1.289750	5.153610
H	-1.069540	1.318430	8.753750	H	-6.272400	0.123730	5.533840
C	-6.669290	0.215900	4.306050	C	1.535720	-0.635990	7.798480
H	-6.694750	0.478000	5.381200	H	1.515660	-1.640580	7.322060
H	-6.364360	1.118340	3.731040	H	2.155740	0.036490	7.168350
H	-7.709050	-0.042430	4.002950	H	2.058490	-0.730320	8.775240
C	-6.128140	-2.203150	4.863170	C	-0.509990	-0.994990	9.133560
H	-6.021590	-2.000500	5.947470	H	0.160010	-1.003750	10.021780
H	-7.187610	-2.476120	4.657200	H	-1.514700	-0.676230	9.465550
H	-5.495520	-3.082110	4.607820	H	-0.601040	-2.041110	8.767110
C	-5.948000	-1.362820	2.527790	C	0.263440	1.367520	8.549340
H	-5.764980	-0.519530	1.828500	H	0.775020	1.994590	7.785930
H	-5.302730	-2.213670	2.218090	H	-0.706630	1.851050	8.781570
H	-7.005190	-1.679350	2.389760	H	0.881190	1.384490	9.475590

II. Experimental Section

II.1 Materials and Methods

Chromatography stationary phases: Column chromatography was carried out using 0.04 – 0.063 mm mesh silica gel. R_f values were determined by thin layer chromatography on Polygram® Sil G/UV_{254} (0.2 mm particle size).

NMR spectroscopy: NMR spectra were measured in deuterated solvents. Chemical shifts are either calibrated to the internal standard TMS or using residual protonated solvent signals (^{1}H: δ ($CHCl_3$) = 7.26 ppm, δ (CD_3CN) = 1.94 ppm, δ (toluene-d8) = 2.08 ppm; ^{13}C: δ ($CHCl_3$) = 77.16 ppm, δ (CD_3CN) = 1.32 ppm, δ (toluene-d8) = 137.48 ppm; deuteration grade 99.8 %). Reference for ^{19}F NMR spectra is CCl_3F to which the spectrometer frequency is calibrated. Assignments of ^{1}H and ^{13}C nuclei were confirmed by the 2D methods COSY, HSQC and HMBC. The signal multiplicities are abbreviated as s (singlet), d (doublet), t (triplet), q (quartet), quint (quintet), m (multiplet) and br (broad signal).

Mass spectrometry: The high resolution (HR) mass spectra were measured on a time-of-flight (TOF) mass spectrometer with electron ionization (EI).

IR spectroscopy: Infrared spectra were recorded on a FT-IR spectrometer with an ATR unit. Signal intensities were abbreviated with w (weak), m (medium), s (strong) and vs (very strong). Broad signals are additionally labeled with br.

UV-vis spectroscopy: UV-visible absorption spectra were recorded on a two-beam spectrophotometer with a thermostat (T = 20 °C). Measurements were performed in quartz cells of 1 cm optical path length.

Light sources: Irradiation experiments were performed using LED light sources.

II.2 NMR Spectroscopy

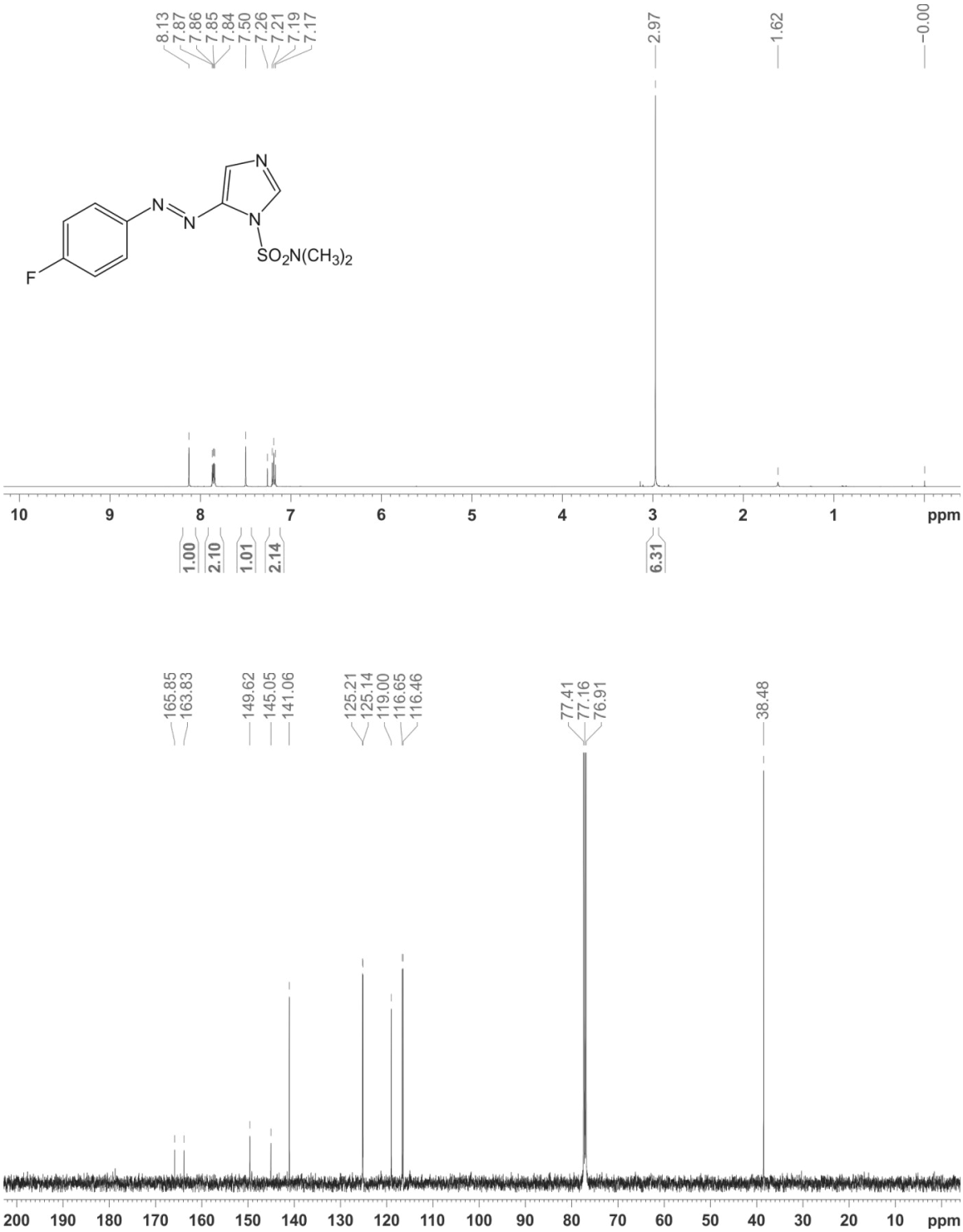

Figure S6. ^{1}H NMR spectrum (top) and ^{13}C NMR spectrum (bottom) of 1-(*N*,*N*-Dimethylsulfamoyl)-5-(4'-fluorophenylazo)imidazole. Spectra were measured in chloroform-d_1 at 300 K.

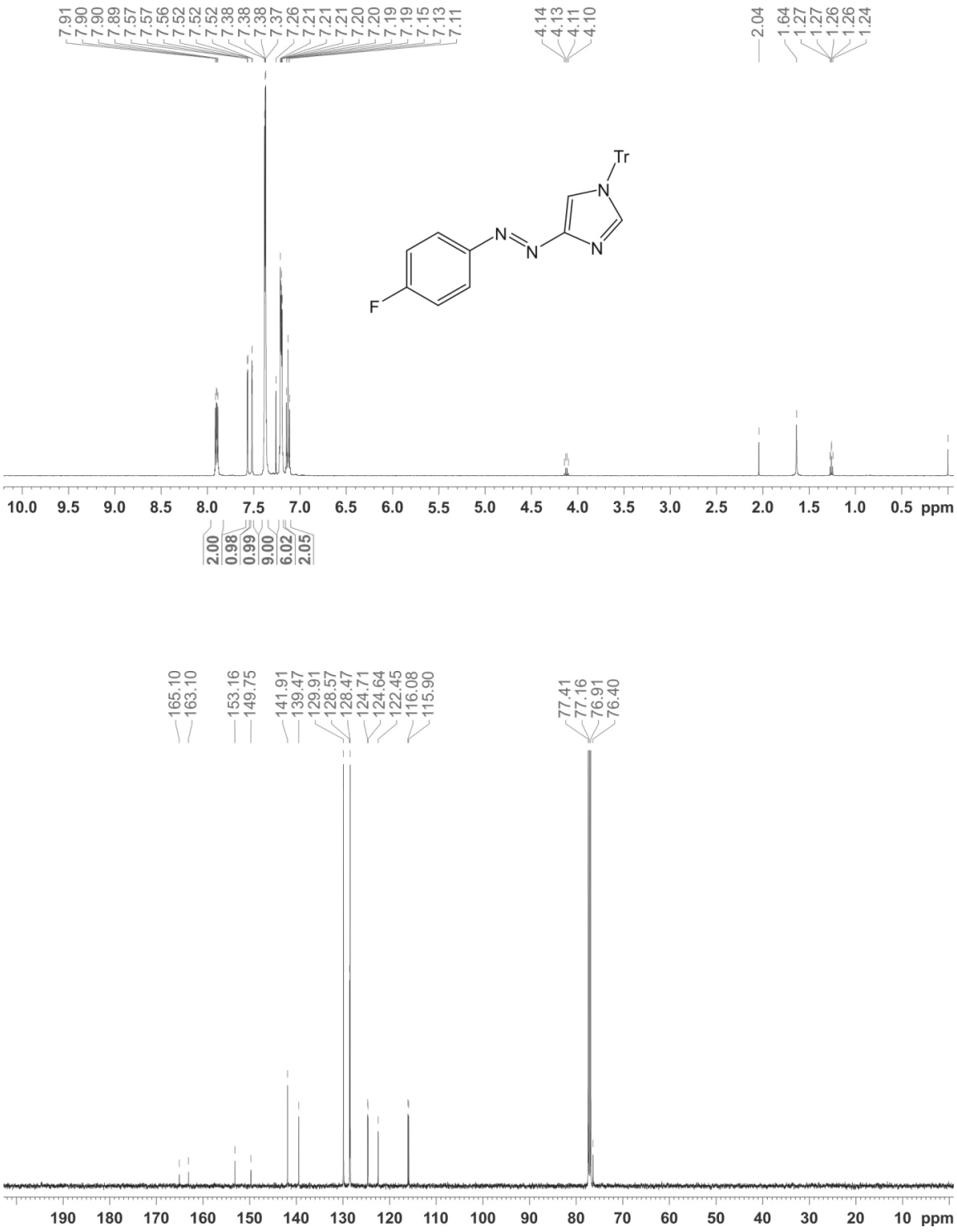

Figure S7. ^{1}H NMR spectrum (top) and ^{13}C NMR spectrum (bottom) of 1-Trityl-4-(4'-fluorophenylazo)imidazole. Spectra were measured in chloroform-d_1 at 300 K.

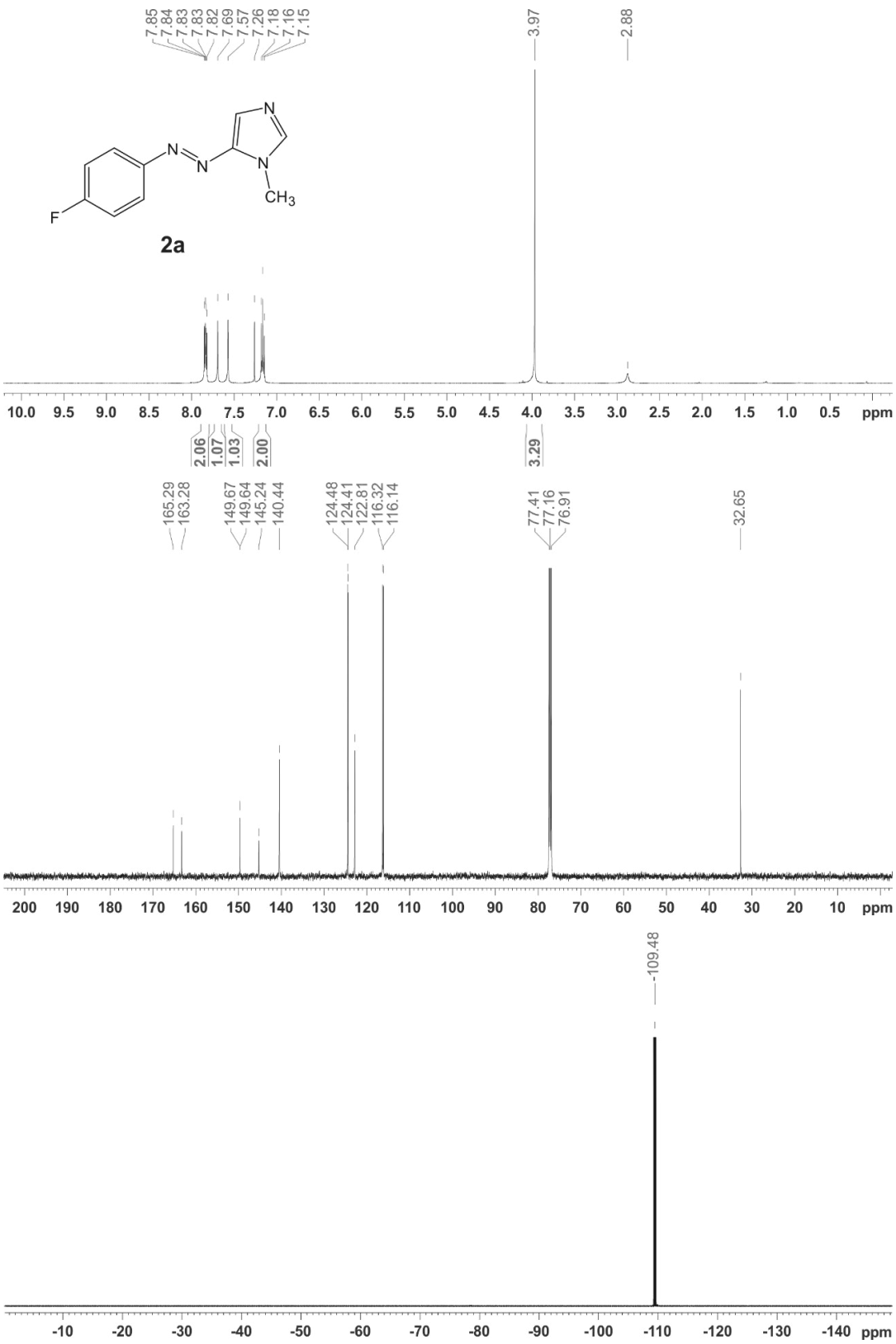

Figure S8. ^{1}H NMR spectrum (top), ^{13}C NMR spectrum (middle) and ^{19}F NMR spectrum (bottom) of 1-Methyl-5-(4'-fluorophenylazo)imidazole (**2a**). Spectra were measured in chloroform-d_1 at 300 K.

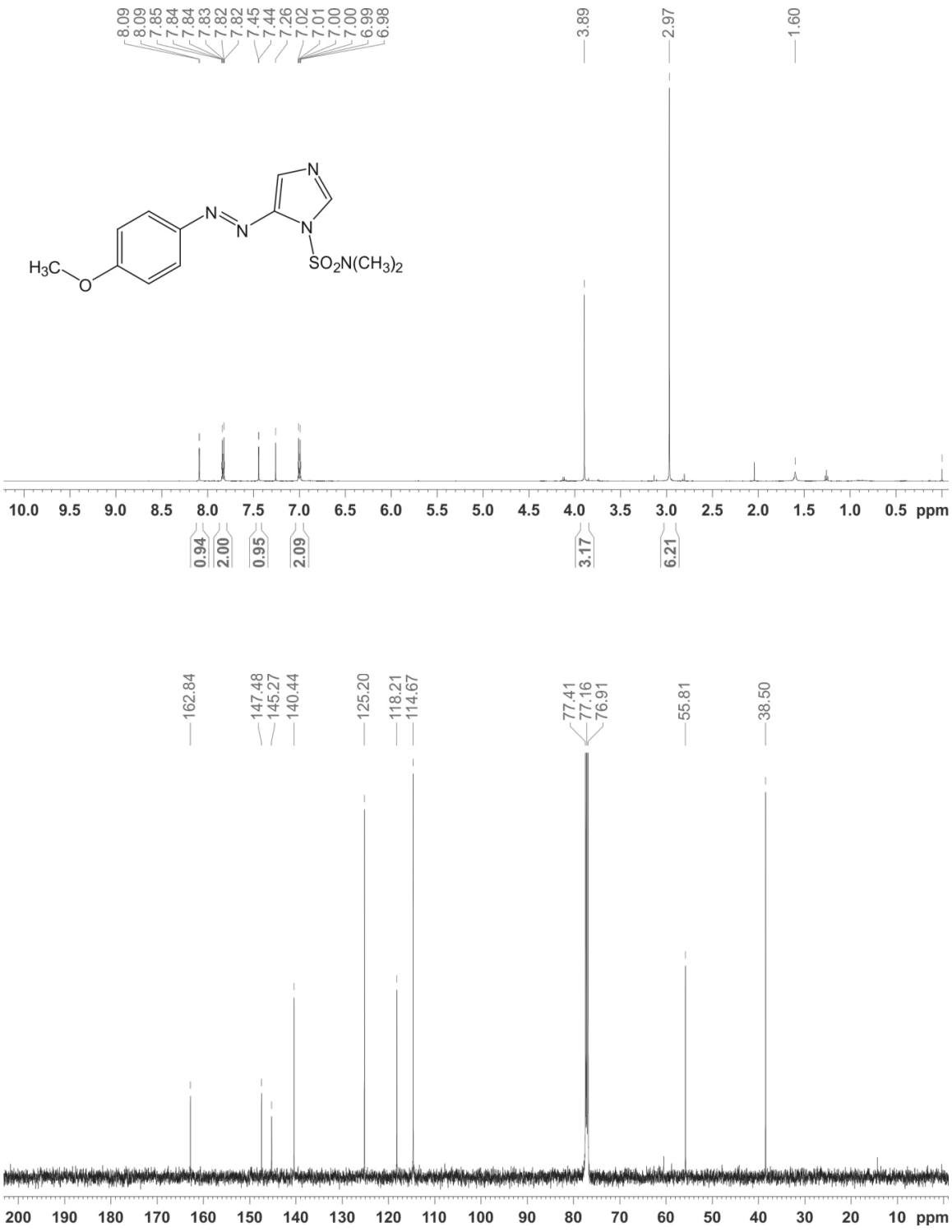

Figure S9. ^{1}H NMR spectrum (top) and ^{13}C NMR spectrum (bottom) of 1-(*N*,*N*-Dimethylsulfamoyl)-5-(4'-methoxyphenylazo)imidazole. Spectra were measured in chloroform-d_1 at 300 K.

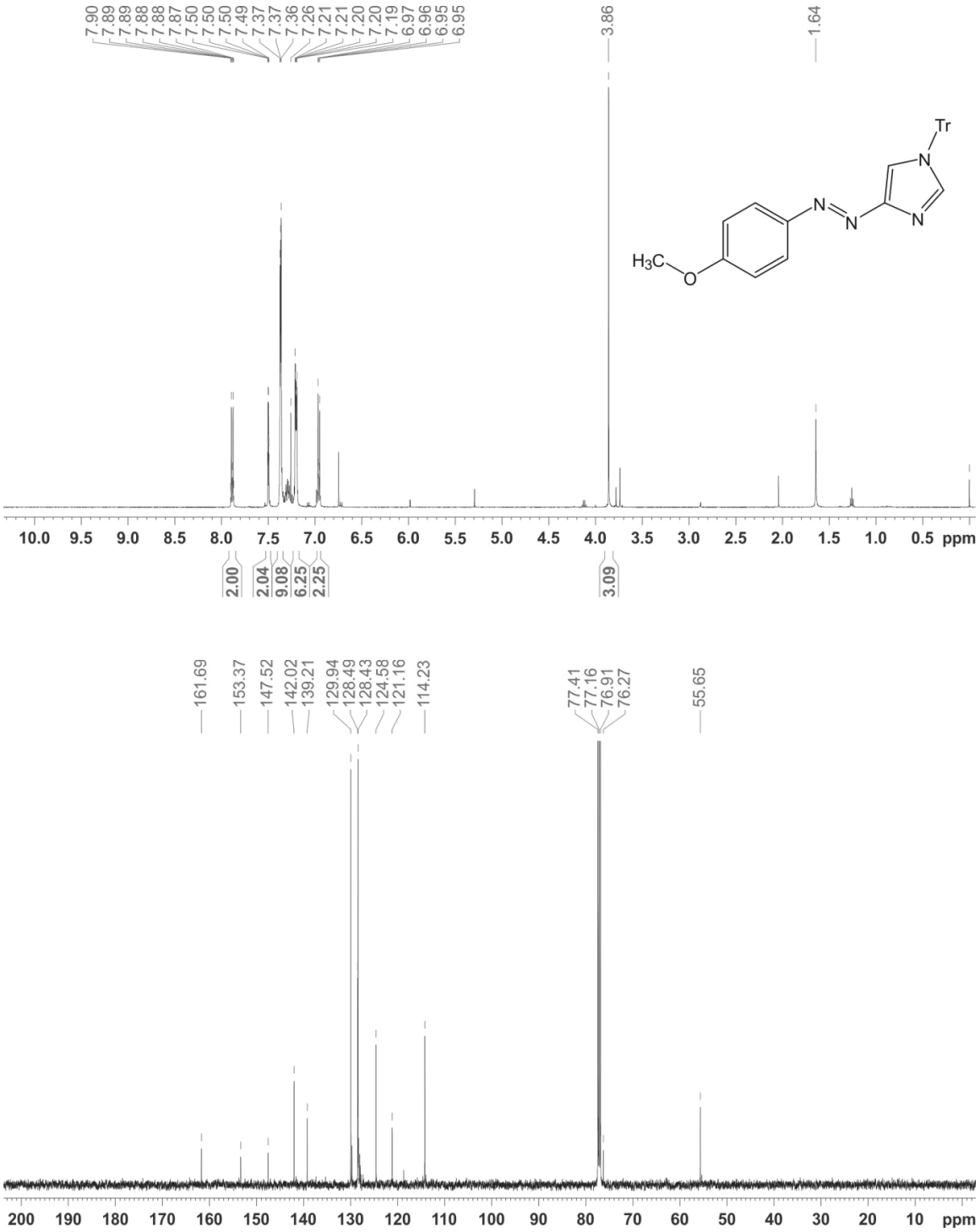

Figure S10. ^{1}H NMR spectrum (top) and ^{13}C NMR spectrum (bottom) of 1-Trityl-4-(4'-methoxyphenylazo)imidazole. Spectra were measured in chloroform-d_1 at 300 K.

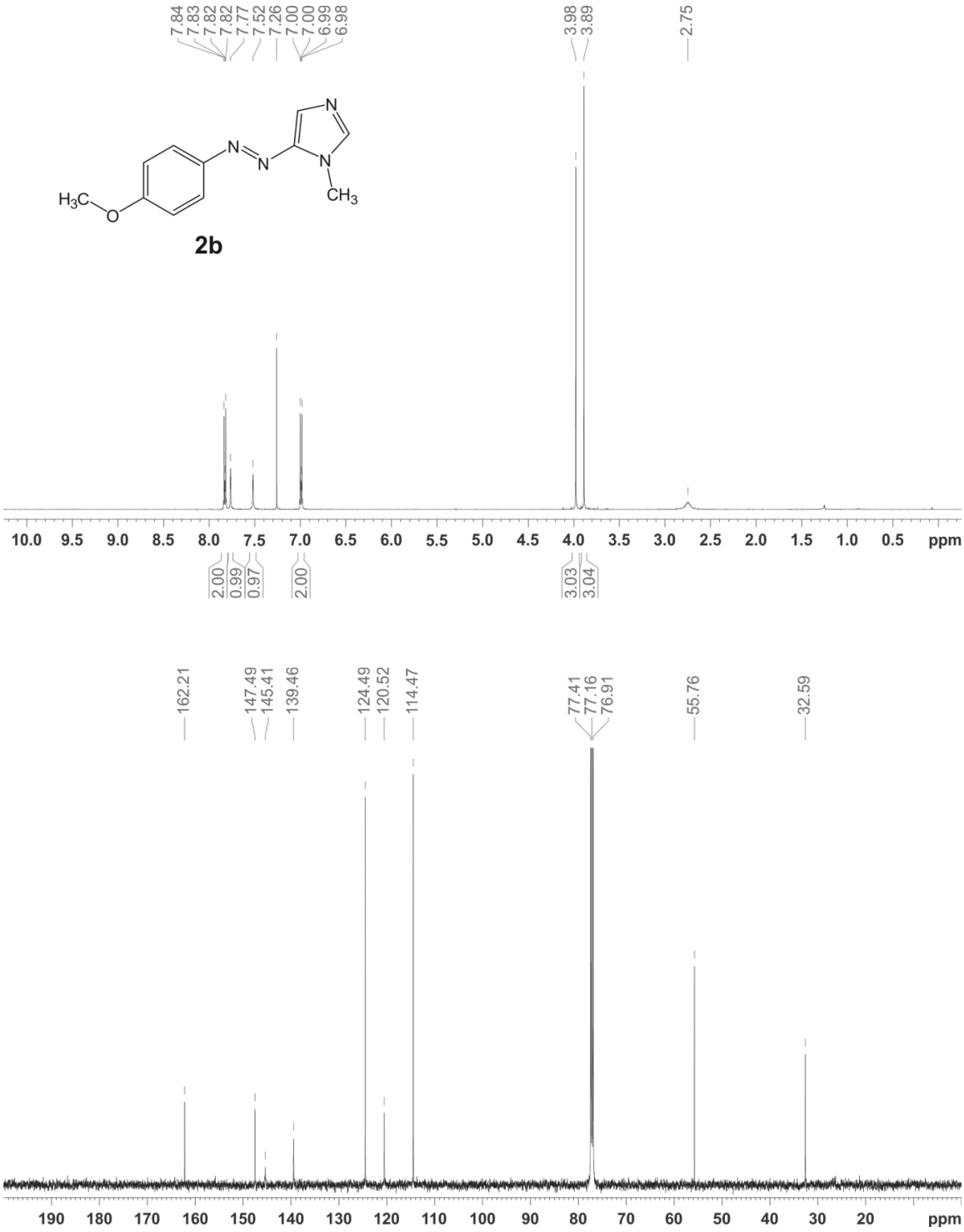

Figure S11. ^{1}H NMR spectrum (top) and ^{13}C NMR spectrum (bottom) of 1-Methyl-5-(4'-methoxyphenylazo)imidazole (**2b**). Spectra were measured in chloroform-d_1 at 300 K.

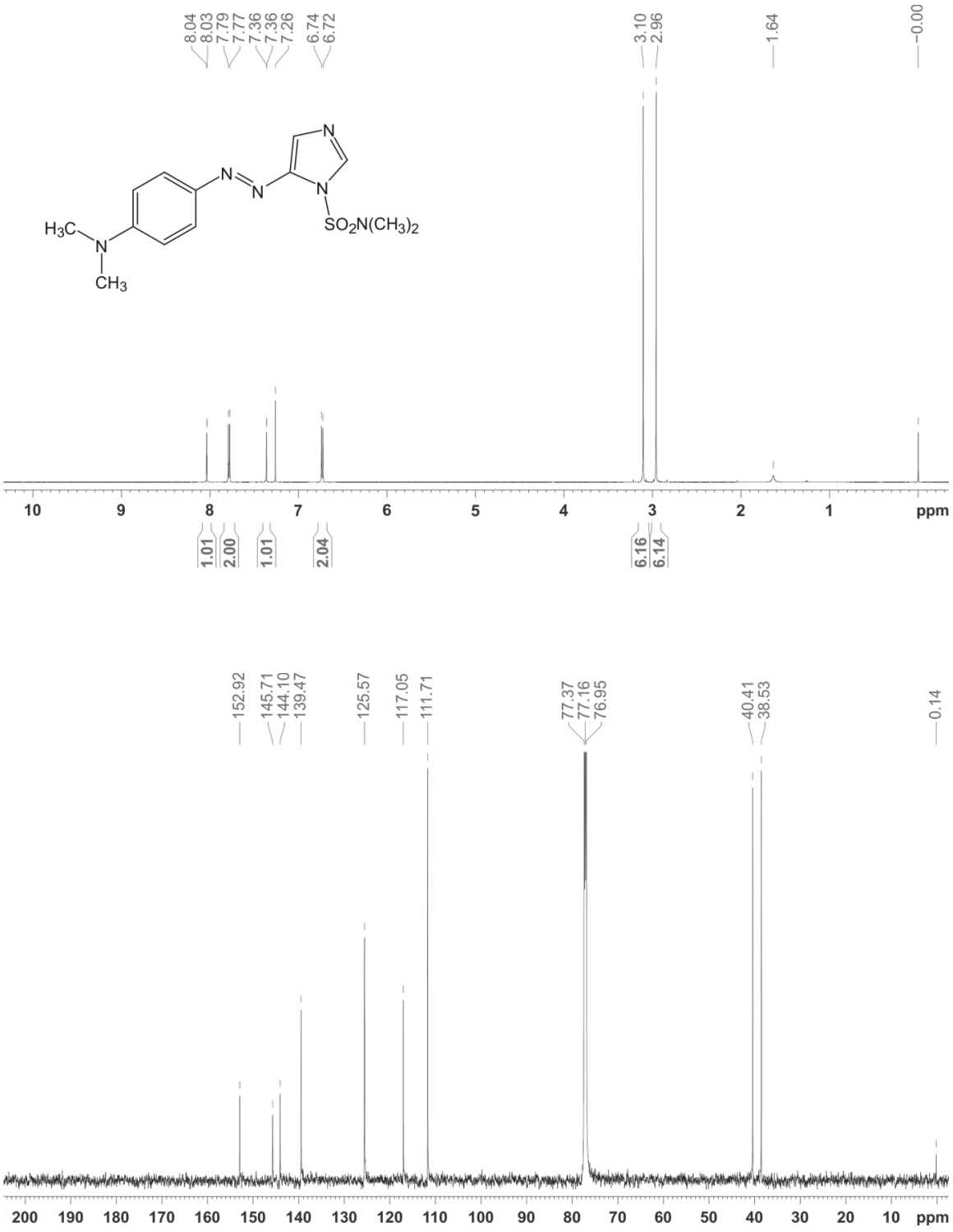

Figure S12. ^{1}H NMR spectrum (top) and ^{13}C NMR spectrum (bottom) of 1-(*N*,*N*-Dimethylsulfamoyl)-5-(4'-*N*,*N*-dimethylaminophenylazo)imidazole**.** Spectra were measured in chloroform-d_1 at 300 K.

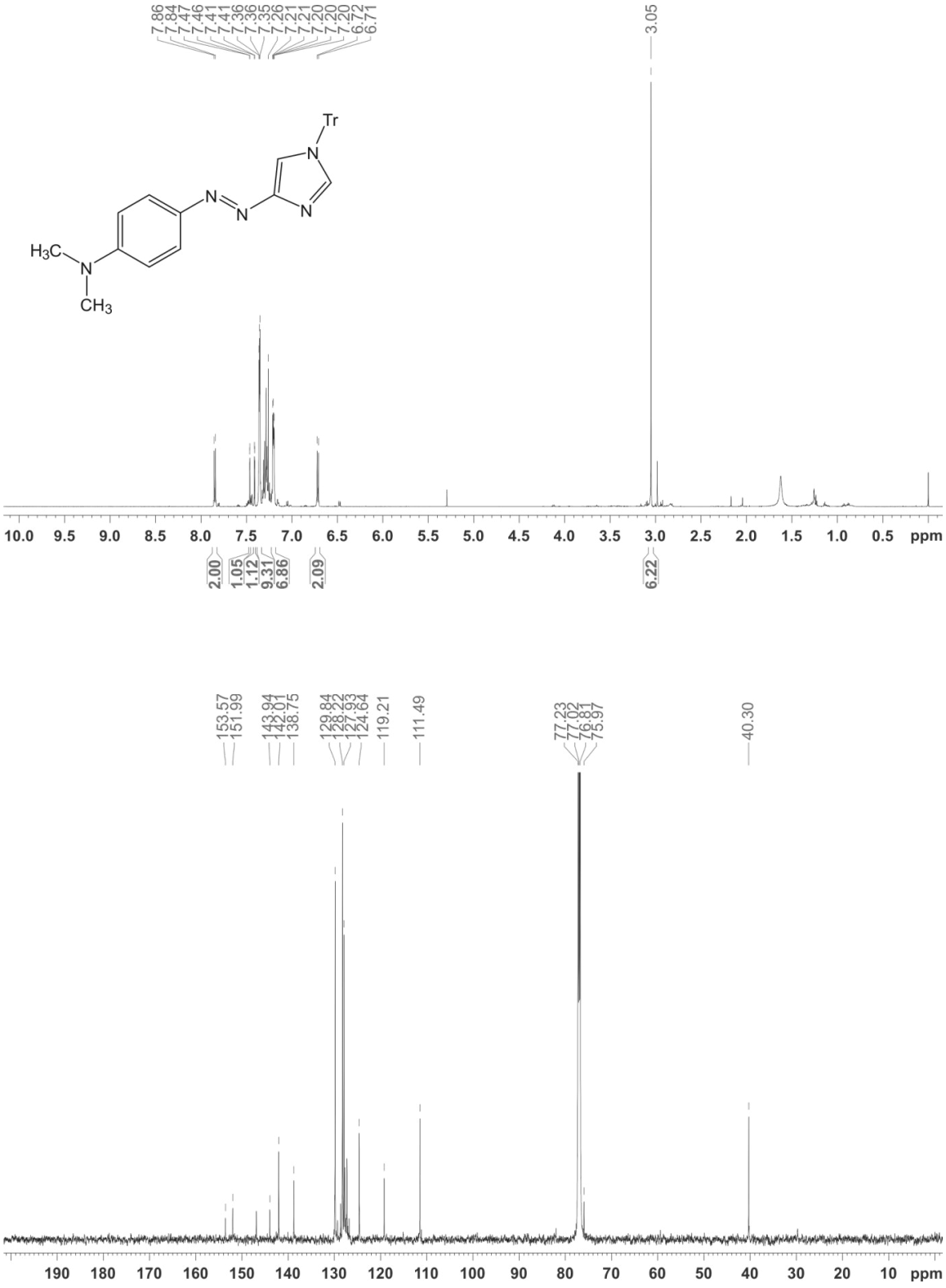

Figure S13. ^{1}H NMR spectrum (top) and ^{13}C NMR spectrum (bottom) of 1-Trityl-4-(4'-*N*,*N*-dimethylaminophenylazo)imidazole**.** Spectra were measured in chloroform-d_1 at 300 K.

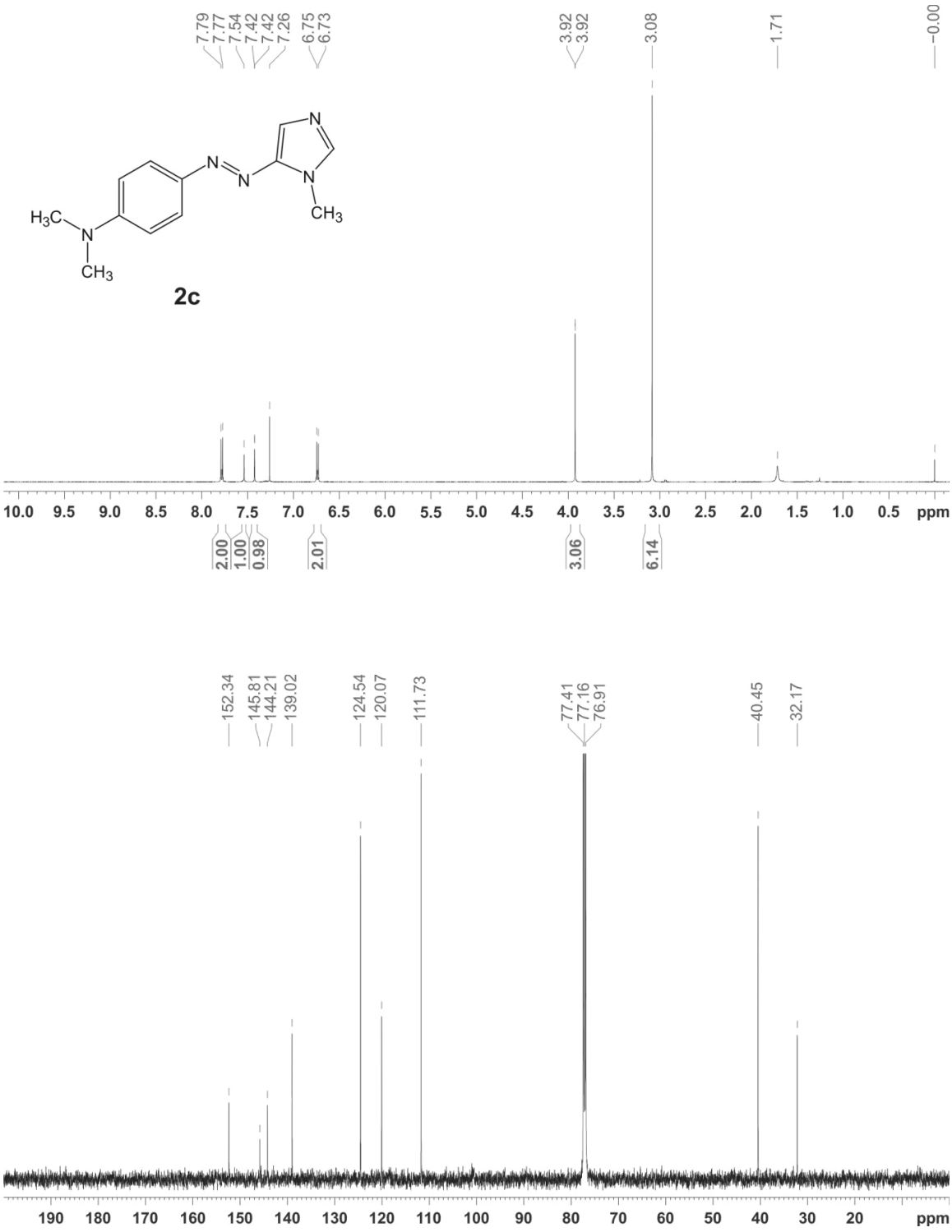

Figure S14. ^{1}H NMR spectrum (top) and ^{13}C NMR spectrum (bottom) of 1-Methyl-5-(4'-*N*,*N*-dimethylaminophenylazo)imidazole **(2c).** Spectra were measured in chloroform-d_1 at 300 K.

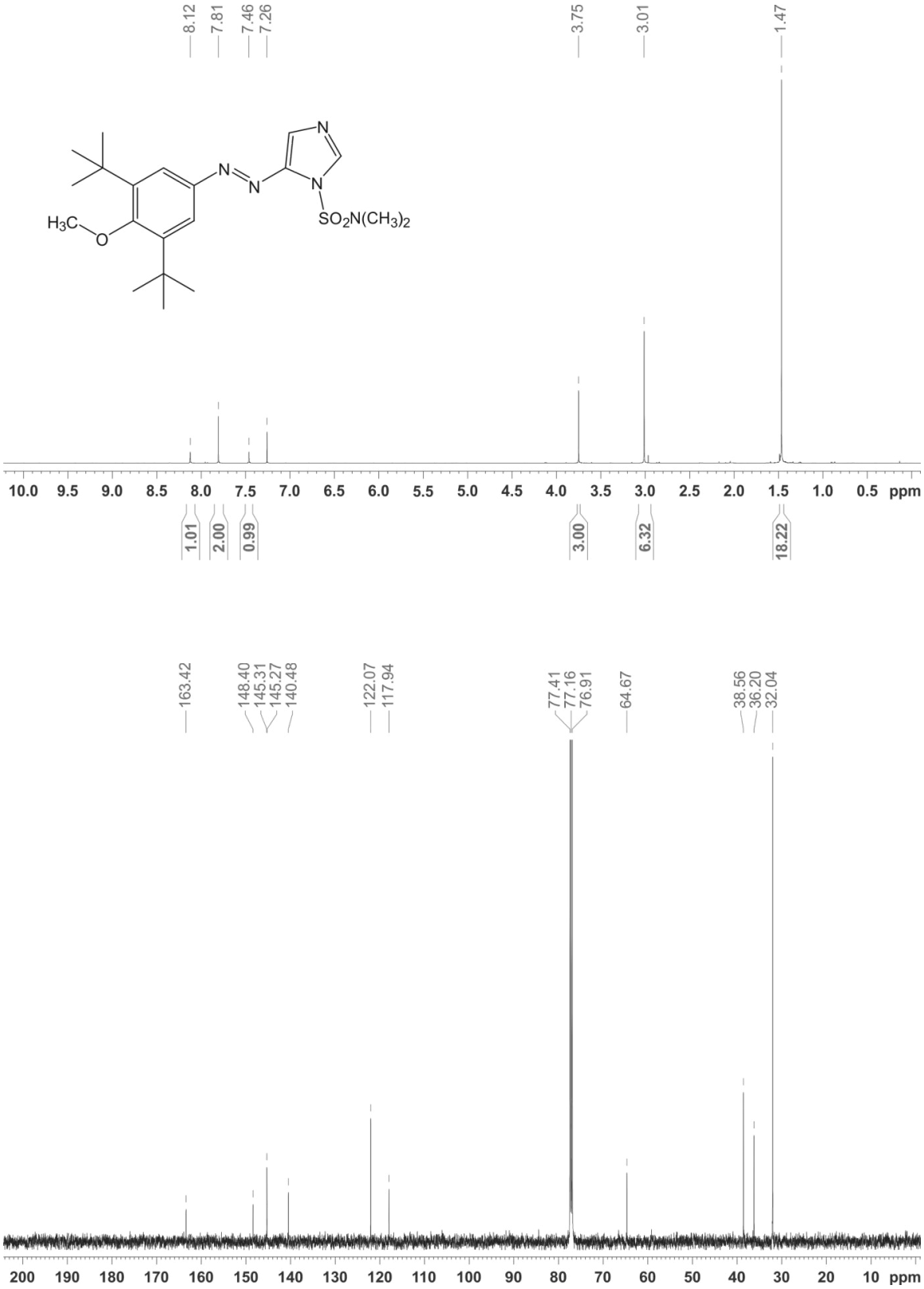

Figure S15. ^{1}H NMR spectrum (top) and ^{13}C NMR spectrum (bottom) of 1-(*N*,*N*-Dimethylsulfamoyl)-5-(3',5'-di-tert-butyl-4'-methoxyphenylazo)imidazole. Spectra were measured in chloroform-d_3 at 300 K.

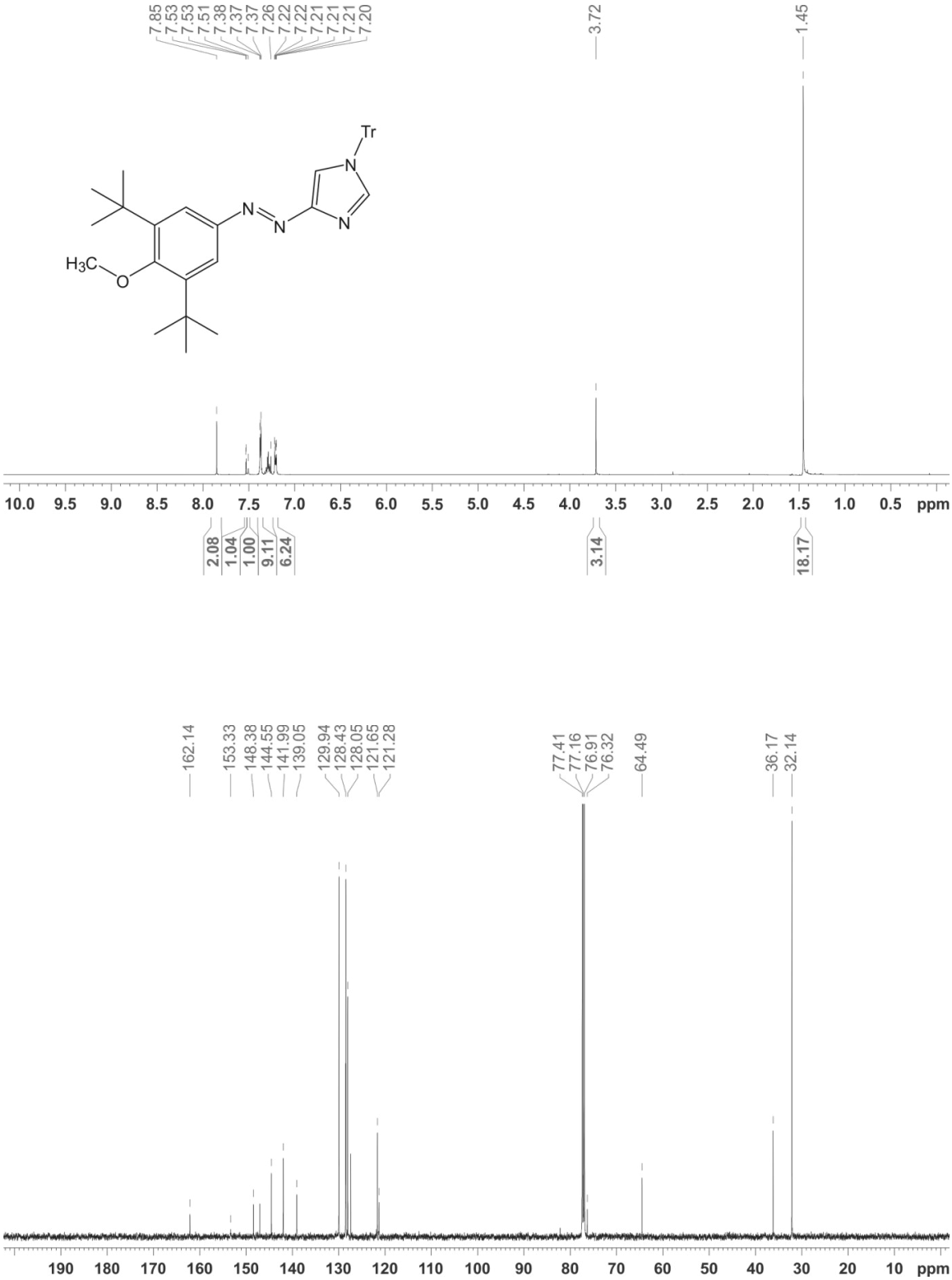

Figure S16. ^{1}H NMR spectrum (top) and ^{13}C NMR spectrum (bottom) of 1-Trityl-4-(3',5'-di-tert-butyl-4'-methoxyphenylazo)imidazole. Spectra were measured in chloroform-d_3 at 300 K.

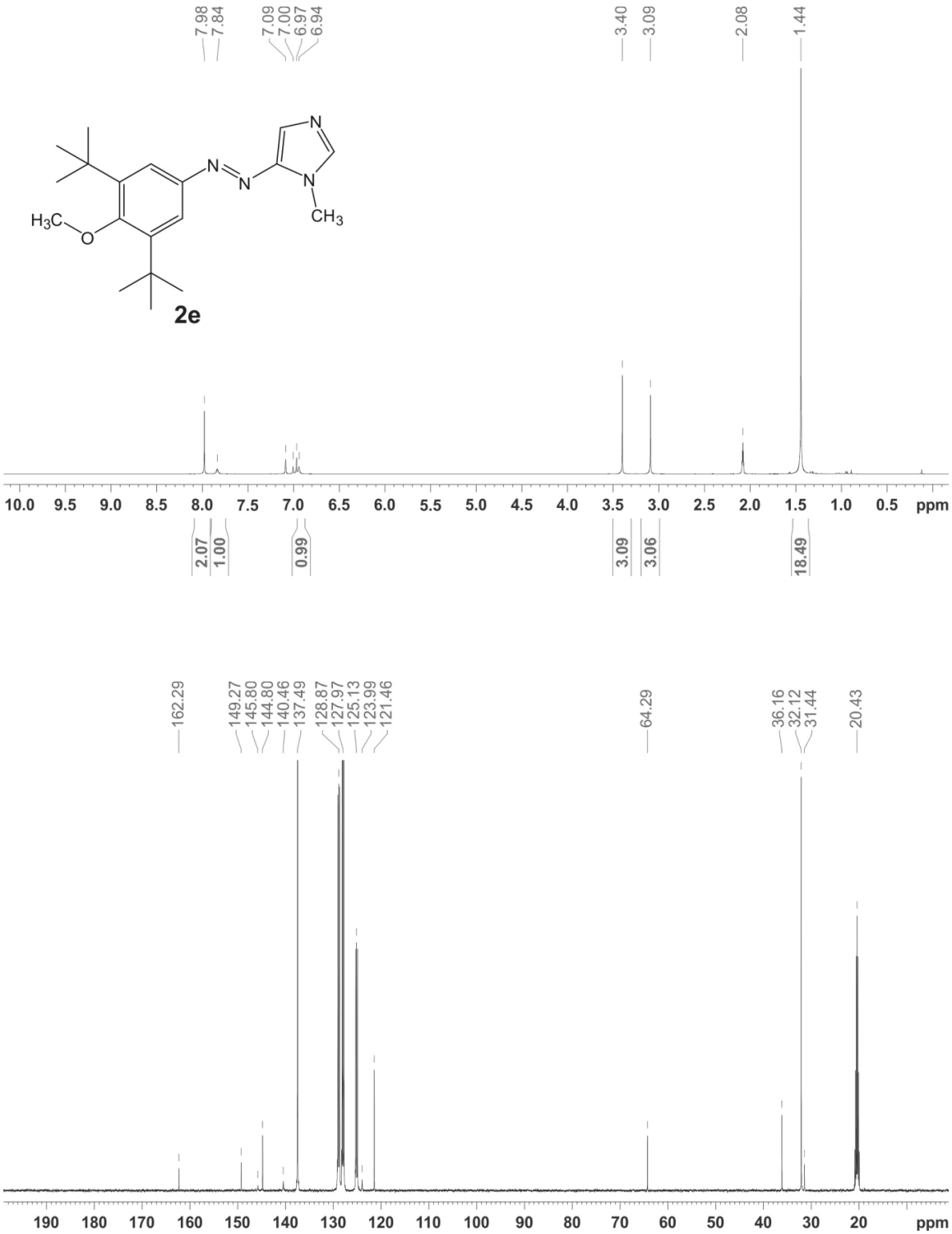

Figure S17. ^{1}H NMR spectrum (top) and ^{13}C NMR spectrum (bottom) of 1-Methyl-5-(3',5'-di-tert-butyl-4'-methoxyphenylazo)imidazole (**2e**). Spectra were measured in toluene-d_8 at 300 K.

II.3 UV-vis Spectroscopy

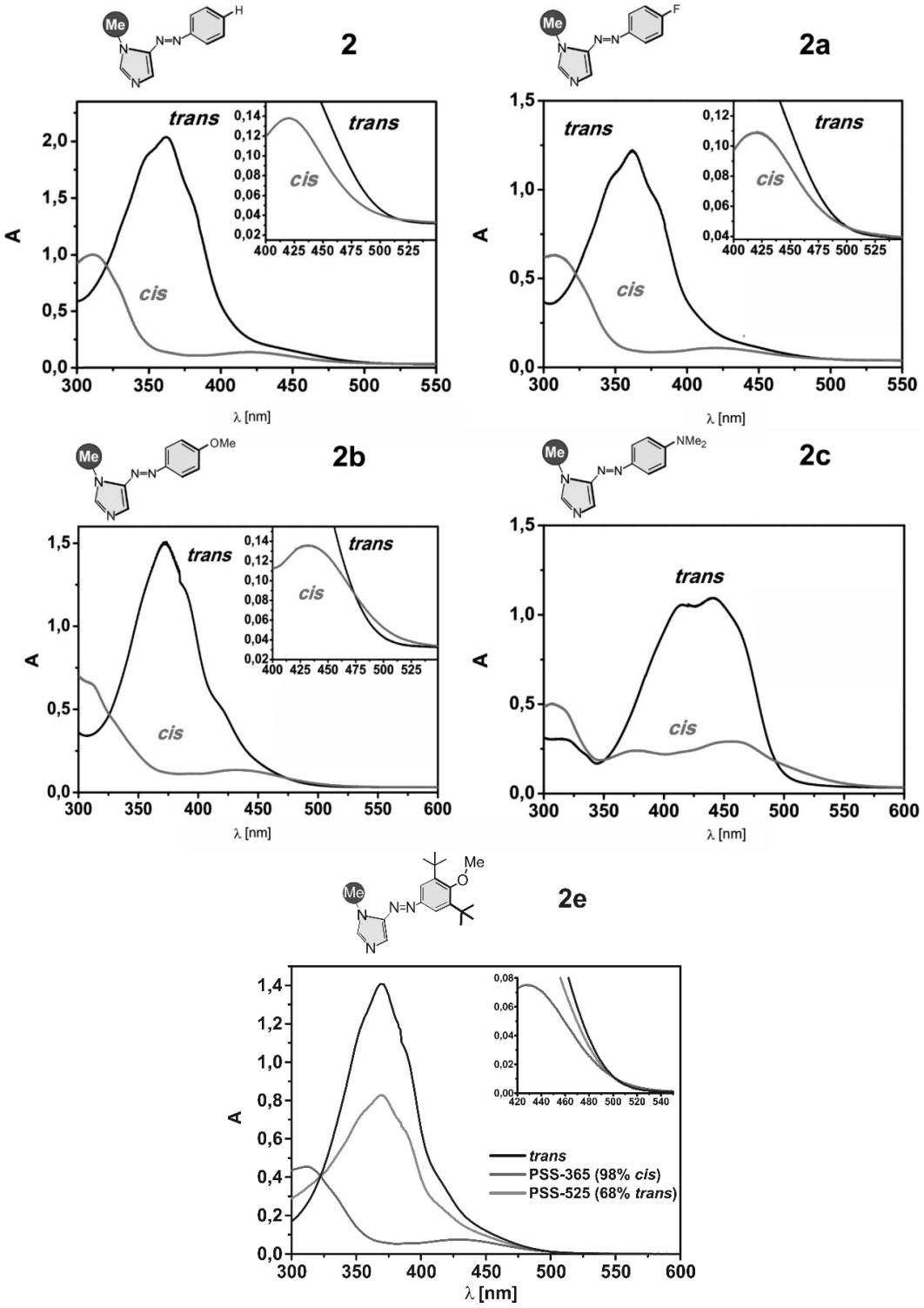

Figure S18. UV-vis spectra of the parent system **2** (top left) and its corresponding derivatives **2a** (top right), **2b** (middle left), **2c** (middle right). The spectrum of the *cis* isomer is presented in red and the spectrum of the *trans* isomer is shown in black. UV-vis spectra of azoimidazole **2e** (bottom). The spectrum of pure *trans* isomer (black line) was measured after storage in the dark for 2 days at 40 °C. The spectra of PSS-365 (violet line) and PSS-525 (green line) were measured after irradiation for 15 minutes with the respective wavelength.

II.4 Thermal reisomerization of Phenylazoimidazoles 2b and 2e

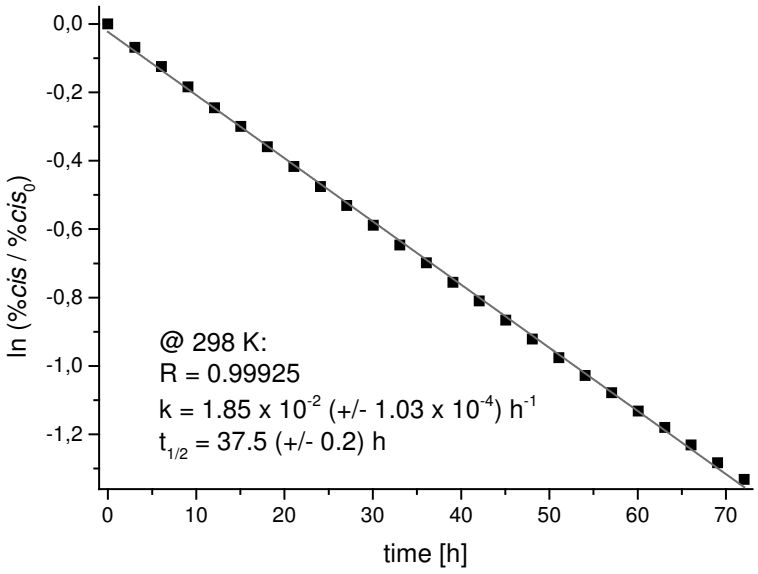

Figure S19. First order kinetics plot for the thermal *cis* to *trans* isomerization of 1-methyl-5-(4'-methoxyphenylazo)imidazole **2b** in toluene-d_8. *Cis* ratios were determined by ^{1}H NMR spectroscopy.

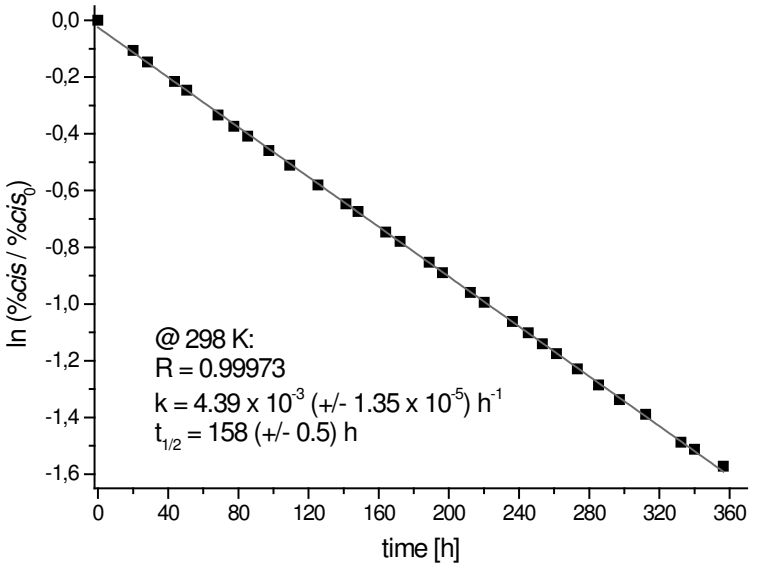

Figure S20. First order kinetics plot for the thermal *cis* to *trans* isomerization of 1-methyl-5-(3',5'-di-*tert*-butyl-4'-methoxyp-henylazo)imidazole **2e** in toluene-d_8. *Cis* ratios were determined by ^{1}H NMR spectroscopy.

II.5 Association Constants and Thermodynamic Parameters[4,5]

As we have described earlier,[4] the paramagnetism of the Ni^{2+} in the penta- and hexacoordinated complexes gives rise to a strong downfield shift and a broadening of the pyrrole proton resonance in porphyrins such as 5,10,15,20-tetrakis(pentafluorophenyl)-nickel(II)porphyrin ($NiTPPF_{20}$). Due to the very rapid coordination/decoordination process a time averaged signal of the dia- and paramagnetic species is observed in the ^1H NMR spectra which can be used to determine the ratio of dia- and paramagnetic Ni-porphyrins. The signal of the pyrrole protons was followed as a function of the axial ligand concentration at four different temperatures (298 K, 308 K, 318 K and 328 K). K_{1S} and K_2 were determined from these data for each temperature using a non-linear curve fitting. Arrhenius plots of the obtained association constants gave the thermodynamic parameters ΔH and ΔS of complex formation. A different NMR tube was used for each ligand concentration. Each ^1H-NMR tube was filled with 25 µL (Experim. with 1-methylimidazole (**1-mim**)) or 100 µL (Experim. with PDLs **2**, **2b** and **2e**), respectively, of a 9.70 mM $NiTPPF_{20}$ solution in toluene-d_8. Then different amounts of a solution of the ligands (**1-mim**: 122 mM; **2**: 267 mM; **2b**: 258 mM; **2e**: 248 mM) in toluene-d_8 were added to obtain ligand/porphyrin ratios between 2:1 and 100:1, and the tubes were filled up to 500 µL with toluene-d_8 and sealed. We measured NMR spectra of the PDL/porphyrin solutions (as described above) after storage in the dark at ≥40 °C overnight (large excess of *trans*) and after irradiation for 20 min with 365 nm (PSS with large excess of *cis*) at four different temperatures (298 K, 308 K, 318 K and 328 K). NMR spectra of the *N*-methylimidazole/porphyrin solutions were measured at four different temperatures (298 K, 308 K, 318 K and 328 K). The data from NMR titration were fitted to a model including all conceivable 1:1 and 1:2 complexes with a non-linear treatment using Excel Speciation Tool.[5]

Table S5: Summary of temperature dependend association constants of 1-methylimidazole and azoimidazoles 2, 2b and 2e with $NiTPPF_{20}$ in toluene-d_8 obtained from non-linear fitting.

	C_{pq}[a]	K_{pq}[a]	T [K]	**1-mim**[d]	**2**	**2b**	**2e**
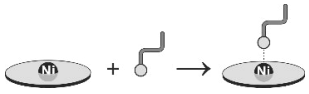	C_{10}	K_{10}[b]	298	355.33	38.31	59.14	60.03[e]
			308	255.78	27.41	43.25	43.14
			318	172.52	18.51	30.29	29.85
			328	116.09	13.50	21.32	21.74
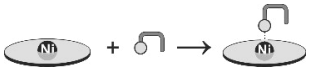	C_{01}	K_{01}[b]	298	-	10,76	15.83	1.37
			308	-	8,35	12.20	1.14
			318	-	6,66	9.61	1.00
			328	-	5,19	7.30	0.85
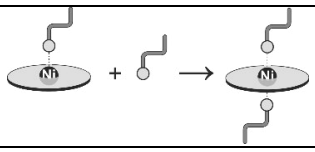	C_{20}	K_{20}[b]	298	93.75	81.58	67.13	65.99[e]
			308	60.59	56.51	47.03	48.30
			318	39.72	38.30	30.43	34.80
			328	35.00	24.92	21.50	22.29
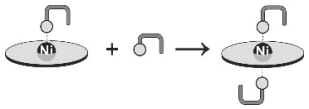	C_{02}	K_{02}[b]	298	-	35,55	44.33	8.15
			308	-	23,94	32.76	4.12
			318	-	17,80	25.22	2.08
			328	-	14,63	19.54	1.16
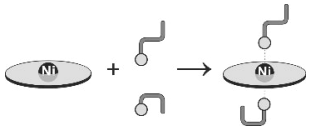	C_{11}	β_{11}[c]	298	-	1342,6	1170.0	524.91
			308	-	702,27	821.92	179.54
			318	-	391,38	537.07	63.67
			328	-	246,95	459.16	37.68

[a] C_{pq} represents the complex composition (p: PDL in *trans* configuration, q: PDL in *cis* configuration), K_{pq} represents the corresponding association constant, [b] [L mol^{-1}]; [c] [L^2 mol^{-2}]; [d] **1-mim** obviously does not provide a *trans* and *cis* species. For the sake of simplicity the data for **1-mim** were filed to the *trans* datasets of PDLs **2**, **2b** & **2e**; [e] 300 K.

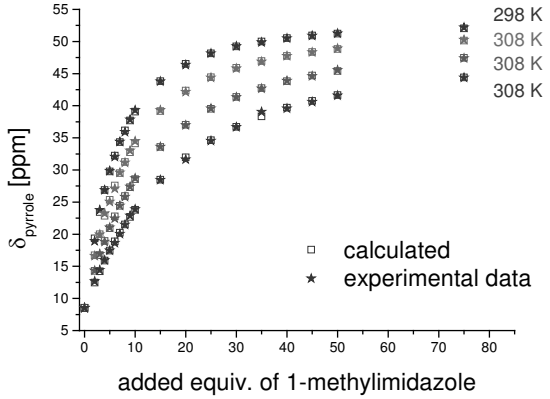

Figure S21: Fitting plots of measured and calculated pyrrole shifts of $NiTPPF_{20}$ upon coordination of 1-methylimidazole.

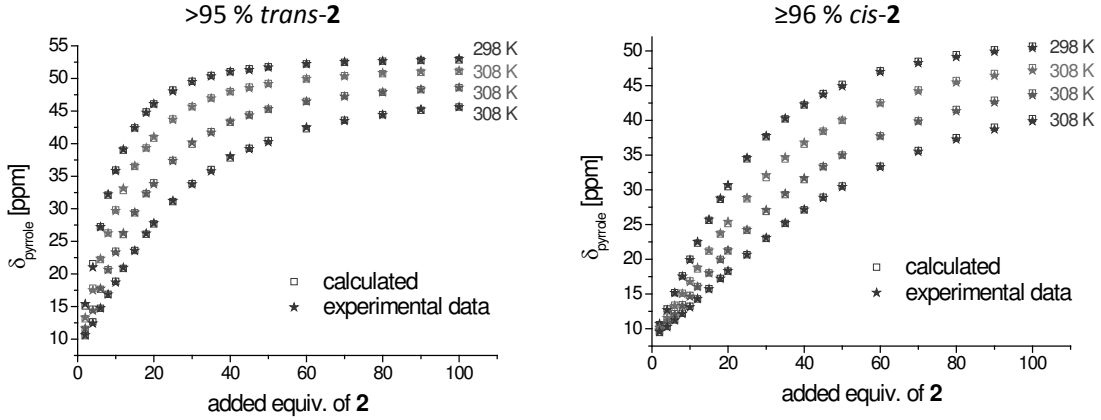

Figure S22: Fitting plots of measured and calculated pyrrole shifts of $NiTPPF_{20}$ upon coordination of *trans* (left) and *cis* (right) 1-methyl-5-phenylazoimidazole **2**.

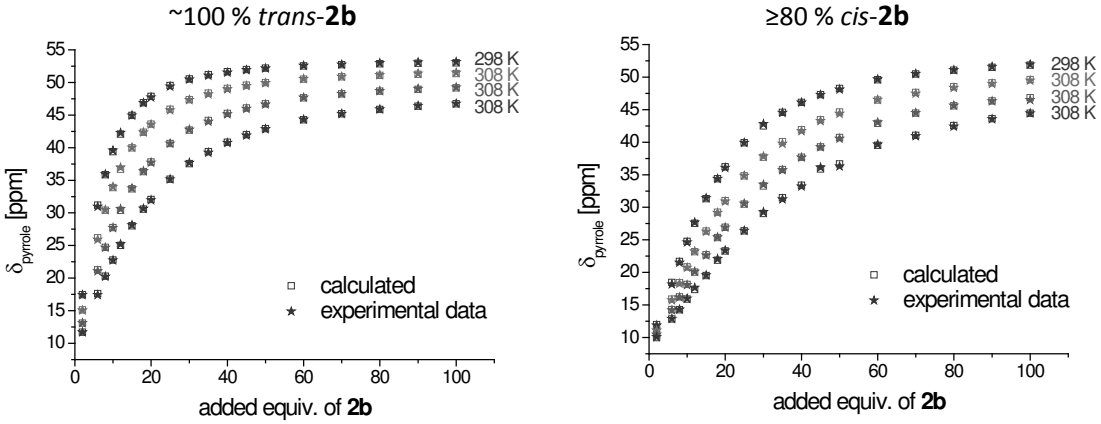

Figure S23: Fitting plots of measured and calculated pyrrole shifts of $NiTPPF_{20}$ upon coordination of *trans* (left) and *cis* (right) 1-methyl-5-(4'-methoxyphenylazo)imidazole **2b**.

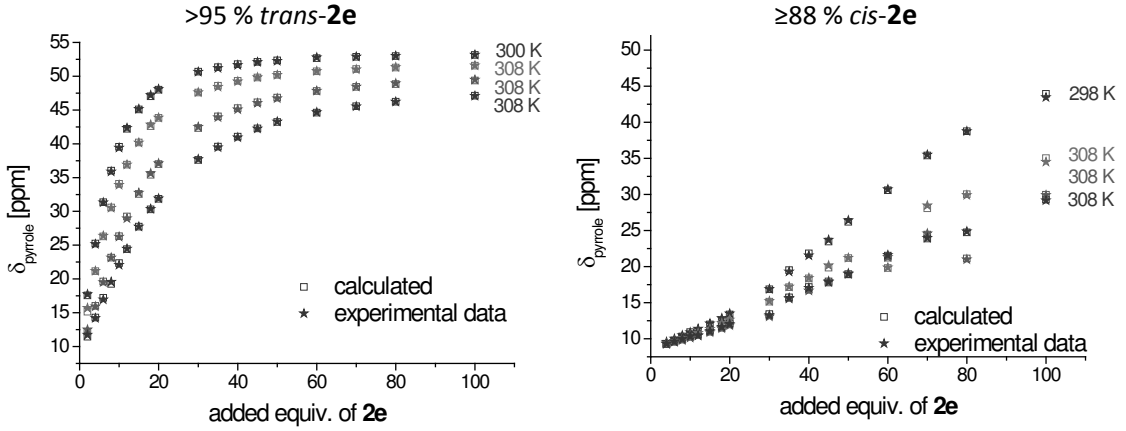

Figure S24: Fitting plots of measured and calculated pyrrole shifts of $NiTPPF_{20}$ upon coordination of *trans* (left) and *cis* (right) 1-methyl-5-(3',5'-di-*tert*-butyl-4'-methoxyphenylazo)imidazole **2e**.

Table S6: Summary of thermodynamic binding parameters of 1-methylimidazole and azoimidazoles 2, 2b and 2e with Ni(II)$TPPF_{20}$ determined from Arrhenius plots of temperature dependent association constants.

		***N*-mim**[a]		**2**		**2b**		**2e**	
		ΔH_f[b]	ΔS_f[c]	ΔH_f[b]	ΔS_f[c]	ΔH_f[b]	ΔS_f[c]	ΔH_f[b]	ΔS_f[c]
trans	K_{1S}	-7.27 (± 0.37)	-12.66 (± 1.17)	-6.84 (± 0.20)	-15.67 (± 0.65)	-6.63 (± 0.26)	-14.09 (± 0.84)	-7.10 (± 0.15)	-15.55 (± 0.49)
	K_2	-6.59 (± 0.91)	-13.20 (± 2.90)	-7.65 (± 0.35)	-16.88 (± 1.11)	-7.48 (± 0.27)	-16.69 (± 0.85)	-7.45 (± 0.57)	-16,49 (± 1.81)
cis	K_{1S}	-	-	-4.67 (± 0.11)	-11.01 (± 0.35)	-4.97 (± 0.16)	-11.19 (± 0.52)	-3.01 (± 0.11)	-9.50 (± 0.34)
	K_2	-	-	-5.77 (± 0.49)	-12.35 (± 1.58)	-5.28 (± 0.06)	-10.20 (± 0.20)	-12.70 (± 0.16)	-38.43 (± 0.52)

[a] **1-MeIm** obviously does not provide a *trans* and *cis* species. For the sake of simplicity the data for **1-MeIm** were filed to the *trans* datasets of PDLs **2**, **2e** & **2g**. [b] [kcal mol^{-1}]; [c] [cal mol^{-1}].

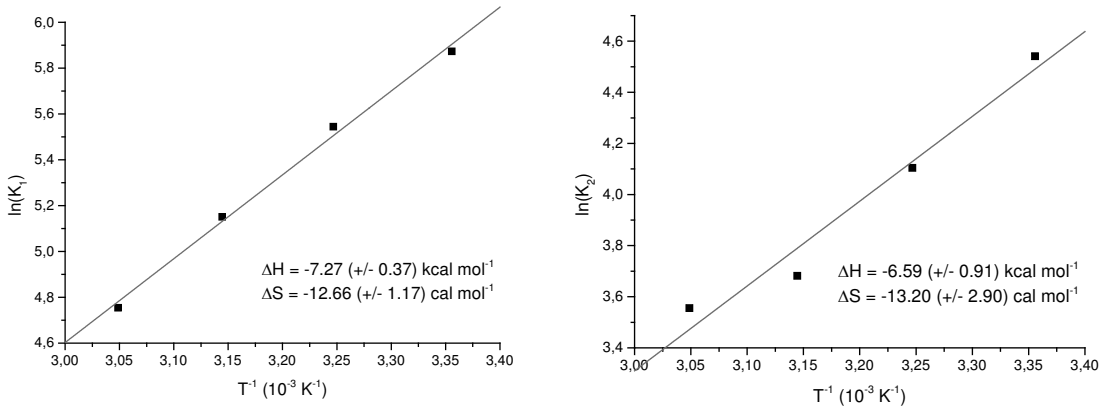

Figure S25: Arrhenius plots for determination of binding enthalpies and entropies for coordination of 1-methylimidazole to $NiTPPF_{20}$.

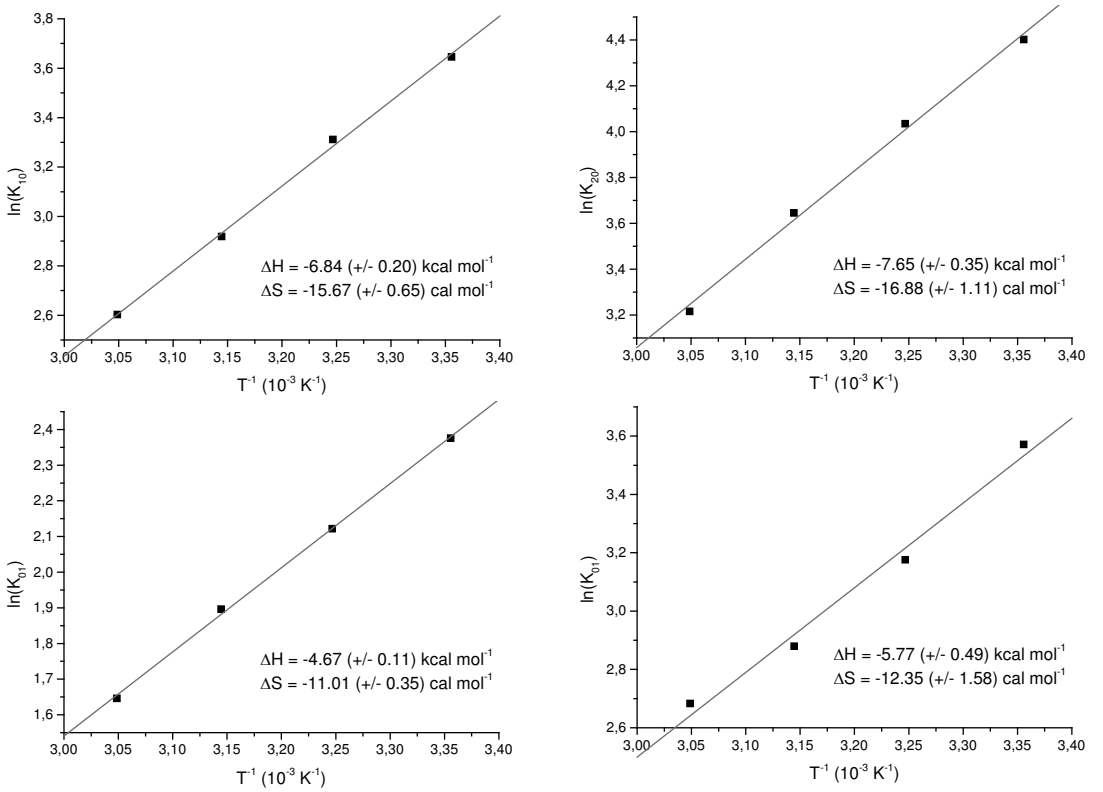

Figure S26: Arrhenius plots for determination of binding enthalpies and entropies for coordination of *trans* (top) and *cis* (down) 1-methyl-5-phenylazoimidazole **2** to $NiTPPF_{20}$.

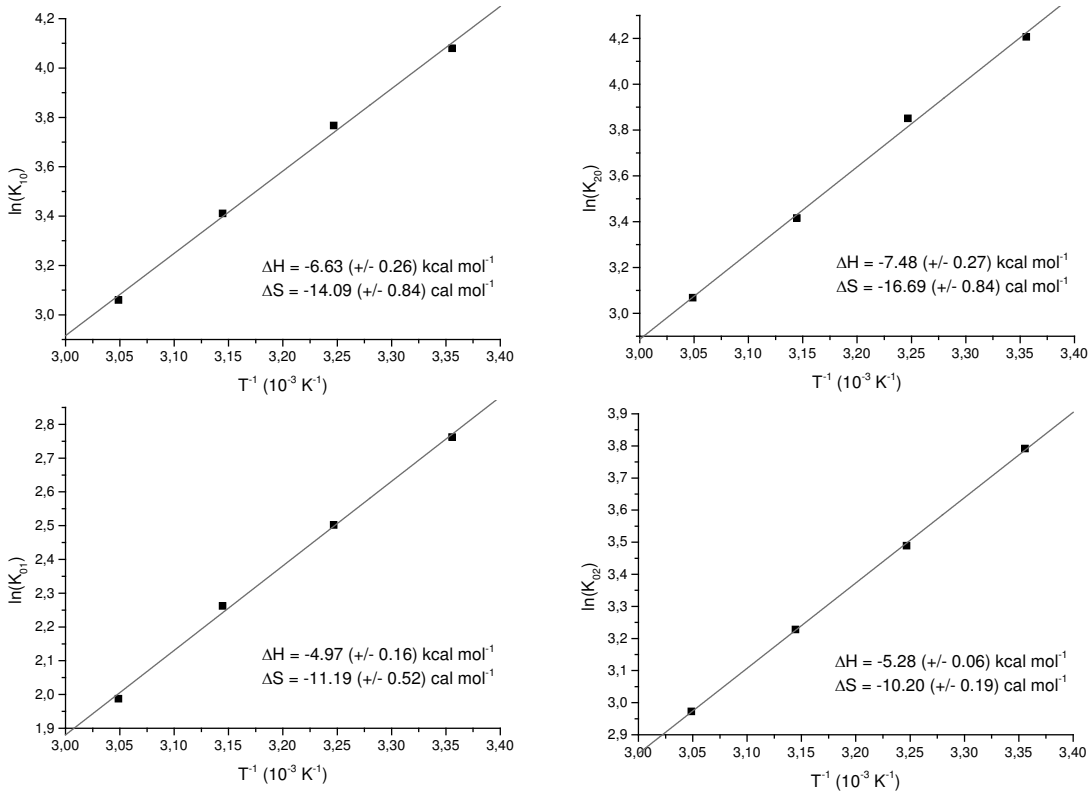

Figure S27: Arrhenius plots for determination of binding enthalpies and entropies for coordination of *trans* (top) and *cis* (down) 1-methyl-5-(4'-methoxyphenylazo)imidazole **2b** to $NiTPPF_{20}$.

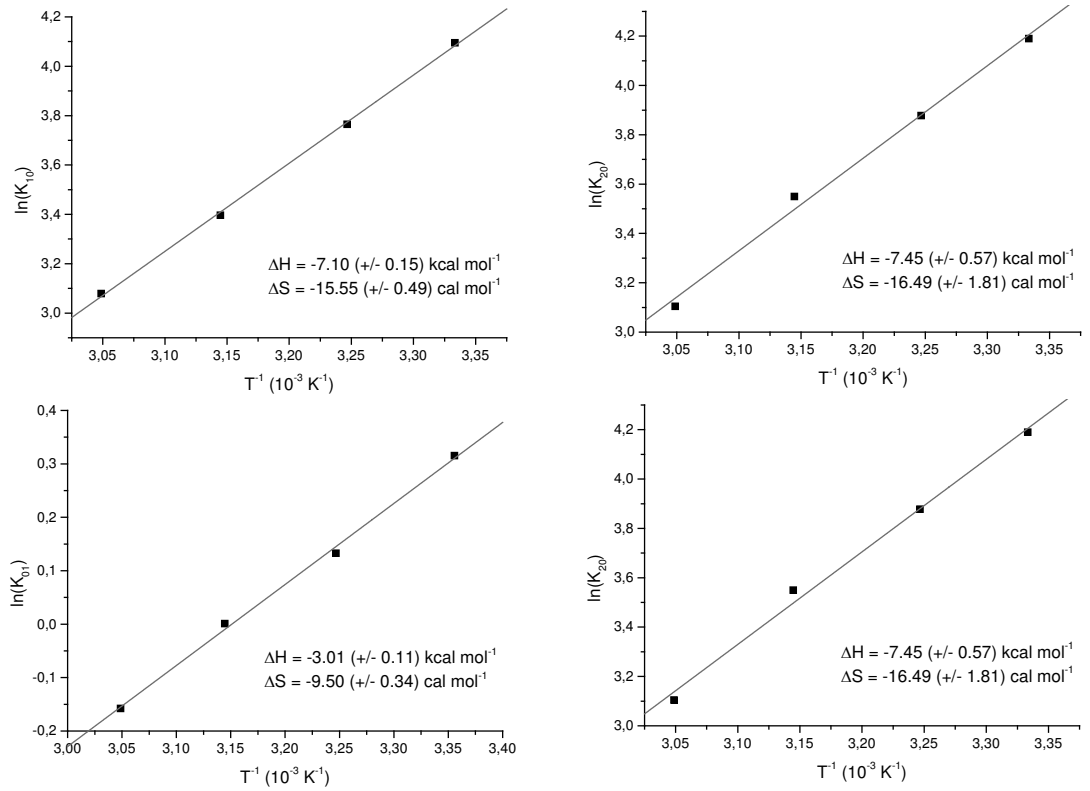

Figure S28: Arrhenius plots for determination of binding enthalpies and entropies for coordination of *trans* (top) and *cis* (down) 1-methyl-5-(3',5'-di-*tert*-butyl-4'-methoxyphenylazo)imidazole **2e** to $NiTPPF_{20}$.

II.6 NMR spin switching experiments

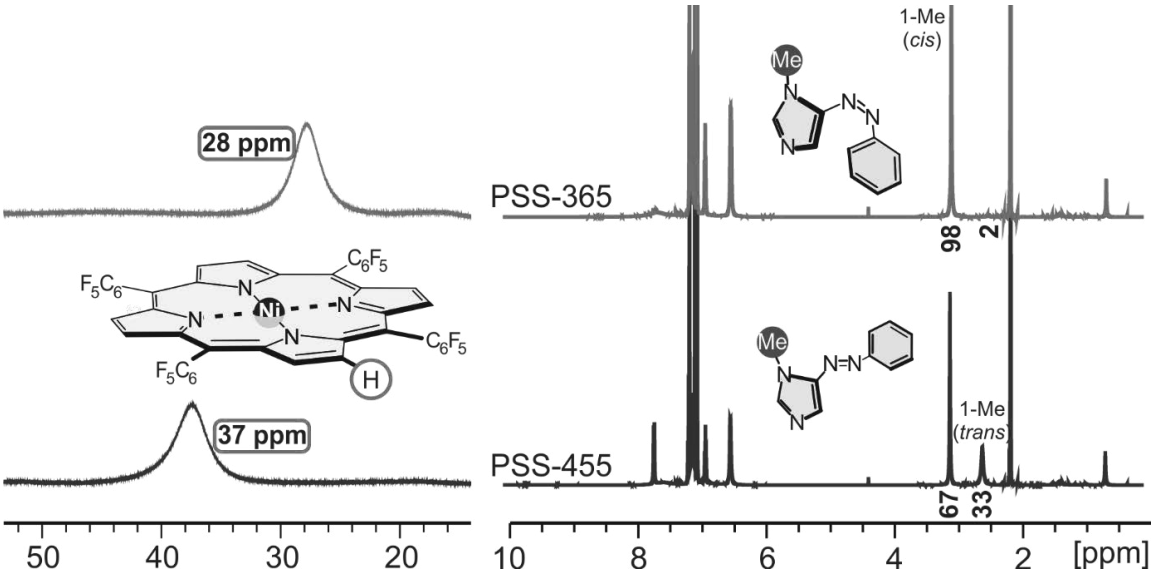

Figure S29: NMR switching experiments with phenylazoimidazole **2** (34.9 mM) and $NiTPPF_{20}$ (1.94 mM) in toluene-d_8. The amount of paramagnetic Ni^{2+} species in both photostationary states (PSS-365 and PSS-455) was calculated from the shift of the porphyrin's pyrrole protons (left). The corresponding *cis*/*trans* ratios were determined from the integrals of the 1-methyl group (right).

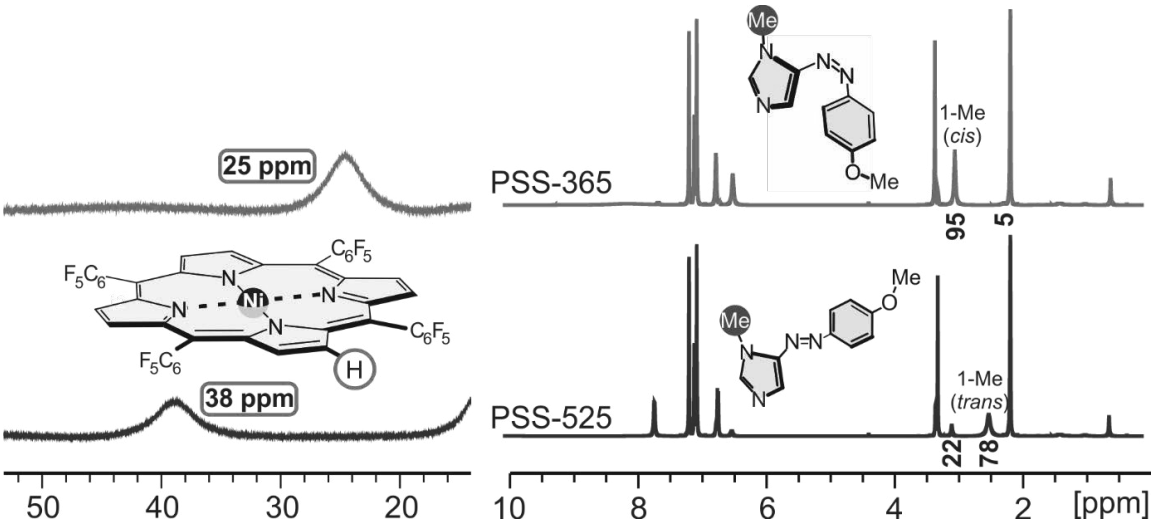

Figure S30: NMR switching experiments with phenylazoimidazole **2b** (19.4 mM) and $NiTPPF_{20}$ (1.94 mM) in toluene-d_8. The amount of paramagnetic Ni^{2+} species in both photostationary states (PSS-365 and PSS-525) was calculated from the shift of the porphyrin's pyrrole protons (left). The corresponding *cis*/*trans* ratios were determined from the integrals of the 1-methyl group (right).

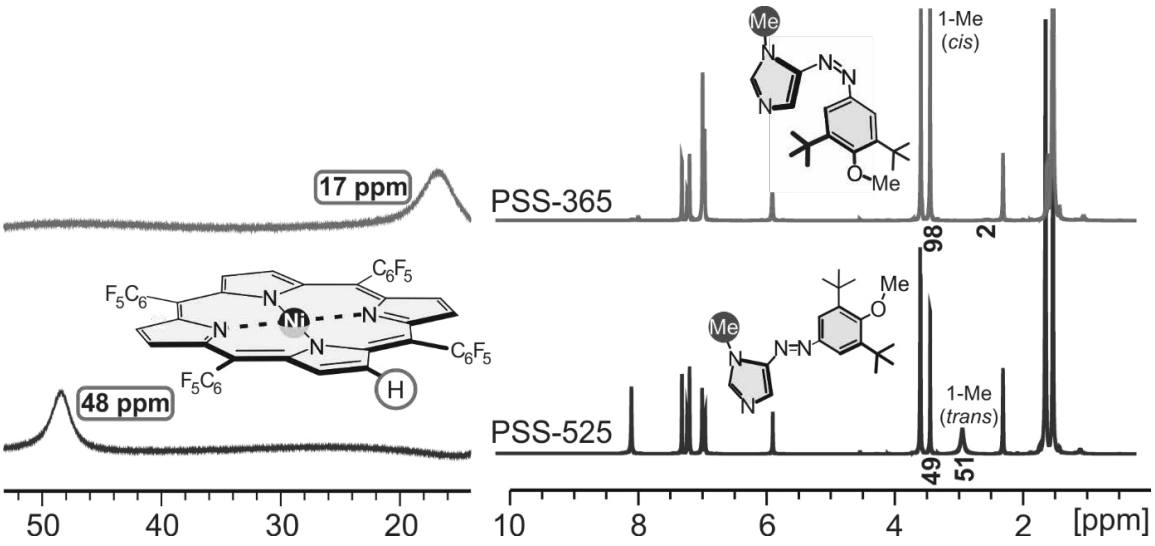

Figure S31: NMR switching experiments with phenylazoimidazole **2e** (67.9 mM) and $NiTPPF_{20}$ (1.94 mM) in toluene-d_8. The amount of paramagnetic Ni^{2+} species in both photostationary states (PSS-365 and PSS-525) was calculated from the shift of the porphyrin's pyrrole protons (left). The corresponding *cis*/*trans* ratios were determined from the integrals of the 1-methyl group (right).

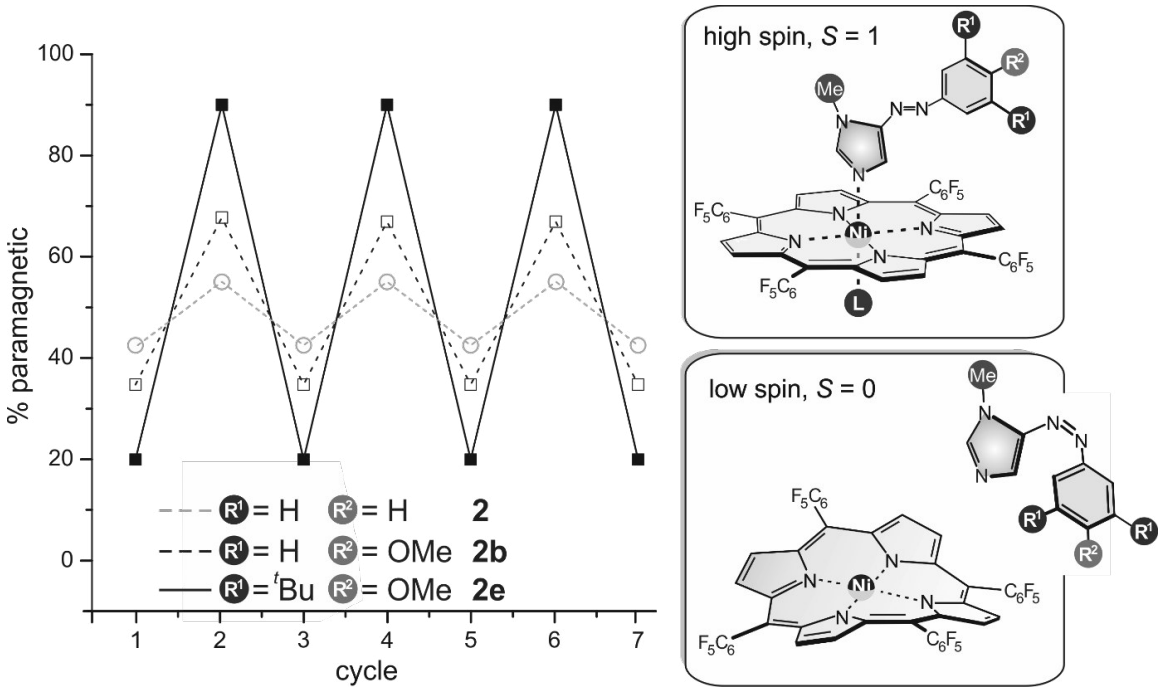

Figure S32: Reversible spin state switching of $NiTPPF_{20}$ with phenylazoimidazoles **2** (parent system), **2b** (4'-methoxy derivative) and **2e** (3',5'-di-*tert*-butyl-4'-methoxy derivative) in toluene-d_8. The proportion of paramagnetic Ni^{2+} species is plotted as a function of the switching cycle. Switching is achieved by irradiation with 365 nm (*trans* → *cis*) and 455 nm for **2** or 525 for **2b** and **2e** (*cis* → *trans*).

III. Literature

[1] TURBOMOLE **V6.3 2011**, a development of University of Karlsruhe and Forschungszentrum Karlsruhe GmbH, 1989-2007, TURBOMOLE GmbH, since 2007; available from http://www.turbomole.com.

[2] Gaussian 09, Revision **D.01**, Frisch, M. J.; Trucks, G. W.; Schlegel, H. B.; Scuseria, G. E.; Robb, M. A.; Cheeseman, J. R.; Scalmani, G.; Barone, V.; Mennucci, B.; Petersson, G. A.; Nakatsuji, H.; Caricato, M.; Li, X.; Hratchian, H. P.; Izmaylov, A. F.; Bloino, J.; Zheng, G.; Sonnenberg, J. L.; Hada, M.; Ehara, M.; Toyota, K.; Fukuda, R.; Hasegawa, J.; Ishida, M.; Nakajima, T.; Honda, Y.; Kitao, O.; Nakai, H.; Vreven, T.; Montgomery, J. A., Jr.; Peralta, J. E.; Ogliaro, F.; Bearpark, M.; Heyd, J. J.; Brothers, E.; Kudin, K. N.; Staroverov, V. N.; Kobayashi, R.; Normand, J.; Raghavachari, K.; Rendell, A.; Burant, J. C.; Iyengar, S. S.; Tomasi, J.; Cossi, M.; Rega, N.; Millam, J. M.; Klene, M.; Knox, J. E.; Cross, J. B.; Bakken, V.; Adamo, C.; Jaramillo, J.; Gomperts, R.; Stratmann, R. E.; Yazyev, O.; Austin, A. J.; Cammi, R.; Pomelli, C.; Ochterski, J. W.; Martin, R. L.; Morokuma, K.; Zakrzewski, V. G.; Voth, G. A.; Salvador, P.; Dannenberg, J. J.; Dapprich, S.; Daniels, A. D.; Farkas, Ö.; Foresman, J. B.; Ortiz, J. V.; Cioslowski, J.; Fox, D. J. Gaussian, Inc., Wallingford CT, **2009**.

[3] Grimme, S.; Parac, M. *ChemPhysChem* **2003**, *4*, 292.

[4] Thies, S.; Sell, H.; Schütt, C.; Bornholdt, C.; Näther, C.; Tuczek, F.; Herges, R. *J. Am. Chem. Soc.* **2011**, *133*, 16243–16250.

[5] del Piero, S.; Melchior, A.; Polese, P.; Portanova, R.; Tolazzi, M. *Annali di Chimica* **2006**, *96*, 29-49.

8.2 Azoimidazole functionalized Ni-porphyrins for molecular spin switching and light responsive MRI contrast agents.

Gernot Heitmann, Christian Schütt, Jens Gröbner, Lukas Huber und Rainer Herges

Supporting Information
Dalton Trans. **2016**, *45*, 11407-11412.
http://dx.doi.org/10.1039/c6dt01727d

Azoimidazole functionalized Ni-porphyrins for molecular spin switching and light responsive MRI contrast agents.

Gernot Heitmann, Christian Schütt, Jens Gröbner, Lukas Huber and Rainer Herges

Table of Contents

I. Coordination Strength and Basicity of Pyridine- and Imidazole-based PDLs

Light-driven coordination-induced spin state switching (LD-CISSS) in water requires a photoswitchable ligand with a high binding affinity (K_L) to the metal center while exhibiting a low basicity (corresponding to the pK_a). Figure S1 shows the association constants (K_L) of several 3-(phenylazo)-pyridine ligands[1] and the parent phenylazoimidazole ligand[2] to $NiTPPF_{20}$ in toluene-d_8 in correlation to their predicted[3] basicity (pK_a*). The azoimidazole ligand provides the most favourable K_L/pK_a ratio and will most likely not be protonated in water (pK_a* = 5.13). The dimethylamino-substituted azopyridine ligand binds stronger to the nickel in toluene; however, its predicted basicity (pK_a* = 8.26) suggests that it will be completely protonated in aqueous media and therefore will not bind.

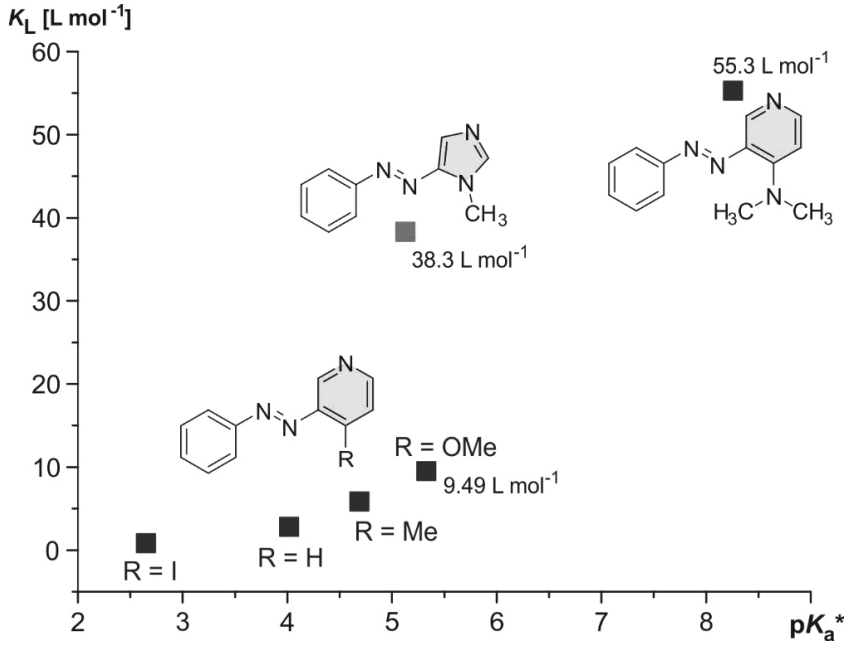

Figure S1: Association constants (K_L) of 3-(phenylazo)pyridines[1] and 5-(phenylazo)-1-methyl-imidazole[2] to Ni(II)$TPPF_{20}$ in toluene in correlation to their calculated[3] pK_a values. The imidazole derivative provides the most favourable K_L/pK_a ratio.

II. Computational Details

II.1 Complex Formation Energy of the Reference System

All calculations have been conducted using Turbomole 6.6.[4] The geometry optimizations were performed at the TPSSh/SVP level of theory. Single point energies using a larger basis set (TPSSh/def2TZVP) were calculated at the optimized geometries. The calculated complex formation energy (ΔE_f) for the formation of the five coordinate complex of tris-pentafluorophenyl-porphyrin ($NiTPPHF_{15}$) with the most stable conformation of *cis*-1-methyl-5-phenylazoimidazole (*cis*-m5p)[2] is given in Figure S2 and Table S1.

Table S1. Complex formation energy (ΔE_f) of the reference system calculated at the TPSSh/def2TZVP//TPSSh/SVP level of theory. ΔE_f is defined according to the following equation: $NiTPPHF_{15}$ (singlet) + *cis*-m5p (singlet) → $NiTPPHF_{15}$ · *cis*-m5p (triplet).

E_{abs} m5p singlet [a.u.]	E_{abs} $NiTPPHF_{15}$ singlet [a.u]	E_{abs} $NiTPPHF_{15}$ singlet [a.u]	ΔE_f [kcal/mol]
-606.28355311	-5286.05067482	-4679.75594046	-7.02

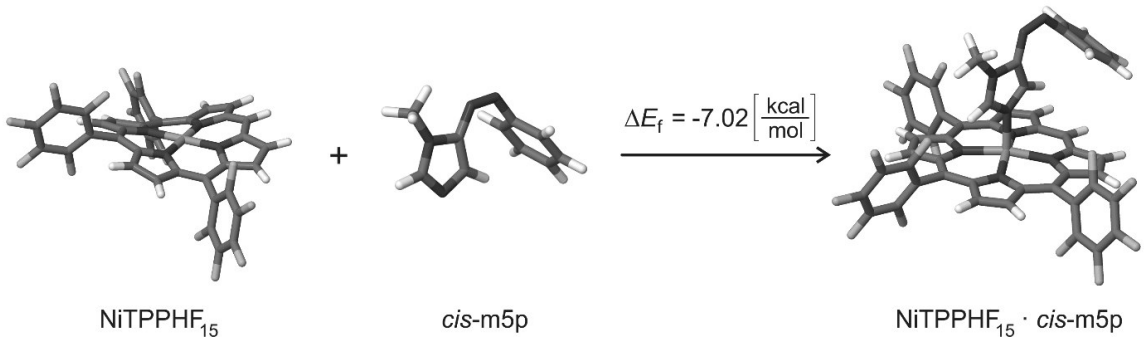

Figure S2: Calculated (TPSSh/def2TZVP//TPSSh/SVP) complex formation energy of the five coordinate complex of *cis*-m5p with $NiTPPHF_{15}$ in kcal/mol.

II.2 Energy Difference of the Magnetic Conformers in cis Configuration

The energy difference ($\Delta\Delta E_f$) of the uncoordinated diamagnetic (*cis*-s-u) and the coordinated paramagnetic *cis* isomer (*cis*-t-k) is indicative of the amount of paramagnetic *cis* species. A higher difference in energy of the magnetic conformers gives rise to a stabilization upon coordination and thus a stronger coordination of the tone arm.

Table S2. Calculated (TPSSh/def2TZVP//TPSSh/SVP) energy difference of the uncoordinated *cis* (singlet) and coordinated *cis* (triplet) species for 1a-c. ($\Delta\Delta E_{f,calc} = \Delta E_{f,calc\text{-}cis\text{-}s\text{-}u} - \Delta E_{f,calc\text{-}cis\text{-}t\text{-}k}$).

	$E_{abs,cis\text{-}s\text{-}u}$ [Hartree]	$E_{abs,cis\text{-}t\text{-}k}$ [Hartree]	$\Delta\Delta E_f$ [kcal/mol]
Biphenyl **4**	-5515.98617580	-5515.98958307	2.14
Biarylthioether **5**	-5914.20203374	-5914.20847273	4.04

II.3 XYZ Coordinates of TPSSh/SVP Optimized Reference System.

$NiTPPHF_{15}$ · 1 *cis*-m5p
$E_{TPSSh/SVP}$ = -5281.59352739 Hartree
NImag = 0

C	0.266560	-3.468100	4.108400
C	-1.033430	-3.799430	3.687930
C	-1.235560	-4.930670	2.893870
C	-0.151520	-5.730600	2.510350
C	1.139590	-5.402250	2.940570
C	1.351960	-4.283980	3.752260
N	0.478370	-2.385780	5.012410
N	0.390980	-1.186690	4.653060
C	0.192970	-0.754850	3.347150
C	0.184630	-1.260280	2.043190
N	0.057630	0.629080	3.199960
N	0.048050	-0.232430	1.164390
C	-0.032760	0.886720	1.885560
H	-1.876780	-3.173230	3.991600
H	-2.249170	-5.186540	2.570760
H	-0.314900	-6.614460	1.886810
H	1.990320	-6.026860	2.651550
H	2.352960	-4.029760	4.110330
H	0.277500	-2.287570	1.703360
H	-0.160100	1.888560	1.476580
C	1.217600	2.516540	-1.136420
N	1.408950	1.161040	-1.173020
C	2.491890	3.205340	-1.186160
C	3.452510	2.240790	-1.266240
C	2.763530	0.966090	-1.249540
C	-0.032650	3.160200	-1.059390
C	-1.282940	2.513540	-1.050510
C	-2.557690	3.201460	-1.031920
C	-3.520820	2.235690	-1.034130
C	-2.832140	0.960640	-1.054780
N	-1.475320	1.157180	-1.065860
Ni	-0.021980	-0.287040	-0.895610
N	1.420570	-1.721340	-1.184440
C	1.220520	-3.076040	-1.229530
C	2.485320	-3.769380	-1.347760
C	3.453980	-2.807770	-1.381550
C	2.772100	-1.531730	-1.279890
C	-3.478910	-0.288930	-1.059980
C	-2.830950	-1.539160	-1.083680
C	-3.512320	-2.818660	-1.149460
C	-2.539940	-3.776030	-1.184230
C	-1.273110	-3.078020	-1.146060
N	-1.475820	-1.724280	-1.082590
C	-0.026110	-3.706580	-1.196280
C	3.412420	-0.279930	-1.303170
H	-4.600830	2.374830	-1.025090
H	-2.696870	4.281800	-1.034080
H	-4.591780	-2.960520	-1.182500
H	-2.659030	-4.858010	-1.247650
H	4.530820	-2.942380	-1.477270
H	2.604560	-4.851400	-1.409480

***cis*-m5p**
$E_{TPSSh/SVP}$ = -605.618593002 Hartree
Nimag = 0

C	1.537060	0.035830	0.606520
C	2.073990	-1.140650	0.058860
C	2.984140	-1.060000	-0.999180
C	3.372690	0.185210	-1.507880
C	2.850830	1.355900	-0.944250
C	1.939170	1.287940	0.113220
N	0.680020	-0.038310	1.744680
N	-0.570700	-0.081390	1.628610
C	-1.265670	-0.070460	0.431930
C	-1.026140	-0.030040	-0.952930
N	-2.661640	-0.119390	0.543340
N	-2.193300	-0.051820	-1.639540
C	-3.147540	-0.104580	-0.717030
H	1.772610	-2.108920	0.467600
H	3.395640	-1.979730	-1.426770
H	4.086900	0.243490	-2.334420
H	3.157440	2.333710	-1.328830
H	1.533550	2.197940	0.563780
H	-4.218570	-0.133770	-0.925460
C	-3.422460	-0.173220	1.785870
H	-4.039260	-1.086400	1.812770
H	-2.698900	-0.187000	2.612850
H	-4.071830	0.713440	1.872470
H	-0.068020	0.012210	-1.466200

$NiTPPHF_{15}$
$E_{TPSSh/SVP}$ = -4675.95096384 Hartree
NImag = 0

C	-0.352450	-0.078880	3.463820
N	0.686240	0.257860	2.626100
C	0.062380	-0.010250	4.844310
C	1.351160	0.434500	4.841470
C	1.739540	0.558660	3.460080
C	-1.661250	-0.328840	3.043230
C	-2.066710	-0.080570	1.729870
C	-3.447090	0.019360	1.325690
C	-3.445320	0.480280	0.043150
C	-2.063450	0.589170	-0.353110
N	-1.229840	0.256860	0.689930
Ni	0.698330	0.256320	0.690200
N	2.631190	0.248150	0.686840
C	3.468830	-0.078650	-0.352830
C	4.850290	0.012970	0.054990
C	4.846050	0.452000	1.346130
C	3.464400	0.558330	1.738660
C	-1.651310	0.837040	-1.664760
C	-0.340610	0.591120	-2.079470
C	0.062680	0.494490	-3.460360
C	1.342300	0.028590	-3.460720
C	1.746970	-0.068460	-2.080040
N	0.703070	0.261430	-1.243390

H	2.634060	4.284840	-1.170140
H	4.531060	2.378760	-1.328920
C	-0.026380	4.649340	-0.957330
C	4.901940	-0.259750	-1.418940
C	-4.971590	-0.288720	-1.054990
C	-5.697080	-0.645190	0.089190
C	-7.093460	-0.645720	0.108760
C	-7.796970	-0.284550	-1.042310
C	-7.102790	0.074140	-2.199800
C	-5.706010	0.068470	-2.193830
F	-5.051310	-0.991620	1.204020
F	-7.757840	-0.982020	1.212570
F	-9.125630	-0.281700	-1.035960
F	-7.776200	0.413400	-3.296410
F	-5.070260	0.415080	-3.312320
C	5.726030	-0.319070	-0.289080
C	7.117400	-0.249450	-0.387980
C	7.711980	-0.129710	-1.645980
C	6.915620	-0.075390	-2.792090
C	5.526380	-0.144460	-2.666910
F	5.185520	-0.430790	0.924670
F	7.877910	-0.293040	0.703750
F	9.034850	-0.063430	-1.751690
F	7.483160	0.042790	-3.990040
F	4.789860	-0.087560	-3.774890
C	0.270280	5.466110	-2.056040
C	0.312750	6.858500	-1.950390
C	0.046670	7.465180	-0.720800
C	-0.257190	6.678490	0.392910
C	-0.291640	5.289950	0.259330
F	0.529620	4.917400	-3.241160
F	0.604460	7.607990	-3.009570
F	0.085350	8.788100	-0.608800
F	-0.501620	7.254870	1.567950
F	-0.578130	4.562650	1.348210
C	0.018240	1.604050	4.285490
H	-0.883430	1.452110	4.898000
H	0.905670	1.480700	4.922510
H	0.002820	2.609230	3.839320
H	-0.026990	-4.798800	-1.242210
C	3.057000	-0.319410	-1.666490
C	3.044010	0.783200	3.042000
H	-4.298790	0.693660	-0.598280
H	-4.302670	-0.199590	1.962390
H	-0.570110	0.718970	-4.316850
H	1.973820	-0.196570	-4.317900
H	5.694410	0.658280	1.998490
H	5.705130	-0.197040	-0.585950
H	-0.567890	-0.245130	5.700080
H	2.006850	0.626860	5.690490
C	-2.681960	-0.776730	4.031740
C	-2.671610	1.265930	-2.663270
C	4.071290	-0.760740	-2.664820
C	4.513320	-2.090740	-2.679430
C	5.458520	-2.543440	-3.601470
C	5.986450	-1.652110	-4.537920
C	5.570570	-0.318550	-4.543820
C	4.624310	0.111250	-3.611020
F	4.023850	-2.962570	-1.799980
F	5.854280	-3.813260	-3.597470
F	6.883330	-2.074210	-5.421400
F	6.077670	0.532170	-5.432260
F	4.248740	1.389760	-3.638720
C	-3.222700	0.383080	-3.600800
C	-4.180110	0.798050	-4.529020
C	-4.609280	2.127420	-4.527880
C	-4.083070	3.029390	-3.600670
C	-3.126520	2.591420	-2.682970
F	-2.835940	-0.892090	-3.623140
F	-4.685470	-0.062610	-5.408760
F	-5.517310	2.534970	-5.406800
F	-4.491270	4.295300	-3.601080
F	-2.640600	3.472630	-1.810930
C	-3.237560	0.089760	4.981470
C	-4.196360	-0.342250	5.900290
C	-4.620510	-1.673050	5.878090
C	-4.089210	-2.559170	4.938570
C	-3.132170	-2.104170	4.029930
F	-2.855330	1.365830	5.023150
F	-4.707500	0.503820	6.790830
F	-5.528830	-2.097350	6.748750
F	-4.492910	-3.826370	4.919180
F	-2.641010	-2.970850	3.146350
H	3.797780	1.014840	3.797490

II.4 XYZ Coordinates of TPSSh/SVP Optimized Record Player Type Molecules.

II.4.1 Magnetic Conformers of Biphenyl RP **4**

***cis*$_{\mathbf{dia}}$**
$E_{TPSSh/SVP}$ = -5511.28035583 Hartree
NImag = 0

C	-0.772220	-2.996780	2.692220
N	-1.509020	-2.058540	2.004550
C	-1.503850	-4.232880	2.816510
C	-2.680320	-4.056940	2.152290
C	-2.688730	-2.692840	1.685730
C	0.549540	-2.832030	3.103780
C	1.318520	-1.738870	2.698810
C	2.752120	-1.683080	2.829600
C	3.165460	-0.593240	2.122490
C	1.975640	0.051820	1.624870
N	0.850500	-0.662150	1.979610
Ni	-0.991060	-0.247450	1.560250
N	-2.838290	0.186880	1.195400
C	-3.393550	1.442390	1.096800
C	-4.813270	1.356860	0.858230
C	-5.109770	0.031990	0.747740
C	-3.883490	-0.685460	0.992930
C	1.979060	1.273930	0.945490
C	0.796970	1.994440	0.757400
C	0.770620	3.392720	0.405210
C	-0.514580	3.812590	0.570810
C	-1.282070	2.651650	0.945620
N	-0.470650	1.546330	1.064930
C	-2.674720	2.637450	1.052940
C	-3.810290	-2.071280	1.135730
H	4.180720	-0.234570	1.963850
H	3.360330	-2.411720	3.363120
H	1.642540	3.975560	0.114460
H	-0.920950	4.811940	0.426350
H	-6.075290	-0.428860	0.546160
H	-5.481800	2.209020	0.747660
H	-1.142690	-5.125180	3.325240
H	-3.492680	-4.768920	2.015620
C	1.202930	-3.925190	3.880200
C	-5.015390	-2.891410	0.822430
C	3.284000	1.901190	0.559850
C	-3.436500	3.917820	1.002430
C	-3.981320	4.464940	2.171630
C	-4.731610	5.642270	2.153620
C	-4.950420	6.299320	0.940890
C	-4.418680	5.778720	-0.241280
C	-3.670280	4.600350	-0.198180
F	-3.793310	3.856570	3.341420
F	-5.235560	6.140520	3.279350
F	-5.666790	7.417070	0.912360
F	-4.631690	6.402810	-1.397010
F	-3.182700	4.121480	-1.341340
C	-6.024160	-3.102920	1.770460
C	-7.162980	-3.855960	1.477530

***cis*$_{\mathbf{para}}$**
$E_{TPSSh/SVP}$ = -5511.29817707 Hartree
NImag = 0

C	3.350850	0.546430	3.653890
C	3.856360	0.086790	2.423440
C	4.641320	0.930260	1.618740
C	4.903240	2.240820	2.063180
C	4.396250	2.697180	3.283190
C	3.638990	1.849610	4.092450
N	2.703830	-0.320620	4.583580
N	1.601340	-0.881000	4.372330
C	0.793590	-0.697020	3.261380
C	0.743850	0.083830	2.105770
N	-0.372640	-1.473770	3.223120
N	-0.373320	-0.224570	1.396900
C	-1.024000	-1.159120	2.091970
H	3.662120	-0.942130	2.108410
H	5.510340	2.905200	1.441540
H	4.606060	3.718990	3.612900
H	3.267050	2.176740	5.066650
H	1.450130	0.825820	1.747670
H	-1.956370	-1.628130	1.782410
C	-0.762190	-2.490440	4.198060
C	0.782560	2.796850	-0.932280
N	0.976550	1.443410	-0.847930
C	2.055680	3.482200	-1.010010
C	3.020820	2.519420	-0.971110
C	2.336940	1.247820	-0.857930
C	-0.467550	3.445450	-0.937320
C	-1.717840	2.803480	-0.918570
C	-2.990430	3.496890	-0.957450
C	-3.957490	2.536910	-0.956820
C	-3.272400	1.260010	-0.932850
N	-1.916510	1.448600	-0.901340
Ni	-0.479580	0.010370	-0.661850
N	0.978390	-1.434630	-0.869330
C	0.778090	-2.788290	-0.855890
C	2.046280	-3.483750	-0.781550
C	3.014930	-2.524000	-0.733050
C	2.335160	-1.244610	-0.793480
C	-3.921660	0.013050	-0.964750
C	-3.274070	-1.235640	-0.989720
C	-3.959890	-2.508540	-1.067750
C	-2.995640	-3.473690	-1.049570
C	-1.722420	-2.786970	-0.972970
N	-1.918330	-1.429580	-0.942410
C	-0.474130	-3.431320	-0.907710
C	2.992470	0.002560	-0.780090
H	-5.036760	2.679430	-0.981530
H	-3.125780	4.576770	-0.991930
H	-5.037960	-2.646190	-1.137960
H	-3.136370	-4.552510	-1.094270

C	-7.305390	-4.418180	0.206630	H	4.092550	-2.664600	-0.670080
C	-6.314030	-4.226750	-0.758010	H	2.179260	-4.564780	-0.773840
C	-5.184120	-3.469140	-0.441800	H	2.193300	4.559180	-1.092020
F	-5.910310	-2.574030	2.987730	H	4.099750	2.650700	-1.030420
F	-8.108350	-4.039740	2.395250	C	-0.470970	4.938280	-0.975070
F	-8.384270	-5.134760	-0.086440	C	4.492330	0.002990	-0.768050
F	-6.454150	-4.763960	-1.966940	C	-5.414360	0.008570	-0.973190
F	-4.255120	-3.298880	-1.380260	C	-0.484760	-4.923340	-0.856730
C	4.039860	2.544630	1.556090	C	-0.232180	-5.607150	0.339190
C	5.242570	3.188500	1.255880	C	-0.265890	-7.000070	0.420230
C	5.705880	3.197180	-0.063280	C	-0.561080	-7.745760	-0.723540
C	4.964430	2.563310	-1.061620	C	-0.818050	-7.094630	-1.932060
C	3.750070	1.905320	-0.779340	C	-0.773040	-5.699450	-1.986680
C	1.873330	-4.975840	3.241490	C	-6.141700	-0.356460	0.167200
C	2.489190	-6.000790	3.962110	C	-7.537790	-0.367470	0.182750
C	2.440910	-5.983810	5.358140	C	-8.239550	-0.008450	-0.970250
C	1.777640	-4.949810	6.022660	C	-7.543800	0.357800	-2.124440
C	1.167540	-3.935970	5.279880	C	-6.146780	0.362630	-2.113880
F	1.934780	-5.012220	1.910940	C	5.253000	0.456420	0.338950
F	3.119790	-6.988780	3.332630	C	6.657180	0.481740	0.230770
F	3.027250	-6.952450	6.052090	C	7.310210	0.059280	-0.928910
F	1.732560	-4.936710	7.352340	C	6.559500	-0.397260	-2.016370
F	0.541820	-2.960810	5.935900	C	5.165820	-0.419880	-1.929620
H	3.660680	2.546660	2.582440	C	-0.152590	5.644250	-2.142540
H	5.811180	3.683280	2.048820	C	-0.165080	7.040300	-2.187980
H	6.648840	3.691090	-0.316130	C	-0.505070	7.762530	-1.042060
H	5.341340	2.551280	-2.088580	C	-0.828660	7.087410	0.136790
C	3.016230	1.247580	-1.898990	C	-0.806880	5.691270	0.157700
C	2.849770	1.935210	-3.115090	H	-1.821930	-2.355340	4.463680
C	2.522860	-0.067780	-1.798420	H	-0.125330	-2.360310	5.083170
C	1.864860	-0.663440	-2.878930	H	-0.606740	-3.494240	3.770950
C	1.704030	0.022130	-4.085040	F	-8.215910	0.694060	-3.222550
C	2.221520	1.320970	-4.207140	F	-9.568060	-0.015680	-0.968790
H	3.203950	2.964420	-3.219490	F	-8.203620	-0.712490	1.282820
H	2.667110	-0.635870	-0.877520	F	-5.495850	-0.705540	1.282780
H	1.480190	-1.683130	-2.780980	F	-5.509430	0.715250	-3.229370
H	1.189520	-0.438200	-4.932470	F	-1.103080	-7.805590	-3.019720
N	2.019030	2.061520	-5.410060	F	-1.023530	-5.107710	-3.153580
N	2.825090	1.970660	-6.371000	F	-0.599780	-9.072070	-0.661220
C	3.976990	1.198810	-6.374670	F	-0.027750	-7.618880	1.574900
N	4.708680	1.245290	-7.564020	F	0.044990	-4.919670	1.453490
C	4.727150	0.355630	-5.534550	F	-1.120770	5.073800	1.297080
N	5.840800	-0.081260	-6.170220	F	-1.150900	7.777900	1.228380
C	5.797060	0.466370	-7.379170	F	0.172840	4.980980	-3.251680
C	4.342860	1.992890	-8.758900	F	0.139380	7.686210	-3.311390
H	4.505450	0.055130	-4.512630	F	-0.520830	9.090860	-1.073010
H	6.544700	0.320820	-8.161270	H	4.571830	-0.754980	-2.785000
H	4.229470	3.060130	-8.516620	H	7.054700	-0.727560	-2.934410
H	3.389070	1.621400	-9.163880	H	8.402810	0.083950	-0.979940
H	5.141430	1.859770	-9.504300	H	7.242440	0.824630	1.089420

II.4.2 Magnetic Conformers of Biphenyl Thioether RP **5**

***cis*$_{\mathbf{dia}}$**
$E_{TPSSh/SVP}$ = -5909.35804047 Hartree
NImag = 0

C	-0.679150	-3.306580	2.911930
N	-1.487480	-2.363040	2.322040
C	-1.416030	-4.519950	3.166710
C	-2.668710	-4.328100	2.663530
C	-2.712520	-2.971870	2.176950
C	0.702100	-3.184090	3.081460
C	1.422090	-2.146250	2.484380
C	2.854480	-2.145060	2.317240
C	3.150150	-1.099860	1.494170
C	1.906830	-0.416070	1.233450
N	0.857420	-1.070730	1.836610
Ni	-1.002650	-0.576630	1.788140
N	-2.865790	-0.088260	1.745030
C	-3.396160	1.180530	1.751890
C	-4.837030	1.129220	1.704850
C	-5.177520	-0.186260	1.600270
C	-3.947920	-0.935490	1.664730
C	1.827330	0.825330	0.592850
C	0.680640	1.619130	0.702030
C	0.643210	3.028260	0.397200
C	-0.564550	3.489430	0.829310
C	-1.297010	2.343780	1.308210
N	-0.517060	1.210720	1.247410
C	-2.657250	2.360650	1.630940
C	-3.882670	-2.325920	1.773240
H	4.122600	-0.782880	1.121590
H	3.536500	-2.876350	2.747720
H	1.458770	3.588850	-0.055520
H	-0.946580	4.507990	0.792690
H	-6.172900	-0.619610	1.518720
H	-5.495680	1.996050	1.705960
H	-1.007290	-5.414110	3.634830
H	-3.506900	-5.023160	2.654160
C	1.427200	-4.268070	3.802650
C	-5.112220	-3.135300	1.539880
C	3.027400	1.340560	-0.136000
C	-3.391520	3.655340	1.706390
C	-3.843160	4.146000	2.939350
C	-4.578520	5.329190	3.038240
C	-4.875020	6.052650	1.881070
C	-4.438210	5.589610	0.638060
C	-3.706750	4.402530	0.563500
F	-3.577880	3.474010	4.058300
F	-4.996070	5.770670	4.221570
F	-5.574660	7.178770	1.960290
F	-4.729520	6.276750	-0.463740
F	-3.318450	3.978830	-0.638860
C	-6.099100	-3.310830	2.517250
C	-7.248290	-4.066800	2.273160
C	-7.425890	-4.664840	1.023240
C	-6.456500	-4.509770	0.030220

***cis*$_{\mathbf{para}}$**
$E_{TPSSh/SVP}$ = -5909.37624370 Hartree
NImag = 0

H	-2.351860	-4.763160	-0.708790
H	-4.273350	-2.866890	-0.722840
C	-4.675250	-0.196540	-0.787290
C	-3.175620	-0.198440	-0.756440
C	-0.954900	-2.983160	-0.736400
H	4.849830	2.462620	-1.358820
H	2.932020	4.352550	-1.415800
C	0.289080	4.710870	-1.317820
H	-4.279260	2.468890	-0.916190
H	-2.366470	4.353890	-1.179320
C	-3.201300	2.324000	-0.951260
C	-2.521080	1.045740	-0.872040
C	-2.234170	3.277210	-1.080800
C	-0.964590	2.582530	-1.073530
N	-1.161700	1.232880	-0.941600
C	0.282110	3.221250	-1.204440
C	1.532540	2.579900	-1.240090
C	2.801190	3.273960	-1.340960
C	3.771710	2.317050	-1.312190
C	3.091760	1.041280	-1.207450
N	1.735640	1.228500	-1.167330
C	3.741970	-0.205210	-1.147850
C	5.233540	-0.211050	-1.147660
C	3.094460	-1.452540	-1.060880
N	1.741270	-1.637080	-0.951520
C	1.542010	-2.991020	-0.888610
C	2.808350	-3.688410	-0.970520
C	3.774800	-2.730780	-1.078380
H	4.848970	-2.877820	-1.182470
H	2.939950	-4.769560	-0.961180
C	0.293570	-3.627330	-0.774290
C	-2.224240	-3.681440	-0.711390
C	-3.194160	-2.724360	-0.716250
C	-2.515020	-1.443160	-0.729270
N	-1.155790	-1.628010	-0.749890
Ni	0.310250	-0.183440	-0.726690
N	0.531930	-0.024180	1.314840
C	-0.403230	0.452860	2.174630
C	1.558990	-0.447620	2.053630
N	1.326790	-0.259870	3.363710
C	0.055530	0.310790	3.487480
C	2.217380	-0.605160	4.467470
H	-1.336890	0.866760	1.808490
H	2.475710	-0.884960	1.659900
N	-0.331180	0.613880	4.788240
H	3.208510	-0.834580	4.049610
H	1.828180	-1.480770	5.010540
H	2.281610	0.244350	5.161790
N	-1.448290	1.081820	5.122750
C	-2.496550	1.267360	4.173950
C	-2.955920	2.568790	3.920180

C	-5.315470	-3.751510	0.298160	C	-3.105050	0.165460	3.554680
F	-5.954910	-2.747430	3.716030	C	-4.138860	0.367960	2.630110
F	-8.171890	-4.220640	3.218510	C	-4.586890	1.670330	2.352520
F	-8.517110	-5.380760	0.777360	C	-3.990830	2.757200	2.999230
F	-6.628060	-5.079250	-1.159530	H	-2.485660	3.414020	4.428090
F	-4.407730	-3.614060	-0.665910	H	-2.740110	-0.844940	3.758790
C	3.877490	2.303530	0.431900	S	-4.835070	-1.096320	1.887680
C	4.991190	2.785380	-0.263050	H	-5.399680	1.828720	1.639560
C	5.273890	2.291280	-1.541730	H	-4.343460	3.770330	2.783980
C	4.453790	1.316830	-2.114830	C	-5.494360	-0.529850	0.320810
C	3.325420	0.843680	-1.427240	C	-5.313550	0.144640	-1.994800
C	2.117620	-5.281980	3.126050	C	-6.706010	0.143590	-2.118410
C	2.774090	-6.307170	3.810240	C	-7.502420	-0.196080	-1.021330
C	2.747590	-6.329510	5.206570	C	-6.893820	-0.526940	0.192300
C	2.066260	-5.333010	5.908850	H	-4.691690	0.398520	-2.858050
C	1.415460	-4.318910	5.202890	H	-7.165470	0.402510	-3.076980
F	2.153790	-5.288440	1.794000	H	-8.593130	-0.201880	-1.105330
F	3.418590	-7.262660	3.145280	H	-7.499400	-0.787750	1.064440
F	3.370050	-7.300280	5.865050	C	0.309710	-5.118840	-0.679760
F	2.043890	-5.355150	7.239020	C	0.416510	-5.754400	0.562830
F	0.770920	-3.381260	5.895000	C	0.484050	-7.144090	0.678010
H	3.650840	2.676640	1.435290	C	0.436470	-7.930760	-0.475080
H	6.139150	2.653990	-2.104650	C	0.325610	-7.325430	-1.728760
H	4.690240	0.923370	-3.105590	C	0.259270	-5.932800	-1.817470
S	2.252310	-0.430270	-2.075650	F	0.469610	-5.025860	1.678800
C	2.457650	-0.316560	-3.846950	F	0.596570	-7.720940	1.872670
C	2.184680	0.870610	-4.541390	F	0.500660	-9.254510	-0.379990
C	2.783900	-1.487260	-4.551360	F	0.287290	-8.077290	-2.826070
C	2.810070	-1.468790	-5.950970	F	0.155330	-5.382480	-3.026060
C	2.533180	-0.293190	-6.652490	C	0.194590	5.529730	-0.185960
C	2.250150	0.887060	-5.943920	C	0.251220	6.922120	-0.276350
H	1.907290	1.777590	-3.998270	C	0.390970	7.524240	-1.528710
H	3.001890	-2.405840	-4.000500	C	0.479330	6.733820	-2.676830
H	3.048460	-2.384620	-6.500150	C	0.425970	5.343130	-2.559740
H	2.536990	-0.272310	-7.745140	F	0.613720	7.308510	-3.869740
N	1.868940	2.056730	-6.664140	F	0.516610	4.613520	-3.670490
N	2.569580	3.100060	-6.657670	F	0.060340	4.982320	1.022480
C	3.830900	3.203850	-6.093280	F	0.177660	7.676650	0.818170
N	4.360520	4.493440	-6.015550	F	0.443220	8.848380	-1.626890
C	4.879040	2.366360	-5.680680	C	5.949820	-0.538960	0.011330
N	5.973820	3.096940	-5.356840	C	7.344920	-0.550250	0.045510
C	5.625540	4.363280	-5.555010	C	8.060520	-0.221640	-1.108250
C	3.645840	5.724410	-6.324990	C	7.377770	0.110840	-2.280290
H	4.887020	1.278760	-5.640410	C	5.980640	0.111090	-2.288550
H	6.267070	5.226870	-5.371930	F	8.062040	0.420550	-3.378210
H	3.037640	6.047990	-5.463560	F	5.358680	0.427950	-3.422980
H	2.979800	5.537550	-7.179120	F	5.292650	-0.849380	1.136240
H	4.379440	6.505970	-6.572580	F	7.996190	-0.862320	1.164050
H	5.637050	3.539740	0.195570	F	9.388690	-0.225620	-1.090130

III. Experimental Section

III.1 General Information

Commercially available solvents and starting materials were used as received. THF was distilled from benzophenone-Na. Dichloromethane was distilled from CaH_2. Column chromatography was carried out using 0.04 – 0.063 mm mesh silica gel (Merck). R_f values were determined by thin layer chromatography on Polygram® Sil G/UV_{254} (Macherey-Nagel, 0.2 mm particle size).

NMR spectra were measured in Schott Economic NMR tubes using deuterated solvents (Deutero). The degree of deuteration is given in parentheses. Chemical shifts are calibrated to residual protonated solvent signals (^{1}H: δ ($CHCl_3$) = 7.26 ppm, δ (CD_2Cl_2) = 5.32 ppm, δ (CD_3CN) = 1.94 ppm, δ (acetone-d_6) = 2.05 ppm, δ (DMSO-d_6) = 2.50 ppm; ^{13}C: δ ($CHCl_3$) = 77.16 ppm, δ (CD_2Cl_2) = 53.84 ppm, δ (CD_3CN) = 1.32 ppm, δ (acetone-d_6) = 29.84 ppm, δ (DMSO-d_6) = 39.52 ppm; deuteration grade 99.8 %). Reference for ^{19}F NMR spectra is CCl_3F to which the spectrometer frequency is calibrated. The signal multiplicities are abbreviated as s (singlet), d (doublet), t (triplet), q (quartet), quint (quintet), sept (septet), m (multiplet) and br (broad signal). Measurements were performed with a Bruker DRX 500 (^{1}H NMR: 500 MHz, ^{13}C NMR: 125 MHz, ^{19}F NMR: 470 MHz) and a Bruker AV 600 (^{1}H NMR: 600 MHz, ^{13}C NMR: 150 MHz).

The high resolution (HR) mass spectra were measured with an APEX 3 FT-ICR with a 7.05 T magnet by co. Bruker Daltonics (ESI) or with an AccuTOF by co. Jeol (EI). Low resolution mass spectra were measured with a MAT 8230 by co. Finnigan (EI/CI), an AccuTOF by co. Jeol (EI), an LCQ Classic by co. Thermo Finnigan (ESI) or an AutoflexSpeed by co. Bruker (MALDI-TOF).

Infrared spectra were recorded on a Perkin-Elmer ATR spectrometer with a Golden-Gate-Diamond-ATR A531-G for neat samples. Signal intensities were abbreviated with w (weak), m (medium), s (strong) and vs (very strong). Broad signals are additionally labeled with br.

UV-visible absorption spectra were recorded on a Perkin-Elmer Lambda-14 spectrophotometer with a Büchi thermostat using quartz cells of 1 cm path length.

The amount of carbon, hydrogen, sulfur and nitrogen in a compound was determined with a CHNS-Elementaranalysator Euro EA 3000 Series by co. Euro Vector.

Irradiation experiments were performed with LED light sources.

Melting points were measured with a Melting Point B-540 by co. Büchi.

III.2 Synthetic procedures

3-Bromobenzenediazonium tetrafluoroborate (8).[5] A suspension of 3-bromoaniline (**6**) (8.25 g, 48.0 mmol) in tetrafluoroboric acid (50 wt-%, 30 mL) was diluted with water until a clear solution was obtained. The solution was cooled to 0 °C and a solution of sodium nitrite (3.71 g, 53.8 mmol) in water (7.5 mL) was added dropwise under vigorous stirring. The precipitate was filtered off and was consecutively washed with water (50 mL), ethanol (50 mL) and diethyl ether (150 mL) before being dried in vacuo. The desired product (11.9 g, 43.8 mmol, 91 %) was obtained as a white solid.

Mp: 139 °C (decomp.).

IR (ATR): ν = 3098 (m), 2304 (m), 1575 (w), 1562 (w), 1463 (m), 1422 (w), 1281 (w), 1173 (w), 1024 (ss, br), 887 (m), 788 (s), 664 (m), 651 (s), 556 (m), 521 (s), 504 (w) cm^{-1}.

^{1}H NMR (500 MHz, CD_3CN, 300 K): δ = 8.63 (t, ^4J = 2.00 Hz, 1H, 2-H), 8.49 (ddd, ^3J = 8.38 Hz, ^4J = 2.05 Hz, ^4J = 0.93 Hz, 1H, 4-H), 8.40 (ddd, ^3J = 8.29 Hz, ^4J = 1.91 Hz, ^4J = 0.94 Hz, 1H, 6-H), 7.84 (t, ^3J = 8.35, 1H, 5-H) ppm.

^{13}C NMR (125 MHz, CD_3CN, 300 K): δ = 146.3 (C-6), 134.9 (C-2), 134.1 (C-5), 132.6 (C-4), 124.5 (C-3), 117.1 (C-1) ppm.

MS (EI, 70 eV): m/z (%) = 175.9/173.9 (99/100) $[C_6H_4BrF]^{\bullet+}$.

HR-MS (EI): m/z $[M]^{\bullet+}$ calcd for $C_6H_4{}^{79}BrF$, 173.9480; found 173.9481; calcd for $C_6H_4{}^{81}BrF$, 175.9460; found 175.9460.

Diazonium tetrafluoroborates undergoe a BALTZ SCHIEMANN reaction during the vaporization process in EI-MS. Therefore, only the fluorinated derivative is found.

5-(3'-Bromophenylazo)-1-(*N,N*-dimethylsulfamoyl)imidazole (9). 1-(*N*,*N*-Dimethylsulfamoyl)imidazole[6] (**7**) (1.50 g, 8.57 mmol) was dissolved in dry THF (45 mL) and cooled to -78 °C. *n*-Butyllithium (3.45 mL, 8.63 mmol) in *n*-hexane was added dropwise over a period of 15 minutes. After 30 minutes of stirring at -78 °C, dimethylthexylchlorosilane (1.86 mL, 12.5 mmol) was added. The reaction mixture was stirred at -78 °C for 60 minutes and at room temperature for 16 hours. It was again cooled to -78 °C and *n*-butyllithium (3.75 mL, 9.38 mmol) in *n*-hexane was added dropwise over a period of 10 minutes. After 30 minutes of stirring at -78 °C, 3-bromobenzenediazonium tetrafluoroborate (**8**) (2.31 g, 8.52 mmol) was added as a solid in one portion, and the reaction mixture immediately turned from light yellow to deep red. It was stirred at -78 °C for 60 minutes and at room temperature for 7 hours. Then, half saturated aqueous sodium bicarbonate solution (60 mL) was added, layers were separated and the aqueous layer was extracted once with THF (40 mL). The combined organic layers were treated with tetra-*n*-butylammoniumfluoride trihydrate (2.93 g, 9.27 mmol) and the mixture was stirred at room temperature for 16 hours. Then, half saturated aqueous sodium bicarbonate solution (60 mL) was added,

layers were separated and the aqueous layer was extracted three times with chloroform (each 40 mL). The combined organic layers were dried over magnesium sulfate and evaporated. The resulting crude product was purified via column chromatography on silica gel (methylene chloride, 10 vol-% ethyl acetate, $R_f = 0.58$). The desired product was obtained as orange solid (1.83 g, 5.11 mmol, 60 %).

Mp: 105 – 106 °C.

IR (ATR): ν = 3130 (w), 1470 (m), 1450 (m), 1383 (s), 1342 (m), 1274 (m), 1252 (m), 1171 (s), 1117 (m), 1089 (s), 1055 (m), 976 (s), 896 (m), 870 (m), 844 (m), 813 (m), 796 (s), 726 (s), 679 (m), 664 (m), 637 (m), 593 (s), 564 (s), 546 (s), 505 (s) cm^{-1}.

^{1}H-NMR (500 MHz, $CDCl_3$, 300 K): δ = 8.15 (d, ^4J = 0.60 Hz, 1H, 2-*H*), 7.96 (t, ^4J = 1.85 Hz, 1H, 2′-*H*), 7.78 (ddd, ^3J = 8.00 Hz, ^4J = 1.70 Hz, ^4J = 1.00 Hz, 1H, 6′-*H*), 7.60 (ddd, ^3J = 7.94 Hz, ^4J = 1.86 Hz, ^4J = 0.96 Hz, 1H, 4′-*H*), 7.53 (d, ^4J = 0.65 Hz, 1H, 4-*H*), 7.34 (t, ^3J = 7.95 Hz, 1H, 5′-*H*), 2.99 (s, 6H, -N(CH_3)$_2$) ppm.

^{13}C-NMR (125 MHz, $CDCl_3$, 300 K): δ = 153.9 (*C*-3′), 145.0 (*C*-5), 141.6 (*C*-2), 134.4 (*C*-4′), 130.8 (*C*-5′), 125.5 (*C*-2′), 123.4 (*C*-1′), 122.4 (*C*-6′), 119.7 (*C*-4), 38.5 (-N(*C*H$_3$)$_2$) ppm.

MS (EI, 70 eV): m/z (%) = 359.0/357.0 (12/12) $[M]^{\bullet+}$, 252.0/250.0 (31/34) $[M\text{-}SO_2N(CH_3)_2+H]^{\bullet+}$, 157.0/155.0 (58/61) $[PhBr]^{\bullet+}$, 108.0 (100) $[SO_2N(CH_3)_2]^{\bullet+}$.

HR-MS (EI): m/z $[M]^{\bullet+}$ calcd for $C_{11}H_{12}N_5O_2S^{79}Br$, 356.9895; found 356.9887; calcd for $C_6H_4{}^{81}BrF$, 358.9875; found 358.9867.

UV/Vis (toluene): λ_{max} (lg ε) = 360 (4.177) nm.

Anal. Calcd. For $C_{11}H_{12}N_5O_2SBr$ (356.99): cal. C 36.88, H 3.38, N 19.55, S 8.95, found C 37.15, H 3.34, N 19.43, S 8.91 %.

4(5)-(3'-Bromophenylazo)imidazole (10). The sulfamoyl-protected azoimidazole **9** (697 mg, 1.95 mmol) was dissolved in ethanol (30 mL) and ethanolic hydrochloric acid (4 M, 30 mL) was added. The reaction mixture was stirred at 55 °C for 1 hour. It was then cooled to 0 °C and potassium hydroxide solution (40 %, 10 mL) was added dropwise. The solution was treated with saturated aqueous sodium bicarbonate solution (80 mL) and stirring at 0 °C was continued for 15 minutes. Chloroform (100 mL) was added and the layers were separated. The aqueous layer was extracted twice with chloroform (50 mL) and the combined organic layers were dried over magnesium sulfate before being evaporated to dryness. The obtained crude product may be purified via column chromatography on silica gel (ethyl acetate, $R_f = 0.20$) to give the desired deprotected azoimidazole **10** (390 mg, 1.55 mmol, 80 %) as yellow powder. However, using the crude product in the following step has found to give comparable yields so that purification on this stage is not essential.

Mp: 135 – 140 °C (decomp.).

IR (ATR): ν (cm^{-1}) = 1568 (w), 1514 (m), 1450 (w), 1427 (s), 1322 (w), 1308 (w), 1296 (w), 1234 (m), 1151 (m), 1094 (m), 1059 (w), 1003 (m), 913 (m), 838 (s), 801 (s), 772 (s), 700 (m), 671 (s), 624 (s), 588 (m), 565 (m), 534 (m), 517 (w) cm^{-1}.

^{1}H-NMR (600 MHz, DMSO-d6, 298 K): δ = 12.66 (s, br, 1H, N*H*), 7.98 (s, 1H, 4-*H*), 7.88 (s, 1H, 2-*H*), 7.87-7.85 (m, 1H, 2′-*H*), 7.82-7.77 (m, 1H, 6′-H), 7.67-7.63 (m, 1H, 4′-H), 7.51 (t, ^3J = 7.92 Hz, 1H, 5′-H) ppm.

^{13}C-NMR (150 MHz, DMSO-d6, 298 K): δ = 153.8 (*C*-1′, *C*-4(5)), 137.3 (*C*-2), 132.5 (*C*-4′), 131.5 (*C*-5′), 122.9 (*C*-2′), 122.5 (*C*-6′, *C*-3′), 118.9 (*C*-5(4)) ppm.

MS (EI, 70 eV): m/z (%) = 252.0/250.0 (46/46) $[M]^{\bullet+}$, 171.1 (18) $[M\text{-}Br]^{\bullet+}$, 157.0/155.0 (39/40) $[PhBr]^{\bullet+}$, 95.0 (100) $[C_3H_3N_4]^{\bullet+}$.

HR-MS (EI): m/z $[M]^{\bullet+}$ calcd for $C_9H_7N_4{}^{79}Br$, 249.9854; found 249.9846; calcd for $C_9H_7N_4{}^{81}Br$, 251.9834; found 251.9834.

UV/Vis (toluene): λ_{max} (lg ε) = 351 (4.337) nm.

4-(3'-Bromophenylazo)-1-(triphenylmethyl)imidazole (11). A suspension of 4(5)-(3'-bromophenylazo)imidazole (**10**) (346 mg, 1.38 mmol) and triphenylchloromethane (404 mg, 1.45 mmol) in methylene chloride (15 mL) was treated with 12rimethylamine (248 µL, 1.79 mmol). Stirring at room temperature for 16 hours gave a deep red solution which was diluted with ethyl acetate (50 mL) and washed three times with half saturated sodium bicarbonate solution (each 30 mL). The organic layer was dried over magnesium sulfate and evaporated to dryness. Purification of the crude product via column chromatography on silica gel (cyclohexane/ethyl acetate, 3:1, R_f = 0.17) gave an orange solid (666 mg, 1.35 mmol, 98 %).

Mp: 68 – 70 °C.

IR (ATR): ν (cm^{-1}) = 1568 (w), 1489 (m), 1444 (m), 1287 (m), 1118 (m), 1087 (m), 991 (m), 904 (m), 865 (m), 745 (s), 698 (s), 676 (s), 658 (s), 638 (m), 616 (m), 560 (m), 506 (m) cm^{-1}.

^{1}H-NMR (600 MHz, $CDCl_3$, 298 K): δ = 8.00 (t, ^4J = 1.83 Hz, 1H, 2′-*H*), 7.87 (ddd, ^3J = 7.95 Hz, ^4J = 1.56 Hz, ^4J = 0.95 Hz, 1H, 6′-*H*), 7.62 (d, ^4J = 1.33 Hz, 1H, 5-*H*), 7.54 (d, ^4J = 1.35 Hz, 1H, 2-*H*), 7.52 (ddd, ^3J = 7.92 Hz, ^4J = 1.71 Hz, ^4J = 0.84 Hz, 1H, 4′-*H*), 7.40-7.36 (m, 9H, Tr-*m*-*H*, Tr-*p*-*H*), 7.34 (t, ^3J = 7.98 Hz, 1H, 5′-*H*), 7.22-7.18 (m, 6H, Tr-*o*-*H*) ppm.

^{13}C-NMR (150 MHz, $CDCl_3$, 298 K): δ = 154.1 (*C*-1′), 152.9 (*C*-4), 141.7 (*C*-*i*-Tr), 139.6 (*C*-2), 132.9 (*C*-4′), 130.3 (*C*-5′), 129.8 (*C*-*o*-Tr), 128.5 (*C*-*p*-Tr), 128.4 (*C*-*m*-Tr), 123.8 (*C*-2′), 123.5 (*C*-5), 123.4 (*C*-6′), 123.0 (*C*-3′), 76.4 (-*C*Ph_3) ppm.

MS (EI, 70 eV): m/z (%) = 250.0 (1) $[M- C(Ph)_3+H]^{\bullet+}$, 243.1 (100) $[C(Ph)_3]^{\bullet+}$.

MS (CI, isobutane): m/z (%) = 495.0/493.0 (7/6) $[M+H]^+$, 243.1 (100) $[C(Ph)_3]^+$, 167.1 (34) $[C(Ph)_2+H]^+$.

4-(3′-(2″-Formylphenyl)phenylazo)-1-(triphenylmethyl)imidazole (12). 4-(3′-Bromophenylazo)-1-(triphenylmethyl)imidazole (**11**) (230 mg, 466 µmol) was dissolved in toluene (15 mL) and purged with nitrogen for 20 min. 2-Formylphenylboronic acid (77.0 mg, 514 µmol) and [1,1′-Bis(diphenylphosphino)ferrocene]dichloropalladium(II) (17.0 mg, 23.3 µmol) were added and purging with nitrogen was continued for another 15 min. Potassium carbonate (212 mg, 1.54 mmol, in 4 mL H_2O) was added and the reaction mixture was stirred at 95 °C overnight under an atmosphere of nitrogen. After cooling down to room temperature ethyl acetate (50 mL) was added, followed by filtration over celite. The organic layer was washed three times with water (each 50 mL), dried over magnesium sulfate and evaporated to dryness. Purification via column chromatography on silica gel (chloroform, R_f = 0.36) gave a yellow solid (236 mg, 455 µmol, 98 %).

Mp: 86 – 88 °C.

IR (ATR): ν (cm^{-1}) = 3080 (w), 2843 (w), 1695 (m), 1595 (m), 1490 (m), 1441 (m), 1389 (w), 1297 (m), 1197 (m), 1121 (m), 1036 (w), 1001 (w), 911 (w), 805 (w), 762 (s), 749 (s), 699 (s), 661 (s), 640 (m), 617 (m), 562 (w), 519 (w), 510 (m) cm^{-1}.

^{1}H-NMR (500 MHz, $CDCl_3$, 300 K): δ = 10.02 (d, ^4J = 0.75 Hz, 1H, -C*H*O), 8.03 (dd, ^3J = 7.78 Hz, ^4J = 1.03 Hz, 1H, 3″-*H*), 8.00 (ddd, ^3J = 8.00 Hz, ^4J = 1.90 Hz, ^4J = 1.10 Hz, 1H, 6′-*H*), 7.92 (t, ^4J = 1.75 Hz, 1H, 2′-*H*), 7.63 (td, ^3J = 7.53 Hz, ^4J = 1.45 Hz, 1H, 5″-*H*), 7.61 (d, ^4J = 1.45 Hz, 1H, 5-*H*), 7.57 (t, ^3J = 7.78 Hz, 1H, 5′-*H*), 7.54 (d, ^4J = 1.45 Hz, 1H, 2-*H*), 7.52-7.46 (m, 2H, 4″-*H*, 6″-*H*), 7.41 (ddd, ^3J = 7.53 Hz, ^4J = 1.73 Hz, ^4J = 1.13 Hz, 1H, 4′-H), 7.40-7.35 (m, 9H, Tr-*m*-*H*, Tr-*p*-*H*), 7.23-7.17 (m, 6H, Tr-*o*-*H*) ppm.

^{13}C-NMR (125 MHz, $CDCl_3$, 300 K): δ = 192.2 (-*C*HO), 153.1 (*C*-1′), 153.0 (*C*-4), 145.3 (*C*-1″), 141.7 (*C*-*i*-Tr), 139.5 (*C*-2), 138.6 (*C*-3′), 133.7 (*C*-2″), 133.6 (*C*-5″), 131.8 (*C*-4′), 130.8 (*C*-6″), 129.8 (*C*-*o*-Tr), 129.1 (*C*-5′), 128.4 (*C*-*p*-Tr), 128.3 (*C*-*m*-Tr), 128.0 (*C*-4″), 127.6 (*C*-3″), 123.2 (*C*-6′, *C*-5, *C*-2′), 76.3 (-*C*Ph_3) ppm.

MS (EI, 70 eV): m/z (%) = 518.1 (<1) $[M+H]^{\bullet+}$, 276.1 (4) $[M-C(Ph)_3+H]^{\bullet+}$, 243.1 (100) $[C(Ph)_3]^{\bullet+}$.

MS (CI, isobutane): m/z (%) = 519.1 (2) $[M+H]^+$, 243.1 (100) $[C(Ph)_3]^+$.

Anal. Calcd. For [$C_{35}H_{26}N_4O$ + 0.45 $CHCl_3$] (572.32): cal. C 74.39, H 4.66, N 9.79, found C 74.34, H 4.41, N 9.86 %.

5-(3′-(2″-Formylphenyl)phenylazo)-1-methylimidazole (13). The tritylated biphenylazoimidazole **12** (530 mg, 1.02 mmol) was dissolved in dry methylene chloride (12 mL) and methyl trifluoromethanesulfonate (170 µL, 1.50 mmol) was added under an atmosphere of nitrogen. It was stirred at room temperature overnight, followed by the addition of acetone/H_2O (2:1, 36 mL) and further stirring for 4 h at 40 °C. Saturated sodium bicarbonate solution (5 mL) was added, layers were separated and the aqueous layer was extracted twice with dichloromethane (each 20 mL). The combined organic layers were dried over magnesium sulfate and were evaporated to dryness. Purification via column chromatography on silica gel (ethyl acetate, $R_f = 0.27$) gave an orange solid (271 mg, 933 µmol, 91 %).

Mp: 119 °C.

IR (ATR): ν (cm^{-1}) = 3113 (w), 3062 (w), 2924 (m), 2852 (m), 2751 (w), 16889 (vs), 1596 (m), 1518 (m), 1505 (m), 1467 (m), 1402 (m), 1340 (s), 1282 (m), 1223 (s), 1196 (m), 1115 (vs), 907 (m), 820 (m), 764 (s), 728 (s), 699 (s), 648 (s), 518 (m) cm^{-1}.

^{1}H-NMR (600 MHz, $CDCl_3$, 298 K): δ = 10.03 (s, 1H, -C*H*O), 8.05 (dd, ^3J = 7.83 Hz, ^4J = 1.05 Hz 1H, 3″-*H*), 7.90 (ddd, ^3J = 7.98 Hz, ^4J = 1.65 Hz, ^4J = 1.08 Hz 1H, 6′-*H*), 7.83 (t, ^4J = 1.71 Hz, 1H, 2′-*H*), 7.67 (dt, ^3J = 7.50 Hz, ^4J = 1.38 Hz, 1H, 5″-*H*), 7.62 (s, 2H, 2-*H*, 4-*H*), 7.59 (t, ^3J = 7.77 Hz, 1H, 5′-*H*), 7.54 (t, ^3J = 7.59 Hz, 1H, 4″-*H*), 7.50 (d, ^3J = 7.62 Hz, 1H, 6″-*H*), 7.44 (td, ^3J = 7.50 Hz, ^4J = 1.26 Hz, 1H, 4′-*H*), 3.96 (s, 3H, -CH_3) ppm.

^{13}C-NMR (150 MHz, $CDCl_3$, 300 K): δ = 192.1 (-*C*HO), 152.9 (*C*-1′), 145.2 (*C*-5), 145.0 (*C*-1″), 140.9 (*C*-2), 138.8 (*C*-3′), 133.8-133.6 (*C*-5″, *C*-2″), 131.9 (*C*-4′), 130.7 (*C*-6″), 129.2 (*C*-5′), 128.2 (*C*-4″), 127.8 (*C*-3″), 124.2 (*C*-4), 123.4 (*C*-2′), 122.4 (*C*-6′), 32.6 (-*C*H_3) ppm.

MS (EI, 70 eV): m/z (%) = 290.1 (100) $[M]^{\bullet+}$, 195.1 (40) $[C_{13}H_9ON]^{\bullet+}$, 152 (70) $[C_{12}H_8]^{\bullet+}$, 109 (73) $[C_4H_5N_4]^{\bullet+}$.

HR-MS (EI): m/z $[M]^{\bullet+}$ calcd for $C_{17}H_{14}N_4O$, 290.1168; found 290.1167.

UV/Vis (acetonitrile): λ_{max} (lg ε) = 210 (4.431), 228 (4.396), 362 (4.373) nm.

5-(Biphenylazo-*N*-methylimidazole)-10,15,20-tris(pentafluorophenyl)porphyrin (mf-4). To a solution of biphenyl tonearm **13** (453 mg, 1.56 mmol) and pentafluorobenzaldehyde (306 mg, 1.56 mmol) in chloroform (200 mL) was added borontrifluoride diethyletherate (406 µL, 3.20 mmol) under an atmosphere of nitrogen. Pentafluorophenyl dipyrromethane (974 mg, 3.12 mmol) in chloroform (20 mL) was added to the stirred solution over 1 h at room temperature. Stirring under nitrogen at room temperature was continued for additional 6 h and the solution turned from dark red to black. Afterwards, chloranil (808 mg, 3.28 mmol) was added and the solution was stirred at reflux for 16 h. After cooling down to room temperature 14rimethylamine (880 µL) was added and stirring was continued for 30 min. The solution was filtrated over celite and evaporated to dryness. Filtration of the

crude product over silica gel (chloroform) and subsequent column chromatography on silica gel (cyclohexane/ethyl acetate, 6:4, R_f = 0.19) gave a purple solid (77.0 mg, 72.0 µmol, 5 %).

Mp: 251 °C.

IR (ATR): ν (cm^{-1}) = 2922 (w), 1725 (w), 1650 (w), 1515 (s), 1494 (vs), 1438 (m), 1342 (m), 1224 (m), 1112 (m), 1077 (m), 1044 (m), 987 (vs), 973 (s), 917 (vs), 903 (m), 804 (s), 765 (s), 750 (s), 724 (s), 699 (m), 650(m), 549 (m) cm^{-1}.

^{1}H-NMR (500 MHz, acetone-d6, 300 K): δ = 9.25 (s, br, 4H, 12-*H*, 13-*H*, 17-*H*, 18-*H*), 9.16 (s, br, 2H, 3-*H*, 7-*H*), 9.08 (d, ^3J = 4.30 Hz, 2H, 2-*H*, 8-*H*), 8.31 (dd, ^3J = 7.53 Hz, ^4J = 0.98 Hz, 1H, 6′-*H*), 8.04 (td, ^3J = 7.70 Hz, ^4J = 1.32 Hz, 1H, 4′-*H*), 7.99 (dd, ^3J = 7.93 Hz, ^4J = 1.13 Hz, 1H, 3′-*H*), 7.88 (td, ^3J = 7.51 Hz, ^4J = 1.45 Hz, 1H, 5′-*H*), 7.54 (t, ^4J = 1.73 Hz, 1H, 2″-*H*), 7.50 (s, 1H, 2‴-*H*), 7.22 (ddd, ^3J = 7.81 Hz, ^4J = 1.66 Hz, ^4J = 1.14 Hz, 1H, 6″-*H*), 6.93 (ddd, ^3J = 7.93 Hz, ^4J = 1.93 Hz, ^4J = 1.10 Hz, 1H, 4″-*H*), 6.89 (d, ^4J = 0.75 Hz, 1H, 4‴-*H*), 6.67 (t, ^3J = 7.88 Hz, 1H, 5″-*H*), 3.30 (s, 3H, -CH_3) , -2.91 (s, 2H, pyrrole-N*H*) ppm.

^{19}F-NMR (470 MHz, acetone-d6, 300 K) δ = -139.74 (dd, ^3J = 23.6 Hz, ^4J = 6.52 Hz, 2F, A-*o*-F), -139.84 (dd, ^3J = 23.9 Hz, ^4J = 7.72 Hz, 1F, B-*o*-F), -140.01 (dd, ^3J = 24.4 Hz, ^4J = 7.69 Hz, 1F, B-*o'*-F), -140.12 (dd, ^3J = 23.4 Hz, ^4J = 7.29 Hz, 2F, A-*o'*-F), -155.69 (t, ^3J = 20.2 Hz, 2F, A-*p*-F), -155.76 (t, ^3J = 20.0 Hz, 1F, B-*p*-F),-164.53 (td, ^3J = 22.1 Hz, ^4J = 7.72 Hz, 2F, B-*m*-F, B-*m'*-F), -164.60 to -164.85 (m, 4F, A-*m*-F, A-*m'*-F) ppm.

MS (EI, 70 eV): m/z (%) = 1068.1 (100) $[M]^{\bullet+}$, 958.6 (4) $[M\text{-}C_4H_5N_4]^{\bullet+}$, 534.0 (15) $[M]^{2+}$.

MS (CI, isobutane): m/z (%) = 1069.4 (72) $[M+H]^+$.

5-(Biphenylazo-*N*-methylimidazole)-10,15,20-tris(pentafluorophenyl)nickel(II)porphyrin (4). The metal free biphenyl record player (77.0 mg, 72.0 µmol) was dissolved in toluene (80 mL) and nickel(II)acetylacetonate (185 mg, 720 µmol) was added. The resulting mixture was stirred at reflux for 3 d after which time no starting material was detectable via MALDI-TOF-MS. The reaction mixture was evaporated to dryness and the crude product was purified via column chromatography on silica gel (chloroform, R_f = 0.76 (*cis*), 0.22 (*trans*)). The product was obtained as purple solid (56.0 mg, 49.8 µmol, 69 %) which is deep red in solution.

Mp: 255 °C.

IR (ATR): ν (cm^{-1}) = 2951 (m), 2923 (m), 2853 (m), 1650 (w), 1518 (s), 1489 (s), 1342 (m), 1261 (m), 1226 (w), 1163 (w), 1071 (m), 1053 (m), 986 (vs), 956 (m), 938 (s), 799 (m), 762 (s), 743 (m), 705 (m) cm^{-1}.

^{1}H-NMR (600 MHz, acetone-d6, 300 K): δ = 10.57-8.52 (s, br, 8H, pyrrole-*H*), 8.27 (d, ^3J = 7.32, 1H, 6′-*H*), 7.99 (t, ^3J = 7.71 Hz, 1H, 4′-*H*), 7.91 (d, ^3J = 7.50 Hz, 1H, 3′-*H*), 7.87 (t, ^3J = 7.26 Hz, 1H, 5′-*H*),

7.34 (s, br, 1H, 2″-*H*), 7.07 (d, ^3J = 7.50 Hz, 1H, 6″-*H*), 6.96 (d, ^3J = 7.68 Hz, 1H, 4″-*H*), 6.71 (t, ^3J = 7.71 Hz, 1H, 5″-*H*), 3.08 (s, br, 3H, -CH_3) ppm.

The ^{1}H NMR signals experience strong line broadening which is due to intermolecular coordination. The imidazole protons (2‴-*H*, 4‴-*H*) are too broad and cannot be assigned. Trifluoroacetic acid (TFA, 10µL) was added to protonate the imidazole and consequently inhibit intermolecular coordination.

^{1}H-NMR (500 MHz, acetone-d6, TFA, 300 K): δ = 9.17-9.13 (m, 4H, pyrrole-*H*), 9.09 (s, br, 1H, 2‴-*H*), 9.06 (d, ^3J = 4.95 Hz, 2H, pyrrole-*H*), 8.99 (d, ^3J = 5.00 Hz, 2H, pyrrole-*H*), 8.35 (m, 1H, 6′-*H*), 8.01 (m, 1H, 4′-*H*), 7.93-7.88 (m, 2H, 3′-*H*, 5′-*H*), 7.50 (d, 4J = 1.35 Hz, 1H, 4‴-*H*), 7.36 (t, ^4J = 1.75 Hz, 1H, 2″-*H*), 7.34 (m, 1H, 6″-*H*), 7.14 (ddd, ^3J = 7.94 Hz, ^4J = 1.91 Hz, ^4J = 1.09 Hz, 1H, 4″-*H*), 6.90 (t, ^3J = 7.90 Hz, 1H, 5″-*H*), 3.54 (s, 3H, -CH_3) ppm.

^{19}F-NMR (470 MHz, acetone-d6, 300 K) δ = -139.10 to -139.70 (m, 3F, A-*o*-F, B-*o*-F), -139.80 to -140.25 (m, 3F, B-*o'*-F, A-*o'*-F), -155.60 to -155.85 (m, 3F, A-*p*-F, B-*p*-F), -164.10 to -164.80 (m, 6F, B-*m*-F, B-*m'*-F, A-*m*-F, A-*m'*-F) ppm.

MS (EI, 70 eV): m/z (%) = 1124.0 (100) $[M]^{\bullet+}$, 1015.3 (20) $[M\text{-}C_4H_5N_4]^{\bullet+}$, 562.0 (7) $[M]^{2+}$.

MS (CI, isobutane): m/z (%) = 1125.1 (51) $[M+H]^+$.

HR-MS (ESI, EtOH, 0.1 % HCOOH)**:** m/z $[M+H]^+$ calcd for $[C_{54}H_{21}F_{15}N_8Ni+H]^+$, 1125.108; found 1125.107.

UV/Vis (acetonitrile): λ_{max} (lg ε) = 406 (5.264), 524 (4.156), 557 (3.966) nm.

4-(3′-(Triisopropylsilylthio)phenylazo)-1-(triphenylmethyl)imidazole (14). Under an atmosphere of nitrogen the tritylated azoimidazole **11** (200 mg, 0.405 mmol) was dissolved in dry toluene (11 mL) and Cesium carbonate (172 mg, 0.527 mmol), [1,1′-Bis(diphenylphosphino)ferrocene]dichloro-palladium(II) (15.0 mg, 20.3 µmol) and triisopropylsilylthiole (113 µL, 0.537 mmol) were then added subsequently. The resulting mixture was stirred at 100 °C for 4 h, [1,1′-Bis(diphenylphosphino)-ferrocene]dichloropalladium(II) (15.0 mg, 20.3 µmol) was added again and stirring at 100 °C was continued for another 5 h. After cooling down to room temperature and further stirring at room temperature overnight ethyl acetate (40 mL) was added. The reaction mixture was filtrated over celite and evaporated to dryness. Purification of the crude product via column chromatography on silica gel (cyclohexane/ethyl acetate, 4:1, R_f = 0.25) gave a yellow solid (224 mg, 0.373 mmol, 92 %).

Mp: 253 °C.

IR (ATR): ν (cm^{-1}) = 2943 (m), 2865 (m), 1738 (w), 1582 (w), 1522 (m), 1493 (m), 1438 (s), 1349 (m), 1280 (m), 1227 (m), 1186 (m), 1152 (m), 1117 (m), 1086 (m), 991 (m), 881 (m), 856 (m), 792 (s), 748 (s), 699 (s), 683 (s), 657 (s), 639 (s), 577 (m), 547 (m), 512 (s), 490 (m), 456 (m) cm^{-1}.

^{1}H-NMR (600 MHz, CD_2Cl_2, 298 K): δ = 7.95 (t, ^4J = 1.74 Hz, 1H, 2′-*H*), 7.65 (ddd, ^3J = 7.98 Hz, ^4J = 1.77 Hz, ^4J = 0.99 Hz, 1H, 6′-*H*), 7.55 (d, ^4J = 1.38 Hz, 1H, 5-*H*), 7.55-7.52 (m, 2H, 4′-*H,* 2-*H*), 7.42-7.38 (m, 9H, *m*-Tr-*H*, *p*-Tr-*H*), 7.32 (t, ^3J = 7.80 Hz, 1H, 5′-*H*), 7.25-7.21 (m, 6H, *o*-Tr-*H*), 1.28 (sept., ^3J = 7.45 Hz, 3H, 3x –C*H*(CH_3)$_2$), 1.08 (d, ^3J = 7.50 Hz, 18H, 3x –CH(C*H*$_3$)$_2$) ppm.

^{13}C-NMR (150 MHz, CD_2Cl_2, 298 K): δ = 153.9 (*C*-4), 153.6 (*C*-1′), 142.3 (*C*-*i*-Tr), 139.6 (*C*-2), 137.4 (*C*-4′), 133.3 (*C*-3′), 130.2 (*C*-*o*-Tr), 130.1 (*C*-2′), 129.4 (*C*-5′), 128.7 (*C*-*p*-Tr, *C*-*m*-Tr), 121.9 (*C*-5), 120.7 (*C*-6′), 76.6 (-*C*Ph$_3$), 18.6 (-*C*H(CH_3)$_2$), 13.5 (-CH(*C*H$_3$)$_2$) ppm.

MS (ESI, methanol): m/z (%) = 642.0 (4) $[M+K]^+$, 625.0 (31) $[M+Na]^+$, 602.7 (12) $[M+H]^+$, 243.1 (100) $[CPh_3]^+$.

Anal. Calcd. For [$C_{37}H_{42}N_4Ssi$ + 0.25 EtOAc] (624.93): cal. C 73.03, H 7.10, N 8.97, S 5.13, found C 72.99, H 7.14, N 9.19, S 4.92 %.

4-(3′-(2″-Formylthiophenyl)phenylazo)-1-(triphenylmethyl)imidazole (15). Under an atmosphere of nitrogen the thiol-functionalized azoimidazole **14** (576 mg, 955 µmol) was dissolved in DMF (25 mL). Potassium carbonate (145 mg, 1.05 mmol) and cesium fluoride (160 mg, 1.05 mmol) were added and the resulting mixture was stirred for 10 min at room temperature. 2-Fluorobenzaldehyde (111 µL, 1.05 mmol) was added and the mixture was heated to 100 °C for 5 h. After cooling down to room temperature half saturated ammonium chloride solution (aq., 40 mL) and diethyl ether (40 mL) were added and layers were separated. The aqueous layer was extracted once with diethylether (30 mL) and the combined organic layers were washed two times with water (each 50 mL), dried over magnesium sulfate and evaporated to dryness. Purification of the crude product via column chromatography on silica gel (cyclohexane/ethyl acetate, 7:3, R_f = 0.32) gave a yellow solid (457 mg, 0.830 mmol, 87 %).

Mp: 216 °C.

IR (ATR): ν (cm^{-1}) = 3122 (w), 3058 (w), 2864 (w), 2161 (w), 1736 (w), 1695 (s), 1588 (m), 1561 (w), 1524 (w), 1489 (m), 1464 (w), 1437 (s), 1410 (w), 1391 (w), 1327 (w), 1275 (s), 1241 (w), 1200 (m), 1188 (m), 1155 (m), 1128 (s), 1087 (w), 1056 (m), 1034 (m), 1001 (m), 988 (m), 921 (m), 904 (w), 889)w), 863 (m), 849 (w), 826 (m), 785 (m), 760 (vs), 751 (vs), 701 (vs), 687 (s), 677 (s), 657 (s), 640 (s), 556 (m), 509 (m), 432 (m), 409 (m) cm^{-1}.

^{1}H-NMR (600 MHz, DMSO-d6, 298 K): δ = 10.26 (s, 1H, -C*H*O), 7.97 (dd, ^3J = 7.62 Hz, ^4J = 1.44 Hz, 1H, 3″-*H*), 7.82 (d, ^3J = 7.92 Hz, 1H, 6′-*H*), 7.76 (t, ^4J = 1.71 Hz, 1H, 2′-*H*), 7.65-7.61 (m, 3H, 2-*H*, 5-*H*, 5′-*H*), 7.58-7.54 (m, 2H, 4′-*H*, 5″-*H*), 7.49-7.37 (m, 10H, 4″-*H*, *m*-Tr-*H*, *p*-Tr-*H*), 7.20-7.15 (m, 6H, *o*-Tr-*H*), 7.07 (d, ^3J = 7.92 Hz, 1H, 6″-*H*) ppm.

^{13}C-NMR (150 MHz, DMSO-d6, 298 K): δ = 192.1 (-*C*HO), 153.4 (*C*-1′), 152.9 (*C*-4), 141.6 (*C*-*i*-Tr), 139.7 (*C*-1″), 139.4 (*C*-2), 134.9 (*C*-4′), 134.6 (*C*-5″), 133.9 (*C*-3′), 133.3 (*C*-3″), 133.2 (*C*-2″), 131.1 (*C*-5′), 129.4 (*C*-6″), 129.2 (*C*-*o*-Tr), 128.5 (*C*-*m*-Tr), 128.3 (*C*-*p*-Tr), 126.7 (*C*-4″), 125.7 (*C*-2′), 123.1

(*C*-6′), 120.8 (*C*-5), 75.7 (-*C*Ph$_3$) ppm.

MS (ESI, methanol): m/z (%) = 588.9 (8) [M+K]$^+$, 573.0 (82) [M+Na]$^+$, 550.7 (9) [M+H]$^+$, 243.1 (100) [CPh$_3$].

Anal. Calcd. For [$C_{35}H_{26}N_4OS$ + 0.25 EtOAc] (572.70): cal. C 75.50, H 4.93, N 9.78, S 5.47, found C 75.38, H 4.89, N 10.02, S 5.47 %.

5-(3′-(2″-Formylthiophenyl)phenylazo)-1-methylimidazole (16). Under an atmosphere of nitrogen the biphenylthioether azoimidazole **15** (347 mg, 630 µmol) was dissolved in dry methylene chloride (12 mL). Methyl trifluoromethanesulfonate (71.0 µL, 630 µmol) was added dropwise and it was stirred at room temperature for 90 min. Acetone/H_2O (2:1, 36 mL) was added and stirring was continued for 16 h. Saturated Sodium bicarbonate solution (aq., 5 mL) was added, layers were separated and the aqueous layer was extracted two times with methylene chloride (each 20 mL). The combined organic layers were dried over magnesium sulfate and evaporated to dryness. Purification via column chromatography on silica gel (ethyl acetate, R_f = 0.15) gave an orange solid (176 mg, 546 µmol, 87 %).

Mp: 135 °C.

IR (ATR): ν (cm^{-1}) = 3112 (w), 2848 (w), 2747 (m), 1698 (m), 1678 (vs), 1588 (m), 1557 (m), 1504 (m), 1458 (m), 1410 (m), 1395 (m), 1339 (s), 1293 (s), 1225 (s), 1198 (vs), 1125 (vs), 1043 (s), 996 (m), 971 (m), 909 (s), 846 (s), 827 (s), 772 (vs), 687 (s), 677 ((s), 658 (vs), 639 (vs), 597 (m), 531 (vs), 468 (m) cm^{-1}.

^{1}H-NMR (500 MHz, CD_2Cl_2, 300 K): δ = 10.39 (s, 1H, -C*H*O), 7.91 (dd, ^3J = 7.65 Hz, ^4J = 1.60 Hz, 1H, 3″-*H*), 7.87 (t, ^4J = 1.83 Hz, 1H, 2′-*H*), 7.82 (ddd, ^3J = 7.82 Hz, ^4J = 1.95 Hz, ^4J = 1.19 Hz, 1H, 6′-*H*), 7.61 (s, 1H, 2-*H*), 7.55-7.50 (m, 2H, 4-*H*, 5′-*H*), 7.49-7.45 (m, 2H, 4′-*H*, 5″-*H*), 7.39 (dt, ^3J = 7.49 Hz, ^4J = 1.11 Hz, 1H, 4″-*H*), 7.23 (dd, ^3J = 7.93 Hz, ^4J = 1.13 Hz, 1H, 6″-*H*), 3.91 (s, 3H, -C*H*$_3$) ppm.

^{13}C-NMR (125 MHz, CD_2Cl_2, 300 K): δ = 191.8 (-*C*HO), 154.4 (*C*-1′), 145.8 (*C*-5), 141.6 (C-2), 140.7 (*C*-1″), 135.6 (*C*-3′), 134.7-134.5 (*C*-4′, *C*-2″, *C*-5″), 132.3 (*C*-3″), 131.4 (*C*-6″), 130.7 (*C*-5′), 127.3 (*C*-4″), 126.0 (*C*-2′), 124.0 (*C*-4), 123.1 (*C*-6′), 32.8 (-*C*H$_3$) ppm.

MS (EI): m/z (%) = 322.1 (100) [M]$^+$, 293.1 (20) [M-CHO]$^+$, 227.0 (24) [M-$C_4H_5N_3$]$^+$, 184.0 (51) [$C_{12}H_8S$]$^+$, 109.1 (76) [$C_4H_5N_4$]$^+$.

HR-MS (EI): m/z [M]$^{\bullet+}$ calcd for $C_{17}H_{14}N_4OS$, 322.0888; found 322.0881.

UV/Vis (acetonitrile): λ_{max} (lg ε) = 210 (4.460), 236 (4.380), 362 (4.365) nm.

Anal. Calcd. For [$C_{17}H_{14}N_4OS$ + 0.2 EtOAc] (340.01): cal. C 62.88, H 4.62, N 16.48, S 9.43, found C 63.08, H 4.34, N 16.32, S 9.63 %.

5-(Phenyl-2'-(thiophenyl-3"-(azo-*N*-methylimidazole)))-10,15,20-tris(pentafluorophenyl)-porphyrin (mf-5). To a solution of biphenylthioether tonearm **16** (484 mg, 1.52 mmol) and pentafluorobenzaldehyde (271 mg, 1.38 mmol) in methylene chloride (200 mL) was added borontrifluoride diethyletherate (257 µL, 2.03 mmol) under an atmosphere of nitrogen. Pentafluorophenyl dipyrromethane (862 mg, 2.76 mmol) in methylene chloride (40 mL) was added to the stirred solution over 1 h at room temperature. Stirring under nitrogen at room temperature was continued for additional 6 h and the solution turned from dark red to black. Afterwards, chloranil (713 mg, 2.90 mmol) was added and the solution was stirred at reflux for 2 h and at room temperature for 16 h. Triethylamine (1 mL) was added and stirring was continued for 30 min. The reaction mixture was evaporated to dryness and the crude product was filtrated over silica gel (methylene chloride). Subsequent column chromatography on silica gel (cyclohexane/ethyl acetate, 6:4 → 1:1, R_f = 0.22 → 0:1) gave a purple solid (44.0 mg, 40.0 µmol, 3 %).

Mp: 154 °C.

IR (ATR): ν (cm^{-1}) = 3316 (w), 2963 (w), 2926 (w), 2855 (w), 1981 (w), 1728 (w), 1704 (w), 1652 (w), 1679 (w), 1517 (s), 1495 (s), 1435 (m), 1403 (m), 1341 (m), 1259 (s), 1226 (m), 1192 (w), 1143 (m), 1113 (m), 1079 (s), 1063 (s), 1043 (s), 1033 (s), 1026 (s), 985 (vs), 936 (m), 917 (s), 801 (s), 756 (vs), 740 (s), 687 (s), 644 (m), 531 (m), 497 (m), 432 (m), 423 (m) cm^{-1}.

^{1}H-NMR (600 MHz, acetone-d6, 300 K): δ = 9.28 (s, br, 4H, pyrrole-*H*), 9.15 (s, br, 2H, pyrrole-*H*), 8.90 (s, br, 2H, pyrrole-*H*), 8.31 (dd, ^3J = 7.41 Hz, ^4J = 1.23 Hz, 1H, 6′-*H*), 7.93 (td, ^3J = 7.46 Hz, ^4J = 1.35 Hz, 1H, 4′-*H*), 7.88 (dd, ^3J = 8.16 Hz, ^4J = 1.14 Hz, 1H, 3′-*H*), 7.84 (td, ^3J = 7.85 Hz, ^4J = 1.49 Hz, 1H, 5′-*H*), 7.68 (s, 1H, 2-*H*), 7.38 (ddd, ^3J = 7.83 Hz, ^4J = 1.62 Hz, ^4J = 1.00 Hz, 1H, 4″-*H*), 7.21 (s, 1H, 4-*H*), 7.14 (t, ^4J = 1.68 Hz, 1H, 2″-*H*), 7.03 (t, ^3J = 7.83 Hz, 1H, 5″-*H*), 6.90 (ddd, ^3J = 7.72 Hz, ^4J = 1.66 Hz, ^4J = 1.04 Hz, 1H, 6″-*H*), 3.55 (s, 3H, -CH_3) , -2.83 (s, 2H, pyrrole-N*H*) ppm.

^{19}F-NMR (470 MHz, acetone-d6, 300 K) δ = -139.57 (dd, ^3J = 24.2 Hz, ^4J = 7.65 Hz, 2F, A-*o*-F), -139.69 (dd, ^3J = 23.8 Hz, ^4J = 7.63 Hz, 1F, B-*o*-F), -139.98 (dd, ^3J = 23.7 Hz, ^4J = 7.53 Hz, 1F, B-*o'*-F), -140.09 (dd, ^3J = 23.8 Hz, ^4J = 7.51 Hz, 2F, A-*o'*-F), -155.66 (t, ^3J = 20.3 Hz, 2F, A-*p*-F), -155.69 (t, ^3J = 20.2 Hz, 1F, B-*p*-F), -164.51 to -164.80 (m, 6F, B-*m*-F, B-*m'*-F, A-*m*-F, A-*m'*-F) ppm.

MS (MALDI-TOF): m/z (%) = 1123.7 (12) $[M + Na]^+$, 1101.7 (100) $[M + H]^+$.

5-(Phenyl-2'-(thiophenyl-3"-(azo-*N*-methylimidazole)))-10,15,20-tris(pentafluorophenyl)-nickel(II)porphyrin (5). The metal free biphenylthioether record player (39.0 mg, 35.4 µmol) was dissolved in toluene (40 mL) and nickel(II)acetylacetonate (91.0 mg, 354 µmol) was added. The resulting mixture was stirred at reflux for 2.5 d after which time no starting material was detectable via MALDI-TOF-MS. The reaction mixture was evaporated to dryness and the crude product was purified

via column chromatography on silica gel (chloroform → chloroform, 5 % methanol, R_f = 0.50 (*cis*), 0.25 (*trans*)). The product was obtained as purple solid (10.0 mg, 8.64 µmol, 24 %) which is deep red in solution.

Mp: 253 °C.

IR (ATR): ν (cm^{-1}) = 1652 (w), 1583 (w), 1518 (s), 1486 (s), 1429 (m), 1342 (m), 1317 (w), 1278 (w), 1262 (w), 1225 (m), 1164 (w), 1142 (w), 1114 (m), 1074 (m), 1060 (m), 1005 (m), 984 (vs), 958 (s), 938 (s), 925 (s), 854 (m), 839 (m), 799 (m), 762 (vs), 745 (s), 703 (s), 686 (m), 641 (m), 585 (w), 503 (w) cm^{-1}.

^{1}H-NMR (600 MHz, acetone-d6, 300 K): δ = 9.44 (s, br, 4H, pyrrole-*H*), 9.32 (s, br, 2H, pyrrole-*H*), 9.09 (s, br, 2H, pyrrole-*H*), 8.24 (dd, ^3J = 7.35 Hz, ^4J = 1.23 Hz, 1H, 6′-*H*), 7.96 (s, br, 1H, 2-*H*), 7.86 (td, ^3J = 7.84 Hz, ^4J = 1.32 Hz, 1H, 4′-*H*), 7.81 (td, ^3J = 7.53 Hz, ^4J = 1.39 Hz, 1H, 5′-*H*) 7.79 (dd, ^3J = 7.83 Hz, ^4J = 1.25 Hz, 1H, 3′-*H*), 7.62 (s, br, 1H, 4-*H*), 7.31 (d, ^3J = 8.22 Hz, 1H, 4″-*H*), 7.08-7.06 (m, 1H, 2″-*H*), 6.99 (t, ^3J = 7.77 Hz, 1H, 5″-*H*), 6.90 (d, ^3J = 7.86 Hz, 6″-*H*), 3.60 (s, 3H, -CH_3) ppm.

^{19}F-NMR (470 MHz, acetone-d6, 300 K) δ = -139.44 (dd, ^3J = 23.4 Hz, ^4J = 7.01 Hz, 2F, A-*o*-F), -139.74 (dd, ^3J = 23.6 Hz, ^4J = 7.20 Hz, 1F, B-*o*-F), -139.87 (dd, ^3J = 23.7 Hz, ^4J = 7.10 Hz, 1F, B-*o'*-F), -140.22 (dd, ^3J = 23.1 Hz, ^4J = 6.82 Hz, 2F, A-*o'*-F), -155.74 (t, ^3J = 20.4 Hz, 2F, A-*p*-F), -155.76 (t, ^3J = 20.2 Hz, 1F, B-*p*-F), -164.35 to –164.72 (m, 6F, B-*m*-F, B-*m'*-F, A-*m*-F, A-*m'*-F) ppm.

HR-MS (ESI, EtOH, 0.1 % HCOOH)**:** m/z $[M+H]^+$ calcd for $[C_{54}H_{21}F_{15}N_8SNi+H]$, 1157.079; found 1157.078.

UV/Vis (acetonitrile): λ_{max} (lg ε) = 406 (5.184), 524 (4.085), 558 (3.951) nm.

III.3 NMR spectra

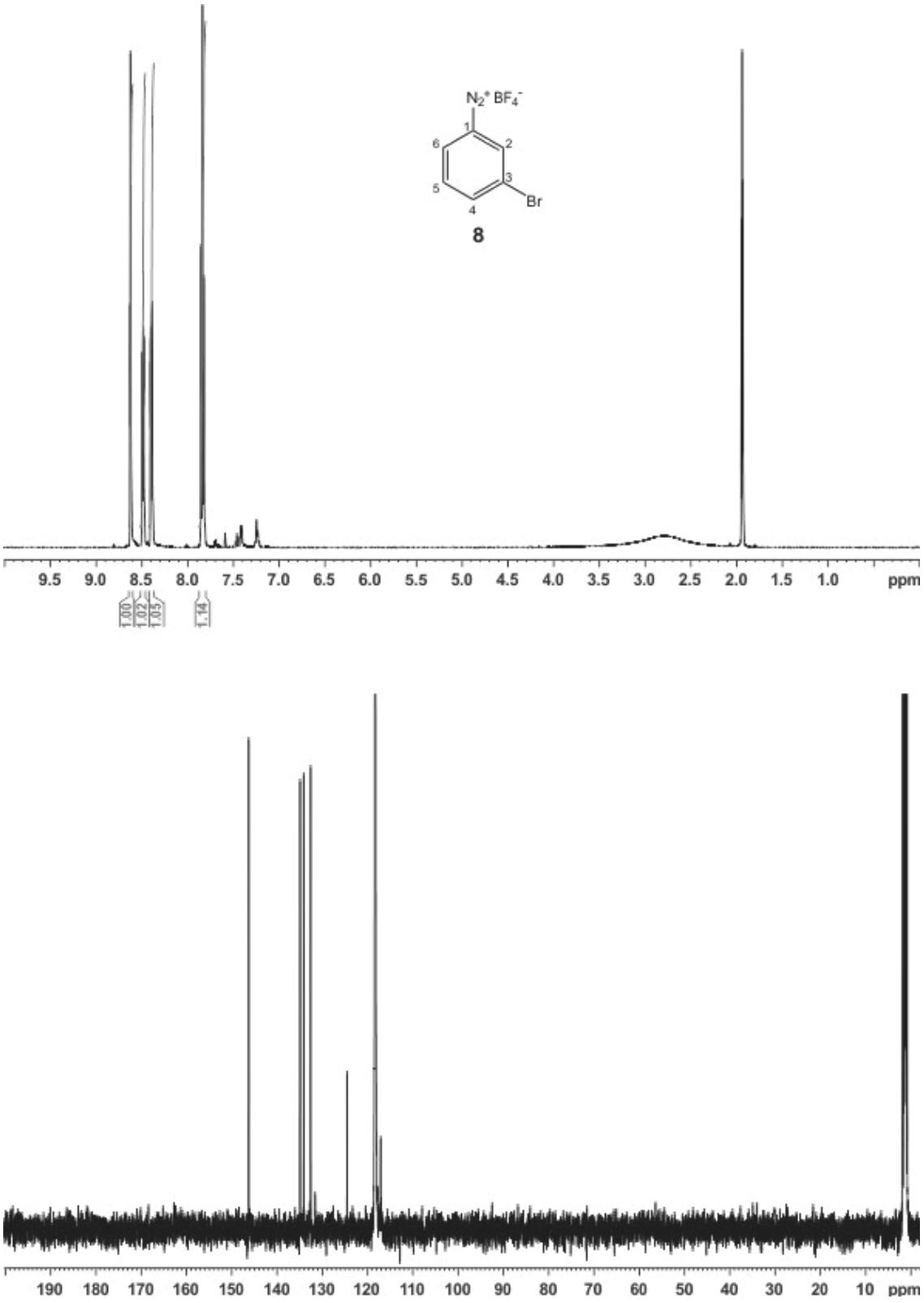

Figure S3: ^{1}H NMR (top) and ^{13}C NMR (bottom) spectra of 3-bromobenzenediazonium tetrafluoroborate **8**. Spectra were measured in acetonitrile-d_3 at 300 K.

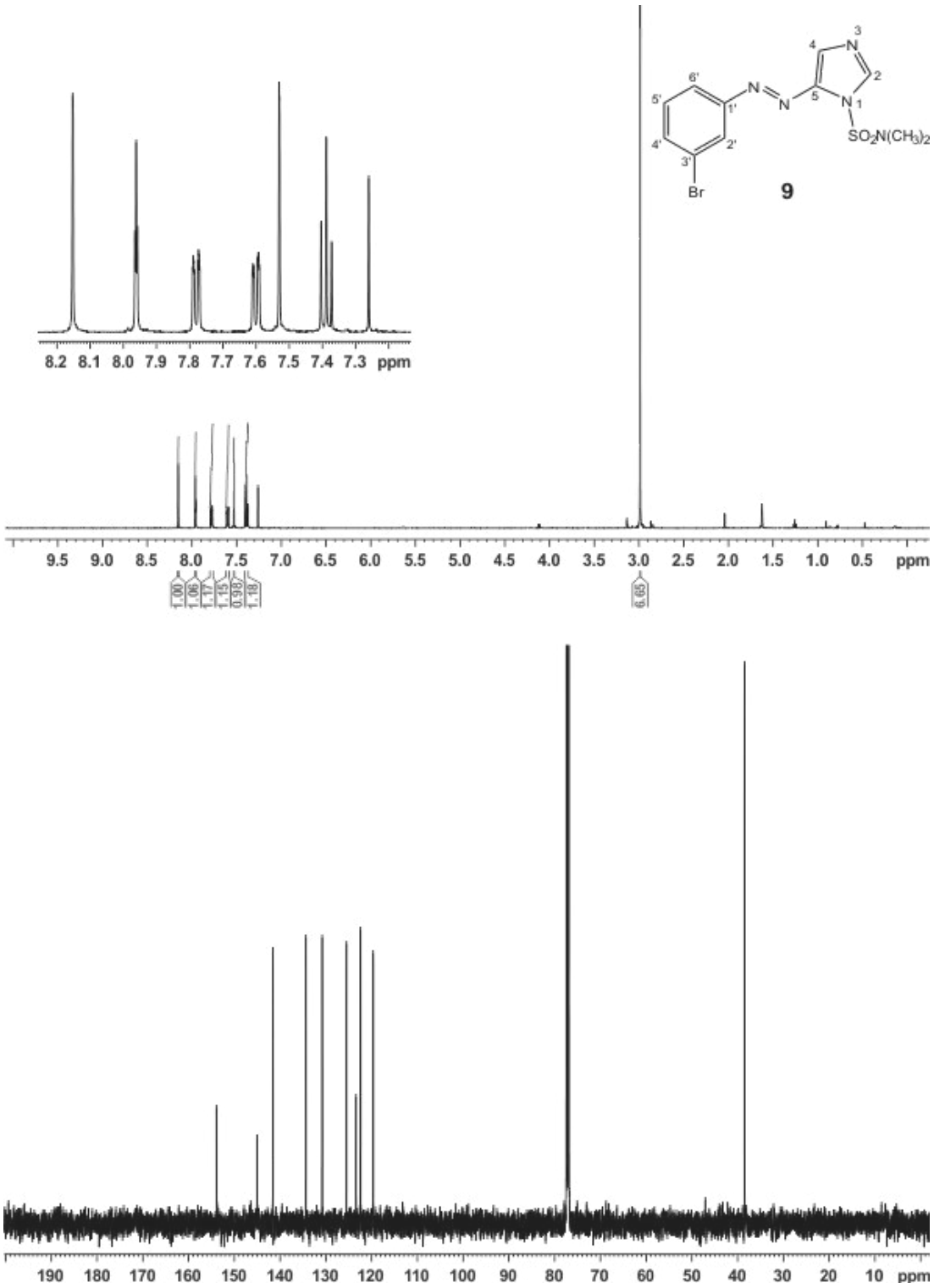

Figure S4: ^{1}H NMR (top) and ^{13}C NMR (bottom) spectra of 5-(3'-Bromophenylazo)-1-(*N,N*-dimethylsulfamoyl)imidazole (**9**). Spectra were measured in $CDCl_3$ at 300 K.

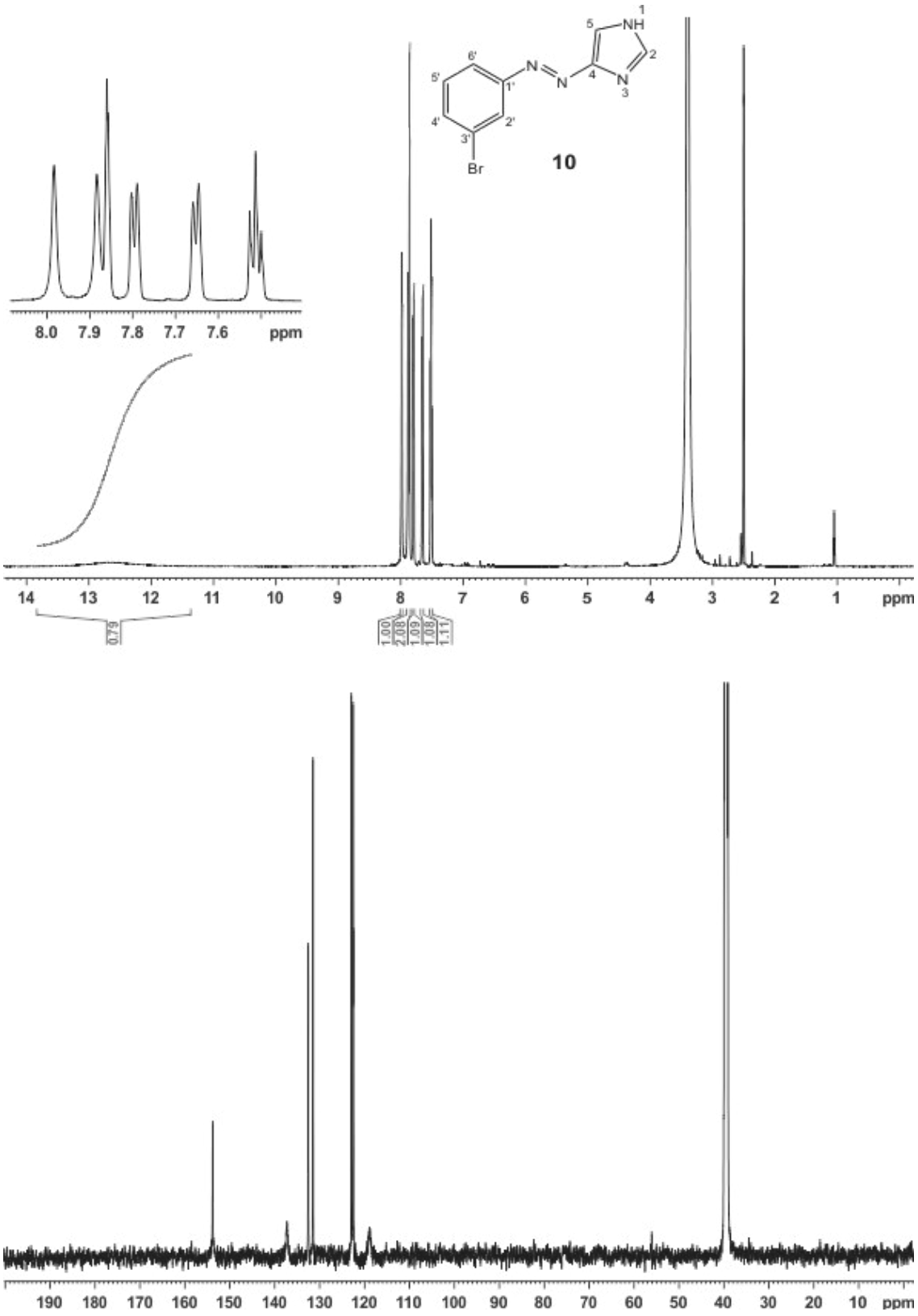

Figure S5: ^{1}H NMR (top) and ^{13}C NMR (bottom) spectra of 4(5)-(3'-Bromophenylazo)imid-azole (**10**). Spectra were measured in DMSO-d_6 at 298 K.

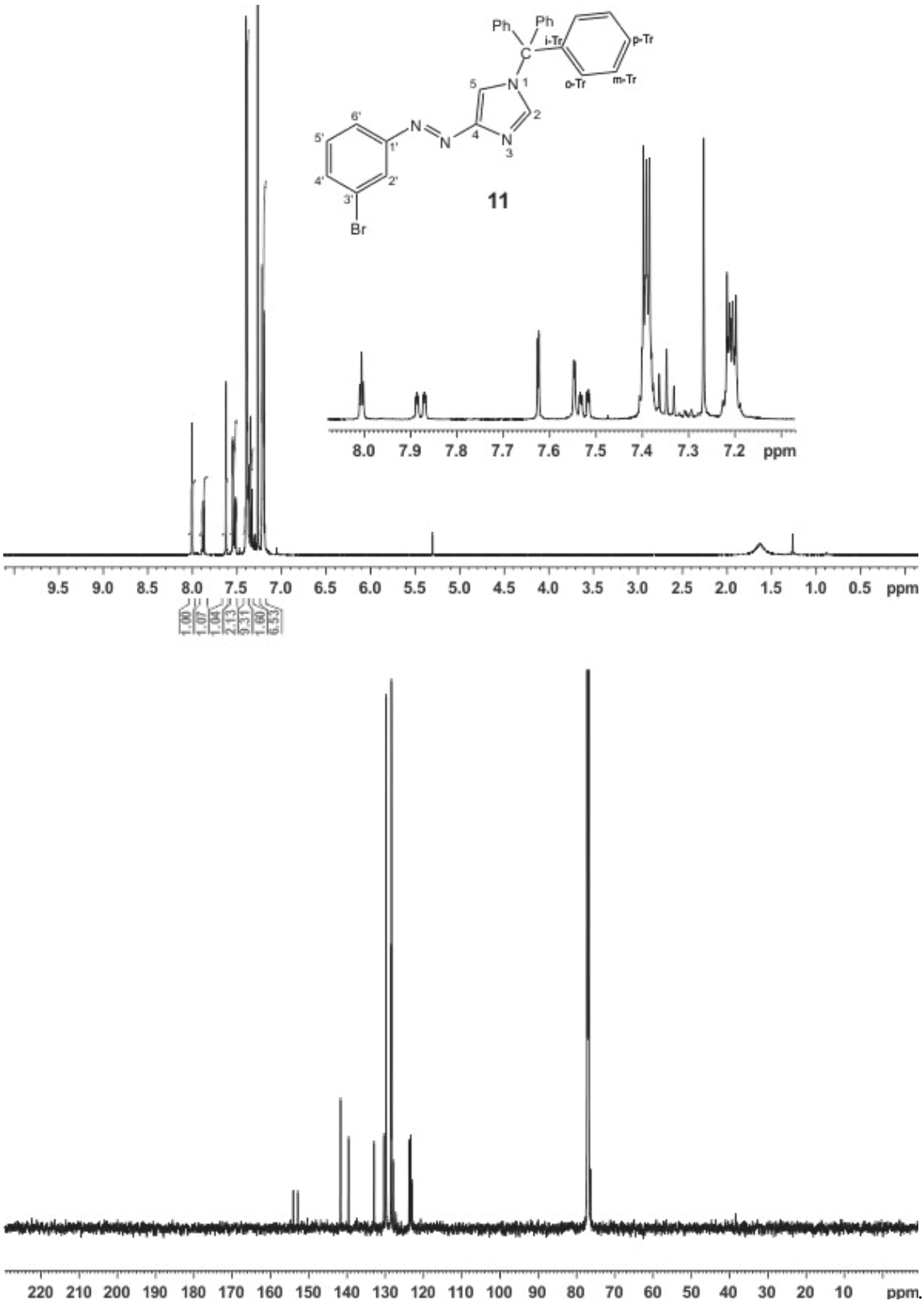

Figure S6: ^{1}H NMR (top) and ^{13}C NMR (bottom) spectra of 4-(3'-Bromophenylazo)-1-(triphenylmethyl)imidazole (**11**). Spectra were measured in $CDCl_3$ at 298 K.

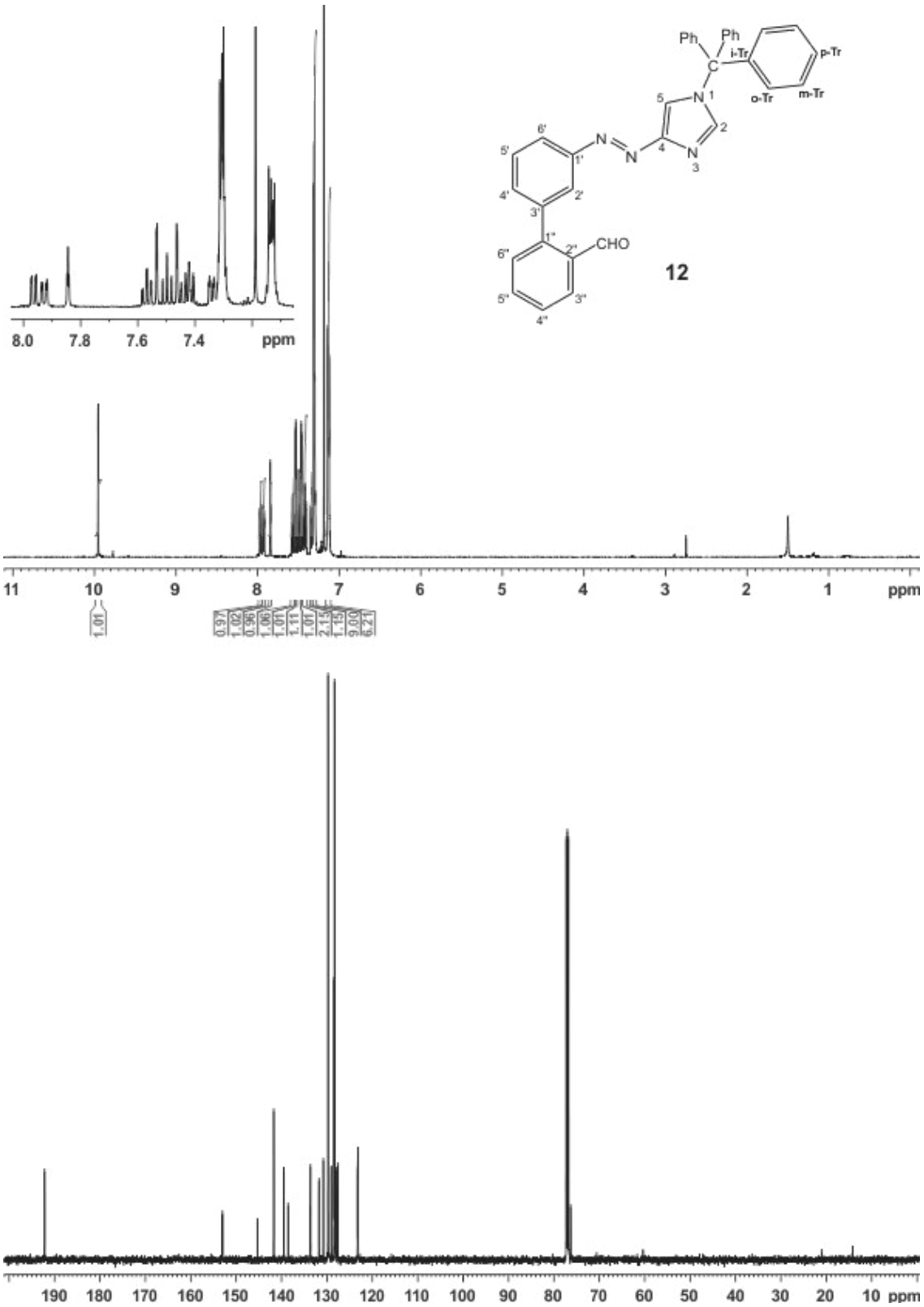

Figure S7: ^{1}H NMR (top) and ^{13}C NMR (bottom) spectra of 4-(3'-(2''-formylphenyl)phenylazo)-1-(triphenylmethyl)imidazole (**12**). Spectra were measured in $CDCl_3$ at 300 K.

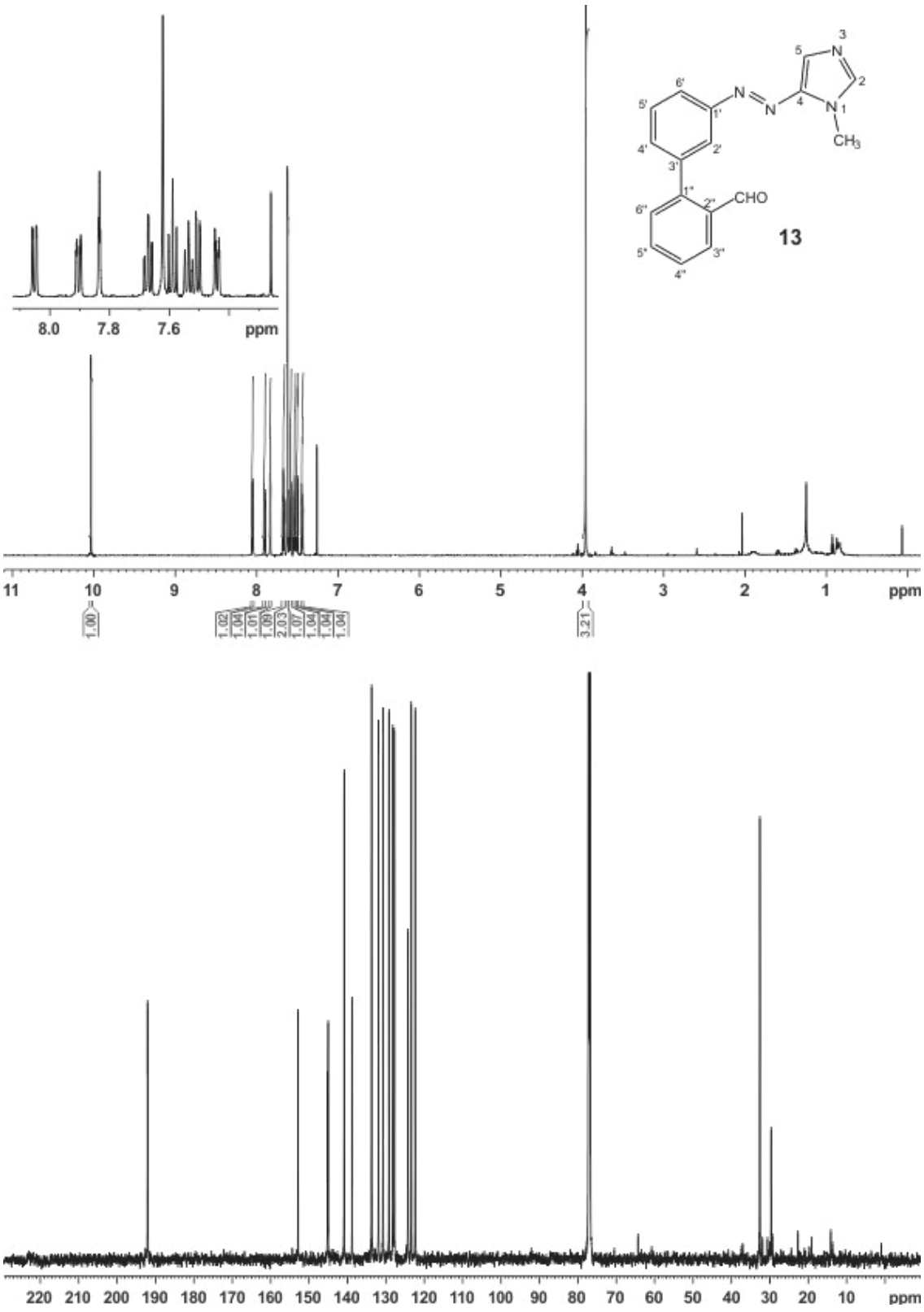

Figure S8: ^{1}H NMR (top) and ^{13}C NMR (bottom) spectra of 5-(3'-(2''-formylphenyl)phenylazo)-1-methylimidazole (**13**). Spectra were measured in $CDCl_3$ at 298 K.

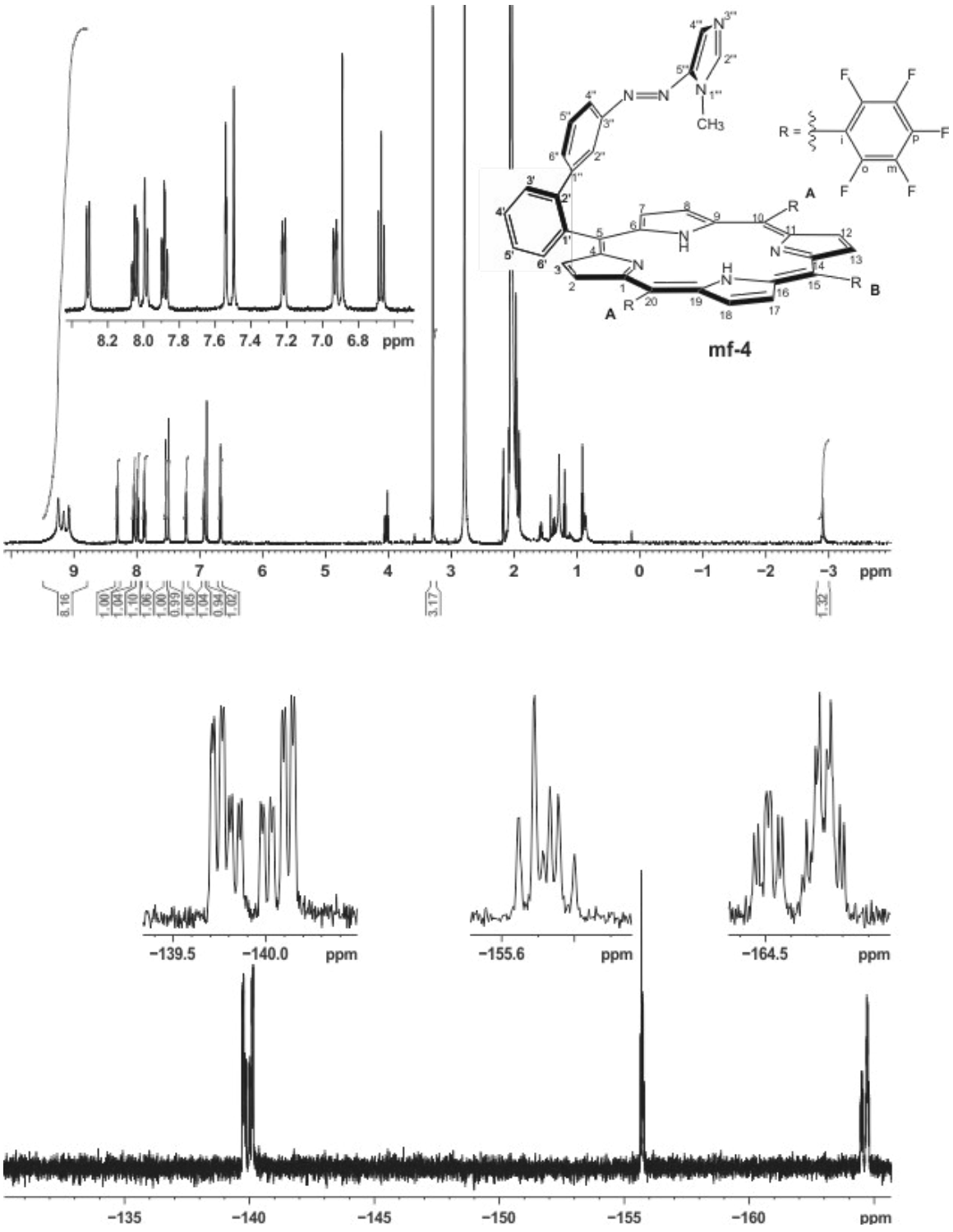

Figure S9: ^{1}H NMR (top) and ^{19}F NMR (bottom) spectra of metal-free biphenyl record player (mf-**4**). Spectra were measured in acetone-d_6 at 300 K.

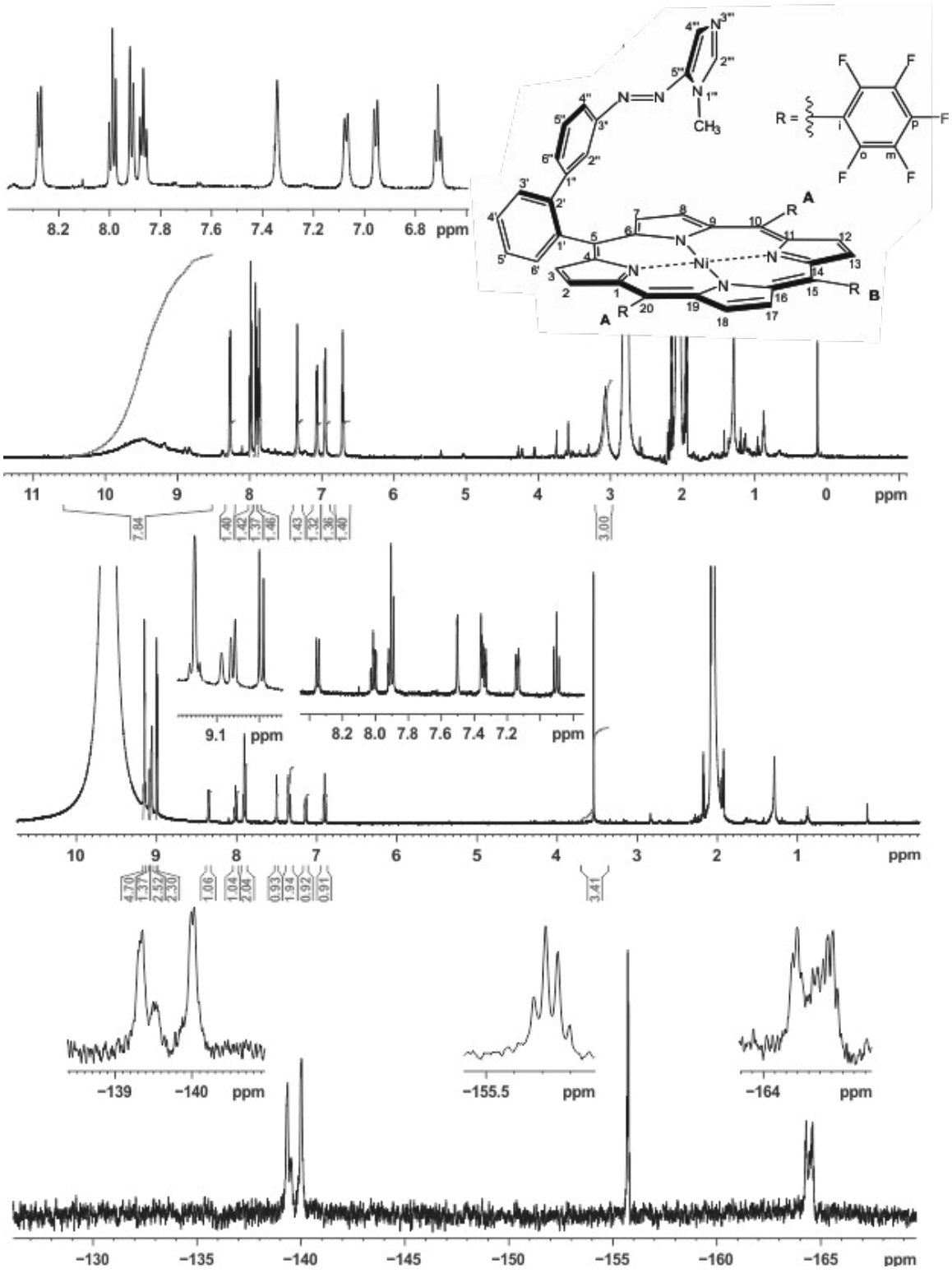

Figure S10: ^{1}H NMR (top), ^{1}H NMR with 10 µL trifluoroacetic acid (middle) and ^{19}F NMR (bottom) spectra of *trans* biphenyl record player (**4**). Spectra were measured in acetone-d_6 at 300 K.

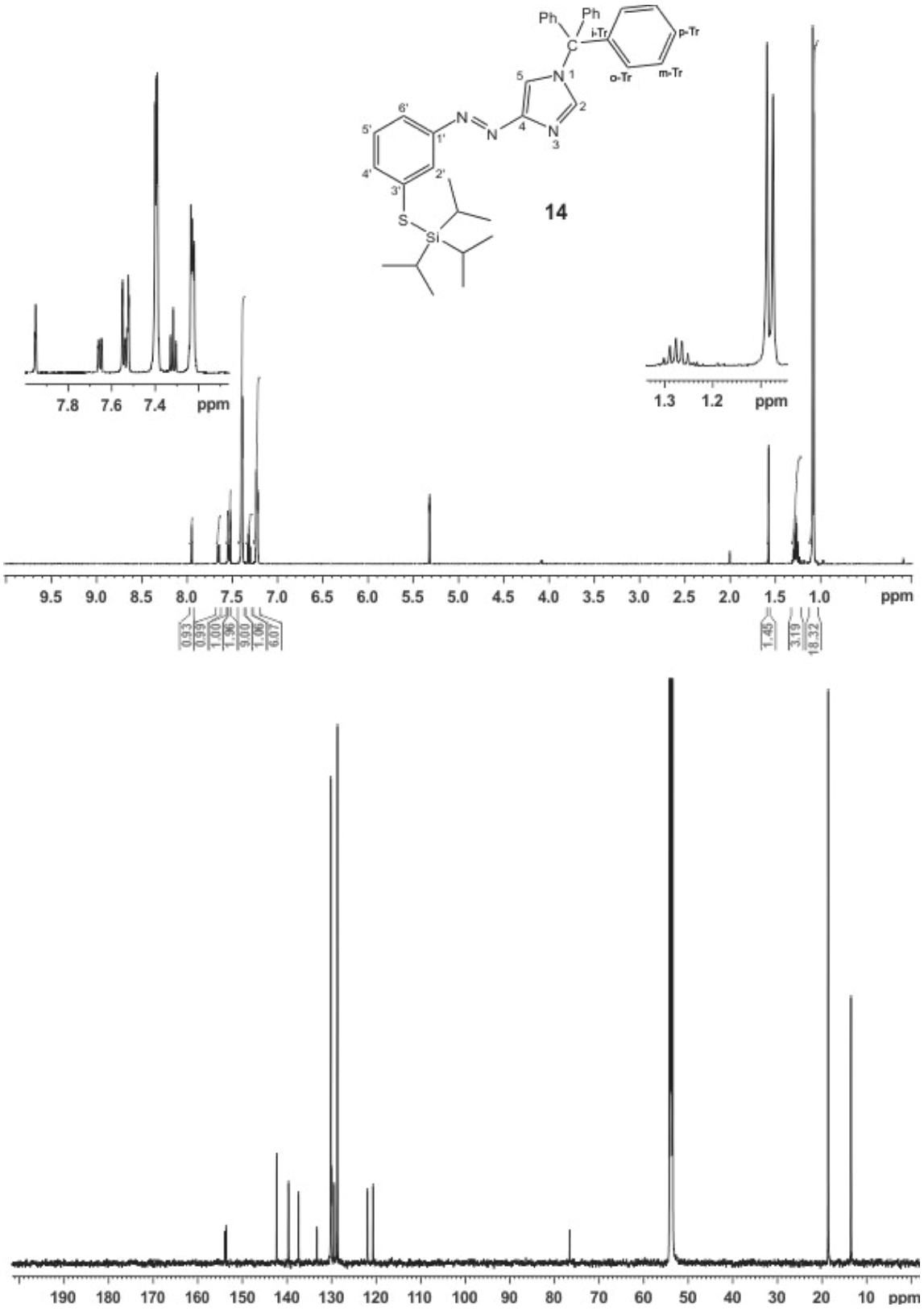

Figure S11: ^{1}H NMR (top) and ^{13}C NMR (bottom) spectra of 4-(3'-(triisopropylsilylthio)phenylazo)-1-(triphenylmethyl)imidazole (**14**). Spectra were measured in CD_2Cl_2 at 298 K.

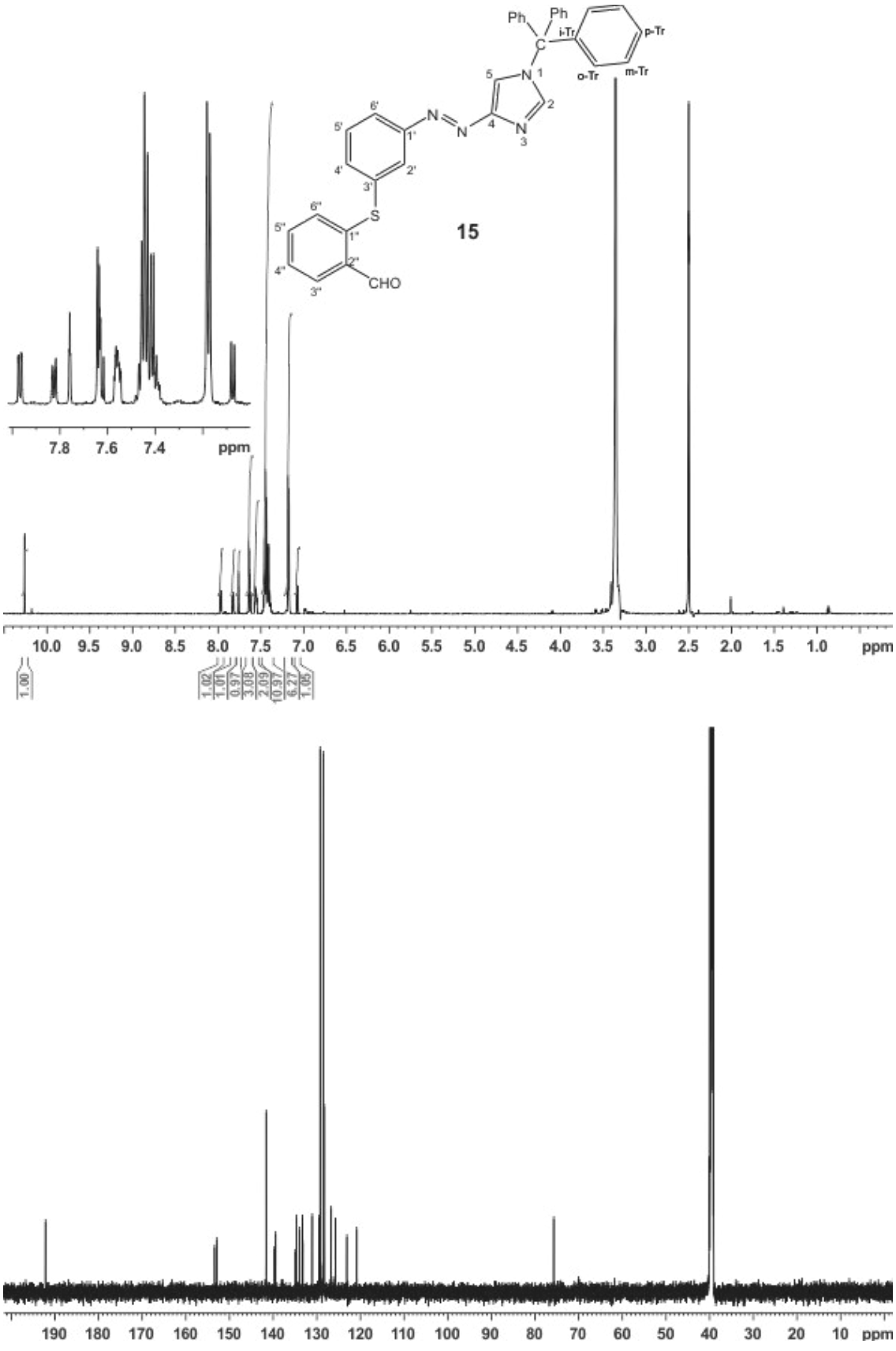

Figure S12: ^{1}H NMR (top) and ^{13}C NMR (bottom) spectra of 4-(3'-(2''-formylthiophenyl)phenylazo)-1-(triphenylmethyl)imidazole (**15**). Spectra were measured in DMSO-d_6 at 298 K.

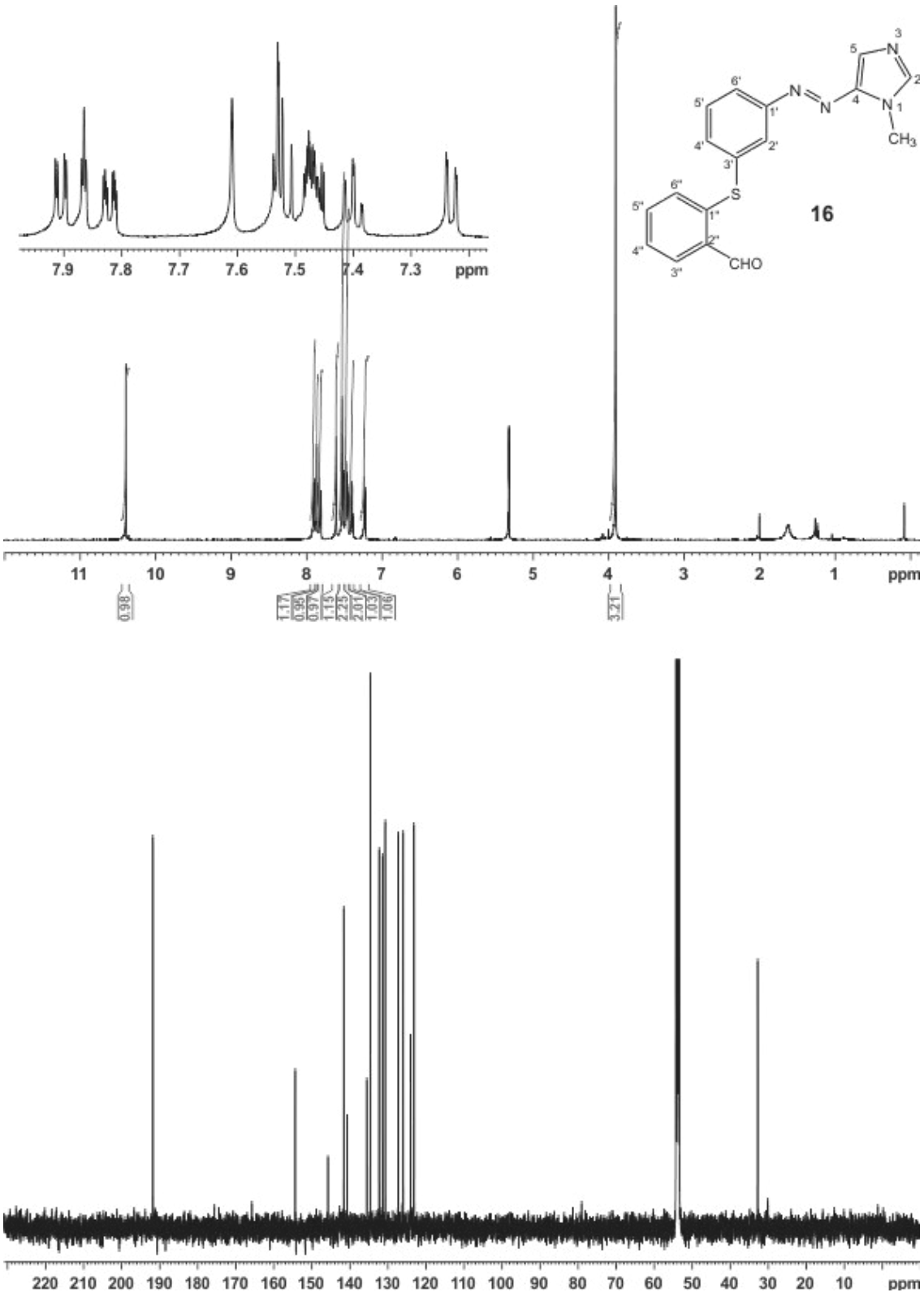

Figure S13: ^{1}H NMR (top) and ^{13}C NMR (bottom) spectra of 5-(3'-(2''-formylthiophenyl)phenylazo)-1-methylimidazole (**16**). Spectra were measured in dichloromethane-d_2 at 300 K.

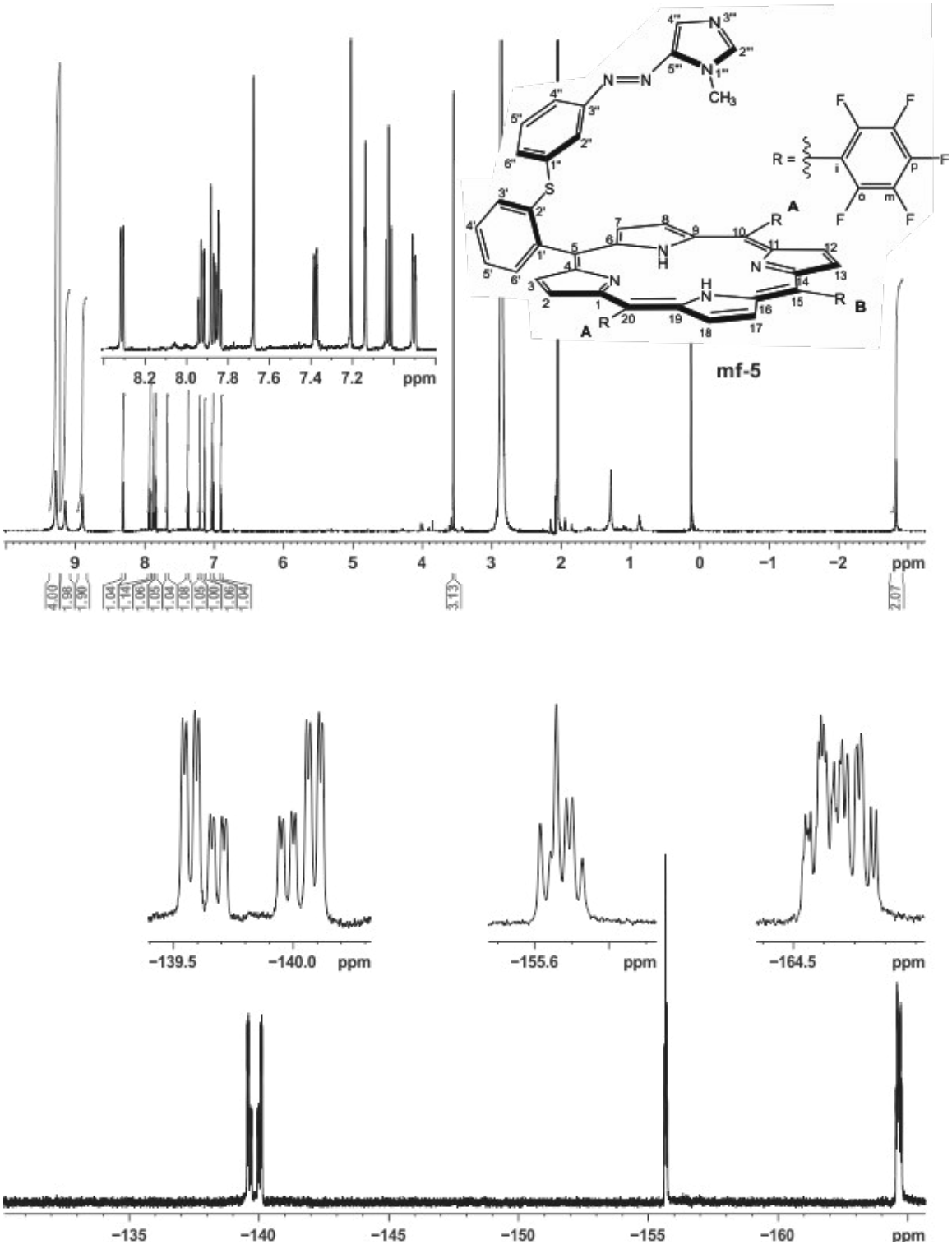

Figure S14: ^{1}H NMR (top) and ^{19}F NMR (bottom) spectra of metal-free biphenyl thioether record player (mf-**5**). Spectra were measured in acetone-d_6 at 300 K.

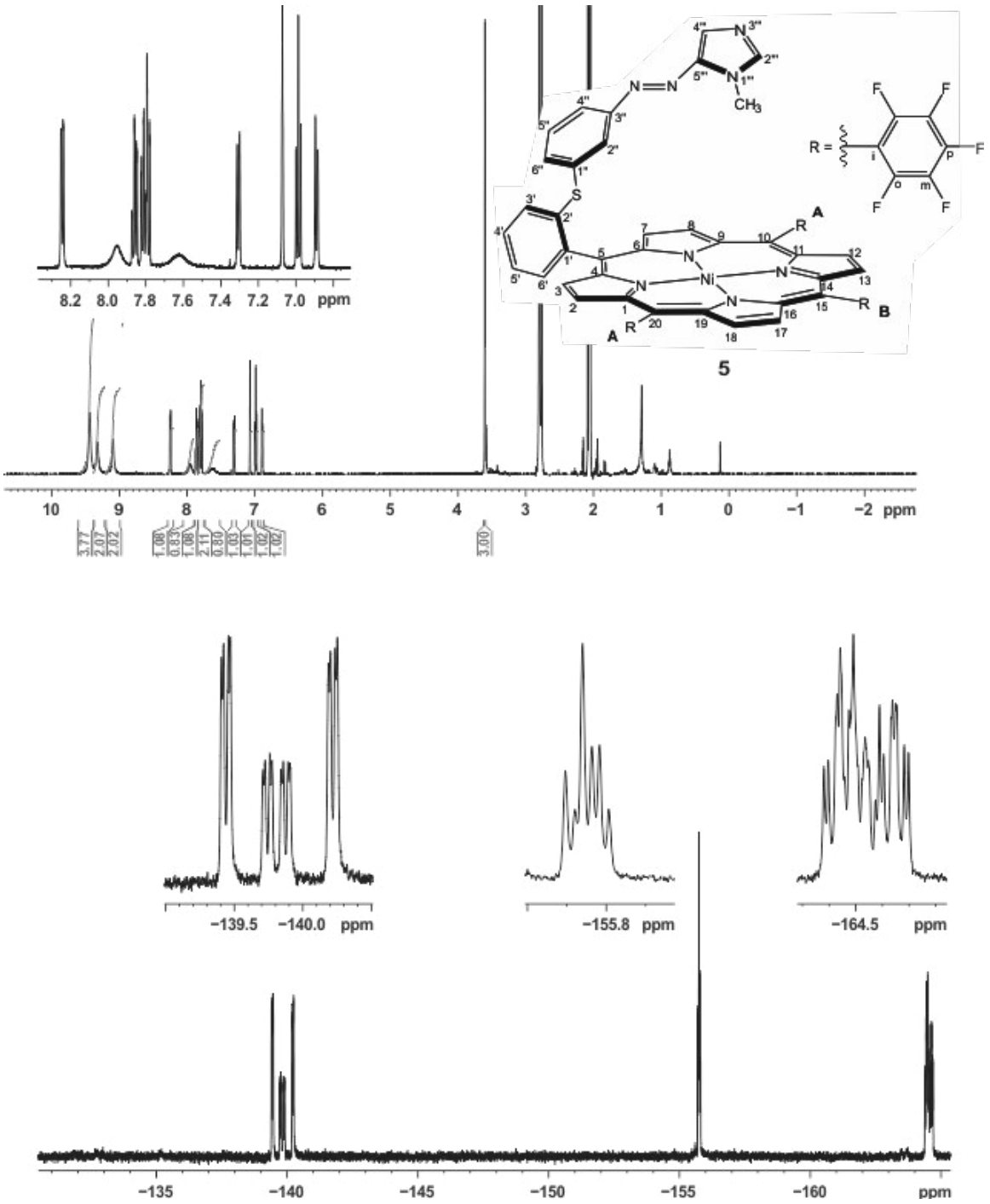

Figure S15: ^{1}H NMR (top) and ^{19}F NMR (bottom) spectra of biphenyl thioether record player (**5**). Spectra were measured in acetone-d_6 at 300 K.

III.4 UV-vis spectra and UV-vis switching experiments.

III.4.1 UV-vis spectra and switching experiments of biphenyl record player (**4**).

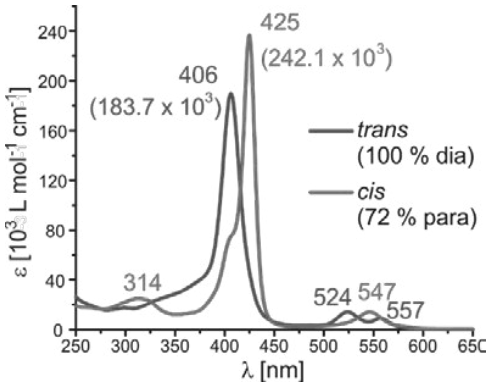

Figure S16: Extinction coefficients of *trans*-**4** (red) and *cis*-**4** (blue) in acetonitrile. The extinction coefficients of pure *trans*-**4** were measured after storage in the dark at 40 °C for 2 weeks. The extinction coefficients of *cis*-**4** were determined by subtracting the absorption of residual *trans*-**4** (15%) from the PSS-365 solutions.

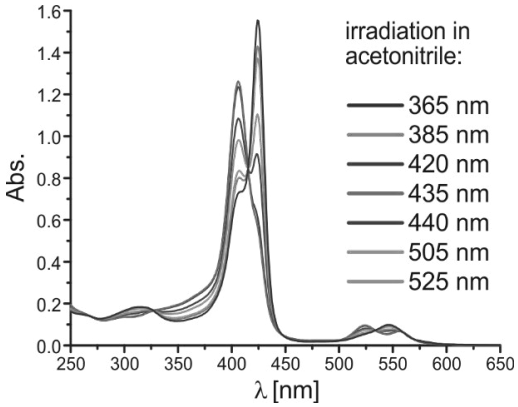

Figure S17: Switching experiments of a 7 µM solution of **4** in acetonitrile (irradiation time: > 1 min). *Trans*→*cis* isomerization is most effective with 365 nm, followed by 385 nm and 505 nm. Back isomerization (*cis*→*trans*) is achieved by irradiation with 435 nm or 420 nm.

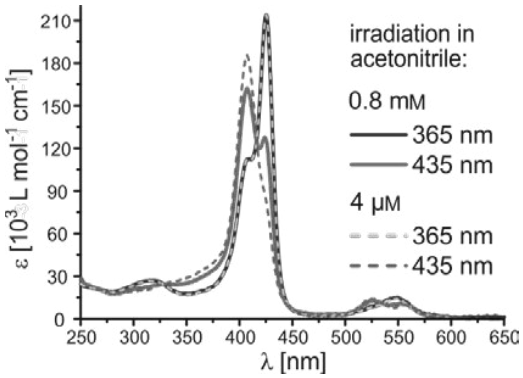

Figure S18: Concentration dependency of photostationary states (365 nm and 435 nm) of **4**. *Cis*→*trans* isomerization with 435 nm is reduced at higher concentrations whereas *trans*→*cis* isomerization with 365 nm remains unaffected (irradiation times: > 30 min).

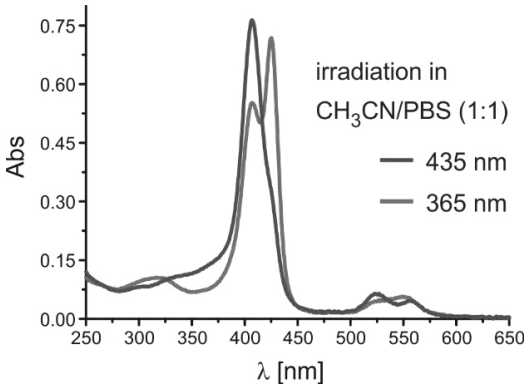

Figure S19: Switching experiments of a 4 µM solution of **4** in acetonitrile/PBS (pH 7.4) (1:1). Intramolecular coordination of *cis*-**4** is reduced in comparison to the measurements in pure acetonitrile (irradiation time: > 1 min).

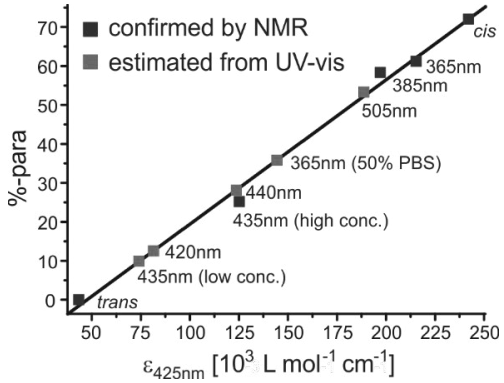

Figure S20: Amount of paramagnetic species (%-para) of **4** in correlation to the UV-vis extinction (ε_{425nm}) at 426 nm (Soret band of the paramagnetic species). A linear relationship between %-para and ε_{426nm} allows the estimation of %-para for samples which are not measurable with NMR.

III.4.2 UV-vis spectra and switching experiments of biphenyl thioether record player (**5**).

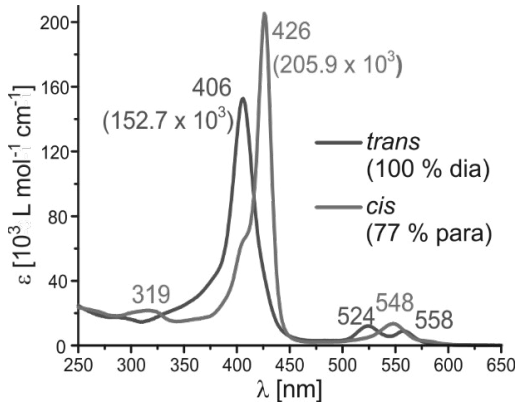

Figure S21: Extinction coefficients of *trans*-**5** (red) and *cis*-**5** (blue) in acetonitrile. The extinction coefficients of pure *trans*-**5** were measured after storage in the dark at 40 °C for 2 weeks. The extinction coefficients of *cis*-**5** were determined by subtracting the absorption of residual *trans*-**5** (15%) from the PSS-365 solutions.

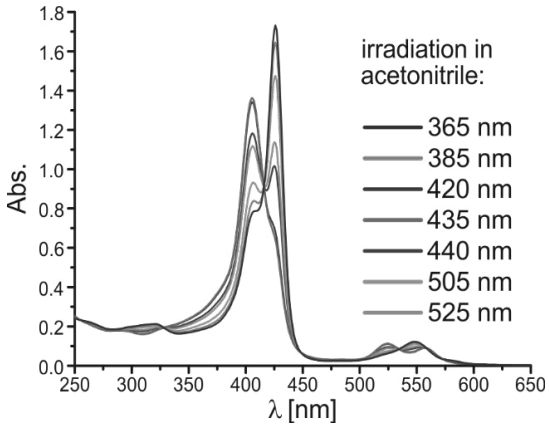

Figure S22: Switching experiments of a 10 µM solution of **5** in acetonitrile (irradiation time: > 1 min). *Trans*→*cis* isomerization is most effective with 365 nm, followed by 385 nm and 505 nm. Back isomerization (*cis*→*trans*) is achieved by irradiation with 435 nm or 420 nm.

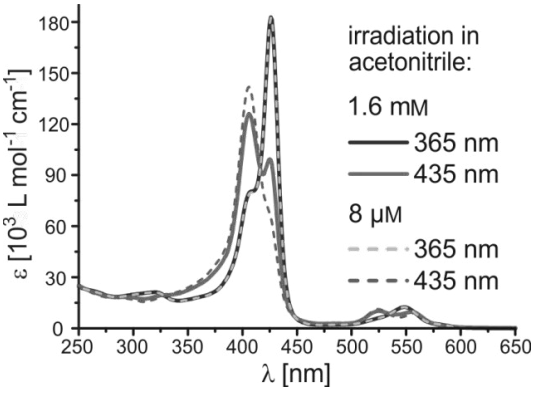

Figure S23: Concentration dependency of photostationary states (365 nm and 435 nm) of **5**. *Cis*→*trans* isomerization with 435 nm is reduced at higher concentrations whereas *trans*→*cis* isomerization with 365 nm remains unaffected (irradiation time: > 30 min).

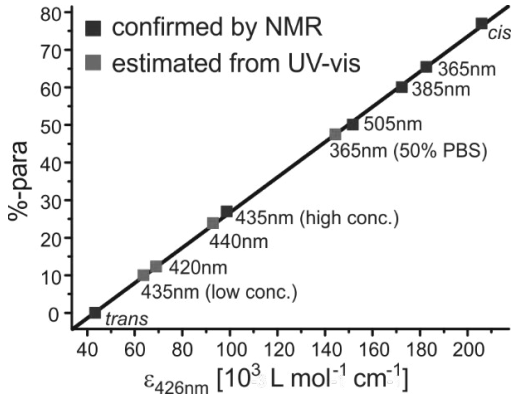

Figure S24: Amount of paramagnetic species (%-para) of **5** in correlation to the UV-vis extinction (ε_{426nm}) at 426 nm (Soret band of the paramagnetic species). A linear relationship between %-para and ε_{426nm} allows the estimation of %-para for samples which are not measurable with NMR.

III.5 NMR switching experiments.

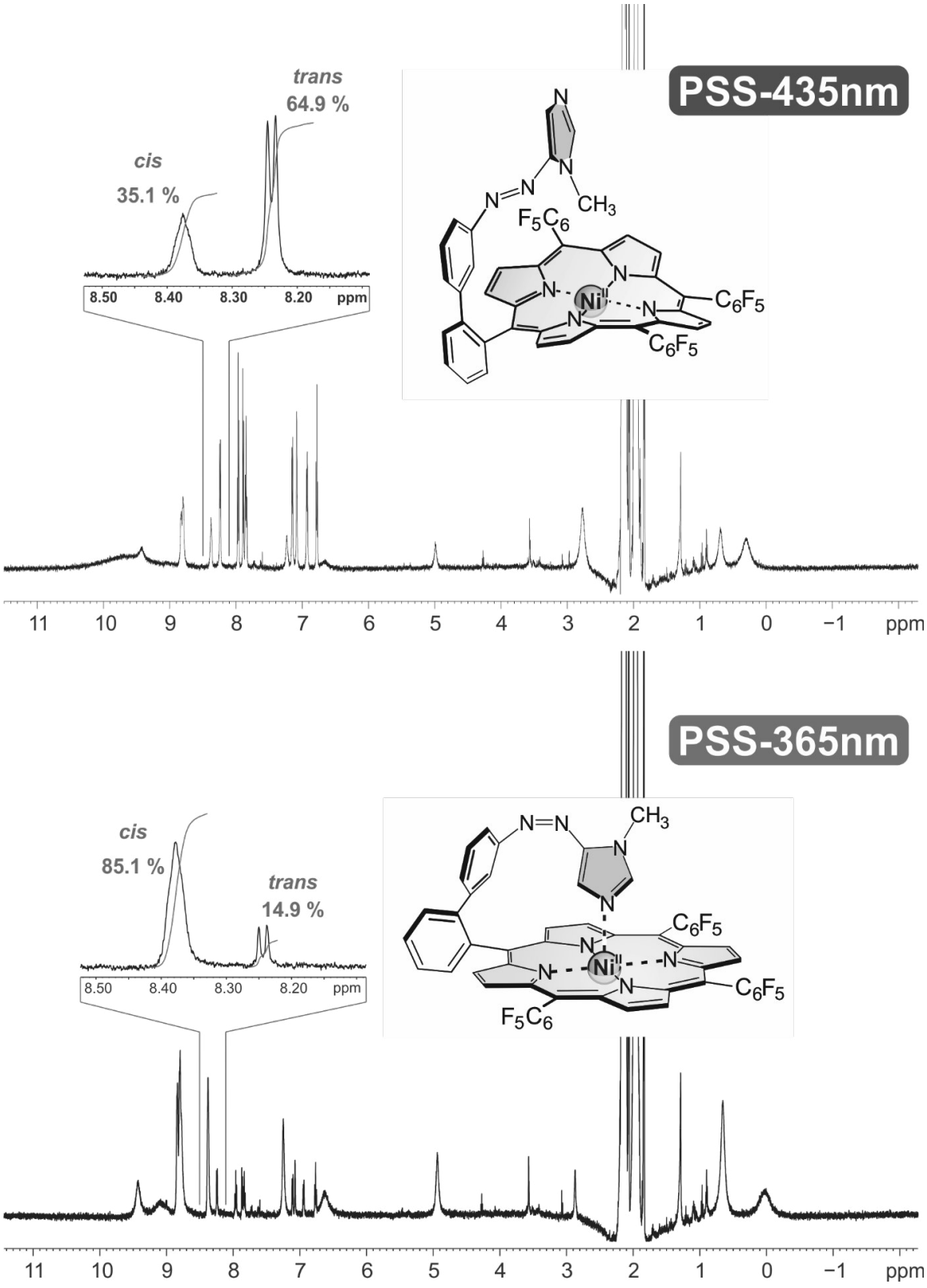

Figure S25: ^{1}H NMR spectra of biphenyl record player (**4**) upon irradiation with 435 nm (top) and 365 nm (bottom). The predominant species of each PSS is shown as molecular structure. Spectra were measured in acetonitrile-d_3 at 300 K.

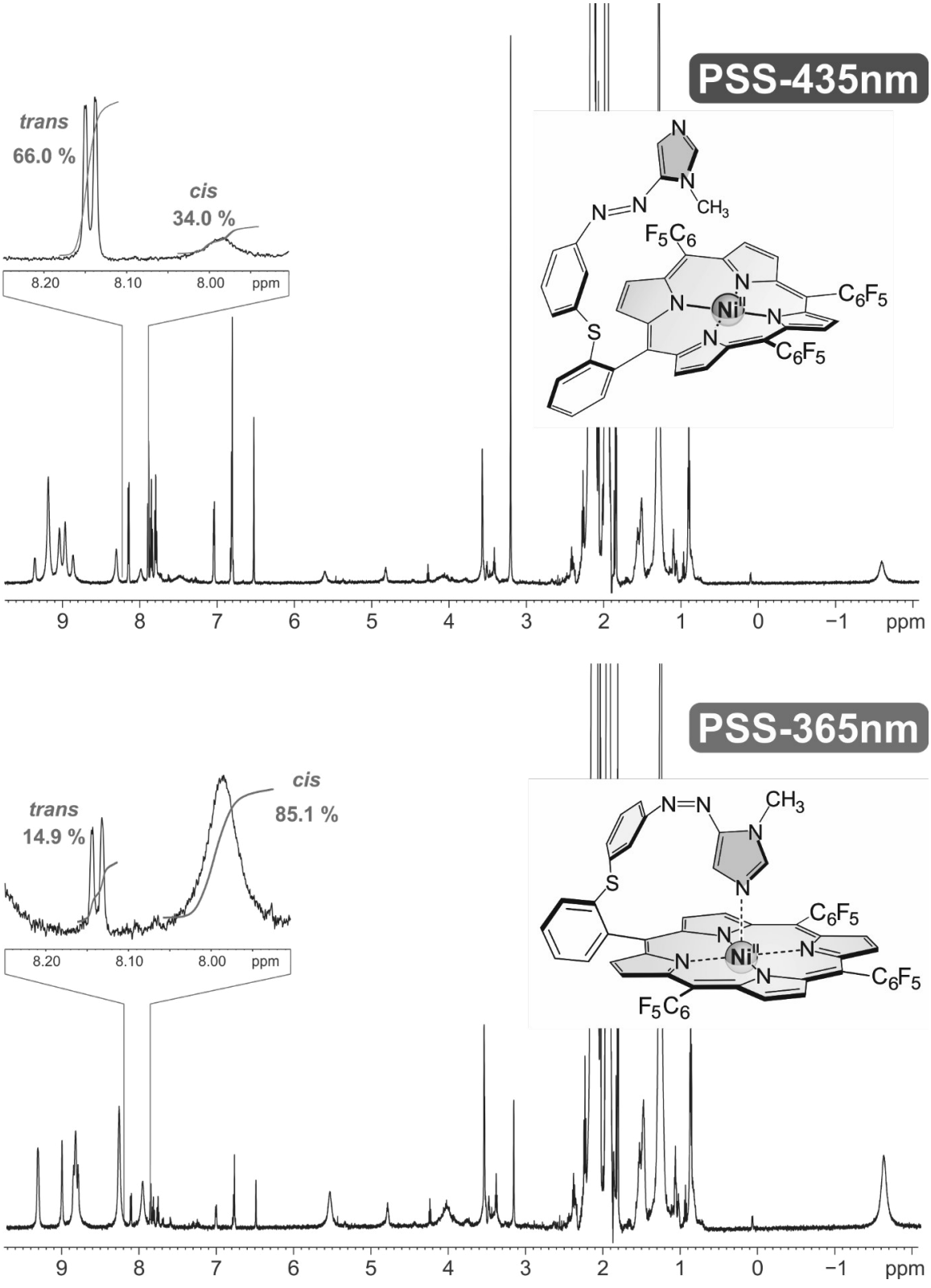

Figure S26: ^{1}H NMR spectra of biphenyl record player (**5**) upon irradiation with 435 nm (top) and 365 nm (bottom). The predominant species of each PSS is shown as molecular structure. Spectra were measured in acetonitrile-d_3 at 300 K.

III.6 Thermal half-lives of *cis*-4 and *cis*-5 and of tonearms *cis*-13 and *cis*-16.

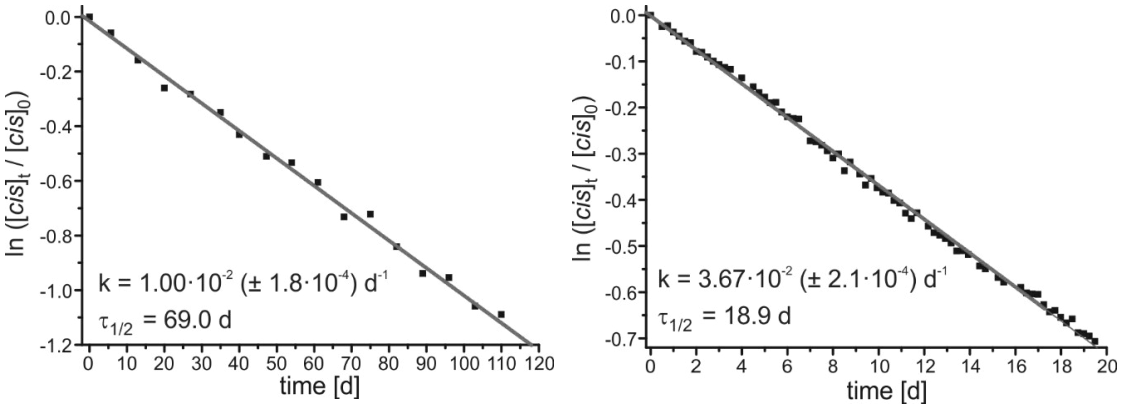

Figure S27: First order kinetics plot for the thermal reisomerization of *cis*-biphenyl rp **4** (left) and of the respective *cis*-biphenyl tonearm **13** (right) in DMSO-d_6 at 25 °C.

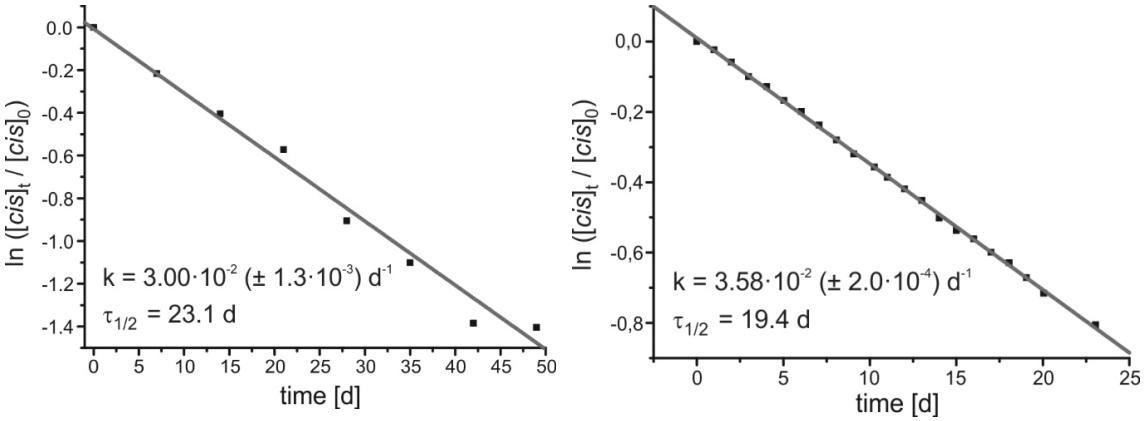

Figure S28: First order kinetics plot for the thermal reisomerization of *cis*-biphenyl thioether rp **5** (left) and of the respective *cis*-biphenyl thioether tonearm **16** (right) in DMSO-d_6 at 25 °C.

III.7 Intramolecular coordination in *cis* record players 4 and 5.

As we described earlier the ratio of the paramagnetic *cis*-species can easily be derived from the NMR shift (δ) of the pyrrole protons of the porphyrin system.[7,8] In a diamagnetic, square planar coordination sphere the pyrrole protons signals appear at 9 ppm (δ_{dia}) and are shifted to ca. 54.5 ppm (δ_{para}) in the paramagnetic, octahedral complex with two additional axial ligands (at 300 K). Since the coordination/de-coordination of axial ligands is fast on nmr time scale only the time-averaged pyrrole shift is observed which represents the respective equilibrium between both magnetic species (see figure S29). The ratio of paramagnetic *cis* species (cis_{para}) correlates linearly with the time-averaged *cis* pyrrole shift (δ_{cis}) following equation S1.

$$cis_{para} = \frac{\delta_{cis} - \delta_{dia}}{\delta_{para} - \delta_{dia}} \tag{S1}$$

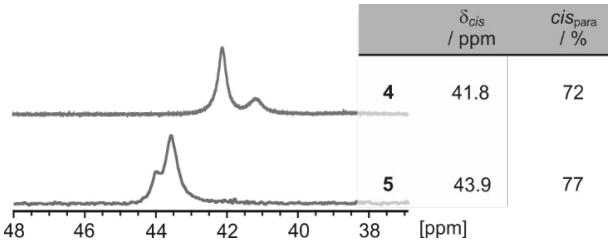

Figure S29: Averaged pyrrole protons shifts (δ_{cis}) of *cis*-**4** and *cis*-**5** in acetonitrile-d_3 at 300 K. The ratios (cis_{para}) of paramagnetic *cis* species correlate linearly with δ_{cis} following equation S1.

To determine the thermodynamic parameters ΔH and ΔS of the coordination event in *cis* record players **4** and **5** (see figure S30) the respective association constant (K) was measured as a function of temperature in acetonitrile-d_3 (see tables S3 and S4). K can be calculated from the pyrrole protons NMR shifts of the *cis* isomer (δ_{cis}) of the record player molecule (see equation S2).[8] The maximum pyrrole protons shifts (δ_{para}) were measured by an analogous experiment in pure pyridine-d_5 for each temperature. The thermodynamic parameters ΔH and ΔS were then obtained by Gibbs free enthalpy plots (see equation S3, figures S31 and S32).

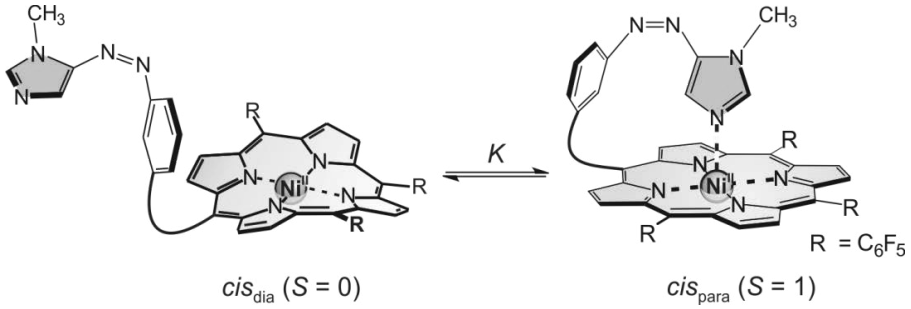

Figure S30: Equilibrium between the magnetic conformers cis_{dia} and cis_{para} of imidazole "record player" molecules.

$$K = \frac{cis_{para}}{cis_{dia}} = \frac{\delta_{cis} - \delta_{dia}}{\delta_{para} - \delta_{cis}} \tag{S2}$$

$$\Delta G = \Delta H - T\Delta S = -RT \ln(K) \tag{S3}$$

Table S3. Determination of intramolecular association constants of biphenyl record player (**4**) in acetonitrile-d_3 from *cis*-pyrrole proton shifts (δ_{cis}). The respective maximum shift (δ_{max}) was found by measurement in pure pyridine-d_5.

T / K	T^{-1} / K^{-1}	δ_{cis} / ppm	δ_{max} / ppm	*cis*-4_{para} / %	*cis*-4_{dia} / %	*K*	ln(K)
300.1	0.00333	41.81	54.42	72.2	27.8	2.6019	0.9562
310.0	0.00323	39.65	52.75	70.1	29.9	2.3397	0.8500
320.1	0.00312	37.70	51.27	67.9	32.1	2.1150	0.7490
330.0	0.00303	36.07	50.12	65.8	34.2	1.9267	0.6558
340.1	0.00294	34.48	48.89	63.9	36.1	1.7682	0.5700

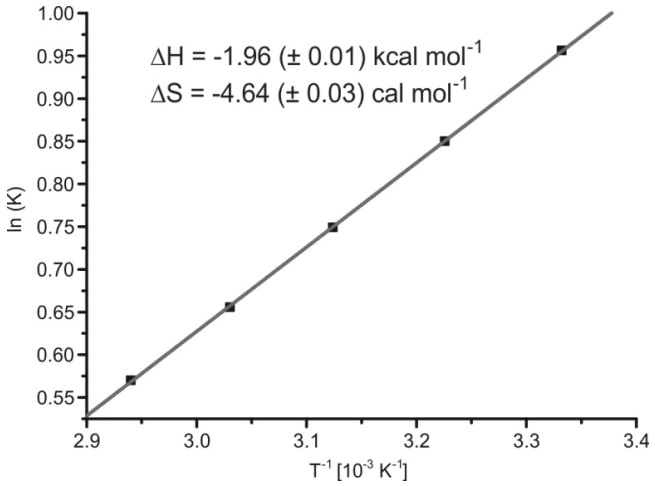

Figure S31: Gibbs free enthalpy plot for the determination of thermodynamic parameters ΔH and ΔS for the coordination event in *cis*-biphenyl rp (**4**).

Table S4. Determination of intramolecular association constants of biphenyl thioether record player (**5**) in acetonitrile-d_3 from *cis*-pyrrole proton shifts (δ_{cis}). The respective maximum shift (δ_{max}) was found by measurement in pure pyridine-d_5.

T / K	T^{-1} / K^{-1}	δ_{cis} / ppm	δ_{max} / ppm	*cis*-5_{para} / %	*cis*-5_{dia} / %	*K*	ln(K)
300.1	0.00333	43.87	54.59	76.5	23.5	3.2528	1.1795
310.0	0.00323	41.46	52.94	73.9	26.1	2.8275	1.0394
320.0	0.00313	39.17	51.46	71.1	28.9	2.4548	0.8981
330.1	0.00303	36.96	49.99	68.2	31.8	2.1458	0.7635
340.1	0.00294	35.06	48.85	65.4	34.6	1.8898	0.6365

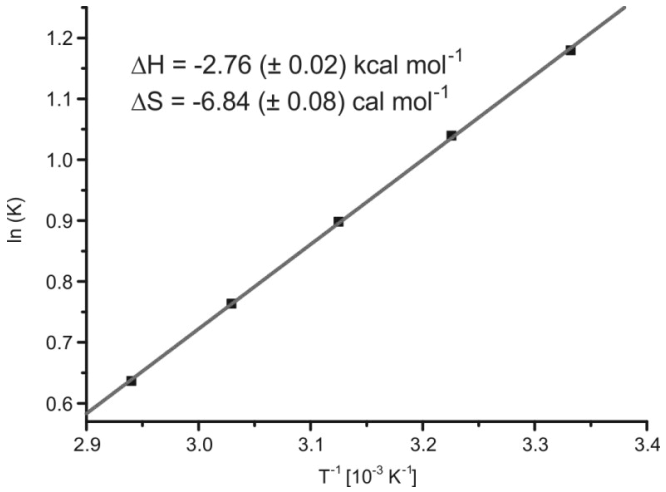

Figure S32: Gibbs free enthalpy plot for the determination of thermodynamic parameters ΔH and ΔS for the coordination event in *cis*-biphenyl thioether rp (**5**).

III.8 MRI measurements with record players 4 and 5.

MRI experiments were performed on a 7T small animal MRI system (ClinScan 70/30 USR by co. Bruker Biospin, Ettlingen, Germany). Samples of record players **4** and **5** were irradiated with the respective wavelengths (435nm or 365nm, irradiation time > 2h) and transferred into NMR tubes which were immobilized in an agarose gel phantom (1 wt.-% agarose in H_2O/D_2O, 1:1). Acetonitrile and H_2O/D_2O (1:1) in NMR tubes were placed into the phantom as well for reference measurements. We used H_2O/D_2O (1:1) instead of pure H_2O to adjust the proton density and therefore the signal strength of the phantom and reference to that of acetonitrile. Measurements were performed with an inversion recovery gradient echo sequence (scan parameters: acquisition type = 2D, TE = 6.3 ms, TR = 3000 ms, flip angle = 90°, FoV = 39 mm^2, matrix = 208×208 px, slice thickness = 2 mm, BW = 775 Hz/px, averages = 5) with varying inversion times (TI = 1500 ms, 2000 ms, 2500 ms). The obtained MR images are shown in figure S33. The signal intensities of all samples were quantified within a 0.1cm^2 area in the centre of the respective sample spot and were referenced to acetonitrile (signal intensity of acetonitrile = 100 % for every TI, see table S5). The thioether record player (**5**) allows switching of the signal intensity from 115 % (PSS-435nm) to 139-133 % (PSS-365nm) with respect to pure acetonitrile and therefore provides an MRI contrast switching efficiency of 24-18 % depending on the inversion time (TI). The biphenyl record player (**4**) switches the signal intensity from 122-123 % (PSS-435nm) to 133-128 % (PSS-365nm) and therefore provides an MRI contrast switching efficiency of 11-5 %. The highest contrast switching efficiencies (24 % for **5**, 11 % for **4**) were obtained for TI = 1500 ms.

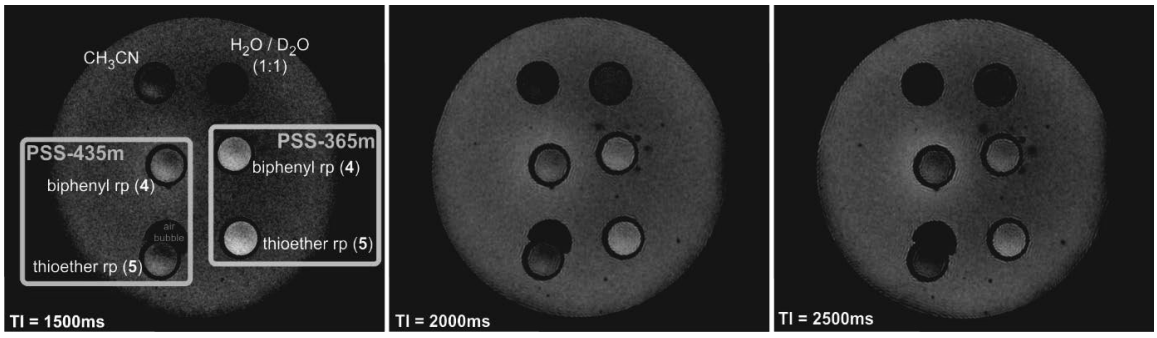

Figure S33: Magnetic resonance images (gradient echo sequence) of record players **4** (location within phantom: middle) and **5** (bottom) in both switching states, plus acetonitrile (top left) and H_2O/D_2O (1:1) (top right) as references with three different inversion times (left image: 1500 ms, middle: 2000 ms, right: 2500 ms). The samples were placed in an agarose gel phantom (1 wt.-% in H_2O/D_2O, 1:1).

Table S5: Inversion time (TI) dependent signal intensities (arbitrary units) within a 0.1cm^2 area in the center of the respective sample spot. For a better comparability the signal intensities were referenced to 100 % signal intensity of the acetonitrile reference.

	Signal intensity / a.u.			**signal intensity / %**		
TI / ms	1500	2000	2500	1500	2000	2500
acetonitrile	52.21	92.18	128.86	100	100	100
H2O / D2O (1:1)	47.77	98.94	145.40	91	107	113
4 (PSS-435nm)	63.51	113.34	158.51	122	123	123
4 (PSS-365nm)	69.69	119.92	164.34	133	130	128
5 (PSS-435nm)	59.90	105.96	148.67	115	115	115
5 (PSS-365nm)	72.34	124.38	170.99	139	135	133
noise	2.42	2.62	2.66	4.6	2.8	2.1

IV. Literature

1 S. Thies, H. Sell, C. Bornholdt, C. Schütt, F. Köhler, F. Tuczek and R. Herges, *Chem. Eur. J.*, 2012, **18**, 16358–16368.

2 C. Schütt, G. Heitmann, T. Wendler, B. Krahwinkel and R. Herges, *J. Org. Chem.*, 2016, **81**, 1206–1215.

3 *Calculated using Advanced Chemistry Development (ACD/Labs) Software V11.02 (© 1994-2016 ACD/Labs).*

4 *TURBOMOLE V6.6 2014, a development of University of Karlsruhe and Forschungszentrum Karlsruhe GmbH, 1989-2007, TURBOMOLE GmbH, since 2007; available from http://www.turbomole.com.*

5 M. F. W. Dunker, E. B. Starkey and G. L. Jenkins, *Journal of the American Chemical Society*, 1936, **58**, 2308–2309.

6 D. J. Chadwick and R. I. Ngochindo, *J. Chem. Soc. Perkin Trans. 1*, 1984, 481–486.

7 S. Thies, H. Sell, C. Schütt, C. Bornholdt, C. Näther, F. Tuczek and R. Herges, *J. Am. Chem. Soc.*, 2011, **133**, 16243–16250.

8 M. Dommaschk, C. Schütt, S. Venkataramani, U. Jana, C. Näther, F. D. Sönnichsen and R. Herges, *Dalton Trans.*, 2014, **43**, 17395–17405.

8.3 Spin State Switching in Solution with an Azoimidazole-Functionalized Nickel(II)-Porphyrin

Gernot Heitmann, Christian Schütt und Rainer Herges

Supporting Information
Eur. J. Org. Chem **2016**, *22*, 3817-3823.
http://dx.doi.org/10.1002/ejoc.201600548

Eur. J. Org. Chem. **2016** · ISSN 1099–0690

SUPPORTING INFORMATION

DOI: 10.1002/ejoc.201600548
Title: Spin State Switching in Solution with an Azoimidazole-Functionalized Nickel(II)-Porphyrin
Author(s): Gernot Heitmann, Christian Schütt, Rainer Herges*

Table of Contents

I. Computational Details

I.1 Theoretical analysis of the ideal binding situation

The ideal binding situation has been analysed in a previous study.[1] A reference structure (NiTPPHF$_{15}$·*cis*-m5p) consisting of tris-pentafluorophenyl-Ni(II)porphyrin (NiTPPHF$_{15}$) and the free ligand *cis*-1-methyl-5-phenylazoimidazole (*cis*-m5p)[2] was calculated using Turbomole 6.6.[3] The geometry optimizations were performed at the TPSSh/SVP level of theory. Single point energies using a larger basis set (TPSSh/def2TZVP) were calculated at the optimized geometries of the porphyrin, the azoimidazole and the complex to determine the stabilization energy upon binding the ligand to the Ni^{2+} (ΔH_{calc}). The reference structure NiTPPHF$_{15}$·*cis*-m5p exhibits an unstrained coordination geometry with ideal coordination parameters (Ni-N distance: 2.062 Å, deviation from orthogonal binding: 0.66°) and the maximum binding energy (ΔH_{calc} = -7.02 kcal/mol, see Figure S1).

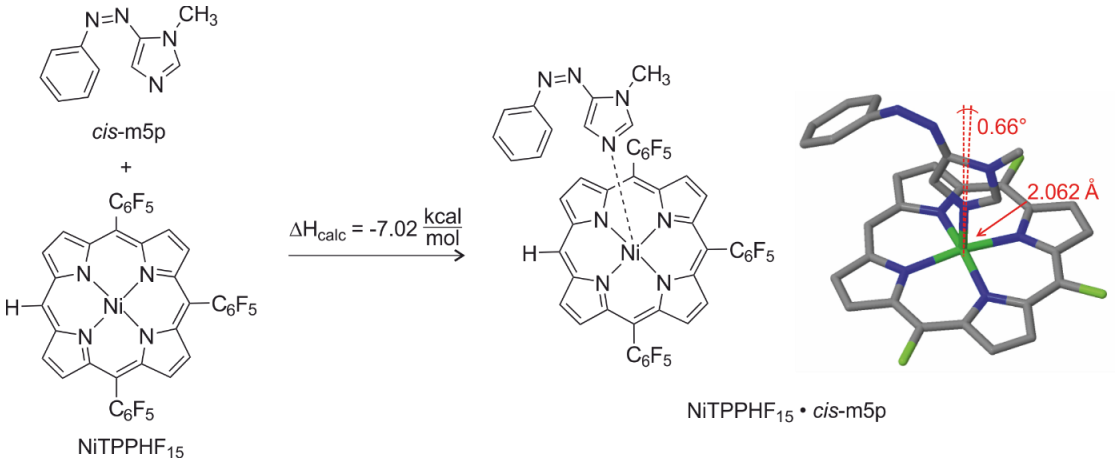

Figure S1: Coordination of free *cis*-phenylazoimidazole (*cis*-m5p) to tris-pentafluorophenyl-Ni(II)porphyrin (NiTPPHF$_{15}$) results in the reference complex (NiTPPHF$_{15}$·*cis*-m5p) which represents the ideal binding situation for imidazole "record player" molecules such as biphenyl ether "record player" **1** (for the sake of clarity, the pentafluorophenyl substituents in the calculated structure are depicted as fluorine substituents).[1]

I.2 Theoretical Description of Imidazole Biphenyl Ether Record Player 1

All calculations have been performed using Turbomole 6.6.[3] The geometry optimizations were performed at the TPSSh/SVP level of theory. Single point energies using a larger basis set (TPSSh/def2TZVP) were calculated at the optimized geometries.

*I.2.1 Energy Difference of the Magnetic Conformers of **1** in cis Configuration*

The energy difference (ΔH_{calc}) of the uncoordinated diamagnetic (*cis*-s-u) and the coordinated paramagnetic *cis* isomer (*cis*-t-k) is indicative of the amount of paramagnetic *cis* species (see Figure S2, $\Delta H_{calc} = E_{cis\text{-}t\text{-}k} - E_{cis\text{-}s\text{-}u}$). A higher difference in energy of the magnetic conformers indicates a stronger coordination of the tone arm.

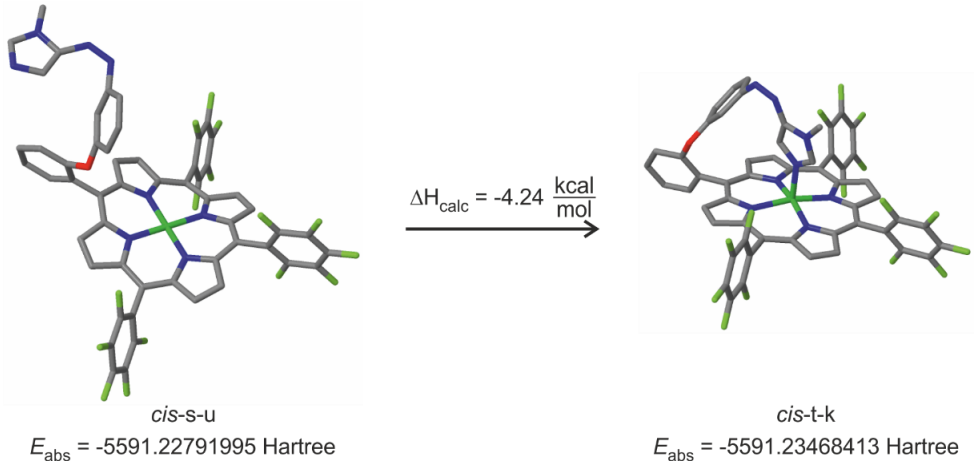

Figure S2: Intramolecular coordination in *cis* imidazole biphenyl ether "record player" **1**. According to DFT calculations (Turbomole 6.6,[3] TPSSh/def2TZVP//TPSSh/SVP) the coordinated *cis*-species (*cis*-t-k) is stabilized by 4.24 kcal/mol with regard to the uncoordinated *cis*-species (*cis*-s-u).

*I.2.2 XYZ Coordinates of TPSSh/SVP Optimized "Record Player" **1***

***cis*$_{dia}$**
$E_{TPSSh/SVP}$ = -5586.43477743 Hartree
NImag = 0

C	-0.609340	-3.314000	2.684630
N	-1.428950	-2.351790	2.141200
C	-1.315720	-4.562210	2.832110
C	-2.563960	-4.366470	2.320720
C	-2.634280	-2.981400	1.928990
C	0.759500	-3.164210	2.919150
C	1.467680	-2.058860	2.441820
C	2.906100	-1.988610	2.372250
C	3.206720	-0.878740	1.641750
C	1.954500	-0.231760	1.339730
N	0.897550	-0.962510	1.832150
Ni	-0.977890	-0.520890	1.727060

***cis*$_{para}$**
$E_{TPSSh/SVP}$ = -5586.45420976 Hartree
NImag = 0

H	-2.345210	-4.658440	-0.415500
H	-4.254340	-2.749600	-0.465690
C	-4.643100	-0.101820	-0.771860
C	-3.144000	-0.102940	-0.768500
C	-0.940400	-2.896650	-0.624280
H	4.901140	2.495370	-1.347590
H	3.004020	4.404230	-1.395010
C	0.335880	4.781290	-1.367460
H	-4.236910	2.543210	-1.144290
H	-2.316700	4.414840	-1.423590
C	-3.158330	2.399070	-1.126620
C	-2.482770	1.127930	-0.958890

N	-2.856680	-0.080850	1.640280	C	-2.186370	3.345550	-1.263200
C	-3.423620	1.172370	1.675010	C	-0.917580	2.654200	-1.173090
C	-4.860730	1.085190	1.589600	N	-1.121040	1.310960	-0.996050
C	-5.162240	-0.234090	1.434390	C	0.334940	3.292090	-1.268240
C	-3.914200	-0.951990	1.502350	C	1.583310	2.643760	-1.269300
C	1.866680	1.036350	0.758140	C	2.860280	3.326290	-1.340090
C	0.684540	1.778860	0.822510	C	3.821130	2.359730	-1.314880
C	0.606720	3.193740	0.552520	C	3.128140	1.089390	-1.233960
C	-0.638930	3.595480	0.930990	N	1.773610	1.289730	-1.203880
C	-1.347390	2.410060	1.343230	C	3.766330	-0.164010	-1.188900
N	-0.524750	1.307590	1.289700	C	5.257840	-0.183430	-1.199840
C	-2.718450	2.375620	1.610700	C	3.108660	-1.406260	-1.101040
C	-3.815050	-2.343260	1.545780	N	1.756520	-1.578450	-0.967070
H	4.186330	-0.497280	1.359430	C	1.548330	-2.929780	-0.875500
H	3.591670	-2.716370	2.802550	C	2.807050	-3.638530	-0.977690
H	1.419890	3.798710	0.156550	C	3.778230	-2.690470	-1.119430
H	-1.059980	4.598750	0.899900	H	4.849050	-2.847430	-1.241900
H	-6.142890	-0.690390	1.311400	H	2.930530	-4.720420	-0.952850
H	-5.541870	1.934320	1.602170	C	0.301370	-3.552550	-0.692920
H	-0.891360	-5.477500	3.241690	C	-2.211150	-3.580420	-0.495350
H	-3.383170	-5.079810	2.245760	C	-3.175490	-2.617170	-0.520430
C	1.491400	-4.284210	3.574450	C	-2.490360	-1.346690	-0.654990
C	-5.026610	-3.168120	1.276340	N	-1.133740	-1.543660	-0.713030
C	3.089830	1.635130	0.144580	Ni	0.342150	-0.107860	-0.747920
C	-3.492140	3.647950	1.677810	N	0.549800	0.005620	1.298910
C	-3.968550	4.133560	2.902680	C	-0.459380	0.300230	2.156990
C	-4.731460	5.300620	2.985940	C	1.576110	-0.420620	2.037170
C	-5.031950	6.009780	1.820970	N	1.268520	-0.420670	3.344860
C	-4.570630	5.550580	0.585390	C	-0.049710	0.031340	3.466590
C	-3.810840	4.380760	0.526740	C	2.132280	-0.830670	4.447720
F	-3.700590	3.473580	4.028190	H	-1.408940	0.674960	1.790130
F	-5.170800	5.740600	4.161960	H	2.543600	-0.732690	1.644830
F	-5.758660	7.119530	1.885210	N	-0.541220	0.065540	4.766990
F	-4.863940	6.225900	-0.523040	H	3.125170	-1.062410	4.035500
F	-3.394920	3.959360	-0.666730	H	1.713030	-1.719610	4.942480
C	-6.026010	-3.363500	2.237420	H	2.207850	-0.016510	5.183060
C	-7.164140	-4.127640	1.969960	N	-1.701190	0.426250	5.086900
C	-7.316710	-4.716370	0.712380	C	-2.644550	0.828630	4.092240
C	-6.333910	-4.543050	-0.264310	C	-2.924860	2.196510	3.944110
C	-5.204160	-3.776120	0.026860	C	-3.310020	-0.129250	3.317370
F	-5.904830	-2.809580	3.443140	C	-4.213690	0.296430	2.336620
F	-8.099840	-4.297790	2.900330	C	-4.494180	1.659170	2.162520
F	-8.396770	-5.440640	0.443070	C	-3.846480	2.596290	2.974090
F	-6.483230	-5.103540	-1.461410	H	-2.410290	2.925260	4.574350
F	-4.283630	-3.622300	-0.922620	H	-3.100280	-1.195050	3.429070
C	3.832110	2.647720	0.775230	O	-4.797710	-0.691220	1.581230
C	4.968550	3.194410	0.171100	H	-5.211130	1.979440	1.403660
C	5.382220	2.723170	-1.080550	H	-4.064370	3.660160	2.841910
C	4.669190	1.707840	-1.723350	C	-5.409800	-0.372390	0.381320
C	3.529520	1.168700	-1.111370	C	-5.341290	0.138860	-1.970050
C	2.309270	-5.161810	2.849960	C	-6.737850	0.109840	-2.024490
C	2.979830	-6.221760	3.463540	C	-7.474170	-0.168150	-0.868060
C	2.832170	-6.425810	4.837440	C	-6.807200	-0.407060	0.336350
C	2.018490	-5.572320	5.585690	H	-4.763590	0.336800	-2.877730
C	1.359260	-4.518040	4.950200	H	-8.567120	-0.199610	-0.900830
F	2.459290	-5.002260	1.535260	H	-7.352150	-0.627450	1.257370

F	3.748830	-7.038510	2.748010	C	0.305840	-5.040520	-0.553250
F	3.463580	-7.430880	5.432800	C	0.366940	-5.643490	0.708510
F	1.879140	-5.767080	6.894350	C	0.409060	-7.030420	0.863040
F	0.588410	-3.722740	5.689430	C	0.383040	-7.847590	-0.269440
H	3.505750	3.003550	1.756660	C	0.318120	-7.275010	-1.541650
H	6.274060	3.137160	-1.560190	C	0.278810	-5.884510	-1.669750
H	4.995770	1.327880	-2.694550	F	0.395920	-4.886060	1.806110
O	2.834500	0.114880	-1.654820	F	0.478280	-7.576030	2.075600
C	2.533700	0.041990	-2.995660	F	0.422980	-9.169040	-0.136260
C	2.281800	1.175400	-3.774180	F	0.296790	-8.054790	-2.619620
C	2.417370	-1.245420	-3.538360	F	0.221340	-5.366080	-2.895420
C	2.029860	-1.390120	-4.872480	C	-0.014830	5.580610	-0.270750
C	1.764840	-0.271380	-5.669350	C	-0.014400	6.974900	-0.341530
C	1.914640	1.010830	-5.120280	C	0.343830	7.603380	-1.536130
H	2.356110	2.176840	-3.344350	C	0.696140	6.835480	-2.648070
H	2.613210	-2.109000	-2.899200	C	0.688890	5.441890	-2.552160
H	1.926520	-2.393230	-5.296850	F	1.031000	7.435490	-3.788210
H	1.448680	-0.377080	-6.709690	F	1.027340	4.737330	-3.631110
N	1.562350	2.150370	-5.901290	F	-0.357740	5.012080	0.886130
N	2.425840	2.973690	-6.296800	F	-0.346780	7.706840	0.719680
C	3.795280	2.827960	-6.137770	F	0.348730	8.929780	-1.614390
N	4.565340	3.925630	-6.528750	C	5.980590	-0.522330	-0.048140
C	4.736120	1.838300	-5.806970	C	7.375760	-0.545790	-0.025470
N	5.997520	2.304850	-5.973480	C	8.084570	-0.220800	-1.184450
C	5.859410	3.556650	-6.394790	C	7.395240	0.121420	-2.349840
C	4.047430	5.218590	-6.954980	C	5.998100	0.135140	-2.346180
H	4.545820	0.816270	-5.484660	F	8.073310	0.427400	-3.452630
H	6.681890	4.239220	-6.615670	F	5.369130	0.461470	-3.473810
H	3.733530	5.817740	-6.083890	F	5.330100	-0.829470	1.081520
H	3.176030	5.057960	-7.605270	F	8.033640	-0.866420	1.086700
H	4.840710	5.750320	-7.501540	F	9.412710	-0.237000	-1.177270
H	5.532730	3.980990	0.679920	H	-7.248660	0.293050	-2.974140

II. NMR Spectra

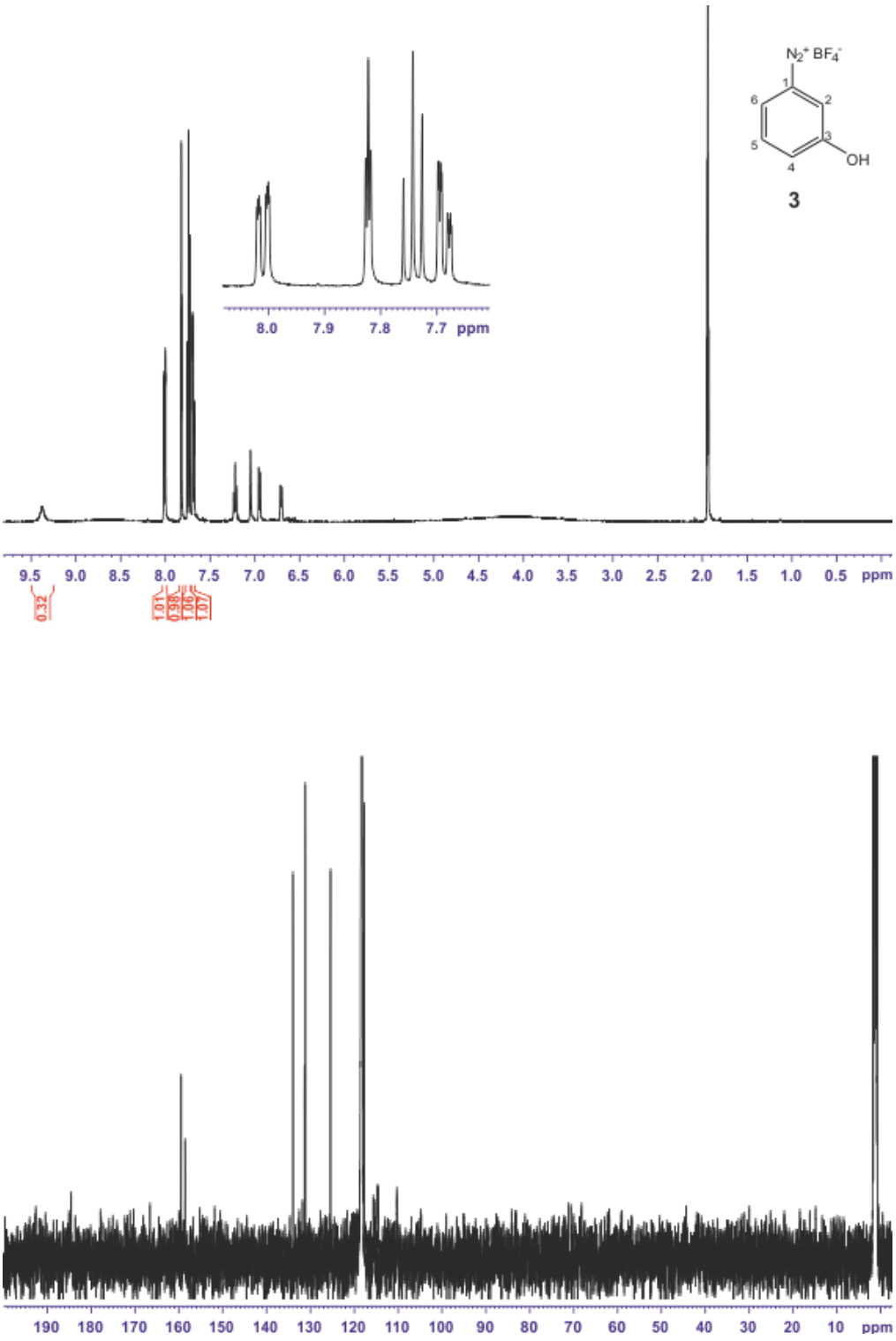

Figure S3: ^{1}H NMR (top) and ^{13}C NMR (bottom) of 3-Hydroxybenzenediazonium tetrafluoroborate (**3**). Spectra were measured in CD_3CN at 300 K.

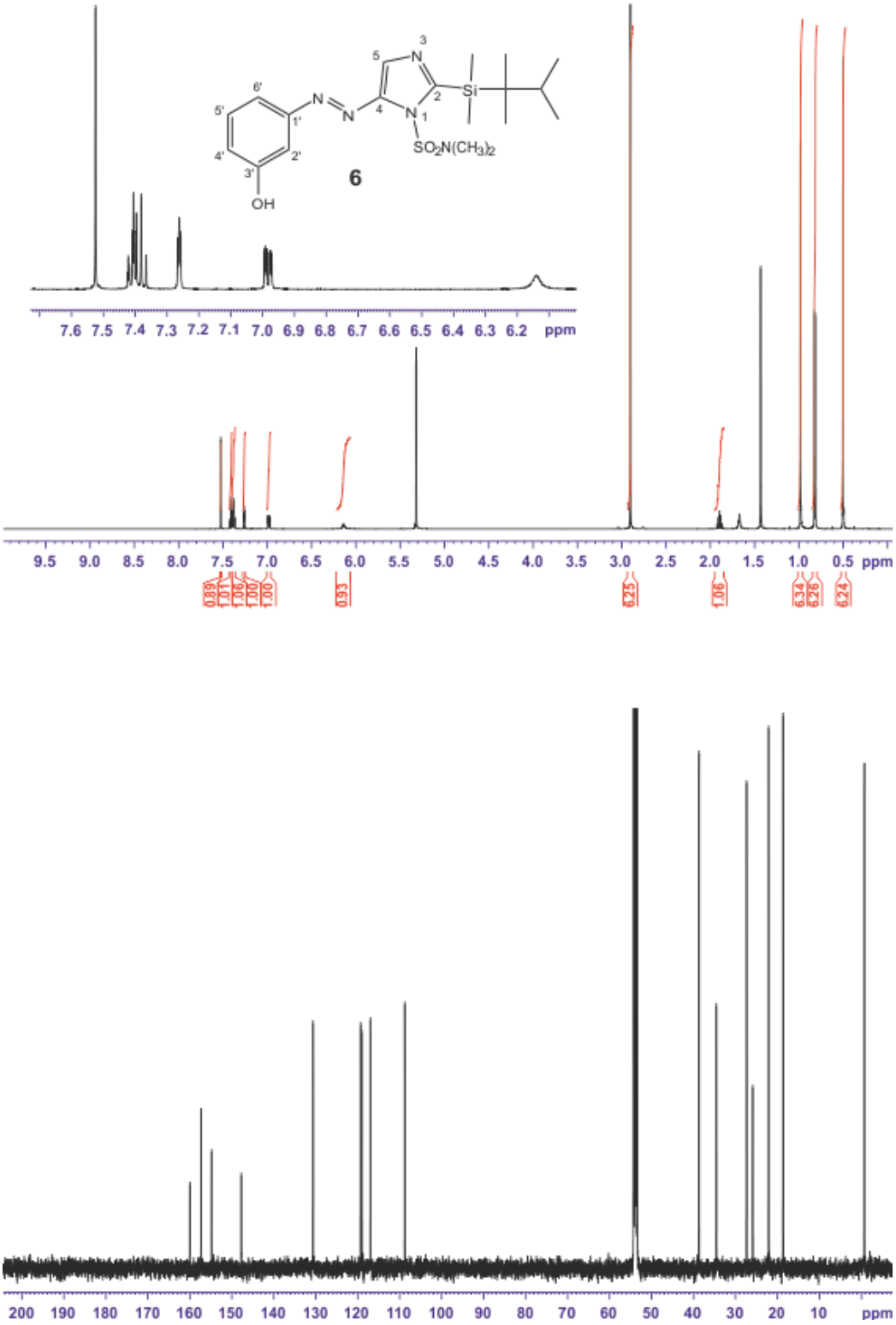

Figure S4: ^{1}H NMR (top) and ^{13}C NMR (bottom) of 5-(3'-Hydroxyphenylazo)-1-(*N*,*N*-dimethylsulfamoyl)-2-(dimethylthexylsilyl)imidazole (**6**). Spectra were measured in CD_2Cl_2 at 300 K.

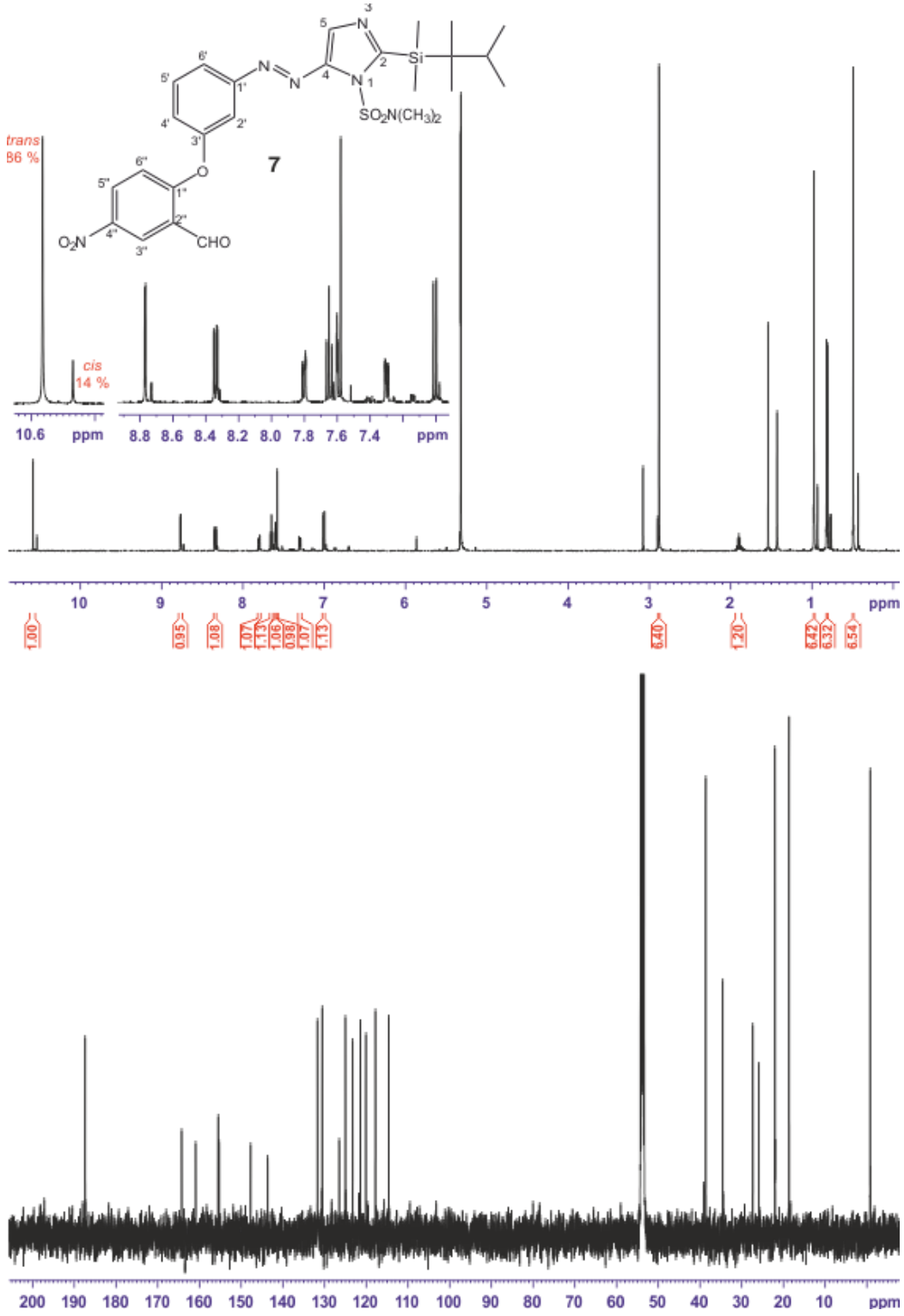

Figure S5: ^{1}H NMR (top) and ^{13}C NMR (bottom) of 5-(3'-(2''-Formyl-4''nitrophenoxy)phenylazo)-1-(N,N-dimethylsulfamoyl)-2-(dimethylthexylsilyl)imidazole (**7**). Spectra were measured in CD_2Cl_2 at 300 K.

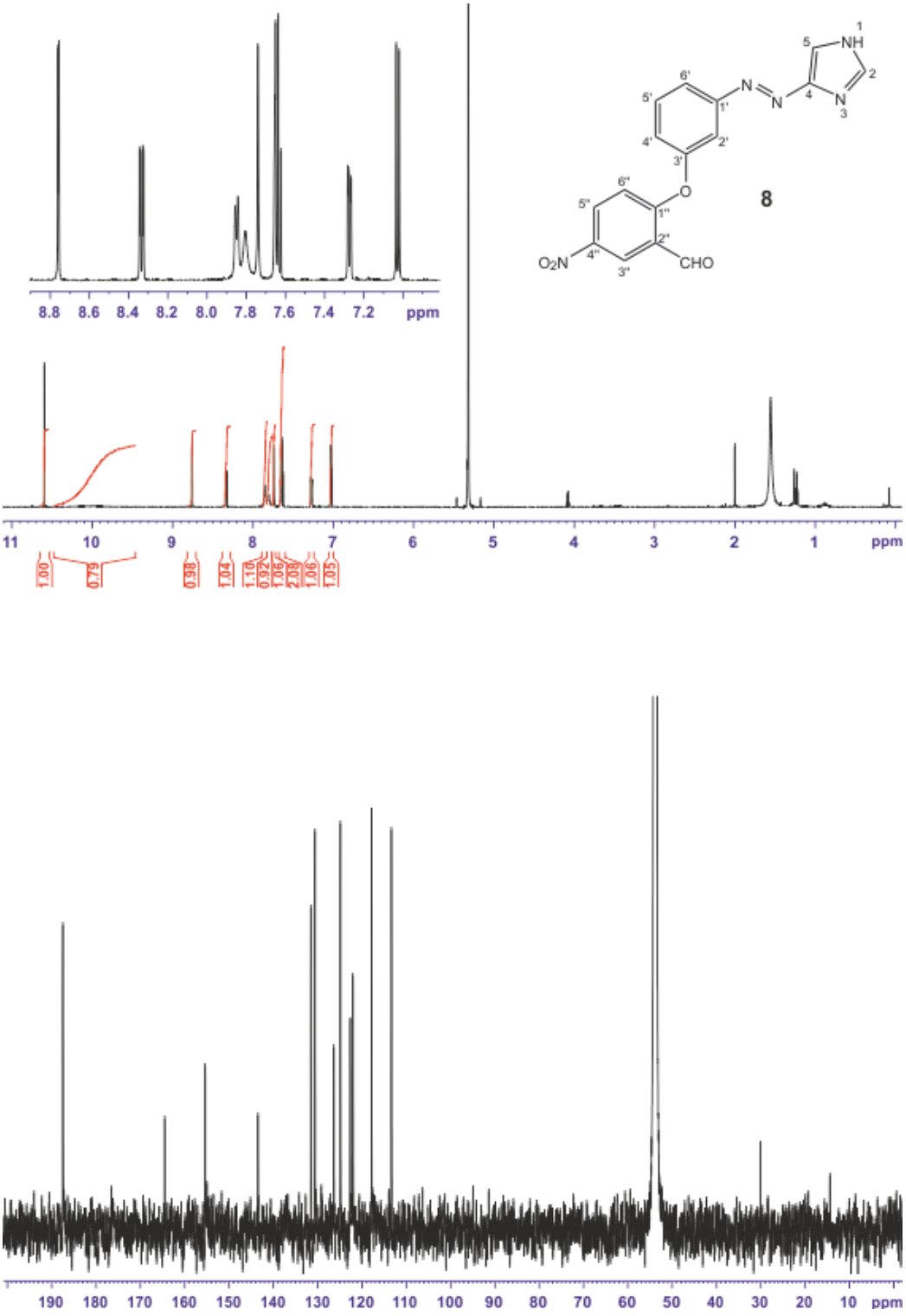

Figure S6: ^{1}H NMR (top) and ^{13}C NMR (bottom) of 4(5)-(3'-(2''-Formyl-4''nitrophenoxy)-phenylazo)imidazole (**8**). Spectra were measured in CD_2Cl_2 at 300 K.

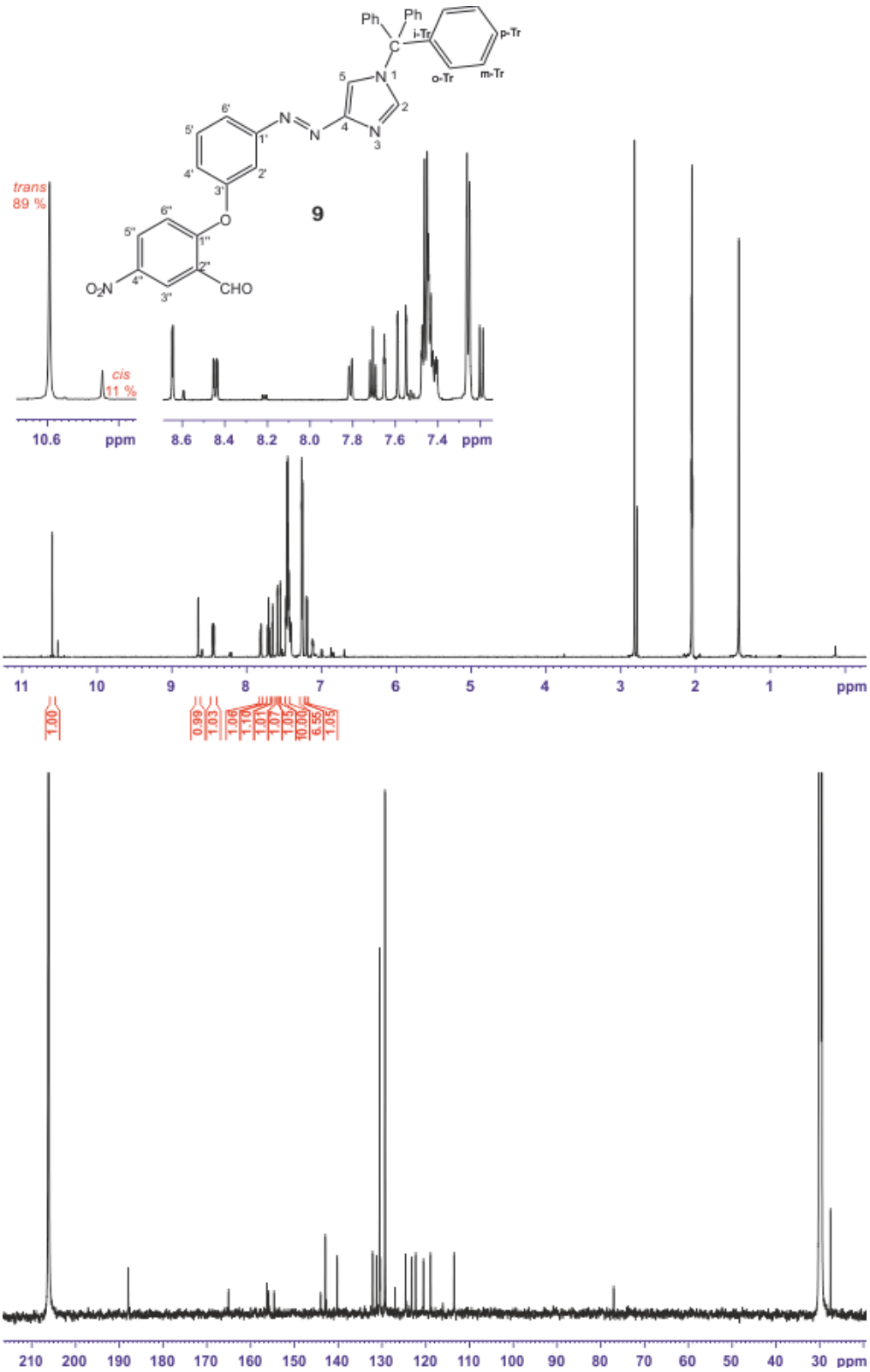

Figure S7: ^{1}H NMR (top) and ^{13}C NMR (bottom) of 4-(3'-(2''-Formyl-4''nitrophenoxy)phenylazo)-1-(triphenylmethyl)imidazole (**9**). Spectra were measured in acetone-d_6 at 298 K.

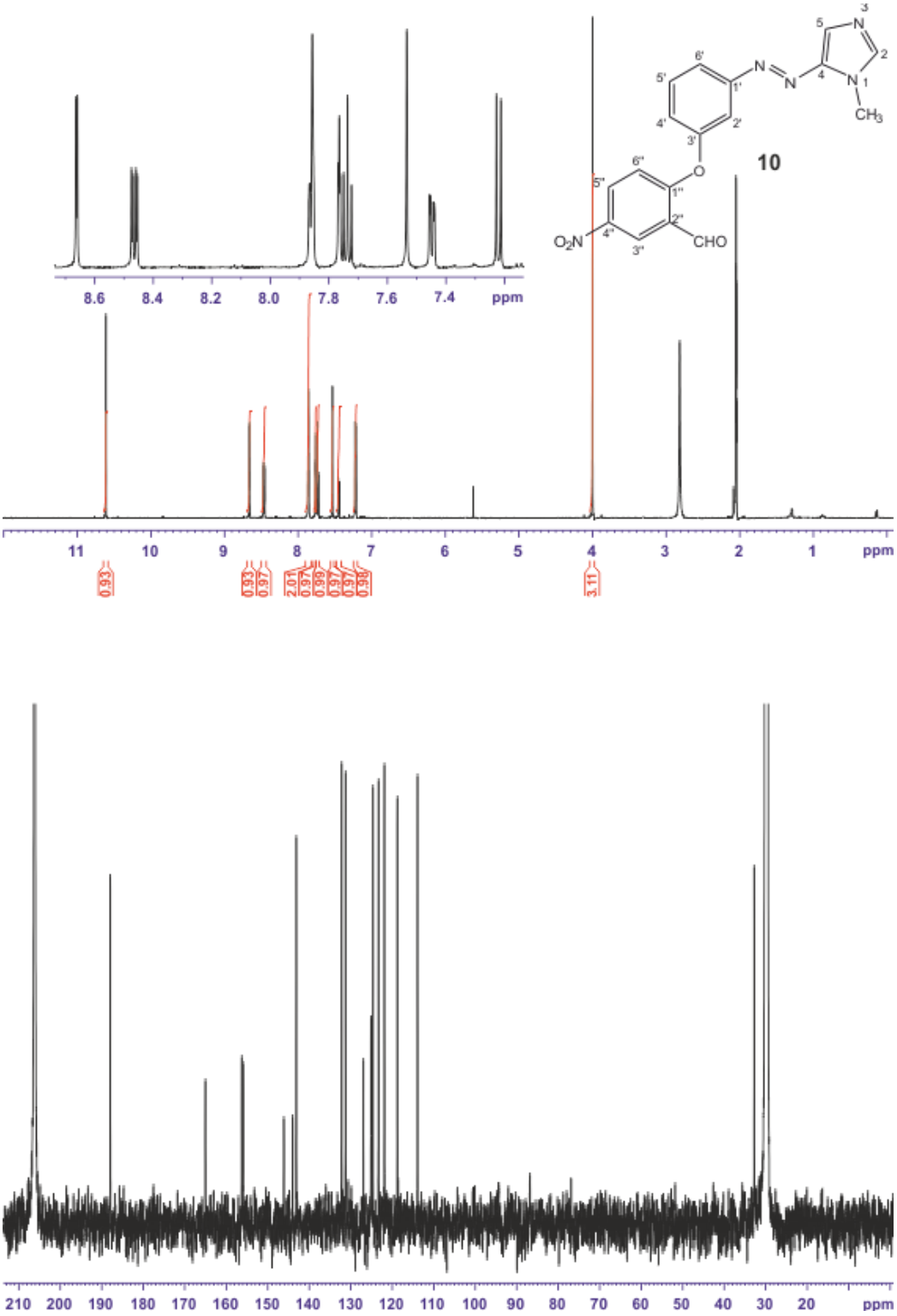

Figure S8: ^{1}H NMR (top) and ^{13}C NMR (bottom) of 5-(3′-(2″-Formyl-4″-nitrophenoxy)phenylazo)-1-methylimidazole (**10**). Spectra were measured in acetone-d_6 at 298 K.

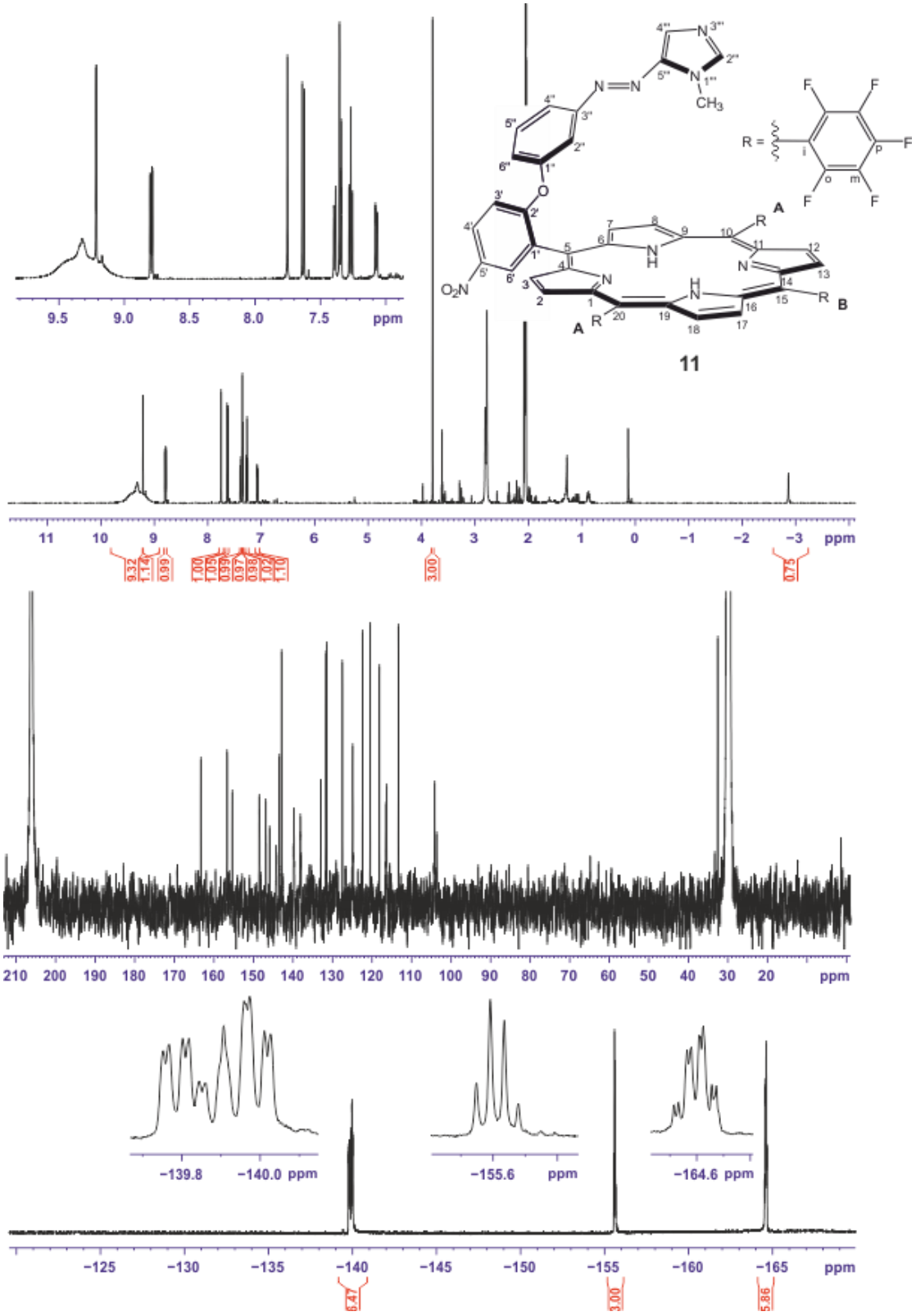

Figure S9: ^{1}H NMR (top), ^{13}C NMR (middle) and ^{19}F NMR (bottom) of metal-free record player **11**. Spectra were measured in acetone-d_6 at 300 K.

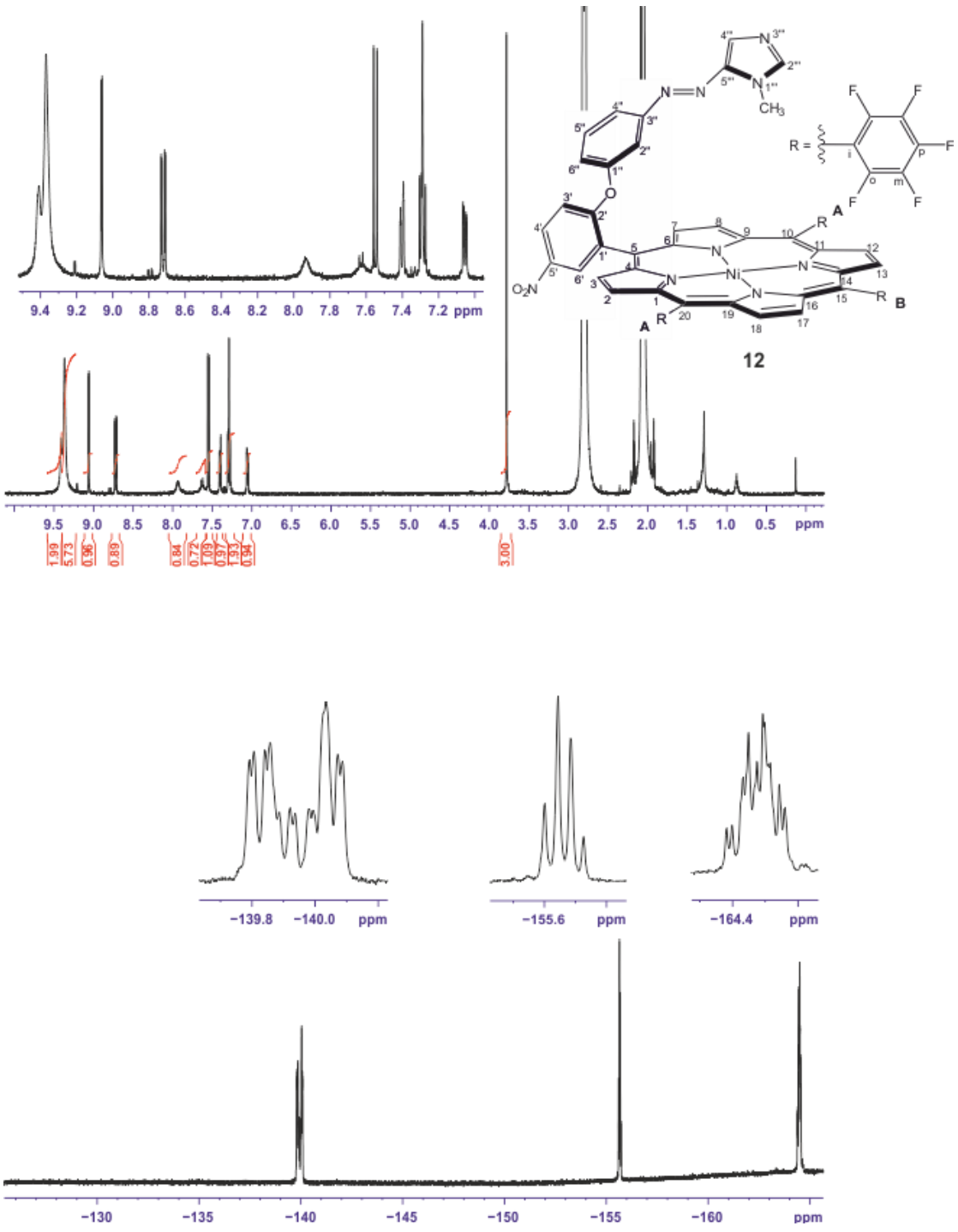

Figure S10: ^{1}H NMR (top) and ^{19}F NMR (bottom) of record player **12**. Spectra were measured in acetone-d_6 at 300 K.

III. Literature

[1] G. Heitmann, C. Schütt, J. Gröbner, L. Huber, R. Herges, *Dalton Trans.* **2016**.

[2] C. Schütt, G. Heitmann, T. Wendler, B. Krahwinkel, R. Herges, *J. Org. Chem.* **2016**, *81*, 1206–1215.

[3] *TURBOMOLE V6.6 2014, a development of University of Karlsruhe and Forschungszentrum Karlsruhe GmbH, 1989-2007, TURBOMOLE GmbH, since 2007; available from http://www.turbomole.com.*

8.4 Modular Synthetic Route to Monofunctionalized Porphyrin Architectures.

Gernot Heitmann, Marcel Dommaschk, Roland Löw und Rainer Herges

Supporting Information
Org. Lett. **2016**, *18*, 5228-5231.
http://dx.doi.org/10.1021/acs.orglett.6b02507

A Modular Synthetic Route to Monofunctionalized Porphyrin Architectures.

Gernot Heitmann, Marcel Dommaschk, Roland Löw and Rainer Herges

Table of Contents

I. Synthesis of halogenated azo compounds 6, 8 and 9

I.1 Synthesis of azobenzenes 6

The iodinated azobenzenes **6** were prepared according to a literature-known procedure.[1] Nitrosobenzene was reacted with the respective iodo aniline in a Mills reaction under acidic conditions (see scheme S1).

Scheme S1. Synthesis of iodinated azobenzenes 6.

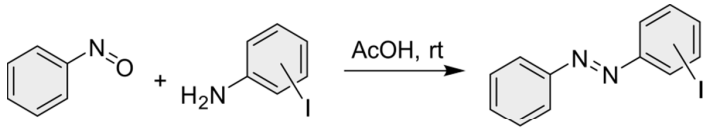

o-I (**6a**): **29 %**
m-I (**6b**): **97 %**
p-I (**6c**): **83 %**

I.2 Synthesis of azopyridines 8

Azopyridine-based switching units **8a** and **8d** are obtained via a Mills reaction under basic conditions of *in-situ* prepared 3-bromonitrobenzene with the respective 3-aminopyridine (see scheme S2). The chlorinated azopyridine **8d** gives the ether-functionalized azopyridines **8b** and **8c** upon nucleophilic aromatic substitution with the respective alcohol.

Scheme S2. Synthesis of azopyridine switching units 8.

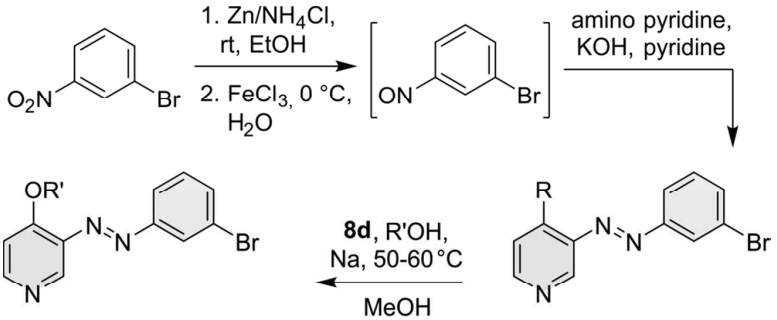

R = Me (**8b**): **97 %**
*i*Pr (**8c**): **91 %**

R = H (**8a**): **35 %**
Cl (**8d**): **65 %**

I.3 Synthesis of azoimidazoles 9

The synthesis of azoimidazole-based switching units **9** (see Scheme S3) starts from *N*,*N*-dimethylsulfamoyl protected imidazole which is *in-situ* silyl-protected in 2-position and consequently reacted with the respective diazonium salt after *in-situ* lithiation in 5-position. After stepwise deprotection an unsubstituted azoimidazole is obtained, which is regioselectively trityl-protected to give a 1,4-substitution pattern on the imidazole ring. Subsequent methylation and trityl-deprotection yields the desired 1-methyl-5-phenylazoderivatives **9a** and **9b**. The fluorinated derivative **9b** can further be modified by nucleophilic aromatic substitution with an alcohol, which gives the ether derivatives **9c** and **9d**.

Scheme S3. Synthesis of azo-*N*-methylimidazole switching units 9.

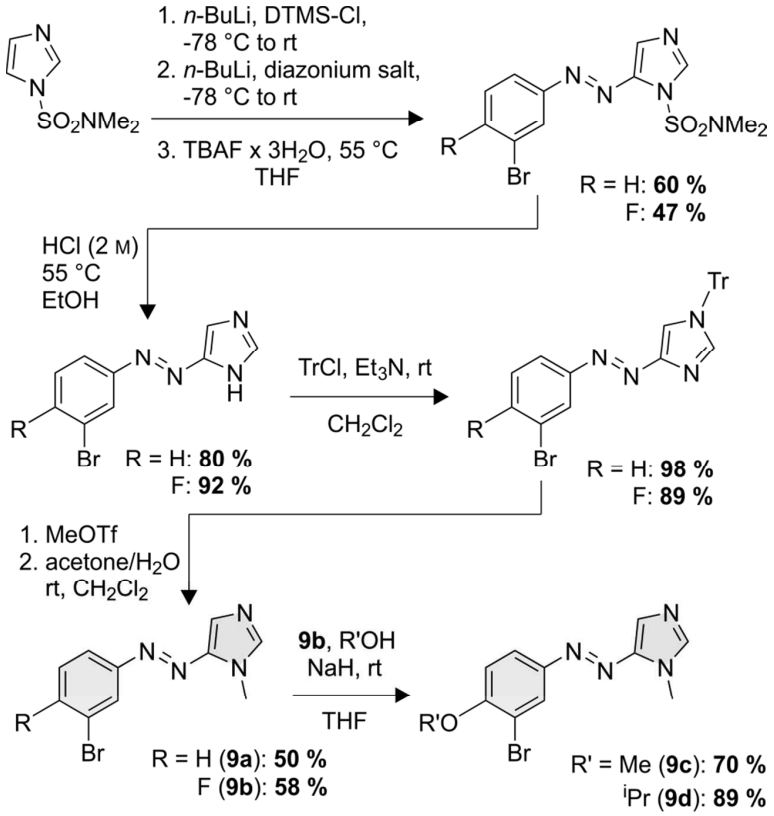

II. Experimental Section

II.1 General Information

Commercially available solvents and starting materials were used as received. THF was distilled from benzophenone-Na. Dichloromethane was distilled from CaH_2. Column chromatography was carried out using 0.04 – 0.063 mm mesh silica gel (Merck). R_f values were determined by thin layer chromatography on Polygram® Sil G/UV_{254} (Macherey-Nagel, 0.2 mm particle size).

NMR spectra were measured in Schott Economic NMR tubes using deuterated solvents (Deutero). The degree of deuteration is given in parentheses. Chemical shifts are calibrated to residual protonated solvent signals (^{1}H: δ (acetone-d_6) = 2.05 ppm, δ (DMSO-d_6) = 2.50 ppm, δ ($CDCl_3$) = 7.26 ppm, δ (CD_2Cl_2) = 5.32 ppm, δ (methanol-d_4) = 3.31 ppm; ^{13}C: δ (acetone-d_6) = 29.84 ppm, δ (DMSO-d_6) = 39.52 ppm, δ ($CDCl_3$) = 77.16 ppm, δ (CD_2Cl_2) = 53.84 ppm, δ (methanol-d_4) = 49.00 ppm; deuteration grade 99.8 %). Reference for ^{19}F NMR spectra is CCl_3F to which the spectrometer frequency is calibrated. The signal multiplicities are abbreviated as s (singlet), d (doublet), t (triplet), q (quartet), quint (quintet), m (multiplet) and br (broad signal). ^{13}C NMR and ^{19}F NMR spectra were measured ^{1}H-decoupled. Measurements were performed with a Bruker DRX 500 (^{1}H NMR: 500 MHz, ^{13}C NMR: 125 MHz, ^{19}F NMR: 470 MHz, ^{11}B NMR: 160 MHz) and a Bruker AV 600 (^{1}H NMR: 600 MHz, ^{13}C NMR: 150 MHz).

The high resolution (HR) mass spectra were measured with an AccuTOF by co. Jeol (EI). Low resolution mass spectra were measured with an AccuTOF by co. Jeol (EI), a LCQ Classic by co. Thermo Finnigan (ESI) or an AutoflexSpeed by co. Bruker (MALDI-TOF).

Infrared spectra were recorded on a Perkin-Elmer ATR spectrometer with a Golden-Gate-Diamond-ATR A531-G for neat samples. Signal intensities were abbreviated with w (weak), m (medium), s (strong) and vs (very strong). Broad signals are additionally labeled with br.

UV-visible absorption spectra were recorded on a Perkin-Elmer Lambda-14 spectrophotometer with a Büchi thermostat using quartz cells of 1 cm path length.

The amount of carbon, hydrogen, sulfur and nitrogen in a compound was determined with a CHNS-Elementaranalysator Euro EA 3000 Series by co. Euro Vector.

Melting points were measured with a Melting Point B-540 (Büchi).

II.2 Synthetic procedures

General Procedure A: Suzuki cross coupling of precursor 5 with azobenzenes 6 and azopyridines 8. The porphyrin precursor **5** and the halogenated azo compound (1.3-2.0 equiv.) were weighted out in a round-bottomed flask and set under nitrogen atmosphere. Toluene (4.4 mL per 28.1 µmol **5**) and Ethanol (1.6 mL per 28.1 µmol **5**) were added and the solution was treated with aqueous (1 mL per 28.1 µmol **5**) potassium carbonate (3.3 equiv.) and catalytic amounts of tetrakis(triphenylphosphine)palladium(0). The reaction mixture was stirred at 90-95 °C overnight under an atmosphere of nitrogen. After cooling to room temperature water was added and the mixture was extracted with dichloromethane twice. The combined organic layer were dried over magnesium sulfate and the solvent was removed under reduced pressure.

General Procedure B: Suzuki cross coupling of precursor 5 with azoimidazoles 9. The porphyrin precursor **5** and the azoimidazole-based switching unit (1.3-1.6 equiv.) were weighted out in a round-bottomed flask and set under nitrogen atmosphere. Dry 1,4-dioxane (~12 mL per 50 µmol **5**) was added and the solution was treated with aqueous (1.3 mL per 50 µmol **5**) cesium carbonate (3 equiv.) and catalytic amounts of $PdCl_2$(dppf). The reaction mixture was stirred at 90-95 °C overnight under an atmosphere of nitrogen. After cooling down to room temperature an excess of ethyl acetate was added and the mixture was filtrated over diatomaceous earth. The organic layer was washed twice with water, dried over magnesium sulfate and the solvent was removed under reduced pressure.

5-(Phenyl-2'-(boronic acid pinacol ester))-10,15,20-tris(pentafluorophenyl)-porphyrin (4). A solution of 2-formylphenylboronic acid pinacol ester (**1**) (564 mg, 2.43 mmol), pentafluoro-benzaldehyde (**2**) (1.42 g, 7.29 mmol) and freshly distilled pyrrole (**3**) (700 µL, 10.1 mmol) in degassed dichloromethane (400 mL) was treated with borontrifluoride diethyl etherate (150 µL, 1.19 mmol) and the reaction mixture was stirred overnight at 37 °C under an atmosphere of nitrogen. Chloranil (1.90 g, 7.73 mmol) was added and stirring at 37 °C was continued overnight. The reaction mixture was filtrated over diatomaceous earth and the solvent was removed in vacuo. Purification via column chromatography on silica gel (*n*-pentane/dichloromethane, 9:1 → 6:4, R_f = 0.20) gave a purple solid (580 mg, 574 µmol, 24 %).

Mp: 221 °C.

FT-IR (layer): υ = 3324 (w), 3316 (w), 2977 (w), 1650 (w), 1595 (w), 1567 (w), 1517 (s), 1495 (vs), 1480 (s), 1437 (m), 1402 (m), 1387 (m), 1353 (s), 1317 (s), 1267 (m), 1246 (w), 1230 (w), 1165 (m), 1143 (m), 1116 (m), 1082 (m), 1072 (m), 1061 (m), 1043 (m), 985 (vs), 936 (m), 918 (vs), 857 (m), 832 (w), 804 (s), 758 (s), 750 (s), 738 (s), 703 (m), 660 (m), 636 (m), 580 (m), 569 (m), 556 (w), 548 (w), 539 (w), 528 (w), 518 (m), 503 (w), 496 (m), 483 (w), 469 (w), 427 (m), 412 (m) cm^{-1}.

^{1}H NMR (500 MHz, acetone-d_6, 300 K): δ = 9.30 (s, br, 4H, Por*H*,), 9.17 (s, br, 2H, Por*H*), 8.80 (d, ^{3}J = 3.75 Hz, 2H, Por*H*), 8.34-8.28 (m, 1H, PorCC*H*), 8.23-8.17 (m, 1H, PorCCC*H*), 7.95-7.86 (m, 2H, PorCCCHC*H*, PorCCHC*H*), 0.14 (s, 12H, 4x -CH_3) ppm.

^{13}C NMR (125 MHz, acetone-d_6, 300 K): δ = 147.1 (Por*C*), 135.6 (PorC*C*H), 134.7 (PorCC*C*H), 129.7 (PorCCH*C*H), 128.7 (PorCCCH*C*H), 126.2 (PorC*C*), 83.6 (-*C*(CH_3)$_2$), 23.9 (-C(*C*H_3)$_2$) ppm. The C atoms of the porphyrin and the C atoms of the pentafluorophenyl substituents cannot be assigned.

^{19}F NMR (470 MHz, acetone-d_6, 300 K): δ = -139.83 to -139.96 (m, 2F, Por-Ar-*o*-*F*), -140.00 (dd, ^{3}J = 23.7 Hz, ^{4}J = 7.81 Hz, 2F, Por-Ar-*o*-*F*), -140.21 (dd, ^{3}J = 23.8 Hz, ^{4}J = 7.79 Hz, 2F, Por-Ar-*o*-*F*), -155.80 (t, ^{3}J = 20.4 Hz, 3F, Por-Ar-*p*-*F*), -164.56 to -164.89 (m, 6F, Por-Ar-*m*-*F*) ppm.

^{11}B NMR (160 MHz, CD_2Cl_2, 300 K): δ = 30.45 (s, 1B, -*B*Pin) ppm.

HR-MS (EI, TOF-Q): m/z $[M]^{+\cdot}$ calcd for $C_{50}H_{26}F_{15}BN_4O_2$, 1010.1909; found 1010.1889 (-2.0 ppm).

Anal. Calcd for $C_{50}H_{26}BF_{15}N_4O_2$: C, 59.43; H, 2.59; N, 5.54. Found: C, 59.64; H, 2.60; N, 5.57.

5-(Phenyl-2'-(boronic acid pinacol ester))-10,15,20-tris(pentafluorophenyl)-Ni(II)-porphyrin (5). The metal free precursor porphyrin **4** (426 mg, 422 µmol) was dissolved in toluene (45 mL) and treated with nickel(II)acetylacetonate (1.08 g, 4.22 mmol). The resulting mixture was stirred at reflux and the progress of the reaction was followed by MALDI-TOF-MS. After 4 days, no starting material was detectable and the reaction mixture was evaporated to dryness. Purification via column chromatography on silica gel (chloroform, R_f = 0.73) gave a purple solid (420 mg, 394 µmol, 93 %).

Mp: 207 °C.

FT-IR (layer): υ = 2978 (w), 1652 (w), 1595 (w), 1519 (s), 1487 (s), 1434 (m), 1350 (s), 1320 (m), 1270 (w), 1215 (w), 1168 (w), 1144 (m), 1117 (w), 1077 (m), 1061 (m), 1006 (m), 987 (vs), 960 (m), 941 (s), 928 (s), 857 (m), 842 (m), 802 (m), 764 (s), 745 (m), 726 (m), 702 (m), 660 (m), 544 (w), 491 (w), 412 (w) cm^{-1}.

^{1}H NMR (500 MHz, acetone-d_6, 300 K): δ = 9.19-9.15 (m, 4H, Por*H*,), 9.05 (d, ^{3}J = 4.95 Hz, 2H, Por*H*), 8.80 (d, ^{3}J = 5.00 Hz, 2H, Por*H*), 8.25 (ddd, ^{3}J = 7.43 Hz, ^{4}J = 1.22 Hz, ^{4}J = 0.60 Hz, 1H, PorCC*H*), 8.08 (ddd, ^{3}J = 7.49 Hz, ^{4}J = 1.63 Hz, ^{4}J = 0.60 Hz, 1H, PorCCC*H*), 7.88 (td, ^{3}J = 7.52 Hz, ^{4}J = 1.58 Hz, 1H, PorCCHC*H*), 7.82 (td, ^{3}J = 7.51 Hz, ^{4}J = 1.23 Hz, 1H, PorCCCHC*H*), 0.14 (s, 12H, 4x -CH_3) ppm.

^{13}C NMR (125 MHz, acetone-d_6, 300 K): δ = 146.1 (Por*C*CH), 145.6 (*C*-Por), 144.2 (*C*-Por), 143.9 (*C*-Por), 143.7 (*C*-Por), 135.2 (*C*H-Por), 134.6 (PorCC*C*H), 134.2 (PorC*C*H), 133.5 (*C*H-Por), 133.2 (*C*H-Por), 132.3 (*C*H-Por), 129.8 (PorCCH*C*H), 128.7 (PorCCCH*C*H), 124.6 (PorC*C*CH), 103.6 (*C*-

Por), 102.8 (*C*-Por), 83.5 (-*C*(CH_3)$_2$), 23.9 (-C(*C*H_3)$_2$) ppm. The the C atoms of the pentafluorophenyl substituents could not be assigned.

^{19}F NMR (470 MHz, acetone-d_6, 300 K): δ = -139.94 (dd, ^3J = 24.0 Hz, ^4J = 7.75 Hz, 1F, Por-Ar-*o*-*F*), -140.09 to -140.30 (m, 5F, Por-Ar-*o*-*F*), -155.86 (t, ^3J = 20.4 Hz, 3F, Por-Ar-*p*-*F*), -164.51 to -164.74 (m, 6F, Por-Ar-*m*-*F*) ppm.

^{11}B NMR (160 MHz, CD_2Cl_2, 300 K): δ = 30.27 (s, 1B, -*B*Pin) ppm.

HR-MS (EI, TOF-Q): m/z $[M]^{\bullet+}$ calcd for $C_{50}H_{24}F_{15}BN_4O_2Ni$, 1066.1106; found 1066.1109 (+0.2 ppm).

UV-vis (CH_3CN): λ_{max} (lg ε) = 294 (4.146), 403 (5.357), 522 (4.193), 556 (4.003) nm.

Anal. Calcd for $C_{50}H_{24}BF_{15}N_4O_2Ni$: C, 56.27; H, 2.27; N, 5.25. Found: C, 56.90; H, 2.25; N, 5.34.

***o*-Iodoazobenzene (6a).**[1] 2-Iodoaniline (3.65 g, 16.7 mmol) and nitrosobenzene (3.26 g, 30.4 mmol) were stirred in acetic acid (180 mL) overnight at room temperature. The solvent was removed under reduced pressure. The crude product was purified via column chromatography on silica gel (*n*-pentane/dichloromethane, 3:1). The product was obtained as a red solid (1.48 g, 4.80 mmol, 29 %).

^{1}H NMR (500 MHz, $CDCl_3$, 300 K): δ = 8.04 (dd, ^3J = 7.9 Hz, ^4J = 1.3 Hz, 1H, ICC*H*), 8.02 (d, ^3J = 7.7 Hz, 2H, N_2CC*H*), 7.66 (dd, ^3J = 8.0 Hz, ^4J = 1.6 Hz, 1H, ICCC*H*), 7.55 (t, ^3J = 7.4 Hz, 2H, N_2CCHC*H*), 7.51 (t, ^3J = 7.1 Hz, 1H, N_2CCHCHC*H*), 7.43 (td, ^3J = 7.7 Hz, ^4J = 1.3 Hz, 1H, ICCCHC*H*), 7.17 (td, ^3J = 7.6 Hz, ^4J = 1.6 Hz, 1H, ICCHC*H*) ppm.

^{13}C NMR (125 MHz, $CDCl_3$, 300 K): δ = 152.3 (N_2C), 151.3 (IC*C*), 139.8 (ICCH), 132.2 (ICCHC*H*), 131.6 (N_2CCHCHCH), 129.2 (N_2CCHCH), 128.9 (ICCCHCH), 123.5 (N_2CCH), 117.3 (ICCCH), 102.5 (I*C*) ppm.

Anal. Calcd for $C_{12}H_9N_2I$: C, 46.78; H, 2.94; N, 9.09. Found: C, 46.79; H, 2.80; N, 9.06.

***m*-Iodoazobenzene (6b).**[1] 3-Iodoaniline (5.08 g, 23.2 mmol) and nitrosobenzene (3.23 g, 30.2 mmol) were stirred in acetic acid (250 mL) overnight at room temperature. The solvent was removed under reduced pressure. The crude product was purified via column chromatography on silica gel (dichloromethane). The product was obtained as an orange solid (6.96 g, 22.6 mmol, 97 %).

^{1}H NMR (500 MHz, $CDCl_3$, 300 K): δ = 8.25 (t, ^4J = 1.7 Hz, 1H, ICC*H*C), 7.92 (d, ^3J = 8.0 Hz, 2H, N_2CC*H*), 7.92 (ddd, ^3J = 7.9 Hz, ^4J = 1.7 Hz, ^4J = 1.1 Hz, 1H, ICCHCC*H*), 7.80 (ddd, ^3J = 7.9 Hz, ^4J = 1.7 Hz, ^4J = 1.0 Hz, 1H, ICC*H*CH), 7.55-7.48 (m, 3H, N_2CCHC*H*, N_2CCHCHC*H*), 7.28 (t, ^3J = 7.9 Hz, 1H, ICCHC*H*) ppm.

^{13}C-NMR (125 MHz, $CDCl_3$, 300 K): δ = 153.4 (ICCH*C*), 152.3 (N_2C), 139.5 (IC*C*HCH), 131.5 (N_2CCHCHC*H*), 130.6 (IC*C*HC), 130.6 (ICCH*C*H), 129.2 (N_2CCH*C*H), 123.5 (ICCHC*C*H), 123.0 (N_2C*C*H), 94.6 (I*C*) ppm.

Anal. Calcd for $C_{12}H_9N_2I$: C, 46.78; H, 2.94; N, 9.09. Found: C, 47.03; H, 2.84; N, 9.13.

***p*-Iodoazobenzene (6c).**[1] 4-Iodoaniline (4.38 g, 20.0 mmol) and nitrosobenzene (2.14 g, 20.0 mmol) were stirred in acetic acid (100 mL) overnight at room temperature. The precipitate was filtered of and recrystallized from ethanol. The product was obtained as an orange solid (5.14 g, 16.7 mmol, 83 %).

^{1}H NMR (500 MHz, $CDCl_3$, 300 K): δ = 7.91 (d, ^3J = 7.9 Hz, 2H, N_2CC*H*), 7.87 (d, ^3J = 8.6 Hz, 2H, ICC*H*), 7.66 (d, ^3J = 8.6 Hz, 2H, ICCHC*H*), 7.52 (t, ^3J = 7.0 Hz, 2H, N_2CCHC*H*), 7.49 (t, ^3J = 7.1 Hz, 1H, N_2CCHCHC*H*) ppm.

^{13}C NMR (125 MHz, $CDCl_3$, 300 K): δ = 152.0 (N_2C), 151.5 (ICCHCH*C*), 138.4 (IC*C*H), 131.4 (N_2CCHCH*C*H), 129.2 (N_2CCH*C*H), 124.5 (ICCH*C*H), 123.0 (N_2C*C*H), 97.6 (I*C*) ppm.

Anal. Calcd for $C_{12}H_9N_2I$: C, 46.78; H, 2.94; N, 9.09. Found: C, 46.49; H, 2.80; N, 9.04.

5-(Biphenyl-*o*-azobenzene)-10,15,20-tris(pentafluorophenyl)-nickel(II)porphyrin (7a). The Ni-porphyrin precursor **5** (30 mg, 28.1 µmol) and 2-iodoazobenzene (**6a**)[1] (40 mg, 130 µmol) were deployed for a Suzuki cross-coupling reaction according to the general procedure A. The product was purified by column chromatography (cyclohexane/ethyl acetate = 9:1, R_f = 0.40). The product was obtained as a purple solid (29.6 mg, 26.4 µmol, 94%).

Mp: 171 °C.

FT-IR (layer): υ = 1650 (w), 1517 (m), 1486 (s), 1351 (w), 1167 (w), 1080 (w), 1060 (m), 986 (vs), 959 (m), 940 (s), 927 (s), 841 (w), 802 (w), 763 (vs), 702 (m), 687 (m), 539 (w) cm^{-1}.

^{1}H NMR (500 MHz, acetone-d_6, 300 K): δ = 9.20-8.48 (m, br, 8H, Por*H*), 8.33 (dd, ^3J = 7.0 Hz, ^4J = 1.7 Hz, 1H, PorCC*H*), 7.91-7.86 (m, 2H, PorCCHC*H*, PorCCCHC*H*), 7.74-7.73 (m, 2H *o*Ph*H*), 7.66 (dd, ^3J = 7.5 Hz, ^4J = 1.7 Hz, 1H, PorCCC*H*), 7.63-7.60 (m, 3H, *m*Ph*H*, *p*Ph*H*), 7.10 (dd, ^3J = 8.0 Hz, ^4J = 1.1 Hz, 1H, N_2CC*H*), 6.96 (dd, ^3J = 7.9 Hz, ^4J = 1.3 Hz, 1H, N_2CCC*H*), 6.61 (td, ^3J = 7.8 Hz, ^4J = 1.3 Hz, 1H, N_2CCHC*H*), 6.45 (dd, ^3J = 7.6 Hz, ^4J = 1.1 Hz, 1H, N_2CCCHC*H*) ppm.

^{19}F NMR (470 MHz, acetone-d_6, 300 K) δ = -139.00 to -139. 60 (m, br, 2F, *o*Ar*F*), -139.78 (dd, ^3J = 23.5 Hz, ^5J = 7.2 Hz, 1F, *o*Ar*F*), -140.27 (dd, ^3J = 23.6 Hz, ^5J = 7.1 Hz, 1F, *o*Ar*F*), -140.35 to -140.45 (m, br, 2F, *o*Ar*F*), -155.69 to -155.80 (m, 3F, *p*Ar*F*), -164.41 to -164.70 (m, 6F, *m*Ar*F*) ppm.

Due to the highly diluted NMR samples, the large number of quarternary C atoms and the large number of ^{19}F-coupled C atoms, ^{13}C NMR spectroscopy of **7a** did not provide sufficient signal

intensities. Therefore, the **^{13}C-NMR (125 MHz, acetone-d$_6$, 300 K)** spectrum was not analyzable. However, ^{1}H-^{13}C correlation experiments (HMBC, HSQC) confirmed the assignments of the ^{1}H-NMR signals.

HRMS (EI, TOF-Q) *m/z*: $[M]^+$ calcd for $C_{56}H_{21}F_{15}N_6Ni$ 1120.0942, found: 1120.0924.

Anal. Calcd for $C_{56}H_{21}F_{15}N_6Ni$: C, 59.97; H, 1.89; N, 7.49. Found: C, 60.17; H, 2.14; N, 7.44.

$t_{1/2}$ of *cis* isomer (acetone, 20 °C): 86 h.

5-(Biphenyl-*m*-azobenzene)-10,15,20-tris(pentafluorophenyl)-nickel(II)porphyrin (7b). The Ni-porphyrin precursor **5** (30 mg, 28.1 µmol) and 3-iodoazobenzene (**6b**)[1] (30 mg, 97.4 µmol) were deployed for a Suzuki cross-coupling reaction according to the general procedure A. The product was purified by column chromatography (cyclohexane/ethyl acetate = 9:1, R_f = 0.34). The product was obtained as a purple solid (30.3 mg, 27.0 µmol, 97%).

Mp: 186 °C.

FT-IR (layer): υ = 2964 (w), 1711 (w), 1517 (s), 1486 (vs), 1430 (m), 1349 (m), 1319 (w), 1261 (w), 1166 (w), 1080 (m), 1060 (m), 986 (vs), 959 (m), 939 (s), 926 (m), 802 (m), 762 (vs), 696 (s), 657 (w), 621 (w) cm^{-1}.

^{1}H NMR (500 MHz, acetone-d$_6$, 300 K): δ = 9.16 (d, ^{3}J = 5.0 Hz, 2H, Por*H*), 9.13 (d, ^{3}J = 5.0 Hz, 2H, Por*H*), 9.06 (d, ^{3}J = 5.0 Hz, 2H, Por*H*), 8.97 (d, ^{3}J = 5.0 Hz, 2H, Por*H*), 8.30 (dd, ^{3}J = 7.6 Hz, ^{4}J = 1.4 Hz, 1H, PorCC*H*C), 7.95 (td, ^{3}J = 7.7 Hz, ^{4}J = 1.4 Hz, 1H, PorCCCHC*H*), 7.89 (dd, ^{3}J = 7.9 Hz, ^{4}J = 1.5 Hz, 1H, PorCCC*H*), 7.83 (td, ^{3}J = 7.5 Hz, ^{4}J = 1.5 Hz, 1H, PorCCHC*H*), 7.29 (t, ^{4}J = 1.9 Hz, 1H, N_2CC*H*), 7.28 (tt, ^{3}J = 7.4 Hz, ^{4}J = 1.3 Hz, 1H, *p*Ph*H*), 7.18 (t, ^{3}J = 7.9 Hz, 2H, *m*Ph*H*), 7.16 (ddd, ^{3}J = 7.8 Hz, ^{4}J = 1.9, 1.1 Hz, 1H, N_2CC*H*CH), 7.08 (ddd, ^{3}J = 7.8 Hz, ^{4}J = 1.9, 1.1 Hz, 1H, N2CCHCC*H*), 6.93 (dd, ^{3}J = 8.4 Hz, ^{4}J = 1.3 Hz, 2H, *o*Ph*H*), 6.80 (t, ^{3}J = 7.8 Hz, 1H, N_2CCHC*H*) ppm.

^{13}C NMR (125 MHz, acetone-d$_6$, 300 K): δ = 152.5 (*C*-*i*Ph), 152.3 (N_2C), 148.3 (C_6F_5), 146.3 (C_6F_5), 145.2 (*C*-Por), 144.3 (*C*-Por), 144.2 (PorC*C*CH), 143.9 (*C*-Por), 143.8 (*C*-Por), 142.9 (N_2CCH*C*CH), 139.8 (C_6F_5), 139.0 (Por*C*CH), 137.8 (C_6F_5), 136.0 (PorC*C*H), 135.1 (*C*H-Por), 133.7 (*C*H-Por), 133.5 (*C*H-Por), 132.9 (*C*H-Por), 132.5 (N_2C*C*H), 131.7 (*C*-*p*Ph), 130.6 (PorCC*C*H), 130.4 (PorCCCH*C*H), 129.6 (*C*-*m*Ph), 129.3 (N_2CCH*C*H), 127.3 (PorCCH*C*H), 122.9 (N2CCHC*C*H, *C*-*o*Ph), 122.7 (N_2C*C*HC), 121.5 (*C*-Por), 115.5 (C_6F_5), 103.8 (*C*-Por), 103.1 (*C*-Por) ppm.

^{19}F NMR (470 MHz, acetone-d$_6$, 300 K) δ = -139.33 (dd, ^{3}J = 23.6 Hz, ^{5}J = 7.9 Hz, 2F, *o*Ar*F*), -139.83 (dd, ^{3}J = 23.6 Hz, ^{5}J = 7.9 Hz, 1F, *o*Ar*F*), -139.96 (dd, ^{3}J = 23.6 Hz, ^{5}J = 7.9 Hz, 1F, *o*Ar*F*), -140.33 (dd, ^{3}J = 23.6 Hz, ^{5}J = 7.8 Hz, 2F, *o*Ar*F*), -155.73 (t, ^{3}J = 20.5 Hz, 2F, *p*Ar*F*), -155.77 (t, ^{3}J = 20.3 Hz,

1F, *p*Ar*F*), -164.32 (ddd, ^3J = 23.6, 20.5 Hz, ^5J = 8.0 Hz, 2F, *m*Ar*F*), -164.47 to -164.65 (m, 2F, *m*Ar*F*), -164.67 (ddd, ^3J = 23.5, 20.5 Hz, ^5J = 8.0 Hz, 2F, *m*Ar*F*) ppm.

HRMS (EI, TOF-Q) *m/z*: $[M]^+$ calcd for $C_{56}H_{21}F_{15}N_6Ni$ 1120.0942, found: 1120.0922.

$\mathbf{t_{1/2}}$ of *cis* isomer (acetone, 20 °C): 642 h.

5-(Biphenyl-*p*-azobenzene)-10,15,20-tris(pentafluorophenyl)-nickel(II)porphyrin (7c). The Ni-porphyrin precursor **5** (30 mg, 28.1 µmol) and 4-iodoazobenzene (**6c**)[1] (15 mg, 48.7 µmol) were deployed for a Suzuki cross-coupling reaction according to the general procedure A. The product was purified by column chromatography (cyclohexane/ethyl acetate = 9:1, R_f = 0.31). The product was obtained as a purple solid (29.1 mg, 25.9 µmol, 93%).

Mp: 370 °C.

FT-IR (layer): υ = 1517 (s), 1486 (s), 1352 (m), 1086 (w), 986 (vs), 957 (m), 924 (s), 852 (w), 802 (m), 763 (vs), 700 (m), 867 (m), 571 (w) cm^{-1}.

^{1}H NMR (500 MHz, acetone-d_6, 300 K): δ = 9.16-9.13 (m, 4H, Por*H*), 9.05 (d, ^3J = 5.0 Hz, 2H, Por*H*), 8.97 (d, ^3J = 5.0 Hz, 2H, Por*H*), 8.26 (dd, ^3J = 7.5 Hz, ^4J = 1.3 Hz, 1H, PorCC*H*), 7.93 (td, ^3J = 7.7 Hz, ^4J = 1.4 Hz, 1H, PorCCCHC*H*), 7.85 (dd, ^3J = 7.9 Hz, ^4J = 1.4 Hz, 1H, PorCCC*H*), 7.82 (td, ^3J = 7.5 Hz, ^4J = 1.4 Hz, 1H, PorCCHC*H*), 7.47-7.45 (m, 2H, *o*Ph*H*), 7.31-7.28 (m, 3H, *m*Ph*H*, *p*Ph*H*), 7.12 (d, ^3J = 8.8 Hz, 2H, N_2CC*H*), 7.08 (d, ^3J = 8.8 Hz, 2H, N_2CCHC*H*) ppm.

^{13}C NMR (125 MHz, acetone-d_6, 300 K): δ = 153.1 (*C*-*i*Ph), 151.2 (N_2C), 148.2 (C_6F_5), 146.3 (C_6F_5), 145.2 (*C*-Por), 145.0 (N_2CCHCH*C*), 144.3 (*C*-Por, PorC*C*CH), 143.8 (*C*-Por), 142.3 (C_6F_5), 139.9 (C_6F_5), 139.0 (Por*C*CH), 137.9 (C_6F_5), 136.3 (PorC*C*H), 135.2 (*C*H-Por), 133.8 (*C*H-Por), 133.5 (*C*H-Por), 132.9 (*C*H-Por), 131.8 (*C*-*p*Ph), 130.9 (N_2C*C*H), 130.6 (PorCC*C*H), 130.3 (PorCCCH*C*H), 129.8 (*C*-*m*Ph), 127.4 (PorCCH*C*H), 123.2 (*C*-*o*Ph), 122.7 (N_2CCH*C*H), 121.5 (*C*-Por), 115.5 (C_6F_5), 103.8 (*C*-Por), 103.1 (*C*-Por) ppm.

^{19}F NMR (470 MHz, acetone-d_6, 300 K) δ = -139.44 (dd, ^3J = 23.6 Hz, ^5J = 7.8 Hz, 2F, *o*Ar*F*), -139.85 (dd, ^3J = 23.7 Hz, ^5J = 7.9 Hz, 1F, *o*Ar*F*), -140.05 (dd, ^3J = 23.6 Hz, ^5J = 7.6 Hz, 1F, *o*Ar*F*), -140.32 (dd, ^3J = 23.6 Hz, ^5J = 7.7 Hz, 2F, *o*Ar*F*), -155.70 (t, ^3J = 20.6 Hz, 2F, *p*Ar*F*), -155.74 (t, ^3J = 20.4 Hz, 1F, *p*Ar*F*), -164.36 (ddd, ^3J = 23.6, 20.6 Hz, ^5J = 7.9 Hz, 2F, *m*Ar*F*), -164.44 to -164.57 (m, 2F, *m*Ar*F*), -164.65 (ddd, ^3J = 23.6, 20.6 Hz, ^5J = 7.9 Hz, 2F, *m*Ar*F*) ppm.

HRMS (EI, TOF-Q) *m/z*: $[M]^+$ calcd for $C_{56}H_{21}F_{15}N_6Ni$ 1120.0942, found: 1120.0973.

$\mathbf{t_{1/2}}$ of *cis* isomer (acetone, 20 °C): 387 h.

3-(3'-Bromophenylazo)pyridine (8a)[2] and **3-(3'-bromophenylazo)-4-methoxypyridine (8b)**[3] were synthesized and characterized as previously reported.

3-(3'-Bromophenylazo)-4-isopropoxypyridine (8c). Sodium (1.00 g, 44 mmol) was dissolved in isopropanol (150 mL). 3-(3'-bromophenylazo)-4-chloropyridine (700 mg, 2.36 mmol) was added and the solution was stirred overnight at 60 °C. The major amount of the solvent was removed under reduced pressure. Water were added and the aqueous layer was extracted with dichloromethane twice. The combined organic layers were dried over magnesium sulfate. The solvent was removed under reduced pressure and the crude product was purified via column chromatography on silica gel (ethyl acetate). The product was obtained as an orange solid (689 mg, 2.15 mmol, 91 %).

^{1}H NMR (500 MHz, $CDCl_3$, 300 K): δ = 8.63 (s, 1H, Py*H*-2), 8.49 (d, ^3J = 5.8 Hz, 1H, Py*H*-6), 8.03 (t, ^4J = 1.9 Hz, 1H, N_2CCHC), 7.88 (ddd, ^3J = 8.0 Hz, ^4J = 1.8 Hz, ^4J = 1.1 Hz, 1H, N_2CCHCH), 7.61 (ddd, ^3J = 8.0 Hz, ^4J = 2.0 Hz, ^4J = 1.0 Hz, 1H, $N_2CCHCCH$), 7.41 (t, ^3J = 8.0 Hz, 1H, N_2CCHCH), 7.00 (d, ^3J = 5.0 Hz, 1H, Py*H*-5), 4.85 (sept, ^3J = 6.1 Hz, 1H, $OCH(CH_3)_2$), 1.50 (d, ^3J = 6.1 Hz, 1H, $OCH(CH_3)_2$) ppm.

^{13}C NMR (125 MHz, $CDCl_3$, 300 K): δ = 160.8 (Py*C*-4), 153.9 (N_2C), 153.1 (Py*C*-6), 139.5 (Py*C*-2), 138.7 (Py*C*-3), 133.9 ($N_2CCHCCH$), 130.5 (N_2CCHCH), 125.1 (N_2CCHC), 123.3 (N_2CCHCH), 110.1 (Br-*C*), 72.2 ($OCH(CH_3)_2$) , 22.0 ($OCH(CH_3)_2$) ppm.

MS (EI): m/z (%) = 319 (5) $[M]^{\bullet+}$, 182 (10) $[BrPhN_2]^{\bullet+}$, 152 (59) $[BrPh]^{\bullet+}$, 149 (100) $[M\text{-}PhBrN]^{\bullet+}$.

Anal. Calcd for $C_{14}H_{14}BrN_3O$: C, 52.52; H, 4.41; N, 13.12. Found: C, 52.78; H, 4.41; N, 13.31.

5-(3′-Bromophenylazo)-1-methylimidazole (9a). 4-(3'-Bromophenylazo)-1-(triphenylmethyl)-imidazole[4] (381 mg, 772 µmol) was dissolved in dry methylene chloride (12 mL) under an atmosphere of nitrogen and methyl trifluoromethanesulfonate (140 µL, 1.24 mmol) was added via syringe. The solution was stirred at room temperature overnight. Acetone/H_2O (2:1, 36 mL) was added and stirring was continued for 4 h at 40 °C. Saturated sodium bicarbonate solution (5 mL) was added, layers were separated and the aqueous layer was extracted twice with dichloromethane (each 20 mL). The combined organic layers were dried over magnesium sulfate and were evaporated to dryness. Purification via column chromatography on silica gel (ethyl acetate, R_f = 0.25) gave an orange solid (103 mg, 389 µmol, 50 %).

Mp: 105 °C.

FT-IR (layer): υ = 3081 (m), 2360 (w), 1719 (w), 1566 (m), 1522 (m), 1503 (m), 1460 (m), 1432 (m), 1400 (m), 1340 (s), 1281 (m), 1234 (s), 1211 (m), 1125 (s), 1052 (m), 992 (m), 904 (s), 882 (s), 860 (s), 781 (ss), 680 (ss), 675 (m), 670 (m), 641 (ss), 571 (m), 530 (s) cm^{-1}.

^{1}H NMR (600 MHz, DMSO-d_6, 298 K): δ = 8.03 (s, 1H, 2-*H*), 7.94 (s, 1H, 2′-*H*), 7.83 (d, ^{3}J = 7.92 Hz, 1H, 6′-*H*), 7.69 (d, ^{3}J = 7.92 Hz, 1H, 4′-*H*), 7.57 (s, 1H, 4-*H*), 7.53 (t, ^{3}J = 7.95 Hz, 1H, 5′-*H*), 3.94 (s, 3H, -CH_3) ppm.

^{13}C NMR (150 MHz, DMSO-d_6, 298 K): δ = 153.7 (*C*-3′), 144.8 (*C*-5), 142.6 (*C*-2), 133.0 (*C*-4′), 131.4 (*C*-5′), 123.8 (*C*-4), 123.6 (*C*-6), 123.5 (*C*-11), 123.1 (*C*-7), 32.3 (-*C*H_3) ppm.

MS (EI, 70 eV): m/z (%) = 266.0/264.0 (57/58) $[M]^{\bullet+}$, 186.0/184.0 (13/14) $[PhBrN_2+H]^{\bullet+}$, 157.0/155.0 (35/37) $[PhBr]^{\bullet+}$, 109 (100) $[M\text{-}PhBr]^{\bullet+}$.

HR-MS (EI, TOF-Q): m/z $[M]^{\bullet+}$ calcd for $C_{10}H_9N_4{}^{79}Br$, 264.0011; found 264.0010 (-0.3 ppm); calcd for $C_{10}H_9N_4{}^{81}Br$, 265.9990; found 265.9990 (±0 ppm).

5-(3′-Bromo-4'-fluorophenylazo)-1-methylimidazole (9b). Step 1: 3-Bromo-4-fluorobenzenediazonium tetrafluoroborate. A solution of 3-bromo-4-fluoroaniline (3.00 g, 15.8 mmol) in a mixture of ethanol and tetrafluoroboric acid (50 wt-%) (60 mL, 7:3) was cooled to 0 °C and isopentylnitrite (2.55 mL, 18.9 mmol) was added dropwise over 10 min. Diethyl ether (210 mL) was added and stirring at 0 °C was continued for 45 min. The precipitate was filtered off and washed thoroughly with diethyl ether (300 mL) before being dried in vacuo. The desired product (2.74 g, 9.49 mmol, 60 %) was obtained as a white solid which is thermally unstable and therefore was used in the following step immediately after preparation.

FT-IR (layer): υ = 3101 (w), 2301 (m), 1569 (m), 1474 (m), 1413 (w), 1307 (w), 1272 (m), 1135 (w), 1027 (vs, br), 891 (m), 857 (m), 825 (s), 733 (m), 559 (m), 524 (m), 464 (m), 403 (s) cm^{-1}.

^{1}H NMR (500 MHz, acetone-d_6, 300 K): δ = 9.28 (dd, $^{4}J_{H\rightarrow F}$ = 5.63 Hz, $^{4}J_{H\rightarrow H}$ = 2.58 Hz, 1H, 2-*H*), 9.03 (ddd, $^{3}J_{H\rightarrow H}$ = 9.21 Hz, $^{4}J_{H\rightarrow F}$ = 3.91 Hz, $^{4}J_{H\rightarrow H}$ = 2.59 Hz, 1H, 6-*H*), 8.03 (dd, $^{3}J_{H\rightarrow H}$ = 9.20 Hz, $^{3}J_{H\rightarrow F}$ = 7.95 Hz, 1H, 5-*H*) ppm.

^{13}C NMR (125 MHz, acetone-d_6, 300 K): δ = 167.6 (d, ^{1}J = 268.3 Hz, *C*-4), 139.6 (d, ^{3}J = 4.01 Hz, *C*-2), 137.1 (d, ^{3}J = 11.8 Hz, *C*-6), 121.1 (d, ^{2}J = 26.4 Hz, *C*-5), 113.4 (s, *C*-1), 112.6 (d, ^{2}J = 24.6 Hz, *C*-3) ppm.

^{11}B NMR (160 MHz, acetone-d_6, 300 K): δ = -0.95 (1B, *B*F_4^-) ppm.

^{19}F NMR (470 MHz, acetone-d_6, 300 K): δ = -81.64 (s, 1F, 4-*F*), -150.86 (s, 1F, BF_4^-), -150.92 (s, 3F, BF_4^-) ppm.

MS (EI, 70 eV): m/z (%) = 191.9/193.9 (100/98) $[C_6H_3BrF_2]^{\bullet+}$.

HR-MS (EI): m/z $[M]^{\bullet+}$ calcd for $C_6H_3{}^{79}BrF_2$, 191.9386; found 191.9394 (+4.1 ppm); calcd for $C_6H_3{}^{81}BrF_2$, 193.9366; found 193.9375 (+4.6 ppm).

Diazonium tetrafluoroborates undergo a Baltz Schiemann reaction during the vaporization process in EI-MS. Therefore, only the fluorinated derivative is found.

Step 2: 5-(3'-Bromo-4'-fluorophenylazo)-1-(*N,N*-dimethylsulfamoyl)imidazole. 1-(*N,N*-Dimethylsulfamoyl)imidazole[5] (1.00 g, 5.71 mmol) was dissolved in dry THF (30 mL) and cooled to -78 °C. *n*-Butyllithium (2.30 mL, 5.75 mmol, 2.5 M in *n*-hexane) was added dropwise over a period of 15 minutes. After 30 minutes of stirring at -78 °C, dimethylthexylchlorosilane (1.24 mL, 6.31 mmol) was added. The reaction mixture was stirred at -78 °C for 60 minutes and at room temperature for 15 hours. It was again cooled to -78 °C and *n*-butyllithium (2.50 mL, 6.25 mmol, 2.5 M in *n*-hexane) was added dropwise over a period of 10 minutes. After 30 minutes of stirring at -78 °C, 3-bromo-4-fluorobenzenediazonium tetrafluoroborate (1.65 g, 5.71 mmol) was added as a solid in one portion, and the reaction mixture immediately turned from light yellow to deep red. It was stirred at -78 °C for 60 minutes and at room temperature for 5 hours. Then, half saturated aqueous sodium bicarbonate solution (30 mL) was added, layers were separated and the aqueous layer was extracted once with THF (40 mL). The combined organic layers were treated with tetra-*n*-butylammoniumfluoride trihydrate (1.95 g, 6.18 mmol) and the mixture was stirred at 55 °C for 90 min and at room temperature for 15 hours. Then, half saturated aqueous sodium bicarbonate solution (60 mL) was added, layers were separated and the aqueous layer was extracted three times with chloroform (each 40 mL). The combined organic layers were dried over magnesium sulfate and evaporated. The resulting crude product was purified via column chromatography on silica gel (methylene chloride, 10 vol-% ethyl acetate, R_f = 0.42 (*cis*) & 0.33 (*trans*)). The desired product was obtained as orange solid (1.02 g, 2.71 mmol, 47 %).

Mp: 110 °C.

FT-IR (layer): υ = 3130 (w), 3070 (w), 3030 (w), 2947 (w), 1582 (w), 1482 (m), 1451 (m), 1390 (s), 1375 (s), 1340 (m), 1289 (m), 1255 (s), 1238 (m), 1182 (m), 1159 (vs), 1118 (s), 1091 (vs), 1033 (m), 980 (s), 887 (m), 844 (s), 820 (m), 759 (m), 729 (vs), 704 (m), 634 (m), 594 (s), 584 (vs), 575 (vs), 544 (vs), 536 (vs), 514 (vs), 473 (vs), 447 (m) cm^{-1}.

^{1}H NMR (600 MHz, CD_2Cl_2, 300 K): δ = 8.13 (s, 1H, 2-*H*), 8.07 (dd, $^4J_{H\rightarrow F}$ = 6.48 Hz, $^4J_{H\rightarrow H}$ = 2.34 Hz, 1H, 2′-*H*), 7.83 (ddd, $^3J_{H\rightarrow H}$ = 8.76 Hz, $^4J_{H\rightarrow F}$ = 4.62 Hz, $^4J_{H\rightarrow H}$ = 2.40 Hz, 1H, 6′-*H*), 7.50 (s, 1H, 4-*H*), 7.30 (dd(t), $^3J_{H\rightarrow F}$ = 8.40 Hz, $^3J_{H\rightarrow H}$ = 8.40 Hz, 1H, 5′-*H*), 2.97 (s, 6H, N(CH_3)$_2$) ppm.

^{13}C NMR (150 MHz, CD_2Cl_2, 300 K): δ = 161.2 (d, ^1J = 253.7 Hz, *C*-4′), 150.3 (s, *C*-1′), 145.3 (s, *C*-5), 141.8 (*C*-2), 128.1 (s, *C*-2′), 124.6 (d, ^3J = 7.73 Hz, *C*-6′), 119.8 (s, *C*-4), 117.6 (d, ^2J = 24.0 Hz, *C*-5′), 110.5 (d, ^2J = 23.0 Hz, *C*-3′), 38.7 (s, N(CH_3)$_2$) ppm.

^{19}F NMR (470 MHz, CD_2Cl_2, 300 K): δ = -103.30 ppm.

MS (EI, 70 eV): m/z (%) = 377.0/375.0 (18/17) $[M]^{\bullet+}$, 270.0/268.0 (36/37) $[M\text{-}SO_2N(CH_3)_2+H]^{\bullet+}$, 175.0/173.0 (32/32) $[PhFBr]^{\bullet+}$, 108.0 (100) $[SO_2N(CH_3)_2]^{\bullet+}$.

HR-MS (EI, TOF-Q): m/z $[M]^{\bullet+}$ calcd for $C_{11}H_{11}N_5O_2FS^{79}Br$, 374.9801; found 374.9800 (-0.2 ppm); calcd for $C_{11}H_{11}N_5O_2FS^{81}Br$, 376.9780; found 376.9780 (±0 ppm).

Step 3: 4(5)-(3'-Bromo-4'-fluorophenylazo)imidazole. The sulfamoyl-protected azoimidazole (857 mg, 2.28 mmol) was dissolved in ethanol (30 mL) and ethanolic hydrochloric acid (4 M, 30 mL) was added. The reaction mixture was stirred at 55 °C for 1 hour, then cooled to 0 °C and potassium hydroxide solution (40 %, 12 mL) was added dropwise. The solution was treated with saturated aqueous sodium bicarbonate solution (80 mL) and stirring at 0 °C was continued for 15 minutes. Methylene chloride (100 mL) was added and the layers were separated. The aqueous layer was extracted twice with methylene chloride (50 mL) and the combined organic layers were dried over magnesium sulfate before being evaporated to dryness. Purification via column chromatography on silica gel (ethyl acetate, $R_f = 0.14$) gave the desired deprotected azoimidazole (564 mg, 2.10 mmol, 92 %) as yellow powder.

Mp: 229 °C (decomp.).

FT-IR (layer): υ = 1592 (w), 1515 (w), 1487 (m), 1432 (vs), 1391 (m), 1324 (m), 1255 (s), 1228 (s), 1175 (m), 1149 (m), 1121 (m), 1093 (m), 1035(m), 1003 (s), 914 (m), 837 (vs), 822 (s), 798 (s), 755 (s), 707 (m), 688 (w), 668 (m), 623 (vs), 578 (m), 552 (m), 541 (m) cm^{-1}.

^{1}H NMR (600 MHz, CD_3OD, 300 K): δ = 8.11 (dd, $^4J_{H\rightarrow F}$ = 6.54 Hz, $^4J_{H\rightarrow H}$ = 2.40 Hz, 1H, 2′-*H*), 7.90 (ddd, $^3J_{H\rightarrow H}$ = 8.73 Hz, $^4J_{H\rightarrow F}$ = 4.59 Hz, $^4J_{H\rightarrow H}$ = 2.40 Hz, 1H, 6′-*H*), 7.86 (s, br, 1H, 5(4)-*H*), 7.83 (s, br, 1H, 2-*H*), 7.38 (dd(t), $^3J_{H\rightarrow F}$ = 8.52 Hz, $^3J_{H\rightarrow H}$ = 8.52 Hz, 1H, 5′-*H*) ppm. The *N*H signal is not found due to fast proton-deuterium exchange in CD_3OD.

^{13}C NMR (150 MHz, CD_3OD, 300 K): δ = 161.4 (d, ^1J = 250.2 Hz, *C*-4′), 155.0 (s, *C*-4(5)), 151.4 (s, *C*-1′), 138.0 (*C*-2), 127.5 (s, *C*-2′), 125.5 (d, ^3J = 6.45 Hz, *C*-6′), 119.4 (s, *C*-5(4)), 118.0 (d, ^2J = 24.0 Hz, *C*-5′), 110.6 (d, ^2J = 22.7 Hz, *C*-3′) ppm.

^{19}F NMR (470 MHz, CD_3OD, 300 K): δ = -107.51 ppm.

MS (EI, 70 eV): m/z (%) = 270.0/268.0 (49/50) $[M]^{\bullet+}$, 174.9/172.9 (40/42) $[PhFBr]^{\bullet+}$, 95.0 (100) $[C_3H_3N_4]^{\bullet+}$.

HR-MS (EI, TOF-Q): m/z $[M]^{\bullet+}$ calcd for $C_9H_6N_4{}^{79}Br$, 267.9760; found 267.9763 (+1.2 ppm); calcd for $C_9H_6N_4{}^{81}Br$, 269.9739; found 269.9748 (+3.3 ppm).

Anal. Calcd for $C_9H_6BrFN_4$: C, 40.17; H, 2.25; N, 20.82. Found: C, 39.76; H, 2.27; N, 20.70.

Step 4: 4-(3'-Bromo-4'-fluorophenylazo)-1-(triphenylmethyl)imidazole. A suspension of 4(5)-(3'-

bromo-4'-fluorophenylazo)imidazole (512 mg, 1.90 mmol) and triphenylchloromethane (557 mg, 2.00 mmol) in methylene chloride (25 mL) was treated with triethylamine (342 µL, 2.47 mmol). Stirring at room temperature for 19 hours gave a deep red solution. Half saturated sodium bicarbonate solution (30 mL) was added, layers were separated and the aqueous layer was extracted twice with methylene chloride (each 30 mL). The combined organic layers were dried over magnesium sulfate and evaporated to dryness. Purification of the crude product via column chromatography on silica gel (cyclohexane/ethyl acetate, 7:3, R_f = 0.38) gave a yellow solid (863 mg, 1.69 mmol, 89 %).

Mp: 85 °C.

FT-IR (layer): υ = 3088 (w), 3060 (w), 3032 (w), 2295 (w), 1582 (w), 1526 (w), 1480 (m), 1444 (s), 1393 (w), 1353 (w), 1323 (w), 1296 (m), 1252 (m), 1230 (m), 1155 (w), 1116 (s), 1087 (m), 1035 (m), 1001 (w), 991 (w), 927 (w), 887 (w), 866 (m), 838 (m), 823 (m), 755 (s), 742 (vs), 699 (vs), 677 (s), 656 (s), 639 (m), 619 (w), 586 (w), 555 (w), 539 (m), 508 (m), 491 (w), 474 (m) cm^{-1}.

^{1}H NMR (500 MHz, CD_2Cl_2, 300 K): δ = 8.06 (dd, $^4J_{H\rightarrow F}$ = 6.55 Hz, $^4J_{H\rightarrow H}$ = 2.40 Hz, 1H, 2′-*H*), 7.83 (ddd, $^3J_{H\rightarrow H}$ = 8.76 Hz, $^4J_{H\rightarrow F}$ = 4.64 Hz, $^4J_{H\rightarrow H}$ = 2.44 Hz, 1H, 6′-*H*), 7.56 (d, ^4J = 1.45 Hz, 1H, 5-*H*), 7.53 (d, ^4J = 1.45 Hz, 1H, 2-*H*), 7.42-7.36 (m, 9H, *m*-Tr-*H*, *p*-Tr-*H*), 7.27-7.19 (m, 7H, 5′-*H*, *o*-Tr-*H*) ppm.

^{13}C NMR (125 MHz, CD_2Cl_2, 300 K): δ = 160.4 (*C*-4′, identified by HMBC), 153.6 (s, *C*-4), 150.5 (s, *C*-1′), 142.2 (s, *C*-*i*-Tr), 139.8 (s, *C*-2), 130.2 (s, *C*-*o*-Tr), 128.8 (s, *C*-*p*-Tr), 128.7 (s, *C*-*m*-Tr), 126.6 (s, *C*-2′), 125.0 (d, ^3J = 7.70 Hz, *C*-6′), 122.4 (s, *C*-5), 117.1 (d, ^2J = 23.7 Hz, *C*-5′), 110.1 (d, ^2J = 22.4 Hz, *C*-3′), 76.7 (s, *C*Ph_3) ppm.

^{19}F NMR (470 MHz, CD_2Cl_2, 300 K): δ = -106.06 ppm.

MS (ESI-TOF, methanol): m/z (%) = 534.8/532.8 (93/100) $[M+Na]^+$, 243.1 (67) $[CPh_3]^+$.

Anal. Calcd. for $C_{28}H_{21}N_4Br$ (492.09): cal. C 65.76, H 3.94, N 10.96, found C 66.52, H 4.43, N 11.19 %.

Step 5: 5-(3′-Bromo-4'-fluorophenylazo)-1-methylimidazole (9b). The tritylated phenylazo-imidazole (410 mg, 802 µmol) was dissolved in dry methylene chloride (12 mL) and methyl trifluoromethanesulfonate (100 µL, 882 µmol) was added under an atmosphere of nitrogen. It was stirred at room temperature for 40 min, followed by the addition of acetone/H_2O (1:1, 24 mL) and further stirring at room temperature for 30 min. Saturated sodium bicarbonate solution (3 mL) was added, layers were separated and the aqueous layer was extracted twice with dichloromethane (each 20 mL). The combined organic layers were dried over magnesium sulfate and were evaporated to dryness. Purification via column chromatography on silica gel (ethyl acetate, R_f = 0.15) gave a yellow solid (132 mg, 466 µmol, 58 %).

Mp: 112 °C.

FT-IR (layer): υ = 3118 (w), 3090 (w), 3052 (w), 3031 (w), 2958 (w), 2360 (w), 2291 (w), 1650 (w), 1581 (m), 1515 (m), 1506 (m), 1474 (s), 1424 (m), 1409 (s), 1387 (m), 1377 (w), 1339 (s), 1301 (m), 1281 (m), 1257 (s), 1244 (s), 1221 (s), 1207 (s), 1171 (m), 1118 (vs), 1067 (m), 1036 (s), 950 (m), 905 (m), 850 (s), 814 (vs), 762 (m), 707 (m), 696 (m), 660 (vs), 640 (vs), 579 (m), 561 (m), 544 (s), 519 (m), 472 (vs) cm^{-1}.

^{1}H NMR (500 MHz, CD_2Cl_2, 300 K): δ = 8.07 (dd, $^{4}J_{H\rightarrow F}$ = 6.55 Hz, $^{4}J_{H\rightarrow H}$ = 2.40 Hz, 1H, 2′-*H*), 7.82 (ddd, $^{3}J_{H\rightarrow H}$ = 8.75 Hz, $^{4}J_{H\rightarrow F}$ = 4.65 Hz, $^{4}J_{H\rightarrow H}$ = 2.40 Hz, 1H, 6′-*H*), 7.62 (s, 1H, 2-*H*), 7.55 (d, ^{4}J = 0.75 Hz, 1H, 4-*H*), 7.27 (dd, $^{3}J_{H\rightarrow H}$ = 8.73 Hz, $^{3}J_{H\rightarrow F}$ = 8.13 Hz, 1H, 5′-*H*), 3.94 (d, ^{4}J = 0.55 Hz, 3H, -CH_3) ppm.

^{13}C NMR (125 MHz, CD_2Cl_2, 298 K): δ = 160.4 (d, ^{1}J = 251.6 Hz, *C*-4′), 150.5 (s, *C*-1′), 145.6 (s, *C*-5), 141.7 (*C*-2), 126.5 (s, *C*-2′), 124.8 (d, ^{3}J = 7.71 Hz, *C*-6′), 124.5 (s, *C*-4), 117.2 (d, ^{2}J = 23.9 Hz, *C*-5′), 110.3 (d, ^{2}J = 22.8 Hz, *C*-3′), 32.9 (s, -*C*H_3) ppm.

^{19}F NMR (470 MHz, CD_2Cl_2, 300 K): δ = -105.45 ppm.

MS (EI, 70 eV): m/z (%) = 284.0/282.0 (86/88) $[M]^{\bullet+}$, 204.0/202.0 (18/20) $[PhFBrN_2+H]^{\bullet+}$, 175.0/173.0 (46/47) $[PhFBr]^{\bullet+}$, 109.1 (100) $[C_4H_5N_4]^{\bullet+}$.

HR-MS (EI, TOF-Q): m/z $[M]^{\bullet+}$ calcd for $C_{10}H_8N_4F^{79}Br$, 281.9916; found 281.9914 (-0.7 ppm); calcd for $C_{10}H_8N_4F^{81}Br$, 283.9896; found 283.9895 (-0.4 ppm).

UV-vis (CH_3CN): λ_{max} (lg ε) = 205 (4.138), 247 (3.872), 361 (4.314) nm.

5-(3′-Bromo-4’-methoxyphenylazo)-1-methylimidazole (9c). Under an atmosphere of nitrogen methanol (17.2 µL, 424 µmol) was dissolved in dry DMF (4 mL) and sodium hydride (12.7 mg, 318 µmol, 60% in mineral oil) was added. After 30 min of stirring at room temperature, the fluorinated phenylazoimidazole **9b** (30.0 mg, 106 µmol) was added and stirring at room temperature was continued overnight. The reaction mixture was diluted with diethyl ether (20 mL) and washed once with half saturated ammonium chloride solution (20 mL) and once with water (20 mL). The aqueous layer was extracted twice with diethyl ether (each 15 mL) and the combined organic layers were dried over magnesium sulfate and evaporated to dryness. Purification via column chromatography on silica gel (ethyl acetate, R_f = 0.13) gave an orange solid (22.0 mg, 74.5 µmol, 70 %).

Mp: 121 °C.

FT-IR (layer): υ = 3102 (w), 2945 (w), 2841 (w), 1657 (w), 1589 (m), 1505 (m), 1493 (s), 1484 (s), 1467 (m), 1440 (m), 1341 (m), 1269 (s), 1260 (s), 1251 (s), 1224 (s), 1165 (m), 1139 (m), 1108 (vs), 1039 (s), 1011 (s), 909 (m), 890 (m), 873 (m), 846 (m), 832 (s), 805 (vs), 747 (m), 712 (m), 694 (m), 671 (m), 661 (s), 645 (s), 579 (s), 555 (s), 532 (vs), 510 (vs) cm^{-1}.

^{1}H NMR (500 MHz, acetone-d_6, 300 K): δ = 8.06 (d, ^4J = 2.40 Hz, 1H, 2′-*H*), 7.88 (dd, ^3J = 8.75 Hz, ^4J = 2.35 Hz, 1H, 6′-*H*), 7.79 (s, br, 1H, 2-*H*), 7.44 (d, ^4J = 0.80 Hz, 1H, 4-*H*), 7.26 (d, ^3J = 8.80 Hz, 1H, 5′-*H*), 4.01-3.99 (m, 6H, -OCH_3, NCH_3) ppm.

^{13}C NMR (125 MHz, acetone-d_6, 300 K): δ = 158.6 (*C*-4′), 148.5 (*C*-1′), 146.1 (*C*-5), 142.2 (*C*-2), 126.1 (*C*-6′), 125.7 (*C*-2′), 123.5 (*C*-4), 113.1 (*C*-5′), 113.0 (*C*-3′), 57.1 (O*C*H$_3$), 32.6 (N*C*H$_3$) ppm.

MS (EI, 70 eV): m/z (%) = 296.0/294.0 (99/100) $[M]^{\bullet+}$, 281.0/279.0 (4/4) $[M\text{-}CH_3]^{\bullet+}$, 216.0/214.0 (13/14) $[PhOCH_3BrN_2+H]^{\bullet+}$, 187.0/185.0 (38/38) $[PhOCH_3Br]^{\bullet+}$, 109.1 (79) $[C_4H_5N_4]^{\bullet+}$.

HR-MS (EI, TOF-Q): m/z $[M]^{\bullet+}$ calcd for $C_{11}H_{11}N_4O^{79}Br$, 294.0116; found 294.0116 (+0.1 ppm); calcd for $C_{11}H_{11}N_4O^{81}Br$, 296.0096; found 296.0099 (+1.2 ppm).

UV-vis (CH_3CN): λ_{max} (lg ε) = 256 (3.951), 370 (4.422) nm.

5-(3′-Bromo-4’-isopropoxyphenylazo)-1-methylimidazole (9d). Under an atmosphere of nitrogen isopropanol (25.0 µL, 324 µmol) was dissolved in dry THF (3 mL) and sodium hydride (8.00 mg, 200 µmol, 60% in mineral oil) was added. After 30 min of stirring at room temperature, the fluorinated phenylazoimidazole **9b** (32.0 mg, 113 µmol) was added and stirring at room temperature was continued for 16 h. The reaction mixture was diluted with ethyl acetate (20 mL) and washed once with half saturated ammonium chloride solution (20 mL) and three times with water (each 20 mL). The organic layer was dried over magnesium sulfate and evaporated to dryness. Purification via column chromatography on silica gel (ethyl acetate, R_f = 0.31) gave an orange solid (30.0 mg, 92.8 µmol, 82 %).

Mp: 100 °C.

FT-IR (layer): υ = 3105 (w), 3082 (w), 3039 (w), 2978 (m), 2965 (w), 2928 (w), 2870 (w), 1710 (w), 1589 (m), 1564 (m), 1514 (w), 1499 (m), 1479 (s), 1463 (s), 1427 (m), 1413 (w), 1383 (w), 1373 (m), 1345 (m), 1336 (m), 1313 (w), 1282 (s), 1273(s), 1249 (s), 1225 (vs), 1165 (m), 1147 (s), 1135 (m), 1114 (vs), 1104 (vs), 1066 (m), 1033 (s), 947 (s), 909 (s), 888 (s), 861 (s), 841 (s), 815 (vs), 757 (m), 716 (m), 685 (w), 674 (m), 666 (vs), 650 (s), 592 (s), 585 (s), 554 (s), 488 (m), 456 (m) cm^{-1}.

^{1}H NMR (500 MHz, CD_2Cl_2, 300 K): δ = 8.07 (d, ^4J = 2.40 Hz, 1H, 2′-*H*), 7.80 (dd, ^3J = 8.78 Hz, ^4J = 2.38 Hz, 1H, 6′-*H*), 7.57 (s, 1H, 2-*H*), 7.46 (d, ^4J = 0.80 Hz, 1H, 4-*H*), 7.03 (d, ^3J = 8.90 Hz, 1H, 5′-*H*), 4.69 (sept., ^3J = 5.99 Hz, 1H, -OC*H*$(CH_3)_2$), 3.93 (s, 3H, NCH_3), 1.42 (d, 3J = 6.05 Hz, 1H, -OCH(C$H_3)_2$) ppm.

^{13}C NMR (125 MHz, CD_2Cl_2, 300 K): δ = 156.8 (*C*-4′), 147.8 (*C*-1′), 145.7 (*C*-5), 140.9 (*C*-2), 125.9 (*C*-2′), 125.3 (*C*-6′), 122.8 (*C*-4), 114.7 (*C*-5′), 114.4 (*C*-3′), 72.8 (O*C*H$(CH_3)_2$), 32.7 (s, N*C*H$_3$), 22.1 (OCH(*C*H$_3)_2$) ppm.

MS (EI, 70 eV): m/z (%) = 324.0/322.0 (38/38) $[M]^{\bullet+}$, 282.0/280.0 (85/85) $[M\text{-}C_3H_7+H]^{\bullet+}$,

202.0/200.0 (8/9) $[C_6H_3OHBrN_2+H]^{\bullet+}$, 172.9/170.9 (12/12) $[C_6H_3OHBr]^{\bullet+}$, 109.1 (100) $[C_4H_5N_4]^{\bullet+}$.

HR-MS (EI, TOF-Q): m/z $[M]^{\bullet+}$ calcd for $C_{13}H_{15}N_4O^{79}Br$, 322.0429; found 322.0429 (±0 ppm); calcd for $C_{13}H_{15}N_4O^{81}Br$, 324.0409; found 324.0402 (-2.1 ppm).

5-(Biphenylazopyridine)-10,15,20-tris(pentafluorophenyl)nickel(II)porphyrin (10a).[2] The Ni-porphyrin precursor **5** (30.0 mg, 28.1 µmol) and 3-(3'-bromophenylazo)pyridine (**8a**)[2] (14.7 mg, 56.2 µmol) were deployed for a Suzuki cross-coupling reaction according to the general procedure A. Purification via column chromatography on silica gel (cyclohexane/ethyl acetate, 4:1, R_f = 0.36 (*cis*-isomer), 0.23 (*trans*-isomer)) gave a purple solid (31.0 mg, 27.6 µmol, 98 %).

^{1}H-NMR (500 MHz, acetone-d_6, TFA-d, 300 K): δ = 9.15 (d, ^3J = 5.1 Hz, 2H, Por-*H*), 9.12 (d, ^3J = 5.1 Hz, 2H, Por-*H*), 9.08 (d, ^3J = 5.6 Hz, 1H, Py*H*-6), 9.01 (d, ^3J = 5.1 Hz, 2H, Por-*H*), 8.99 (d, ^3J = 5.1 Hz, 2H, Por-*H*), 8.91 (s, 1H, Py*H*-2), 8.40 (dd, ^3J = 7.6 Hz, ^4J = 1.3 Hz, 1H, PorCC*H*), 8.07 (dd, ^3J = 8.2 Hz, ^3J = 5.1 Hz, 1H, Py*H*-5), 8.00 (td, ^3J = 7.7 Hz, ^4J = 1.3 Hz, 1H, PorCCHC*H*), 7.92-7.87 (m, 3H, PorCCHC*H*, PorCCC*H*, Py*H*-4), 7.30 (ddd, ^3J = 8.0 Hz, ^4J = 1.7 Hz, ^4J = 1.1 Hz, 1H, N_2CCHCC*H*), 7.30 (t, ^4J = 1.8 Hz, 1H, N_2CC*H*CCH), 7.13 (ddd, ^3J = 8.0 Hz, ^4J = 1.9 Hz, ^4J = 1.1 Hz, 1H, N_2CC*H*CHCH), 6.86 (t, ^3J = 8.0 Hz, 1H, N_2CCHC*H*CH) ppm.

^{19}F-NMR (470 MHz, acetone-d_6, TFA-d, 300 K): δ = -139.75 (dd, ^3J = 23.7 Hz, ^5J = 7.6 Hz, 1F, Por-Ar-*o*-*F*), -139.88 (dd, ^3J = 23.4 Hz, ^5J = 7.5 Hz, 2F, Por-Ar-*o*-*F*), -140.47 (dd, ^3J = 23.6 Hz, ^5J = 7.4 Hz, 1F, Por-Ar-*o*-*F*), -140.57 (dd, ^3J = 23.6 Hz, ^5J = 7.5 Hz, 2F, Por-Ar-*o*-*F*), -155.58 (t, ^3J = 20.6 Hz, 2F, Por-Ar-*p*-*F*), -155.65 (t, ^3J =20.6 Hz, 1F, Por-Ar-*p*-*F*), -164.28 to -164.39 (m, 3F, Por-Ar-*m*-*F*), -164.43 to -164.62 (m, 3F, Por-Ar-*m*-*F*) ppm.

Due to the highly diluted NMR samples, the large number of quarternary C atoms and the large number of ^{19}F-coupled C atoms, ^{13}C NMR spectroscopy of **10b** did not provide sufficient signal intensities. Therefore, the **^{13}C NMR** (125 MHz, acetone-d_6, TFA-d, 300 K) spectrum was not analyzable. However, ^{1}H-^{13}C correlation experiments (HMBC, HSQC) confirmed the assignments of the ^{1}H-NMR signals.

The analytical data are in accordance with the reported data for pyridine record player **10a**.[2]

5-(Biphenylazo-methoxypyridine)-10,15,20-tris(pentafluorophenyl)nickel(II)porphyrin (10b).[3] The Ni-porphyrin precursor **5** (290 mg, 272 µmol) and 3-(3'-bromophenylazo)-4-methoxypyridine (**8b**)[3] (103 mg, 353 µmol) were deployed for a Suzuki cross-coupling reaction according to the general procedure A. Purification via column chromatography on silica gel (cyclohexane/ethyl acetate, 3:2, R_f = 0.13) gave a purple solid (297 mg, 258 µmol, 95 %).

^{1}H NMR (500 MHz, acetone-d_6, TFA-d, 300 K): δ = 9.15-9.13 (m, 4H, Por-*H*), 9.05 (d, ^3J = 5.1 Hz, 2H, Por-*H*), 8.99 (d, ^3J = 5.1 Hz, 2H, Por-*H*), 8.93 (dd, ^3J = 7.0 Hz, ^4J = 1.2 Hz, 1H, Py*H*-6), 8.45 (d, ^4J = 1.2 Hz, 1H, Py*H*-2), 8.33 (dd, ^3J = 7.6 Hz, ^4J = 1.3 Hz, 1H, PorCC*H*), 8.01 (td, ^3J = 7.8 Hz, ^4J = 1.4 Hz, 1H, PorCCHC*H*), 7.90 (td, ^3J = 7.6 Hz, ^4J = 1.3 Hz, 1H, PorCCHC*H*), 7.88 (dd, ^3J = 7.8 Hz, ^4J = 1.4 Hz, 1H, PorCCC*H*), 7.87 (d, ^3J = 7.0 Hz, 1H, Py*H*-5), 7.64 (t, ^4J = 1.8 Hz, 2H, N_2CC*H*CCH), 7.15 (m, 2H, N_2CCHCC*H*, N_2CC*H*CHCH), 6.73 (t, ^3J = 8.0 Hz, 1H, N_2CCHC*H*CH), 4.11 (s, 3H, OCH_3) ppm.

^{19}F NMR (470 MHz, acetone-d_6, TFA-d, 300 K): δ = -139.77 (dd, ^3J = 23.8 Hz, ^5J = 7.8 Hz, 1F, Por-Ar-*o*-*F*), -139.88 (dd, ^3J = 23.6 Hz, ^5J = 7.3 Hz, 2F, Por-Ar-*o*-*F*), -140.22 (dd, ^3J = 23.3 Hz, ^5J = 7.2 Hz, 2F, Por-Ar-*o*-*F*), -140.47 (dd, ^3J = 23.5 Hz, ^5J = 7.3 Hz, 1F, Por-Ar-*o*-*F*), -155.59 (t, ^3J = 20.7 Hz, 2F, Por-Ar-*p*-*F*), -155.66 (t, ^3J =20.5 Hz, 1F, Por-Ar-*p*-*F*), -164.29 to -164.53 (m, 5F, Por-Ar-*m*-*F*), -164.61 (ddd, ^3J = 23.5 Hz, ^3J = 20.5 Hz, ^5J = 7.8 Hz, 1F, Por-Ar-*m*-*F*) ppm.

Due to the highly diluted NMR samples, the large number of quarternary C atoms and the large number of ^{19}F-coupled C atoms, ^{13}C NMR spectroscopy of **10b** did not provide sufficient signal intensities. Therefore, the **^{13}C NMR** (125 MHz, acetone-d_6, TFA-d, 300 K) spectrum was not analyzable. However, ^{1}H-^{13}C correlation experiments (HMBC, HSQC) confirmed the assignments of the ^{1}H-NMR signals.

MS (ESI-TOF, methanol): m/z (%) = 1152 (100) $[M+H]^+$.

The analytical data are in accordance with the reported data for methoxypyridine record player **10b**.[3]

5-(Biphenylazo-isopropoxypyridine)-10,15,20-tris(pentafluorophenyl)nickel(II)porphyrin (10c). The Ni-porphyrin precursor **5** (30.0 mg, 28.1 µmol) and 3-(3'-bromophenylazo)-4-isopropoxy-pyridine (**8c**) (18 mg, 56.2 µmol) were deployed for a Suzuki cross-coupling reaction according to the general procedure A. Purification via column chromatography on silica gel (cyclohexane/ethyl acetate, 4:1, R_f = 0.39 (*cis*-isomer), 0.08 (*trans*-isomer)) gave a purple solid (30.0 mg, 25.4 µmol, 90 %).

Mp: 186.9°C.

FT-IR (layer): υ = 1733 (w), 1652 (w), 1595 (w), 1518 (s), 1486 (s), 1341 (w), 1299 (w), 1243 (w), 1187 (w), 1071 (m), 1053 (m), 985 (vs), 955 (m), 937 (s), 926 (s), 839 (w), 801 (m), 761 (s), 745 (m), 703 (m), 659 (w) cm^{-1}.

^{1}H NMR (500 MHz, acetone-d_6, TFA-d, 300 K): δ = 9.15-9.13 (m, 4H, Por-*H*), 9.05 (d, ^3J = 5.1 Hz, 2H, Por-*H*), 9.00 (d, ^3J = 5.1 Hz, 2H, Por-*H*), 8.88 (dd, ^3J = 7.0 Hz, ^4J = 1.3 Hz, 1H, Py*H*-6), 8.43 (d, ^4J = 1.3 Hz, 1H, Py*H*-2), 8.34 (dd, ^3J = 7.6 Hz, ^4J = 1.4 Hz, 1H, PorCC*H*), 8.01 (td, ^3J = 7.7 Hz, ^4J = 1.4 Hz, 1H, PorCCCHC*H*), 7.91 (td, ^3J = 7.6 Hz, ^4J = 1.4 Hz, 1H, PorCCHC*H*), 7.89 (d, ^3J = 7.8 Hz, 1H, Py*H*-5), 7.87 (dd, ^3J = 7.8 Hz, ^4J = 1.4 Hz, 1H, PorCCC*H*), 7.69 (t, ^4J = 1.8 Hz, 1H, N_2CC*H*CCH),

7.12 (ddd, ^3J = 7.8 Hz, ^4J = 1.7 Hz, ^4J = 1.1 Hz, 1H, $N_2CCHCCH$), 7.10 (ddd, ^3J = 8.0 Hz, ^4J = 1.9 Hz, ^4J = 1.1 Hz, 1H, $N_2CCHCHCH$), 6.71 (t, ^3J = 7.9 Hz, 1H, $N_2CCHCHCH$), 5.22 (sept, ^3J = 6.1 Hz, 1H, $OCH(CH_3)_2$, 1.33 (d, ^3J = 6.1 Hz, 6H, $OCH(CH_3)_2$ ppm.

^{19}F NMR (470 MHz, acetone-d_6, TFA-d, 300 K): δ = -139.75 (dd, ^3J = 23.4 Hz, ^5J = 6.7 Hz, 1F, Por-Ar-*o*-*F*), -139.82 (dd, ^3J = 23.6 Hz, ^5J = 6.5 Hz, 2F, Por-Ar-*o*-*F*), -140.21 (dd, ^3J = 23.8 Hz, ^5J = 7.1 Hz, 2F, Por-Ar-*o*-*F*), -140.52 (dd, ^3J = 23.7 Hz, ^5J = 7.4 Hz, 1F, Por-Ar-*o*-*F*), -155.59 (t, ^3J = 20.4 Hz, 2F, Por-Ar-*p*-*F*), -155.66 (t, ^3J = 20.4 Hz, 1F, Por-Ar-*p*-*F*), -164.34 (ddd, ^3J = 23.4 Hz, ^3J = 20.4 Hz, ^5J = 7.4 Hz, 1F, Por-Ar-*m*-*F*), -164.34 to -164.50 (m, 4F, Por-Ar-*m*-*F*), -164.65 (ddd, ^3J = 23.7 Hz, ^3J = 20.4 Hz, ^5J = 7.4 Hz, 1F, Por-Ar-*m*-*F*) ppm.

Due to the highly diluted NMR samples, the large number of quarternary C atoms and the large number of ^{19}F-coupled C atoms, ^{13}C NMR spectroscopy of **10c** did not provide sufficient signal intensities. Therefore, the **^{13}C NMR** (125 MHz, acetone-d_6, TFA-d, 300 K) spectrum was not analyzable. However, ^{1}H-^{13}C correlation experiments (HMBC, HSQC) confirmed the assignments of the ^{1}H-NMR signals.

HR-MS (EI, TOF-Q): m/z $[M]^{\bullet+}$ calcd for $C_{58}H_{26}F_{15}N_7NiO$, 1179.1313; found 1179.1314 (+0.1 ppm).

5-(Biphenylazo-*N*-methylimidazole)-10,15,20-tris(pentafluorophenyl)nickel(II)porphyrin (11a).[4] The Ni-porphyrin precursor **5** (20.0 mg, 18.7 µmol) and 5-(3'-bromophenylazo)-1-methylimidazole (**9a**) (8.00 mg, 30.2 µmol) were deployed for a Suzuki cross-coupling reaction according to the general procedure B for reactions with azoimidazole-based switching units. Purification of the obtained crude product was achieved via column chromatography on silica gel (cyclohexane/ethyl acetate, 4:1→1:1→2:3, R_f = 0.68 (*cis*) & 0.40 (*trans*)) and yielded a purple solid (19.0 mg, 16.9 µmol, 90 %).

^{1}H NMR (500 MHz, acetone-d_6, 300 K): δ = 10.47-9.07 (m, 8H, Por-*H*), 8.27 (d, ^3J = 7.20, 1H, PorCC*H*), 7.99 (t, ^3J = 7.65 Hz, 1H, PorCCCHC*H*), 7.92 (dd, ^3J = 7.80 Hz, ^3J = 1.06 Hz, 1H, PorCCC*H*), 7.87 (t, ^3J = 7.25 Hz, 1H, PorCCHC*H*), 7.34 (s, br, 1H, $N_2CCHCPh$), 7.08 (d, ^3J = 7.60 Hz, 1H, $N_2CCHCCH$), 6.94 (d, ^3J = 7.95 Hz, 1H, $N_2CCHCHCH$), 6.71 (t, ^3J = 7.80 Hz, 1H, $N_2CCHCHCH$), 3.01 (s, br, 3H, $-NCH_3$) ppm.

The ^{1}H NMR signals experience strong line broadening which is due to intermolecular coordination. The imidazole protons are too broad and cannot be assigned. Deuterated trifluoroacetic acid (TFA-d, 25 µL) was added to protonate the imidazole and consequently inhibit intermolecular coordination.

^{1}H NMR (500 MHz, acetone-d6, TFA-d, 300 K): δ = 9.17-9.12 (m, 4H, Por-*H*), 9.10 (s, br, 1H, CH_3NCHN), 9.05 (d, ^3J = 4.95 Hz, 2H, Por-*H*), 8.99 (d, ^3J = 5.05 Hz, 2H, Por-*H*), 8.36-8.33 (m, 1H, PorCC*H*), 8.03-7.98 (m, 1H, PorCCCHC*H*), 7.92-7.87 (m, 2H, PorCCC*H*, PorCCHC*H*), 7.50 (d, ^{4}J = 1.45 Hz, 1H, N_2CCHN), 7.36-7.32 (m, 2H, $N_2CCHCPh$, $N_2CCHCPhCH$), 7.14 (ddd, ^3J = 7.94 Hz, ^4J =

1.86 Hz, ^4J = 1.19 Hz, 1H, $N_2CCHCHCH$), 6.90 (t, ^3J = 8.13 Hz, 1H, $N_2CCHCHCH$), 3.53 (s, 3H, NCH_3) ppm.

^{19}F NMR (470 MHz, acetone-d6, TFA-d, 300 K): δ = -139.69 (dd, ^3J = 23.7 Hz, ^4J = 7.58 Hz, 1F, Por-Ar-*o*-*F*), -140.02 (dd, ^3J = 23.4 Hz, ^4J = 7.38 Hz, 2F, Por-Ar-*o*-*F*), -140.20 (dd, ^3J = 23.2 Hz, ^4J = 6.71 Hz, 2F, Por-Ar-*o*-*F*), -140.63 (dd, ^3J = 23.6 Hz, ^4J = 6.28 Hz, 1F, Por-Ar-*o*-*F*), -155.55 (t, ^3J = 20.3 Hz, 2F, Por-Ar-*p*-*F*), -155.61 (t, ^3J = 20.4 Hz, 1F, Por-Ar-*p*-*F*), -164.27 (ddd, ^3J = 23.5 Hz, ^3J = 20.5 Hz, ^4J = 8.21 Hz, 1F, Por-Ar-*m*-*F*), -164.34 to -164.57 (m, 4F, Por-Ar-*m*-*F*), -164.67 (ddd, ^3J = 23.5 Hz, ^3J = 20.1 Hz, ^4J = 8.05 Hz, 1F, Por-Ar-*m*-*F*) ppm.

Due to the highly diluted NMR samples, the large number of quarternary C atoms and the large number of ^{19}F-coupled C atoms, ^{13}C NMR spectroscopy of **11a** did not provide sufficient signal intensities. Therefore, the **^{13}C NMR** (150 MHz, acetone-d_6, TFA-d, 300 K) spectrum was not analyzable. However, ^{1}H-^{13}C correlation experiments (HMBC, HSQC) confirmed the assignments of the ^{1}H-NMR signals.

HR-MS (EI, TOF-Q): m/z $[M]^{\bullet+}$ calcd for $C_{54}H_{21}F_{15}N_8Ni$, 1124.1003; found 1124.0989 (-1.2 ppm).

The analytical data are in accordance with the reported data for *N*-methylimidazole record player **11a**.[4]

5-(Biphenyl-*p*-fluoro-azo-*N*-methylimidazole)-10,15,20-tris(pentafluorophenyl)nickel(II)porphyrin (11b). The Ni-porphyrin precursor **5** (19.5 mg, 18.3 µmol) and 5-(3'-bromo-4'-fluorophenylazo)-1-methylimidazole (**9b**) (7.50 mg, 26.5 µmol) were deployed for a Suzuki cross-coupling reaction according to the general procedure B for reactions with azoimidazole-based switching units. Purification of the obtained crude product was achieved via column chromatography on silica gel (cyclohexane/ethyl acetate, 4:1→3:2→2:3, R_f = 0.70 (*cis*) & 0.46 (*trans*)) and yielded a purple solid (17.2 mg, 15.0 µmol, 82 %).

Mp: 250 °C (decomp.).

FT-IR (layer): υ = 1752 (w), 1651 (w), 1518 (s), 1486 (vs), 1430 (m), 1342 (m), 1211 (w), 1164 (w), 1114 (m), 1060 (m), 985 (vs), 956 (m), 938 (vs), 839 (m), 800 (m), 762 (vs), 744 (s), 703 (s), 646 (m), 614 (w), 572 (w) cm^{-1}.

^{1}H NMR (500 MHz, acetone-d_6, 300 K): δ = 9.76 (s, br, 8H, Por-*H*,), 8.36 (d, ^3J = 7.26 Hz, 1H, PorCC*H*), 8.00 (t, ^3J = 7.74 Hz, 1H, PorCCCHC*H*), 7.94 (t, ^3J = 7.08 Hz, 1H, PorCCHC*H*), 7.88 (d, ^3J = 7.62 Hz, 1H, PorCCC*H*), 7.31 (d, $^4J_{H\rightarrow F}$ = 4.92 Hz, 1H, $N_2CCHCCO$), 6.93 (s, br, 1H, $N_2CCHCHCO$), 6.62 (dd(t), $^3J_{H\rightarrow F}$ = 9.00 Hz, $^3J_{H\rightarrow H}$ = 9.00 Hz, 1H, $N_2CCHCHCO$), 3.07 (s, br, 3H, NCH_3) ppm.

The ^{1}H NMR signals experience strong line broadening which is due to intermolecular coordination. The imidazole protons are too broad and cannot be assigned. Deuterated trifluoroacetic acid (TFA-d, 25 µL) was added to protonate the imidazole and consequently inhibit intermolecular coordination.

^{1}H NMR (500 MHz, acetone-d_6, TFA-d, 300 K): δ = 9.15 (dd, ^{4}J = 1.43 Hz, ^{4}J = 0.68 Hz, 1H, CH_3NCHN), 9.14-9.12 (m, 4H, Por-*H*), 9.08 (d, ^{3}J = 5.00 Hz, 2H, Por-*H*), 9.01 (d, ^{3}J = 4.95 Hz, 2H, Por-*H*), 8.44 (dd, ^{3}J = 7.50 Hz, ^{4}J = 1.10 Hz, 1H, PorCC*H*), 8.01 (td, ^{3}J = 7.70 Hz, ^{4}J = 1.48 Hz, 1H, PorCCCHC*H*), 7.96 (td, ^{3}J = 7.57 Hz, ^{4}J = 1.50 Hz, 1H, PorCCHC*H*), 7.86 (d, ^{3}J = 7.80 Hz, 1H, PorCCC*H*), 7.52 (d, ^{4}J = 1.50 Hz, 1H, N_2CCHN), 7.41 (dd, $^{4}J_{H\rightarrow F}$ = 6.88 Hz, $^{4}J_{H\rightarrow H}$ = 2.53 Hz, 1H, $N_2CCHCCO$), 7.17 (ddd, $^{3}J_{H\rightarrow H}$ = 8.77 Hz, $^{4}J_{H\rightarrow F}$ = 4.73 Hz, $^{4}J_{H\rightarrow H}$ = 2.58 Hz, 1H, $N_2CCHCHCO$), 6.75 (dd(t), $^{3}J_{H\rightarrow H}$ = 9.08 Hz, $^{3}J_{H\rightarrow F}$ = 9.08 Hz, 1H, $N_2CCHCHCO$), 3.73 (d, ^{4}J = 0.50 Hz, 3H, NCH_3) ppm.

^{19}F NMR (470 MHz, acetone-d_6, TFA-d, 300 K): δ = -107.32 (s, 1F, $N_2CCHCCF$), -139.68 (dd, ^{3}J = 23.7 Hz, ^{4}J = 7.22 Hz, 1F, Por-Ar-*o*-*F*), -140.11 to -140.30 (m, 4F, Por-Ar-*o*-*F*), -140.69 (dd, ^{3}J = 23.7 Hz, ^{4}J = 7.22 Hz, 1F, Por-Ar-*o*-*F*), -155.60 (t, ^{3}J = 20.3 Hz, 2F, Por-Ar-*p*-*F*), -155.67 (t, ^{3}J = 20.3 Hz, 1F, Por-Ar-*p*-*F*), -164.28 (ddd, ^{3}J = 23.1 Hz, ^{3}J = 20.5 Hz, ^{4}J = 7.84 Hz, 1F, Por-Ar-*m*-*F*), -164.34 to -164.55 (m, 4F, Por-Ar-*m*-*F*), -164.69 (ddd, ^{3}J = 23.3 Hz, ^{3}J = 20.6 Hz, ^{4}J = 7.93 Hz, 1F, Por-Ar-*m*-*F*) ppm.

Due to the highly diluted NMR samples, the large number of quarternary C atoms and the large number of ^{19}F-coupled C atoms, ^{13}C NMR spectroscopy of **11b** did not provide sufficient signal intensities. Therefore, the **^{13}C-NMR (150 MHz, acetone-d_6, 300 K)** spectrum was not analyzable. However, ^{1}H-^{13}C correlation experiments (HMBC, HSQC) confirmed the assignments of the ^{1}H-NMR signals.

HR-MS (EI, TOF-Q): m/z $[M]^{\bullet+}$ calcd for $C_{54}H_{20}F_{16}N_8Ni$, 1142.0909; found 1142.0865 (-3.9 ppm).

UV-vis (CH_3CN): λ_{max} (lg ε) = 298 (4.240), 405 (5.272), 524 (4.138), 557 (3.965) nm.

5-(Biphenyl-*p*-methoxy-azo-*N*-methylimidazole)-10,15,20-tris(pentafluorophenyl)nickel(II)-porphyrin (11c). The Ni-porphyrin precursor **5** (20.0 mg, 18.7 µmol) and 5-(3'-bromo-4'-methoxyphenylazo)-1-methylimidazole (**9c**) (7.20 mg, 24.4 µmol) were deployed for a Suzuki cross-coupling reaction according to the general procedure B for reactions with azoimidazole-based switching units. The general procedure B for Suzuki cross coupling reactions with azoimidazole-based switching units was applied using 5-(3'-bromo-4'-methoxyphenylazo)-1-methylimidazole (**9c**) (7.20 mg, 24.4 µmol). Purification of the obtained crude product was achieved via column chromatography on silica gel (cyclohexane/ethyl acetate, 4:1→3:2→2:3, R_f = 0.68 (*cis*) & 0.39 (*trans*)) and yielded a purple solid (20.0 mg, 17.3 µmol, 93 %).

Mp: >400 °C.

FT-IR (layer): υ = 1751 (w), 1651 (w), 1517 (s), 1486 (vs), 1430 (m), 1345 (m), 1260 (m), 1112 (m), 1060 (m), 985 (vs), 956 (m), 938 (vs), 801 (m), 762 (vs), 744 (m), 703 (s), 660 (w), 507 (m) cm^{-1}.

^{1}H NMR (600 MHz, acetone-d_6, 300 K): δ = 9.35 (s, br, 8H, Por-*H*,), 8.34 (d, ^3J = 7.08 Hz, 1H, PorCC*H*), 7.93 (td, ^3J = 7.80 Hz, ^4J = 1.25 Hz, 1H, PorCCCHC*H*), 7.87 (td, ^3J = 7.69 Hz, ^4J = 1.32 Hz, 1H, PorCCHC*H*), 7.75 (dd, ^3J = 7.80 Hz, ^4J = 1.26 Hz, 1H, PorCCC*H*), 7.48 (d, ^4J = 2.34 Hz, 1H, N_2CC*H*CCO), 6.90 (dd, ^3J = 8.70 Hz, ^4J = 2.16 Hz, 1H, N_2CC*H*CHCO), 6.23 (d, ^3J = 8.76 Hz, 1H, N_2CCHC*H*CO), 3.51 (s, br, 3H, NCH_3), 3.03 (s, 3H, OCH_3) ppm.

The ^{1}H NMR signals experience strong line broadening which is due to intermolecular coordination. The imidazole protons are too broad and cannot be assigned. Deuterated trifluoroacetic acid (TFA-d, 20 µL) was added to protonate the imidazole and consequently inhibit intermolecular coordination.

^{1}H NMR (500 MHz, acetone-d_6, TFA-d, 300 K): δ = 9.18 (dd, ^4J = 1.40 Hz, ^4J = 0.60 Hz, 1H, CH_3NC*H*N), 9.14-9.10 (m, 4H, Por-*H*), 9.08-9.02 (m, 4H, Por-*H*), 8.40 (dd, ^3J = 7.41 Hz, ^4J = 1.50 Hz, 1H, PorCC*H*), 7.94 (td, ^3J = 7.65 Hz, ^4J = 1.53 Hz, 1H, PorCCCHC*H*), 7.91 (td, ^3J = 7.54 Hz, ^4J = 1.53 Hz, 1H, PorCCHC*H*), 7.74 (dd, ^3J = 7.61 Hz, ^4J = 1.48 Hz, 1H, PorCCC*H*), 7.55 (d, ^4J = 1.50 Hz, 1H, N_2CC*H*N), 7.53 (d, ^4J = 2.50 Hz, 1H, N_2CC*H*CCO), 7.07 (dd, ^3J = 8.83 Hz, ^4J = 2.53 Hz, 1H, N_2CC*H*CHCO), 6.37 (d, ^3J = 8.95 Hz, 1H, N_2CCHC*H*CO), 3.95 (d, ^4J = 0.47 Hz, 3H, NCH_3), 3.20 (s, 3H, OCH_3) ppm.

^{19}F NMR (470 MHz, acetone-d_6, TFA-d, 300 K): δ = -139.67 (dd, ^3J = 23.8 Hz, ^4J = 7.65 Hz, 1F, Por-Ar-*o*-*F*), -140.11 to -140.42 (m, 4F, Por-Ar-*o*-*F*), -140.67 (dd, ^3J = 22.9 Hz, ^4J = 6.64 Hz, 1F, Por-Ar-*o*-*F*), -155.54 to -155.73 (m, 3F, Por-Ar-*p*-*F*), -164.24 to -164.64 (m, 5F, Por-Ar-*m*-*F*), -164.72 (ddd, ^3J = 23.2 Hz, ^3J = 20.7 Hz, ^4J = 7.84 Hz, 1F, Por-Ar-*m*-*F*) ppm.

Due to the highly diluted NMR samples, the large number of quarternary C atoms and the large number of ^{19}F-coupled C atoms, ^{13}C NMR spectroscopy of **11c** did not provide sufficient signal intensities. Therefore, the **^{13}C NMR** (150 MHz, acetone-d_6, 300 K) spectrum was not analyzable. However, ^{1}H-^{13}C correlation experiments (HMBC, HSQC) confirmed the assignments of the ^{1}H-NMR signals.

HR-MS (EI, TOF-Q): m/z $[M]^{\bullet+}$ calcd for $C_{55}H_{23}F_{15}N_8ONi$, 1154.1109; found 1154.1073 (-3.1 ppm).

UV-vis (CH_3CN): λ_{max} (lg ε) = 405 (5.290), 524 (4.168), 557 (4.004) nm.

5-(Biphenyl-*p*-isopropoxy-azo-*N*-methylimidazole)-10,15,20-tris(pentafluorophenyl)nickel(II)-porphyrin (11d). The Ni-porphyrin precursor **5** (20.0 mg, 18.7 µmol) and 5-(3'-bromo-4'-isopropoxyphenylazo)-1-methylimidazole (**9d**) (7.55 mg, 23.3 µmol) were deployed for a Suzuki cross-coupling reaction according to the general procedure B for reactions with azoimidazole-based switching units. Purification of the obtained crude product was achieved via column chromatography

on silica gel (cyclohexane/ethyl acetate, 4:1→3:2→2:3, R_f = 0.70 (*cis*) & 0.46 (*trans*)) and yielded a purple solid (14.6 mg, 12.3 µmol, 66 %).

Mp: >400 °C.

FT-IR (layer): υ = 2975 (w), 2932 (w), 1651 (w), 1591 (w), 1518 (s), 1486 (s), 1431 (w), 1345 (m), 1257 (m), 1223 (w), 1164 (w), 1129 (w), 1109 (m), 1075 (m), 1060 (m), 986 (vs), 956 (m), 938 (s), 926 (s), 839 (w), 801 (m), 762 (s), 744 (m), 703 (m), 665 (w), 647 (w), 600 (w), 573 (w), 517 (w) cm^{-1}.

^{1}H NMR (600 MHz, acetone-d_6, 300 K): δ = 9.49 (s, br, 8H, Por-*H*,), 8.31 (d, ^3J = 7.32 Hz, 1H, PorCC*H*), 7.90 (t, ^3J = 7.65 Hz, 1H, PorCCCHC*H*), 7.85 (t, ^3J = 7.38 Hz, 1H, PorCCHC*H*), 7.76 (d, ^3J = 7.68 Hz, 1H, PorCCC*H*), 7.33 (s, 1H, N_2CC*H*CCO), 6.89 (d, ^3J = 8.28 Hz, 1H, N_2CC*H*CHCO), 6.44 (d, ^3J = 8.76 Hz, 1H, N_2CCHC*H*CO), 4.39 (sept., ^3J = 6.01 Hz, 1H, OC*H*(CH_3)$_2$), 3.28 (s, br, 3H, NC*H*$_3$), 0.97 (s, br, 6H, OCH(C*H*$_3$)$_2$) ppm.

^{19}F NMR (470 MHz, acetone-d_6, 300 K): δ = -139.4 to -139.8 (m, 3F, Por-Ar-*o*-*F*), -140.0 to -140.40 (m, 3F, Por-Ar-*o*-*F*), -155.6 to -155.9 (m, 3F, Por-Ar-*p*-*F*), -164.2 to -164.8 (m, 6F, Por-Ar-*m*-*F*) ppm.

The ^{1}H NMR signals experience strong line broadening which is due to intermolecular coordination. The imidazole protons are too broad and cannot be assigned. Deuterated trifluoroacetic acid (TFA-d, 20 µL) was added to protonate the imidazole and consequently inhibit intermolecular coordination.

^{1}H NMR (500 MHz, acetone-d_6, TFA-d, 300 K): δ = 9.13 (dd, ^4J = 1.45 Hz, ^4J = 0.65 Hz, 1H, CH_3NC*H*N), 9.12-9.09 (m, 4H, Por-*H*), 9.09-9.06 (m, 4H, Por-*H*), 8.38 (dd, ^3J = 7.48 Hz, ^4J = 1.50 Hz, 1H, PorCC*H*), 7.93 (td, ^3J = 7.69 Hz, ^4J = 1.50 Hz, 1H, PorCCCHC*H*), 7.88 (td, ^3J = 7.54 Hz, ^4J = 1.49 Hz, 1H, PorCCHC*H*), 7.75 (dd, ^3J = 7.70 Hz, ^4J = 1.50 Hz, 1H, PorCCC*H*), 7.43 (d, 4J = 1.55 Hz, 1H, N_2CC*H*N), 7.40 (d, ^4J = 2.55 Hz, 1H, N_2CC*H*CCO), 7.09 (dd, ^3J = 8.83 Hz, ^4J = 2.58 Hz, 1H, N_2CC*H*CHCO), 6.58 (d, ^3J = 8.88 Hz, 1H, N_2CCHC*H*CO), 4.49 (sept., ^3J = 6.08 Hz, 1H, OC*H*(CH_3)$_2$), 3.83 (d, ^4J = 0.50 Hz, 3H, NC*H*$_3$), 1.04 (s, br, 6H, OCH(C*H*$_3$)$_2$) ppm.

^{19}F NMR (470 MHz, acetone-d_6, TFA-d, 300 K): δ = -139.66 (dd, ^3J = 23.6 Hz, ^4J = 7.93 Hz, 1F, Por-Ar-*o*-*F*), -140.04 to -140.55 (m, 4F, Por-Ar-*o*-*F*), -140.65 (dd, ^3J = 23.0 Hz, ^4J = 7.55 Hz, 1F, Por-Ar-*o*-*F*), -155.58 (t, ^3J = 20.3 Hz, 2F, Por-Ar-*p*-*F*), -155.67 (t, ^3J = 20.3 Hz, 1F, Por-Ar-*p*-*F*), -164.31 (ddd, ^3J = 23.6 Hz, ^3J = 20.4 Hz, ^4J = 7.88 Hz, 1F, Por-Ar-*m*-*F*), -164.43 (s, br, 2F, Por-Ar-*m*-*F*), -164.59 (ddd, ^3J = 23.6 Hz, ^3J = 20.7 Hz, ^4J = 7.84 Hz, 2F, Por-Ar-*m*-*F*), -164.73 (ddd, ^3J = 23.6 Hz, ^3J = 20.5 Hz, ^4J = 7.91 Hz, 1F, Por-Ar-*m*-*F*) ppm.

Due to the highly diluted NMR samples, the large number of quarternary C atoms and the large number of ^{19}F-coupled C atoms, ^{13}C NMR spectroscopy of **11d** did not provide sufficient signal intensities. Therefore, the **^{13}C NMR** (150 MHz, acetone-d_6, 300 K) spectrum was not analyzable. However, ^{1}H-^{13}C correlation experiments (HMBC, HSQC) confirmed the assignments of the ^{1}H-NMR signals.

HR-MS (EI, TOF-Q): m/z $[M]^{\bullet+}$ calcd for $C_{57}H_{27}F_{15}N_8ONi$, 1182.1422; found 1182.1407 (-1.3 ppm).

UV-vis (CH_3CN): λ_{max} (lg ε) = 405 (5.290), 524 (4.169), 557 (3.987) nm.

III. NMR Spectra

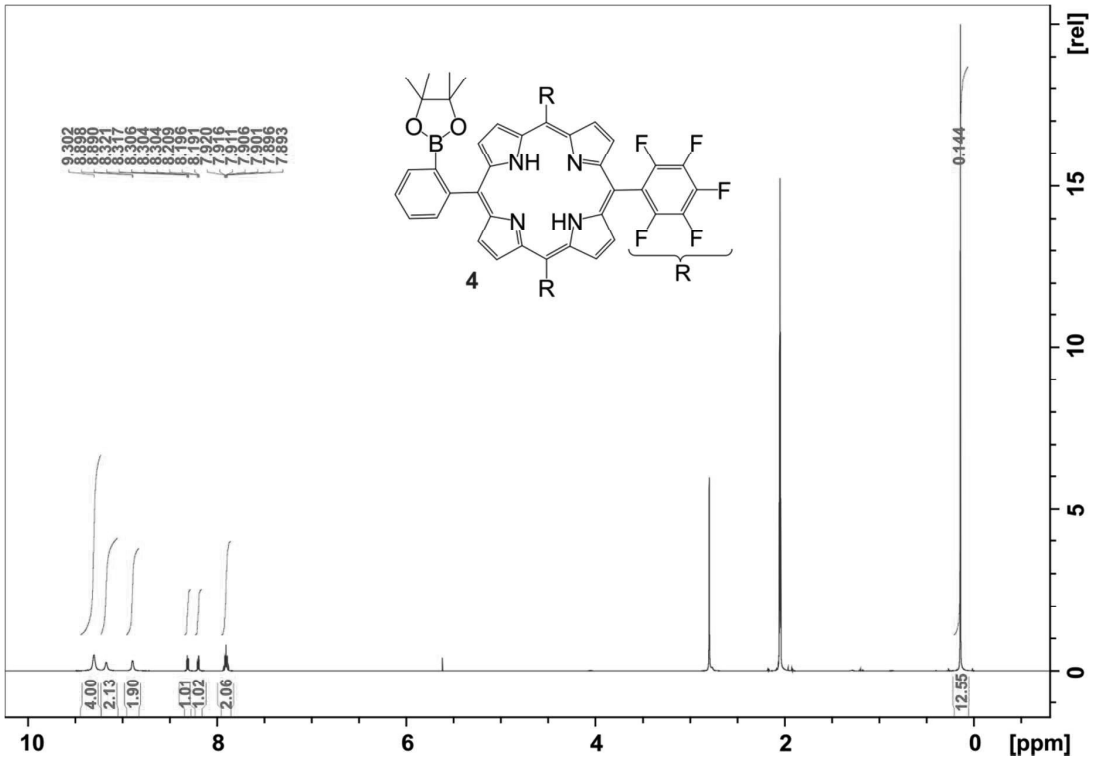

Figure S1. ^{1}H-NMR (500 MHz, acetone-d_6, 300 K) spectrum of **4**.

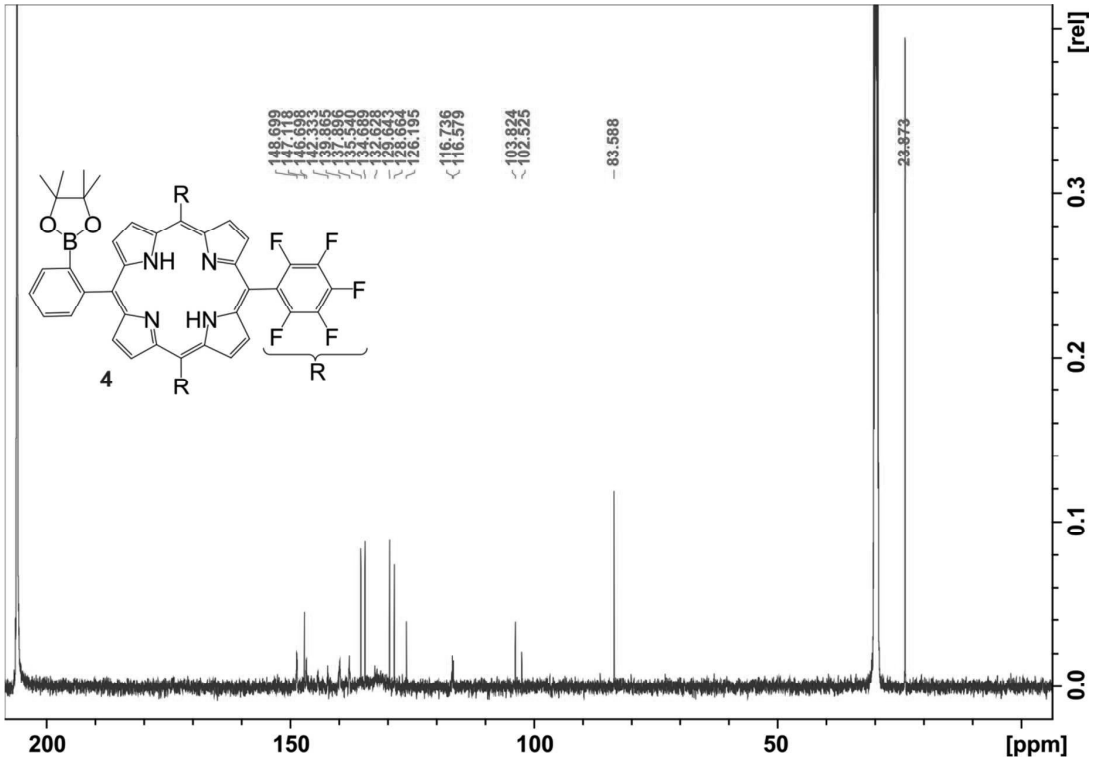

Figure S2. ^{13}C-NMR (125 MHz, acetone-d_6, 300 K) spectrum of **4**.

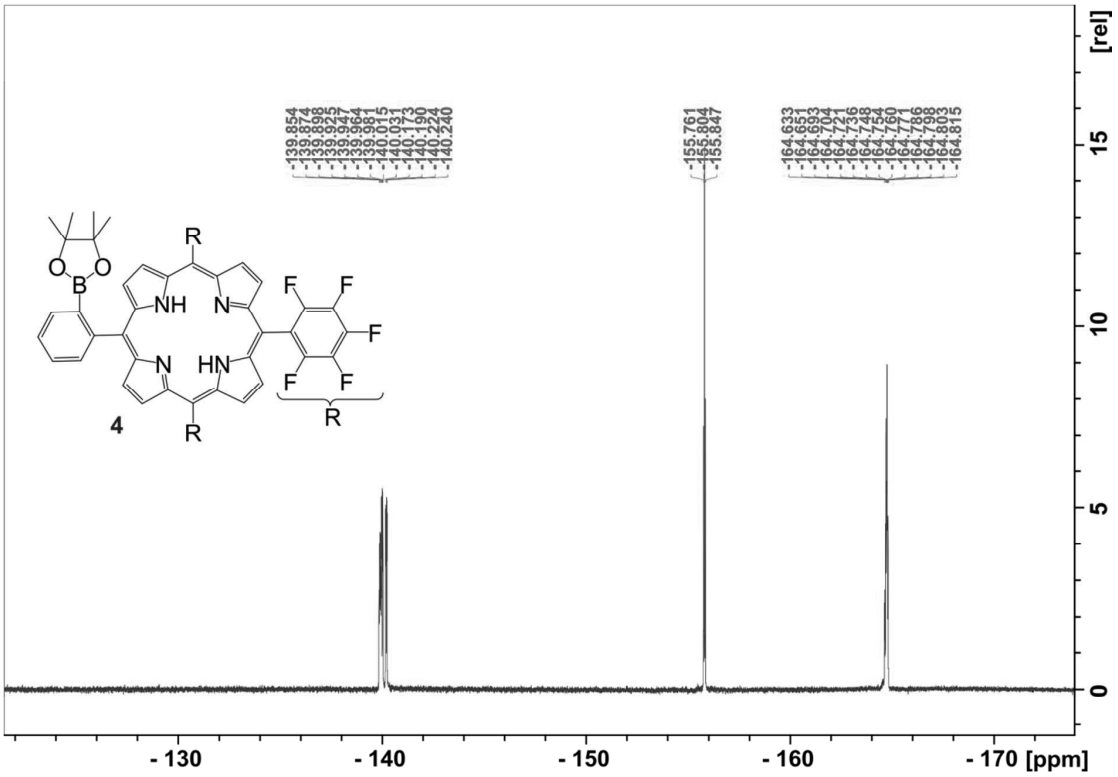

Figure S3. ^{19}F-NMR (470 MHz, acetone-d_6, 300 K) spectrum of **4**.

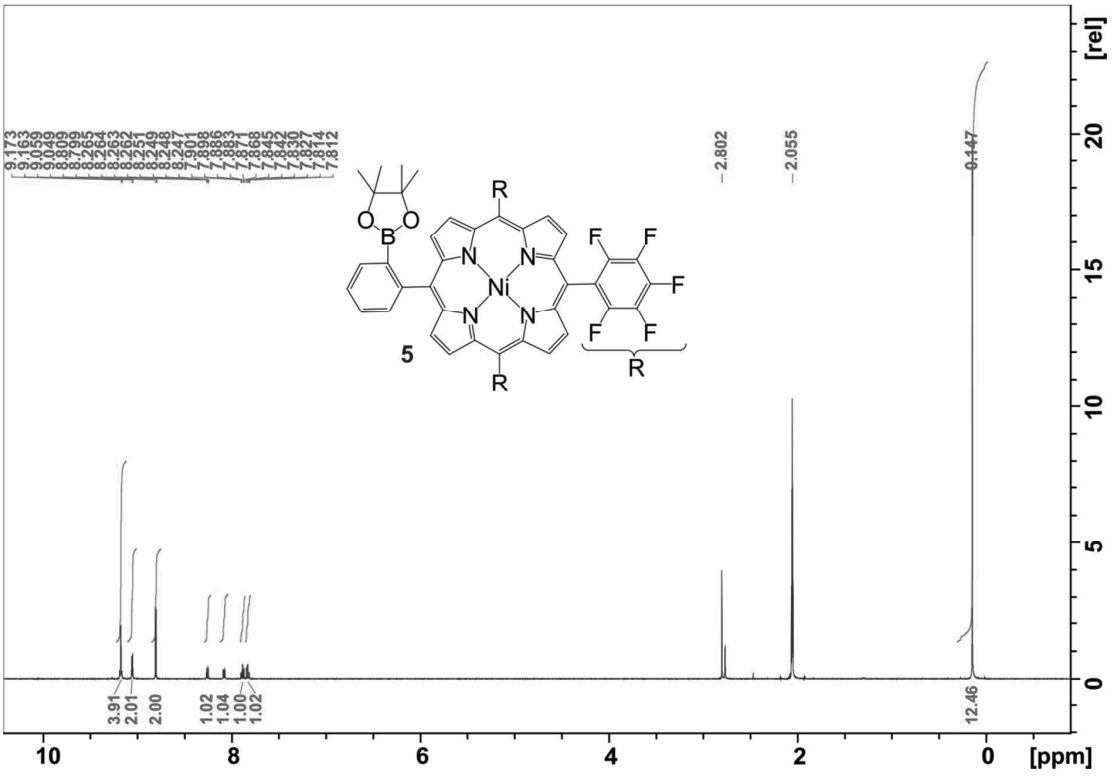

Figure S4. ^{1}H-NMR (500 MHz, acetone-d_6, 300 K) spectrum of **5**.

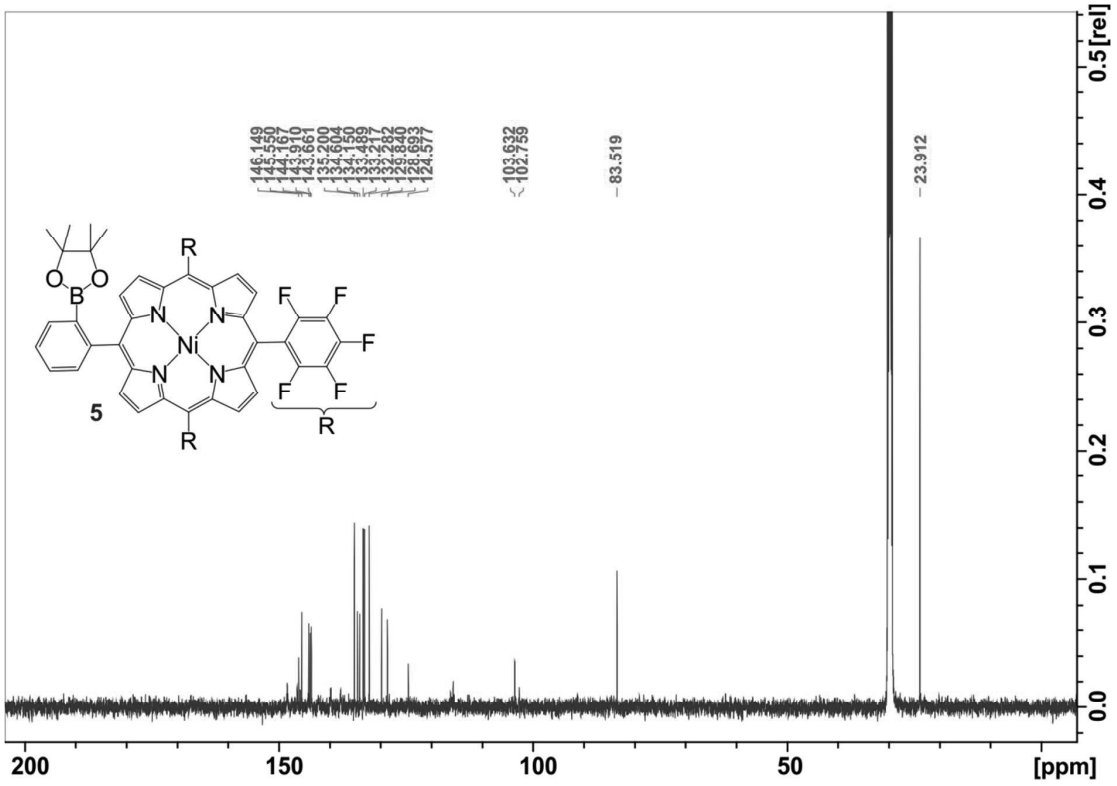

Figure S5. ^{13}C-NMR (125 MHz, acetone-d_6, 300 K) spectrum of **5**.

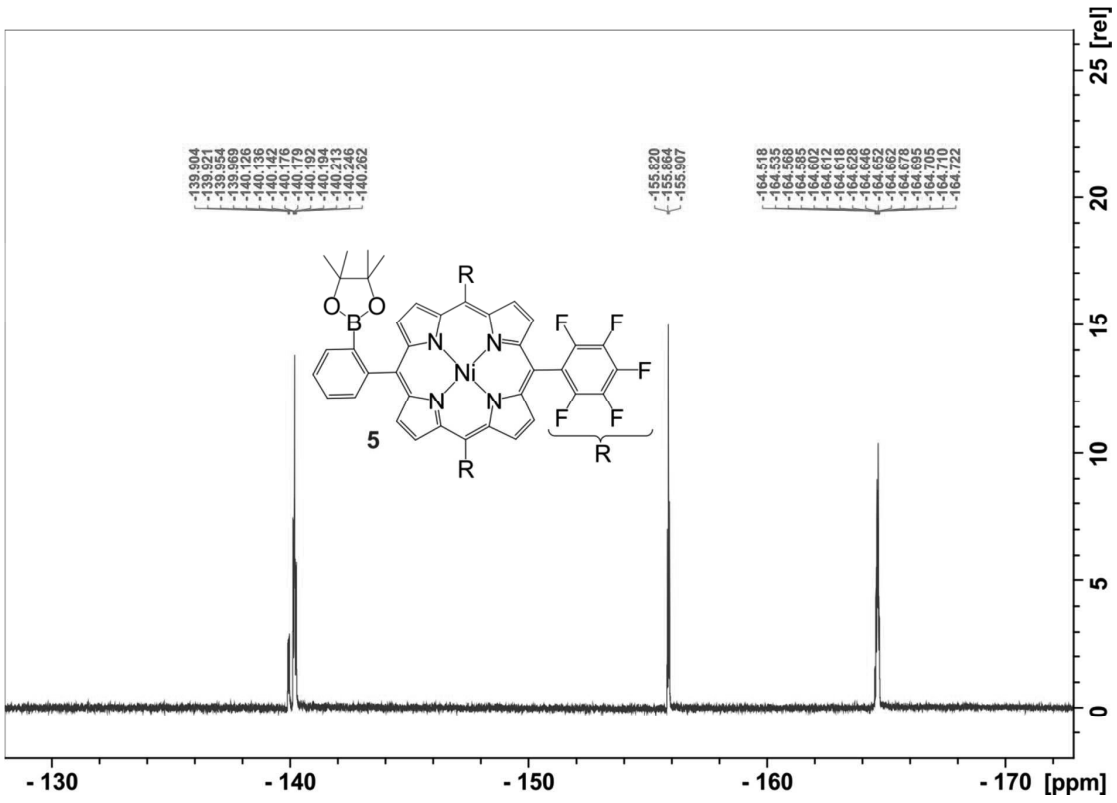

Figure S6. ^{19}F-NMR (470 MHz, acetone-d_6, 300 K) spectrum of **5**.

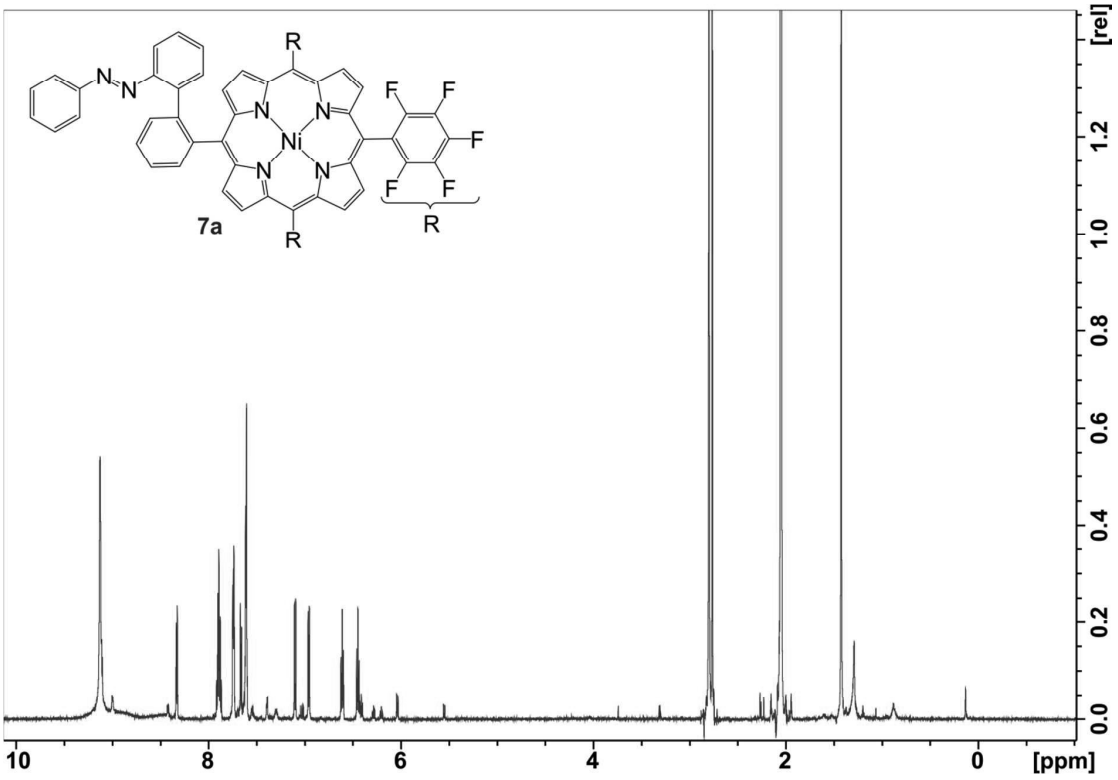

Figure S7. ^{1}H-NMR (500 MHz, acetone-d_6, 300 K) spectrum of **7a**.

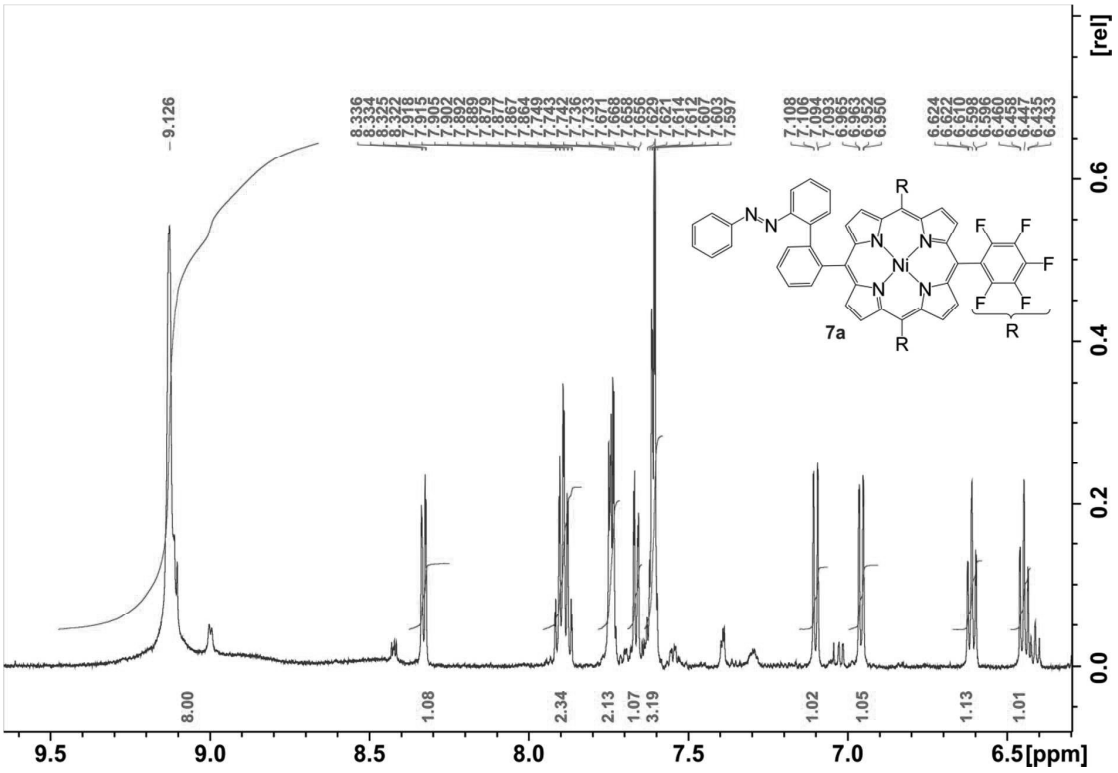

Figure S8. ^{1}H-NMR (500 MHz, acetone-d_6, 300 K) spectrum (aromatic region) of **7a**.

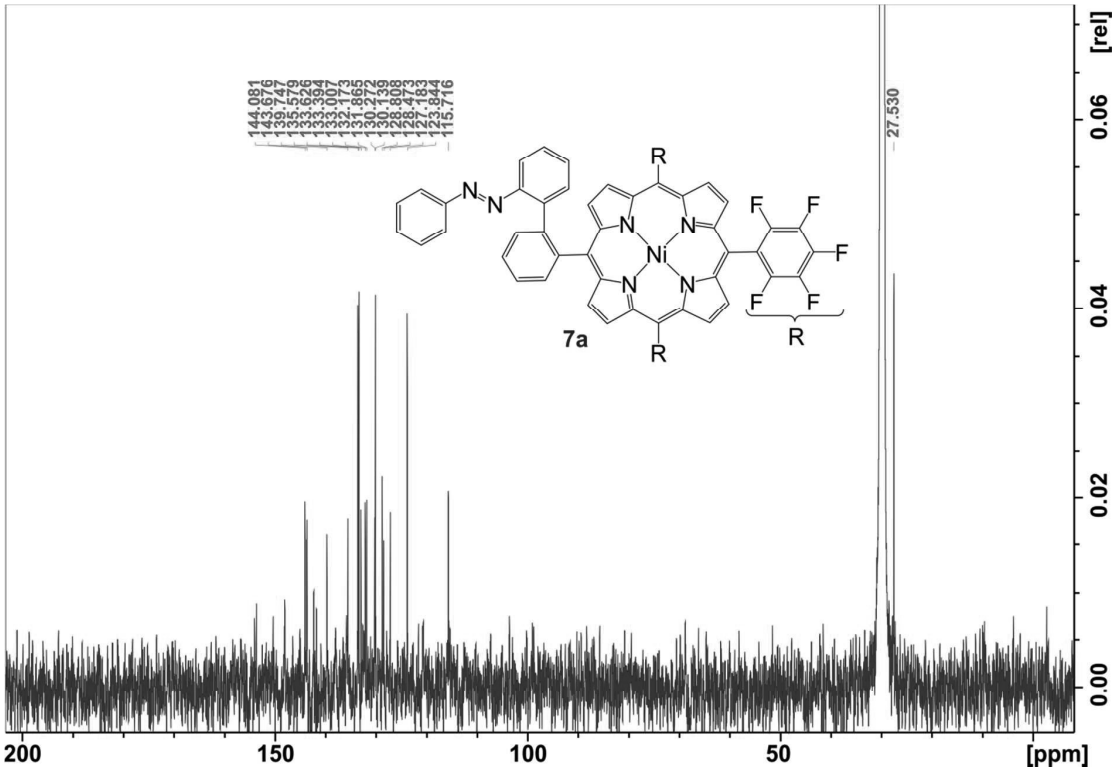

Figure S9. ^{13}C-NMR (125 MHz, acetone-d_6, 300 K) spectrum of **7a**.

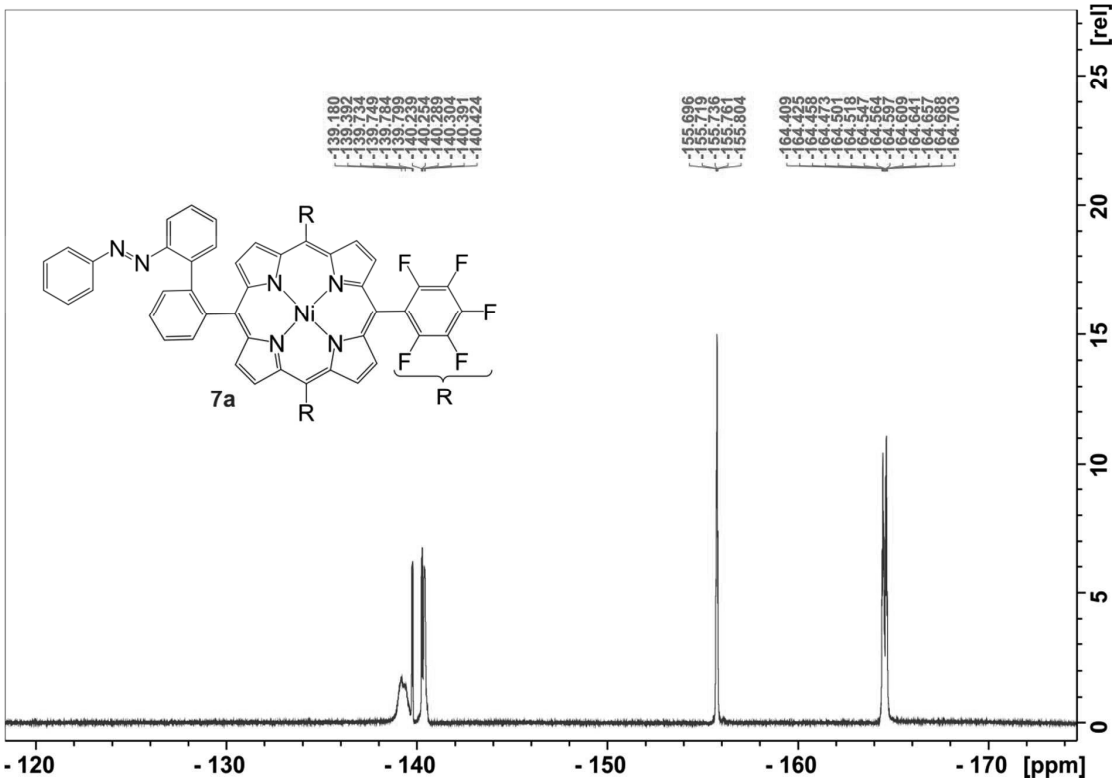

Figure S10. ^{19}F-NMR (470 MHz, acetone-d_6, 300 K) spectrum of **7a**.

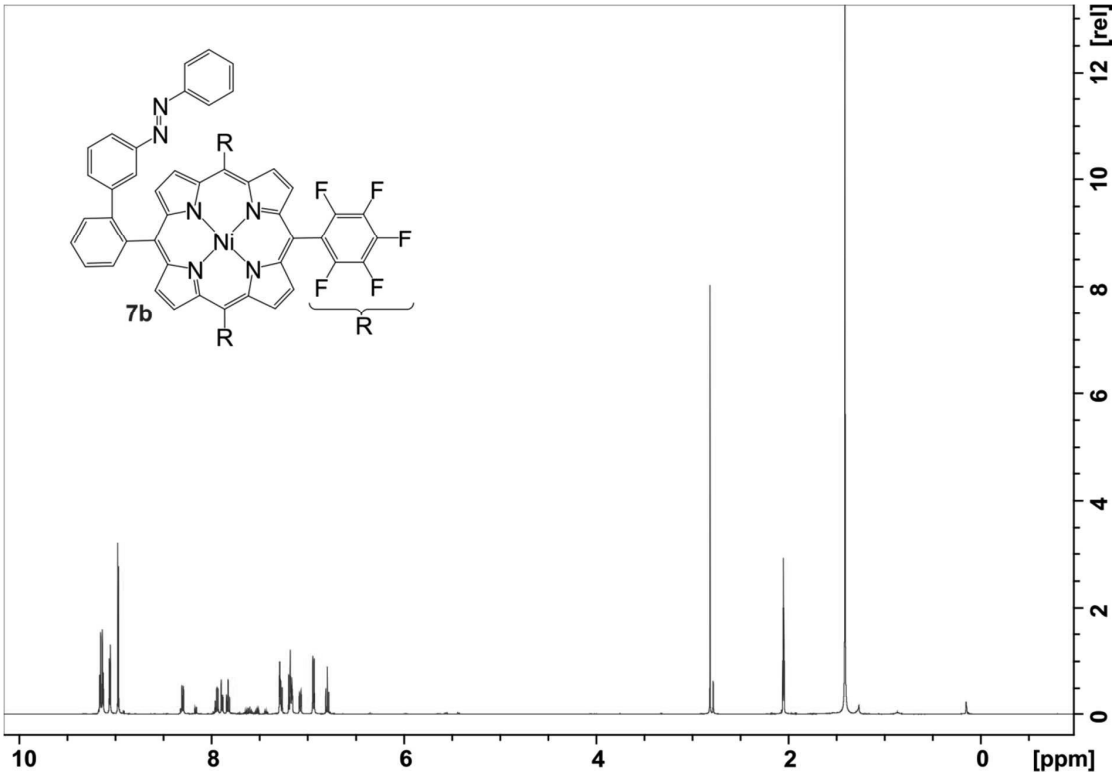

Figure S11. ^{1}H-NMR (500 MHz, acetone-d_6, 300 K) spectrum of **7b**.

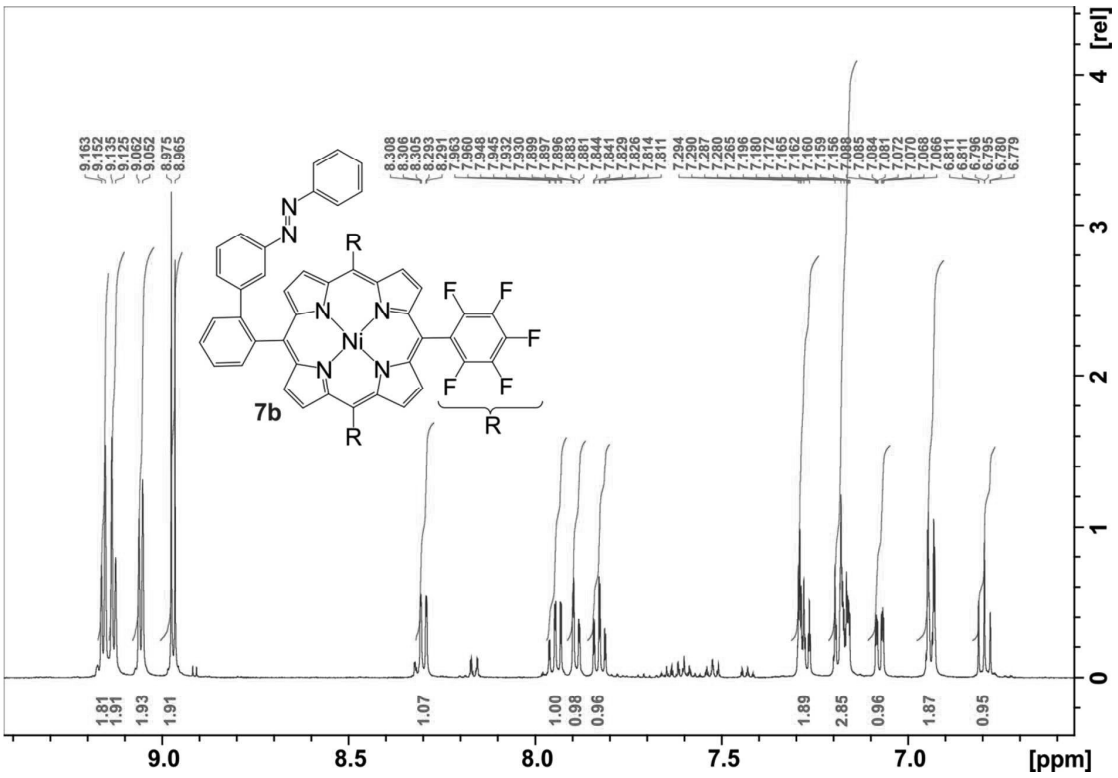

Figure S12. ^{1}H-NMR (500 MHz, acetone-d_6, 300 K) spectrum (aromatic region) of **7b**.

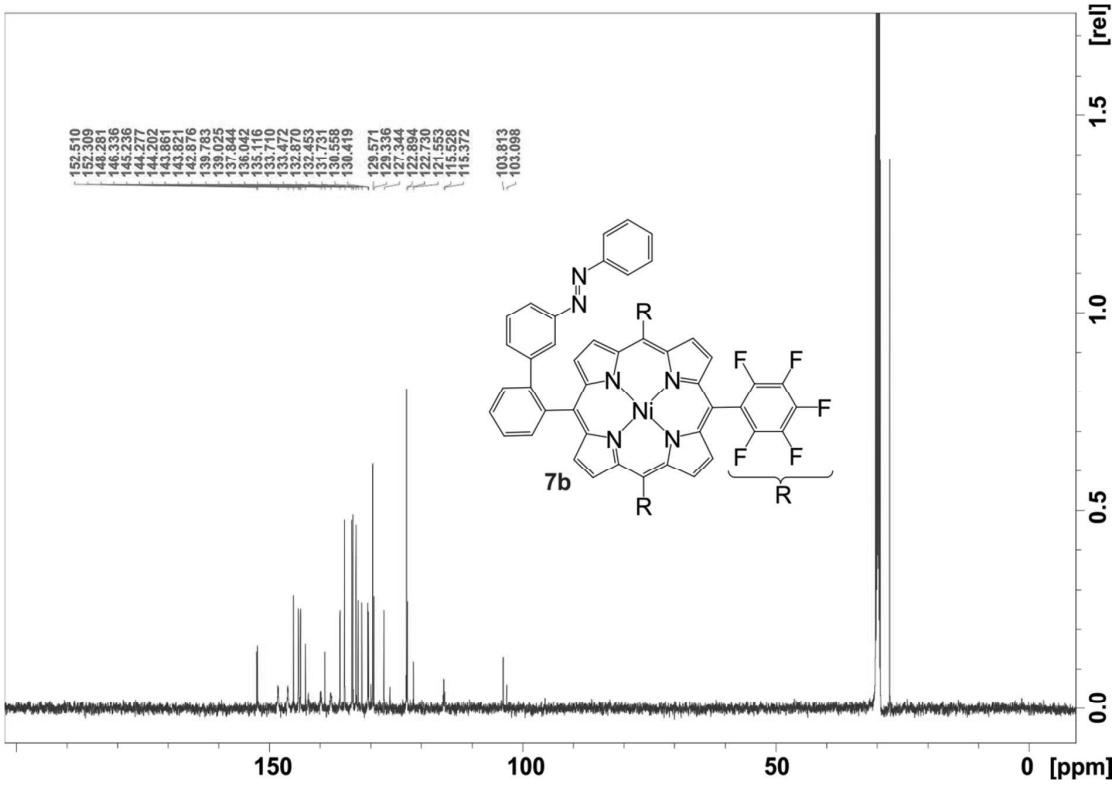

Figure S13. ^{13}C-NMR (125 MHz, acetone-d_6, 300 K) spectrum of **7b**.

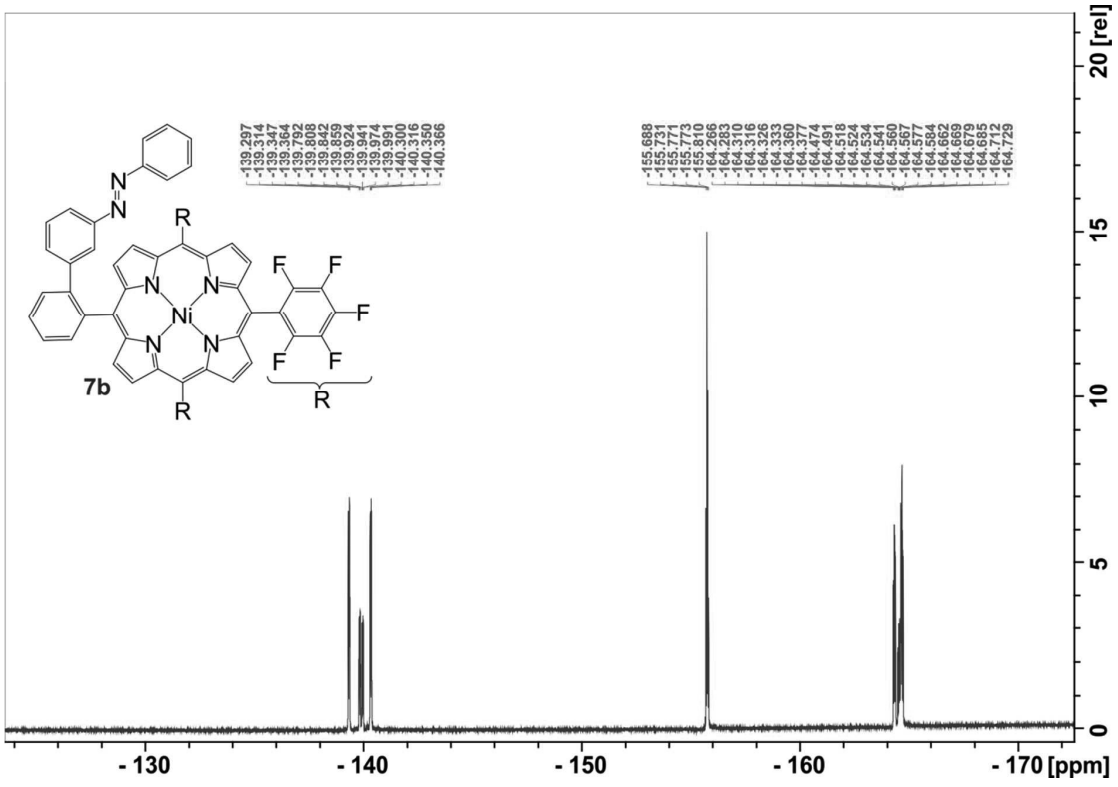

Figure S14. ^{19}F-NMR (470 MHz, acetone-d_6, 300 K) spectrum of **7b**.

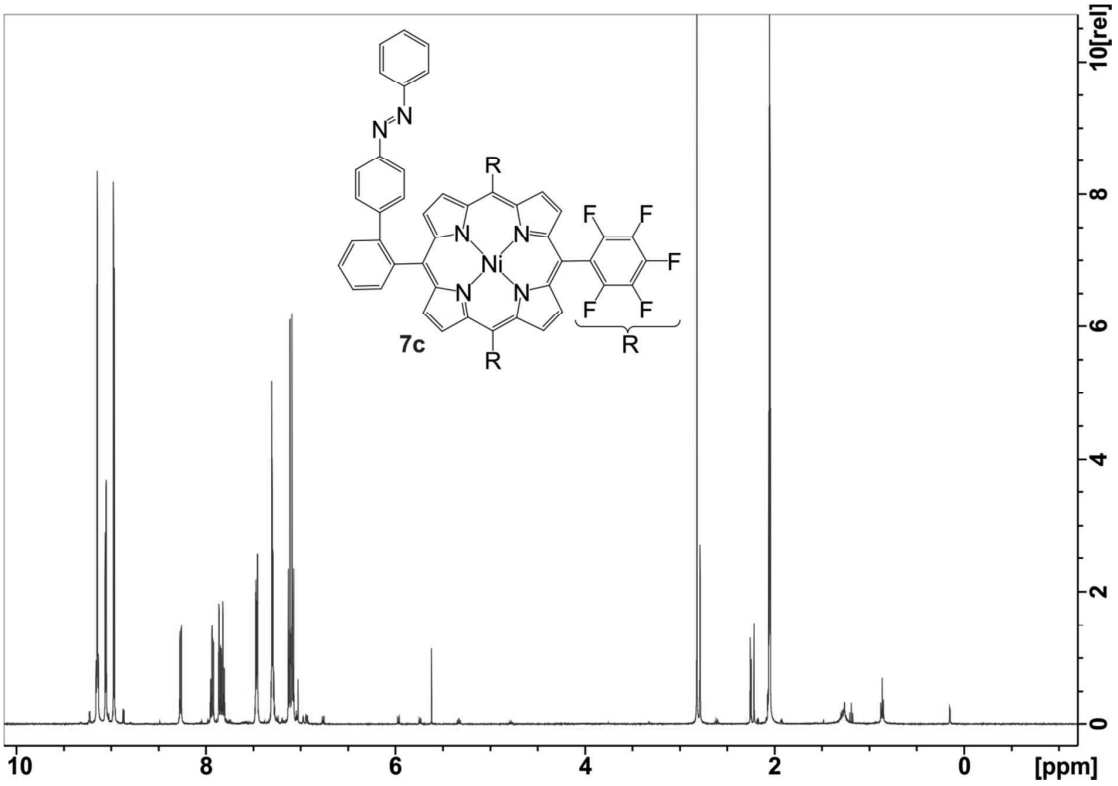

Figure S15. ^{1}H-NMR (500 MHz, acetone-d_6, 300 K) spectrum of **7c**.

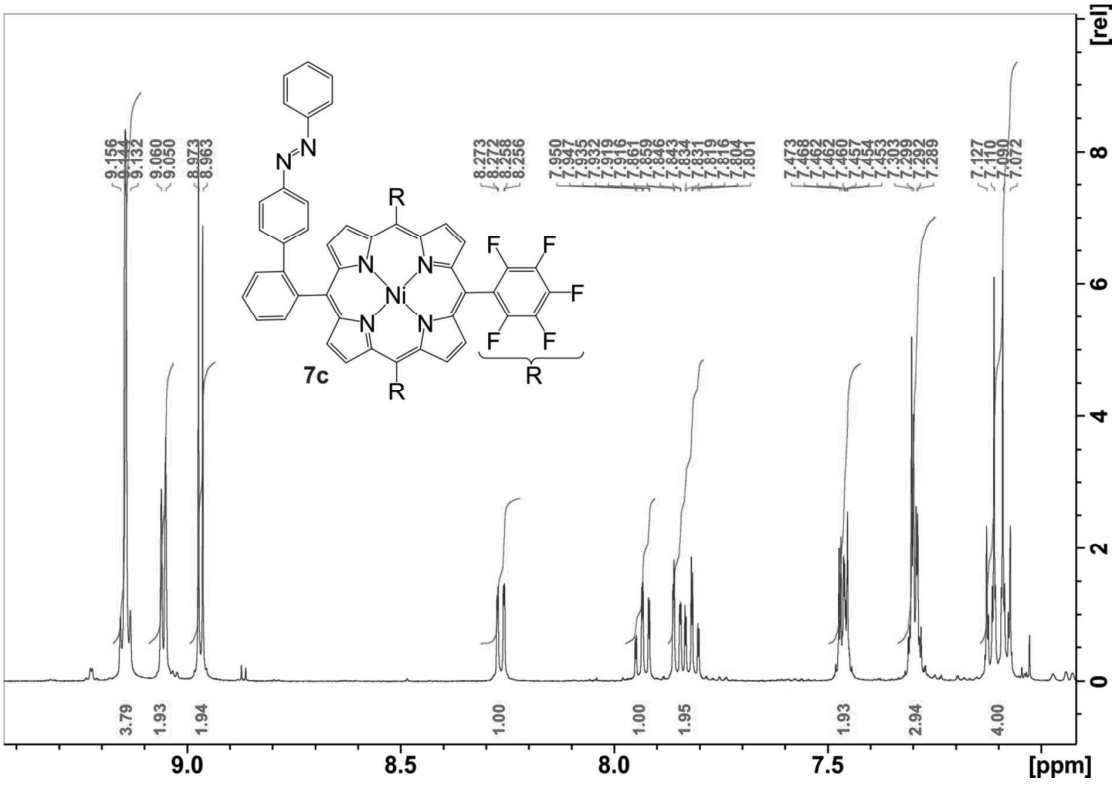

Figure S16. ^{1}H-NMR (500 MHz, acetone-d_6, 300 K) spectrum (aromatic region) of **7c**.

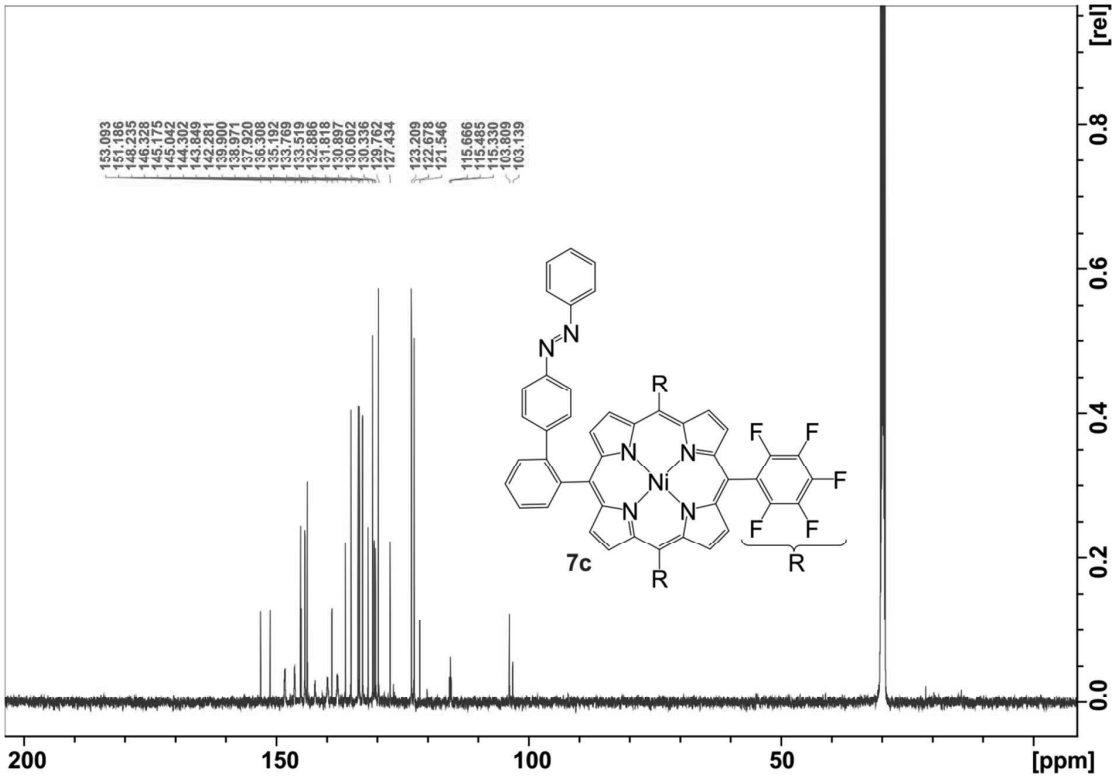

Figure S17. ^{13}C-NMR (125 MHz, acetone-d_6, 300 K) spectrum of **7c**.

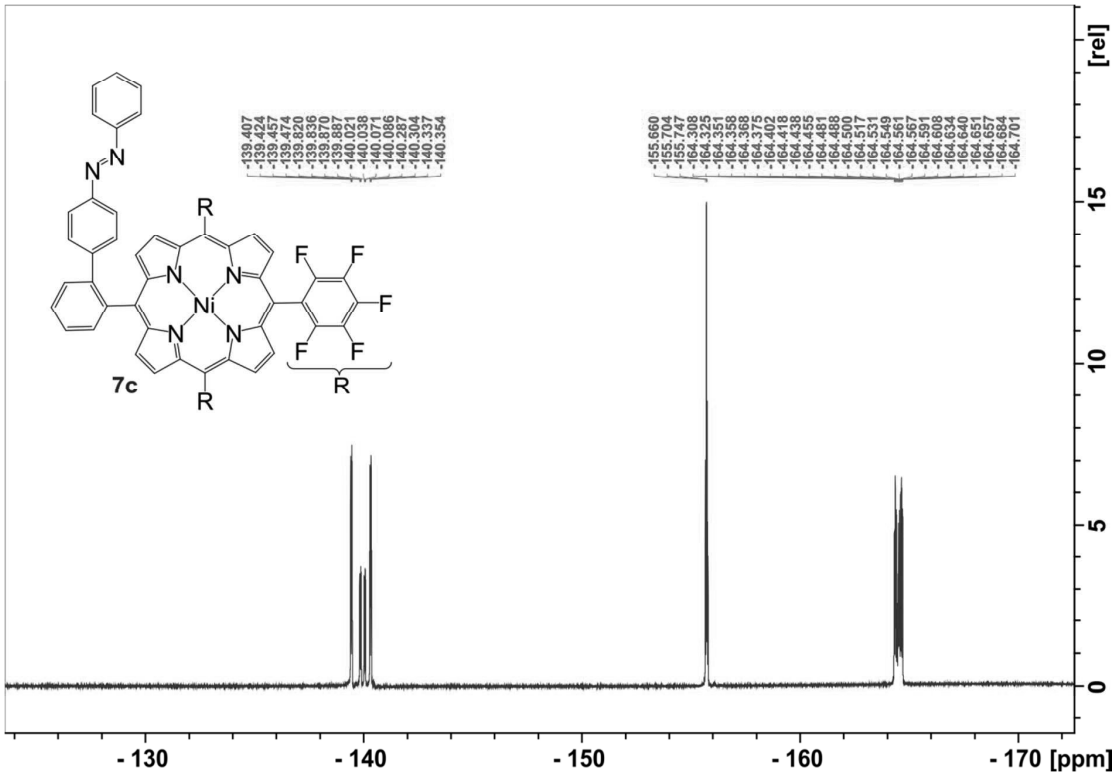

Figure S18. ^{19}F-NMR (470 MHz, acetone-d_6, 300 K) spectrum of **7c**.

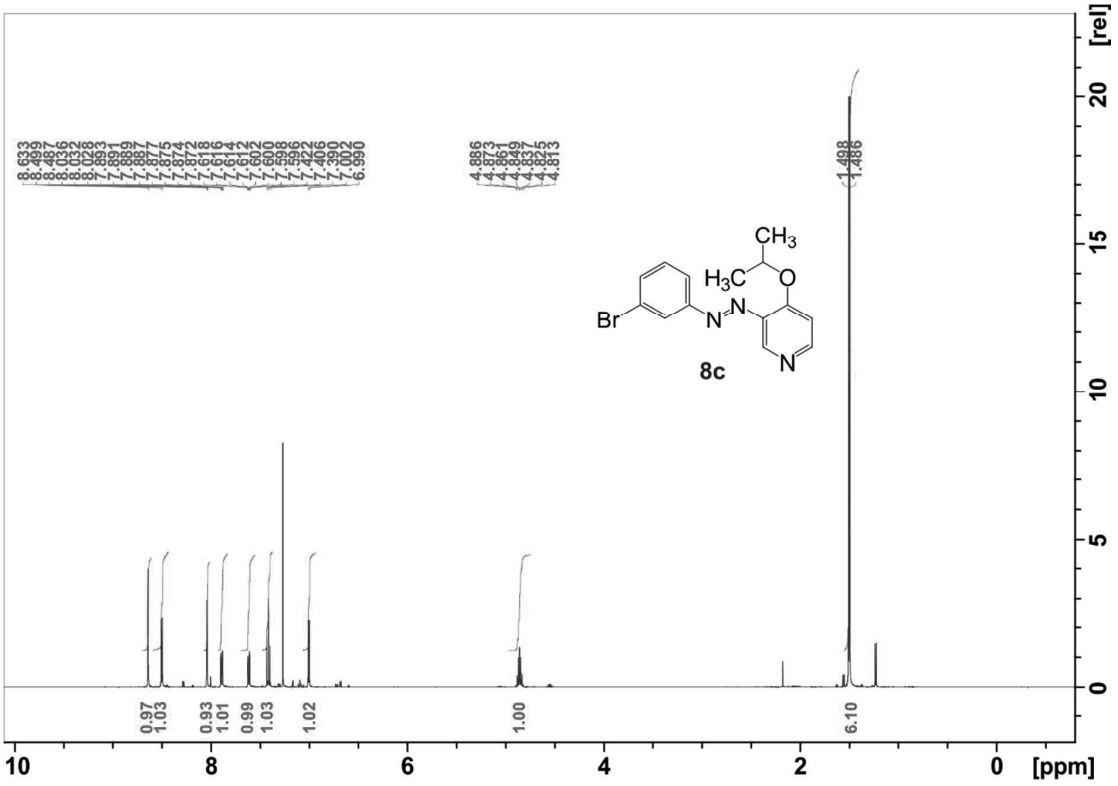

Figure S19. ^{1}H-NMR (500 MHz, $CDCl_3$, 300 K) spectrum of **8c**.

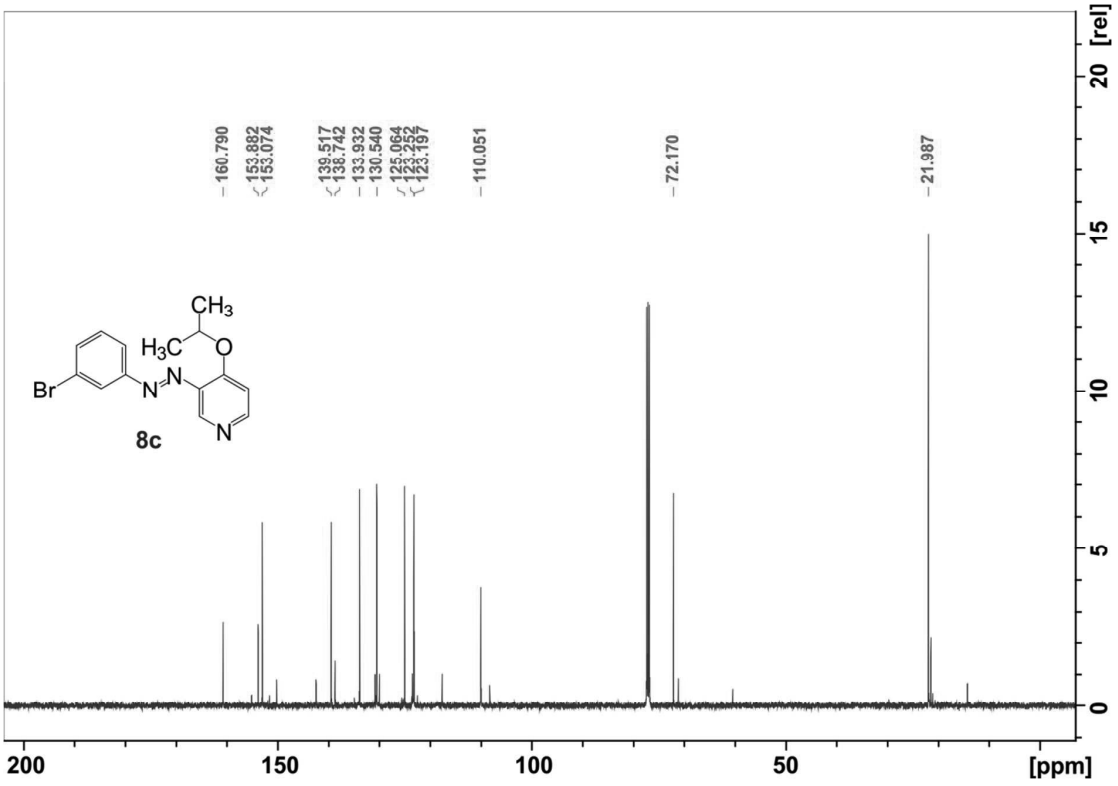

Figure S20. ^{13}C-NMR (125 MHz, $CDCl_3$, 300 K) spectrum of **8c**.

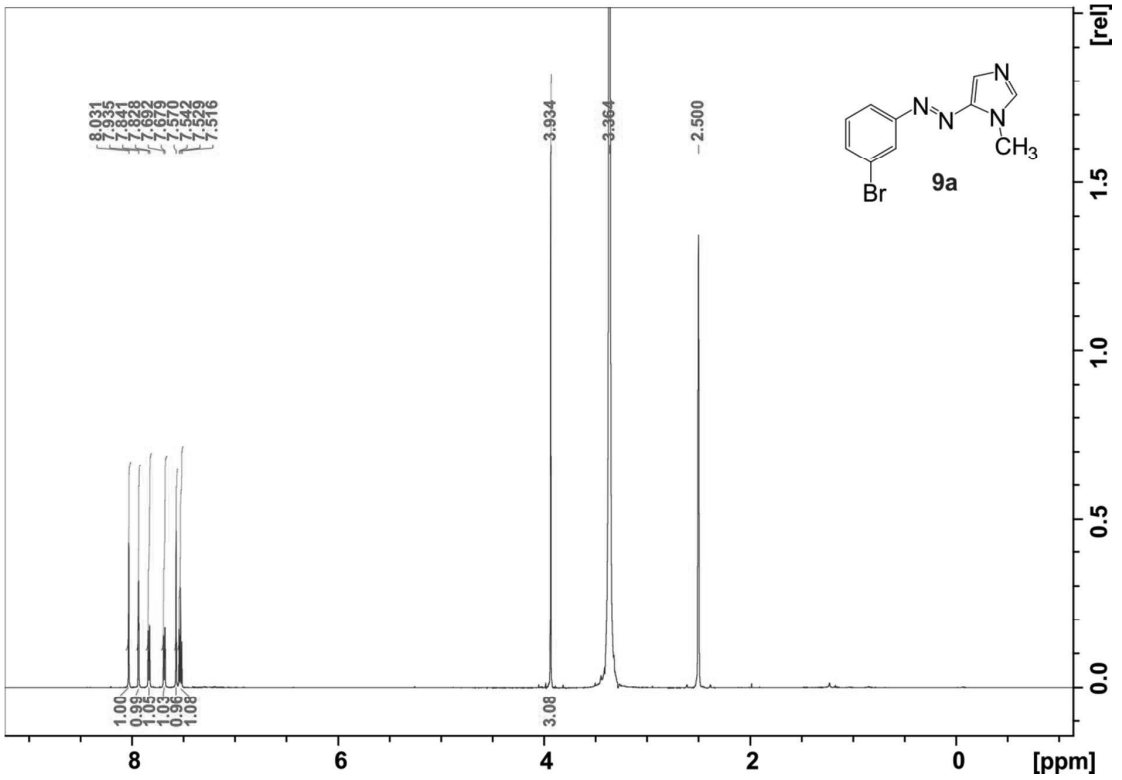

Figure S21. ^{1}H-NMR (600 MHz, DMSO-d_6, 298 K) spectrum of **9a**.

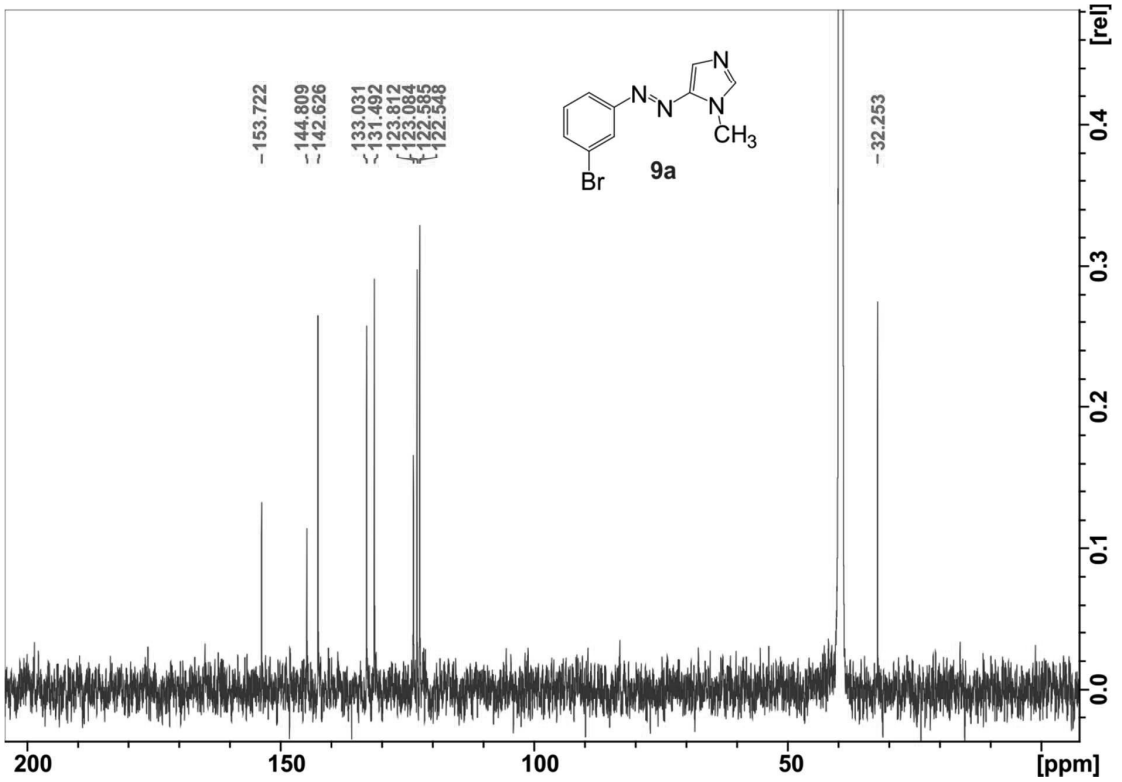

Figure S22. ^{13}C-NMR (150 MHz, DMSO-d_6, 298 K) spectrum of **9a**.

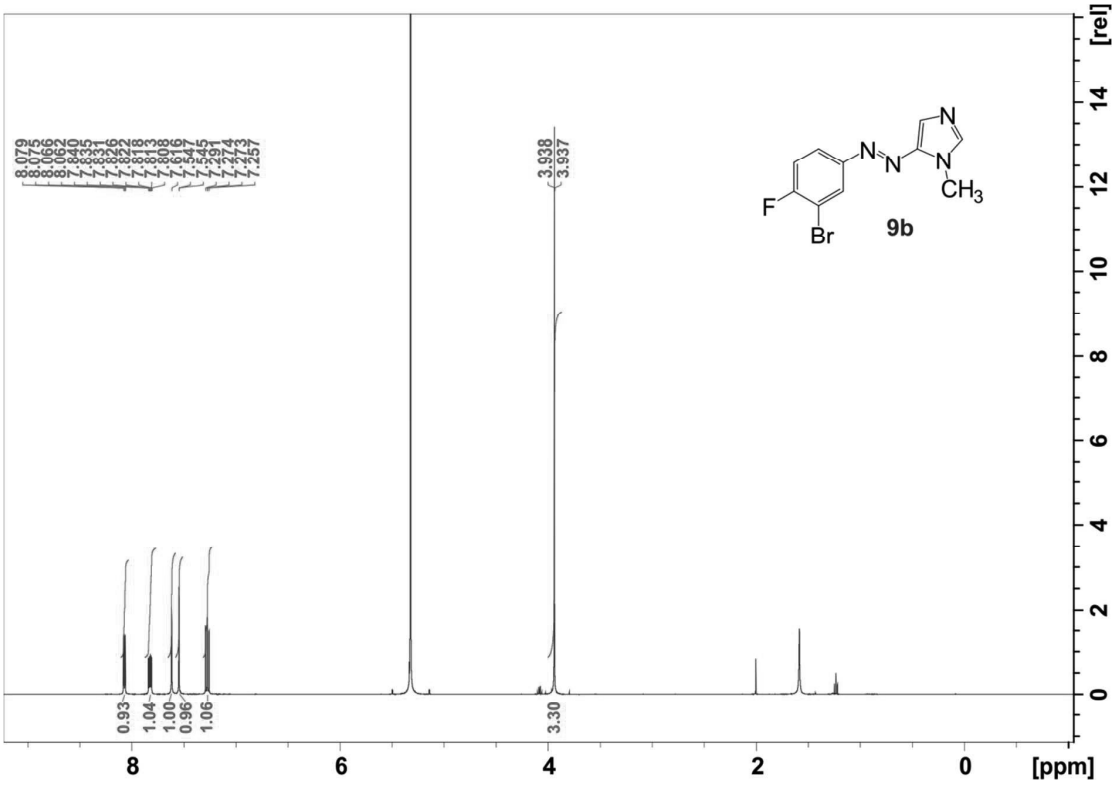

Figure S23. ^{1}H-NMR (500 MHz, CD_2Cl_2, 300 K) spectrum of **9b**.

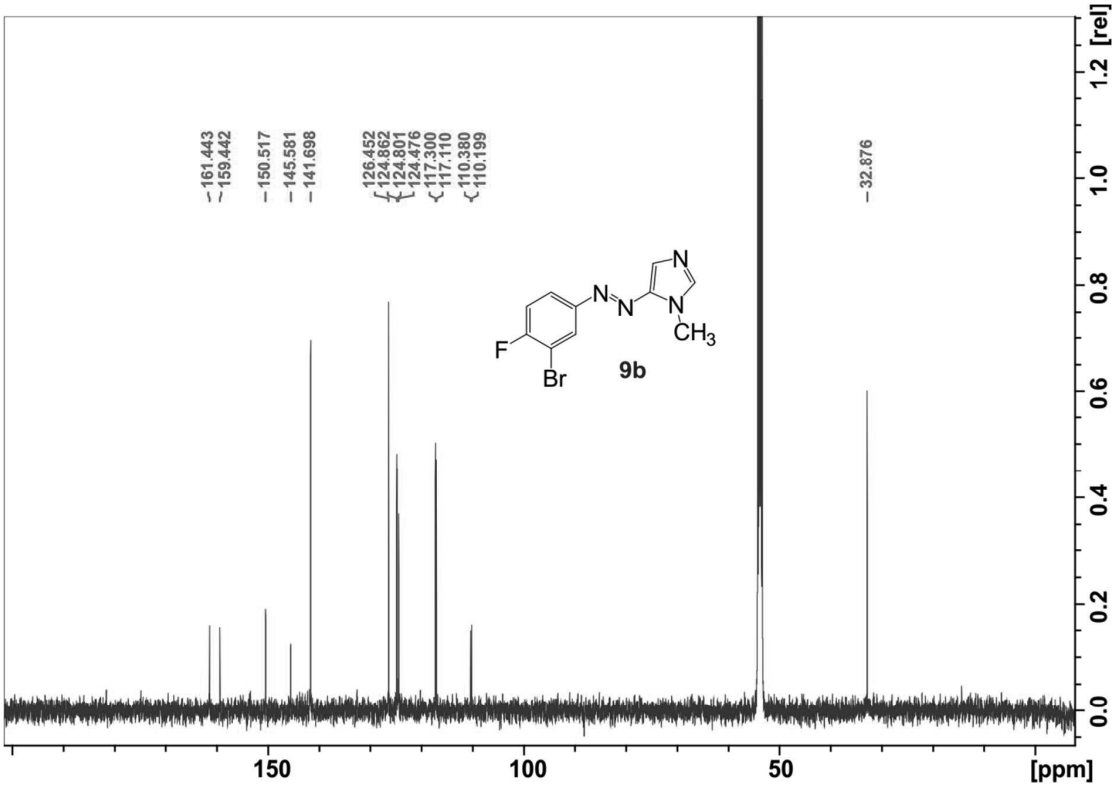

Figure S24. ^{13}C-NMR (125 MHz, CD_2Cl_2, 300 K) spectrum of **9b**.

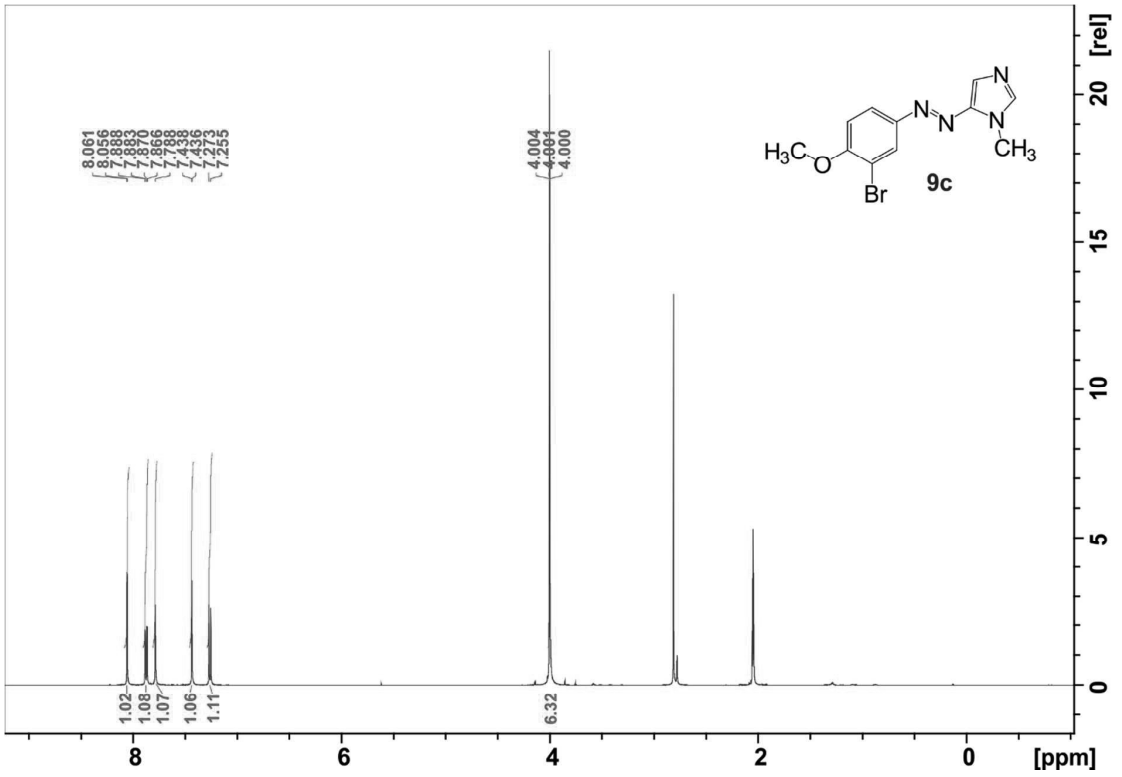

Figure S25. [1]H-NMR (500 MHz, acetone-d_6, 300 K) spectrum of **9c**.

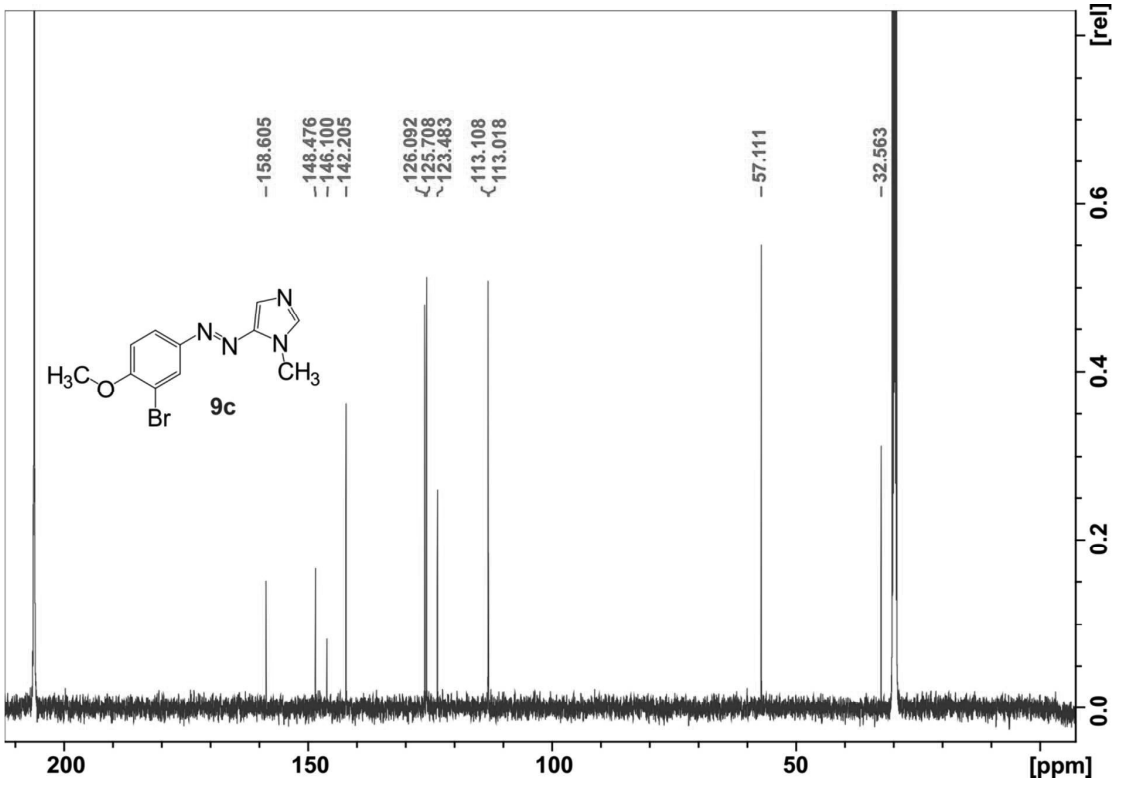

Figure S26. [13]C-NMR (125 MHz, acetone-d_6, 300 K) spectrum of **9c**.

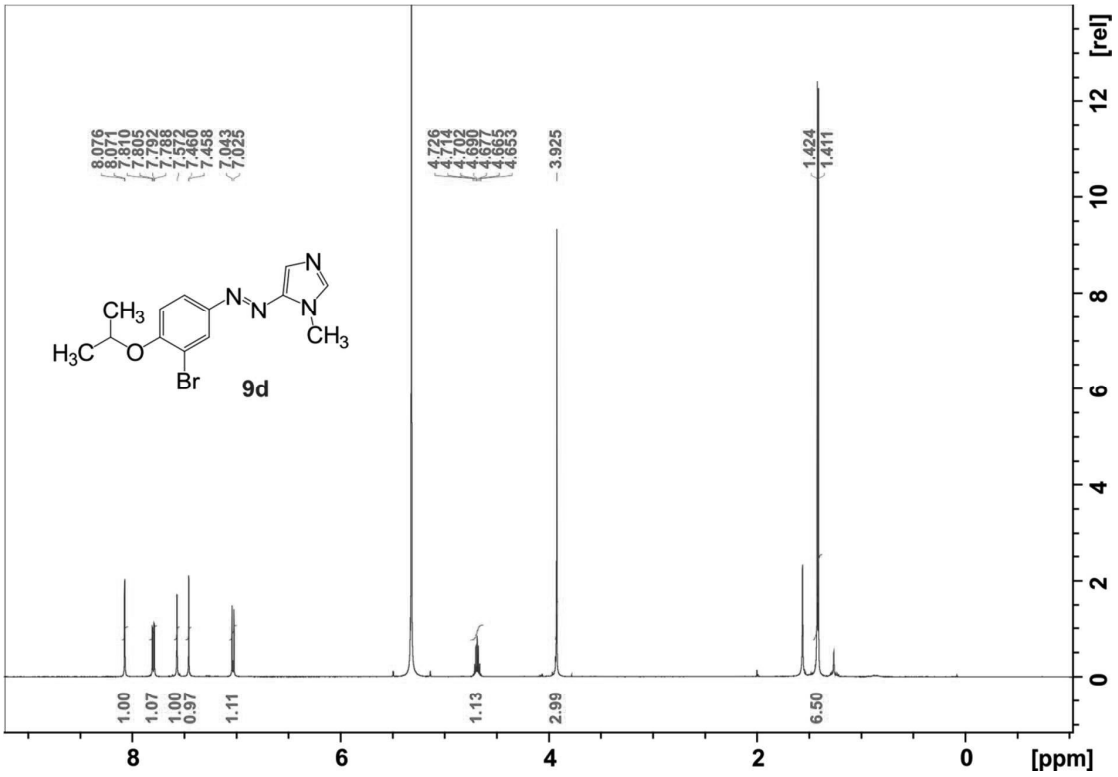

Figure S27. ^{1}H-NMR (500 MHz, CD_2Cl_2, 300 K) spectrum of **9d**.

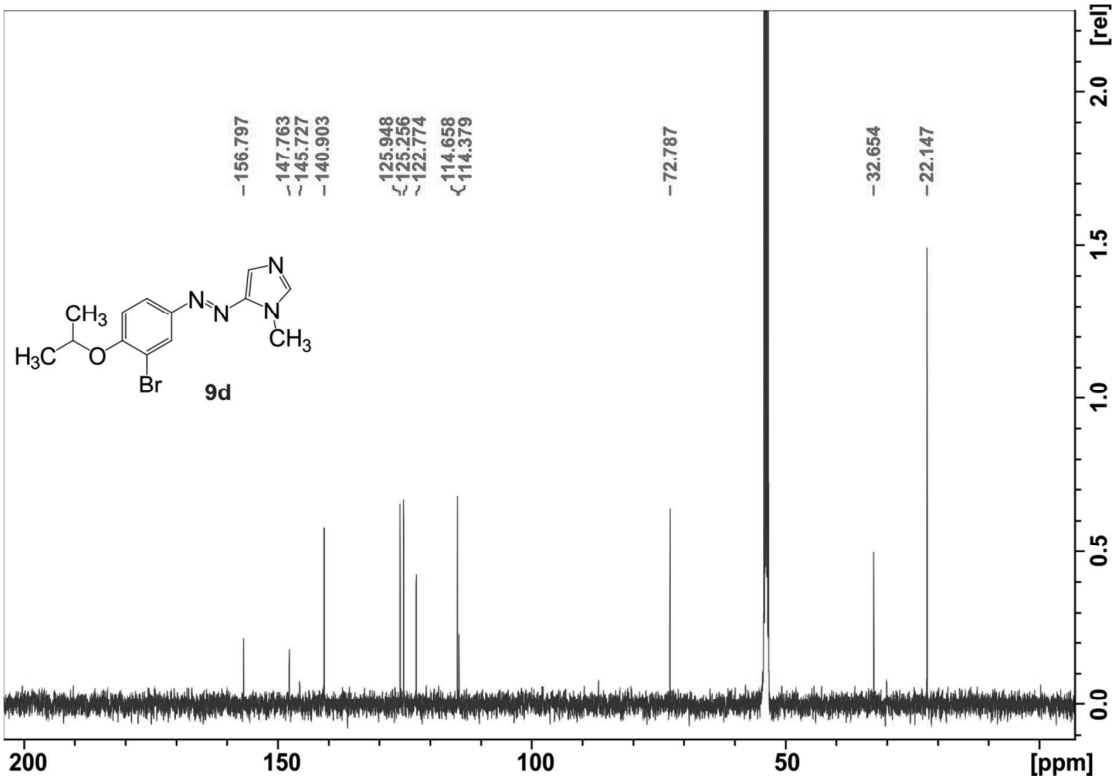

Figure S28. ^{13}C-NMR (125 MHz, CD_2Cl_2, 300 K) spectrum of **9d**.

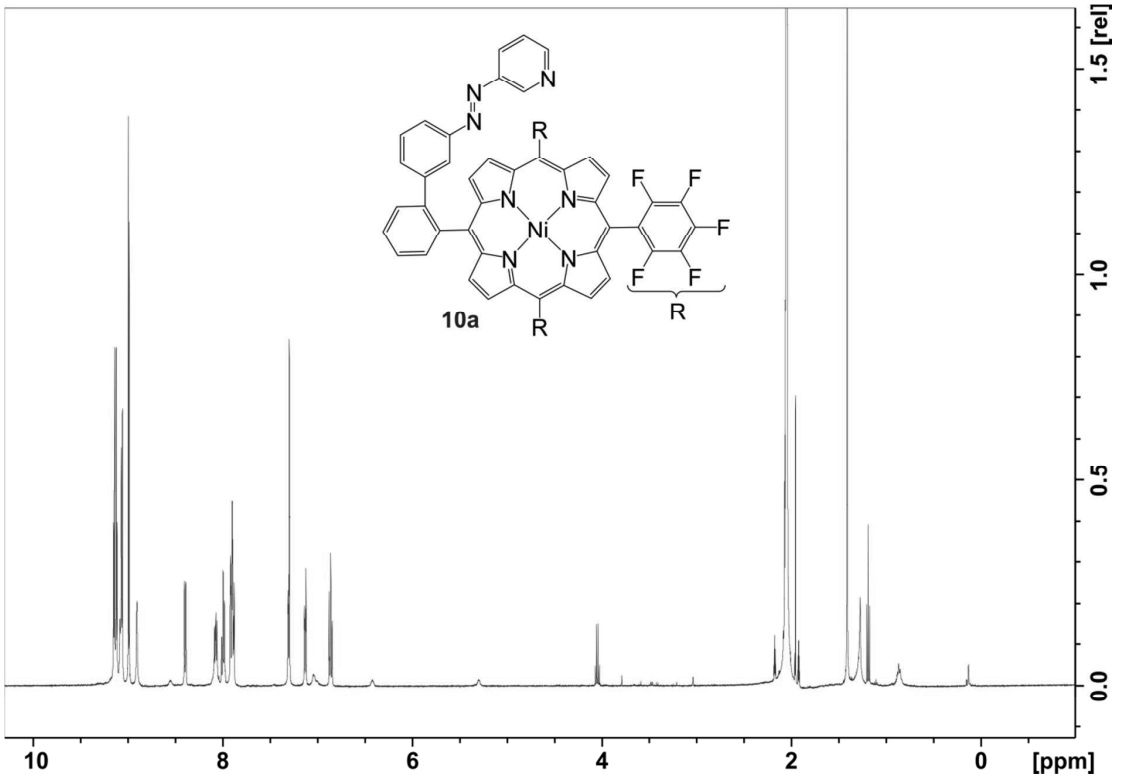

Figure S29. ^{1}H-NMR (500 MHz, acetone-d_6, TFA-d, 300 K) spectrum of **10a**.

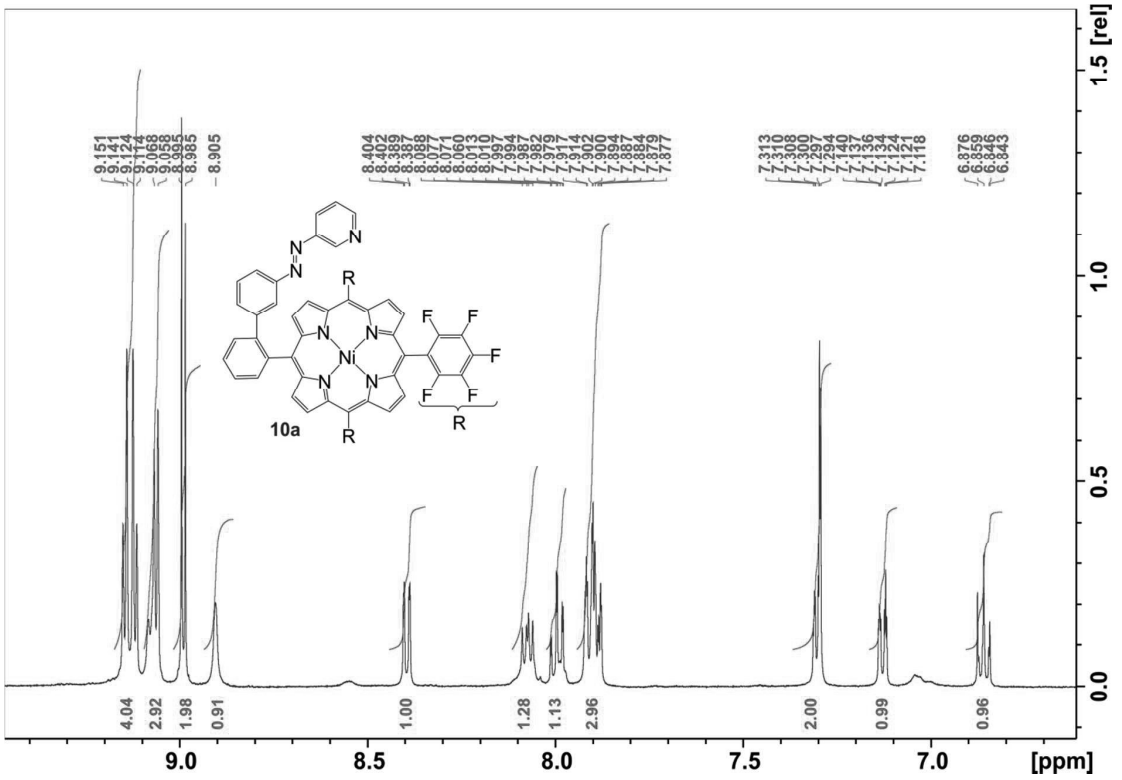

Figure S30. ^{1}H-NMR (500 MHz, acetone-d_6, TFA-d, 300 K) spectrum (aromatic region) of **10a**.

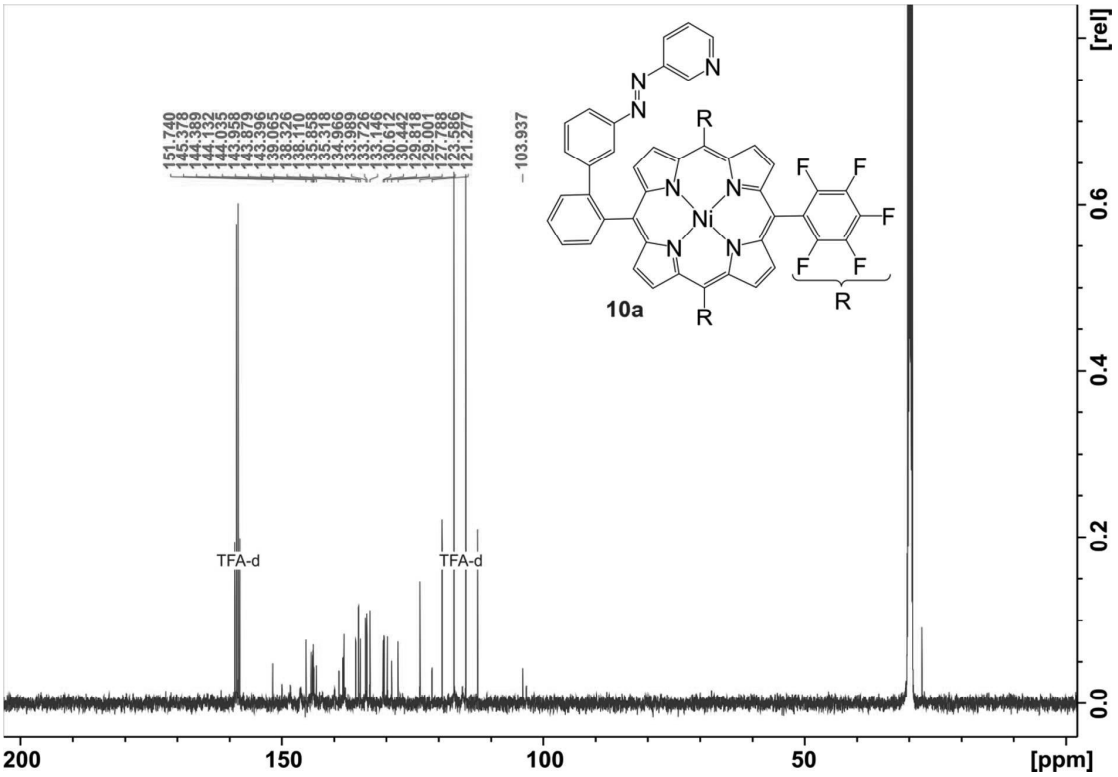

Figure S31. ^{13}C-NMR (125 MHz, acetone-d_6, TFA-d, 300 K) spectrum of **10a**.

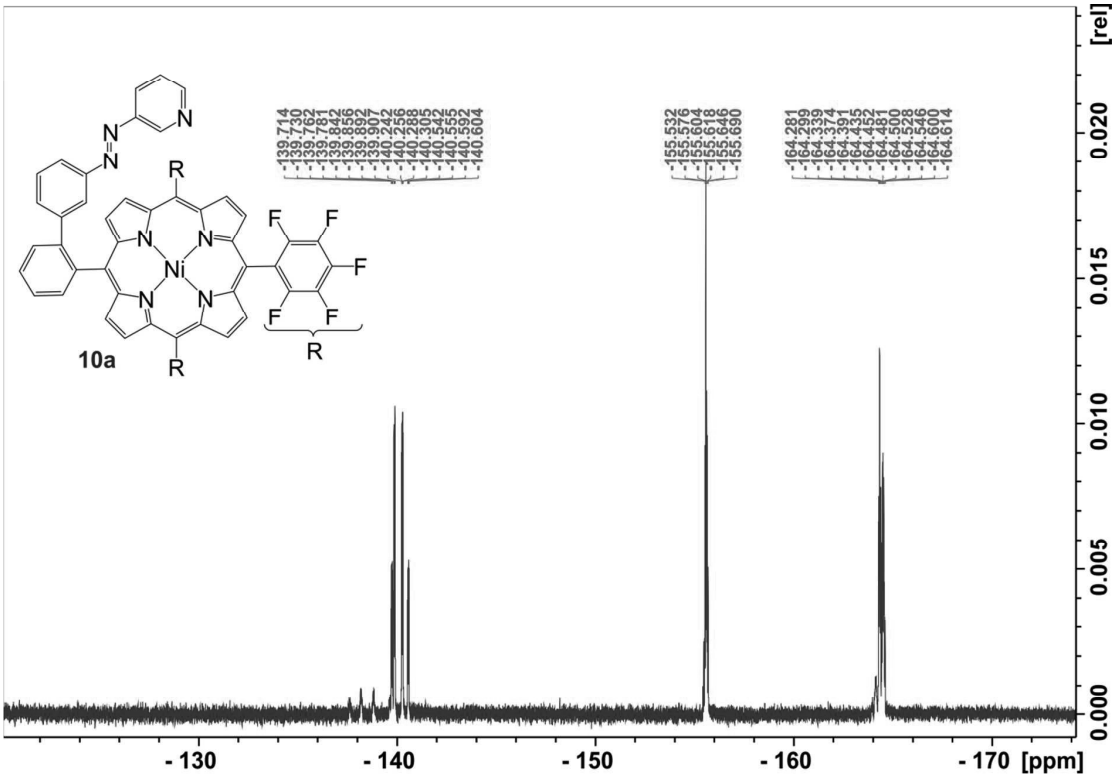

Figure S32. ^{19}F-NMR (470 MHz, acetone-d_6, TFA-d, 300 K) spectrum of **10a**.

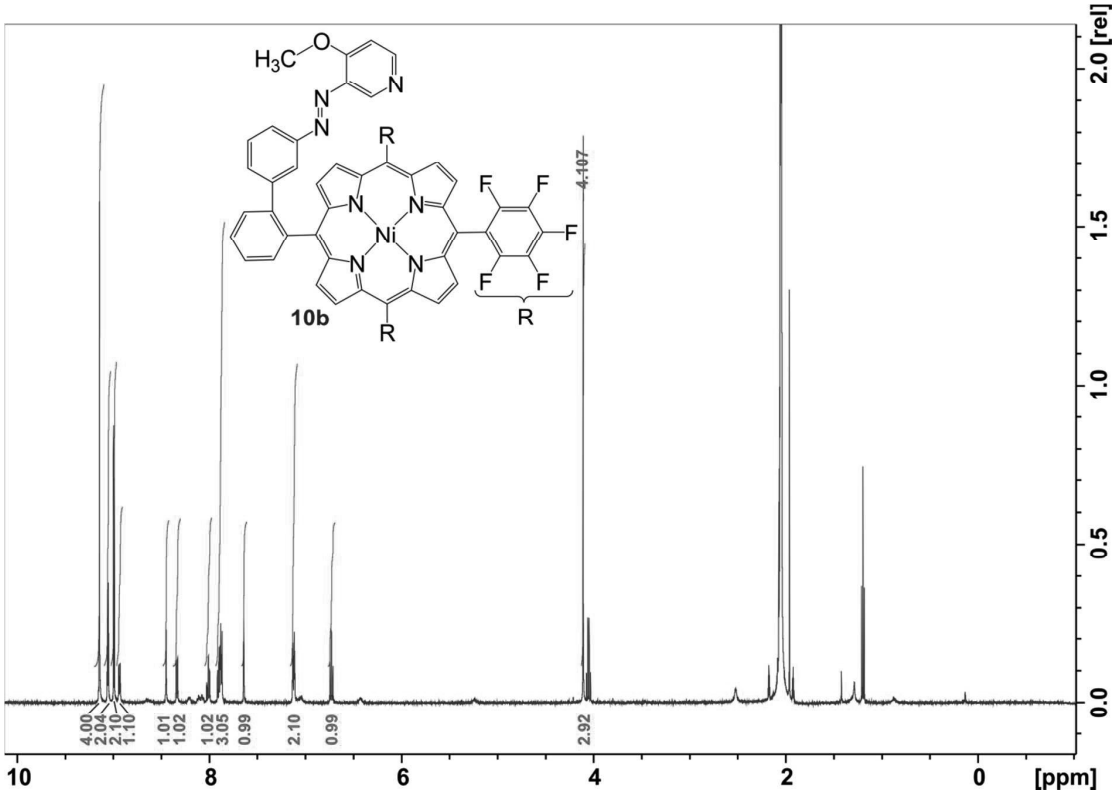

Figure S33. [1]H-NMR (500 MHz, acetone-d_6, TFA-d, 300 K) spectrum of **10b**.

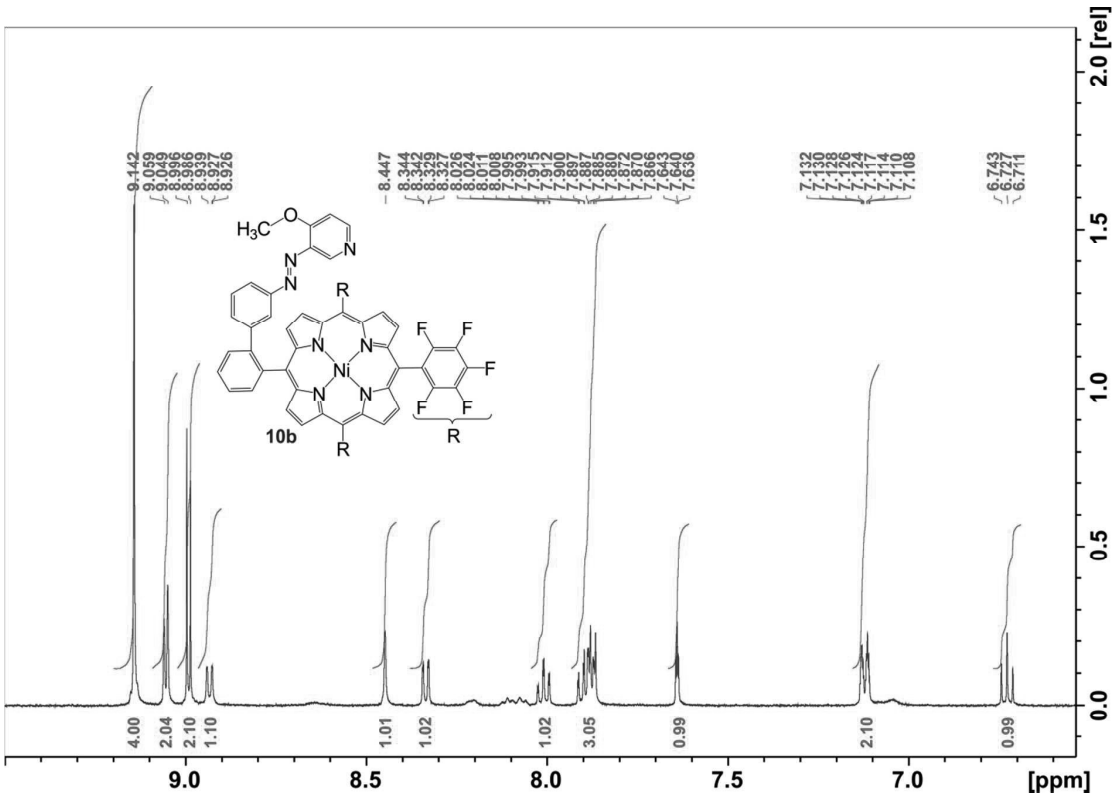

Figure S34. [1]H-NMR (500 MHz, acetone-d_6, TFA-d, 300 K) spectrum (aromatic region) of **10b**.

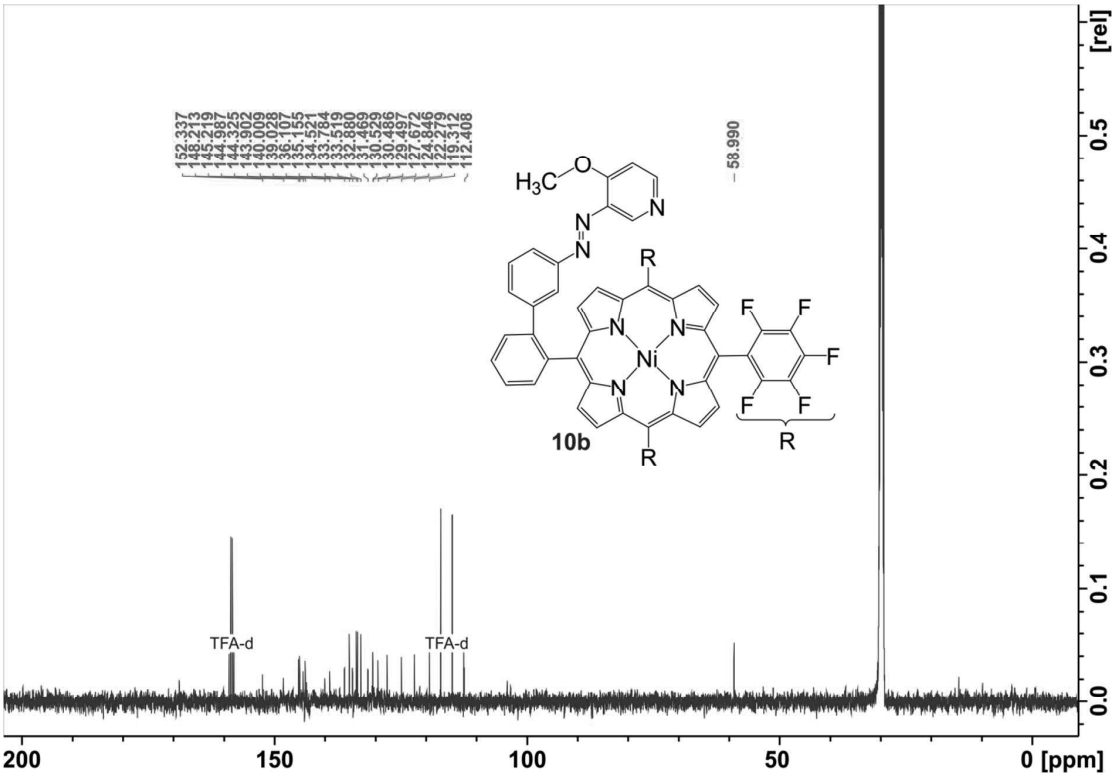

Figure S35. ^{13}C-NMR (125 MHz, acetone-d_6, TFA-d, 300 K) spectrum of **10b**.

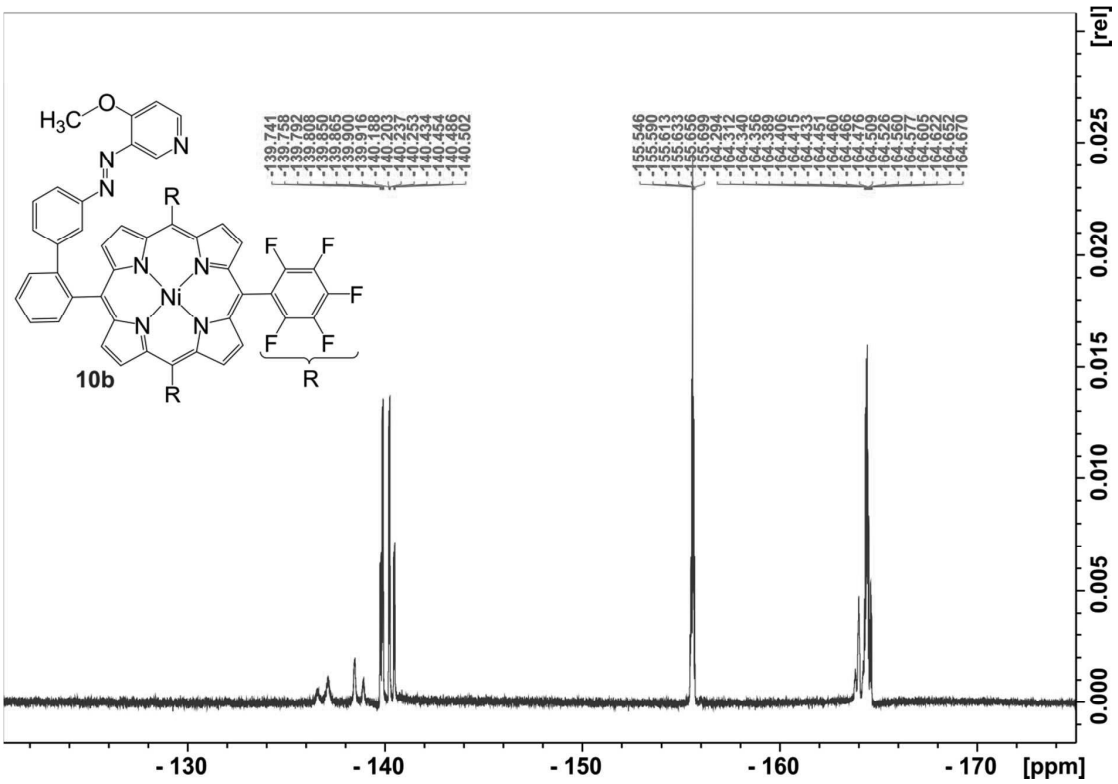

Figure S36. ^{19}F-NMR (470 MHz, acetone-d_6, TFA-d, 300 K) spectrum of **10b**.

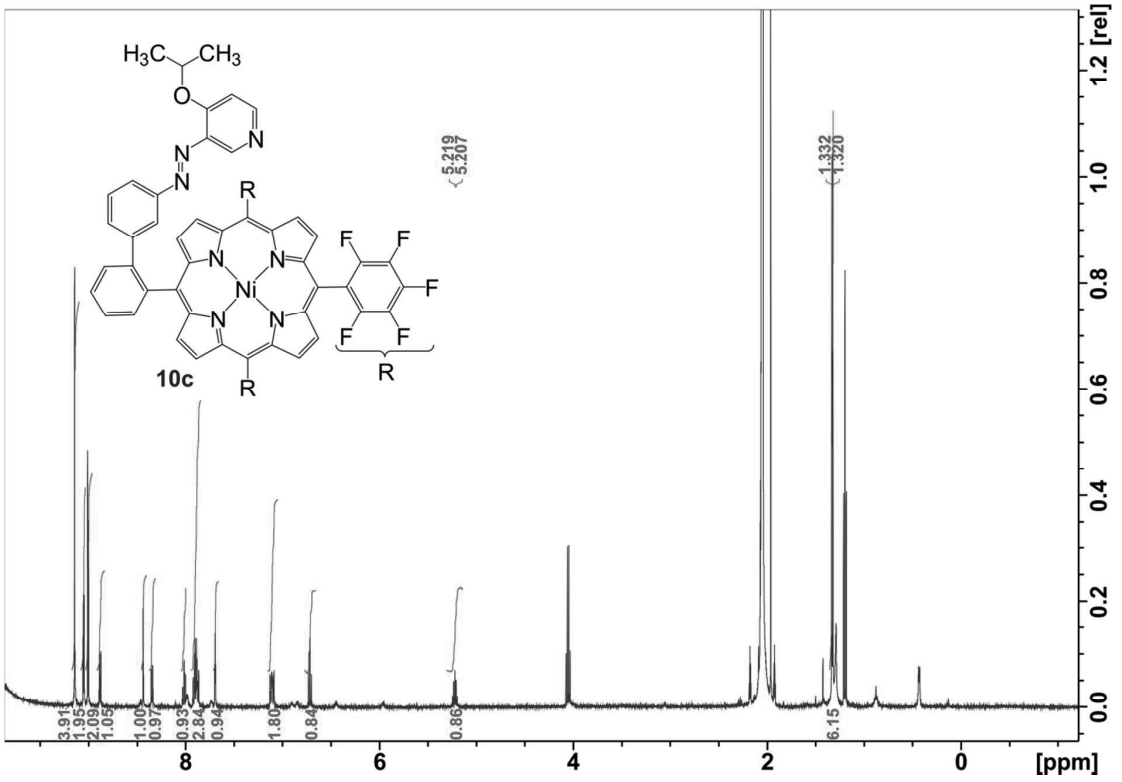

Figure S37. [1]H-NMR (500 MHz, acetone-d_6, TFA-d, 300 K) spectrum of **10c**.

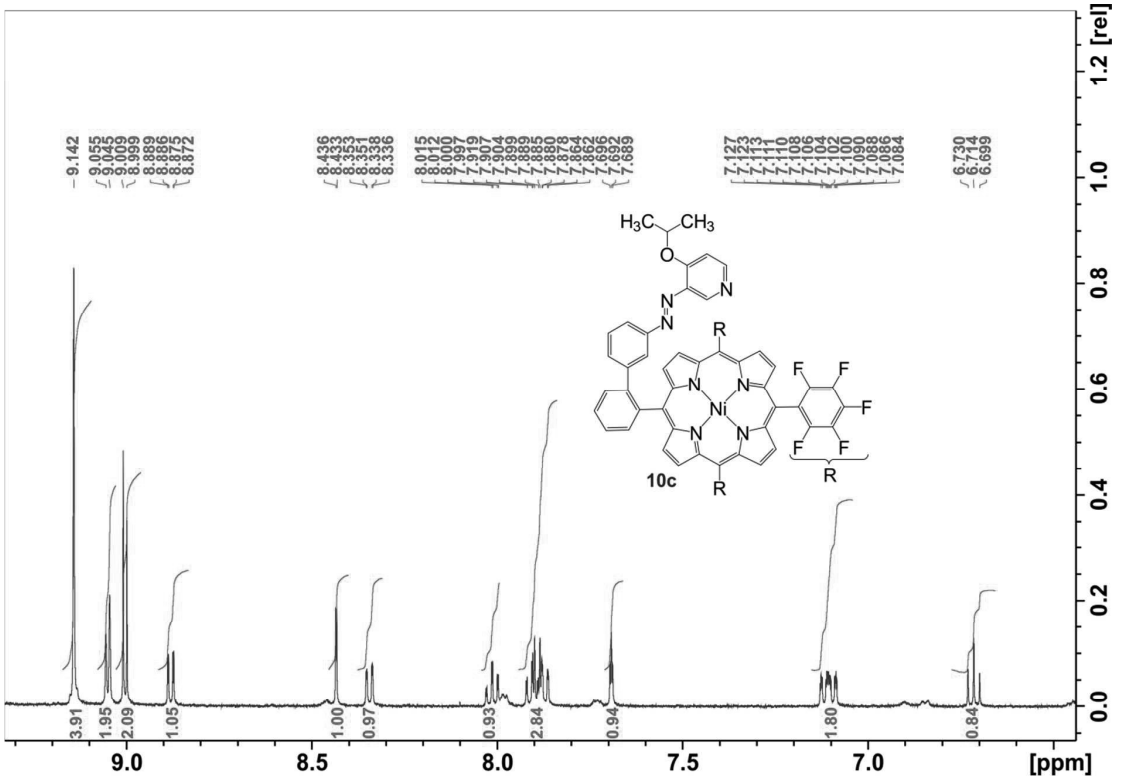

Figure S38. [1]H-NMR (500 MHz, acetone-d_6, TFA-d, 300 K) spectrum (aromatic region) of **10c**.

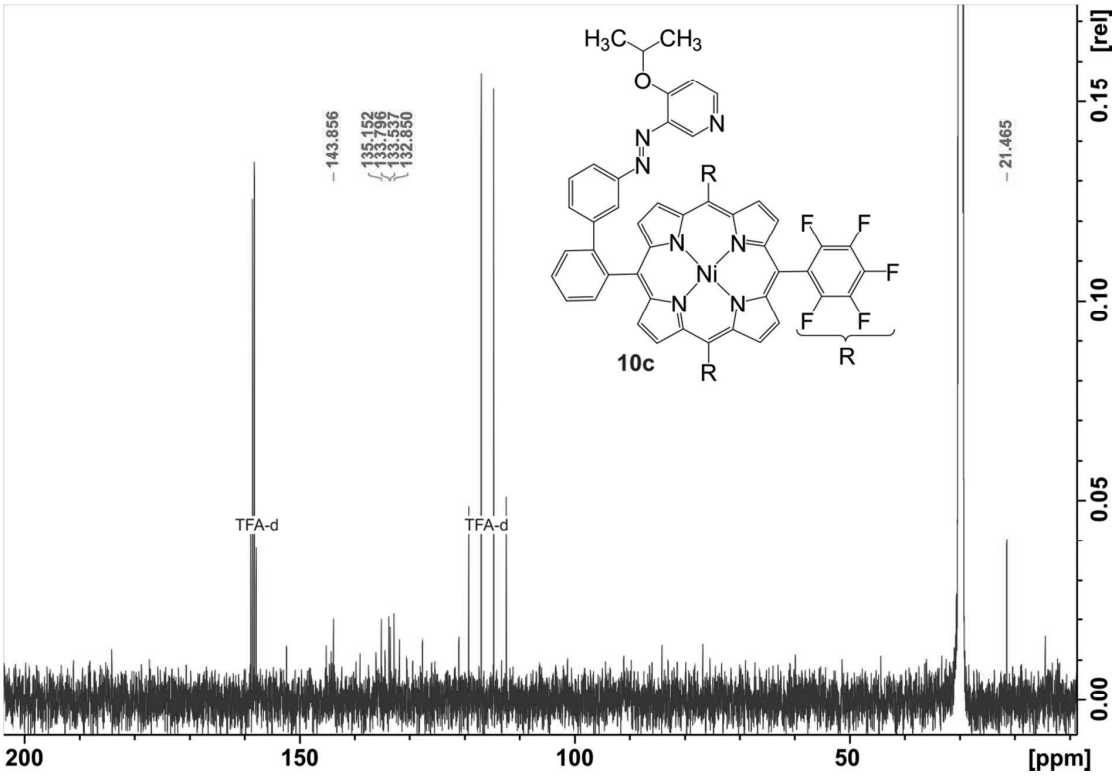

Figure S39. ^{13}C-NMR (125 MHz, acetone-d_6, TFA-d, 300 K) spectrum of **10c**.

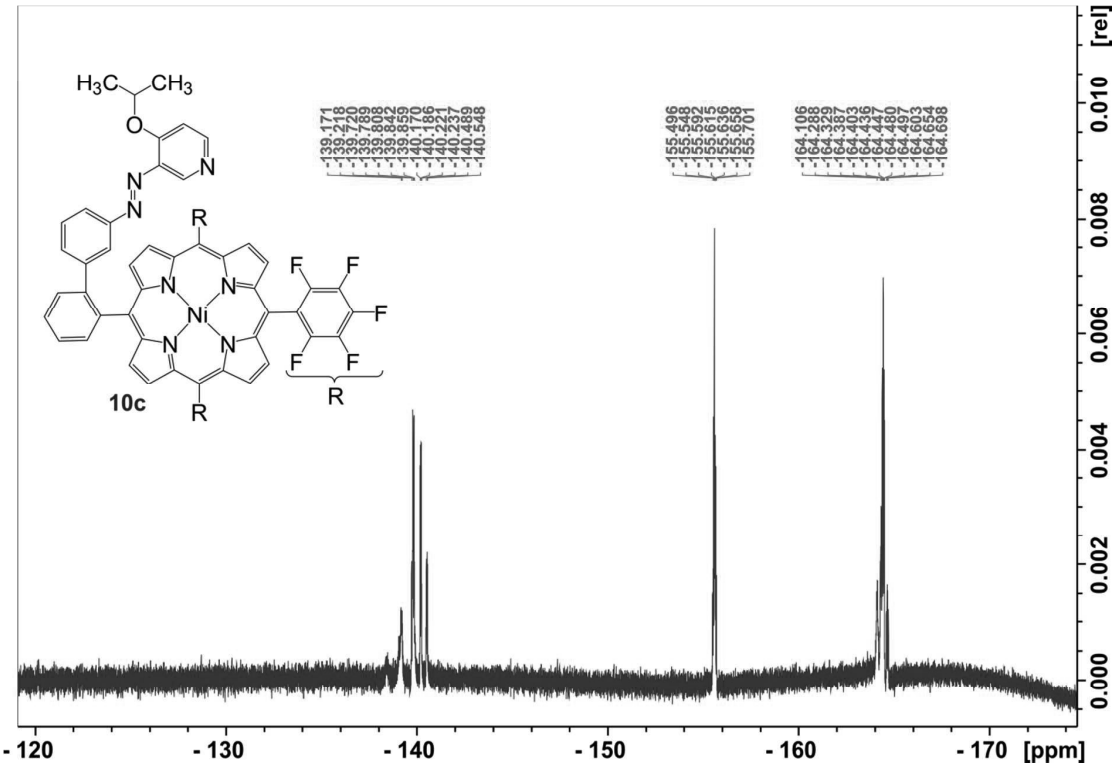

Figure S40. ^{19}F-NMR (470 MHz, acetone-d_6, TFA-d, 300 K) spectrum of **10c**.

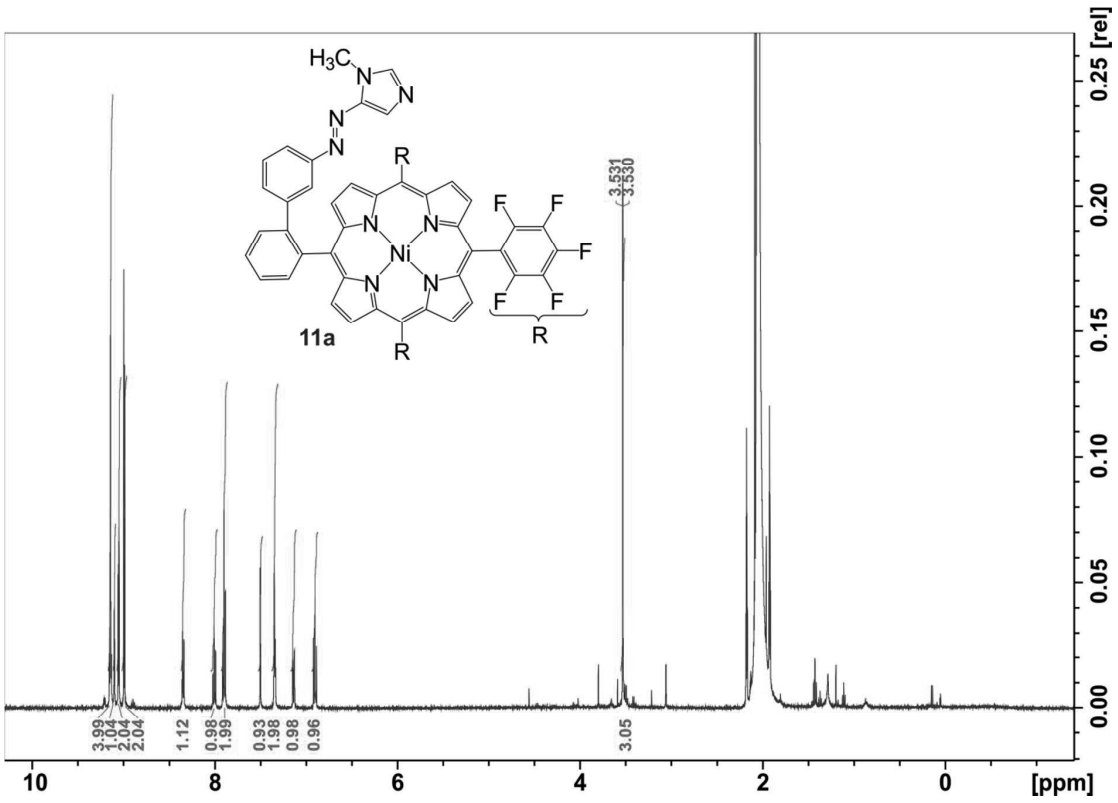

Figure S41. ^{1}H-NMR (500 MHz, acetone-d_6, TFA-d, 300 K) spectrum of **11a**.

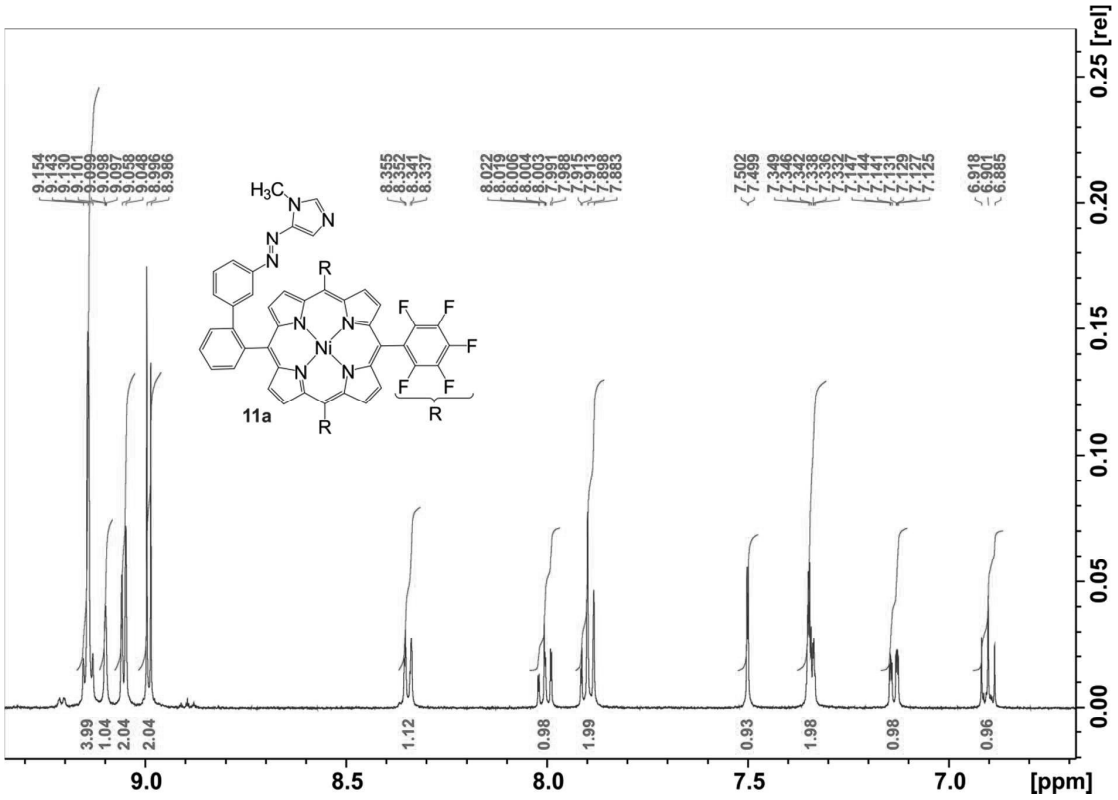

Figure S42. ^{1}H-NMR (500 MHz, acetone-d_6, TFA-d, 300 K) spectrum (aromatic region) of **11a**.

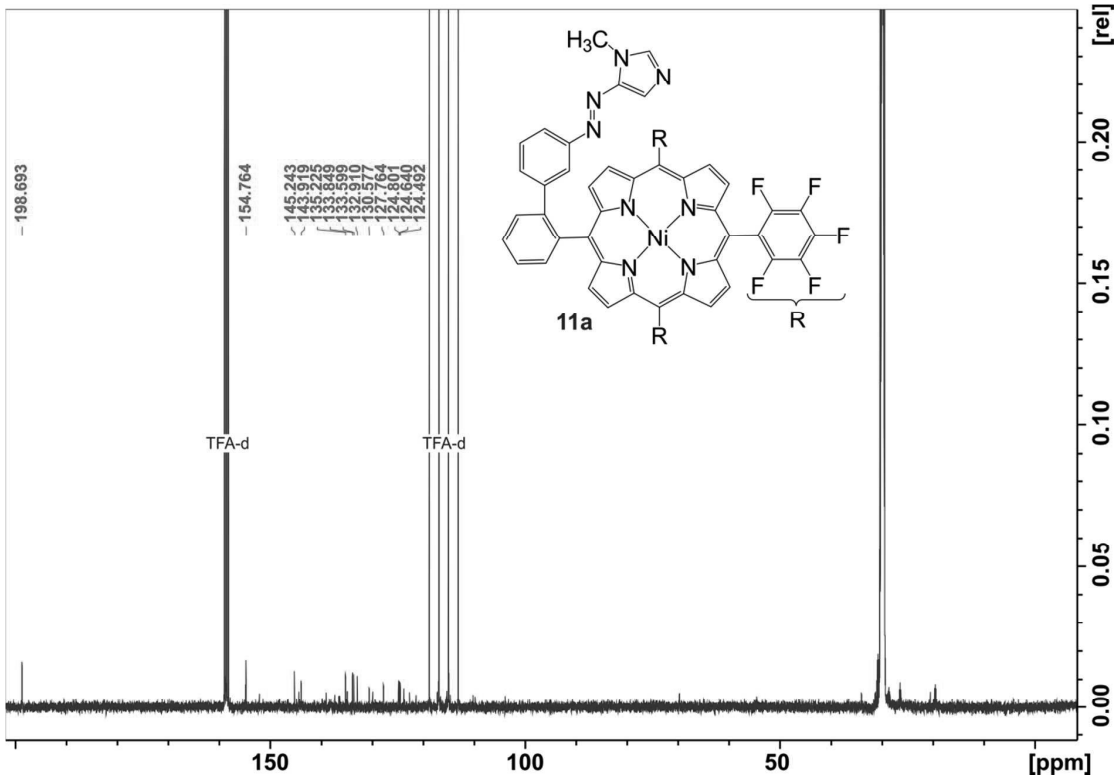

Figure S43. ^{13}C-NMR (150 MHz, acetone-d_6, TFA-d, 300 K) spectrum of **11a**.

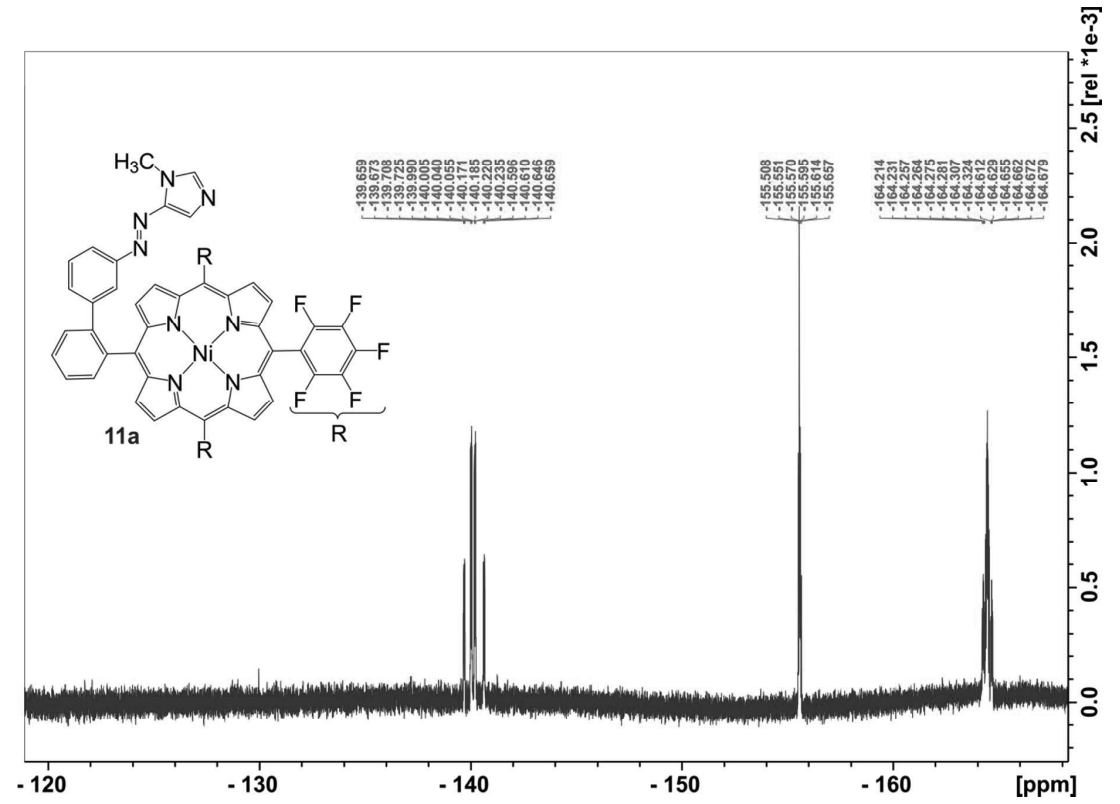

Figure S44. ^{19}F-NMR (470 MHz, acetone-d_6, TFA-d, 300 K) spectrum of **11a**.

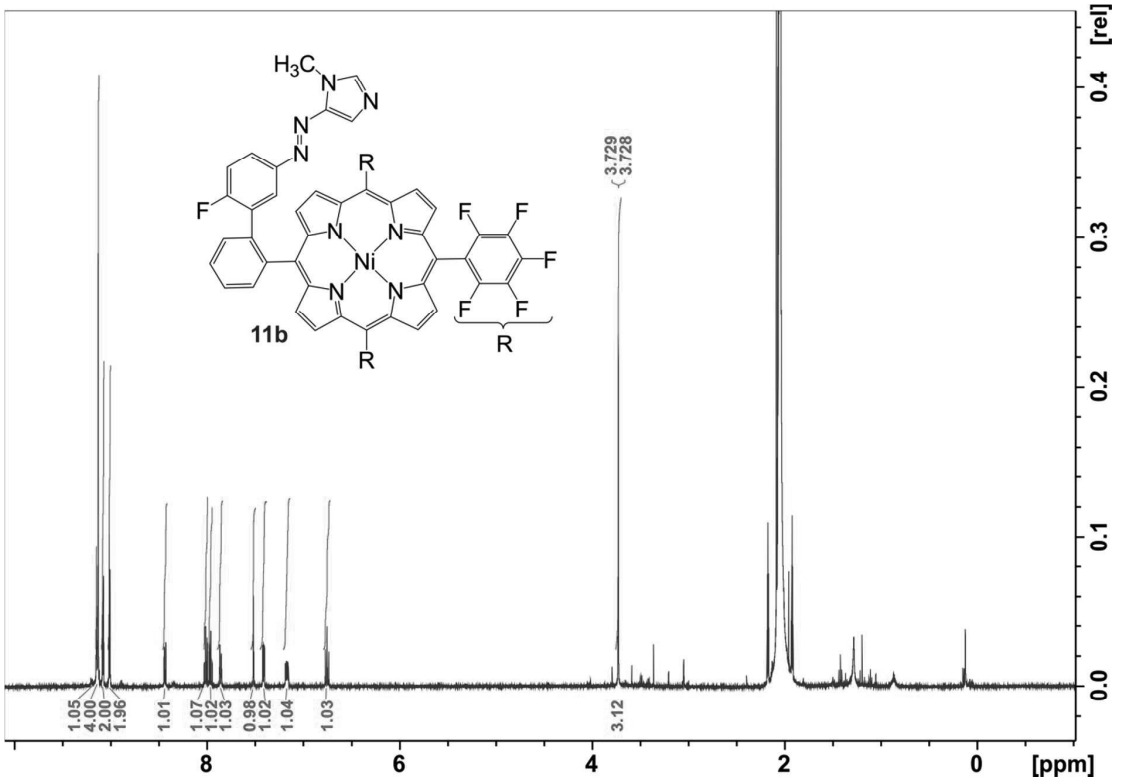

Figure S45. ^{1}H-NMR (500 MHz, acetone-d_6, TFA-d, 300 K) spectrum of **11b**.

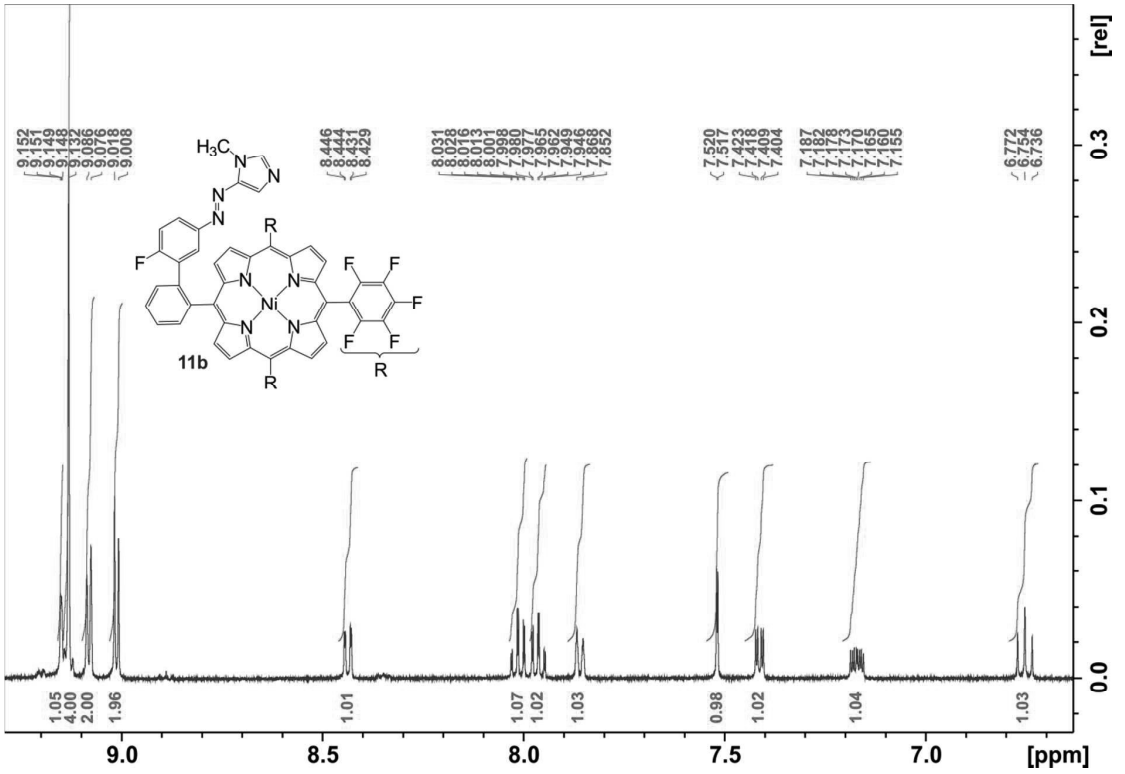

Figure S46. ^{1}H-NMR (500 MHz, acetone-d_6, TFA-d, 300 K) spectrum (aromatic region) of **11b**.

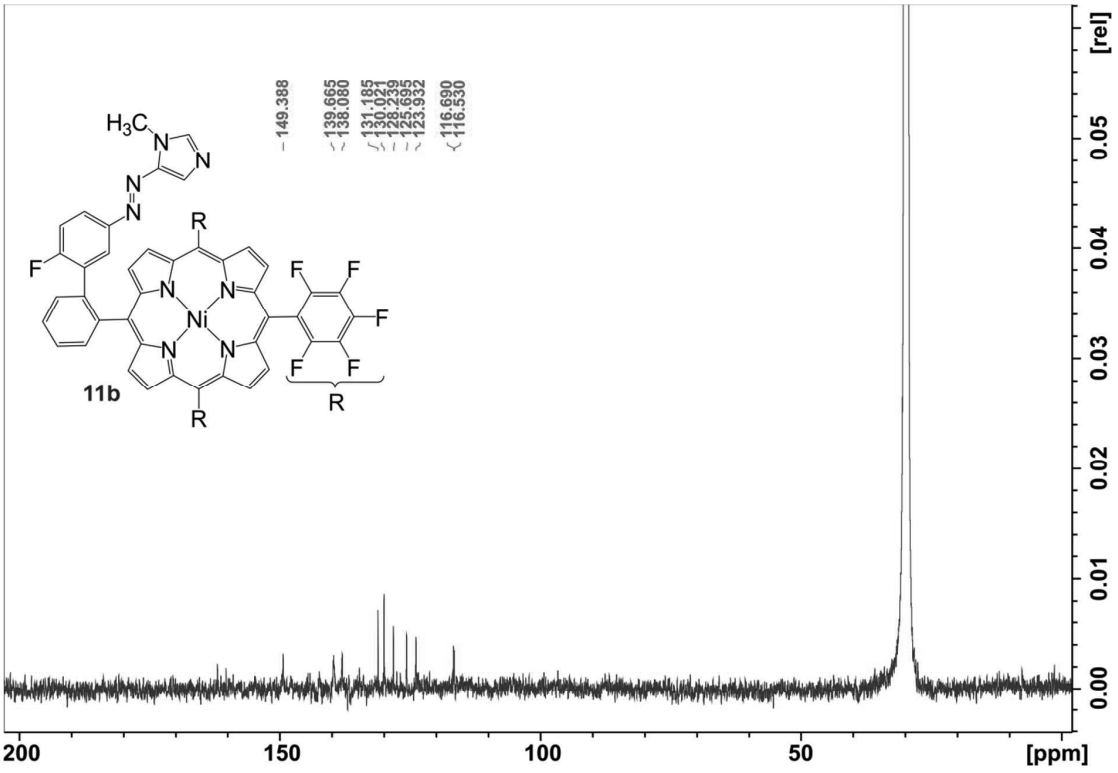

Figure S47. ^{13}C-NMR (150 MHz, acetone-d_6, 300 K) spectrum of **11b**.

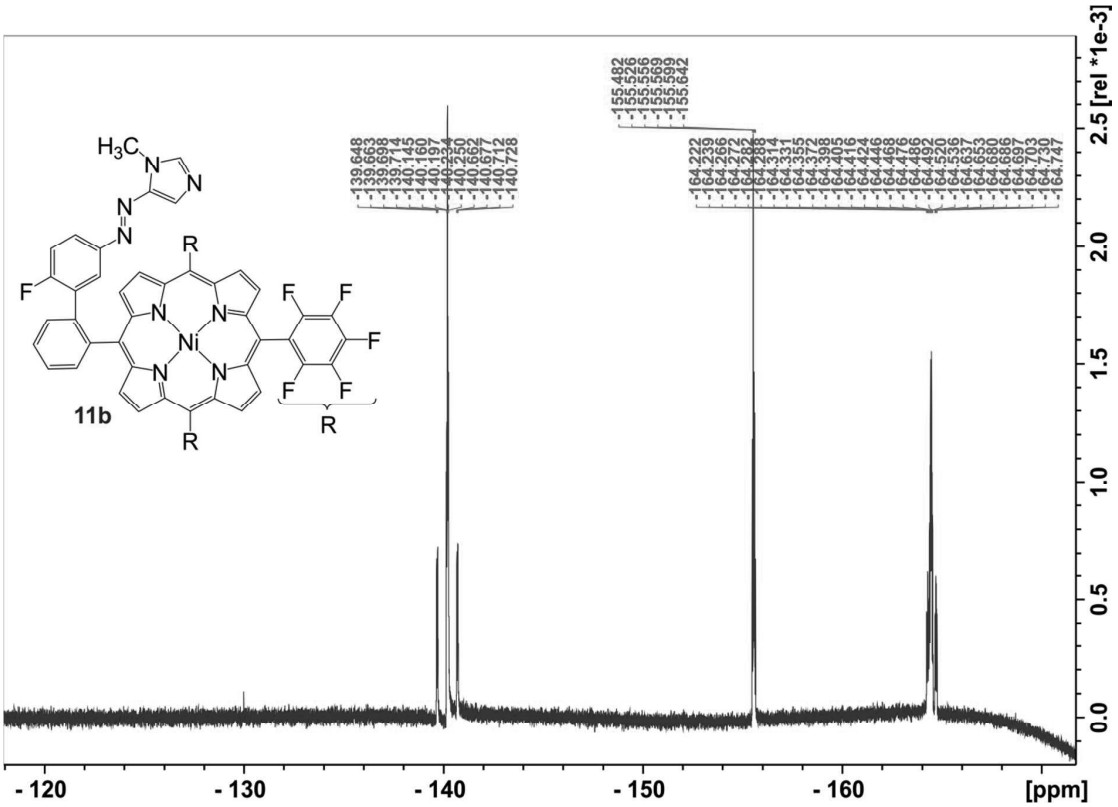

Figure S48. ^{19}F-NMR (470 MHz, acetone-d_6, TFA-d, 300 K) spectrum of **11b**.

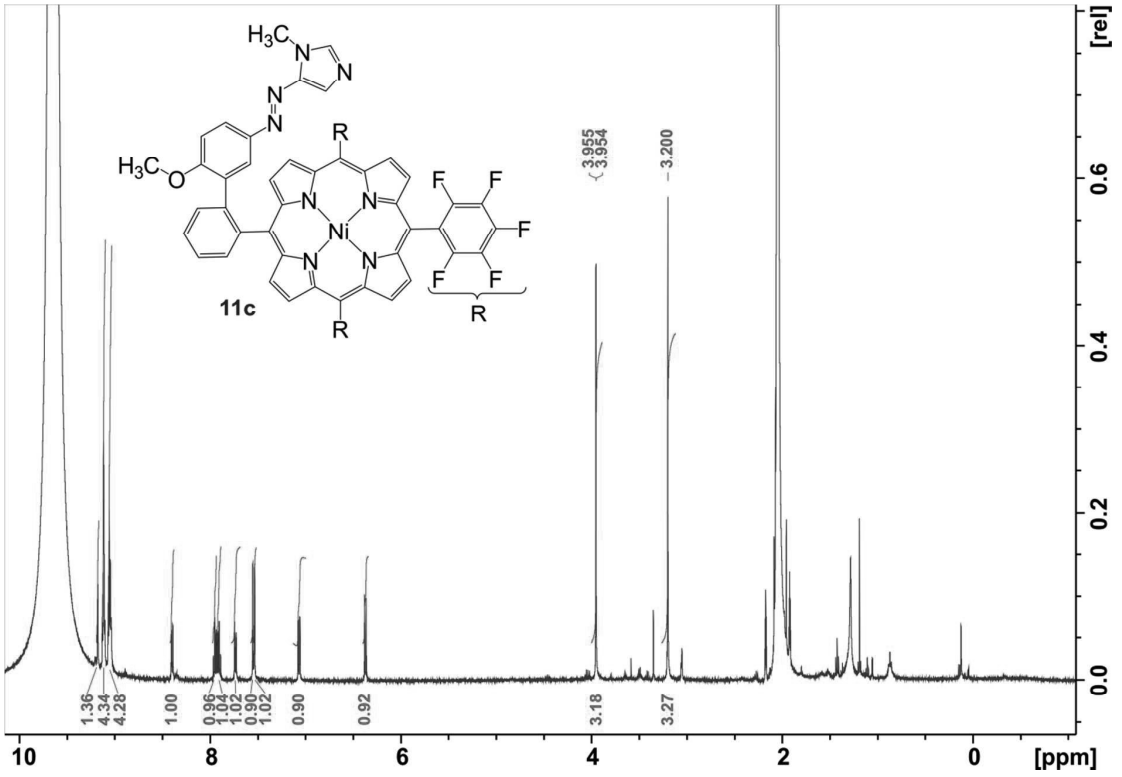

Figure S49. ^{1}H-NMR (500 MHz, acetone-d_6, TFA-d, 300 K) spectrum of **11c**.

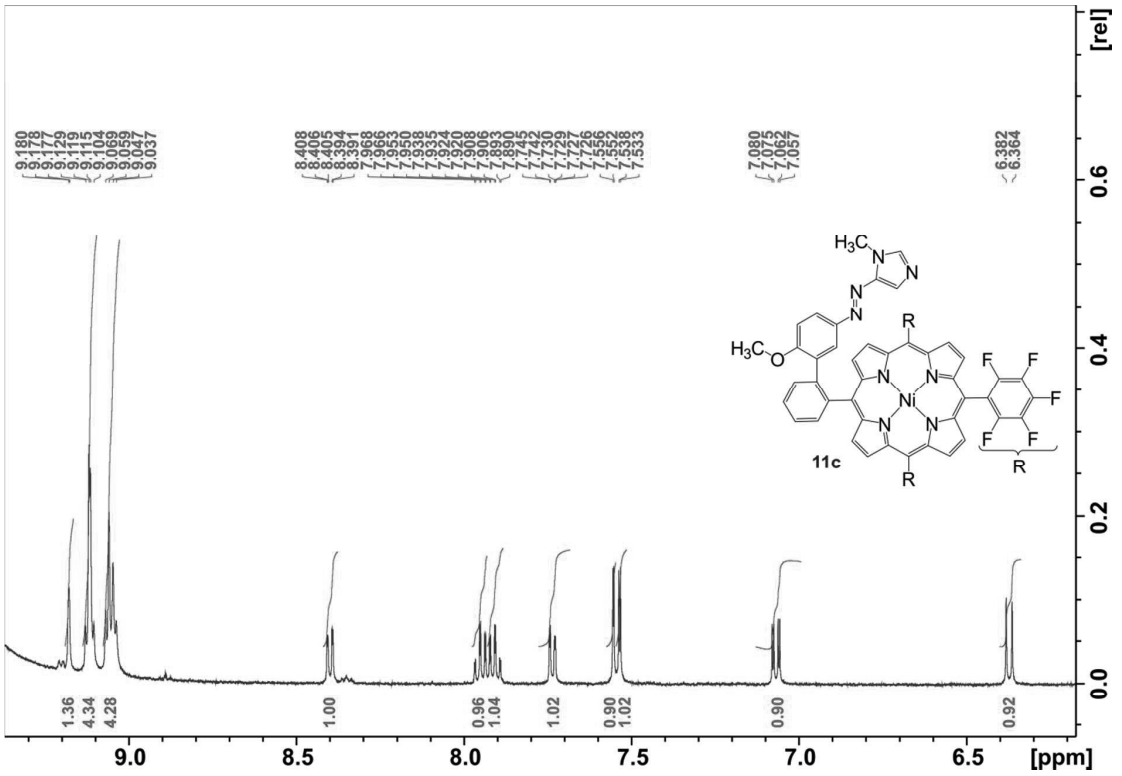

Figure S50. ^{1}H-NMR (500 MHz, acetone-d_6, TFA-d, 300 K) spectrum (aromatic region) of **11c**.

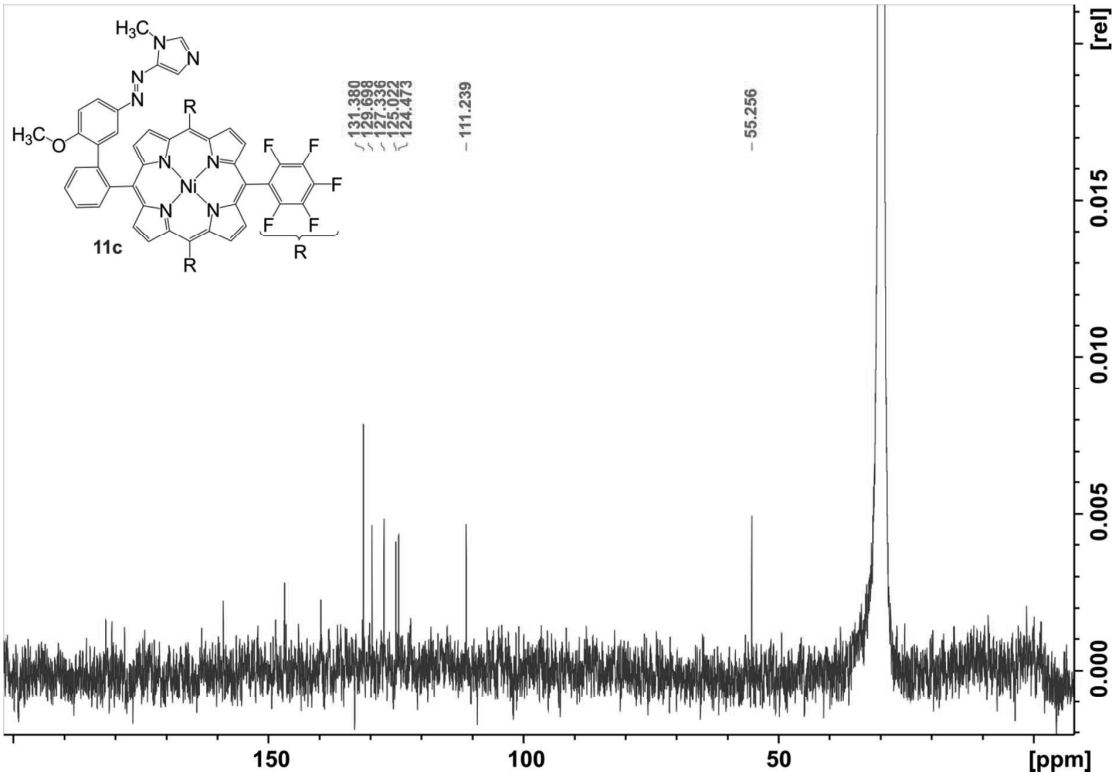

Figure S51. ^{13}C-NMR (150 MHz, acetone-d_6, 300 K) spectrum of **11c**.

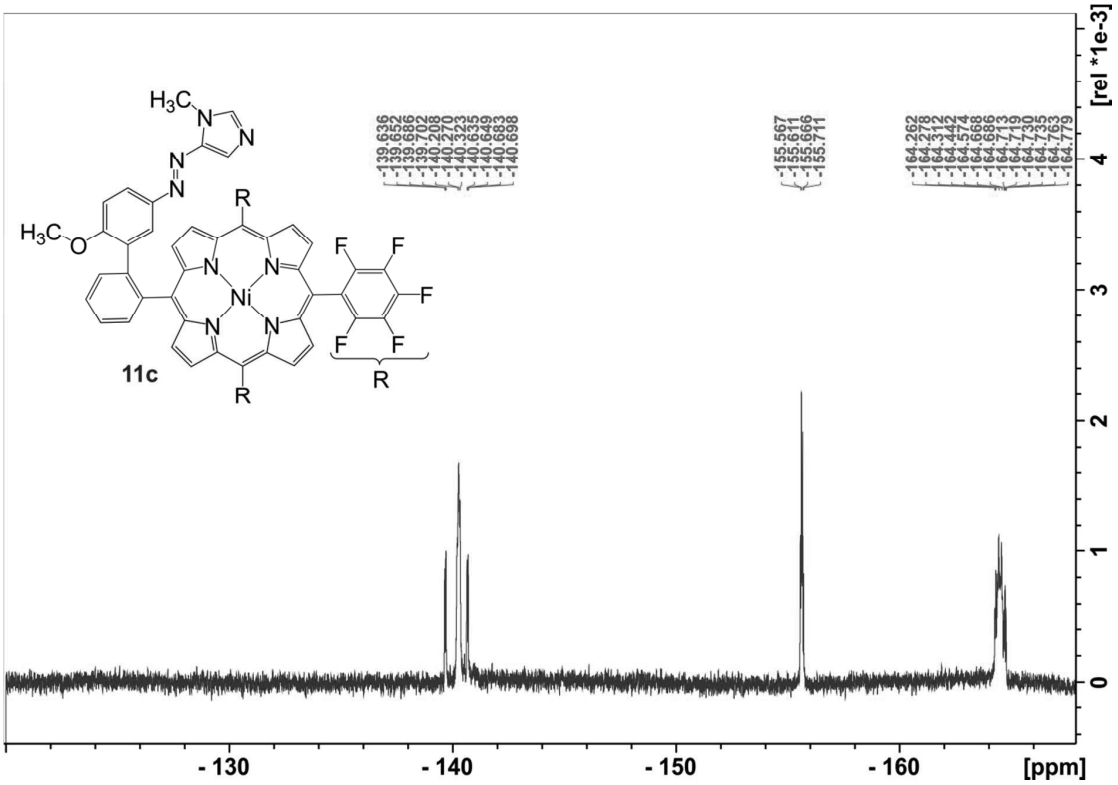

Figure S52. ^{19}F-NMR (470 MHz, acetone-d_6, TFA-d, 300 K) spectrum of **11c**.

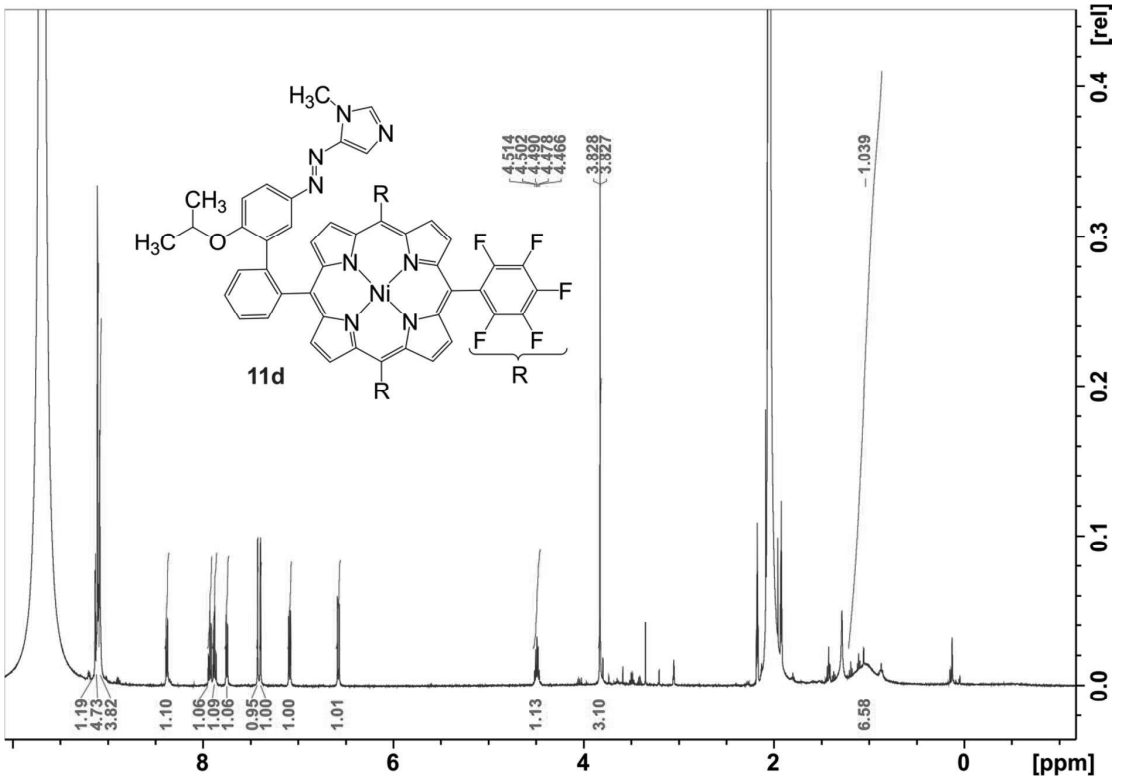

Figure S53. ^{1}H-NMR (500 MHz, acetone-d_6, TFA-d, 300 K) spectrum of **11d**.

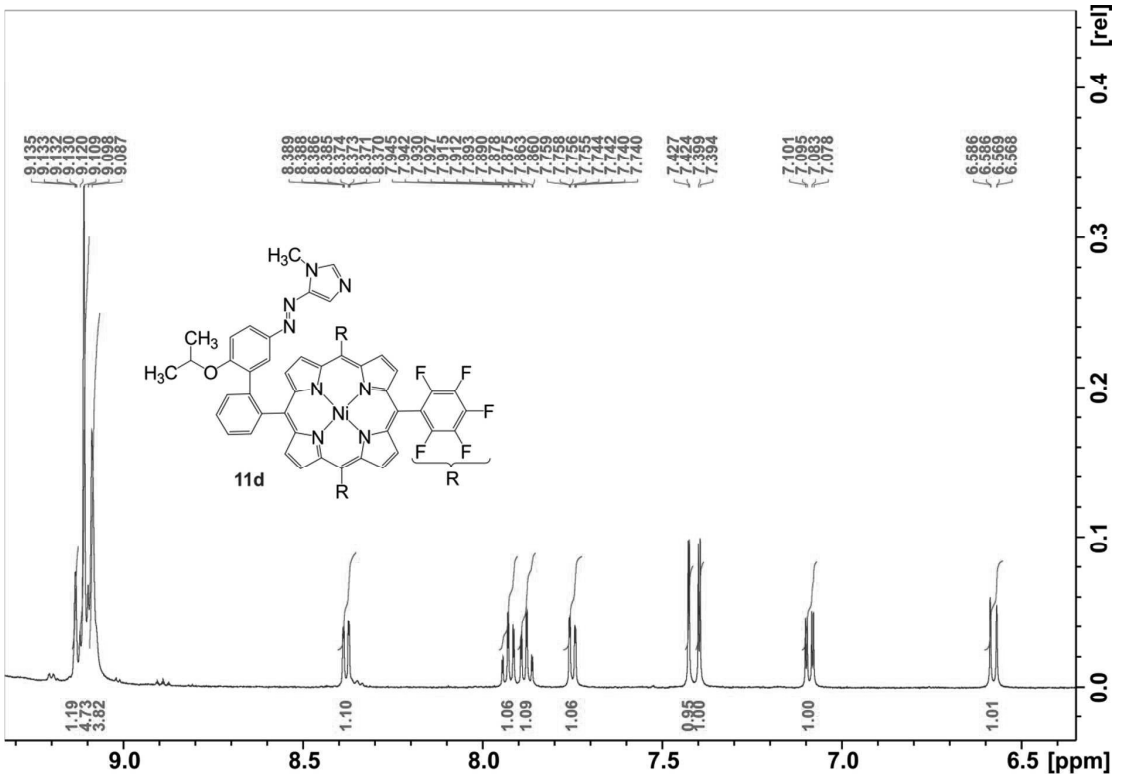

Figure S54. ^{1}H-NMR (500 MHz, acetone-d_6, TFA-d, 300 K) spectrum (aromatic region) of **11d**.

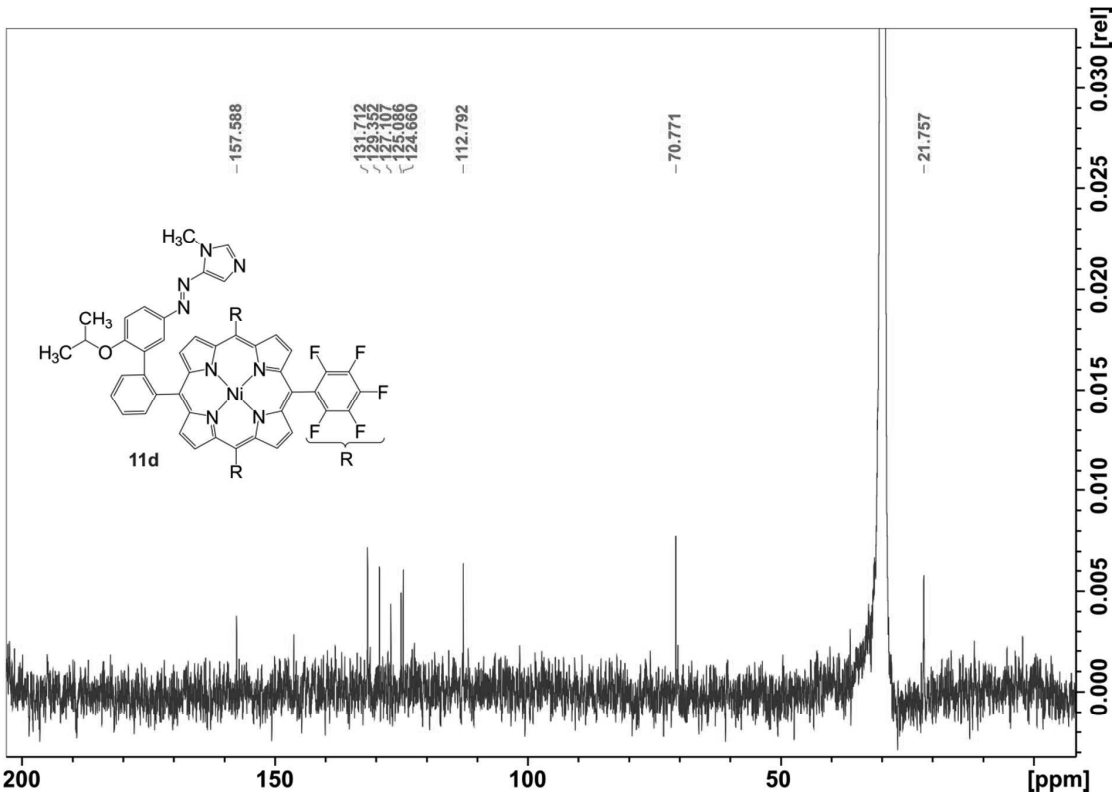

Figure S55. ^{13}C-NMR (150 MHz, acetone-d_6, 300 K) spectrum of **11d**.

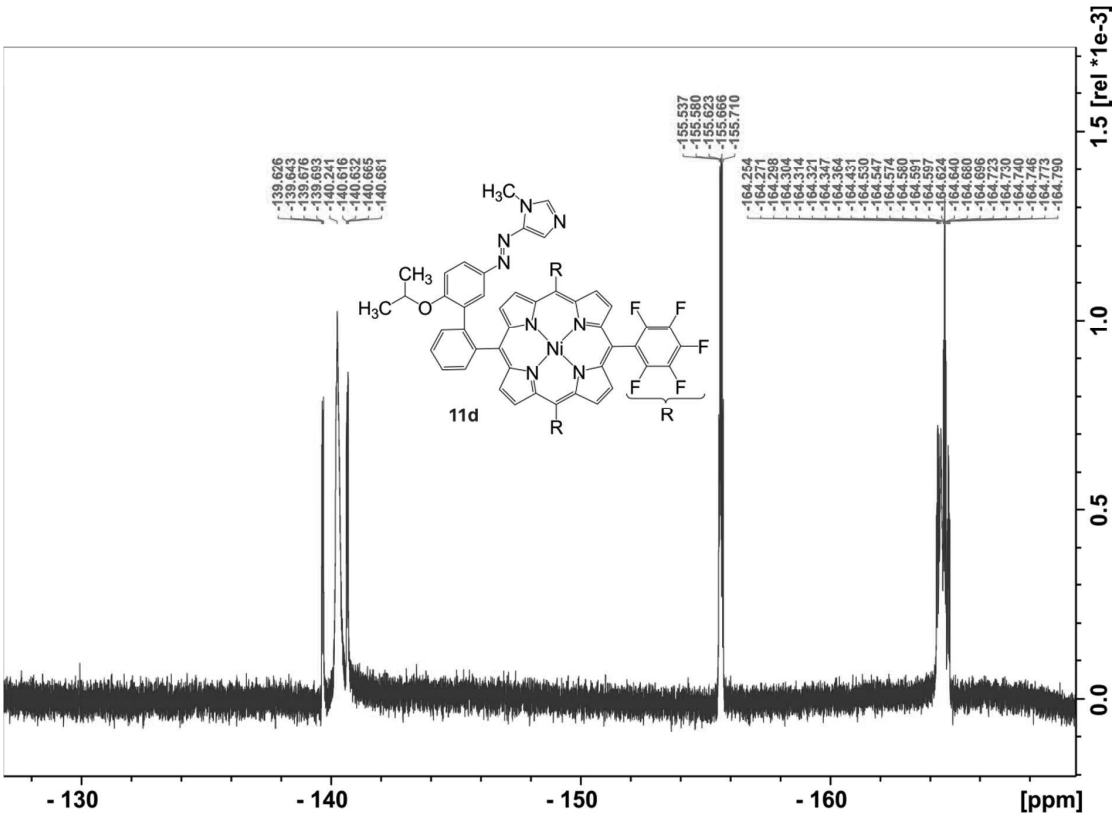

Figure S56. ^{19}F-NMR (470 MHz, acetone-d_6, TFA-d, 300 K) spectrum of **11d**.

IV. Literature

(1) Strueben, J.; Lipfert, M.; Springer, J.-O.; Gould, C. A.; Gates, P. J.; Sönnichsen, F. D.; Staubitz, A. *Chemistry - A European Journal* **2015**, *21*, 11165–11173.

(2) Venkataramani, S.; Jana, U.; Dommaschk, M.; Sönnichsen, F. D.; Tuczek, F.; Herges, R. *Science* **2011**, *331*, 445–448.

(3) Dommaschk, M.; Peters, M.; Gutzeit, F.; Schütt, C.; Näther, C.; Sönnichsen, F. D.; Tiwari, S.; Riedel, C.; Boretius, S.; Herges, R. *J. Am. Chem. Soc.* **2015**, *137*, 7552–7555.

(4) Heitmann, G.; Schütt, C.; Gröbner, J.; Huber, L. M.; Herges, R. *Dalton Trans.* **2016**, *45*, 11407–11412.

(5) Chadwick, D. J.; Ngochindo, R. I. *J. Chem. Soc. Perkin Trans. 1* **1984**, 481–486.

9 Literaturverzeichnis

[1] P. Gütlich, H. A. Goodwin, *Spin Crossover in Transition Metal Compounds I-III*, Topics in Current Chemistry, Springer-Verlag Berlin Heidelberg New York **2004**.

[2] M. A. Halcrow, *Spin-Crossover Materials: Properties and Applications*, John Wiley & Sons Ltd **2013**.

[3] O. Kahn, *Science* **1998**, *279*, 44–48.

[4] A. Bousseksou, G. Molnár, P. Demont, J. Menegotto, *J. Mater. Chem.* **2003**, *13*, 2069–2071.

[5] A. Bousseksou, C. Vieu, J.-F. Letard, P. Demont, J.-P. Tuchagues, L. Malaquin, J. Menegotto, L. Salmon, Molecular memory and method for making same. Patent WO 2003019695 A1, **06.03.2003**.

[6] Y. Garcia, V. Ksenofontov, P. Gütlich, *Hyperfine Interact.* **2002**, *139/140*, 543–551.

[7] S. Sanvito, *Chem. Soc. Rev.* **2011**, *40*, 3336–3355.

[8] K. A. Mirica, S. S. Shevkoplyas, S. T. Phillips, M. Gupta, G. M. Whitesides, *J. Am. Chem. Soc.* **2009**, *131*, 10049–10058.

[9] G. Fanucci, D. Cafiso, *Curr. Opin. Struct. Biol.* **2006**, *16*, 644–653.

[10] R. Herges, *Nachr. Chem.* **2011**, *59*, 817–821.

[11] R. N. Muller, L. V. Elst, S. Laurent, *J. Am. Chem. Soc.* **2003**, *125*, 8405–8407.

[12] D. Weishaupt, V. D. Köchli, B. Marincek, *Wie funktioniert MRI?*, 7. Aufl., Springer-Verlag Berlin Heidelberg **2014**.

[13] P. C. Lauterbur, *Nature* **1973**, *242*, 190–191.

[14] A. N. Garroway, P. K. Grannell, P. Mansfield, *J. Phys. C: Solid State Phys.* **1974**, *7*, L457–L462.

[15] P. Mansfield, *J. Phys. C: Solid State Phys.* **1977**, *10*, L55–L58.

[16] C. G. Fry, *J. Chem. Educ.* **2004**, *81*, 922–932.

[17] B. M. Dale, M. A. Brown, R. C. Semelka, *MRI: Basic Principles and Applications*, 5. Aufl., Wiley-Blackwell **2015**.

[18] L. M. Fletcher, J. B. Barsotti, J. P. Hornak, *Magn. Reson. Med.* **1993**, *29*, 623–630.

[19] R. Damadian, *Science* **1971**, *171*, 1151–1153.

[20] F. Bloch, W. W. Hansen, M. Packard, *Phys. Rev.* **1946**, *70*, 474–485.

[21] N. Bloembergen, E. M. Purcell, R. V. Pound, *Phys. Rev.* **1948**, *73*, 679–712.

[22] P. Reimer, R. Vosshenrich, *Der Radiologe* **2004**, *44*, 273–283.

[23] Hellerhoff, Bluthirnschranke nach Infarkt nativ und KM.png, Online-Material **2010**, URL `https://commons.wikimedia.org/wiki/File%3ABluthirnschranke_nach_Infarkt_nativ_und_KM.png`, Abgerufen am 24.08.2016.

[24] R. B. Lauffer, *Chem. Rev.* **1987**, *87*, 901–927.

[25] C. de Haen, *Top. Magn. Reson. Imaging* **2001**, *12*, 221–230.

[26] P. Caravan, J. J. Ellison, T. J. McMurry, R. B. Lauffer, *Chem. Rev.* **1999**, *99*, 2293–2352.

[27] J.-M. Idée, M. Port, I. Raynal, M. Schaefer, S. L. Greneur, C. Corot, *Fundam. Clin. Pharmacol.* **2006**, *20*, 563–576.

[28] T. Meade, *Curr. Opin. Neurobiol.* **2003**, *13*, 597–602.

[29] L. M. D. Leon-Rodriguez, A. J. M. Lubag, C. R. Malloy, G. V. Martinez, R. J. Gillies, A. D. Sherry, *Acc. Chem. Res.* **2009**, *42*, 948–957.

[30] E. L. Que, C. J. Chang, *Chem. Soc. Rev.* **2010**, *39*, 51–60.

[31] J. Hall, R. Häner, S. Aime, M. Botta, S. Faulkner, D. Parker, A. S. de Sousa, *New J. Chem.* **1998**, *22*, 627–631.

[32] S. Zhang, K. Wu, A. D. Sherry, *Angew. Chem. Int. Ed.* **1999**, *38*, 3192–3194.

[33] S. Aime, S. G. Crich, M. Botta, G. Giovenzana, G. Palmisano, M. Sisti, *Chem. Commun.* **1999**, 1577–1578.

[34] M. P. Lowe, D. Parker, O. Reany, S. Aime, M. Botta, G. Castellano, E. Gianolio, R. Pagliarin, *J. Am. Chem. Soc.* **2001**, *123*, 7601–7609.

[35] M. Woods, G. E. Kiefer, S. Bott, A. Castillo-Muzquiz, C. Eshelbrenner, L. Michaudet, K. McMillan, S. D. K. Mudigunda, D. Ogrin, G. Tircsó, S. Zhang, P. Zhao, A. D. Sherry, *J. Am. Chem. Soc.* **2004**, *126*, 9248–9256.

[36] E. Tóth, R. D. Bolskar, A. Borel, G. González, L. Helm, A. E. Merbach, B. Sitharaman, L. J. Wilson, *J. Am. Chem. Soc.* **2005**, *127*, 799–805.

[37] D. D. Castelli, E. Terreno, S. Aime, *Angew. Chem. Int. Ed.* **2011**, *50*, 1798–1800.

[38] I.-R. Jeon, J. G. Park, C. R. Haney, T. D. Harris, *Chem. Sci.* **2014**, *5*, 2461.

[39] R. A. Moats, S. E. Fraser, T. J. Meade, *Angew. Chem. Int. Ed.* **1997**, *36*, 726–728.

[40] A. Y. Louie, M. M. Hüber, E. T. Ahrens, U. Rothbächer, R. Moats, R. E. Jacobs, S. E. Fraser, T. J. Meade, *Nat. Biotechnol.* **2000**, *18*, 321–325.

[41] J. A. Duimstra, F. J. Femia, T. J. Meade, *J. Am. Chem. Soc.* **2005**, *127*, 12847–12855.

[42] M. Querol, J. W. Chen, R. Weissleder, A. Bogdanov, *Org. Lett.* **2005**, *7*, 1719–1722.

[43] M. Giardiello, M. P. Lowe, M. Botta, *Chem. Commun.* **2007**, 4044–4046.

[44] K. Hanaoka, K. Kikuchi, T. Terai, T. Komatsu, T. Nagano, *Chem. Eur. J.* **2008**, *14*, 987–995.

[45] S. Mizukami, R. Takikawa, F. Sugihara, Y. Hori, H. Tochio, M. Wälchli, M. Shirakawa, K. Kikuchi, *J. Am. Chem. Soc.* **2008**, *130*, 794–795.

[46] F. Touti, P. Maurin, J. Hasserodt, *Angew. Chem. Int. Ed.* **2013**, *52*, 4654–4658.

[47] C. Carrera, G. Digilio, S. Baroni, D. Burgio, S. Consol, F. Fedeli, D. Longo, A. Mortillaro, S. Aime, *Dalton Trans.* **2007**, 4980–4987.

[48] S. Aime, D. D. Castelli, F. Fedeli, E. Terreno, *J. Am. Chem. Soc.* **2002**, *124*, 9364–9365.

[49] R. Trokowski, S. Zhang, A. D. Sherry, *Bioconjugate Chem.* **2004**, *15*, 1431–1440.

[50] W. Li, S. E. Fraser, T. J. Meade, *J. Am. Chem. Soc.* **1999**, *121*, 1413–1414.

[51] K. Dhingra, M. E. Maier, M. Beyerlein, G. Angelovski, N. K. Logothetis, *Chem. Commun.* **2008**, 3444–3446.

[52] G. Angelovski, P. Fousková, I. Mamedov, S. Canals, E. Tóth, N. K. Logothetis, *ChemBioChem* **2008**, *9*, 1729–1734.

[53] E. L. Que, E. Gianolio, S. L. Baker, A. P. Wong, S. Aime, C. J. Chang, *J. Am. Chem. Soc.* **2009**, *131*, 8527–8536.

[54] K. Hanaoka, K. Kikuchi, Y. Urano, T. Nagano, *J. Chem. Soc., Perkin Trans. 2* **2001**, 1840–1843.

[55] J. L. Major, G. Parigi, C. Luchinat, T. J. Meade, *Proc. Natl. Acad. Sci. U.S.A.* **2007**, *104*, 13881–13886.

[56] H. Hifumi, A. Tanimoto, D. Citterio, H. Komatsu, K. Suzuki, *The Analyst* **2007**, *132*, 1153–1160.

[57] C. Shen, E. J. New, *Curr. Opin. Chem. Biol.* **2013**, *17*, 158–166.

[58] S. Zhang, M. Merritt, D. E. Woessner, R. E. Lenkinski, A. D. Sherry, *Acc. Chem. Res.* **2003**, *36*, 783–790.

[59] K. R. Thulborn, J. C. Waterton, P. M. Matthews, G. K. Radda, *BBA - Gen. Subjects* **1982**, *714*, 265–270.

[60] J. W. Belliveau, B. R. Rosen, H. L. Kantor, R. R. Rzedzian, D. N. Kennedy, R. C. McKinstry, J. M. Vevea, M. S. Cohen, I. L. Pykett, T. J. Brady, *Magn. Reson. Med.* **1990**, *14*, 538–546.

[61] S. Ogawa, T. M. Lee, A. R. Kay, D. W. Tank, *Proc. Natl. Acad. Sci. U.S.A.* **1990**, *87*, 9868–9872.

[62] S. Ogawa, T.-M. Lee, A. S. Nayak, P. Glynn, *Magn. Reson. Med.* **1990**, *14*, 68–78.

[63] N. K. Logothetis, J. Pauls, M. Augath, T. Trinath, A. Oeltermann, *Nature* **2001**, *412*, 150–157.

[64] A. H. Mahnken, K. E. Wilhelm, J. Ricke, *CT- and MR-Guided Interventions in Radiology*, 2. Aufl., Springer-Verlag Berlin Heidelberg **2013**.

[65] D. Bléger, S. Hecht, *Angew. Chem. Int. Ed.* **2015**, *54*, 11338–11349.

[66] M. Banghart, K. Borges, E. Isacoff, D. Trauner, R. H. Kramer, *Nat. Neurosci.* **2004**, *7*, 1381–1386.

[67] A. A. Beharry, G. A. Woolley, *Chem. Soc. Rev.* **2011**, *40*, 4422–4437.

[68] A. Polosukhina, J. Litt, I. Tochitsky, J. Nemargut, Y. Sychev, I. D. Kouchkovsky, T. Huang, K. Borges, D. Trauner, R. N. V. Gelder, R. H. Kramer, *Neuron* **2012**, *75*, 271–282.

[69] W. Szymanski, J. M. Beierle, H. A. V. Kistemaker, W. A. Velema, B. L. Feringa, *Chem. Rev.* **2013**, *113*, 6114–6178.

[70] L. Möckl, A. Müller, C. Bräuchle, T. K. Lindhorst, *Chem. Commun.* **2016**, *52*, 1254–1257.

[71] C. Tu, A. Y. Louie, *Chem. Commun.* **2007**, 1331–1333.

[72] C. Tu, E. A. Osborne, A. Y. Louie, *Tetrahedron* **2009**, *65*, 1241–1246.

[73] F. Hund, *Zeitschrift für Physik* **1925**, *33*, 345–371.

[74] L. Cambi, L. Szegö, *Ber. dtsch. Chem. Ges. A/B* **1931**, *64*, 2591–2598.

[75] L. Cambi, A. Cagnasso, *Atti Accad. Naz. Lincei* **1931**, *13*, 809–813.

[76] C. D. Coryell, F. Stitt, L. Pauling, *J. Am. Chem. Soc.* **1937**, *59*, 633–642.

[77] R. C. Stoufer, D. H. Busch, W. B. Hadley, *J. Am. Chem. Soc.* **1961**, *83*, 3732–3734.

[78] A. H. Ewald, R. L. Martin, I. G. Ross, A. H. White, *Proc. R. Soc. London, Ser. A* **1964**, *280*, 235–257.

[79] E. Koenig, K. Madeja, *Inorg. Chem.* **1967**, *6*, 48–55.

[80] S. Decurtins, P. Gütlich, C. Köhler, H. Spiering, A. Hauser, *Chem. Phys. Lett.* **1984**, *105*, 1–4.

[81] J. Krober, E. Codjovi, O. Kahn, F. Groliere, C. Jay, *J. Am. Chem. Soc.* **1993**, *115*, 9810–9811.

[82] T. Granier, B. Gallois, J. Gaultier, J. A. Real, J. Zarembowitch, *Inorg. Chem.* **1993**, *32*, 5305–5312.

[83] C. Roux, J. Zarembowitch, B. Gallois, T. Granier, R. Claude, *Inorg. Chem.* **1994**, *33*, 2273–2279.

[84] E. Coronado, J. R. Galán-Mascarós, M. Monrabal-Capilla, J. García-Martínez, P. Pardo-Ibáñez, *Adv. Mater.* **2007**, *19*, 1359–1361.

[85] M. Nihei, T. Shiga, Y. Maeda, H. Oshido, *Coord. Chem. Rev.* **2007**, *251*, 2606–2621.

[86] A. Bousseksou, G. Molnár, L. Salmon, W. Nicolazzi, *Chem. Soc. Rev.* **2011**, *40*, 3313.

[87] P. Gütlich, *Eur. J. Inorg. Chem.* **2013**, *2013*, 581–591.

[88] P. Gütlich, A. B. Gaspar, Y. Garcia, *Beilstein J. Org. Chem.* **2013**, *9*, 342–391.

[89] P. Gütlich, A. Hauser, H. Spiering, *Angew. Chem. Int. Ed.* **1994**, *33*, 2024–2054.

[90] P. Gütlich, Y. Garcia, H. A. Goodwin, *Chem. Soc. Rev.* **2000**, *29*, 419–427.

[91] J. A. Real, A. B. Gaspar, V. Niel, M. Muñoz, *Coord. Chem. Rev.* **2003**, *236*, 121–141.

[92] M. A. Halcrow, *Polyhedron* **2007**, *26*, 3523–3576.

[93] Y. Garcia, P. J. van Koningsbruggen, E. Codjovi, R. Lapouyade, O. Kahn, L. Rabardel, *J. Mater. Chem.* **1997**, *7*, 857–858.

[94] M. A. Halcrow, *Chem. Lett.* **2014**, *43*, 1178–1188.

[95] J. Zarembowitch, C. Roux, M.-L. Boillot, R. Claude, J.-P. Itie, A. Polian, M. Bolte, *Mol. Cryst. Liq. Cryst. Sci. Technol., Sect. A* **1993**, *234*, 247–254.

[96] J. A. Real, A. B. Gaspar, M. C. Muñoz, *Dalton Trans.* **2005**, 2062.

[97] O. Sato, J. Tao, Y.-Z. Zhang, *Angew. Chem. Int. Ed.* **2007**, *46*, 2152–2187.

[98] M. Khusniyarov, *Elsevier Reference Module in Chemistry, Molecular Sciences and Chemical Engineering*, Kap. Light-Induced Spin-crossover, Elsevier Waltham (MA) **2015**.

[99] M. M. Khusniyarov, *Chem. Eur. J.* **2016**, *22*, 15178–15191.

[100] S. Decurtins, P. Gütlich, K. M. Hasselbach, A. Hauser, H. Spiering, *Inorg. Chem.* **1985**, *24*, 2174–2178.

[101] A. Hauser, *Chem. Phys. Lett.* **1986**, *124*, 543–548.

[102] J. J. McGravey, I. Lawthers, *J. Chem. Soc., Chem. Commun.* **1982**, 906–907.

[103] M.-L. Boillot, C. Roux, J.-P. Audière, A. Dausse, J. Zarembowitch, *Inorg. Chem.* **1996**, *35*, 3975–3980.

[104] M.-L. Boillot, J. Zarembowitch, A. Sour, *Spin Crossover in Transition Metal Compounds II*, Bd. 234 von *Topics in Current Chemistry*, Kap. Ligand-Driven Light-Induced Spin Change (LD-LISC): A Promising Photomagnetic Effect, Springer-Verlag Berlin Heidelberg **2004**, 261–276.

[105] K. Takahashi, Y. Hasegawa, R. Sakamoto, M. Nishikawa, S. Kume, E. Nishibori, H. Nishihara, *Inorg. Chem.* **2012**, *51*, 5188–5198.

[106] B. Rösner, M. Milek, A. Witt, B. Gobaut, P. Torelli, R. H. Fink, M. M. Khusniyarov, *Angew. Chem. Int. Ed.* **2015**, *54*, 12976–12980.

[107] M.-L. Boillot, S. Chantraine, J. Zarembowitch, J.-Y. Lallemand, J. Prunet, *New J. Chem.* **1999**, *23*, 179–184.

[108] R. M. Buchanan, C. G. Pierpont, *J. Am. Chem. Soc.* **1980**, *102*, 4951–4957.

[109] D. N. Hendrickson, C. G. Pierpont, *Spin Crossover in Transition Metal Compounds II*, Bd. 234 von *Topics in Current Chemistry*, Kap. Valence Tautomeric Transition Metal Complexes, Springer-Verlag Berlin Heidelberg **2004**, 63–95.

[110] E. Evangelio, D. Ruiz-Molina, *Eur. J. Inorg. Chem.* **2005**, *2005*, 2957–2971.

[111] O. Sato, A. Cui, R. Matsuda, J. Tao, S. Hayami, *Acc. Chem. Res.* **2007**, *40*, 361–369.

[112] T. Tezgerevska, K. G. Alley, C. Boskovic, *Coord. Chem. Rev.* **2014**, *268*, 23–40.

[113] D. M. Adams, B. Li, J. D. Simon, D. N. Hendrickson, *Angew. Chem. Int. Ed.* **1995**, *34*, 1481–1483.

[114] A. Witt, F. W. Heinemann, S. Sproules, M. M. Khusniyarov, *Chem. Eur. J.* **2014**, *20*, 11149–11162.

[115] A. Witt, F. W. Heinemann, M. M. Khusniyarov, *Chem. Sci.* **2015**, *6*, 4599–4609.

[116] S. Thies, H. Sell, C. Schütt, C. Bornholdt, C. Näther, F. Tuczek, R. Herges, *J. Am. Chem. Soc.* **2011**, *133*, 16243–16250.

[117] S. Venkataramani, U. Jana, M. Dommaschk, F. D. Sönnichsen, F. Tuczek, R. Herges, *Science* **2011**, *331*, 445–448.

[118] S. Thies, C. Bornholdt, F. Köhler, F. D. Sönnichsen, C. Näther, F. Tuczek, R. Herges, *Chem. Eur. J.* **2010**, *16*, 10074–10083.

[119] M. Dommaschk, F. Gutzeit, S. Boretius, R. Haag, R. Herges, *Chem. Commun.* **2014**, *50*, 12476–12478.

[120] M. Dommaschk, V. Thoms, C. Schütt, C. Näther, R. Puttreddy, K. Rissanen, R. Herges, *Inorg. Chem.* **2015**, *54*, 9390–9392.

[121] C. Lochenie, K. G. Wagner, M. Karg, B. Weber, *J. Mater. Chem. C* **2015**, *3*, 7925–7935.

[122] K. Bütje, K. Nakamoto, *Inorg. Chim. Acta* **1990**, *167*, 97–108.

[123] F. A. Walker, E. Hui, J. M. Walker, *J. Am. Chem. Soc.* **1975**, *97*, 2390–2397.

[124] Y. Song, R. E. Haddad, S.-L. Jia, S. Hok, M. M. Olmstead, D. J. Nurco, N. E. Schore, J. Zhang, J.-G. Ma, K. M. Smith, S. Gazeau, J. Pécaut, J.-C. Marchon, C. J. Medforth, J. A. Shelnutt, *J. Am. Chem. Soc.* **2005**, *127*, 1179–1192.

[125] B. D. McLees, W. S. Caughey, *Biochemistry* **1968**, *7*, 642–652.

[126] D. Kim, Y. O. Su, T. G. Spiro, *Inorg. Chem.* **1986**, *25*, 3988–3993.

[127] W. A. Kaplan, R. A. Scott, K. S. Suslick, *J. Am. Chem. Soc.* **1990**, *112*, 1283–1285.

[128] W. S. Caughey, W. Y. Fujimoto, B. P. Johnson, *Biochemistry* **1966**, *5*, 3830–3843.

[129] W. S. Caughey, R. M. Deal, B. D. McLees, J. O. Alben, *J. Am. Chem. Soc.* **1962**, *84*, 1735–1736.

[130] E. W. Baker, M. S. Brookhart, A. H. Corwin, *J. Am. Chem. Soc.* **1964**, *86*, 4587–4590.

[131] C. Bornholdt, *Dissertation*, Christian-Albrechts-Universität zu Kiel **2008**.

[132] G. C. Hampson, J. M. Robertson, *J. Chem. Soc.* **1941**, 409–413.

[133] A. Mostad, C. Roemming, *Acta Chem. Scand.* **1971**, *25*, 3561–3568.

[134] T. Umemoto, Y. Ohtani, T. Tsukamoto, T. Shimada, S. Takagi, *Chem. Commun.* **2014**, *50*, 314–316.

[135] S. Thies, H. Sell, C. Bornholdt, C. Schütt, F. Köhler, F. Tuczek, R. Herges, *Chem. Eur. J.* **2012**, *18*, 16358–16368.

[136] W. G. Levine, *Drug Metab. Revi.* **1991**, *23*, 253–309.

[137] M. A. Brown, S. C. D. Vito, *Crit. Rev. Env. Sci. Tec.* **1993**, *23*, 249–324.

[138] M. Dommaschk, M. Peters, F. Gutzeit, C. Schütt, C. Näther, F. D. Sönnichsen, S. Tiwari, C. Riedel, S. Boretius, R. Herges, *J. Am. Chem. Soc.* **2015**, *137*, 7552–7555.

[139] M. Dommaschk, C. Näther, R. Herges, *J. Org. Chem.* **2015**, *80*, 8496–8500.

[140] M. Dommaschk, C. Schütt, S. Venkataramani, U. Jana, C. Näther, F. D. Sönnichsen, R. Herges, *Dalton Trans.* **2014**, *43*, 17395–17405.

[141] T. La, R. A. Richards, R. S. Lu, R. Bau, G. M. Miskelly, *Inorg. Chem.* **1995**, *34*, 5632–5640.

[142] T. Wendler, C. Schütt, C. Näther, R. Herges, *J. Org. Chem.* **2012**, *77*, 3284–3287.

[143] T. Wendler, *Dissertation*, Christian-Albrechts-Universität zu Kiel **2013**.

[144] J. Otsuki, K. Suwa, K. K. Sarker, C. Sinha, *J. Phys. Chem. A* **2007**, *111*, 1403–1409.

[145] J. Otsuki, K. Narutaki, J. M. Bakke, *Chem. Lett.* **2004**, *33*, 356–357.

[146] J. Otsuki, K. Narutaki, *Bull. Chem. Soc. Jpn.* **2004**, *77*, 1537–1544.

[147] K. Suwa, J. Otsuki, K. Goto, *Tetrahedron Lett.* **2009**, *50*, 2106–2108.

[148] T. Hirose, F. Helmich, E. W. Meijer, *Angew. Chem. Int. Ed.* **2012**, *52*, 304–309.

[149] J. Otsuki, T. Akasaka, K. Araki, *Coord. Chem. Rev.* **2008**, *252*, 32–56.

[150] W. A. Velema, W. Szymanski, B. L. Feringa, *J. Am. Chem. Soc.* **2014**, *136*, 2178–2191.

[151] J. Broichhagen, J. A. Frank, D. Trauner, *Acc. Chem. Res.* **2015**, *48*, 1947–1960.

[152] M. M. Lerch, M. J. Hansen, G. M. van Dam, W. Szymanski, B. L. Feringa, *Angew. Chem. Int. Ed.* **2016**, *55*, 10978–10999.

[153] J. Broichhagen, I. Jurastow, K. Iwan, W. Kummer, D. Trauner, *Angew. Chem. Int. Ed.* **2014**, *53*, 7657–7660.

[154] M. J. Hansen, W. A. Velema, G. de Bruin, H. S. Overkleeft, W. Szymanski, B. L. Feringa, *ChemBioChem* **2014**, *15*, 2053–2057.

[155] M. Borowiak, W. Nahaboo, M. Reynders, K. Nekolla, P. Jalinot, J. Hasserodt, M. Rehberg, M. Delattre, S. Zahler, A. Vollmar, D. Trauner, O. Thorn-Seshold, *Cell* **2015**, *162*, 403–411.

[156] W. Szymanski, M. E. Ourailidou, W. A. Velema, F. J. Dekker, B. L. Feringa, *Chem. Eur. J.* **2015**, *21*, 16517–16524.

[157] R. Ferreira, J. R. Nilsson, C. Solano, J. Andréasson, M. Grotli, *Sci. Rep.* **2015**, *5*, 9769.

[158] R. Huckvale, M. Mortensen, D. Pryde, T. G. Smart, J. R. Baker, *Org. Biomol. Chem.* **2016**, *14*, 6676–6678.

[159] C. Schütt, G. Heitmann, T. Wendler, B. Krahwinkel, R. Herges, *J. Org. Chem.* **2016**, *81*, 1206–1215.

[160] P. Rothemund, *J. Am. Chem. Soc.* **1935**, *57*, 2010–2011.

[161] P. Rothemund, A. R. Menotti, *J. Am. Chem. Soc.* **1941**, *63*, 267–270.

[162] A. D. Adler, F. R. Longo, J. D. Finarelli, J. Goldmacher, J. Assour, L. Korsakoff, *J. Org. Chem.* **1967**, *32*, 476.

[163] J. S. Lindsey, I. C. Schreiman, H. C. Hsu, P. C. Kearney, A. M. Marguerettaz, *J. Org. Chem.* **1987**, *52*, 827–836.

[164] J. S. Lindsey, R. W. Wagner, *J. Org. Chem.* **1989**, *54*, 828–836.

[165] M. O. Senge, M. Fazekas, E. G. A. Notaras, W. J. Blau, M. Zawadzka, O. B. Locos, E. M. N. Mhuircheartaigh, *Adv. Mater.* **2007**, *19*, 2737–2774.

[166] J. P. Celli, B. Q. Spring, I. Rizvi, C. L. Evans, K. S. Samkoe, S. Verma, B. W. Pogue, T. Hasan, *Chem. Rev.* **2010**, *110*, 2795–2838.

[167] M. O. Senge, *Chem. Commun.* **2011**, *47*, 1943–1960.

[168] G. Heitmann, C. Schütt, J. Gröbner, L. Huber, R. Herges, *Dalton Trans.* **2016**, *45*, 11407–11412.

[169] G. Heitmann, C. Schütt, R. Herges, *Eur. J. Org. Chem.* **2016**, *2016*, 3817–3823.

[170] G. Alcover-Fortuny, C. de Graaf, R. Caballol, *Phys. Chem. Chem. Phys.* **2015**, *17*, 217–225.

[171] M. Dommaschk, C. Schütt, R. Herges, *unveröffentlichte Ergebnisse* **2016**, Christian–Albrechts–Universität zu Kiel.

[172] G. Heitmann, M. Dommaschk, R. Löw, R. Herges, *Org. Lett.* **2016**, *18*, 5228–5231.

[173] M. Dommaschk, *unveröffentlichte Ergebnisse* **2016**, Christian–Albrechts–Universität zu Kiel.

[174] G. Heitmann, *unveröffentlichte Ergebnisse* **2016**, Christian–Albrechts–Universität zu Kiel.

[175] J. Ludwig, *unveröffentlichte Ergebnisse* **2016**, Christian–Albrechts–Universität zu Kiel.

[176] V. Thoms, *unveröffentlichte Ergebnisse* **2016**, Christian–Albrechts–Universität zu Kiel.

[177] G. Heitmann, C. Schütt, *unveröffentlichte Ergebnisse* **2016**, Christian–Albrechts–Universität zu Kiel.

[178] H. Kropp, A. Scheurer, F. W. Heinemann, J. Bendix, K. Meyer, *Inorg. Chem.* **2015**, *54*, 3562–3572.

[179] K. Shikama, *Coord. Chem. Rev.* **1988**, *83*, 73–91.

[180] R. Huszank, O. Horvath, *Chem. Commun.* **2005**, 224–226.

[181] L. Christiansen, D. N. Hendrickson, H. Toftlund, S. R. Wilson, C. L. Xie, *Inorg. Chem.* **1986**, *25*, 2813–2818.

[182] L. Spiccia, G. D. Fallon, M. J. Grannas, P. J. Nichols, E. R. T. Tiekink, *Inorg. Chim. Acta* **1998**, *279*, 192–199.

[183] V. Stavila, M. Allali, L. Canaple, Y. Stortz, C. Franc, P. Maurin, O. Beuf, O. Dufay, J. Samarut, M. Janier, J. Hasserodt, *New J. Chem.* **2008**, *32*, 428–435.

[184] P. B. Tsitovich, J. M. Cox, J. B. Benedict, J. R. Morrow, *Inorg. Chem.* **2016**, *55*, 700–716.

[185] F. Touti, A. K. Singh, P. Maurin, L. Canaple, O. Beuf, J. Samarut, J. Hasserodt, *J. Med. Chem.* **2011**, *54*, 4274–4278.

[186] J. Wang, C. Gondrand, F. Touti, J. Hasserodt, *Dalton Trans.* **2015**, *44*, 15391–15395.

[187] C. Gondrand, F. Touti, E. Godart, Y. Berezhanskyy, E. Jeanneau, P. Maurin, J. Hasserodt, *Eur. J. Inorg. Chem.* **2015**, *2015*, 1376–1382.

[188] F. Touti, P. Maurin, L. Canaple, O. Beuf, J. Hasserodt, *Inorg. Chem.* **2012**, *51*, 31–33.

[189] C. E. Weston, R. D. Richardson, P. J. Haycock, A. J. P. White, M. J. Fuchter, *J. Am. Chem. Soc.* **2014**, *136*, 11878–11881.

[190] C. E. Weston, R. D. Richardson, M. J. Fuchter, *Chem. Commun.* **2016**, *52*, 4521–4524.

[191] R. Siewertsen, H. Neumann, B. Buchheim-Stehn, R. Herges, C. Nather, F. Renth, F. Temps, *J. Am. Chem. Soc.* **2009**, *131*, 15594–15595.